UNIVERSIDAD NACIONAL DE COLOMBIA

Grupo de Campos y Partículas
Facultad de Ciencias

Limitantes desde estabilidad del vacío, unitariedad perturbativa y parámetros oblicuos en el modelo con dos dobletes de Higgs

Andrés Castillo
Departamento de Física
Universidad Nacional de Colombia

Director: Dr. John Morales Aponte

Tesis sometida para optar al titulo de Doctor en Ciencias-Física

UNIVERSIDAD NACIONAL DE COLOMBIA

Grupo de Campos y Partículas
Facultad de Ciencias

Theoretical and phenomenological analyses from vacuum stability, perturbative unitarity, and oblique parameters in the Two Higgs Doublet Model

Andrés Castillo
Departamento de Física
Universidad Nacional de Colombia

Advisor: Dr. John Morales Aponte

This dissertation is submitted for the degree of Doctor of Philosophy-Physics

To my family

"Non est ad astra mollis e terris via"
Seneca

Contents

List of Figures

List of Tables

Acronyms List

In the following table, we define relevant acronyms that shall be used along the text:

Acronym	**Meaning**	***Context and Benchmarks***
QFT	Quantum Filed Theory	Mathematical frameworks for quantum interactions in space-time
QED	Quantum Electrodynamics	QFT based on the interactions among photons and charged particles
SM	Standard Model	Fundamental QFT to Particles Interactions: EW plus QCD
EW	Electroweak	QED plus weak interactions based on $SU(2)_L \times U(1)_Y$ gauge group
QCD	Quantum Cromodynamics	Strong interactions based on the $SU(3)_C$ gauge group
2HDM(s)	Two Higgs Doublet Model(s)	Next non-trivial extension to Higgs sector of SM
VEV	Vacuum Expectation Values	Average of a field operator in the vacuum
SSB	Spontaneous Symmetry Breaking	Physical processes to break a symmetry by the vacuum realization
CP(T)	Charge-Parity (Temporal Inversion)	Discrete Symmetries related to space-time and internal degrees
FCNC(s)	Flavor Changing Neutral Current(s)	Experimental constrained Flavor Physics processes
LO	Leading Order	Zero order in perturbation theory in QFT
NLO	Next to Leading Order	First level in perturbation theory in QFT
NNLO	Next to Next to Leading Order	Second level in perturbation theory in QFT
RGE(s)	Renormalization Group Equations	Differential equations for dependence of couplings with energy scale
GUT	Grand Unification Theories	High energy-QFTs describing scale for QCD and EW unification
EFT	Effective Field Theories	QFTs with relevant freedom degrees up to some energy (cut) scale
LHC	Large Hadron Collider	Most important experiment in Particle Physics so far

Declaration

I with this declare that, except where specific reference is given to the work of others in the bibliography, the contents of this dissertation are original and have not been submitted in whole or in part for consideration for any degree or qualification in this, or any other university. This dissertation is my work and contains nothing which is the outcome of work done in collaboration with others, except as specified in the text and Acknowledgments.

Andrés Castillo

Acknowledgments

I am strongly indebted to my former advisor Dr. Rodolfo Diaz for his academical, personal support throughout my career, master and Ph.D. programs. He taught me -both consciously and unconsciously- many things in science, physics, and life; several immutable, invaluable, and ineradicable footprints, which I will never forget. This thesis contains an important part of his legacy. He left us, perhaps, to get another place where his kindness, intelligence, smartness, and other outstanding virtues might be more appreciated. The most remarkable tribute what I can give him: Trying to be a great human being and one great physicist.

It is my wish to thank my current advisor, Dr. John Morales Aponte, who faced the task to guiding me in the last stages of my thesis development. Both, Professors Rodolfo and John, always believed in my as great professional and they lead introducing me to research in Theoretical Particle Physics. Their guidance and collaboration helped me in all the time of researching and writing of this thesis. I could not have imagined having better advisors and mentors for my Ph.D. studies.

I also want to thank Dr. Carlos Quimbay, Dr. Raffaele Fazio, Dr. Justo Lopez and Dr. Rafael Hurtado as well as to other members of the group of "Campos y Partículas" staff, for fruitful and idoneous conversations and his continuous both personal and professional encouragement during these years of my formation.

I acknolewdge to my thesis examiners: Drs. Antonio Dobado, Carlos Quimbay and Fredy Ochoa for their usefull questions and pieces of advice to improve this work. I would like to express my special appreciation and thanks to my qualifying exam referees, Drs. Diego Restrepo, Fredy Ochoa and Raffaele Fazio by their suggestions and elaborated questions about fundamental topics here implemented: Chiral anomalies, perturbative unitarity, and vacuum stability. Qualifying scenario gave me several clues and drawn many paths to solve many issues about these important formalisms. I also acknowledge to Drs. Vicente Pleitez, Carlos Avila and Fredy Ochoa for their comments about the thesis proposal.

I am grateful to all members of the group of "Teorías Efectivas en Física Moderna" of the Universidad Complutense de Madrid for their kind hospitality, especially to Drs. Felipe Llanes Estrada and Antonio Dobado Gonzalez for giving me the opportunity to interact and to collaborate with them and some other colleagues at the Departamento de Física Teórica I at the same university. I am very grateful to Rafael Delgado, who taught me many aspects of the computational implementation of radiative corrections in effective theories. I would like thank to Drs. Jose Ruiz Cembranos and Antonio Lopez Maroto for professional and relevant scientific conversations. Furthermore, I am indebted with other young researchers at the same place: Santos Nuñez Jareño, Oscar Viyuela, Markus Muller, Alvaro Cruz Dombriz, Prado Martin, Arkaitz Rodas, Ismael Ayuzo and Alexandre Dauphin for giving me personal and professional support during my stay in Spain.

I also acknowledge the privilege to stay in the Theory Division of Fermi National Laboratory, learning about new, both theoretical and experimental, challenges in high energy physics. Mainly, I acknowledge to Dr. Felix Yu for supporting and teaching of many aspects of effective theories with two Higgs doublet models and their relation to lepton flavor violation. I also thank Olivia Vizcarra for her kindness and patience to guide me at Fermilab.

I thank the many friends whose support I have relied on during the long course of this project. I am particularly grateful with Carlos Gomez Tarazona and José David Tamara for their patience, criticism, and suggestions during these years of my academical and professional formation. I am strongly indebted to my family, in particular to my brother and mother. They always confer me several outstanding pieces of advice about life and profession.

Finally, but no less important, I thank Universidad Nacional de Colombia for accepting me in its Ph.D. program as a young researcher of the group Campos y Partículas. I am also heartily grateful with Colciencias and its Program of *Doctorados Nacionales* to give me all fundamentals funding to carry out my Ph.D. program and financial support for stays and scientific events. I am indebted to Harvard and Boston Universities for the financial aid to assist at the International Conference on Neutrino Physics and Astrophysics (Neutrino-2014) held in Boston-Massachusetts. I also acknowledge as well to Sociedad Mexicana de Física, ICTP and Mitchell Institute for its invitation and financial support to participate at the Joint School: BCVSPIN Advanced School in Particle Physics and Cosmology / XVI Mexican School of Particles and Fields done in Manzanillo. I am grateful to ICTP for the financial support to participate in the Summer School on Particles Physics-2015 and Particles-Strings and Cosmology PASCOS conference, both held in Trieste (Italy). In a similar way James Joyce did, the landscapes of Trieste and Adriatic sea inspired me to write several important parts of this thesis.

Abstract

In light of the new results from experiments like the ones coming from the Large Hadron Collider (LHC), theoretical and phenomenological implications are comprehensively studied from an extended scalar sector given by the Two Higgs Doublet Model. A review and a brief status based on symmetries and Spontaneous Symmetry Breaking patterns are discussed. By using the hidden reparametrization invariance, we focused our analyses on Higgs potential behavior at tree level and Next to Leading Order. Particularly, positivity constraints to get a bounded from below Higgs potential are broadly analyzed. Moreover, since metastable states might be present even at tree level, compatible parameter space can be discussed from new limits; being this fact pointed out to an improvement of Next to Leading Order results. Exclusions over parameter space coming from to avoid limiting charge violation vacua scenarios are converted in complementary studies to whose associated with vacuum stability analyses. Besides these studies, we also consider the strongest conditions from perturbativity unitarity analyses in scattering processes for the scalar sector. Further, since brief surveys over unitarity is possible to introduce the concept of fermion mass scale as well as to study its realization in general Yukawa couplings in the 2HDMs. Besides, this treatment allows tackling the problem of perturbative unitarity in fermion-antifermion scattering. As a central point, we discussed unitarity bounds over flavor changing neutral currents couplings, which are compatible with those yielded by perturbativity in renormalization group equations. The most important feature of these bounds is the independence with Higgs masses and mixing angles.

As a prototypical and realistic example incorporating all fundamentals described above, we present one complete scanning from vacuum analyses of several parameters spaces in an inert-2HDM with Z_2 and $U(1)$ symmetries. For scalar mass splittings in different zones of parameter space, we focused over stability bounds and described the evolution of instabilities and non-perturbative zones (yielding possible Landau poles). Moreover, we present new constraints to find one global minimum in the theory of the inert scenario. We apply a methodology based on reparameterization group formalism for the Higgs potential in 2HDMs. Bounds established by metastability analyses are evaluated regarding allowed zones compatible with one loop level studies for vacuum stability and unitarity systematics. All these regions are also analyzed from several phenomenological realizations and oblique parameters.

Other archetypes scenarios to study the vacuum behavior of an extended Higgs sector are the two Higgs doublet models under the implementation of a softly broken $U(1)$ global symmetry. The soft term is induced to forbid massless-axion particles arising when the global symmetry becomes spontaneously broken. 2HDMs with a soft breaking of $U(1)$ global symmetry have metastability regions through the possible presence of multiple non-degenerate minima. Metastable states are unwanted from the phenomenological point of view if the other local minima are not long-lived enough. The analysis of this fact leads to find possible exclusion limits over parameter space of quartic couplings. It improves the individual behavior of initial conditions for renormalization group equations; also determining unstable zones for the Higgs potential at one loop level. Besides vacuum stability analyses, the influence of absence of charge violation minima is considered in all studies. Extremal cases for the model as well as criticality phenomena are comprehensively discussed using relation among Higgs masses or splittings among them. From vacuum behavior and LHC results, phenomenological aspects in the searching of charged and heavier Higgs bosons are considered to evaluate the scalar alignment regimen of the two Higgs doublet model.

Keywords: Extended Higgs sectors, Vacuum stability, Precision tests in High Energy Physics, Perturbative Unitarity, Spontaneous Symmetry Breaking and Gauge Theories

Introduction

When you teach any branch of physics you must motivate the formalism - it isn't any good just to present the formalism and say that it agrees with experiment- you have to explain to the students why this the way the world is.
Stephen Weinberg

The Standard Model (SM), formulated by Weinberg, Glashow, Salam, with one Higgs doublet is the simplest realization of electroweak symmetry breaking and provides an excellent description of almost all data collected so far at hadron and lepton colliders. Current information data includes measurements associated with the recently discovered 125 GeV scalar boson at the LHC. SM is thus converting into an important benchmark to study fundamental interactions since it allows describe almost all phenomena existing in the high energy physics. Nevertheless, there are many problems in High Energy Physics (HEP) to be addressed and what are out the scope of the SM. Outstanding examples of these unexplained features are the neutrino oscillations determined from solar and long baseline measurements and whose mechanism emerges by the small masses of neutrinos. Neutrino masses are absent in the SM formalism since these fermions enter into the theory only with their left chirality components (approximately neutrinos with negative helicity), while the spontaneous symmetry breaking requires both sectors, left and right handed projections, to get appropriate massive structures. Another incompatible observation with SM precision measurements is the baryonic asymmetry of the universe (BAU), whose mechanism can not be explained by the current experimental scenario of the SM with a single Higgs boson. Another issue of the SM is the absence of dark matter candidates or possible portals and interactions, which are invoked to explain the outstanding amount of non-baryonic processes as well as other astrophysical and cosmological constraints (emerging mainly from gravitational lensing or Cosmic Microwave Background observables).

After the discovery of a Higgs boson-like particle, it is also now time to confront possible extensions in the Higgs sector of the standard model with LHC data (as the first approach to other scenarios of new physics), which might be electroweak completions to SM that lead some solutions to latter issues. For instance, one of the simplest ways to extend the typical scalar sector is by adding one more complex doublet to the model. The resulting two Higgs doublet models (2HDMs) can provide additional CP-violation sources coming from the scalar sector and can also easily originate dark matter candidates compatible with the typical bounds.

Furthermore from Yukawa sector, the presence of an additional doublet might lead Flavor Changing Neutral Currents, which are processes highly restricted from experimental studies. Another interesting feature is that more developed models with other fields and symmetries realization contain a 2HDM like scalar sector - as e.g. in the case of the most restricted version of Susy- the Minimal Supersymmetric Standard Model. By counting the physical degrees of freedom, it is very easy to note that 2HDMs have particle spectrum containing two charged and three neutral scalars; it leads to a significant number of interactions between those fields and therefore it is also translated into a richer phenomenology. From the 2HDM fundamentals, our primary goal is to study what influence have these couplings and interactions in the theoretical framework for the model and phenomenology in the particular cases of unitarity and vacuum stability analyses. Also, we will be taking into account possible phenomenological consequences from the behavior of critical precision test parameters, which are related with accidental or several explicit symmetries present in different sectors of the 2HDM-Lagrangian.

Scalar signal compatible with a Higgs hypothesis and favored by the experimental data in CMS and ATLAS leads to a mass close to 125 GeV [1–4]. This mass region has been studied comprehensively from vacuum analysis at next to leading order (NLO) [5] and in the most contemporary analysis at next to next to leading order (NNLO) [6–11]. The first approach relies on two loop renormalization group equations and one loop threshold corrections at the electroweak scale improved with two loop terms from pure QCD corrections. On the other hand, the NNLO incorporates higher order corrections in the strong, top Yukawa and Higgs quartic couplings; considering mainly full three loop beta functions for all SM gauge couplings and the leading terms three loop beta functions in the RG evolution. Moreover, NNLO terms have an important piece of the vacuum stability analysis that comes from two-loop corrections to quartic coupling at the weak scale due to QCD and top Yukawa interactions, because such couplings are sizable at low energy scales. With these computations, absolute stability of the Higgs potential is excluded at 98% C.L. for $m_h < 126$ GeV while quartic

coupling at the Planck scale is close to zero, which is associated with critical phenomena [6]. Indeed, in the current mass region for Higgs and top quark, there is a significant preference for *metastability* of the SM potential [12]. This situation takes place when the true minimum of the scalar potential is deeper than the standard electroweak minimum, but the latter has a lifetime that is larger than the age of the universe [13, 14].

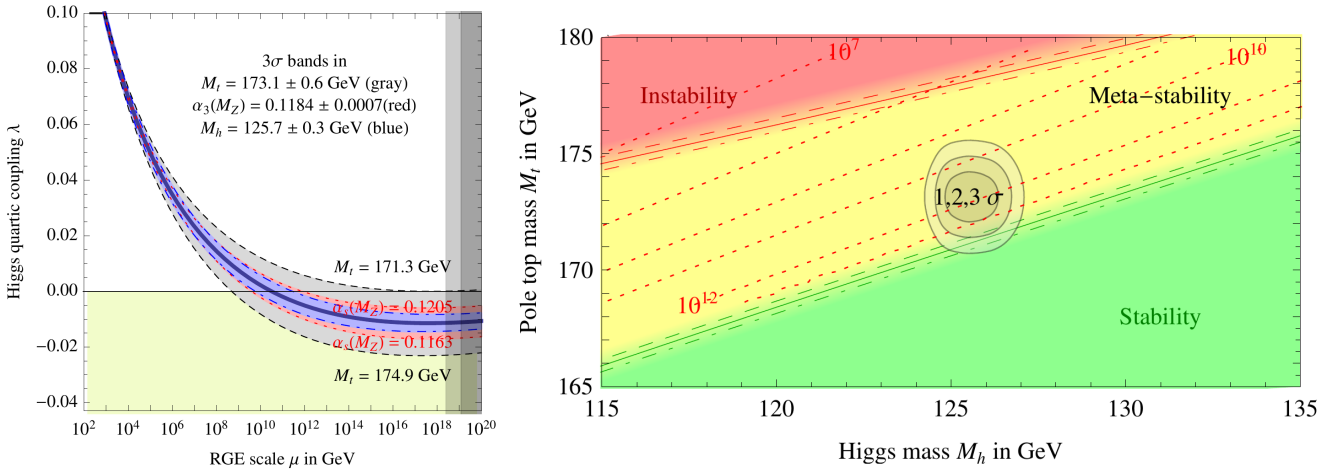

Figure A: ***(Left)*** *RG evolution of λ varying m_t (top quark mass), m_{h^0} (Higgs mass) and α_s by 3σ reported in [6].* ***(Right)*** *Regions of absolute stability, metastability and instability of the SM vacuum-minimum in the $m_t - m_{h^0}$ plane. This region has been zoomed in the preferred experimental range of m_{h^0} and m_t plane (the gray areas denote the allowed region at 1σ, 2σ, and 3σ). The three boundary lines correspond to $\alpha_s(m_z) = 0.1184 \pm 0.0007$, and the grading scale of the colors indicates the size of the theoretical error. The dotted contour lines show the instability scale Λ_I in GeV assuming $\alpha_s(m_z) = 0.1184$.*

The occurrence of criticality (metastability-stability boundary) for couplings at higher energy scales could be a consequence of symmetry, a fine tuning or a dynamical effect among new parameters from an Extended Higgs Sector of the Inert Two Higgs Doublet Model (IHDM), for instance. The last one is the primary motivation for our work: try to understand some limits of this criticality phenomena through of extended models respecting the minimality principle -wherein the typical scales for SM and the Inert Two Higgs Doublet Model are the same-. Moreover, those analyses would be involved in the threshold corrections in the study of phenomenology in other models beyond SM sharing a similar Higgs spectrum (with the decoupling other particle states).

Criticality in our case reflects as the boundary separating the stability and instability behaviors in the effective potential for the extended Higgs sector. By plotting different combinations of new quartic couplings of extended parameter space, we analyze the behavior of criticality with energy scales. Since these couplings also depend on measurements for Higgs boson and top quark masses, the improvement for the precision level of these parameters leads to describing most accurately mechanisms and principles behind of phase diagrams.

The 2HDM includes two complex doublets with identical quantum numbers and represents the next non-trivial extension compatible with the gauge invariance and with the Electroweak-Spontaneous Symmetry Breaking (EW-SSB) in the SM. Therefore in 2HDMs there are eight real fields. By Higgs mechanism, three must become the longitudinal components of the $W^{\pm}$ and Z^0 bosons after the SSB (in the unitary gauge). Five physical Higgs scalars will remain: a charged scalar $H^{\pm}$ and three neutral scalars h^0, A^0 and another neutral pseudoscalar A^0 (CP conserving scenario). Other motivations to introduce an extended Higgs sector with two doublets are the additional sources either spontaneous and explicit CP violation; being both outstanding mechanisms to explain baryon asymmetry of the universe (BAU) from baryogenesis processes [15]. The non-compatibility of SM dynamics consequences with Sackarov conditions -notably the absence of a strong enough First Order Phase Transition- is a significant failure of the minimal model with one doublet [16, 17]. Besides mechanisms to take into account BAU through Sackarov conditions realization require a complete study of vacuum structures of extended models, translating both, stability and baryogenesis plausibility, into relevant frames to limit a feasible parameter space.

As was introduced and motivated above, another crucial consequence with additional Higgs doublets is the possibility of flavor-changing neutral currents (FCNC). It is well known that FCNCs are highly constrained by the charged current processes like mesons oscillations, so it would be desirable to "naturally"suppress them in these models. For instance, if

[0]The parameter $\rho \equiv m_w^2/m_z^2 \cos^2\theta_w$ is a critical piece sensitive to the scalar structure of EWSSB. A splendid feature of models with extra $SU(2)$ doublets (or singlets) is that they do not break the custodial $SU(2)$ global symmetry, that protects $\rho = 1$ at tree-level.

all fermions with the same quantum numbers couple to the same scalar doublet, then FCNC will be avoided. A condition (necessary and sufficient), leading to an absence of FCNCs at tree level, is all fermions of a specified charge and helicity transform regarding the same irreducible representation of $SU(2)-$group; corresponding to the same eigenvalue of the third component of isospin operator. Hence exist a basis in which fermions receive their contributions in the mass matrix from a single source [18]. From quark sector in the Yukawa part, we can see two possibilities: All quarks couple to just one doublet or the up type right-handed quarks couple to one doublet (e.g. Φ_2) and the down type right-handed quarks couple to other (Φ_1). The first choice is called the 2HDM type I, and the last model is known as the 2HDM type II. In the moment of these structures extends to the leptonic sector, it is taken the charged leptons couple to the same Higgs multiplet as the $Q = -1/3$ quarks. Although this condition is not necessary to avoid FCNCs. There are other two possibilities to construct models with natural flavor conservation indeed. In the lepton-specific model, the RH quarks couple to Φ_2 and the RH leptons couple to Φ_1. In the flipped model (or Y-2HDM), the $Q = 2/3$ right-handed quarks and charged leptons couples to the same doublet (say Φ_1), and the $Q = -1/3$ right handed quarks couple to Φ_2 [19]. In this dissertation, we concentrate on the traditional types I and II 2HDMs and the corresponding extension to lepton sector, since for these 2HDMs, the considered symmetries are accomplished either Higgs potential and Yukawa sector. Nevertheless, in our discussion about foundations of 2HDMs will make some phenomenological studies over these four models with natural flavor conservation (Type I, II, X, Y-2HDMs). Moreover, we will see the possibility of having FCNCs in the new measurements for Higgs boson coming from run1 data at LHC.

Because of the Higgs mass in SM is becoming measured and limited even more as a result of precision tests performed in LHC, one might ask how the new scalar free parameters in the 2HDM are constrained by the general vacuum behavior [20]. There are more self-couplings (which could diverge by the unification scale leads to possible Landau poles) and more directions in field space where an instability in the Higgs potential could arise. Limits of model parameters or splittings (mass differences) generated depend on mass eigenstates hierarchy in 2HDM and thus of symmetries implemented in the Higgs potential. Mainly, the first scenario interpreting the vacuum behavior as a threshold correction with significant phenomenological consequences is the inert Higgs doublet model. To constrain masses of new charged and pseudoscalar particles (or splittings), we can identify the lighter Higgs with the current signal for Higgs boson and study the remain directions in the parameter space. This structure form for analysis is a parallel one to the constraints over parameter space of 2HDM, which have been examined before [21], but the Higgs mass was unknown at the time (different values from 50 GeV up to about 150 GeV for the Higgs mass were considered).

Other features for the inert-Higgs doublet model have been introduced with the aim to set a Higgs boson (H^0) of mass between 400 and 600 GeV. This choice lifts the divergence of the Higgs radiative corrections beyond the TeV scale. In such range, new physics is supposed to render the theory natural and convert the Higgs quartic coupling perturbative [22]. The perturbative unitarity bounds for m_{H^0}, m_{A^0} and $m_{H^\pm}$ are near to 700 GeV for models compatible with a inert 2HDM [23], hence the interval to interpret naturalness problem is according to this tree level bound. By using the constraints from the electroweak precision, data implies to introduce a second inert Higgs doublet is introduced (Φ_2). Although Φ_2 has weak and quartic interactions just as in the ordinary 2HDM, it does not acquire a VEV (its minimum is at $(0, 0)$), nor it has any other couplings to matter. The inert-2HDM describes one particular class of Type-I 2HDMs. The Φ_2 doublet transforms odd under a novel unbroken parity symmetry, Z_2, while all the SM fields have even Z_2 parity. As a consequence, the lightest inert scalar (LIP) (H^0 or A^0) is stable and a suitable dark matter candidate [24].

In addition to the standard issues in the stability conditions, the 2HDM has a richer vacuum structure wherein metastable states could be present. This effect is a consequence of relating the number of critical points in the Higgs potential, which particularly in its minimum consists on the composition of two vacuum expectation values, also depending on stationary points nature. The scalar potential of 2HDM might have simultaneously two neutral minima, two CP conserving or two CP violating [25][1]. In those cases, from a vacuum state belonging in a local metastable-minimum, there would be the possibility of decaying later into a deeper minimum. Descriptions of metastability with underlying two Higgs doublet dynamics focused on formal aspects have been broadly studied in [26–30]. Phenomenological aspects of the possibility of two global minima have been treated comprehensively in [31,32]. Nonetheless, relevant studies about vacuum metastability in softly $U(1)$ models have been carried out, comparison among one loop behavior of the effective Higgs potential and the presence of two neutral minima is still an issued to be addressed. In this direction, recently in [33] studied the impact of considering a softly breaking term to get stable zones in energies $\mu > 10^{10}$ GeV. For Inert models, in [34] has been shown as the parameter space compatible with the coexistence of both possible neutral vacua is larger than the predicted by the tree-level analyses; also demonstrating how the nature of vacuum can change at one loop level

[0] In 2HDM type II, selection of inert vacuum prevents to down-type fermions to acquire mass. Therefore and how we are interested in to study effects of down fermions in RGEs, we would consider only the 2HDM type I.

[1] In 2HDMs exist the possibility of having charge violating critical points. Despite these stationary points must be avoided and coexistence with normal ones is forbidden, we consider limiting where this vacuum is possibly generated as one assumption to describe hierarchical structures in scalar masses computed in a neutral-minimum.

concerning established at tree level. Therefore, potential regions investigated by vacuum stability can be constrained by the presence of an inert-like vacuum (where fermions are massless) at one loop level.

In the moment of building a model containing a Higgs potential with several distinct neutral minima breaking the same symmetries, possibility of taking a metastable minimum as a physically acceptable vacuum state is also allowed if this effect is suppressed by the fact of having a long lived enough minimum state. This lead to describe the masses for particles in a realistic approach, without being concerned about the tunneling effects changing this phenomenological scenario. Nevertheless, from a cosmological point of view, the metastable regime of 2HDM could bring many consequences and issues in baryogenesis mechanisms. For instance, the critical temperature for a strong phase EW transition might have an ambiguous definition if possible minima of the effective Higgs potential are not considered properly [16]. However, LHC-phenomenology analyses as decays ratios of new physics could give some information about suppression metastable states [32] in 2HDMs. Moreover, LHC collaborations have given contours in the measured golden-decays with a good confidence level [35]. These regions can be used to extract plausible frameworks in the vacua realization for 2HDMs.

Although experimental accessibility is now significant, many possible scenarios of 2HDM remain unknown from the phenomenological point of view. Hence, theoretical constraints might be obtained by making further fundamental assumptions on the Quantum Field Theory background of the 2HDM. In addition to the vacuum stability behavior, triviality, oblique parameters, and the unitarity at the tree level can be used to study parameter space regimes widely. Triviality bounds rely on the fact that the quartic couplings in the potential remain finite up to large scales of energy to avoid divergences associated with Landau poles. The condition of vacuum stability requires that some couplings (e.g. the associated couplings to self-terms: $(\Phi_i^\dagger \Phi_i)$ with $i = 1, 2$) in the Higgs potential must be positive in all field space directions for their asymptotically large values, otherwise the potential would be unbounded from below and does not have a minimum [36, 37].

On the other hand, $S-$matrix unitarity is embodied in all perturbative levels due to the Optical Theorem (OT) [38–40]. Especially for asymptotically flat models (wherein scattering amplitudes do not exhibit any power-like growth in the high energy limit), leading contributions lie at the tree level. Theoretical constraints are thus ensured through the correct reliability of perturbation theory in gauge theories.

Perturbative unitarity bounds are derived from the Lee-Quigg-Thacker (LQT) method which shows that if the Higgs boson mass m_{η^0} exceeds critical values obtained from partial wave decomposition, unitarity is violated at the tree level for different binary scattering processes $p_2 p_1 \to p_3 p_4$ at high energies, $s >> m_{\eta^0}^2$ [23, 41–44].

These unitarity constraints have been commonly applied to bosonic scalar and bosonic vectorial sectors because the unitarity limits emerge from Partial Waves Decomposition, which is only valid for spinless particles (for vector bosons formalism applies because of the theorem of equivalence). For fermionic Yukawa couplings, it is necessary to introduce a General Partial Waves Decomposition where different spin states are involved. The Jacob-Wick expansion is the most natural and simplified method for partial diagonalization in the angular momentum basis since such systematics relies on the appropriate choice of physical states in the initial characterization of scattering processes [45].

With the aid of these fundamental points, this work would be expected by converting into a well-grounded frame to analyze new extended Higgs sectors and the respective phenomenological properties for observables like masses, splittings, mixing angles and production or decays of physical states. This dissertation has also the purpose of giving to model building relevant scenarios to take into account besides to analysis from current searches for new physics beyond SM.

With the aim to incorporate all concepts systematically, this thesis is organized as follow. In chapter 1, fundamentals of 2HDM are considered, as well as particular cases of an Abelian and non-Abelian global and discrete symmetries for Higgs potential and Yukawa sector; discussing phenomenological scenarios for different models and making a review of new Higgs bosons searches. With this essential discussion and examination, in chapter 2, vacuum structures in 2HDMs analyses are established comprehensively. Loop corrections to study NLO-effective Higgs potential behavior are considered in chapter 3. To make an improvement over typical studies and to determine a proper behavior of scattering amplitudes at high energies, in chapter 4 we review unitarity constraints and perturbative behavior for general quantum field theories and the particular case of 2HDMs. By applying all fundamental in these parts, in chapter 5 contours (built up to emulate a bounded from below effective Higgs potential) and several analyses for couplings are considered in different energy scales up to GUT and Planck scales- for inert 2HDMs. Similarly, in chapter 6 we discuss phenomenological aspects in the searching of possible metastable states in the Higgs potential of 2HDM with softly breaking of a $U(1)$ symmetry. Finally, in the conclusions and remarks, we discuss the influence of our treatments in the interpretation of vacuum, perturbative unitarity, and electroweak precision tests globally. Additional discussions, description of generalizations of formalisms and relevant demonstrations for 2HDMs-fundamentals, vacuum stability, oblique parameters, perturbative unitarity, and phenomenology are respectively considered in appendices A-M.

1. 2HDM Fundamentals

From new experimental analyses, standard model (SM) has become a primary benchmark to study fundamental interactions since it allows describe almost all phenomena existing in the high energy physics with a high level of accuracy. For instance, small deviations ($< 68\%$ C.L:) from SM couplings of Higgs bosons to gauge bosons and fermions are present in data from run 1 of LHC, as we can see in Fig. 1.1.

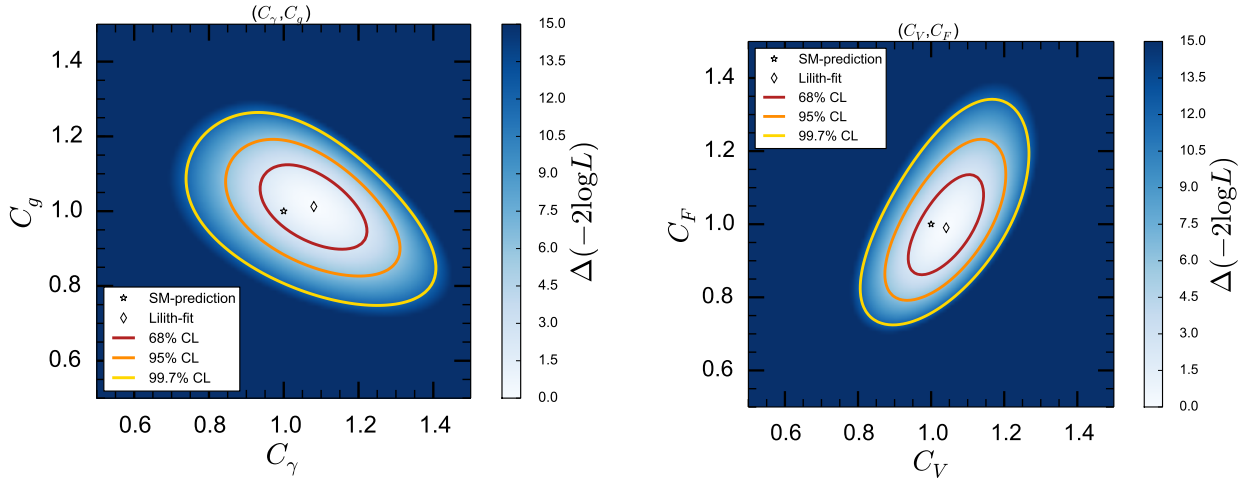

Figure 1.1.: *Likelihood proof for (C_γ, C_g) (left) and (C_V , CF) (right) effective couplings fits using data from the LHC-run 1 combination [35]. C_γ and C_g describe effective LO couplings for Higgs boson to two photons and two gluons, respectively. C_V and C_F are the effective couplings form Higgs boson to EW-gauge bosons ($W^\pm$, Z^0). The red, orange and yellow color-scaled filled surfaces correspond to the 68% C.L., 97% C.L. and 99% C.L. regions obtained by Lilith. The black diamond indicates the position of the Lilith best-fit point and the white circle shows the SM prediction. To build up these compatibility-contours, we have assumed $m_h = 125.04$ GeV.*

Nevertheless, there are many problems in High Energy Physics to be addressed and what are out the scope of the SM. One notable example is the neutrino oscillations, determined from solar and long baseline measurements [46–48]. This phenomenon arises from the massive character of the neutrinos and their tiny size; features that are not implemented naturally in the SM formalism. Another relevant observation is the baryonic asymmetry of the universe (BAU), whose mechanism to yield strong first order phase transitions can not explaining by the current experimental scenario of the SM (primarily in the Higgs mass around of 125 GeV). Another issue of the SM is the absence of dark matter candidates or possible portals and interactions to explain the outstanding amount of non-baryonic processes [49].

After the discovery [1,2,50] of a Higgs boson at LHC, it is now time to confront possible extensions of the with data and reconstructions derived from them. One of the simplest ways to extend the scalar sector of the SM is by adding one more complex multiplet ($N = 2$) to the model. The resulting two Higgs doublet models (2HDMs) can provide CP-violation sources coming from the scalar sector and can also easily originate dark matter candidates compatible with the typical bounds [51–53]. Besides, 2HDMs could induce suitable scenarios to yield baryogenesis processes by the realization of EW-Strong First Order Phase Transitions [16, 54, 55].

Another benchmark point is that 2HDMs could have spontaneous and explicit CP violation sources. Both effects could generate compatible scenario with baryogenesis processes since Sackarov conditions demand new sources of CP violation to establish an accurate number of Baryonic Asymmetry of Universe.

Besides to these phenomena, the presence of an additional doublet might lead Flavor Changing Neutral Currents (FCNCs). Despite the fact that these processes are highly constrained from experimental studies, the 2HDMs framework would result in investigating the origin of precise suppression mechanisms for them. Another interesting feature is that

more evolved models with an additional content of fields and symmetries have a 2HDM like scalar-Higgs sector - as in the case- of The Minimal Supersymmetric Standard Model (MSSM) and Grand Unification theories[1] or Left-Right symmetric theories. In these cases, 2HDMs are considered as low energy effective theories of the model with more relevant degrees of freedom.

Recently, electromagnetic form factors for neutrinos have been studied in frames provided by 2HDMs, showing how these models with flavor conservation have higher contributions than expected by a minimal SM with massive neutrinos; being them potential frameworks to compare available parameter spaces for 2HDMs with precision measurements for magnetic dipole moment of tau neutrino [56, 57].

Furthermore, 2HDMs have a richer particle spectrum with two charged and three neutral scalars; it leads to a significant number of interactions between those fields and therefore it translates into an extensive phenomenology. From the 2HDM fundamentals our primary goal is to study what influence have these couplings and interactions in the theoretical framework for the model and phenomenology; in the particular cases of unitarity and vacuum stability analyses. Furthermore, we are taking into account possible phenomenological consequences from the behavior of significant precision test-parameters connected with accidental symmetries belonging in different sectors of the 2HDM-Lagrangian. For example, we handle the custodial symmetry behavior in various parts of the 2HDM as well as its realization in the oblique parameters.

Finally, we make a review of some relevant phenomenological analyses for searches of new physics and the constraints mainly obtained by the recent data of LHC-collaborations. These include compatibility level studies between different types of 2HDM with flavor conservation and LHC results; incorporating the so-called type I and type II 2HDMs as well as lepton-specific and flipped cases. Also, we summarize searches for FCNCs, charged and pseudoscalar Higgs bosons.

1.1. 2HDM: Fields content and kinetic sector

To build up a general 2HDM and to achieve the Spontaneous Symmetry Breaking of EW-gauge group $SU(2)_L \times U(1)_Y \to U(1)_Q$, we add a copy of the first doublet with the same quantum numbers, i.e., the same hypercharges $Y_1 = Y_2 = 1$ and isospin $I = 1/2$,[2]

$$\Phi_1 = \begin{pmatrix} \phi_1^+ \\ \phi_1^0 \end{pmatrix}; \qquad \Phi_2 = \begin{pmatrix} \phi_2^+ \\ \phi_2^0 \end{pmatrix}. \tag{1.1.1}$$

In a general scenario, both doublets could acquire VEVs, where a possible case is such that neutral components can be parameterized in a generic form by

$$\langle \Phi_1 \rangle_0 = \frac{v_1}{\sqrt{2}}; \qquad \langle \Phi_2 \rangle_0 = \frac{v_2}{\sqrt{2}} e^{i\theta}. \tag{1.1.2}$$

The multiplets can be written regarding eight fields associated with the freedom degrees introduced by the complex doublets of $SU(2)$

$$\Phi_1 = \begin{pmatrix} \phi_1^+ \\ \frac{h_1 + v_1 + i\eta_1}{\sqrt{2}} \end{pmatrix}; \qquad \Phi_2 = \begin{pmatrix} \phi_2^+ \\ \frac{h_2 + v_2 e^{i\theta} + i\eta_2}{\sqrt{2}} \end{pmatrix}. \tag{1.1.3}$$

where θ is a phase parameter, which is connected with a possible spontaneous breaking of CP symmetry. When the gauge symmetry breaks spontaneously by the Higgs mechanism, the eight degrees of freedom from the $SU(2)$ doublets Φ_1 and Φ_2 are usually re-expressed in states with definite physical properties. Then, the spectrum contains three Goldstone modes: $G^\pm$ and G^0, which are absorbed (in the unitary gauge) to turn on mass to the gauge bosons $W^\pm$ and Z^0, reducing the number of physical Higgs states to five. Three of these scalars are neutral, of which two (h^o and H^0, with $m_{h^0} \leq m_{H^0}$) are CP-even, and one is CP-odd typically denoted as A^0[3]. The remaining two states are a pair of charged

[1] The MSSM requires a second Higgs doublet to ensure the removal of gauge anomalies. So, the Higgs sector of this model is a 2HDM which contains two chiral Higgs super-multiplets distinguished by the sign of their hyper-charge. In grand unification theories, we need to break the Lie group to the $SU(3)_C \times SU(2)_L \times U(1)_Y$ group. To implement so, the model requires different Higgs representations. In general, this implies the presence of an extended scalar sector at the electroweak scale. For example, a two-Higgs-doublet model is needed to break $SO(10)$ to the SM group .

[2] These quantum number assignments $(1, 1/2)$ are compatible with a *non-normalized in Y Gell Mann-Nishijima formula:* $Q = I_3 + Y/2$

[3] The CP-quantum numbers assignment before fermions introduction is the following :

$$\begin{array}{ccc} J^{PC} & \to & \text{Field} \\ 0^{++} & \to & H^0 \\ 0^{++} & \to & h^0 \\ 0^{-+} & \to & A^0 \end{array}$$

Higgs bosons ($H^{\pm}$). The charged and pseudoscalar Higgs bosons are a characteristic of the 2HDM that is not present in the minimal SM. Then, its discovery would be a major signal of physics beyond and it might drive out to models with higher symmetries to be more constrained.

The model implementation requires the construction of a kinetic Lagrangian and the Higgs potential V_H. These parts of the scalar sector have the following Lagrangian

$$\mathcal{L} = (\mathcal{D}_\mu \Phi_1)^\dagger (\mathcal{D}^\mu \Phi_1) + (\mathcal{D}_\mu \Phi_2)^\dagger (\mathcal{D}^\mu \Phi_2) - V_H \tag{1.1.4}$$

The kinetic sector defines interactions among scalars and gauge bosons as well as after SSB their respective mass terms. For our studies about vacuum stability, the scalar potential would receive special attention, and thus their representations and symmetries will be treated comprehensively in the next section. Through developments on Higgs potential in the general formalism, we study Yukawa interactions and their relations with symmetries and basis transformations.

1.2. The Higgs potential in 2HDMs

The Higgs potential determines the SSB structure as well as the anatomy for scalar spectrum (Higgs eigenstates), the self-interactions among scalars and the vacuum behavior at leading order. Since this sector remains largely unknown from phenomenological scenarios, theoretical methods should be considered to limit all its free parameters. The number of free parameters would depend on of the Higgs-potential structure based on the symmetries imposed on this sector [58]. To study this fact we introduce different notations for the Higgs potential and after we shall establish several symmetries class associated with the global nature of the model [4]. The most general Higgs potential, renormalizable (with dimension two and dimension four terms) and $SU(2)_L \times U(1)_Y$ gauge invariant is given by

$$\begin{aligned} V(\Phi_1,\Phi_2) = {} & m_{11}^2 \Phi_1^\dagger \Phi_1 + m_{22}^2 \Phi_2^\dagger \Phi_2 - \left[m_{12}^2 \Phi_1^\dagger \Phi_2 + m_{12}^{*2} \Phi_2^\dagger \Phi_1 \right] + \frac{\lambda_1}{2} \left(\Phi_1^\dagger \Phi_1 \right)^2 + \frac{\lambda_2}{2} \left(\Phi_2^\dagger \Phi_2 \right)^2 \\ & + \lambda_3 \left(\Phi_1^\dagger \Phi_1 \right) \left(\Phi_2^\dagger \Phi_2 \right) + \lambda_4 \left(\Phi_1^\dagger \Phi_2 \right) \left(\Phi_2^\dagger \Phi_1 \right) + \frac{1}{2} \left[\lambda_5 \left(\Phi_1^\dagger \Phi_2 \right)^2 + \lambda_5^* \left(\Phi_2^\dagger \Phi_1 \right)^2 \right] \\ & + \left[\lambda_6 \left(\Phi_1^\dagger \Phi_1 \right) \left(\Phi_1^\dagger \Phi_2 \right) + \lambda_6^* \left(\Phi_1^\dagger \Phi_1 \right) \left(\Phi_2^\dagger \Phi_1 \right) \right] + \left[\lambda_7 \left(\Phi_2^\dagger \Phi_2 \right) \left(\Phi_1^\dagger \Phi_2 \right) + \lambda_7^* \left(\Phi_2^\dagger \Phi_2 \right) \left(\Phi_2^\dagger \Phi_1 \right) \right]. \end{aligned} \tag{1.2.1}$$

Terms m_{11}^2, m_{22}^2 and λ_{1234} are real (by hermiticity property), while, m_{12}^2 and λ_{567} are -in general- complex values. This potential has fourteen free parameters, but it could be reduced by symmetry arguments as we will discuss below. This form is an important tool to determine the Feynman rules for scalar-scalar interactions. The Higgs potential in a generic basis (1.2.1), could be written in a more compact form through bilinears combinations of the doublets [59]:

$$V(\Phi) = \sum_{i,j=1}^{n_H=2} \mu_{ij} \Phi_i^\dagger \Phi_j + \frac{1}{2} \sum_{m,j,k,l=1}^{n_H=2} \Lambda_{km}^{jl} (\Phi_j^\dagger \Phi_k)(\Phi_l^\dagger \Phi_m). \tag{1.2.2}$$

This structure for the Higgs potential is useful to determine invariants, basis transformations, and symmetries [60]. By definition

$$\Lambda_{km}^{jl} = \Lambda_{mk}^{lj} \tag{1.2.3}$$

Moreover, hermiticity of the Higgs potential implies:

$$\mu_{ij} = \mu_{ji}^*, \quad \text{and} \quad \Lambda_{km}^{jl} = \left(\Lambda_{mk}^{jl} \right)^* \tag{1.2.4}$$

With these features over bilinears couplings, it is possible to present the correspondence between both forms (1.2.1) and (1.2.2) of the Higgs potential,

$$\begin{aligned} & \mu_{11} = m_{11}^2, \quad \mu_{22} = m_{22}^2, \quad \mu_{12} = -m_{12}^2, \quad \mu_{21} = -m_{12}^{*2} \\ & \Lambda_{11}^{11} = \lambda_1, \ \Lambda_{22}^{22} = \lambda_2, \quad \Lambda_{12}^{12} = \Lambda_{12}^{12} = \lambda_3, \quad \Lambda_{12}^{21} = \Lambda_{12}^{12} = \lambda_4 \\ & \Lambda_{22}^{11} = \lambda_5, \ \Lambda_{11}^{22} = \lambda_5^*, \ \Lambda_{21}^{11} = \Lambda_{12}^{11} = \lambda_6, \ \Lambda_{11}^{12} = \Lambda_{11}^{21} = \lambda_6^*, \ \Lambda_{22}^{12} = \Lambda_{22}^{21} = \lambda_7, \Lambda_{12}^{22} = \Lambda_{21}^{22} = \lambda_7^* \ . \end{aligned} \tag{1.2.5}$$

These equivalences will be used to write symmetries relations and the respective Renormalization Group Equations (RGEs).

[4] Relevant systematics of the formalism in this chapter follow the lines shown by Sher et al in [19]

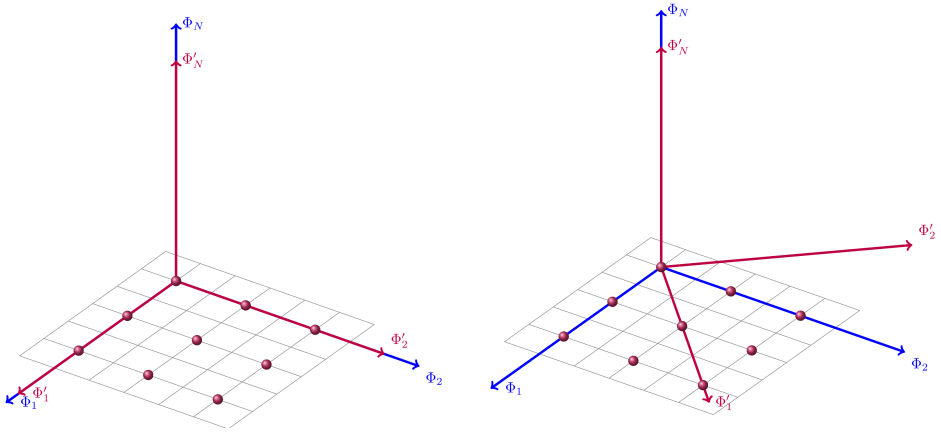

Figure 1.2.: *Illustration for a basis transformation on 2HDM from an original one identified by blue axis. The red axis corresponds to a primed coplanar basis (rotated from an orthogonal axis Φ_N in the right part). The red points are possible combinations for doublets seeing from both coordinate frameworks (passive transformation).*

1.2.1. Basis Transformations

Since only the scalar mass eigenstates and possible mixing angles are physical observables, any combination of the doublets which respect the symmetries imposed on the Higgs potential will produce the same physical predictions. To introduce the basis transformations, we construct all possibles combinations of (Φ_1, Φ_2) as a *basis* for the doublets space [5]. It is possible to rewrite the potential regarding the new doublets Φ'_a, which have been obtained from the original doublets from a global basis transformation

$$\Phi'_a = \sum_{b=1}^{2} U_{ab}\Phi_b. \tag{1.2.7}$$

U is a 2×2 unitary matrix. We illustrate this situation in Fig. (1.2) using a passive transformation point of view.

Now, it is need to study the form in which coefficients inside Higgs potential transform under a basis transformation. In the compact notation (1.2.2), the couplings and mass terms behave

$$\mu'_{ij} = \sum_{c,d=1}^{2} U_{ic}\mu_{cd}U^*_{jd} = \left(U\mu U^\dagger\right)_{ij}, \tag{1.2.8}$$

$$\Lambda^{jl}_{km} = \sum_{e,f,g,h=1}^{2} U_{je}U_{\lg}\Lambda^{eg}_{fh}U^*_{kf}U^*_{mh}. \tag{1.2.9}$$

From (1.2.8) and (1.2.9), we can see that the overall phase of U does not influence the change of the parameters in the Higgs potential. Hence, we may consider $U \in SU(2)$. This fact leads to,

$$U = \begin{pmatrix} e^{i\chi}\cos\psi & e^{i(\chi-\xi)}\sin\psi \\ -e^{i(\xi-\chi)}\sin\psi & e^{-i\chi}\cos\psi. \end{pmatrix}. \tag{1.2.10}$$

A basis transformation may be used to avoid some of the degrees of freedom in the scalar potential. This overcounting implies that not all the parameters in that potential have physical significance. Thus, three parameters in Eq. (1.2.10) may be used to extract three out of the 14 parameters in the scalar potential. As a result of this procedure in the general approach, there are only 11 physical degrees of freedom in the potential and, thus, only 11 independent observables. Although we are still discussing the most general potential; when a global symmetry on the 2HDM is imposing, the number of parameters which may be eliminated through basis transformations may even be less than three.

[5] For instance, we seldom use a basis of Hermitian, gauge invariant operators to expand the 2HDM-Higgs potential:

$$\Phi_1^\dagger\Phi_1; \Phi_2^\dagger\Phi_2; \mathrm{Re}\left(\Phi_1^\dagger\Phi_2\right); \mathrm{Im}\left(\Phi_1^\dagger\Phi_2\right) \tag{1.2.6}$$

This basis leads us to construct all possible Hermitian bilinear and quartic interactions compatible with gauge invariance.

1.2.2. Higgs potential symmetries

The large number of free parameters in the scalar potential of the 2HDM reduces the theory's predictive nature. It is necessary designing a strategy to search phenomenological relevant information behind of the theoretical model. Likewise, theoretical constraints (vacuum stability analyses, perturbative unitarity) and any well-grounded symmetry that we may impose on the 2HDM to constrain its scalar potential shall be therefore a valuable tool to control plausible parameter spaces. Also, as we discussed in previous sections, the 2HDM is in general plethoric of Flavor-Changing Neutral Currents (FCNC); however, they may be actively suppressed by imposing an internal symmetry on the 2HDM [61]. Similarly, those models might or not contain either explicit or spontaneous CP symmetry violation sources, which have broad consequences in phenomenology like dark matter behavior, strong-CP problem and baryogenesis mechanisms [16]. As we will see, many global symmetries (some whose lead to FCNC suppression) of the Higgs potential yield absence of CP violation. The set of symmetries lead to kinetic terms unchanged may be of either two types:

1. Φ_a relates with Φ_b through some unitary transformation,

$$\Phi_a \to \Phi_a^S = \sum_{b=1}^{2} S_{ab}\Phi_b, \tag{1.2.11}$$

where S is a unitary matrix. This linear transformation is an isomorphism since S maps Φ in itself, i.e., S: $V \to V$. Therefore, we demand that the Higgs potential to be invariant under this transformation. As a result of this invariance, the couplings inside the Higgs potential (1.2.2) are given by

$$\mu_{ij} = \sum_{c,d=1}^{2} S_{ic}\mu_{ij}S_{jd}^*, \tag{1.2.12}$$

$$\Lambda_{km}^{jl} = \sum_{e,f,g,h=1}^{2} S_{je}S_{lf}\Lambda_{gh}^{ef}S_{kg}^*S_{mh}^*. \tag{1.2.13}$$

They are known as Higgs Family (HF) symmetries. This scenario is not the situation considered in eqs. (1.2.7)-(1.2.9). There, the coefficients of the Lagrangian do change under the transformation. In contrast, eqs. (1.2.11)-(1.2.13) imply the existence of a HF symmetry of the scalar potential because the coefficients of V_H are unchanged.

2. Φ_a relates with Φ_b^* through some unitary transformation,

$$\Phi_a \to \Phi_a^{GCP} = \sum_{b=1}^{2} X_{ab}\Phi_b^*. \tag{1.2.14}$$

X is an arbitrary unitary matrix. Here X transforms a vector space in its complex counterpart. Superscript GCP corresponds to CP transformations [6]. Hence, the potential would be invariant under this symmetry:

$$\mu_{ij} = \sum_{c,d=1}^{2} X_{ac}\mu_{ij}^*X_{bd}^*, \tag{1.2.16}$$

$$\Lambda_{km}^{jl} = \sum_{e,f,g,h=1}^{2} X_{je}X_{lf}\Lambda_{gh}^{ef}X_{kg}^*X_{mh}^* \tag{1.2.17}$$

These are known as GCP symmetries.

Under a basis transformation $\Phi_a \to \Phi'_a = U_{ab}\Phi_b$ in eq (1.2.7) the specific forms of the HF and GCP symmetries get altered, respectively, into:

$$S' = USU^\dagger \tag{1.2.18}$$

$$X' = UXU^\dagger \tag{1.2.19}$$

[6] The standard CP transformation for a Higgs one reads:

$$\Phi(t,\mathbf{x}) \to \Phi^{CP}(t,\mathbf{x}) = \Phi^*(t,-\mathbf{x}) \tag{1.2.15}$$

Presence of identical multiplets requires a definition of CP ($\Phi_1^{CP} = \Phi_1^*$ and $\Phi_2^{CP} = \Phi_2^*$ in a basis of (Φ_1,Φ_2)) and it should be preserved under basis changes. CP-symmetry definition is a motivation to introduce general CP transformations [19, 62, 63].

Class	Symmetry	m_{11}^2	m_{22}^2	m_{12}^2	λ_1	λ_2	λ_3	λ_4	λ_5	λ_6	λ_7	n
I	$U(2)$		m_{11}^2	0		λ_1		$\lambda_1-\lambda_3$	0	0	0	3
II	CP3		m_{11}^2	0		λ_1			$\lambda_1-\lambda_3-\lambda_4$	0	0	4
III	CP2		m_{11}^2	0		λ_1					$-\lambda_6$	5
IV	$U(1)$			0					0	0	0	6
V	Z_2			0						0	0	7
VI	CP1			real					real	real	real	8

Table 1.1.: *The six classes of symmetries (I–VI) of the scalar potential and a practical example in each one. The number in the last column is the minimal number of parameters (n) in the scalar potential, which can be gotten on a specific basis [19, 60].*

Therefore, a symmetry relation among the coefficients of the scalar potential will appear as a distinct link if the coefficients of the potential are written by using a different basis for the Higgs doublets. Equation (1.2.18) constitutes a conjugacy relation within the $U(2)$ group. Thus, HF symmetries associated with matrices S and S' which are in the same conjugacy class of $U(2)$ correspond to the same model. Moreover, symmetries S and S' related by an overall phase transformation ($S' = e^{i\xi}S$) also lead to the same physics, since that overall phase transformation does not affect the bilinears $\Phi_a^\dagger \Phi_b$. One may, of course, impose on a theory several HF symmetries and GCP symmetries simultaneously. Nevertheless, in [36] has been shown that, no matter what combination of HF and/or GCP symmetries imposed on the scalar potential of the 2HDM, they always end up with one of six distinct classes of constrained Higgs potentials. Table 1.1 despites an example in each of the six categories of symmetries found in [36], and the constraints on the parameters of the potential following from that particular symmetry. The number of physical parameters in the potential may in general, within each one of Ivanov's classes, be even more reduced by choosing a specific basis for the scalar doublets. In the same way, as the general 2HDM potential has 14 parameters which may, however, be reduced to 11 through a suitable basis choice. We have organized these classes in a table 1.1, showing the number of physical parameters for each class in the last column. The respective structures for the symmetries are the following set of transformations:

- $U(2)$ is the most general HF symmetry, whose representation for S matrix in (1.2.11):

$$S = \begin{pmatrix} e^{-i\xi}\cos\theta & e^{-i\psi}\sin\theta \\ -e^{i\psi}\sin\theta & e^{i\xi}\cos\theta \end{pmatrix}, \text{ where } \mathrm{Tr}\,(S) = 2\cos\theta\cos\xi \text{ and } \det(S) = \pm 1 \tag{1.2.20}$$

  ξ, θ, and ψ are arbitrary parameters.

- $U(1)$ is a restricted version of the HF symmetry of eq. (1.2.20) with

$$S = \begin{pmatrix} e^{-i\xi} & 0 \\ 0 & e^{i\xi} \end{pmatrix}, \text{ where } \mathrm{Tr}\,(S) = 2\cos\xi \text{ and } \det(S) = 1 \tag{1.2.21}$$

  ξ is an arbitrary parameter. Hence, as a possible connexion, it corresponds to take $\theta = 0$ in (1.2.20).

- Z_2 is the symmetry under $\Phi_1 \to \Phi_1$ and $\Phi_2 \to -\Phi_2$ (associated to the cyclic group of order 2),

$$S = \begin{pmatrix} 1 & 0 \\ 0 & -1 \end{pmatrix}, \text{ where } \mathrm{Tr}\,(S) = 0 \text{ and } \det(S) = -1 \tag{1.2.22}$$

- $CP3$ is a GCP symmetry

$$X = \begin{pmatrix} \cos\theta & \sin\theta \\ -\sin\theta & \cos\theta \end{pmatrix}, \tag{1.2.23}$$

  θ belongs in the first quadrant and it is different from the two limit values 0 and $\pi/2$. We can assume this symmetry from a $SO(2)$ -like global transformation.

- $CP2$ is a GCP symmetry specifying of $CP3$ with $\theta = \pi/2$. This leads to

$$X = \begin{pmatrix} 0 & 1 \\ -1 & 0 \end{pmatrix}. \tag{1.2.24}$$

- $CP1$ is the standard CP symmetry, with

$$X = \begin{pmatrix} 1 & 0 \\ 0 & 1 \end{pmatrix}. \tag{1.2.25}$$

The introduction of the discrete Z_2 symmetry in the quark sector avoids FCNCs, while enforces in the Higgs potential: $m_{12}^2 = 0$ and $\lambda_6 = \lambda_7 = 0$. It is reasonable to consider the Z_2 symmetry in a different scalar basis:

$$\Phi_1' = \frac{1}{\sqrt{2}}(\Phi_1 + \Phi_2). \tag{1.2.26a}$$

$$\Phi_2' = \frac{1}{\sqrt{2}}(\Phi_1 - \Phi_2). \tag{1.2.26b}$$

obtaining the interchange symmetry

$$\Pi_2 : \ \Phi_1' \leftrightarrow \Phi_2' \tag{1.2.27}$$

This is equivalent to apply $S' = USU^\dagger$ in the form

$$\frac{1}{2}\begin{pmatrix} 1 & 1 \\ 1 & -1 \end{pmatrix}\begin{pmatrix} 1 & 0 \\ 0 & -1 \end{pmatrix}\begin{pmatrix} 1 & 1 \\ 1 & -1 \end{pmatrix} = \begin{pmatrix} 0 & 1 \\ 1 & 0 \end{pmatrix}. \tag{1.2.28}$$

The Π_2 symmetry enforces in the Higgs potential $m_{11}^2 = m_{22}^2$, Im $(m_{12}^2) = 0$, $\lambda_1 = \lambda_2$, $\lambda_6^* = \lambda_7$, and $\mathrm{Im}(\lambda_5) = 0$. Thus, the constraints obtained by applying Z_2 are apparently different from those achieved by applying Π_2. However, the two symmetries are equivalent, since applying Z_2 in a given basis is the same as applying Π_2 in a basis obtained from the first one through the transformation (1.2.27). Hence, the Z_2-symmetric and Π_2 -symmetric potentials must lead to the same physical predictions -we say that they are in the same class- because physical observables cannot depend on the basis in which we choose to write the Higgs doublets. The discrete Z_2 symmetry and a continuous $U(1)$ symmetry are related by a single generator

$$\Phi_1 \to e^{i\theta}\Phi_1, \ \Phi_2 \to e^{-i\theta}\Phi_2 \tag{1.2.29}$$

for an arbitrary θ. $U(1)$ global symmetry, originally introduced by Peccei and Quinn, is in connection with the strong-CP problem [64–66]. The Higgs potential invariant under $U(1)$ has $m_{12}^2 = 0$ and $\lambda_5 = \lambda_6 = \lambda_7 = 0$ and is therefore also invariant under Z_2. In addition, Z_2 and $U(1)$ symmetries could be defined as those that does not allow transitions between doublets $\Phi_1 \to \Phi_2$. It is important to note that, for instance, a potential invariant under

$$S_{2/3} = \begin{pmatrix} e^{-i2\pi/3} & 0 \\ 0 & e^{i2\pi/3} \end{pmatrix} \tag{1.2.30}$$

which is automatically invariant under the full Peccei-Quinn $U(1)$ group. Even though we only want to enforce symmetry group $Z_3 = \left\{S_{2/3}, S_{2/3}^2, S_{2/3}^3 = 1\right\}$, getting automatically a potential with full $U(1)$ symmetry. In fact, invariance under any Z_n group, with $n > 2$, will lead us to a $U(1)$-invariant potential. Another possibility of obtaining the same result is to choose an irrational multiple of π for the angle θ in Eq. (1.2.29). This discussion is an important point because continuous symmetries when they are broken, may lead to massless scalars (Goldstone bosons). An implementation of a discrete symmetry may have the same effect on the scalar potential as a continuous symmetry and therefore arises the possibility of undesired massless scalars (associated with possible topological defects in the theory). Nevertheless, the eigenstates construction can be an aid describing when is possible to lead a parameter space compatible with a massless (or quasi-massless) scalar; and treat to interpret its behavior in the theory. Moreover, we shall search the compatibility of those models and their particular parameter spaces with vacuum and perturbativity behaviors in the next chapters.

It is worthwhile to point out one caveat to the discussion in the preceding paragraph. Firstly, in this treatment has been assumed a renormalizable theory, from which we exclude all terms in the potential with a dimension larger than four [60, 67]. However in a first view, we take the reasonable assumption that the 2HDM is just the low-energy limit of a larger theory. So, we decide to include effective operators of dimensions five, six, or above. Then the equivalence between different symmetries (such as the Z_n with $n > 2$, all of them leading to the same $U(1)$-invariant scalar potential) might no longer be verified. Another possible issue is connected with the fermionic sector: with a particular symmetry of the scalar sector, there are in general many ways of extending that symmetry to the fermion sector, often with completely different effects on the Yukawa terms indeed. It shall comprehensively describe in section 1.3.

On the other hand, by imposing a symmetry with multiple generators on the scalar potential. For example, the scalar potential invariant under both Z_2 and Π_2 on the same basis has a parameter space constrained by $m_{11}^2 = m_{22}^2$, $m_{12}^2 = 0$, $\lambda_1 = \lambda_2$, and $\lambda_6 = \lambda_7 = \mathrm{Im}(\lambda_5) = 0$. Thus, the potential invariant under $Z_2 \times \Pi_2$ only has five parameters

$(m_{11}^2, \lambda_1, \lambda_3, \lambda_4, \mathrm{Re}(\lambda_5))$ and, it is possible to show that it is equivalent to a potential with CP2 symmetry written in another basis; hence $Z_2 \times \Pi_2 \Leftrightarrow CP2$. The $U(2)$-invariant potential may similarly be obtained through the imposition of the $CP3$ and $U(1)$ symmetries in the same basis, as can easily be seen in table 1.1. One can also prove that the existence of either the Z_2 (or, equivalently, Π_2), $U(1)$, or $U(2)$ symmetries is sufficient to guarantee the existence of a basis choice in which all the parameters of the scalar potential are real. That is, the corresponding scalar Higgs sectors are explicitly CP-conserving. Therefore, all models belonging to the classes in table 1.1 have CP-conserving scalar Higgs potentials [60,67]. The potential CP1 results from applying the GCP symmetry with the matrix X in Eq. (1.2.23) with $\theta = 0$. This leads to $\Phi_1 \to \Phi_1^*$ and $\Phi_2 \to \Phi_2^*$ standard CP symmetry, which forces all coefficients in the potential to be real. The potential CP2 arises from applying the GCP symmetry with the matrix X in Eq. (1.2.23) with $\theta = \pi/2$; being for the doublets $\Phi_1 \to \Phi_2^*$ and $\Phi_2 \to \Phi_1^*$. On the other hand, the potential in the CP3-scenario results from applying the GCP symmetry with any other (arbitrary) angle $\theta \neq 0, \pi/2$. The theories with symmetry CP2 and CP3 are (of course) CP-conserving, but they have potentials more restrictive than CP1-scenario. In the CP3 symmetry, if one wants to extend the CP symmetry to the Yukawa sector, different values of θ will have different consequences for the quark masses how for instance only $\theta = \pi/3$ allows six massive quarks after symmetry implementation.

As was mentioned, it is possible to reach class CP2 of 2HDM scalar potentials either by requiring symmetry under the GCP transformation of Eq. (1.2.24) or, alternatively, by requiring joint symmetry under Z_2 and Π_2. There are, indeed, many other ways to obtain this form for scalar potential. For $CP3 \Leftrightarrow U(1) \times \Pi_2$. In general, there are many possible symmetries leading into any of the six classes of constrained 2HDM potentials. The different symmetries are equivalent concerning the scalar potential, but they may differ when one tries to extend them to the Yukawa sector.

1.3. The Yukawa Lagrangian in 2HDMs

From pure scalar sector analyses, we now study the fermion-scalar interactions and also lepton-quark masses mechanisms from SSB scenarios. The Yukawa Lagrangian compatible with gauge invariance and renormalizability has the general form:

$$-\mathcal{L}_Y = \tilde{\eta}_{i,j}^{U,0} \bar{Q}_{iL}^0 \tilde{\Phi}_1' U_{jR}^0 + \tilde{\eta}_{i,j}^{D,0} \bar{Q}_{iL}^0 \Phi_1' D_{jR}^0 + \tilde{\xi}_{i,j}^{U,0} \bar{Q}_{iL}^0 \tilde{\Phi}_2' U_{jR}^0 + \tilde{\xi}_{i,j}^{D,0} \bar{Q}_{iL}^0 \Phi_2' D_{jR}^0 + \tilde{\eta}_{i,j}^{E,0} \bar{L}_{iL}^0 \Phi_1' E_{jR}^0 + \tilde{\xi}_{i,j}^{E,0} \bar{L}_{iL}^0 \Phi_2' E_{jR}^0 + h.c. \quad (1.3.1)$$

Here $\tilde{\Phi}_{1,2} \equiv i\sigma_2 \Phi_{1,2}$. $\tilde{\eta}$ and $\tilde{\xi}$ are non diagonal 3×3 matrices and i, j denote family indexes. D_R^0 refers to the three down type weak isospin quarks singlets $D_R^0 \equiv \left(d_R^0, s_R^0, b_R^0\right)^T$, U refers to the three up type weak isospin quark singlets $U_R^0 \equiv \left(u_R^0, c_R^0, t_R^0\right)$ and $E_R^0 = \left(e_R^0, \mu_R^0, \tau_R^0\right)$ the three charged leptons. Finally, $\bar{Q}_{iL}^0$, $\bar{L}_{iL}^0$ denote the quark and lepton weak isospin left-handed doublets respectively. The superscript 0 labels the fact that the fields are not mass eigenstates yet. In the SM, diagonalizing the mass matrix also diagonalizes the Yukawa interactions, therefore there are no tree-level FCNC. For the model described by Lagrangian (1.3.1) has been considered that, in a general case, both Higgs doublets couple to the up and down sectors simultaneously. However, this fact leads to processes with flavor changing neutral currents (FCNC) at tree level, since by rotating the fermion gauge eigenstates to get the mass eigenstates we are not able to diagonalize both coupling matrices η and ξ simultaneously. In other words, FCNC presence is due to general 2HDM structure. Nothing does not ensure the alignment of the fermion mass terms with the neutral changing Yukawa couplings. In the following we describe the origin of FCNC couplings. The most generic Yukawa interactions for 2HDM can be written in a more compact form by

$$\mathcal{L}_Y = -\sum_{j=1}^{2} \left[\bar{Q}_L \left(\Phi_j Y_j^d D_R + \tilde{\Phi}_j Y_j^u U_R \right) + \bar{L}_L \Phi_j Y_j^e E_R \right] + h.c. \quad (1.3.2)$$

In this equation, $\widetilde{\Phi}_j = i\tau_2 \Phi_j^*$; Q_L (quark doublet), L_L (lepton doublet), D_R (negative charged quarks), U_R (positively charged quarks) and E_R (negatively charged leptons) are 3-vector in flavor space. For simplicity and as a first glance, we have not included the neutrino sector by their smallness mass size; although this condition can be relaxed through different mechanisms. Besides, $Y_j^{d,u,e}$ are generic 3×3 complex matrices containing the Yukawa couplings, for the down, up and leptonic sector respectively. In part, almost all develops over quark sector can be extended to the leptonic sector, we only assume the absence of right part of neutrinos (as a first assumption). It does impossible to describe mass terms for neutrinos [7]. With the Yukawa lagrangian defined by Eq. 1.3.2, it is possible to build up the scalar-fermionic interactions in the Higgs basis (H_1, H_2) defining by H_1 having vev equal to $v/\sqrt{2}$ while has vanishing vev[8]. We begin

[7] Construction of 2HDM taking into account hierarchical neutrino masses has been described in [68, 69]

[8] In a reduced part of the literature have used the term of "fundamental parametrization" to referring the Higgs basis. In our treatment, the former term will be employed when the 2HDM type III become introduced. In the symmetries formalism, we use the Higgs basis term.

with the vacuum expectation value definition in general terms ($\tilde{v}_1$ and $\tilde{v}_2$ are allowed to be complex)

$$v = \sqrt{|\tilde{v}_1|^2 + |\tilde{v}_2|^2}. \tag{1.3.3}$$

It is well known as v related to Fermi's constant has been measured with high precision, for example in muon decay measurements [4]. The most typical value for v is 246 GeV, being by definition a real and a positive quantity. The relevant transformations for the doublets from a generic basis to Higgs basis are

$$\Phi_1 = \frac{1}{v}\left(\tilde{v}_1 H_1 + \tilde{v}_2^* H_2\right), \tag{1.3.4a}$$

$$\Phi_2 = \frac{1}{v}\left(\tilde{v}_2 H_1 - \tilde{v}_1^* H_2\right). \tag{1.3.4b}$$

Defining the matrices for down quarks sector

$$\bar{M}^d = \frac{1}{\sqrt{2}}\left(\tilde{v}_1 Y_1^d + \tilde{v}_2 Y_2^d\right), \tag{1.3.5a}$$

$$\bar{N}^d = \frac{1}{\sqrt{2}}\left(\tilde{v}_2^* Y_1^d - \tilde{v}_1^* Y_2^d\right). \tag{1.3.5b}$$

Moreover, it is possible to compute the term composed by a doublet and the respective Yukawa coupling

$$\begin{aligned}\sum_{j=1}^{2}\Phi_j Y_j^d &= \frac{1}{v}\left(\tilde{v}_1 H_1 + \tilde{v}_2^* H_2\right) Y_1^d + \frac{1}{v}\left(\tilde{v}_2 H_1 - \tilde{v}_1^* H_2\right) Y_2^d, \\ &= \frac{1}{v}\left(\tilde{v}_1 Y_1^d + \tilde{v}_2 Y_2^d\right) H_1 + \frac{1}{v}\left(\tilde{v}_2^* Y_1^d - \tilde{v}_1^* Y_2^d\right) H_2, \\ &= \frac{\sqrt{2}}{v}\left(\bar{M}^d H_1 + \bar{N}^d H_2\right).\end{aligned} \tag{1.3.6}$$

In a similar way, the up-quarks sector behaves as

$$\sum_{j=1}^{2}\Phi_j Y_j^u = \frac{\sqrt{2}}{v}\left(\bar{M}^u \tilde{H}_1 + \bar{N}^u \tilde{H}_2\right). \tag{1.3.7}$$

where $H_i = i\sigma_2 H_i^*$, with $i = 1, 2$. We can translate these matrices into the mass basis of quarks, in which the mass matrices are diagonal. Hence we perform a bi-unitary transformation over M^d and M^u, through rotations on the left-handed and right-handed quarks fields, where $k = u, d$:

$$V_L^{k\dagger}\bar{M}^k V_R^k = M^k \tag{1.3.8a}$$

$$V_L^{k\dagger}\bar{N}^k V_R^k = \bar{M}^k \tag{1.3.8b}$$

Both diagonal matrices M^d =diag(m_d, m_s, m_b) and M^u =diag(m_u, m_c, m_t) have real and positive diagonal elements. In general, even if after bi-diagonalization, matrices N^d and N^u are not diagonal, then there will be scalar FCNCs at tree level in both quark sectors. In the Higgs basis, the FCNC couplings for those interactions are obtained from N^u and N^d elements. This basis can also be extrapolated to charged leptonic sector. On a generic basis like associated to original Lagrangian (1.3.2), the FCNC's absence could be derived from commuting Y_1^i and Y_2^i matrices $i = u, d$)[9]. For instance, that condition is trivially satisfied when $Y_2^i = 0$, as could occur when a discrete symmetry like Z_2 is introduced in the Yukawa Lagrangian as we discuss below. This implementation can be translated into a sufficient condition, based on the assumption of all fermions become coupled to just one doublet, originating mass terms uniquely. It is well known that FCNCs are highly constrained compared with the charged current processes like mesons oscillations. Therefore it would be viable to "naturally"suppress them in these models. If all fermions with the same quantum numbers couple

[9] This statement can be shown by the fact that FCNCs are absent both matrices might be diagonalized simultaneously if and only if Yukawa matrices are represented regarding the linear combinations of a complete set of orthogonal matrices of the same dimensionality of Yukawa matrices [70].

to the same scalar multiplet, then FCNC will be absent. In other words, all quarks and leptons of a given charge and helicity must transform with the same irreducible representation of $SU(2)$ isospin group. This fact is corresponding to having the same eigenvalue of the third component of isospin operator. The latter ensures the existence of a basis in which fermions receive their contributions in the mass matrix from a single source [40]. To accomplish this condition, we invoke an unbroken intrinsic parity symmetry in the fields, Z_2, which could be introduced by the SM fields and doublets in even or odd transformations [19].

From above discussion in the quark sector of 2HDM, we can see two possibilities. i) All quarks become coupled to just one doublet (here it has been chosen to be Φ_1) or ii) the up type right-handed quarks couple to one doublet (e.g. Φ_1) and the down type right-handed quarks couple to other (Φ_2). The first scenario is called the 2HDM type I, meanwhile, the last model is known as the 2HDM type II. Both models are outlined in Fig. (1.3).

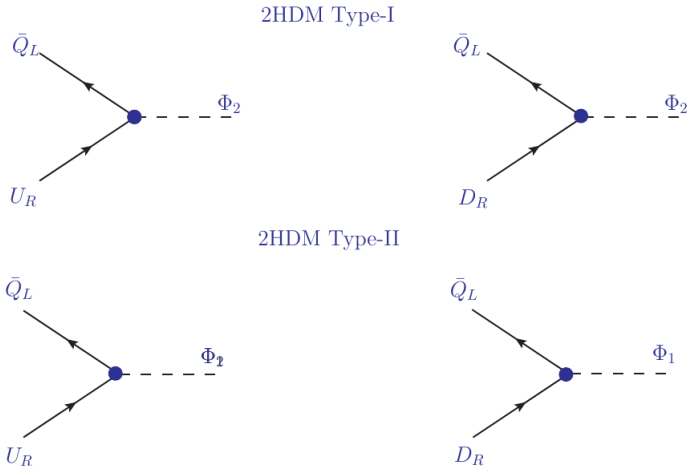

Figure 1.3.: *Couplings structure in models with flavor conservation. (**Up**) Type I and (**Down**) type II models in the quark sector.*

When these structures for symmetries implementations are extended to the leptonic sector, the charged leptons couple to the same scalar doublet as the $Q = -1/3$ quarks although this condition is not necessary to avoid FCNCs at tree level. Nonetheless, there are other two possibilities to construct models with natural flavor conservation. In the lepton-specific model, the RH quarks couple to Φ_2 and the RH leptons couple to Φ_1. In the flipped model, the $Q = 2/3$ right-handed quarks and charged leptons couples to the same doublet (say Φ_1), and the $Q = -1/3$ right handed quarks are coupled to Φ_2 [19]. In this work, we are focused on the traditional types I and II 2HDMs with flavor conservation and the corresponding extension to lepton sector[10].

1.3.1. Basis transformations and Yukawa couplings

From section 1.2.1, we have seen as the basis transformations change the coefficients in the Higgs potential (1.2.2). Now, we are focused on the basis change in the Yukawa Lagrangian taken as a guide the basis transformations over Higgs potential terms. The Yukawa lagrangian (1.3.2) can be written regarding new fields obtained from the original ones by simple basis changes over doublets

$$\Phi_a \to \Phi'_a = \sum_{\alpha=1}^{2} V_{a\alpha}\Phi_\alpha, \tag{1.3.11}$$

meanwhile for fermions doublets

[10]It is important to point out that the Yukawa Lagrangian type I and II can also be generated from a continuous global symmetry. The set of transformations

$$\Phi_1 \to e^{i\varphi}\Phi_1 \text{ and } \Phi_2 \to -\Phi_2 \tag{1.3.9}$$

$$D_{jR} \to e^{-i\omega}D_{jR} \text{ and } U_{jR} \to e^{-i\varphi}U_{jR} \tag{1.3.10}$$

with $\omega = \varphi, \pi/2$, yields models type I and type II respectively. Here D_R is labeling the three down type weak isospin quark singlets and U_R is applying to the three up type weak isospin quark singlets.

$$Q_L \rightarrow Q'_L = V_L Q_L; \tag{1.3.12}$$
$$L_L \rightarrow L'_L = \bar{V}_L L_L. \tag{1.3.13}$$

For singlets representations of fermions, we have

$$D_R \rightarrow D'_R = V_{DR} D_R, \quad U_R \rightarrow U'_R = V_{UR} U_R, \quad E_R \rightarrow E'_R = V_{ER} E_R. \tag{1.3.14}$$

where $V \in U(2)$ is a 2×2 unitary matrix and $\mathcal{V} \equiv \left\{V_L, \bar{V}_L, V_{DR}, V_{UR}, V_{ER}\right\} \in U(3)$ are 3×3 unitary matrices. The gauge-kinetic terms are unchanged by basis transformations and the coefficients of the Higgs potential are transformed in the following way

$$\mu'_{ij} = \sum_{\alpha,\beta=1}^{2} V_{i\alpha} \mu_{\alpha\beta} V^*_{b\beta} = \left(V \mu V^\dagger\right)_{ij}, \tag{1.3.15a}$$

$$\Lambda^{jl}_{km} = \sum_{\alpha,\beta,\gamma,\delta=1}^{2} V_{j\alpha} V_{l\gamma} \Lambda^{\alpha\gamma}_{\beta\delta} V^*_{k\beta} V^*_{m\delta}. \tag{1.3.15b}$$

Then, Yukawa matrices are transformed by

$$\begin{aligned} Y^d_a &\rightarrow Y^{d'}_a = \sum_{\alpha=1}^{2} V_L Y^d_\alpha V^\dagger_{DR} \left(V^\dagger\right)_{\alpha a}, \\ Y^u_a &\rightarrow Y^{u'}_a = \sum_{\alpha=1}^{2} V_L Y^u_\alpha V^\dagger_{UR} \left(V^T\right)_{\alpha a}, \\ Y^e_a &\rightarrow Y^{e'}_a = \sum_{\alpha=1}^{2} \bar{V}_L Y^e_\alpha V^\dagger_{ER} \left(V^\dagger\right)_{\alpha a}. \end{aligned} \tag{1.3.16}$$

In all transformations, we show the indexes explicitly in scalars space while we have used matrix formulation in the flavor space for fermions.

1.3.2. Yukawa couplings and Symmetries

We have studied in section 1.2.2 as six symmetries (Family and CP) classes arose in the Higgs potential by the realization of $SL(2, C)$ re-parameterization group of 2HDM. Hence, to this point correspond to study as those symmetries could be extended to the full Lagrangian. By definition, these symmetries leave out the gauge terms invariant, but in the Yukawa sector and by coupling structures among fermions and doublets, they might affect Yukawa terms. We review as Higgs family and CP-symmetries are extended to the Yukawa Lagrangian and how the phenomenology associated with fermions-scalars interactions is modified by that kind of implementations.

Family symmetries

The main assumptions belong in assuming that the Lagrangian (1.3.2) is invariant under the symmetry transformations (1.2.11)

$$\Phi_a \rightarrow \Phi^S_a = \sum_{b=1}^{2} S_{ab} \Phi_b. \tag{1.3.17}$$

i.e. Φ_a relates with Φ_b through a unitary matrix 2×2, S. The fermion fields (doublets) transform according to

$$Q_L \rightarrow Q^S_L = S_L Q_L, \tag{1.3.18a}$$
$$L_L \rightarrow L^S_L = \bar{S}_L L_L. \tag{1.3.18b}$$

while the singlets transform as

$$\begin{aligned} D_R &\rightarrow D_R^S = S_{DR} D_R, \\ U_R &\rightarrow U_R^S = S_{UR} U_R, \\ L_R &\rightarrow E_R^S = S_{ER} E_R. \end{aligned} \tag{1.3.19}$$

where $S \in U(2)$ and $\mathcal{S} = \left\{S_L, \bar{S}_L, D_R, U_R, E_R\right\} \in U(3)$. Trough applications of these transformations, the parameters of Higgs potential and Yukawa matrices obey the following equations:

$$\mu_{ij} = \sum_{\alpha,\beta}^{2} S_{i\alpha} \mu_{\alpha\beta} S_{j\beta}^{*}, \tag{1.3.20a}$$

$$\Lambda_{km}^{jl} = \sum_{e,f,g,h=1}^{2} S_{j\alpha} S_{l\gamma} \Lambda_{\alpha\gamma}^{\beta\delta} S_{k\beta}^{*} S_{m\delta}^{*}. \tag{1.3.20b}$$

and the Yukawa couplings for down, up and charged lepton sectors transforming according to

$$\begin{aligned} Y_a^d &= \sum_{\alpha=1}^{2} S_L Y_\alpha^d S_{DR}^{\dagger} \left(S^{\dagger}\right)_{\alpha a}, \\ Y_a^u &= \sum_{\alpha=1}^{2} S_L Y_\alpha^u S_{UR}^{\dagger} \left(S^{\dagger}\right)_{\alpha a}, \\ Y_a^e &= \sum_{\alpha=1}^{2} \bar{S}_L Y_\alpha^e S_{ER}^{\dagger} \left(S^{\dagger}\right)_{\alpha a}. \end{aligned} \tag{1.3.21}$$

With the basis transformations presented in Eqs. (1.3.11), (1.3.12) and (1.3.14), symmetry transformations in doublets are changed by

$$\begin{aligned} S' &= V S V^{\dagger}, \\ S'_L &= V_L S V_L^{\dagger}, \\ \bar{S}_L &= \bar{V}_L \bar{S}_L V_L^{\dagger}. \end{aligned} \tag{1.3.22}$$

while in singlets sectors we get

$$\begin{aligned} S'_{DR} &= V_{DR} S_{DR} V_{DR}^{\dagger}, \\ S'_{DR} &= V_{UR} S_{UR} V_{UR}^{\dagger}, \\ S'_{ER} &= V_{ER} S_{ER} V_{ER}^{\dagger}. \end{aligned} \tag{1.3.23}$$

We are looking for the general way to extend Higgs potential symmetries Higgs family ones) into Yukawa Lagrangian. For this purpose, a particular set of one symmetry $\mathcal{S}$ is considered on some basis. In the case of an Abelian symmetry, Eq (1.3.17) is translated into a diagonal transformation

$$\begin{pmatrix} \Phi_1^S \\ \Phi_2^S \end{pmatrix} = \begin{pmatrix} e^{i\theta_1} & 0 \\ 0 & e^{i\theta_2} \end{pmatrix} \begin{pmatrix} \Phi_1 \\ \Phi_2 \end{pmatrix}. \tag{1.3.24}$$

From a particular choice of $\{\mathcal{V}\}$, the symmetry in all fields can be parametrized by the following diagonal matrices

$$S = \mathrm{diag}\left(e^{i\theta_1}, e^{i\theta_2}\right), \quad S_L = \mathrm{diag}\left(e^{i\alpha_1}, e^{i\alpha_2}, e^{i\alpha_3}\right), \quad \bar{S}_L = \mathrm{diag}\left(e^{i\bar{\alpha}_1}, e^{i\bar{\alpha}_2}, e^{i\bar{\alpha}_3}\right), \tag{1.3.25a}$$

$$S_{DR} = \mathrm{diag}\left(e^{i\beta_1}, e^{i\beta_2}, e^{i\beta_3}\right), \quad S_{UR} = \mathrm{diag}\left(e^{i\gamma_1}, e^{i\gamma_2}, e^{i\gamma_3}\right), \quad S_{ER} = \mathrm{diag}\left(e^{i\delta_1}, e^{i\delta_2}, e^{i\delta_3}\right). \tag{1.3.25b}$$

An overall phase change has no effect on the symmetry. For example, taking $V = e^{i\theta} I_{2\times 2}$, leaves $S\prime = S$. On the other hand, we can see from Eqs (1.3.20a)-(1.3.21) that the symmetry

$$\tilde{S} = e^{i\tilde{\theta}} S, \quad \tilde{S}_L = e^{i\tilde{\alpha}} S_L, \quad \tilde{S}_L = e^{i\tilde{\alpha}} \bar{S}_L, \tag{1.3.26a}$$

$$\tilde{S}_{DR} = e^{i\tilde{\beta}} S_{DR}, \quad \tilde{S}_{UR} = e^{i\tilde{\gamma}} S_{UR}, \quad \tilde{S}_{ER} = e^{i\tilde{\delta}} S_{ER}, \tag{1.3.26b}$$

imposes the same constraints on the Lagrangian as the symmetry set $\mathcal{S}$, as long as

$$e^{i\left(\tilde{\beta}-\tilde{\alpha}-\tilde{\theta}\right)} = 1; \; e^{i\left(\tilde{\gamma}-\tilde{\alpha}+\tilde{\theta}\right)} = 1 \text{ and } e^{i\left(\tilde{\beta}-\tilde{\alpha}-\tilde{\theta}\right)} = 1. \tag{1.3.27}$$

This can be used to translated Eqs. (1.3.25b) into the forms

$$S = \text{diag}\left(1, e^{i\theta}\right), \quad S_L = \text{diag}\left(e^{i\alpha_1}, e^{i\alpha_2}, e^{i\alpha_3}\right), \quad \bar{S}_L = \text{diag}\left(e^{i\bar{\alpha}_1}, e^{i\bar{\alpha}_2}, e^{i\bar{\alpha}_3}\right); \tag{1.3.28a}$$

$$S_{DR} = \text{diag}\left(e^{i\beta_1}, e^{i\beta_2}, e^{i\beta_3}\right), \quad S_{UR} = \text{diag}\left(e^{i\gamma_1}, e^{i\gamma_2}, e^{i\gamma_3}\right), \quad S_{ER} = \text{diag}\left(e^{i\delta_1}, e^{i\delta_2}, e^{i\delta_3}\right). \tag{1.3.28b}$$

with $\alpha_1 = 0$ and $\bar{\alpha}_1 = 0$. Thus, all the freedom in choosing the fermion transformation laws is reduced to the choice of the arbitrary phases. Despite immense simplification, these sets of parameters yield even many possibilities to specify symmetry implementations, which is translated to many different models. However, since constraints as CKM entries and requirements of six massive quarks, the number of possible models is highly reduced. In the former fact, the reason for this reduction is that the effect of the phases α_i on the CKM matrix, or in the quark squared mass matrices, is equivalent to setting many entries equal to zero. For $\theta = \pi$, S =diag$(1, -1)$ leads to the usual Z_2 Higgs potential. Any other value of $0 < \theta < 2\pi$, leads to the full $U(1)$ symmetric Higgs potential. For example, with $\theta = 2/3$, $S^3 = I_2$, and a Z_3 symmetry is assumed on the scalar fields. Nonetheless, due to the scalar potential only has quadratic and quartic terms, the resulting Higgs potential has the full $U(1)$ Peccei-Quinn symmetry. As we discussed before, if this symmetry is spontaneously broken by the vacuum, the spectrum would have massless particles. In consequence, great care must be taken when imposing what may look like discrete symmetries in models with multi doublets. Substituting Eqs. (1.3.25b) in Eqs. (1.3.21), these symmetries satisfy

$$\begin{aligned} \left(Y_a^d\right)_{ij} &= e^{i(\alpha_i - \beta_j - \theta_a)} \left(Y_a^d\right)_{ij}, \\ \left(Y_a^u\right)_{ij} &= e^{i(\alpha_i - \gamma_j + \theta_a)} \left(Y_a^u\right)_{ij}, \\ \left(Y_a^e\right)_{ij} &= e^{i(\bar{\alpha}_i - \delta_j - \theta_a)} \left(Y_a^e\right)_{ij}, \end{aligned} \tag{1.3.29}$$

where no sum over i and j indexes is explicit on the right-hand sides. For the simplified form in Eq. (1.3.28b) we set $\theta_1 = 0$ and $\theta_2 = \theta$. Furthermore, we will always take $\theta \neq 0 \pmod{2\pi}$ since we are only interested in symmetries which do transform the scalar fields. It will prove useful to keep α_1 explicitly, having in mind that it can be set equal to zero without loss of generality.

1.3.3. CP symmetries in the Yukawa sector

With the aim to study as CP violation phases arise in a general 2HDM, we introduce symmetry operations in the Yukawa sector for fermion and scalar interactions. As SSB is not achieved yet, we restrict our review in one based on explicit symmetry transformations. Moreover, these discussions would lead to discriminate the role and the intimate relation among Yukawa structure and their CP symmetries with FCNC processes. In this treatment, the primary assumption is that Yukawa Lagrangian (1.3.2) is invariant under the CP symmetry,

$$\Phi_a \to \sum_{\alpha=1}^{2} X_{a\alpha} \Phi_\alpha^*, \tag{1.3.30}$$

from discussion given in section 1.2.2, this operation relates the doublet Φ_a with the complex conjugate of $\Phi_b \to \Phi_b^*$. For fermionic fields, we can obtain

$$Q_L \to X_L \gamma^0 C Q_L^*, \tag{1.3.31a}$$

$$L_L \to \bar{X}_L \gamma^0 C L_L^*, \tag{1.3.31b}$$

where X is a 2×2 unitary matrix and X_L and $\bar{X}_L$ are arbitrary 3×3 unitary matrices. $C = i\gamma_2\gamma_0$ is the charge conjugation operator. For singlet representations

$$\begin{aligned} D_R &\to X_{DR}\gamma^0 C D_R^*, \\ U_R &\to X_{UR}\gamma^0 C U_R^*, \\ E_R &\to X_{ER}\gamma^0 C E_R^*, \end{aligned} \tag{1.3.32}$$

where $\{X_{DR}, X_{UR}, X_{ER}\}$ are 3×3 unitary matrices. A result of these transformations is that scalar couplings in the lagrangian must satisfy

$$\mu_{ij}^* = \sum_{\alpha,\beta=1}^{2} X_{\alpha i}^* \mu_{\alpha\beta} X_{\beta j}, \tag{1.3.33a}$$

$$\left(\Lambda_{km}^{jl}\right)^* = \sum_{e,f,g,h=1}^{2} X_{k\alpha}^* X_{m\gamma}^* \Lambda_{\alpha\gamma}^{\beta\delta} X_{j\beta} X_{l\delta}, \tag{1.3.33b}$$

In the same way for fermionic couplings, we get

$$\begin{aligned} Y_i^{d*} &= \sum_{\alpha=1}^{2} X_{i\alpha} X_L Y_\alpha^d X_{DR}^\dagger, \\ Y_i^{u*} &= \sum_{\alpha=1}^{2} X_{i\alpha}^* X_L Y_\alpha^u X_{UR}^\dagger, \\ Y_i^{e} &= \sum_{\alpha=1}^{2} X_{i\alpha} \bar{X}_L Y_\alpha^e X_{ER}^\dagger. \end{aligned} \tag{1.3.34}$$

Under basis change of Eqs. (1.3.11), (1.3.12) and (1.3.14), *CP* symmetry transformations are altered by

$$X' = VXV^T, \quad X'_L = V_L X_L V_L^T, \quad \bar{X}_L = \bar{V}_L \bar{X}_L \bar{V}_L^T, \tag{1.3.35a}$$

$$X_{DR} = V_{DR} X_{DR} V_{DR}^T, \quad X_{UR} = V_{UR} X_{UR} V_{UR}^T, \quad X_{ER} = V_{ER} X_{ER} V_{ER}^T. \tag{1.3.35b}$$

Comparing with Higgs-family symmetries, it is much simpler to extend the three possible scalar GCP symmetries to the Yukawa sector. In fact, as we discussed in section 1.2.2, any GCP transformation on the doublets can be reduced to a simple rotation matrix of the form

$$X^{CP} = \begin{pmatrix} \cos\theta & \sin\theta \\ -\sin\theta & \cos\theta \end{pmatrix}. \tag{1.3.36}$$

That is, it is always possible, through a judicious choice of basis of quark fields (flavor space), to reduce the transformation matrix of the left doublets to the form

$$X_L = \begin{pmatrix} \cos\alpha & \sin\alpha & 0 \\ -\sin\alpha & \cos\alpha & 0 \\ 0 & 0 & 1 \end{pmatrix}, \tag{1.3.37}$$

with some angle $0 \leq \alpha \leq \pi/2$. A similar form is obtained for the matrices X_{DR} and X_{UR} in eqs. (1.3.34), with independent angles β and γ in the same range as α. A quite simple form of the fermion transformation matrices imposes severe constraints on the Yukawa couplings. In fact, the restrictions are so serious that no ambiguity occurs in the fermionic sector when one extends the scalar GCP symmetries to it; each of the three GCP models has only one possible implementation on the fermion sector. Recalling that the three GCP scalar models can be parameterized regarding the angle θ in the simplified GCP transformation of Eq. (1.3.36), it was concluded that [67]:

- For the CP1 situation, with $\theta = 0$, there is only one way to extend the scalar symmetry to the fermion sector which does not entail massless quarks or charged leptons: by forcing all Yukawa couplings to be real. We are thus left with a Lagrangian with real generic matrices Y_j^d - as such the model has tree-level scalar FCNCs, which are not in any way "naturally suppressed ". In this model, CP violation must arise spontaneously, through a relative phase between the two vevs (as will be exposed in the following chapter).

- For the CP2 symmetry, with $\theta = \pi/2$, there is no way to extend the symmetry to the Yukawa sector without obtaining at least one massless charged fermion. As such, the CP2 model may be considered ruled out by experiment. However, one might also take the point of view that the CP2 symmetry is an approximate one, broken by some manner of mechanism, and as such the massless fermions it predicts will acquire a (small) mass somehow, corresponding to the first generations of particles.
- For the CP3 model, with any $0 < \theta < \pi/2$, a remarkable effect takes place: all values of $\theta \neq \pi/3$ lead to massless quarks or charged leptons. Only $\theta = \pi/3$ leads to an acceptable fermion mass spectrum with a strict hierarchy. The Yukawa matrices which result from such a symmetry are extremely constrained - the quark sector ends up depending only on ten independent parameters (seven moduli and three phases). Nevertheless, this model is compatible with the fitting all quark masses and the elements of the CKM matrix with relative phases. The model does possess tree-level FCNC, but they end up being entirely suppressed, in a "natural"way. The model also has a unique feature, in the sense that CP violation arises in a relatively novel way - through computing Jarlskog invariant [11]. However, the value of the Jarlskog invariant predicted by this model is several orders of magnitude below of its SM value, which leads to values of the unitarity triangle angles inα and β (in the Euler parametrization of CKM matrix) practically equal - a prediction of the model in contradiction with the most recent experimental data. This fact rules out this scenario.

In conclusion, when one extends the three GCP scalar symmetries to the Yukawa sector, one obtains: i) arbitrary FCNCs for the CP1 case. ii) The model spectrum has massless quarks and charged leptons for the CP2 scenario; a single CP3 symmetry leading to three massive generations of fermions, with naturally small FCNC but predictions for heavy meson phenomenology which does not agree with experiment data.

1.4. Custodial Symmetry and Electroweak Oblique Parameters

Once considered relevant sectors of 2HDM from symmetries point of view, our discussion should be focused in as these several models can be tested by precision measurements carry out in several experiments of high-energy physics. Our hypothesis to conduct our phenomenological analyses is that 2HDMs parameter space is compatible with *alignment regime*, where scalar boson found in LHC is consistent in couplings and mass of h^0 (lighter CP-Higgs boson), emulating at the same time all possible properties of SM-Higgs boson. The formal description of scalar alignment for 2HDM with non-zero VEVs is discussed in appendix A. One formalism is based on to establish which is the new physics influence in observables as decays and vector boson masses measurements. These effects could even be present in NLO corrections for well known EW sector. In general, the contribution to appropriate electroweak corrections from the extra $SU(2)$ doublet in the 2HDM is small, since scalar doublets (or singlets) do not break the custodial symmetry which protects the tree-level relation

$$\rho = \frac{m_w^2}{m_z^2 \cos^2\theta_w} = 1. \tag{1.4.1}$$

It is an experimental fact and measured from m_z and m_w pole masses and precision tests [72, 73]. There are many Higgs representations to satisfy the $\rho = 1$ constraint at tree level. The general formula is [74]

$$\rho = \frac{m_w^2}{m_z^2 \cos^2\theta_w} = \frac{\sum_{T,Y}\left[4T\left(T+1\right) - Y^2\right]\left|V_{T,Y}\right|^2 c_{T,Y}}{\sum_{T,Y} 2Y^2 \left|V_{T,Y}\right|^2}. \tag{1.4.2}$$

where $\langle \Phi\left(T,Y\right)\rangle = V_{T,Y}$ defines the vacuum expectation value of each neutral Higgs field, and T and Y specify the total $SU\left(2\right)_L$ isospin and the hypercharge of the Higgs representation to which it belongs. $c_{T,Y}$ depends on representation values

$$c_{T,Y} = \begin{cases} 1, & (T,Y) \in \text{ complex representation} \\ \frac{1}{2}, & (T,Y=0) \in \text{ real representation} \end{cases} \tag{1.4.3}$$

[11] Jarlskog invariant in the quark sector for Hermitian mass matrices is defined as [71]

$$J = \frac{\mathrm{Im}\left(\det\left[M_d, M_u\right]\right)}{2F} \tag{1.3.38}$$

with

$$F = \left(1+2\tilde{m}_{2u}\right)\left(1-\tilde{m}_{1u}\right)\left(\tilde{m}_{1u}+\tilde{m}_{2u}\right)\left(1+\tilde{m}_{2d}\right)\left(1-\tilde{m}_{1d}\right)\left(\tilde{m}_{1d}+\tilde{m}_{2d}\right)$$

here $\tilde{m}_{iq}$ are the quark mass ratios $\tilde{m}_{iq} = m_{iq}/m_{3q}$. Being 3 the index for the third family (top or bottom depending on the sector in the ratio).

The requirement that $\rho = 1$ for arbitrary $V_{T,Y}$ value is

$$(2T+1)^2 - 3Y^2 = 1 \tag{1.4.4}$$

How the custodial symmetry arises in SM can be seen as follows: The left (right) chiral fermions in the SM also transform according to the global symmetry $SU(2)_{L(R)}$. The scalar-Higgs doublet (with four real fields) is a bi-doublet under this global symmetry. Before the spontaneous breaking of $SU(2)_L \times U(1)_Y$ gauge group, the Higgs potential has a global $SO(4) \simeq SU(2)_L \times SU(2)_R$ symmetry which reduces to $SU(2)_V$ [12]when the symmetry is broken. This $SU(2)_V$ symmetry is also isomorphic to $SO(3)$ group under which the triplet $\left(G^{\pm}, G^0\right)$ of Goldstone bosons transforms. This symmetry is not respected by the scalar kinetic terms, in particular, those ones involving the hypercharge coupling g'. Moreover, the $SO(4)$ symmetry is also broken by Yukawa terms, which are linear in Φ, due to up and down quarks have different masses (i.e. isospin violation). Thus $SO(4)$ is not a symmetry of the whole Lagrangian, only of its scalar sector. Since in the scalar sector, $SO(4)$ global symmetry is only broken by small g' terms in the kinetic part, it is regarded as an *approximate* symmetry in the theory. In the most general 2HDM, there is no $SO(4)$ global symmetry because of the presence of new bilinears and their interactions; thus here arises the possibility of substantial contributions to ρ parameter coming from scalar sector alone. If one wants to avoid them, one may impose custodial symmetry on the 2HDM potential which yields particular structure in the scalar sector of the Lagrangian. Besides, large mass splitting between scalar states could induce additional contributions to ρ parameter by including radiative corrections. These effects can be measured by using EW-oblique parameters. We will come back to the last point when the correlation between oblique parameters space is used to constraint parameter space of the 2HDM. To extend the first end, we define the following 2×2 matrix [75]

$$M_{ij} = \left(\tilde{\Phi}_i | \Phi_j\right) = (i\sigma_2 \Phi_i | \Phi_j) = \begin{pmatrix} \varphi_i^{0*} & \varphi_j^{+} \\ -\varphi_i^{-} & \varphi_j^{0} \end{pmatrix}. \tag{1.4.6}$$

with $i, j = 1, 2$. Under $SU(2)_L \times SU(2)_R$ group, these matrices transform as

$$M_{ij} \to U_L M_{ij} U_R^{\dagger} \tag{1.4.7}$$

with $U_L, U_R \in SU(2)$. We know that $\mathrm{tr}\left(M_{ij}^{\dagger} M_{kl}\right) = \mathrm{tr}\left(U_R M_{ij}^{\dagger} U_L^{\dagger} U_L M_{kl} U_R^{\dagger}\right) = \mathrm{tr}\left(M_{ij}^{\dagger} M_{kl}\right)$ are invariant under the full $SU(2)_L \times SU(2)_R$ group transformations which correspond to the same $SO(4)$ symmetry of the SM scalar potential. By introducing a new notation for the most general Higgs potential in Eq. (1.2.1)(with $\lambda_4 = \lambda_5$ and all parameters are real)

$$\begin{aligned} V &= \frac{1}{2} m_{11}^2 \mathrm{tr}\left(M_{11}^{\dagger} M_{11}\right) + \frac{1}{2} m_{22}^2 \mathrm{tr}\left(M_{22}^{\dagger} M_{22}\right) - m_{12}^2 \mathrm{tr}\left(M_{11}^{\dagger} M_{22}\right) + \frac{1}{8}\lambda_1 \left[\mathrm{tr}\left(M_{11}^{\dagger} M_{11}\right)\right]^2 + \frac{1}{8}\lambda_2 \left[\mathrm{tr}\left(M_{22}^{\dagger} M_{22}\right)\right]^2 \\ &+ \frac{1}{4}\lambda_3 \left[\mathrm{tr}\left(M_{11}^{\dagger} M_{11}\right) \mathrm{tr}\left(M_{22}^{\dagger} M_{22}\right)\right] + \frac{1}{2}\lambda_4 \left[\mathrm{tr}\left(M_{11}^{\dagger} M_{22}\right)\right]^2 + \frac{1}{2}\lambda_6 \left[\mathrm{tr}\left(M_{11}^{\dagger} M_{11}\right) \mathrm{tr}\left(M_{11}^{\dagger} M_{22}\right)\right] \\ &+ \frac{1}{2}\lambda_7 \left[\mathrm{tr}\left(M_{22}^{\dagger} M_{22}\right) \mathrm{tr}\left(M_{11}^{\dagger} M_{22}\right)\right]. \end{aligned} \tag{1.4.8}$$

We have used only M_{11} and M_{22} matrices. Here $\mathrm{tr}\left(M_{ii}^{\dagger} M_{jj}\right) = \Phi_i^{\dagger}\Phi_j + \Phi_j^{\dagger}\Phi_i$. This potential is also invariant under $SO(4)$. Now we consider a neutral vacuum $\langle \varphi_i^0 \rangle = v_i$,

$$\langle M_{ij} \rangle = \begin{pmatrix} v_i^* & 0 \\ 0 & v_j \end{pmatrix}. \tag{1.4.9}$$

This vacuum structure (introduced formally in the following chapter) is not invariant under the full group $SU(2)_L \times SU(2)_R$. However, if $v_i^* = v_j$, then $\langle M_{ij} \rangle$ is proportional to the 2×2 identity matrix and the vacuum preserves a group $SU(2)_V$ corresponding to identical matrices, i.e. $U_L = U_R$, in Eq. (1.4.7). This remaining group preserved by the vacuum is the custodial-symmetry group although it often is attributed to the $SU(2)_L \times SU(2)_R$ group.

On the other hand, we can build up the Higgs potential with M_{12} matrix alone. It reads

$$\begin{aligned} V &= \frac{1}{2} m_{11}^2 \mathrm{tr}\left(M_{12}^{\dagger} M_{12}\right) - \left[m_{12}^2 \det\left(M_{12}\right) + h.c.\right] + \frac{1}{2}\lambda_1 \left[\mathrm{tr}\left(M_{12}^{\dagger} M_{12}\right)\right]^2 \\ &+ \lambda_4 \det\left(M_{12}^{\dagger} M_{12}\right) + \frac{1}{2}\left[\lambda_5 \det\left(M_{12}\right)^2 + \lambda_6 \det\left(M_{12}\right) \mathrm{tr}\left(M_{12}^{\dagger} M_{12}\right) + h.c.\right] \end{aligned} \tag{1.4.10}$$

[12] $SU(2)_V$ corresponding to identical matrices (i.e $L = R$) in bi-unitary transformations for matrices

$$M_{ij} \to V_L M_{ij} V_R^{\dagger} \tag{1.4.5}$$

where $m_{11}^2 = m_{22}^2$, $\lambda_1 = \lambda_2 = \lambda_3$ and $\lambda_6 = \lambda_7$. Moreover, in this case $\lambda_5, \lambda_6, \lambda_7$ and m_{12}^2 remain complex. Again a neutral vacuum preserves $SU(2)_V$ if and only if $v_1 = v_2$. In both cases, there is a dramatic prediction for the scalar masses: the charged Higgs $H^\pm$ is degenerate with the pseudoscalar A^0. In both cases of Pomarol and Vega [75], the potential conserves CP, even with the complex couplings of the latter case. Having in mind the CP conserving frame, there is thus a well-defined pseudoscalar particle in the spectrum. In [76] have proposed a *twisted custodial symmetry* which generalizes the formalism presented above. They observed that the transformation matrix U_R need not be the same for M_{11} and M_{22} , namely

$$M_{11} \to U_L M_{11} U_R^\dagger \quad \text{and} \quad M_{22} \to U_L M_{22} U_R^{'\dagger} \tag{1.4.11}$$

This extra freedom has a limitation, though: since the hypercharge is proportional to the diagonal generator of $SU(2)_R$, the matrices U_R and U_R' must be related through $U_R^{'} = X^\dagger U_R X$, with

$$X = \begin{pmatrix} e^{i\gamma/2} & 0 \\ 0 & e^{-i\gamma/2} \end{pmatrix} \tag{1.4.12}$$

A definite choice for the phase γ yields the custodial mass relation $m_{H^\pm}^2 = m_{A^0}^2$; but a different selection imposes a degeneracy between the charged Higgs and one of the CP-even scalars, $m_{H^\pm}^2 = m_{H^0}^2$; providing the natural frame for a light A^0 within the 2HDM. Equivalently, the substitution of the CP-even H^0 for the CP-odd A^0, can be understood concerning a twisted CP symmetry acting on the Higgs field.

1.4.1. Electroweak Oblique Parameters

Having studied the implications of custodial symmetry in 2HDM, we continue analyzing possible measurable effects in precision tests since new scalar spectrum. Indeed, oblique parameters are intended to constrain models of new physics from the Electroweak precision observables. It is assumed that the effects of new physics only appear through vacuum polarization and therefore lead to modified oblique parameters. Most of the effects on electroweak precision observables can be parameterized by three gauge self-energy parameters *(S, T, U)* introduced by Peskin and Takeuchi [77][13]. Hence, the correlation among above parameters could be given regarding electroweak observables and leads to analyze different kind of precision physics, useful to constraint new phenomenology. For instance, we have broadly that

- S describes new physics contributions to neutral current processes at different energy scales.

- T measures the difference between the new physics contributions of neutral and charged current processes at low energies (i.e., sensitive to isospin violation). This parameter is related to the commonly used parameter

$$\rho_0 = \frac{\rho}{\rho_{SM}} \tag{1.4.13}$$

  through the relation

$$\rho_0 = \frac{1}{1 - \alpha T}. \tag{1.4.14}$$

  It thus encodes the departure from the SM value of $\rho_0 = 1$.

- U is only constrained by the W boson mass and its total width. Besides, U is small in new physics models[14]. Therefore, the STU parameter space can often be projected down to a two-dimensional parameter space in which the experimental constraints are easy to visualize.

- $S + U$ describes new physics contributions to charged current processes at different energy scales.

[13] Despite STU are the most useful parameters, there are other EW-quantities associated with vacuum polarization of W and Z boson [78]. It is worthwhile to point out that when new physics contributions are decoupled, these new oblique parameters vanish.
[14] In fact, U quantity is related to a dimension-eight operator, while S and T can be given regarding six dimension operators.

The 2HDM contributions are defined from relations [79]

$$S = \frac{16\pi \cos\theta_w^2}{g^2}\left\{\frac{\bar{A}_{Z^0Z^0}(m_z^2) - \bar{A}_{Z^0Z^0}(0)}{m_z^2} - \frac{\partial \bar{A}_{\gamma\gamma}(q^2)}{\partial q^2}\bigg|_{q^2=0} + \frac{\cos^2\theta_w - \sin^2\theta}{\sin\theta_w\cos\theta_w}\frac{\partial \bar{A}_{\gamma Z^0}(q^2)}{\partial q^2}\bigg|_{q^2=0}\right\} \tag{1.4.15a}$$

$$T = \frac{4\pi}{g^2\sin^2\theta_w}\left[\frac{\bar{A}_{W^+W^-}(0)}{m_w^2} - \frac{\bar{A}_{Z^0Z^0}}{m_z^2}\right] \tag{1.4.15b}$$

$$U = \frac{16\pi}{g^2}\left\{\frac{\bar{A}_{W^+W^-}(m_w^2) - \bar{A}_{W^+W^-}(0)}{m_w^2} - \cos\theta_w^2\frac{\bar{A}_{Z^0Z^0}(m_z^2) - \bar{A}_{Z^0Z^0}}{m_z^2} - \sin^2\theta_w\frac{\partial \bar{A}_{\gamma\gamma}(q^2)}{\partial q^2}\bigg|_{q^2=0}\right.$$
$$\left. + 2\cos\theta_w\sin\theta_w\frac{\partial \bar{A}_{\gamma Z^0}(q^2)}{\partial q^2}\bigg|_{q^2=0}\right\} \tag{1.4.15c}$$

Here the $A_{VV'}$ are the coefficients for $g^{\mu\nu}$ in the vacuum polarization tensors

$$\Pi^{\mu\nu}_{VV'}(q) = g^{\mu\nu}A_{VV'}(q^2) + q^\mu q^\nu B_{VV'}(q^2). \tag{1.4.16}$$

With the subtraction from SM contribution,

$$\bar{A}_{VV''}(q^2) = A_{VV'}(q^2)|_{2HDM} - A_{VV'}(q^2)|_{SM}. \tag{1.4.17}$$

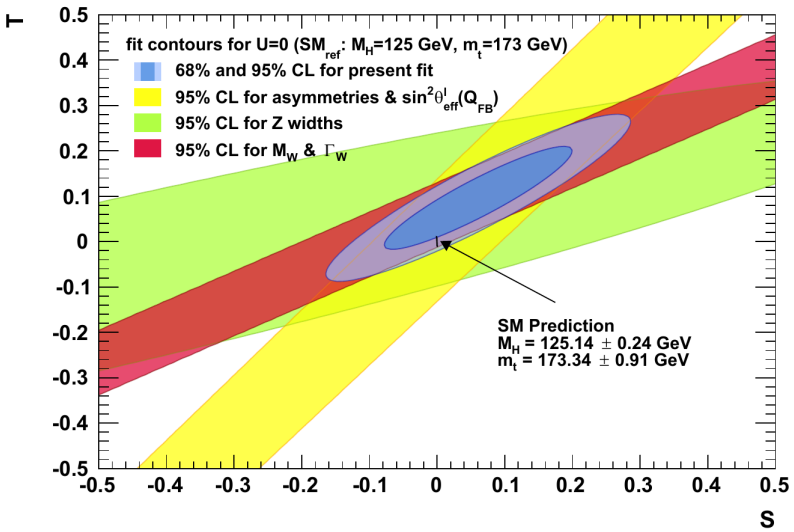

Figure 1.4.: *Constraints on the oblique parameters S and T, fixing $U = 0$ parameter fixed in function of all observables (blue). The thin black stroke indicates the prediction given by SM dynamics (within uncertainties). Single restrictions are depicted using the asymmetry measurements (yellow), the Z-boson partial and total widths (green) and W-boson mass and width (red), with confidence levels drawn for one degree of freedom. Figure is taken from [80]*

Formulas for oblique parameters are summarized in appendix B. Constraints on the STU electroweak parameters are derived from a fit to the electroweak precision data, more details can be found in the most current articles [81–85]. Besides the STU parameters the floating fit parameters are $m_z = 91.1873 \pm 0.0021$ GeV, $\Delta\alpha_{had}(m_z^2) = 0.02757 \pm 0.00010$, and $\alpha_s(m_z^2) = 0.1192 \pm 0.0033$. The following fit results are determined from a fit for a reference Standard Model with $m_{t,ref} = 173$ GeV and $m_{H,ref} = 125$ GeV:

$$S = 0.05 \pm 0.11. \tag{1.4.18}$$

$$T = 0.09 \pm 0.13. \tag{1.4.19}$$

$$U = 0.01 \pm 0.11. \tag{1.4.20}$$

The bounds on S and T for a fixed value of $U = 0$ are shown in Fig. 1.4. This ST contour will be translated into an important framework to test mass splittings in different models realization and also studied from vacuum and unitarity

Model	U_R^i	D_R^i	E_R^i
Type I	Φ_2	Φ_2	Φ_2
Type II	Φ_2	Φ_1	Φ_1
Lepton specific	Φ_2	Φ_2	Φ_1
Flipped	Φ_2	Φ_1	Φ_2

Table 1.2.: *Standard couplings structure for models without FCNC. The i index indicates generation label. By convention, U_R^i always couples to Φ_2.*

analyses. The propagation of the current experimental uncertainties in $m_h \equiv M_H$ and m_t upon the SM dynamics prediction is illustrated by the small black area at about $S = T = 0$.

As we will see in the chapter 5, every step here presented would be a valuable tool to measure the compatibility level of the vacuum behavior predictions with the EW observables and precision tests over them.

1.5. Phenomenological review of the 2HDM realizations

After of the review of some theoretical structures, we shall make an updated summary of experimental searches in the 2HDM realizations.

1.5.1. Studies approaching the Type I and Type II and other 2HDM realizations

Z_2 symmetry implementation over Yukawa sector yields Type I and Type 2HDMs, which conserve flavor symmetry when fermions and scalars couplings become diagonalized. As was discussed before, it is possible to find other two models: Lepton specific and flipped models. In the first models, leptons couple to one doublet different which quarks couple. In the flipped model, leptons are coupled to the same doublet that couples with up-type quarks. All structures are summarized in Table 1.2.

Couplings structure depends on mixing angle α between CP even-neutral eigenstates and $\tan\beta = v_2/v_1$ ratio. β is related to diagonalization angle for charged part and CP-odd-neutral part. With this in mind, doublets in Eq. (1.1.3) can be written by [15]

$$\Phi_1 = \frac{1}{\sqrt{2}} \begin{pmatrix} \sqrt{2}\left(G^+ \cos\beta - H^+ \sin\beta\right) \\ v\cos\beta - h^0 \sin\alpha + H\cos\alpha + i\left(G^0\cos\beta - A^0\sin\beta\right) \end{pmatrix} \tag{1.5.1}$$

$$\Phi_2 = \frac{1}{\sqrt{2}} \begin{pmatrix} \sqrt{2}\left(G^+ \sin\beta + H^+ \cos\beta\right) \\ v\sin\beta + h^0 \cos\alpha + H\sin\alpha + i\left(G^0\sin\beta + A^0\cos\beta\right) \end{pmatrix} \tag{1.5.2}$$

where $v^2 = v_1^2 + v_2^2$. In this general basis, fermion couplings to neutral Higgs h^0, H^0 and A^0 behave as it depicted in Table 1.3

Coupling/Model	Type I	Type II	Lepton-Specific	Flipped
ξ_h^u	$\cos\alpha/\sin\beta$	$\cos\alpha/\sin\beta$	$\cos\alpha/\sin\beta$	$\cos\alpha/\sin\beta$
ξ_h^d	$\cos\alpha/\sin\beta$	$-\sin\alpha/\cos\beta$	$\cos\alpha/\sin\beta$	$-\sin\alpha/\cos\beta$
ξ_h^l	$\cos\alpha/\sin\beta$	$-\sin\alpha/\cos\beta$	$-\sin\alpha/\cos\beta$	$\cos\alpha/\sin\beta$
ξ_H^u	$\sin\alpha/\sin\beta$	$\sin\alpha/\sin\beta$	$\sin\alpha/\sin\beta$	$\sin\alpha/\sin\beta$
ξ_H^d	$\sin\alpha/\sin\beta$	$\cos\alpha/\cos\beta$	$\sin\alpha/\sin\beta$	$\cos\alpha/\cos\beta$
ξ_H^l	$\sin\alpha/\sin\beta$	$\cos\alpha/\cos\beta$	$\cos\alpha/\cos\beta$	$\sin\alpha/\sin\beta$
ξ_A^u	$\cot\beta$	$\cot\beta$	$\cot\beta$	$\cot\beta$
ξ_A^d	$-\cot\beta$	$\tan\beta$	$-\cot\beta$	$\tan\beta$
ξ_A^l	$-\cot\beta$	$\tan\beta$	$\tan\beta$	$-\cot\beta$

Table 1.3.: *Yukawa couplings for fermions to the neutral Higgs bosons h^0, H^0 and A^0 in models without FCNC. All couplings are normalized with respect to the SM Yukawa terms.*

Normalized couplings among gauge bosons and neutral Higgs states:

[15] This parameterization assumes a neutral vacuum for spontaneous symmetry breaking; equivalent to take $\theta = 0$ in (1.1.3). In chapter 2, neutral vacuum structure and features will comprehensively be studied.

$$h^0VV \to \sin(\beta-\alpha) \text{ and } H^0VV \to \cos(\beta-\alpha) \tag{1.5.3}$$

An important feature of a CP-conserving scenario is the absence of couplings at tree level between A^0 and gauge bosons. Since the discussion presented above in Fig. (1.1), new physics scenarios with extended Higgs sectors can be highly constrained by data. All models flavor conserving can be tested to establish different compatibility levels with experimental results.

To investigate the impact of the current Higgs data on 2HDMs, we discuss modifications of the tree-level couplings due to new Higgs appearance evaluated in a scalar *alignment* framework for 2HDMs. The *alignment regime* is based on saturation of fermion and gauge boson couplings for h^0 concerning SM-Higgs ones. Hence, only exist tiny deviations from SM Higgs couplings. The regimen for the mass is interpreted through the scalar signal detected at LHC. Meanwhile, other Higgs boson could be settled in any energy scale. The difference with decoupling regimen is that other Higgs are located in mass scale greater than EW-cut. For details in parameter space choices, see appendix A.

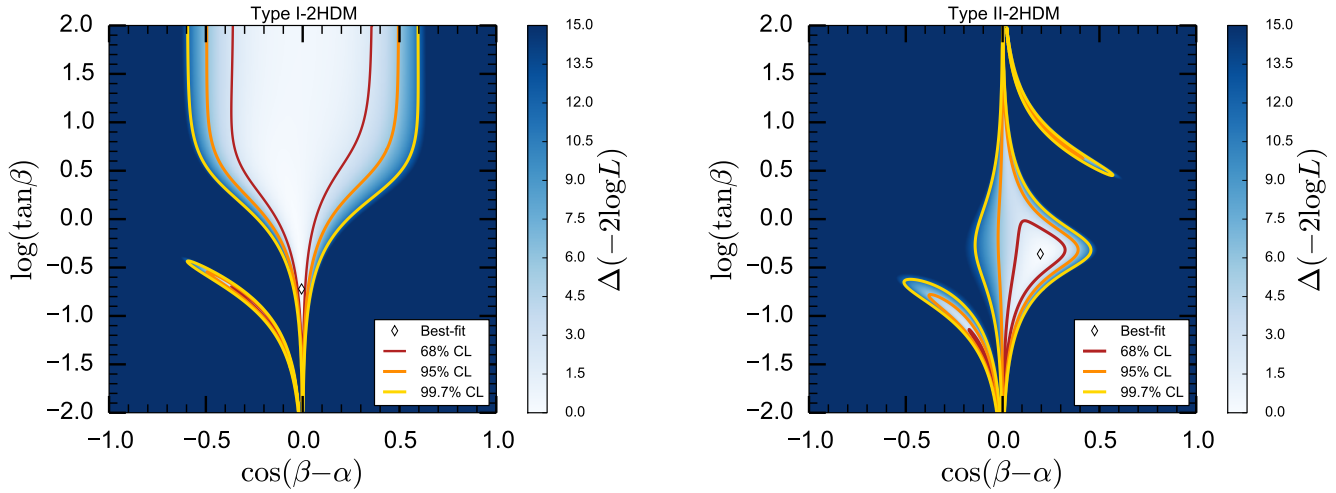

Figure 1.5.: *Fits of* $\cos(\beta-\alpha)$ *and* $\log(\tan\beta)$ *plane by Likelihood proof for type I (**Left**) and II (**Right**) 2HDMs in a Higgs mass for* h^0 *of* 125.04 *GeV. The red, orange and yellow regions are the* 68%, 95% *and* 99.7% *CL regions, respectively. Decays of* h^0 *into new physics particles are assumed to disappear. The best-fit points are marked as white diamonds (taken as a contour with* $\Delta(-2\log L < 0.2)$*). Fits use data stored by* `Lilith` *module [35].*

Varying $\alpha \in [-\pi/2, \pi/2]$ and $\beta \in [0, \pi/2]$, and assuming that there are no contributions from non-SM particles to the loop diagrams for C_γ (associated with diphoton decay of Higgs) and C_g (associated with digluon decay of Higgs) [16], we verify compatibility of these models with LHC data.

The fits results for 2HDMs without FCNCs are shown in Fig. (1.5)-(1.6) for a Higgs with a central mass of 125.04 GeV. h^0 lighter CP-even Higgs state is interpreted as the observed scalar state in LHC, and where possible decays to new physics particles are absent.

In the type I case, we see a high compatibility between data and an alignment scenario for 2HDMs, which is strongly independent of $\tan\beta$ values. Other compatible scenarios appear when $\tan\beta > 0.2$ (close to the best fit point). For $\tan\beta > 1$, at 95% CL, $|\cos(\beta-\alpha)|$ can be large as 0.5, which is slightly higher than limit reported by [86]. This discrepancy is due to the fact the new module take into account the most recent results from run 1 in LHC. Additionally, our results show a second narrow allowed (non-symmetric) contour for $0.3 > \tan\beta > 0.001$, which is compatible with $-0.5 \leq \cos(\beta-\alpha) \leq 0$ at 95% CL. Nevertheless, best-fit computations with both data sets are just different in the chosen interval for $\Delta(-2\log L) < 0.1$.

In the type II 2HDM, all situations differ substantially from the former case. Now, alignment regime is compatible only at 95% C.L. for $\tan\beta > 0.1$. In addition exist three compatible valleys in $\tan\beta - \cos(\beta-\alpha)$ plane. The first region belongs around of $\cos(\beta-\alpha) = 0$ (exact alignment regimen) and with a large deviation in $\tan\beta \geq 0.5(5)$ where $\cos(\beta-\alpha) = 0.4$ at 95% C.L. Other minimum in the likelihood appears with $\tan\beta = 0.3$ where $\cos(\beta-\alpha) = 0.5(0.4)$ at 99% C.L. (95% C.L.). The last minimum belongs in $\tan\beta \leq 0.2(0.06)$ where $\cos(\beta-\alpha) = -0.4$ at 95% C.L. (68% C.L.).

[16] This implicitly implies that charged Higgs bosons in 2HDMs are heavy and decoupled from SM spectrum

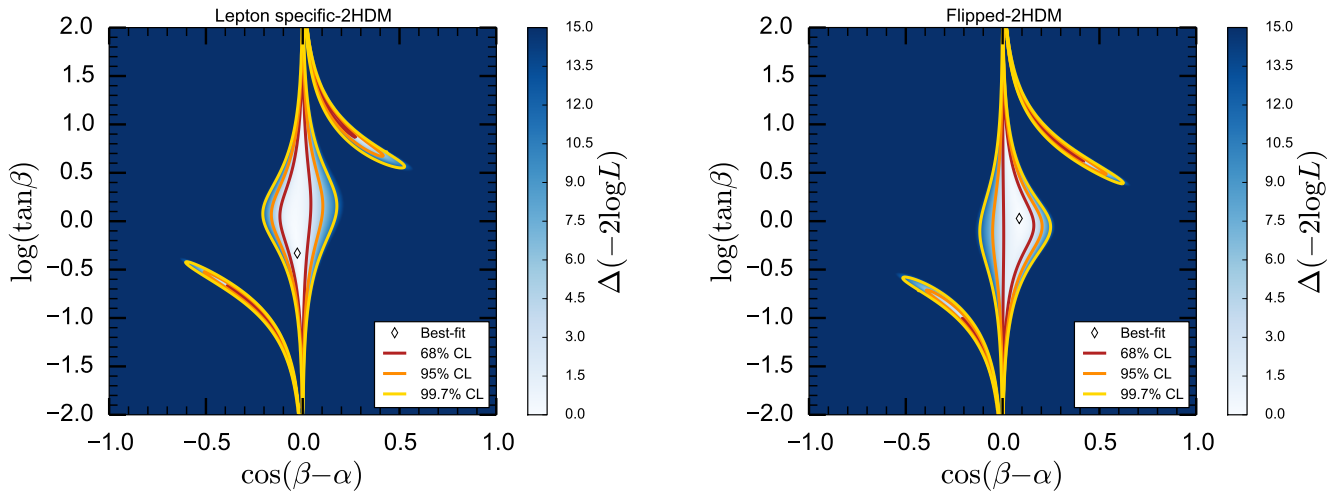

Figure 1.6.: *Fits of* $\cos(\beta-\alpha)$ *and* $\log(\tan\beta)$ *plane by Likelihood proof for Lepton specific (**Left**) and Flipped (**Right**) 2HDMs in a Higgs mass for* h^0 *of* 125.04 *GeV. The red, orange and yellow regions are the* 68%, 95 *and* 99.7 *CL regions, respectively. Decays of* h^0 *into new physics particles are assumed to disappear. The best-fit points are marked as white diamonds* ($\Delta(-2\log L)<0.1$)*. Fits use data stored by* `Lilith` *module [35]*

For Lepton-specific and Flipped models, the shapes of $\cos(\beta-\alpha)$ and $\log(\tan\beta)$ compatible valleys are slightly different to the from gotten by type II-2HDM (see Fig. 1.6). Relevant changes are best fit points and the maximum deviation from alignment regime $\cos(\beta-\alpha)\to 0$; being these models more constrained compared with the type II-2HDM. For instance, in Lepton specific model, the maximum deviation occurs in $\tan\beta$ close to 1 where $-0.15\leq\cos(\beta-\alpha)\leq 0.1$ at 95% CL. Meanwhile for Flipped model, in $\tan\beta=1$, the maximum deviation is in $-0.05\leq\cos(\beta-\alpha)\leq 0.2$ at 95% C.L. Nevertheless, the two additional valleys still appearing for $\tan\beta<0.1$ and for $\tan\beta>1$ for intermediate values of $-0.4<\cos(\beta-\alpha)<0$ and $0<\cos(\beta-\alpha)<0.5$ at 95% CL. respectively[17].

Valleys for $\cos(\beta-\alpha)>0$ and $\tan\beta>0.3$ are related to the phenomenology of a "wrong" Yukawa sign in fermion-scalar couplings for down type quarks indeed. Whereas such a scenario is consistent with current LHC observations, both future running at the LHC and or future experiments might give new information about phenomenological discrepancies originated by this sign. Discrimination and differentiation are possible for two reasons. Firstly, the interference labeling between the b-quark and the t-quark loop contributions to the ggh^0 coupling changes sign. Secondly, and relating to new physics influence, the charged-Higgs loop contribution to the h^0 coupling can be significant and relatively constant up to the largest charged-Higgs mass allowed by tree-level unitarity bounds when the b-quark Yukawa coupling has the opposite sign concerning the SM one. In the latter, we can assume that the change in sign of the interference terms between the b-quark loop and the Ws and t-loops having negligible impact [88]

1.5.2. FCNCs: Phenomenological Constraints

Perhaps, the most important consequence inside Yukawa Lagrangian is the presence of new vertices associated with neutral currents, whose role is yield an admixture between different flavors for quarks and leptons. From observations in distinct processes, these possible predictions are highly constrained. Moreover and as we have broadly discussed, the general Yukawa Lagrangian in (1.3.1) leads to processes with Flavor Changing Neutral Currents (FCNC) even at tree level. Indeed, FCNCs arise because by rotating the down sector of quarks (or up and lepton sectors) to get the mass eigenstates it is not possible to diagonalize both coupling matrices η^0_{ij},ξ^0_{ij} simultaneously. Before to see implications in higher perturbative corrections, vacuum studies or unitarity behavior, correspond to make a phenomenological overview of the several restrictions over possible FCNC reactions. Processes containing FCNCs are strongly limited experimentally, in particular, due to the small K_L-K_S mass difference. In SM, the FCNC are strongly suppressed by virtue of the GIM mechanism [89]. In the 2HDM, several mechanisms to suppress FCNC at tree level were proposed. One of them is to consider the exchange of heavy scalar or pseudoscalar Higgs Fields or by the cancellation of large values with opposite sign. In 2HDM, one mechanism is provided by Glashow and Weinberg, who implemented in the Yukawa Lagrangian a discrete symmetry that automatically forbids the couplings among fermions and scalars that generate such rare decays.

[17]These results are compatible at 95 % CL with experimental fits presented by the CMS collaboration in [87]

λ_{ij}	Process	Assumptions or Origin	Bound	Reference
$\sqrt{\lambda_{bs}\lambda_{\mu\tau}}$	$B \to K\mu\tau$	Precision Tests Validity	$\lesssim \mathcal{O}(10)$	[95]
$\sqrt{\lambda_{ut}\lambda_{ct}}$	$D-\bar{D}$	100 $\leq$scalar masses (GeV)$\leq$ 400	≤ 0.6	[96]
λ_{tt}	$b \to s\gamma$	$\lambda_{ii} = 0$ $i \neq t, b$ and $m_{H^\pm} \leq 300$ GeV	$\lesssim 1.7$	[97, 98]
$\lambda_{\mu\tau}$	$(g-2)_\mu$	$m_{A^0} >> m_{H^0}, m_{h^0}$	$(10, 80)$	[99, 100]
$\lambda_{e\tau}\lambda_{\mu\tau}$	$(g-2)_\mu$	$m_{A^0} >> m_{H^0}, m_{h^0}$	< 0.004	[99, 100]
$\lambda_{e\tau}$	$(g-2)_\mu$	$m_{A^0} >> m_{H^0}, m_{h^0}$	$< 10^{-3}$	[99, 100]

Table 1.4.: *Phenomenological Bounds on Yukawa couplings in the 2HDM type III under Cheng and Sher anzats.*

From $K-\bar{K}$ mixing, as well as many processes involving kaon and muon decays [90], it has been considered that the heaviest fermion set the scale for the entire matrix of Yukawa couplings. This assumption yields many stringent bounds for the heavy scalars, for instance, 150 TeV (lower bound) from $K-\bar{K}$ mixing. However, the most outstanding feature of the fermion masses is their hierarchical structure. If we expect roughly the same hierarchy in the Yukawa couplings, setting all the Flavor Changing (FC) couplings to be of the order of the heaviest-fermion Yukawa couplings is not reliable [19]. From these considerations[18], Cheng, and Sher proposed that FC couplings should be of the order of the geometric mean of the Yukawa couplings of the two fermions. Such anzats leading to a parametrization for the Yukawa couplings of the form

$$\xi_{ij} = \frac{\lambda_{ij}\sqrt{2m_i m_j}}{v}, \tag{1.5.4}$$

because with the Cheng and Sher anzats we expect that $\lambda_{ij} \sim \mathcal{O}(1)$. If the Cheng and Sher anzats is correct, the FCNC coming from the first two generations are strongly constrained since the associated Yukawa couplings are suppressed by the EW-scale. As a consequence, the lower bound on Higgs boson masses is reduced [19, 91]. It is usual to assume the validity of the Cheng and Sher anzats in the 2HDM type III, and to explore its phenomenological implications [61]. Several searches focus on some few specific processes, including Δm_B, $t \to ch$ and $h \to \bar{t}c + \bar{c}t$, rare μ, τ, and B decays ($B \to K\mu\tau$), $\mu \to e\gamma$ at the two loop level, $t \to c\gamma$ and $t \to cZ^0$, muon-electron conversion, and $b \to s\gamma$. If the Cheng and Sher anzats is correct, then one would expect from λ_{ij} to be all of order unity (emulating to SM). This request is very weak since there are unknown mixing angles. In addition, for many phenomenological limits, several scalar masses enter in all specific processes. One of the most stringent experimental constraints on the 2HDM comes from flavor physics. Currently flavor processes have been studied in the LHC from atlas collaboration, where $tc\gamma$ couplings are limited by means of diphotonic-Higgs $H \to \gamma\gamma$ channel [2]. For the 2HDM with general (flavor diagonal) Yukawa couplings, and from the charged Higgs contribution to different transitions such as $b \to s\gamma$ in [92], bounds on $|\lambda_{tt}|$ were found; which must be less or equal to unity when $m_{H^\pm} \lesssim 500$ GeV. With theoretical and experimental assumptions over SM predictions (from QCD lattice) of observables involving $F-\bar{F}$ mixing (with $F \equiv K, D, B_d$ or B_s) and with the measured meson mass differences ΔM_F [93], constraints over flavor space have been computed. Reference [94] considers that the addition between SM and the new contribution does not exceed the experimental values, $\Delta M_{B_d}^{expt} = (3.337 \pm 0.033) \times 10^{-13}$ GeV and $\Delta M_{B_s}^{expt} = (117.0 \pm 0.8) \times 10^{-13}$ GeV, by more than two standard deviations for B_d and B_s systems. This procedure impose upper bounds on ξ_{db} and ξ_{sb} Yukawa couplings. Moreover for K and D systems, in order to obtain the upper bounds on ξ_{ds} and ξ_{uc} it is required that only the 2HDM contribution does not exceed the experimental values, $\Delta M_K^{expt} = (3.476 \pm 0.006) \times 10^{-15}$ GeV and $\Delta M_D^{expt} = (0.95 \pm 0.37) \times 10^{-14}$ GeV, by more than two standard deviations. For a mass degenerate spectrum in neutral scalar and pseudoscalar sector $m_{h^0} = m_{H^0} = m_{A^0} = 120$ GeV those bounds are transformed in limits on Cheng-Sher couplings: $(\lambda_{ds}, \lambda_{uc}, \lambda_{bd}, \lambda_{bs}) \leq (0.1, 0.2, 0.06, 0.06)$. Another phenomenological bounds on Cheng-Sher couplings for quark and leptonic sectors are revised in table 1.4.

New studies on phenomenological constraints of FCNC's have been done in [101], wherein a comprehensive analysis of flavor observables in a 2HDM with generic Yukawa structure (in the decoupling limit of the MSSM) is realized. Here strong bounds over fermionic vertices are obtained for particular values of $\tan\beta$ and charged Higgs mass $m_{H^\pm}$. This review shall be relevant for our studies coming from perturbative unitarity, which will be presented in chapter 4

Besides to these indirect analyses over FCNC couplings, we can make different studies over the possible realization of diagonal FCNC couplings with the aid of compatibility with LHC data. Using Eq. (1.5.4) and Sher-Cheng anzats, we express couplings among up (λ_U) and down (λ_D) type fermions and scalars with additional deviation from FCNC's presence. For simplicity and without loss of generality, we take the fundamental parametrization, i.e., $\beta = 0$[19]. These compatible valleys are depicted in Fig. (1.7). For $\lambda_{U,D}$-$\cos(\bar{\alpha})$ plane, $\alpha = 0$ shows a broad valley, which is independent

[18] All these developments can be settled in the type III-2HDM, which has been considered in appendix C

[19] This choice is the typical Higgs basis, where one doublet generates mass terms, meanwhile the another doublet yields FCNC couplings (see appendix C).

of $\lambda_{U,D}$. Large deviation belong in zones near to $\lambda_{U,D} = 0$ with $|\cos(\bar{\alpha})| < 0.3$ at 68% C.L. Using one of the best fits in $\cos(\bar{\alpha}) = 0.012$, contours for $\lambda_U - \lambda_D$ plane. Here $0 < \lambda_D < 25$ and $-80 < \lambda_U < 10$ are the intervals at 95% C.L. Therefore, compatibility with constrained FCNCs ($\lambda_s = 0$) in one best fit is only valid at 95% C.L. To make a detailed study, we need measurements over flavor violation couplings (e.g., whose involving $h^0 \to \bar{t}c$ decays) in order to construct a complete FCNC matrix. This extrapolation can be done with the data of run 2 in LHC employing top quark decays and with leptonic channels [102].

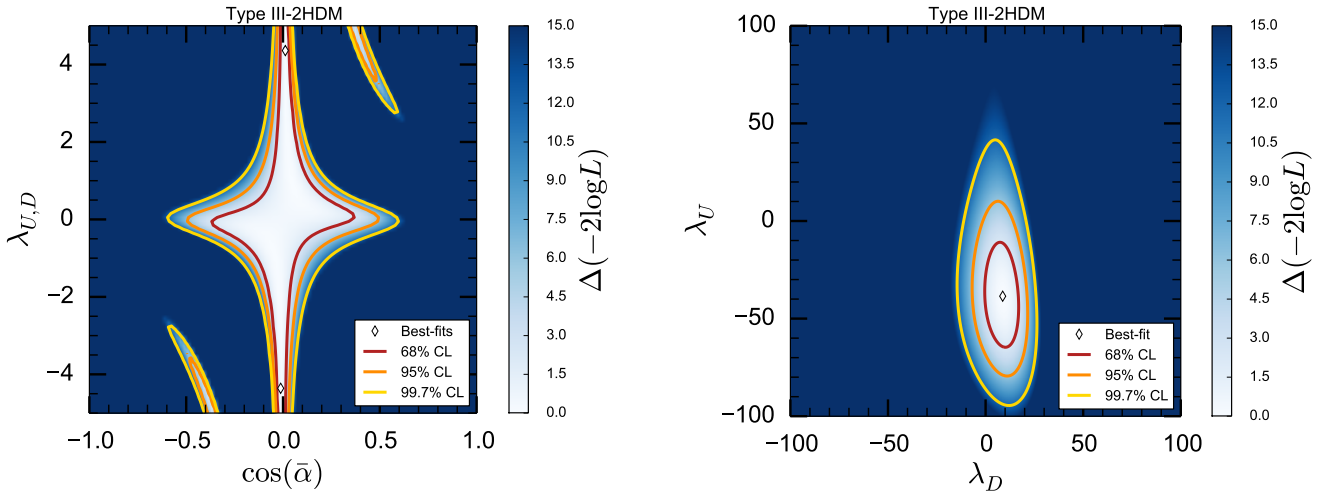

Figure 1.7.: ***(Left)*** *Fit of* $\cos(\bar{\alpha})$ *and* $\lambda_U (= \lambda_D)$ *plane by Likelihood proof for Type III 2HDMs using Cheng and Sher anzats in a Higgs mass for* h^0 *of* 125.04 *GeV.* $\bar{\alpha}$ *is defined as the mixing angle in the fundamental parametrization.* ***(Right)*** *Fit of* λ_U *and* λ_D *couplings for* $\cos(\bar{\alpha}) = 0.012$ *(one best fit). The red, orange and yellow regions are the* 68%, 95 *and* 99.7 *CL regions, respectively. Decays of* h^0 *into new physics particles are assumed to disappear. The best-fit points are marked as white diamonds* ($\Delta(-2\log L) < 0.1$)*. Fits use data stored by* `Lilith` *module [35]*

From this phenomenological review, it is clear that bounds on Yukawa couplings depend strongly on the Higgs mass pattern (and also from other free parameters such as the mixing angles). In chapter 4, we consider a theoretical limit for the fermionic sector through generalized unitarity constraints. There using a helicity formalism, it is possible to find bounds on the general structure of Yukawa couplings. We shall see that, despite those limits are weaker than the phenomenological ones, such limits are independent of the Higgs masses and mixing angles, making them more model independent.

1.5.3. Charged Higgs boson $H^{\pm}$ searches

For charged Higgs bosons studies, the latest and most complete results come from CMS and ATLAS collaborations [103,104] and they are based on the run 1 data[20]. First analyses are based on charged Higgs production in pp collisions of up to ~ 20 fb^{-1} (at $\sqrt{s} = 8$ TeV) using several final states (leptonic and quarks tagged jets). In the absence of evidence of some signal, limits could be settled on cross sections and/or branching ratios, some of which have been interpreted as exclusion of regions in the broad 2HDM parameter space of m_{H^+}, $\tan\beta$ and $m_{H^0} - m_{H^\pm}$.

In the former case, most of the searches for H^+ production at the LHC are so far based on tH^+X channels, focusing mainly in $H^+ \to \tau\nu_\tau$ decays. Since $H^+ \to c\bar{s}$ decay dominates at $\tan\beta < 1$ for m_{H^+}, this channel has also been considered. When a H^+ is produced either in the decay of a pair-produced top quark (if $m_{H^+} < m_t$), or in association with a individually produced top quark (if $m_{H^+} > m_t$), the event features a t that will decay predominantly according to the SM: $t \to W^+b$. In searching for $H^+ \to \tau\nu$, one can exploit hadronic decays of the W as well as leptonic, provided hadronic decays of the τ can be effectively triggered on. All other searches require a prompt lepton (e or μ) from a W decay for triggering as well as off-line suppression of large QCD background. Most searches do not cover $160 < m_H^+(\text{GeV}) < 180$, due to the unavailability of reliable theoretical treatment of H^+ production in that region.

[20] Before LHC, direct searches at LEP described a lower limit on $m_{H^\pm}$ of about 90 GeV [105], meanwhile Tevatron experiments put upper limits over $B(t \to H^+b)$ in the interval of 0.15 to 0.20 for $m_{H^\pm} < m_t$ [106, 107].

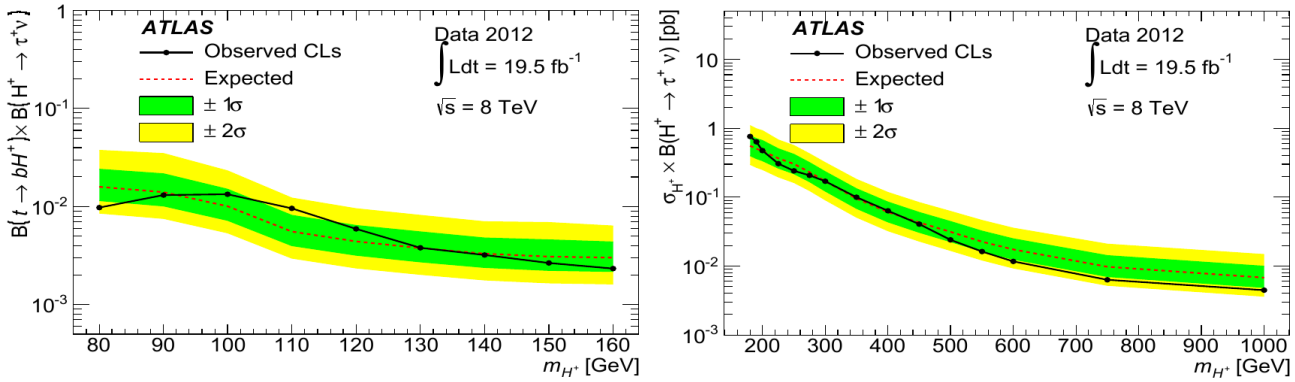

Figure 1.8.: *Observed and expected* 95% *CL upper limits on the production and decay of* H^+ *bosons in the* $\tau\nu$ *final state, as functions of* m_{H^+}*, for low-mass region (**Left**) and high-mass region (**Right**), from the ATLAS experiment. The latter take into account both* H^+ *and* H^- *decays [108].*

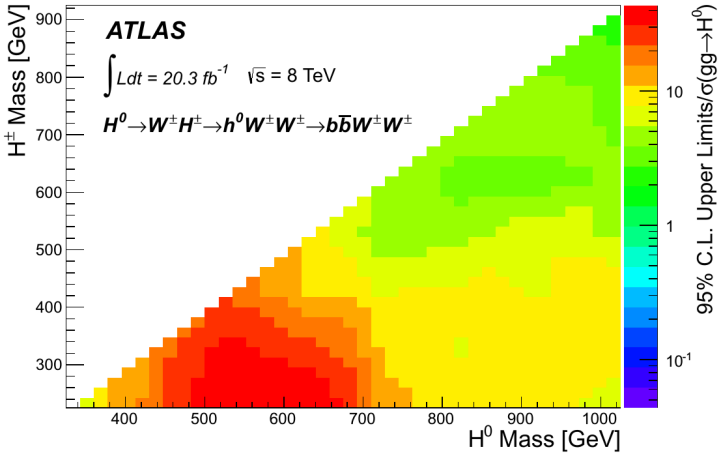

Figure 1.9.: *The ratio of the observed* 95% *CL upper limits imposed on the cross section to the theoretical cross section for a relatively heavy Higgs boson yielded via gluon-gluon fusion at the SM rate, derived by ATLAS analyses from its search for* $pp \to H^0 \to H^{\pm}W^{\mp} \to h^0W^+W^- \to b\bar{b}l\nu jj$ *[109].*

As is shown in Fig. 1.8, comparisons between kinematic distributions of events in data and those expected from signal+background and background-only hypotheses at different points on the m_{H^+} , $\tan\beta$ parameter space using a binned likelihood function and CLs procedure [108] leads to 95% CL upper limits on $B(t \to H^+b) \times B(H^+ \to \tau^+\nu_\tau)$ for $m_{H^+} < m_t$ and $\sigma_{H^+} \times \mathrm{Br}\,(H^+ \to \tau^+\nu_\tau)$ for $m_{H^+} > m_t$. The expected limits correspond to a hypothetical data set that contains no signal.

A fairly model-independent search for charged Higgs bosons in the process $pp \to H^0 \to H^{\pm}W^{\mp} \to h^0W^+W^- \to b\bar{b}l\nu jj$ has been performed by ATLAS using 20.3 fb^{-1} of data at $\sqrt{s} = 8$ TeV [109]. The analysis exploits the di-jet mass constraint $m_{bb} = m_{h^0} = 125$ GeV. Once again, the final state is the same as that of semi-leptonic decays of $t\bar{t}$. The analysis uses a Boosted Decision Tree trained at 36 different values of m_{H^0} to discriminate signal against SM $t\bar{t}$ events. As seen in Fig. 1.9, presently the observed 95% upper limit on the cross section is higher than the theory-predicted cross section everywhere in the m_{H^0}, m_H^+ parameter space, but approaching it for larger values of m_{H^0} and m_H^+.

1.5.4. Pseudoscalar Higgs boson A^0 searches

We make a survey for pseudoscalar Higgs boson searches with the most updated analyses from data of Run I in LHC. An important channel is associated with $A^0 \to Z^{*0}h^{*0} \to l^+l^-b\bar{b}$. The charged leptons (being either e^- or μ^-) coming from Z^{*0} decays, meanwhile the SM-like Higgs boson h^0 decays into the pair $b\bar{b}$. From Fig. 1.10 upper limits at a 95% CL can be derived on the product of a narrow pseudoscalar boson cross section and branching fraction $\sigma_A\mathcal{B}\left(A^0 \to Z^{*0}h^{*0} \to l^+l^-b\bar{b}\right)$, which exclude 30 to 3 fb at the low and high ends of the 250−600 GeV mass range.

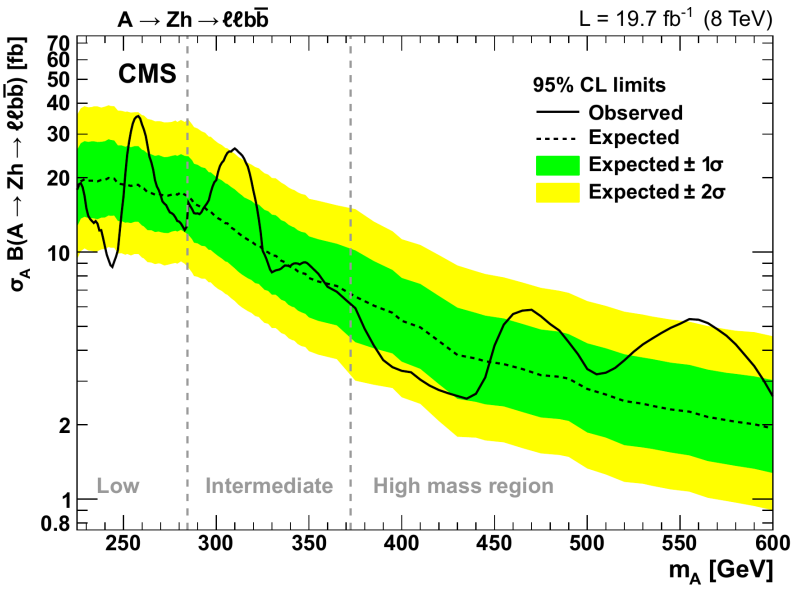

Figure 1.10.: *Measured and expected 95% CL upper limit on* $\sigma_A \mathcal{B}\left(A^0 \to Z^{*0}h^{*0} \to l^+l^-b\bar{b}\right)$ *as a function of pseudoscalar mass in the narrow-width approximation, including all statistical and systematic uncertainties. The green and yellow bands are the* $\pm 1\sigma$ *and* $\pm 2\sigma$ *uncertainty bands on the expected limit [110]..*

1.6. Overview of 2HDM fundamentals

2HDMs are invoked to solve open issues of SM, as hierarchy problem of fermions, as well as to propose dark matter and baryogenesis mechanisms. Furthermore, some models for physics beyond have a low energy limit with a non-minimal Higgs sector similar to those yields by a 2HDM. For instance, at least two Higgs doublets are necessary for supersymmetric and left-right models and besides the so-called 2HDM type II has the same Yukawa couplings as the Minimal Supersymmetric Standard Model (MSSM). In particular, if the supersymmetric particles are heavy enough, the Higgs sector of the MSSM becomes a constrained 2HDM type II at low energies. SUSY models with two Higgs doublets could provide solutions to some problems of the SM such as the Higgs mass behavior at very high scales (*naturalness problem*), the Planck and Electroweak scale hierarchy, the mass hierarchy among fermion families and the existence of masses of neutrinos and neutrino oscillations.

On the other hand, the 2HDM could induce CP violation either explicitly or spontaneously in the Higgs potential. However, restricting the discussion on a CP-conserving framework, which is achieved by a limited number of symmetries over the Higgs potential. These symmetries relate doublets to their complex behavior using particular transformations associated with singular values of $SO(2)$ symmetries group.

An additional mechanism lying in the general 2HDM is based on the study of some processes called Flavor Changing Neutral Currents (FCNC). It is well known that such processes are strongly constrained by experimental data, despite the fact that they seem not to violate any fundamental law of nature. Indeed the processes with FCNC are actively suppressed by some underlying principle still unknown, being it an open question in particle physics. Correspond to give alternative scenarios where suppression is natural or compatible with precision tests. Mechanisms to suppress these FCNCs reactions belonging in the general 2HDM can be proposed based on symmetries, imposed firstly in the Higgs potential and correspondingly extended to Yukawa sector. However, generation of FCNC processes is still compatible with the strong enough experimental limits on them and in the light of new LHC there slight deviations from SM couplings between scalar particle and fermions. Having said that, the presence of FCNC could be an indirect signature of the existence of an extended Higgs sector like 2HDM.

The most general form of the Higgs sector has a broad parameter space. Symmetries implemented CP and for Higgs families leading to simpler models for 2HDM, converting into valuable tools to make predictions from fundamentals. We shall build up systematically these theories analyzing different theoretical and phenomenological implications from them. Those studies could be extended not only to 2HDM behavior but other models with extended Higgs sectors.

Furthermore of symmetries in the Higgs potential coming from Higgs family and CP transformations, we review the effect of extending of custodial symmetry of the Higgs potential SM and the corresponding scalar sector in the 2HDMs. In general, the contribution of the oblique parameters from the extra $SU(2)$ doublet in the 2HDM is tiny since scalar doublets (or singlets) do not break the custodial symmetry. Since the custodial symmetry is broken by Yukawa and

kinetic terms, we consider how splitting in mass eigenstates could induce sizable effects in precision EW parameters even at one loop level. This analysis is implemented defining STU parameters, which constitute a sensitive probe of new physics coupling to the EW gauge bosons.

Because the description of 2HDM fundamentals, it is possible to face other features of extended Higgs sector as vacuum structures and their behavior at high energy scales. This fact will be the *leitmotiv* of the following chapters, where we consider tree level behavior of minima and stationary points in the Higgs potential as well as its possible radiative corrections. Both studies leading to analyze all effects in vacuum stability or instability at NLO for Higgs potential in the field space for different models with different symmetries implementations.

2. Vacuum structure and stability at tree level for extended Higgs sectors

2.1. Vacuum stability behavior in Extended Higgs sectors

The vacuum stability condition is one of the most important features for Spontaneous Symmetry Breaking (SSB) sector since it determines the natural solutions for stationary and minimization equations. For instance in the Standard Model, this condition is such that the Higgs potential in its dimension fourth part is always positive in the field space. This is translated into the quartic coupling would be $\lambda > 0$, for asymptotical values of $|\Phi|$. This condition at tree level can be extrapolated to the effective Higgs potential at, e.g., one loop level or at Next to Next Leading Order (NNLO). Under the use of Renormalization Group Equations for quartic constant, gauge and Yukawa couplings and their simultaneous solution, it is possible to find out the stability regime for effective Higgs potential on the scale of energy μ. In those regimes, the Higgs potential shape may change, and it might drive out to the instabilities in fact. The instability scale can be seen as cut scale where the theory (as a bottom-up approach) is only effective until those energy values, where new degrees of freedom become relevant to the description of physical properties.

For others models, the general procedure to find positivity structure could be more intricate. For example, in two Higgs doublet models, the vacuum stability conditions depend on the asymptotical behavior of the extended field space and also of its possible combinations. Hence, and as will see soon, the consequences over parameter space are more elaborated. Furthermore, the RG equations at one loop level for scalar and Yukawa couplings are too many, complicated and hard to control; and they need additional assumptions as initial conditions over the respective space of free parameter. The last fact is a motivation to introduce other theoretical and phenomenological constraints in the general study of vacuum stability regions for extended models.

In addition to the standard issues in the stability conditions, the 2HDM has a richer vacuum structure wherein metastability states at tree level could be present. This effect is a consequence of relating the number of critical points in the Higgs potential, which particularly in its minimum depends on the composition of two vacuum expectation values and stationary points nature (being minima, or maximums or saddle points). Even at the moment of building a model with a Higgs potential with several distinct minima, the possibility of taking a metastable minimum as a physically acceptable vacuum state is also allowed if this effect is suppressed by the fact of having a long lived enough minimum state, there possible consequences for the phenomenology of the model. This scenario would describe the mass particles in a realistic approach without fear of the tunneling effects changing this phenomenological framework. From a cosmological point of view, the critical temperature of EW-phase transition is defined as the value where Higgs potential minima become degenerate. Therefore, a metastable regime of 2HDM could bring many consequences in baryogenesis mechanisms, since, this critical temperature definition might be ambiguous if EW-minimum is not correctly defined.

The six classes of symmetries considered in the last chapter will be a major framework to analyze the stability. These properties will be further used here in a general way to write a more compact form which is invariant under a parameterization given by the restricted Lorentz group in the future light cone. By the way and under impositions extrapolated to Minkowskian space is possible to find out vacuum stability constraints associated with the requirement at tree level for a bounded from below Higgs potential. Moreover, that covariant form of the Higgs potential yields a suitable frame to analyze the possibility to reach metastability vacua for two normal minima (with real VEVs).

2.2. Vacuum structure of 2HDM

Before to start the study of vacuum stability behavior, it is convenient to analyze multiple forms in which the vacua in 2HDM theories behave. In SM, theory is invariant under $SU(2)_L \otimes U(1)_Y$ group and its spontaneous symmetry breaking can be achieved with a doublet where the VEV is settled in the neutral component (real part), i.e., $\langle \Phi \rangle_0 = v/\sqrt{2}$. The consequence of this choice is that $Q\langle \Phi \rangle = 0$ since the vacuum configuration has not electric charge. If all components of the doublet, charged and neutral, as well as real and imaginary ones, acquire a VEV the consequence would still

be a massless photon, because of remainder symmetry in the vacuum. Hence the electromagnetic $U(1)_{em}$ vacuum configuration can not be broken by just one doublet; where the redefinition of the VEVs in all components would have the effect of a redefinition of the charge operator. The scheme for vacuum invariant structure $SU(2)_L \otimes U(1)_Y \to U(1)_{em}$ also ensures the non-presence of possible phases that lead spontaneous CP violation [27].

When we add a second doublet, scenarios for vacuum configuration are converted into richer ones. Every parametrization for two doublets introduces eight fields, which in a general way all can have VEVs. By using gauge structure $SU(2)_L \otimes U(1)_Y$, it is possible to build the following parametrization for the doublets in the vacuum configuration

$$\langle \Phi_1 \rangle = \begin{pmatrix} 0 \\ v_1 e^{i\theta} \end{pmatrix} \text{ and } \langle \Phi_2 \rangle = \begin{pmatrix} \bar{v} \\ v_2 \end{pmatrix}. \tag{2.2.1}$$

The mass eigenstates for gauge boson matrix now can get all non-zero entries. The mass eigenvalue for photon reads

$$m_\gamma^2 = \frac{1}{8}\left[v^2\left(g^2 + g'^2\right) - \sqrt{v^4\left(g^2+g'^2\right) - 16 g^2 g'^2 v_1^2 \bar{v}^2}\right], \tag{2.2.2}$$

where $v^2 = v_1^2 + v_2^2 + \bar{v}^2$. By taking $v_1 = 0$ (SM case) or $\bar{v} = 0$ (aligned VEVs), otherwise the photon acquires mass and vacuum violates charge conservation.

To analyze CP symmetry behavior, we start by defining a transformation in the sense previously introduced in the last chapter $\Phi_i \to \Phi_i^*$. Therefore, the possible configurations for vacuum can be classified in the following structures: Neutral vacua

$$\langle \Phi_1 \rangle_N = \begin{pmatrix} 0 \\ v_1 \end{pmatrix}; \langle \Phi_2 \rangle_N = \begin{pmatrix} 0 \\ v_2 \end{pmatrix}. \tag{2.2.3}$$

The spontaneous CP breaking configuration has the following structure ,

$$\langle \Phi_2 \rangle_{CP} = \begin{pmatrix} 0 \\ v_1 + i\delta \end{pmatrix}; \langle \Phi_2 \rangle_{CP} = \begin{pmatrix} 0 \\ v_2 \end{pmatrix}. \tag{2.2.4}$$

Finally, the charge breaking configuration

$$\langle \Phi_2 \rangle_{CB} = \begin{pmatrix} 0 \\ v_1 \end{pmatrix}; \langle \Phi_2 \rangle_{CB} = \begin{pmatrix} \alpha \\ v_2 \end{pmatrix}. \tag{2.2.5}$$

Vacua with α and δ simultaneously non-zero are not considered because the minimization conditions of the CP-conserving Higgs potential forbid them. Henceforth we will only be concentrated in normal and CP breaking vacuum-configurations.

2.2.1. Vacuum properties from Higgs potential structure

Because of gauge invariance, it is possible to write the Higgs potential in 2HDM regarding four bilinear: $x_1 = \Phi_1^\dagger \Phi_1$, $x_2 = \Phi_2^\dagger \Phi_2$, $x_3 = \text{Re}\left(\Phi_1^\dagger \Phi_2\right)$ and $x_4 = \text{Im}\left(\Phi_1^\dagger \Phi_2\right)$. Hence the most general Higgs potential

$$\begin{aligned} V = {} & a_1 x_1 + a_2 x_2 + a_3 x_3 + a_4 x_4 + b_{11} x_1^2 + b_{22} x_2^2 + b_{33} x_3^2 + b_{44} x_4^2 \\ & + b_{12} x_1 x_2 + b_{13} x_1 x_3 + b_{23} x_2 x_3 + b_{14} x_1 x_4 + b_{24} x_2 x_4 + b_{34} x_3 x_4. \end{aligned} \tag{2.2.6}$$

More developments in this form of the Higgs potential are presented in Appendix D. Here is also exposed the relations among a_i and b_{ij} parameters with quartic a bilinear couplings of traditional notation for Higgs otential[1]. By seeing this Higgs potential, terms linear in x_4 break CP explicitly. Taking these terms equal to zero, we get a CP-conserving Higgs potential with ten parameters:

$$V = a_1 x_1 + a_2 x_2 + a_3 x_3 + b_{11} x_1^2 + b_{22} x_2^2 + b_{33} x_3^2 + b_{44} x_4^2 + b_{12} x_1 x_2 + b_{13} x_1 x_3 + b_{23} x_2 x_3. \tag{2.2.7}$$

The stationary condition with a CP breaking vacuum structure is given by

$$b_{13}\left(v_1^2 + \delta^2\right) + b_{23} v_2^2 + \left(b_{33} - b_{44}\right) v_1 v_2 = a_3. \tag{2.2.8}$$

[1] By means of Morse' inequalities, notation in bilinears is also a useful tool to determine how many critical points can exist in the Higgs potential as well as the origin of these stationary points. This formalism is presented in Appendix H.

Renormalizability in the Higgs potential forces b_{13} and b_{23} are simultaneously either zero or nonzero. Here, we ask what models without explicit CP violation protect vacuum against spontaneous CP violation. We first note that there are regions in the space parameters where solutions for this equation are absent at all,

$$b_{13} = b_{23} = a_3 = 0 \text{ and } b_{33} \neq b_{44}, \tag{2.2.9a}$$
$$b_{13} = b_{23} = b_{33} - b_{44} = 0 \text{ and } a_3 \neq 0. \tag{2.2.9b}$$

Respectively, each parameter space is induced by the symmetries:

$$\Phi_1 \rightarrow -\Phi_1 \text{ and } \Phi_2 \rightarrow \Phi_2. \tag{2.2.10a}$$
$$\Phi_1 \rightarrow \mathrm{e}^{i\theta}\Phi_1 \text{ and } \Phi_2 \rightarrow \Phi_2. \tag{2.2.10b}$$

Hence, CP-breaking minimum is avoided with two phenomenologically different seven-parameter potentials, with $U(1)$ (softly broken) and Z_2 global symmetries. Besides, when this symmetry is extended to Yukawa Lagrangian sector the FCNC processes at tree level can be suppressed through Weinberg-Glashow mechanism. There other two Higgs potentials: $U(1)$ exact global symmetry or a potential with a Z_2 symmetry broken softly. The second case has the following Higgs potential

$$V_H^{Z_2-soft} = a_1x_1 + a_2x_2 + a_3x_3 + b_{11}x_1^2 + b_{22}x_2^2 + b_{33}x_3^2 + b_{44}x_4^2 + b_{12}x_1x_2. \tag{2.2.11}$$

All models to avoid a CP breaking vacua can be obtained from different limits of $V_H^{Z_2-soft}$. By means of the Higgs mass eigenstates, $\tan\beta$ and α (rotation angle in the CP-even sector) and a_3, and to recover easily the models $U(1)$(softly broken) and Z_2 and $U(1)$ exact, it is necessary to take:

$$\begin{aligned} U(1)\,\text{(softly-broken)} &\rightarrow b_{33} = b_{44},\ a_3 = -\frac{m_A^2}{\sin 2\beta} \\ U(1) &\rightarrow b_{33} = b_{44} \text{ and } a_3 = 0, \\ Z_2 &\rightarrow a_3 = 0. \end{aligned} \tag{2.2.12}$$

2.2.2. Stationary points of different nature

In SM, gauge invariance and renormalizability lead to one unique vacuum. Contrary 2HDMs can have several stationary points. It is possible to ask about the possibility of having different nature to the same parameter set. This fact yields to the possibility of tunneling among these stationary points. Hence it is necessary to study the way of these critical points arise. We compute many relations about differences between possible stationary points in the appendices D-E. For example, when a CP symmetry can be described as a good quantum number the differences between a normal vacuum V_N and a CP vacuum V_{CP} get the form

$$V_{CP} - V_N = \frac{m_A^2}{2v^2}\left[\left(v_1v_2' - v_2v_1'\right)^2 + \delta^2 v_2^2\right]. \tag{2.2.13}$$

The value of pseudo-scalar mass is evaluated at the normal stationary point. If the normal stationary point is a minimum, positivity of m_A^2 ensures that the CP stationary point is above it. Furthermore, in such case, the CP-critical point is a saddle point. Perhaps the main result is that the stability of the normal minimum against tunneling to a deeper CP breaking stationary point is thus ensured in 2HDM. The method extends straightforward to other vacuum structures differences, like one between CP and CB configurations (see appendix F). If a CP breaking stationary point is a minimum, the competing normal and charge breaking critical points are saddle points above it - the CP breaking minimum is then a global one.

2.2.3. Stationary points of the same nature

Now we consider the case of having simultaneously two normal vacua. This effect will be translated in the main corner of the metastability analysis. In 2HDMs, one of the most relevant consequences of the stationary points is the fact of minima of different nature can not coexist. Contrary to CP minima (linear equations in VEVs), normal minima are not uniquely determined; it is possible to find out two patterns for SSB with different masses for gauge bosons [30]. The

stationarity conditions are always a set of two coupled cubic equations. From the general Higgs potential with terms that break the CP-symmetry explicitly (2.2.6), the relation between two normal vacuum N_1 and N_2 is given by

$$V_{N_2} - V_{N_1} = \frac{1}{2}\left[\left(\frac{m^2_{H^\pm}}{v^2}\right)_{N_1} - \left(\frac{m^2_{H^\pm}}{v^2}\right)_{N_2}\right]\left[\left(v_1 v_2' - v_2 v_1'\right)^2 + \delta^2 v_2^2\right]. \tag{2.2.14}$$

where $v^2_{N_1} = v_1^2 + v_2^2$ and $v^2_{N_2} = v_1'^2 + v_2'^2 + \delta^2$ are the VEVs in each vacua, and $\left(m^2_{H^\pm}\right)_{N_1 2,}$ is the charged Higgs masses evaluated in different vacuum configurations. Hence the deepest minimum is characterized by the highest value of charged Higgs mass and the VEV ratio.

2.3. Minkowskian Structure of the 2HDM Higgs Potential

We have seen as multiple structure for vacuum in 2HDM arises for the complex form of the Higgs potential. These forms also yield several relation between minima and saddle points of the same or different nature. In this section, we study as the obtention of these properties are connected with the more general basis transformations of the model. Firstly, we should introduce a brief discussion on notation: though writing the 2HDM potential regarding doublets (manifestly gauge covariant) quoted in Eq. (1.2.1),

$$\begin{aligned} V_H = {} & m_{11}^2\Phi_1^\dagger\Phi_1 + m_{22}^2\Phi_2^\dagger\Phi_2 + \frac{1}{2}\lambda_1\left(\Phi_1^\dagger\Phi_1\right)^2 + \frac{1}{2}\lambda_2\left(\Phi_2^\dagger\Phi_2\right)^2 + \lambda_3\left(\Phi_1^\dagger\Phi_1\right)\left(\Phi_2^\dagger\Phi_2\right) + \lambda_4\left(\Phi_1^\dagger\Phi_2\right)\left(\Phi_2^\dagger\Phi_1\right) \\ & + \left\{\frac{1}{2}\lambda_5\left(\Phi_1^\dagger\Phi_2\right)^2 + \lambda_6\left(\Phi_1^\dagger\Phi_1\right)\left(\Phi_1^\dagger\Phi_2\right) + \lambda_7\left(\Phi_2^\dagger\Phi_2\right)\left(\Phi_1^\dagger\Phi_2\right) - m_{12}^2\Phi_1^\dagger\Phi_2 + h.c.\right\}, \end{aligned} \tag{2.3.1}$$

Here couplings λ_i with $i = 1, 2, 3, 4$ and m^2_{jj} with $j = 1, 2$ are real, while λ_k where $k = 5, 6, 7$ and $m^2_{i,j}$ where $i, j = 1, 2$ and different between them can be in general complex numbers. It is worthwhile point out different points in this 14-dimensional parameter space do not necessarily correspond to distinct physical predictions [36]. Now if we perform any linear transformation between doublets Φ_1 and Φ_2, the 2.3.1 becomes the same generic potential with redefined coefficients, which still corresponds to the same set of physical observables. Those operations were discussed in the section 1.2.2 of the last chapter 1. Thus, the systematics of minimizing the Higgs potential has a reparameterization invariance embedded in a group $GL\,(2, C)$ [2]. To see it in more detail, we first introduce the four-vector

$$r^\mu = (r_0, r_i) = \left(\mathbf{\Phi}^\dagger\mathbf{\Phi}, \mathbf{\Phi}^\dagger\sigma_i\mathbf{\Phi}\right), \tag{2.3.2}$$

where

$$\mathbf{\Phi} = \begin{pmatrix} \Phi_1 \\ \Phi_2 \end{pmatrix}. \tag{2.3.3}$$

which is a 2-dimensional vector Higgs bi-doublet, usually called Higgs field space. σ_i are the Pauli matrices. Finally, r^μ is gauge invariant and lead to parametrize the gauge orbits in the space of the Higgs fields.

On the other hand, the general reparametrization group $GL(2, C)$ can be written as

$$C^* \times SL\,(2, C), \tag{2.3.4}$$

where C^* is the group of simultaneous multiplication of both Φ_i with the same non-zero complex number and $SL(2, C)$ is the special linear transformation group containing all unit determinant transformation matrices. We know that multiplication of both doublets by the same number gives a freedom to rescale r_μ, however, it does not modify the standard structure of the general Higgs potential. The special linear group $SL\,(2, C)$, on the contrary leads to non-trivial changes of the pure scalar potential, and in the subsequent analysis in that we shall focus on it [111].

It is very convenient to switch from the fundamental to the adjoint representation of $SU(2)$. The corresponding decomposition is given by

[2] We consider the following statements:

- $GL\,(n, F)$ the general linear group of degree n is the set of $n \times n$ invertible matrices, together with the operation of ordinary matrix multiplication (in the particular case this is defined in the field C).
- The special linear group, written $SL(n, F)$ is the subgroup of $GL(n, F)$ representing by matrices with a determinant of 1.
- This property is an extension of an earlier identification of re-phasing $U\,(1)$, and unitary reparameterization $U\,(2)$, invariance of the model. It starts with the observation of the internal Minkowski-space structure behind 2HDM.

$$2 \otimes \bar{2} = 3 \oplus 1 \tag{2.3.5}$$

Hence the relevant quantities might form a triplet and a singlet representation. Using the well-known $SU(2) \to SO(3)$ mapping, one maps them (triplet and singlet) into a scalar and a real-valued vector:

$$r_0 = \mathbf{\Phi}^\dagger\, \mathbf{\Phi} = \left(\Phi_1^\dagger \Phi_1 + \Phi_2^\dagger \Phi_2\right), \tag{2.3.6}$$

$$r_i = \mathbf{\Phi}^\dagger \sigma_i\, \mathbf{\Phi} = \begin{pmatrix} \Phi_1^\dagger \Phi_2 + \Phi_2^\dagger \Phi_1 \\ -i\left[\Phi_1^\dagger \Phi_2 - \Phi_2^\dagger \Phi_1\right] \\ \Phi_1^\dagger \Phi_1 - \Phi_2^\dagger \Phi_2 \end{pmatrix}. \tag{2.3.7}$$

The Higgs potential can be now written as

$$V = -M_i r_i - M_0 r_0 + A_{ij} r_i r_j + B_i r_i r_0 + C r_0^2. \tag{2.3.8}$$

where M_i and M_0 contain the mass coefficients, while A_{ij}, B_i and C are composed of quartic couplings λ_i. From this formalism, it is possible to extract the following features:

- This representation already displays some structure in the space of all possible 2HDM, i.e. the space of all free parameters of the potential.
- A $SU(2)$ rotation induces a corresponding $SO(3)$ rotation of the basis in $3D$ space, under which r_i, M_i, B_i transform as vectors, meanwhile A_{ij} transforms as a symmetric tensor, but the value of the potential remains the same.

Considering the largest group of invertible linear transformations $GL(2,C)$ of a complex-valued 2-vector, we can do this decomposition in a more general way. By the quartic part of the Higgs potential contains all possible fourth order terms, an arbitrary linear transformation between the two doublets keeps it unchanged; only up to reparameterization operation. Therefore, the group under which the Higgs potential is reparameterization-invariant is $GL(2,C)$, not just $U(2)$ as usually it is assumed in the literature [29, 36].

Moreover, the subgroup C^*(i.e. overall multiplication by a non-zero complex number) of $GL(2,C)$ is over-determinate for the description of the Higgs potential. Therefore the product of all the fields by the same real non-zero constant yields to a rescaling of all the observables, without changing the fundamental structure of the model, while the global phase rotations have no effect on the Higgs potential. It is its factor group $SL(2,C)$ that encodes all non-trivial transformations and generates interesting symmetries. These properties are useful to study Higgs potential realizations and to establish possible connections with phenomenology and other theoretical analyses.

Consequently, from adjoint representation of $SL(2,C)$ it is possible to induce proper Lorentz group $SO(1,3)$[3]. Apart from the 3D rotations, induced by $SU(2)$, we have also boost-transformations along the three axes. The scalar r^0 and vector r^i now become parts of a single irreducible representation of $SO(1,3)$:

$$r^\mu = (r_0, r_i)\,. \tag{2.3.9}$$

The orbit space (generated by all possible four-vectors r_μ) is equipped with the Minkowski space structure. The covariant and contravariant vectors are related by the metric tensor $g_{\mu\nu}$ =diag$(1,-1,-1,-1)$ (i.e. signature equal to -2).

2.3.1. The orbit gauge space

The orbit space in 2HDM is not the entire Minkowski space; since the square of the 4-vector r^μ is invariant under any proper Lorentz transformation and it is non-negative due to the Schwartz inequality for the product of the doublets,

$$\begin{aligned} r^2 &\equiv r^\mu r_\mu = r_0^2 - r_i^2 = 4\left[\left(\Phi_1^\dagger \Phi_1\right)\left(\Phi_2^\dagger \Phi_2\right)\right] \\ &= \left(\Phi_1^\dagger \Phi_1 + \Phi_2^\dagger \Phi_2\right)^2 - \left(\Phi_1^\dagger \Phi_2 + \Phi_2^\dagger \Phi_1\right)^2 + \left(\Phi_1^\dagger \Phi_2 - \Phi_2^\dagger \Phi_1\right)^2 - \left(\Phi_1^\dagger \Phi_1 - \Phi_2^\dagger \Phi_2\right)^2 \\ &= 4\left(\Phi_1^\dagger \Phi_1\right)\left(\Phi_2^\dagger \Phi_2\right) - 4\left(\Phi_1^\dagger \Phi_2\right)\left(\Phi_2^\dagger \Phi_1\right) \geq 0, \end{aligned} \tag{2.3.10}$$

[3]The restricted Lorentz group consists of Lorentz transformations, boosts or rotations in four dimensions, that preserve the orientation of space and direction of time besides to the quadratic form .

and hence temporal component of cuadrivector

$$r_0 = \Phi_1^\dagger \Phi_1 + \Phi_2^\dagger \Phi_2 \geq 0. \tag{2.3.11}$$

Therefore, the physical field configurations lie inside and on the border of the future lightcone (LC^+) in the Minkowski space.

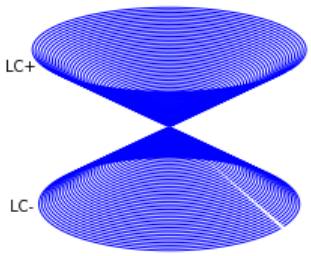

Figure 2.1.: *Geometrical point of view for orbit space consistent with Schwartz inequality for doublets. Because of Schwartz inequalities, the gauge orbit space for 2HDM belongs only in the frontier and inside of the future light cone LC^+.*

The surface of LC^+, $r^2 = 0$, corresponds to the situation when the two Higgs multiplets are proportional to each other. In particular, if a vector r^μ indicates a stationary point (e.g. EW vacuum) of the potential, then r^2 means that the vacuum is electrically neutral. $r^2 > 0$ can be realized only when the two doublets are not proportional; a vacuum solution with $r^2 > 0$ would correspond to the charge-breaking vacuum as we will see soon (another discussion is presented in Appendix G). From (2.3.8), the Higgs potential in the r^μ-gauge orbit space can be written in a very compact form:

$$V_H = -M_\mu r^\mu + \frac{1}{2}\Lambda_{\mu\nu} r^\mu r^\nu. \tag{2.3.12}$$

Here the four-vector M_μ is built from parameters m_{ij}^2 in (2.3.1), while the symmetric four-tensor $\Lambda_{\mu\nu}$ is constructed from the quartic coefficients λ_i.

2.3.2. Properties of $\Lambda^{\mu\nu}$

The positivity constraint on the Higgs potential requires it to be bounded from below in all possible directions of the field space conformed by (Φ_1, Φ_2). These constraints presented as a list of inequalities among different $\lambda's$, which can be gotten from different arguments of variational calculus [112]. Every restriction has been summarized in Table 2.1.

Condition	Lagrange multiplier (Normal vacuum)	Main assumption or Consequence
$\lambda_1 > 0$	No	$\lvert\Phi_1\rvert \to \infty$ and $\lvert\Phi_2\rvert \to 0$
$\lambda_2 > 0$	No	$\lvert\Phi_1\rvert \to 0$ and $\lvert\Phi_2\rvert \to \infty$
$\lambda_3 > -\sqrt{\lambda_1\lambda_2}$	No	$\Phi_1^\dagger\Phi_2 = 0$ (orthogonal)
$\lambda_4 + \lambda_3 + \lambda_5 > -\sqrt{\lambda_1\lambda_2}$	Yes$\to \Lambda_1$	$\mathrm{Re}\left(\Phi_1^\dagger\Phi_2\right) = 0$
$\lambda_4 + \lambda_3 - \lambda_5 > -\sqrt{\lambda_1\lambda_2}$	Yes$\to \Lambda_1$	$\mathrm{Im}\left(\Phi_1^\dagger\Phi_2\right) = 0$

Table 2.1.: *Vacuum stability constraints in the field space for quartic couplings in a general CP-conserving Higgs potential obtained from variational methods [20, 113, 114].*

We should look for a formalism or properties for $SO(1,3)$ representations to ensure that Higgs potential is bounded from below. In the language of the gauge orbits equipped with Minkowskian metric, the positivity constraint for the Higgs potential in Eq. (2.3.12) is given by a single statement: *The tensor $\Lambda^{\mu\nu}$ is positive definite on the future light-cone.* This fact is equivalent to the following set of requirements:

- Tensor $\Lambda^{\mu\nu}$ is diagonalizable by a $SO(1,3)$ transformation,

- the time-like eigenvalue Λ^0 is positive and
- all spacelike eigenvalues Λ_i are smaller than Λ_0.

In other words, there always exists a $SO(1,3)$ transformation that brings $\Lambda^{\mu\nu}$ to

$$\begin{pmatrix} \Lambda_0 & 0 & 0 & 0 \\ 0 & -\Lambda_1 & 0 & 0 \\ 0 & 0 & -\Lambda_2 & 0 \\ 0 & 0 & 0 & -\Lambda_3 \end{pmatrix}, \text{ with } \Lambda_0 > 0, \text{ and } \Lambda_0 > \Lambda i \tag{2.3.13}$$

Note that Λ_i are bounded only from above. The negative values of Λ_i with arbitrary large absolute values are allowed. In particular, all $\Lambda_i < 0$ if and only if $\Lambda^{\mu\nu}$ is positive definite in the entire Minkowski space. The demonstration of these implications has been given in the appendix G.

2.4. CP-Conserving Potential and Minkowskian structure

In section 2.2.1 was naively demonstrated, considering the 2HDM potential regarding doublets from (2.3.1) is extremely useful for many calculations (e.g. everything dealing with the fermion sector) and to get Feynman rules. However, in some instances, a different notation - in which the potential written in terms of gauge bilinear invariants - can be crucial in find out possible symmetries relations in the Higgs potential itself and its stationary points. For instance, by taking $\delta = 0$ in Eq. (2.2.14), the comparison of values of potentials at different vacua

$$V_{N_1} - V_{N_2} = \frac{1}{2}\left[\left(\frac{M^2_{H^\pm}}{v'^2}\right)_{N_2} - \left(\frac{M^2_{H^\pm}}{v'^2}\right)_{N_2}\right]\left[\left(\beta_1 v_2 - \beta_2 v_1\right)^2\right], \tag{2.4.1}$$

it is simple to obtain in the bilinears notation, but extremely intricate to do in the former (2.3.1). In the same way, the conditions for existence of dual minima are far easier to establish in the bilinear formalism, which we have introduced in appendices D-E. As we studied in sections (2.3) and (2.3.1), a outstanding feature of this notation in bilinears is the fact that the 2HDM potential has a hidden Minkowski-like structure, when it is written in terms of gauge invariant bilinears which form a covariant $4-$vector in a Minkowski space, $r_\mu\,(\mu = 0,..,3)$ defined in (2.3.6)-(2.3.7); it arises from reparameterization group $SL\,(2,C)$. Moreover, the allowed vectors $r^\mu = \left(r_0, -r^i\right)$ fill the forward lightcone LC^+ defined by $r_0 \geq 0$ and $r^\mu r_\mu \geq 0$. The apex of this cone regards to the EW symmetric vacuum, meanwhile its surface corresponds to the neutral vacua, and its interior corresponds to charge-breaking vacua [115].

In the CP-conserving case for the Higgs potential written in the Minkowskian bilinears form (2.3.12), the $4-$vector M_μ and the tensor $\Lambda_{\mu\nu}$ are given by

$$M_\mu = (M_0, M_i) = \left(-\frac{1}{2}\left(m^2_{11} + m^2_{22}\right), \mathrm{Re}\left(m^2_{12}\right), 0, \frac{1}{2}\left(m^2_{22} - m^2_{11}\right)\right). \tag{2.4.2}$$

with $M^\mu = (M_0, -M_i)$ and

$$\Lambda_{\mu\nu} = \begin{pmatrix} \frac{\lambda_1+\lambda_2}{2} + \lambda_3 & \lambda_6 + \lambda_7 & 0 & \frac{\lambda_1-\lambda_2}{2} \\ \lambda_6 + \lambda_7 & \lambda_4 + \lambda_5 & 0 & \lambda_6 - \lambda_7 \\ 0 & 0 & \lambda_4 - \lambda_5 & 0 \\ \frac{\lambda_1-\lambda_2}{2} & \lambda_6 - \lambda_7 & 0 & \frac{\lambda_1+\lambda_2}{2} - \lambda_3 \end{pmatrix}. \tag{2.4.3}$$

As we mentioned earlier, Higgs potential belongs on a basis where all parameters are real, which causes the appearance of several zeros in $\Lambda_{\mu\nu}$ and M_μ. This fact is a sufficient condition to avoid explicit CP violation in the Higgs potential. With the notation established here, it is possible to give the preliminary steps required to verify whether or not the most general CP-conserving potential can have two neutral minima [29], and if one of them is a metastable vacuum characterized by a deeper minimum (true-false vacua tension).

- The first step in the systematic is the diagonalization of the tensor of the quartic couplings. Due to the Minkowski indexes, this is achieved via a combination of rotations and Lorentz-like boosts. To achieve it exist a much simpler systematic : Define the matrix $\Lambda = \Lambda_\mu^{\ \nu}$; it is obtained from eq. (2.4.3) by simply make a flipping of the sign of the three last columns. The 4×4 matrix has eigenvalues Λ_a $(a = 1,2,3,4)$ determined by the usual equation,

$$\det\left(\Lambda - \Lambda_a \boldsymbol{I}\right) = 0, \tag{2.4.4}$$

with eigenvectors, $V^{(a)}$ which satisfy (no sum indexes)

$$\Lambda V^{(a)} = \Lambda_a V^{(a)}. \tag{2.4.5}$$

Perhaps solving for the eigenvectors and eigenvalues of Λ could be implemented within any numerical calculation package. Since the matrix Λ is not symmetric anymore, its eigenvalues and eigenvectors are -in general- complex. In particular, this condition shall be translated onto separate conditions for vacuum stability on independent directions for $\Phi_1 - \Phi_2$ space.

- The next step is ensuring that the potential is bounded from below or determining the stability conditions. In these cases, the eigenvalues of Λ must obey the conditions:

$$\begin{aligned} & \text{All eigenvalues must be real} && \text{(2.4.6a)} \\ \Lambda_0 \;&>\; 0, && \text{(2.4.6b)} \\ \Lambda_0 \;&>\; \{\Lambda_1, \Lambda_2, \Lambda_3\}\,. && \text{(2.4.6c)} \end{aligned}$$

- The eigenvectors obtained in (2.4.5) are then real and can be normalized in such a way that one of them is time-like one, the others are space-like ones. Meaning, if the eigenvector referring to the largest eigenvalue Λ_0, obtained in (2.4.5) is given by $V^{(0)} = (v_{00}, v_{10}, v_{20}, v_{30})$, its overall normalization is such that, with our conventions,

$$\left|V^{(0)}\right|^2 = v_{00}^2 - v_{10}^2 - v_{20}^2 - v_{30}^2 = 1, \tag{2.4.7}$$

whereas, for the other three eigenvectors $V^{(i)}$, we must have

$$\left|V^{(i)}\right|^2 = v_{0i}^2 - v_{1i}^2 - v_{2i}^2 - v_{3i}^2 = -1. \tag{2.4.8}$$

- We now build up a rotation matrix O, with the eigenvectors $V^{(a)}$ serving as its columns. Which means, with the coefficients v used in eqs. (2.4.7) and (2.4.8), $O_{ab} = v_{ab}$. This matrix O satisfies

$$O^{-1}\Lambda O = \text{diag}\left(\Lambda_0, \Lambda_1, \Lambda_2, \Lambda_3\right). \tag{2.4.9}$$

We now build up a rotation matrix O, where the eigenvectors $V^{(a)}$ serving as its columns. Which means, with the coefficients v used in eqs. (2.4.7) and (2.4.8), $O_{ab} = v_{ab}$. This matrix O satisfies

$$\begin{pmatrix} \widehat{M}_0 \\ \widehat{M}_1 \\ \widehat{M}_2 \\ \widehat{M}_3 \end{pmatrix} = O^T \begin{pmatrix} -\frac{1}{2}\left(m_{11}^2 + m_{22}^2\right) \\ -\text{Re}\left(m_{12}^2\right) \\ 0 \\ \frac{1}{2}\left(m_{11}^2 - m_{22}^2\right) \end{pmatrix}, \quad \begin{pmatrix} \widehat{r}^0 \\ \widehat{r}^1 \\ \widehat{r}^2 \\ \widehat{r}^3 \end{pmatrix} = O^T \begin{pmatrix} \frac{1}{2}\left(v_1^2 + v_2^2\right) \\ v_1 v_2 \\ 0 \\ \frac{1}{2}\left(v_1^2 - v_2^2\right) \end{pmatrix}. \tag{2.4.10}$$

Thus $\widehat{M}^0 = \widehat{M}_0$, $\widehat{M}^i = -\widehat{M}_i$, etc. Since we began with the CP-conserving potential of eqs. (2.4.2) and (2.4.3), we are guaranteed to obtain $\widehat{M}^2 = \widehat{r}^2 = 0$.

$$\widehat{r}_\mu \widehat{r}^\mu = \widehat{r}_0^2 - \widehat{r}_1^2 - \widehat{r}_3^2 = \frac{1}{4}\left(v_1^2 + v_2^2\right)^2 - v_1^2 v_2^2 - \frac{1}{4}\left(v_1^2 - v_2^2\right)^2 = 0. \tag{2.4.11}$$

Now in possession of the values of the eigenvalues Λ_0, Λ_i; of the rotated quadratic coefficients $\widehat{M}^0$, $\widehat{M}^i$; and of the rotated VEVs $\widehat{r}^0, \widehat{r}^i$, the necessary conditions for the existence of two neutral minima are very simple to write:

$$\begin{aligned} \text{If } \widehat{M}_0 \;&>\; 0 \text{ and } \sqrt[3]{x^2} + \sqrt[3]{y^2} \leq 1, \text{ with} \\ x \;&=\; \frac{\widehat{M}_1\left(\Lambda_0 - \Lambda_3\right)}{\widehat{M}_0\left(\Lambda_3 - \Lambda_1\right)},\; y = \frac{\widehat{M}_3\left(\Lambda_0 - \Lambda_1\right)}{\widehat{M}_0\left(\Lambda_3 - \Lambda_1\right)}. \end{aligned} \tag{2.4.12}$$

Then the potential can have two neutral minima. We emphasize that these are necessary conditions for the existence of two neutral minima (see demonstration in Appendix F) - although they are necessary and sufficient conditions for the existence of four normal stationary points. Remarkably, we have a necessary and sufficient condition to verify the global nature of our minimum - to know whether our $\{v_1, v_2\}$ vacuum is the global minimum of the potential, we need only do the following:

Let us define a discriminant D, given by
$D = \widehat{M}_1 \widehat{M}_3 \widehat{r}_1 \widehat{r}_3$ (2.4.13)
Our vacuum is the global minimum of the potential if and only if $D > 0$

It is simple to verify that this procedure leads to the conditions laid out for the softly broken Peccei-Quinn -like-model in the following section. Unfortunately for the most general Z_2-model with a softly term and λ_5 complex coupling, the diagonalization procedure explained above renders analytical expressions for the bounds inviable. Nevertheless, the formalism treated in this section is quite easy to implement in a numerical way [4].

2.4.1. Lower half space: $\widehat{M}^0 < 0$

Here we show that, if $\widehat{M}^0 < 0$ *in the* $\Lambda_{\mu\nu}$*-diagonal basis, then the potential has only one non-zero stationary point, which behaves as the global minimum in the theory* [36, 115, 117]. Finding neutral extreme of the potential in Eq. (2.3.12), that is, with values of r^μ restricted to the surface of lightcone, $r^\mu r_\mu = 0$ - benefits from using a Lagrange multiplier ζ associated with this constraint. Therefore, we consider an auxiliary potential $\bar{V}$ taking into account the respective restriction

$$\bar{V} = V - \frac{\zeta}{2} r^\mu r_\mu = -M_\mu r^\mu + \frac{1}{2}\Lambda_{\mu\nu} r^\mu r^\nu - \frac{\zeta}{2} r^\mu r_\mu. \tag{2.4.14}$$

The minimization conditions with respect to vectors and Lagrange multiplier are thus

$$\frac{\partial V}{\partial r^\mu} = -M_\mu + \Lambda_{\mu\nu} r^\nu - \zeta r_\mu = 0. \tag{2.4.15}$$
$$\frac{\partial V}{\partial \zeta} = r^\mu r_\mu = 0. \tag{2.4.16}$$

The last condition is the original constraint to get solutions on the frontier of the lightcone. By using the explicit coefficients of the potential in the $\Lambda_{\mu\nu}$-diagonal frame, the stationary conditions become

$$(\Lambda_0 - \zeta)\,\widehat{r}_0 = \widehat{M}_0, \tag{2.4.17}$$
$$(\Lambda_i - \zeta)\,\widehat{r}_i = \widehat{M}_i. \tag{2.4.18}$$

Notice that, because of the potential is CP conserving and no CP spontaneous breaking is being considered, $\widehat{M}_2 = 0$ and $\widehat{r}_2 = 0$. Thus in these stationary equations, we can reduce spatial conditions

$$(\Lambda_1 - \zeta)\,\widehat{r}_1 = \widehat{M}_1, \tag{2.4.19}$$
$$(\Lambda_3 - \zeta)\,\widehat{r}_3 = \widehat{M}_3. \tag{2.4.20}$$

This system has therefore three independent variables ζ, r_1, r_3, while the value of $\widehat{r}_0$ is then expressed as the positive square root of $\widehat{r}_0^2 = \sum_\iota \widehat{r}_i^2$. Since $\widehat{r}_0$ is necessarily positive (taking $\widehat{r}_0$ means we are excluding the trivial solution, where all $\widehat{r}_\mu = 0$), the equation (2.4.17) implies that, if $\widehat{M}_0 < 0$, the solution is found for a value of the Lagrange multiplier $\zeta > \Lambda_0$. The condition $\widehat{r}_0^2 = \sum_\iota \widehat{r}_i^2$ can be rewritten as

$$\sum_i \left(\frac{\Lambda_0 - \zeta}{\Lambda_i - \zeta}\right)^2 \left(\frac{\widehat{M}_i}{\widehat{M}_0}\right)^2 \equiv \sum_i \Omega_i = 1. \tag{2.4.21}$$

This form is a single algebraic equation of fourth order in ζ, and it will be converted in a crucial relation to study stability and metastability conditions in models established in a CP-conserving frame. Nevertheless without solving it

[4] We have followed the formalism, the discussion, and method exposed by Ivanov in [36, 116]

explicitly, we can extract some features for extremal cases of, for instance, a Lagrange multiplier. Thus, by varying the value of ζ from Λ_0 to infinity, the following ranges are found

$$\text{when } \zeta = \Lambda_0 \rightarrow \frac{\zeta - \Lambda_0}{\zeta - \Lambda_i} = 0, \tag{2.4.22}$$

$$\text{when } \zeta \rightarrow \infty \rightarrow \frac{\zeta - \Lambda_0}{\zeta - \Lambda_i} = 1. \tag{2.4.23}$$

($\Lambda_0 > \Lambda_i$ from vacuum stability conditions) hence ζ is increasing, in a monotonous function, from zero (in Λ_0) up to one ($\zeta >> \Lambda_0$). The expression on the left of (2.4.21) is therefore a monotonous function of ζ, and it grows from zero to a maximum equal to

$$\sum_\iota \left(\frac{\widehat{M}_i}{\widehat{M}_0}\right)^2 \text{ when } \zeta \text{ goes to } \infty. \tag{2.4.24}$$

We can, therefore, say that

- If $\widehat{M}_0 < 0$ and $\widehat{M}_\mu \widehat{M}^\mu \geq 0$,

$$\widehat{M}_0^2 - \sum_i \widehat{M}_i^2 \geq 0 \rightarrow \sum_i \left(\frac{\widehat{M}_i}{\widehat{M}_0}\right)^2 \leq 1. \tag{2.4.25}$$

  and from

$$(\Lambda_0 - \zeta)\,\widehat{r}_0 = \widehat{M}_0 < 0 \text{ and } \widehat{r}_0 > 0 \text{ therefore } \zeta > \Lambda_0, \tag{2.4.26}$$

  hence the equation (2.4.21) has no solution in the region $\zeta > \Lambda_0$ (only for $\sum_i \widehat{M}_i^2 = \widehat{M}_0^2$). Thus, the potential has no non-trivial extreme. The only extremum - the global minimum - lies at the apex $r_\mu = 0$, and no electroweak breaking occurs. This situation is physically uninteresting (for our purposes) since theory remains in a non-breaking phase where Goldstone bosons have not incorporated into longitudinal components of gauge bosons to yield their respective masses.

- If $\widehat{M}_0 < 0$ and $\widehat{M}_\mu \widehat{M}^\mu < 0$, therefore

$$\sum_i \left(\frac{\widehat{M}_i}{\widehat{M}_0}\right)^2 > 1, \tag{2.4.27}$$

  and the equation (2.4.21) has only one solution in the region $\zeta > \Lambda_0$. Here $\widehat{M}^\mu$ lies outside of the past lightcone but still in the lower half space, there exists a unique non-zero neutral extremum, which is necessarily the global minimum. Thus, there are no two minima in this situation.

Furthermore, in the lower half-plane exists only one surface of phase transitions, i.e., the past lightcone LC^-, at which the EW-breaking or one restoring phase transition might take place.

In conclusion, $\widehat{M}^0 > 0$ is a condition necessary to get two minima in the Higgs potential, implying from stationary conditions (2.4.21) that $\zeta < \Lambda_0$. The next subsection is devoted to showing additional conditions to have minima in the Higgs potential for the upper half space in the temporal component of bilinear terms.

2.4.2. Upper half space: $\widehat{M}_0 > 0$

For $\widehat{M}_0 > 0$, the geometrical phase diagram is more complex than associated with $\widehat{M}_0 < 0$. To describe and see it, let us introduce the 3-vector $\boldsymbol{m}_i, i = 1, 2, 3$:

$$\boldsymbol{m}_i = \frac{1}{\widehat{M}_0}\left(\widehat{M}_1, \widehat{M}_2, \widehat{M}_3\right). \tag{2.4.28}$$

and it allows showing the phase diagram in the m_i-space. There are two generic cases to consider: i) When all spatial components in diagonal tensor $\Lambda_i < 0$ and ii) One at least $\Lambda_i < 0$. Both cases are displayed in Fig. 2.2.

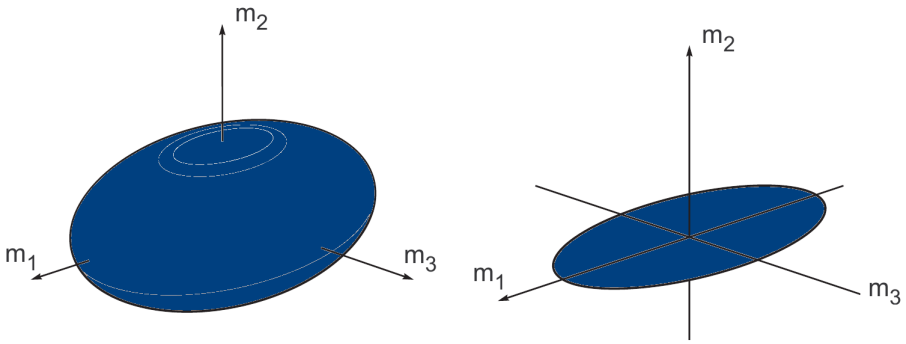

Figure 2.2.: *The phase diagram for vacuum structures in the m_i-space. Left: all $\Lambda_i < 0$, the ellipsoid separates the charge-breaking and the neutral vacua. Right: Λ_2 is positive and greater than Λ_1 and Λ_3. Inside the dark ellipse, the discrete symmetry of the potential V is spontaneously broken [36].*

All $\Lambda_i < 0$

The condition $\Lambda_1, \Lambda_2, \Lambda_3 < 0$ is the necessary condition for the charge-violating minimum to exist [118,119] (see also G). Whether this minimum is realized, depends on m_i, i.e. on the point of the phase diagram. Indeed, in the $\Lambda_{\mu\nu}$ -diagonal frame, equations for extremal condition are now

$$\Lambda_0 \widehat{r}_0 = \widehat{M}_0, \tag{2.4.29}$$
$$\Lambda_i \widehat{r}_i = \widehat{M}_i. \tag{2.4.30}$$

Since the solution $\widehat{r}_\mu$ must lie inside the forward lightcone, one obtains that the charge-breaking phase in the phase diagrams lies inside the ellipsoid

$$\frac{\mathsf{m}_1^2}{a_1^2} + \frac{\mathsf{m}_2^2}{a_2^2} + \frac{\mathsf{m}_3^2}{a_3^2} < 1, \tag{2.4.31}$$

This can be obtained from

$$\widehat{r}_\mu \widehat{r}^\mu > 0; \text{ translated to } \sum_i \left(\frac{\widehat{M}_i}{\Lambda_i}\right)^2 \left(\frac{\Lambda_0}{\widehat{M}_0}\right)^2 < 1 \text{ with } a_i = |\Lambda_i| / \Lambda_0. \tag{2.4.32}$$

This relation is depicted in Fig. 2.2, left. If m_i lies outside ellipsoid (2.4.31), then the vacuum is neutral. The surface of the ellipsoid is thus the locus of the critical points of the phase diagram, at which the second order charge-breaking or charge-restoring phase transition takes place.

At least one $\Lambda_i > 0$

If at least one Λ_i is positive, then the minimum always corresponds to a neutral vacuum and its position satisfies the following equations

$$(\Lambda_0 - \zeta)\, \widehat{r}_0 = \widehat{M}_0, \tag{2.4.33}$$
$$(\Lambda_i - \zeta)\, \widehat{r}_i = \widehat{M}_i. \tag{2.4.34}$$

By writing the vacuum position in gauge orbit space through $\widehat{r}_\mu = \widehat{r}_0\,(1, n_1, n_2, n_3)$, with unitary vector $|\overrightarrow{n}| = 1$. Since we are concern to the lightcone surface $\widehat{r}_\mu \widehat{r}^\mu = 0$ one can eliminate the Lagrange multiplier and to develop the spatial terms

$$\left[(\Lambda_i - \Lambda_0)\, \widehat{r}_0 + \widehat{M}_0\right] n_i = \widehat{M}_i. \tag{2.4.35}$$

The requirement that $\widehat{n}$ is an unit vector can be written as

$$\sum_i \frac{m_i^2}{\left[(\Lambda_i - \Lambda_0)\, \frac{\widehat{r}_0}{\widehat{M}_0} + 1\right]^2} = 1. \tag{2.4.36}$$

This is a sixth order equation for r_0. In a general case, the system cannot be solved exactly. However, the geometrical approach to critical points analyses still allows understanding the structure of the phase diagram. First, if m_i lies on one of the principal planes, then the potential has an additional discrete symmetry. The solutions of (2.4.35) can either conserve or violate this symmetry. From relation (2.4.21), a necessary and sufficient condition for violation of this symmetry, e.g. in the case $\mathsf{m}_2 = 0$ is given by

$$\frac{\mathsf{m}_1^2}{b_1^2} + \frac{\mathsf{m}_3^2}{b_3^2} < 1 \text{ where } b_i = \frac{\Lambda_i - \zeta}{\Lambda_3 - \zeta}. \tag{2.4.37}$$

From spatial stationary conditions (2.4.18), and for $\widehat{M}_{i=2} = 0$, first we consider $\widehat{r}_i \neq 0$, hence $\Lambda_2 = \zeta$. Therefore

$$\frac{\mathsf{m}_1^2}{b_1^2} + \frac{\mathsf{m}_3^2}{b_2^2} < 1 \text{ where } b_i = \frac{\Lambda_i - \Lambda_2}{\Lambda_3 - \Lambda_2}. \tag{2.4.38}$$

Thus, symmetry-violating extreme appear, if m_i lies inside ellipse on one of the principal planes. It was proved that these symmetry-violating extreme are minima, if and only if the corresponding eigenvalue of $\Lambda_{\mu\nu}$ (Λ_2 for $\mathsf{m}_2 = 0$) is positive and is the biggest of all Λ_i. So, when constructing the phase diagram, we should first identify the largest eigenvalue and then consider only the ellipse that lies in the plane orthogonal to the corresponding eigenvector, as it is shown in Fig. 2.2, right. For points lying strictly inside the ellipse, two different degenerate minima exist. In both of them, the discrete symmetry is spontaneously broken. For points in the $(\mathsf{m}_1, \mathsf{m}_3)$ plane outside the ellipse only one minimum exists and the discrete symmetry is preserved. So, if m_i lies strictly on the plane and moves from outside into the ellipse, a symmetry-breaking second-order phase transition takes place.

For the points just above ($\mathsf{m}_2 > 0$) or just below ($\mathsf{m}_2 < 0$) the ellipse have two minima at different depths. So, if m_i lies above the ellipse and moves through it downwards, the relative depth between the two minima changes sign, and a first-order phase transition takes place. Thus, the interior of the ellipse is the locus of the first-order phase transitions, while its boundary is the locus of the second-order phase transitions.

2.4.3. The astroid condition

Here we shall show that for the 2HDM scalar potential to have two normal minima, the values of the parameters in the Higgs potential must be such that we are inside a region of space limited by the astroid curve defined as

$$\sqrt[3]{x^2} + \sqrt[3]{y^2} \leq 1. \tag{2.4.39}$$

where x and y are functions of $\Lambda's$, $\widehat{M}'s$ and $\widehat{r}'s$. We will use the geometric approach to counting solutions of the minimization equations (2.4.21) developed in [115], showing the astroid condition. As a first glance, we are only interested in an extreme with VEVs without any relative phase, thus $\widehat{r}_2 = 0$. Since the existence of a normal minimum forbids a CP-breaking one (see section 2.2.2), meaning that a more global analysis would discover a greater number of saddle points. But restricting ourselves to the $\widehat{r}_2 = 0$ case has no impact on the counting of possible normal minima. The analysis has a subtlety or caveat associated with the ordering of the eigenvalues Λ_i. Hence in a first glance, let us start with the case where $\Lambda_1 > \Lambda_3$.

Eq. (2.4.21) can be seen as defining an ellipse. In fact, if we define the variables $\mathsf{m}_1 = \widehat{M}_1/\widehat{M}_0$ and $\mathsf{m}_3 = \widehat{M}_3/\widehat{M}_0$, the semi-axes of the ellipse depends on ζ and will be given by

$$a_1(\zeta) = \frac{|\Lambda_1 - \zeta|}{\Lambda_0 - \zeta}, \; a_3(\zeta) = \frac{|\Lambda_3 - \zeta|}{\Lambda_0 - \zeta}. \tag{2.4.40}$$

In terms of these new variables eq. (2.4.21) thus it becomes

$$\frac{\mathsf{m}_1^2}{a_1^2} + \frac{\mathsf{m}_3^2}{a_3^2} = 1, \tag{2.4.41}$$

which is the equation describing an ellipse in the $(\mathsf{m}_1, \mathsf{m}_3)$ region. Considering now the family of obtained ellipses when we take all values of the Lagrange multiplier $-\infty < \zeta < \Lambda_0$ and count how many times this family of ellipses crosses a particular point (a, b) in the $(\mathsf{m}_1, \mathsf{m}_3)$ plane. When an ellipse passes by that juncture, Eq. (2.4.41) has a solution, meaning that the Higgs potential has a critical point. Then, the number of times the ellipses cross the stage (a, b) will give us the number of non-trivial extrema of the potential. Also, it has been shown that the larger ζ is, the smaller the value of the potential.

So, as ζ changes from $-\infty$ to , Λ_0 we have:

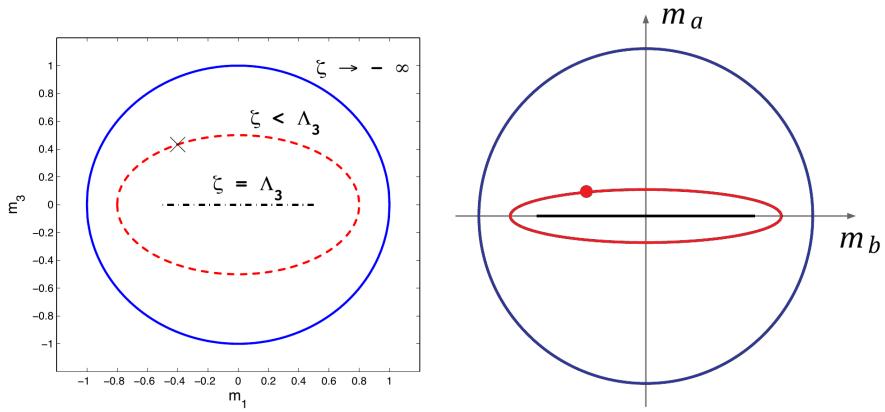

Figure 2.3.: *Example of a geometric representation of the ellipse evolution defined by the condition 2.4.21. In this case* $-\infty < \zeta < \Lambda_3$. ***(Right)*** *Ellipse evolution in arbitrary projection plane for spatial ordering* $\Lambda_a < \Lambda_b < \lambda_c$ *and* $\zeta < \Lambda_a$ *[29]*

- In the limit $\zeta \to -\infty$, $a_1 \to 1$ and $a_3 \to 1$

$$\mathsf{m}_1^2 + \mathsf{m}_3^2 = 1, \tag{2.4.42}$$

the ellipse is just the unit circle. This occurs because the semi-axes a_1 and a_3 tend to one in this limit (solid blue line in figure 2.3).

- As ζ increases, the ellipse shrinks. It shrinks most quickly along the direction of the smallest semi-axis - and since $\Lambda_1 > \Lambda_3$ (first case), then according to Eq. (2.4.40)

$$\frac{\mathsf{m}_1^2}{a_1^2} + \frac{\mathsf{m}_3^2}{a_3^2} = 1, \tag{2.4.43}$$

this relation means that the ellipse is contracting faster along the axis m_3 (dashed red line in figure 2.3).

- As ζ increases further, the ellipse on the $(\mathsf{m}_1, \mathsf{m}_3)$-plane shrinks even more. At $\zeta = \Lambda_3$ the ellipse collapses to a line segment (dot-dashed black line in Fig. 2.3):

$$a_3 = 0, \;\; a_1 = \frac{\Lambda_1 - \Lambda_3}{\Lambda_0 - \Lambda_3}. \tag{2.4.44}$$

or equivalently

$$\mathsf{m}_3 = 0, \;\; |\mathsf{m}_1| \leq \mathsf{m}_1^* = \frac{\Lambda_1 - \Lambda_3}{\Lambda_0 - \Lambda_3}. \tag{2.4.45}$$

- Notice that over the interval $-\infty < \zeta < \Lambda_3$ the ellipses sweep once all points inside the unit circle. For instance, there is only one ellipse passing by the juncture (a, b) marked with a "X" in Fig. 2.3. A single crossing means that in this space there is only one non-trivial solution of the minimization relation for this region of values of the Lagrange multiplier ζ:

  For $\Lambda_3 < \zeta < \Lambda_1$ the situation is different:

- For $\zeta > \Lambda_3$ the line segment again becomes an ellipse. When ζ increase further, $\Lambda_3 < \zeta < \Lambda_1$, the ellipse shrinks along the m_1 axis and grows along m_3 axis (solid blue and dashed red lines in figure, 2.4).

- At $\zeta = \Lambda_1$ the ellipses collapse to another line segment (dot-dashed black line in figure, 2.4):

$$\mathsf{m}_1 = 0, \;\; |\mathsf{m}_3| \leq \mathsf{m}_3^* = \frac{\Lambda_1 - \Lambda_3}{\Lambda_0 - \Lambda_1} > \mathsf{m}_1^* \tag{2.4.46}$$

- During this evolution, the ellipses sweep a particular area in the $(\mathsf{m}_1, \mathsf{m}_3)$-plane, and each point inside this place is crossed twice (see, for instance, the point marked with a "X"in Fig. 2.4).

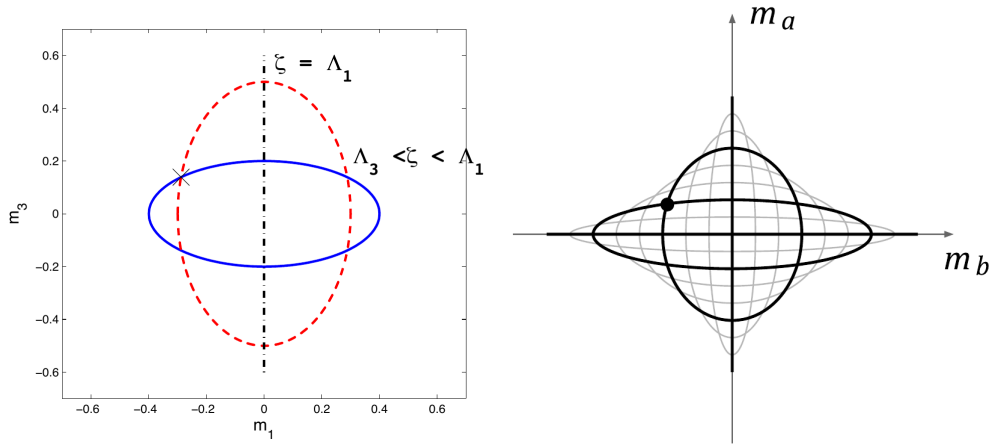

Figure 2.4.: ***(Left)*** *Example of a geometric representation of the ellipse evolution defined by the condition 2.4.21. In this case* $\Lambda_3 < \zeta < \Lambda_1$. ***(Right)*** *Ellipse evolution in arbitrary projection plane for spatial ordering* $\Lambda_a < \Lambda_b < \lambda_c$ *and* $\zeta \in [\Lambda_a, \Lambda_b]$ *[29]*

- Furthermore, it is possible to show (see the following section) that, of these two crossings, one is a critical point labeled as a saddle point and, if we impose further conditions on the parameters, the other can be a minimum.

Finally, when $\Lambda_1 < \zeta < \Lambda_0$, the ellipse grows infinitely (the semi-axes a_1 and a_3 tend to infinity when $\zeta \to \Lambda_0$), and the entire $(\mathsf{m}_1, \mathsf{m}_3)$-plane is covered. But each point of the plane is crossed by an ellipse one single time. And since the last crossing systematics corresponds to the largest value of ζ to yield an extremum, it will lead be the global minimum of the potential. It is worthwhile to emphasize that regardless of whether the latter critical points exist or not, this one is always present in minima structure, and it is the global minimum of the Higgs potential.

All indicates that exists the possibility of two minima. One may lie in the region where $\Lambda_3 < \zeta < \Lambda_1$ (imposing further constraints on the parameters of the potential), another exists (guaranteed) for values of ζ such that $\Lambda_1 < \zeta < \Lambda_0$. By considering the case where $\Lambda_3 > \Lambda_1$, we would have similar conclusions: the figures obtained for that situation would be analogous to those in Fig. 2.3, but rotated by $\pi/2$, and both minima should be found for values of the Lagrange multiplier in the ranges $\Lambda_1 < \zeta < \Lambda_3$ and $\Lambda_3 < \zeta < \Lambda_0$. All is ensuring with two conditions

$$\sqrt[3]{x^2} + \sqrt[3]{y^2} \leq 1 \tag{2.4.47}$$

$$D = \widehat{M}_1 \widehat{M}_3 \widehat{r}_1 \widehat{r}_3 > 0, \tag{2.4.48}$$

Translating into the existence of four normal-stationary points, with one of them being the global minimum of the potential. Making that one of the remaining critical points is the second minimum, we would need additional conditions.

Two neutral minima are a realization if, in the $(\mathsf{m}_1, \mathsf{m}_3)$-plane, the values of the parameters of the Higgs potential are such that we are at a point inside the area covered by intersecting ellipses such as the two shown in Fig. 2.4. The covering region is given by all of those ellipses delimited by the astroid curve given in Eq. (2.4.47)

$$\sqrt[3]{x^2} + \sqrt[3]{y^2} \leq 1 \tag{2.4.49}$$

$$x = \frac{\widehat{M}_1 (\Lambda_0 - \Lambda_3)}{\widehat{M}_0 (\Lambda_3 - \Lambda_1)}, \; y = \frac{\widehat{M}_3 (\Lambda_0 - \Lambda_1)}{\widehat{M}_0 (\Lambda_3 - \Lambda_1)} \tag{2.4.50}$$

To show this, we apply the standard method of finding the envelope of a family of curves. The family of ellipses in question is described by an equation of the form $F(\mathsf{m}_1, \mathsf{m}_3, \zeta) = 0$, and we also need to consider the tangent to these ellipses at each point, determined by $\partial F / \partial \zeta = 0$. Explicitly, the function to solve is the following

$$F(\mathsf{m}_1, \mathsf{m}_3, \zeta) = \frac{\mathsf{m}_1^2}{(\Lambda_1 - \zeta)^2} + \frac{\mathsf{m}_3^2}{(\Lambda_3 - \zeta)^2} - \frac{1}{(\Lambda_0 - \zeta)^2} = 0$$

and the tangent curves

$$\frac{\partial F(\mathsf{m}_1, \mathsf{m}_3, \zeta)}{\partial \zeta} = \frac{2\mathsf{m}_1^2}{(\Lambda_1 - \zeta)^3} + \frac{2\mathsf{m}_3^2}{(\Lambda_3 - \zeta)^3} - \frac{2}{(\Lambda_0 - \zeta)^3} = 0 \tag{2.4.51}$$

To solve these equations, we define the following angles

$$\cos\varphi = \frac{\Lambda_0 - \zeta}{\Lambda_1 - \zeta}\mathsf{m}_1, \quad \sin\varphi = \frac{\Lambda_0 - \zeta}{\Lambda_3 - \zeta}\mathsf{m}_3. \tag{2.4.52}$$

From the second condition (2.4.51) is possible to find out the form of Lagrange multiplier

$$\zeta = \frac{\Lambda_1 \frac{(\Lambda_3 - \Lambda_0)}{(\Lambda_0 - \Lambda_1)} \tan^2\varphi - \Lambda_3}{\left[\frac{(\Lambda_3 - \Lambda_0)}{(\Lambda_0 - \Lambda_1)} \tan^2\varphi - 1\right]}. \tag{2.4.53}$$

and from this result and by defining

$$x = \frac{\Lambda_0 - \Lambda_3}{\Lambda_1 - \Lambda_3}\mathsf{m}_1 \text{ and } y = \frac{\Lambda_0 - \Lambda_1}{\Lambda_3 - \Lambda_1}\mathsf{m}_3. \tag{2.4.54}$$

We can write finally

$$x^{2/3} + y^{2/3} = 1, \tag{2.4.55}$$

which is the boundary of an astroid, associated to combinations of quartic couplings and mass term for Higgs potential.

2.4.4. Metastability condition

The necessary and sufficient conditions for the existence of metastable vacua can be considered by themselves, where is claimed the need to verify whether or not the potential has two minima. To show systematically this fact, let us begin with the case $\Lambda_1 > \{\Lambda_2, \Lambda_3\}$. As we have seen in the previous section, in this situation the several possible stationary points obey the following relations:

- The global minimum (simple minimum) occurs for a value of the Lagrange multiplier, ζ_G , such that $\zeta_G > \Lambda_1 > \Lambda_3$.
- If another local minimum exists, it can only occur for a given value of the Lagrange multiplier, ζ_L , such that $\Lambda_3 < \zeta_L < \Lambda_1$.

  And this is all the information required. Recalling the minimization conditions of the potential (2.4.14), written in terms of the Lagrange multiplier,

$$(\Lambda_0 - \zeta)\,\widehat{r}_0 = \widehat{M}_0, \tag{2.4.56}$$
$$(\Lambda_i - \zeta)\,\widehat{r}_i = \widehat{M}_i, \tag{2.4.57}$$

  at this point we define the following discriminants,

$$D_1 = -\widehat{r}_1\widehat{M}_1, \quad D_3 = -\widehat{r}_3\widehat{M}_3, \; D = D_1 D_3 \tag{2.4.58}$$

  Given the minimization conditions, we can write

$$D_1 = -\widehat{r}_1\widehat{M}_1 = (\zeta - \Lambda_1)\,\widehat{r}_1^2 \tag{2.4.59}$$
$$D_3 = -\widehat{r}_3\widehat{M}_3 = (\zeta - \Lambda_3)\,\widehat{r}_3^2 \tag{2.4.60}$$

  These discriminants can be computed for any minimum, i.e. for any given value of ζ. Then, we see that:

- In the global minimum $\zeta = \zeta_G$.
- Given that $\zeta_G > \Lambda_1 > \Lambda_3$, we will have $D_1 > 0$ and $D_3 > 0$
- Thus, at the global minimum, $D = D_1 D_3 > 0$.
- If the second local minimum exists, it occurs for $\zeta = \zeta_L$
- Since $\Lambda_3 < \zeta_L < \Lambda_1$, we will necessarily have $D_1 < 0$ and $D_3 > 0$.
- Thus, at the local minimum, $D = D_1 D_3 < 0$.

And so we see that the sign of D_1 discriminates between the local and the global minima, while the sign of D_3 does not. If it happens that the potential has only one minimum, it will correspond to the case $D_i > 0$. Also, in the case where $\widehat{M}_0 < 0$ and there is a single minimum with $\zeta_G > \Lambda_0$, already discussed above, both D_1 and D_3 are guaranteed to be positive, given that boundedness from below implies $\Lambda_0 > \{\Lambda_1, \Lambda_3\}$.

Suppose we now have $\Lambda_3 > \Lambda_1$. The demonstration for this case is analogous to the one we have just given, with the following differences: the global minimum is now at $\zeta = \zeta_G > \Lambda_3 > \Lambda_1$; the local minimum, if it exists, corresponds to a Lagrange multiplier $\Lambda_1 < \zeta_L < \Lambda_3$; at the global minimum we will have $D_1 > 0$ and $D_3 > 0$, at the local one $D_1 > 0$ and $D_3 < 0$. Thus, in this case, the sign of D_3 does discriminate between the local and the global minima, but the sign of D_1 does not. In any case, $D = D_1 D_3$ is positive at the global minimum and negative at the local one. In conclusion, the product of D_1 and D_3 is a quantity able to discriminate between the two normal minima. If it is computed at a given minimum and if $D = D_1 D_3 > 0$ is found, that minimum is the global minimum of the potential; $D < 0$, the minimum is local. Thus the conditions are proven:

$$\text{If } \widehat{M}_0 > 0 \text{ and } \sqrt[3]{x^2} + \sqrt[3]{y^2} \leq 1, \text{ with} \tag{2.4.61}$$

$$x = \frac{\widehat{M}_1 (\Lambda_0 - \Lambda_3)}{\widehat{M}_0 (\Lambda_3 - \Lambda_1)},\ y = \frac{\widehat{M}_3 (\Lambda_0 - \Lambda_1)}{\widehat{M}_0 (\Lambda_3 - \Lambda_1)}. \tag{2.4.62}$$

- *Then the potential can have two neutral minima.* To keep the problem in mind, we should like to emphasize that these structures are necessary conditions for the existence of two neutral minima (see a demonstration in Appendix F) - although they are necessary and sufficient conditions for the existence of four normal stationary points. Remarkably, we have a necessary and sufficient condition to verify the global nature of our minimum. to know whether our $\{v_1, v_2\}$ vacuum is the global minimum of the potential, we need only do the following: Let us define a discriminant $D = \widehat{M}_1 \widehat{M}_3 \widehat{r}_1 \widehat{r}_3$, and sweep the parameter space in such a way that $D > 0$.

The systematic for a general case can be a quite more intricate. The following procedure [29] can be used for the most general Higgs potential, where only is involved the computing of eigenvalues of $\Lambda_{\mu\nu}$. Λ_α characterize these eigenvalues, and it is necessary to address which are associated with 0 index. By considering the following projector operator, one for each eigenvalue Λ_α of Λ_{diag}

$$\left(\widehat{P}^\alpha\right)_{\mu\nu} = \prod_{\beta \neq \alpha} \frac{1}{\Lambda_\alpha - \Lambda_\beta} \left(\Lambda_{\mu\nu} - \Lambda_\beta g_{\mu\nu}\right), \tag{2.4.63}$$

- obeying (for $\Lambda_\alpha \in \mathbb{R}$) properties for a projection operator

$$\widehat{P}^\alpha \widehat{P}^\beta = \delta_{\alpha\beta} \widehat{P}^\alpha \text{ and } \sum_\alpha \widehat{P}^\alpha = 1.$$

$\widehat{P}$ is the projection operator into the subspace generated by the eigenvector corresponding to Λ_α. Projection operators are symmetric in the indexes μ, ν. For example for an arbitrary four vector $(l^\mu = (1,0,0,0))$. The new vector

$$l^0_\nu = \left(\widehat{P}^0\right)_{\nu\mu} l^\mu,$$

lies along the eigenvector of Λ_0, and, thus, it is timelike:

$$0 < \left(l^0\right)^\nu l^0_\nu = l^{\mu'} \left(\widehat{P}^0\right)^\nu_{\mu'} \left(\widehat{P}^0\right)_{\nu\mu} l^\mu = l^{\mu'} \left(\widehat{P}^0\right)_{\mu'\mu} l^\mu.$$

Similarly,

$$l^k_\nu = \left(\widehat{P}^k\right)_{\nu\mu} l^\nu.$$

for $k = 1, 2, 3$ lies along the eigenvector of Λ_k, and thus, it is spacelike:

$$\left(l^k\right)^\nu l^k_\nu = l^{\mu'} \left(\widehat{P}^k\right)_{\mu'\mu} l^\mu < 0.$$

This relation is true for any vector l^μ, apart, of course, from the case when the vector is accidentally chosen to be orthogonal to some eigenvector. Choosing the simplest case for $l^\mu = (1,0,0,0)$, means of

$$s_\alpha = \text{sign}\left[\left(\widehat{P}^\alpha\right)_{00}\right].$$

which is positive if and only if $\alpha = 0$. Hence s_α will be positive for only one value of α; the corresponding eigenvalue is the time-like Λ_0. Now from Higgs potential with auxiliary function given in (2.4.14) and minimizing it with respect to r^μ and ζ, yielding the same relation in (2.4.15)

$$\Lambda^\mu{}_\nu r^\nu - M^\mu = \zeta r^\mu$$

Any component of this relation can be used to compute the auxiliary function ζ. In any neutral stationary point ζ is connected with charged Higgs mass by

$$m^2_{H^\pm} = \zeta v^2$$

Our new discriminant is given by

$$D = -\det\left(\Lambda_E - \zeta 1\right)$$

where 1 is the four dimensional identity matrix. Writing Λ_E in the diagonal basis,

$$D = (\Lambda_0 - \zeta)(\zeta - \Lambda_1)(\zeta - \Lambda_2)(\zeta - \Lambda_3)$$

If $D > 0$ is ensured a global minimum in the Higgs potential (see Appendix I). For negative $D < 0$ scenario, excluding negative cases for eigenvalues of Λ_E and from stability conditions for "covariant" Higgs potential; for a global minimum it is needed that

$$\zeta > \Lambda_0$$

2.5. Comments and remarks about vacuum structures and stability

Vacuum behavior at tree level in SM is determined by the behavior of a Higgs potential structure, and just one stationary point enables few properties; where only a normal configuration for vacuum and $\lambda > 0$ condition define its original nature completely. The first feature is a consequence of the gauge invariance of the EW theory and the scheme of SSB, which lead to absorb vacuum phases. By contrast, in 2HDMs exist new vacuum configurations besides to the normal one, the CP and charge breaking structures. The appropriate choice of the initial free parameters can be used to eliminate both possibilities, even the CP breaking vacua connected with spontaneous symmetry breaking in the theory. Then departure of this condition will be a valuable tool to study new sources of CP violation and processes with, e.g. in baryogenesis or leptogenesis mechanisms.

Nevertheless in 2HDMs, it is possible to show that two minima of different nature can not coexist. These minima are related to the spontaneous breaking of various symmetries in the Higgs potential. Furthermore from CP and charge breaking minima, there is no possible to have two simultaneous solutions for stationary and minimum equations. This scenario is the contrary case for the Higgs potential for normal vacua, where high order equations for stationary points lead to having two possible normal vacua of different depths. In this configuration, EW fields properties like gauge bosons, or fermion masses could not be the same. This point would be a central framework for the remainder discussions evaluating the vacuum behavior and scenarios for the stability of the Higgs potential.

On the other hand, the extension of the scalar sector yields to analyze new directions in the field space where possible vacuum instabilities might arise. By using a reparameterization invariance $SL(2, C)$ where the doublets can be organized in a gauge orbit space of the scalar sector of 2HDM, it is straightforward to establish general sufficient conditions to ensure a bounded from below Higgs potential [36]. The same formalism allows determining whether potential might have metastable zones even at tree level. We would implement all these concepts to constrain the parameter in the Higgs potential as well as possible phenomenology belongs in different model-realizations. Before to do that, we must investigate and to clarify the role of the constraints for the Higgs potential stability and metastability (improved from tree-level analysis) at higher perturbative orders. This fact is the primary goal for the following chapter.

3. One loop effects over vacuum stability

Once motivated the study of fundamentals of extended Higgs sectors as 2HDMs from symmetries point of view and study of vacuum structure in the previous chapters, henceforth we shall focus on the one loop effects over Higgs potential. Now since phenomenology over Higgs mass from LHC seem to indicate the existence of Metastability vacuum for SM; we should study the possibility of having additional scalar fields leads to new stability regimes (evaluated from EW scale) for an extended Higgs potential with initial conditions defined in m_Z scale. Behind of this statement, which could relate initial conditions for different couplings between SM and 2HDMs, is the *Minimality Principle* for extended Higgs sectors: Physics from SM and 2HDM is connected with the same energy scale (i.e. scale for electroweak effects).

The vacuum behavior at NLO gives us the way in which RG flow leads to instabilities in all sectors as well as the phenomenology arising in 2HDMs might be constrained.

3.1. Radiative corrections forms for 2HDMs

In this section, we summarize the full mathematical origin of RGEs at one loop level for the Two Higgs Doublet Model. Although many articles have shown how these RGE could be obtained [113, 120–127], we introduce valuable comments and the relevant diagrams to understand the origin of the respective contributions and their influence on vacuum stability behavior of the Higgs potential.

As a general point of view, we know that the RGE are first-order differential equations which give the evolution of the couplings of a model defined at tree level and relative to $t = \ln \mu$. Here μ is the mass parameter used in the dimensional regularization of ultraviolet-divergent integrals in four dimensions. These standard integrals are based on Passarino-Veltmann structures $A_0(m_0)$, $B\left(p^2, m_1, m_2\right)$, $C\left(p_1, p_2, m_1, m_2, m_3\right)$ and $D\left(p_1, p_2, p_3, m_1, m_2, m_3, m_4\right)$ defined in D-dimensions by

$$A_0\left(m_0\right) = \int \frac{d^D q}{\left(q^2 - m_0^2 + i\epsilon\right)} \tag{3.1.1a}$$

$$B_{0;\mu;\mu\nu}\left(p_1, m_1, m_2\right) = \int \frac{d^D q}{\left(q^2 - m_1^2\right)} \frac{1; q_\mu; q_\mu q_\nu}{\left[(q+p_1)^2 - m_2^2\right]} \tag{3.1.1b}$$

$$C_{0;\mu;\mu\nu;\mu\nu\alpha}\left(p_1, p_2, m_1, m_2, m_3\right) = \int \frac{d^D q}{\left(q^2 - m_1^2\right)} \frac{1; q_\mu; q_\mu q_\nu; q_\mu q_\mu q_\alpha}{\left[(q+p_1)^2 - m_2^2\right]\left[(q+p_1+p_2)^2 - m_3^2\right]} \tag{3.1.1c}$$

$$D_{0;\mu;\mu\nu;\mu\nu\alpha;\mu\nu\alpha\beta}\left(p_1, p_2, p_3, m_1, m_2, m_3, m_4\right) = \int \frac{d^D q}{\left(q^2 - m_1^2\right)} \frac{1; q_\mu; q_\mu q_\nu; q_\mu q_\nu q_\alpha; q_\mu q_\nu q_\alpha q_\beta}{\left[(q+p_1)^2 - m_2^2\right]\left[(q+p_1+p_2)^2 - m_3^2\right]\left[(q+p)^2 - m_4^2\right]} \tag{3.1.1d}$$

In all integrals, we have factorized out $\kappa = (2\pi\mu)^\epsilon / i\pi^2$. Here p_i are typical momenta (all incoming in vertices) and m_i are typical masses defining in the loops, and $\epsilon = 4 - D$. In the last integral $p = p_1 + p_2 + p_3$. To describe the solution of these standard integrals, it is useful to know the divergent part of the Passarino-Veltmann scalar forms:

$$\mathrm{Div} A_0\left(m_0\right) = \Delta_\epsilon m_0^2 \tag{3.1.2a}$$

$$\mathrm{Div} B_0\left(p, m_1, m_2\right) = \Delta_\epsilon \tag{3.1.2b}$$

$$\mathrm{Div} C_{00}\left(p_1, p_2, m_1, m_2, m_3\right) = \frac{\Delta_\epsilon}{4} \tag{3.1.2c}$$

$$\mathrm{Div} D_{0000}\left(p_1, p_2, p_3, m_1, m_2, m_3, m_4\right) = \frac{\Delta_\epsilon}{24} \tag{3.1.2d}$$

where $\Delta_\epsilon = 2/\epsilon - \gamma_E + \ln 4\pi$. Some specific results for integrals are[1]

[1]The finite result for the integral in B function in the case of equal masses is

$$\int_0^1 dx \ln\left[\frac{-x(1-x)p^2 + xm^2 + (1-x)m^2}{\mu^2}\right] = \ln\frac{m^2}{\mu^2} + \frac{\sqrt{4m^2 - p^2}}{p} \arctan\left(\frac{p}{\sqrt{4m^2 - p^2}}\right) - 2 \tag{3.1.3}$$

$$A_0\left(m_0^2\right) = m_0^2\left(\Delta_\epsilon + 1 - \ln\frac{m_0^2}{\mu^2}\right) \tag{3.1.4a}$$

$$B_0\left(p, m_1, m_2\right) = \Delta_\epsilon - \int_0^1 dx \ln\left[\frac{-x(1-x)p^2 + xm_2^2 + (1-x)m_1^2}{\mu^2}\right] \tag{3.1.4b}$$

For three point and four point explicit reductions, the reader can found them in the reviews [128, 129]. Our discussion focuses on obtaining coefficients of logarithmic dependence of energy scale μ, for counterterms gotten in the renormalization procedure. β functions can be achieved indeed by derivating these conterterms with respect to μ, i.e.,

$$\beta_i = \mu\frac{\partial\delta_i}{\partial\mu} \equiv \kappa_i \tag{3.1.5}$$

with κ_i the coefficient product of respective couplings and multiplicity factor for each NLO contribution. In practice, β functions encode different infinitesimal RG transformations. It is worthwhile point out that these beta functions are only functions of the couplings themselves and only depend on the energy scale implicitly through the couplings. The one loop β-functions in 2HDM are also discussed employing an algebraic procedure in appendix J.

3.2. Formal definitions from 2HDM-fundamentals

To determine the form of the one-loop contributions, we discuss the structure of the entire scalar sector, quoting relevant results presented in chapter 1. Let the scalar potential (1.2.1) written in a compact form (1.2.2),

$$V = \sum_{j,k}\mu_k^j\left(\Phi_j^\dagger\Phi_k\right) + \frac{1}{2}\sum_{j,k,l,m}\Lambda_{km}^{jl}\left(\Phi_j^\dagger\Phi_k\right)\left(\Phi_l^\dagger\Phi_m\right). \tag{3.2.1}$$

The following properties are satisfied by the coefficients Λ_{km}^{jl} and μ_k^j

$$\Lambda_{km}^{jl} = \Lambda_{mk}^{lj};\;\; \Lambda_{km}^{jl} = \left(\Lambda_{jl}^{km}\right)^*;\;\; \mu_{jk} = \left(\mu_{kj}\right)^* \tag{3.2.2}$$

The last two conditions are consequences of the Higgs potential hermiticity. The kinetic sector described in section (1.1) is

$$\mathcal{L}_K = \sum_{k=1}^{n_H=2}\left(D_\mu\Phi_k\right)^\dagger\left(D^\mu\Phi_k\right). \tag{3.2.3}$$

The covariant derivative is for $SU\left(2\right)_L \times U\left(1\right)_Y$ standard model

$$D_\mu = \partial_\mu - ig\tau_i W_\mu^i - \frac{ig'}{2}YB_\mu. \tag{3.2.4}$$

where τ_i are the generators of $SU\left(2\right)$ group with associated gauge fields W_μ^i. B_μ is the four-vector field associated to the Y generator i.e. the $U(1)_Y$ symmetry. g and g' are coupling strengths associated to W_μ^i and B_μ respectively. Here W_μ^i and B_μ are gauge eigenstates. Expanding the kinetic Lagrangian, we get

$$\begin{aligned}
\sum_k\left(D_\mu\Phi_k\right)^\dagger\left(D^\mu\Phi_k\right) &= \left(\partial_\mu\Phi_k - ig\tau_i W_\mu^i\Phi_k - \frac{ig'}{2}YB_\mu\Phi_k\right)^\dagger\left(\partial^\mu\Phi_k - ig\tau_i W^{i\mu}\Phi_k - \frac{ig'}{2}YB^\mu\Phi_k\right)\\
&= \left(\partial_\mu\Phi_k\right)^\dagger\left(\partial_\mu\Phi_k\right) - \left(\partial_\mu\Phi_k\right)^\dagger\left(ig\tau_i W^{i\mu}\Phi_k\right) - \frac{1}{2}\left(\partial_\mu\Phi_k\right)^\dagger\left(ig'YB^\mu\Phi_k\right)\\
&\quad - \left(ig\tau_i W_\mu^i\Phi_k\right)^\dagger\left(\partial^\mu\Phi_k\right) + \left(ig\tau_i W_\mu^i\Phi_k\right)^\dagger\left(ig\tau_i W^{i\mu}\Phi_k\right) + \frac{1}{2}\left(ig\tau_i W_\mu^i\Phi_k\right)^\dagger\left(ig'YB^\mu\Phi_k\right)\\
&\quad - \frac{1}{2}\left(ig'YB_\mu\Phi_k\right)^\dagger\left(\partial^\mu\Phi_k\right) + \frac{1}{2}\left(ig'YB_\mu\Phi_k\right)^\dagger\left(ig\tau_i W^{i\mu}\Phi_k\right) + \frac{1}{4}\left(ig'YB_\mu\Phi_k\right)^\dagger\left(ig'YB^\mu\Phi_k\right)
\end{aligned} \tag{3.2.5}$$

which is valid in the region $p^2 < 4m^2$.

This sector endows the gauge bosons with mass and provides the interactions among gauge and Higgs bosons. Moreover, this part of the Lagrangian is invariant under charge conjugation as well as under CP and Higgs family symmetries.

The most generic Yukawa interactions for 2HDM, in a compact form by, is

$$\mathcal{L}_Y = -\sum_{j=1}^{2}\left[\bar{Q}_L\left(\Phi_j Y_j^d D_R + \tilde{\Phi}_j Y_j^u U_R\right) + \bar{L}_L \Phi_j Y_j^e E_R\right] + h.c. \tag{3.2.6}$$

Quoting the discussion presented in section 1.3, $\widetilde{\Phi}_j = i\tau_2\Phi_j^*$; Q_L (quark doublet), L_L (lepton doublet), D_R (negative charged quarks), U_R (positively charged quarks) and E_R (negatively charged leptons) are 3-vector in flavor space. For simplicity, we have not included the neutrino sector by their smallness mass size. Although this condition might be relaxed through different mechanisms explaining hierarchical structure among leptons, e.g., the neutrino-specific model[2] [68,130] . Besides, $Y_j^{d,u,e}$ are generic 3×3 complex matrices containing the Yukawa couplings, for the down, up and leptonic sector respectively.

To conserve generality in our procedure, we construct radiative corrections in term of all these structures for couplings (build up with gauge invariance). When scalar and fermionic doublets are expressed regarding physical fields (i.e. eigenstates mass), diagrammatic must be agree with charge conservation and momentum flux in each vertex. This general systematics is consistent in the UV-limit of integrals, where we are interested in to compute the scale dependence of contributions.

3.2.1. RGEs for scalar couplings

Some comments about the structure of the respective conterterms should be made. The first one is that the Feynman rules used come from the general Lagrangian written as gauge invariant terms. As mass eigenstates were not used, the dimensional regularization required a regulator function (treated as a mass scale) in the propagators. The last fact is to get the own energy dependence of the conterterm and thus the respective RGEs. Also, the regularized diagrams are those fields inside doublets in every possible parameterization compatible with charge and momentum fluxes in each vertex.

The one-loop RG equations for the quartic couplings are [131]

$$16\pi^2\frac{d\Lambda_{km}^{jl}}{dt} \equiv \mathcal{D}\Lambda_{km}^{jl} = I_S + I_G + I_{EG} + I_F + I_{EF}. \tag{3.2.7}$$

The I_S is a contribution for pure scalar loops, I_G for gauge loops, I_{EG} is the external scalar lines correction by gauge bosons, I_F is the contribution by fermion boxes and I_{EF} is the correction to the scalar external lines by fermion loops. Contributions I_S, I_G and I_{EG} are based mainly on integrals reduction given by $B-$integrals of Eq. (3.1.1b). Meanwhile, I_F contributions are based on the reducing from D-functions quoted in (3.1.1d).

We shall examine term by term in RGEs explicitly. The scalar loop contribution (s,t,u channels) I_S contains the following structure:

$$I_S = 2\sum_{p,q=1}^{n_H}\left(2\Lambda_{kq}^{jp}\Lambda_{pm}^{ql} + \Lambda_{kq}^{jp}\Lambda_{pm}^{lq} + \Lambda_{qk}^{jp}\Lambda_{pm}^{ql} + \Lambda_{mp}^{qj}\Lambda_{kq}^{pl} + \Lambda_{km}^{pq}\Lambda_{pq}^{lj}\right). \tag{3.2.8}$$

where the first three terms come from the s channel. The fourth term originates from the t channel, while the fifth term derives from the u channel. These contributions are shown in the Figure 3.1. The overall factor is due to the renormalization procedure. The element 2 in front of $\Lambda_{kq}^{jp}\Lambda_{pm}^{ql}$ coupling appears by the multiplicity generated inside of the scalar loop.

I_G are the contributions by gauge bosons in the loops:

$$I_G = \frac{9g^4 + 3g^{'4}}{4}\delta_k^j\delta_m^l + 3g^2g^{'2}\left(\delta_m^j\delta_k^l - \frac{1}{2}\delta_k^j\delta_m^l\right). \tag{3.2.9}$$

From kinetic Lagrangian of (3.2.5), we extract the quartic interactions among scalar and gauge bosons

[2] In this simple model, Dirac neutrinos are coupled to one doublet (e.g. Φ_1) and the remaining leptons are coupled to another doublet (Φ_2), the same that quark sector couples. The small size of neutrino masses is given by choice of a small VEV for the doublet that couples with neutral leptons [56]. Most sophisticated models based on this structure must introduce plausible mechanisms to explain naturalness and hierarchy structure for masses, which carry out to build models compatible with neutrino oscillation measurements.

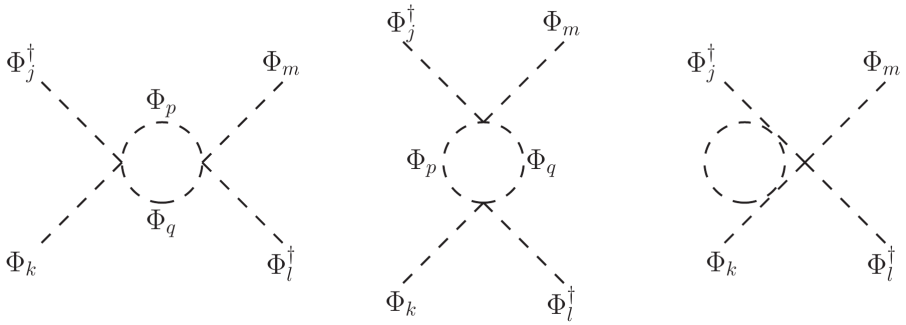

Figure 3.1.: *Scalar (with s, t, u channels) corrections at one loop level to quartic couplings in the Higgs potential. Couplings among physical scalars of the doublets are done in consistency with charge conservation in each vertex.*

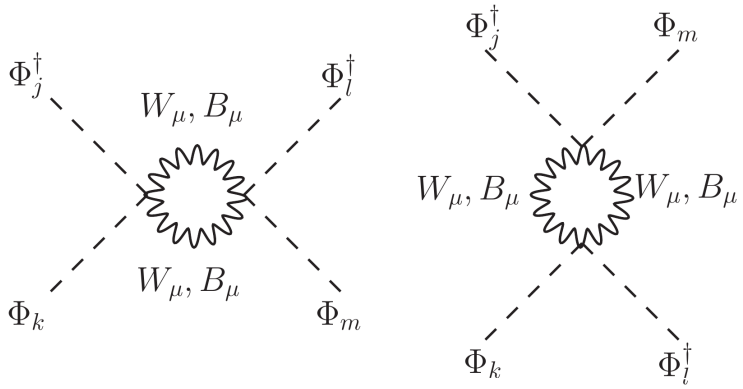

Figure 3.2.: *Gauge bosons (s, t-channels) corrections at one loop level to quartic couplings from the kinetic sector (regarding gauge eigenstates). The t channel is due to the W^μ and B_μ loop. Couplings among physical scalars of the doublets and gauge bosons are done in consistency with charge conservation in each vertex.*

$$\begin{aligned}\mathcal{L}_G &= \left(ig\tau_i W^i_\mu \Phi_k\right)^\dagger \left(ig\tau_i W^{i\mu}\Phi_k\right) + \frac{1}{2}\left(ig\tau_i W^i_\mu \Phi_k\right)^\dagger \left(ig' Y B^\mu \Phi_k\right) \\ &+\frac{1}{2}\left(ig' Y B_\mu \Phi_k\right)^\dagger \left(ig\tau_i W^{i\mu}\Phi_k\right) + \frac{1}{4}\left(ig' Y B_\mu \Phi_k\right)^\dagger \left(ig' Y B^\mu \Phi_k\right) \end{aligned} \tag{3.2.10}$$

Since the form of the interactions among scalars doublets and gauge bosons, the $u-$channel vanishes. On the other hand, interactions from the contribution for the right figure are

$$\begin{aligned}\text{s-channel:} \quad & \eta_p \left(ig\tau_i W^i_\mu \Phi_j\right)^\dagger \left(ig\tau_i W^{i\mu}\Phi_k\right) \delta^j_k \left(ig\tau_a W^a_\mu \Phi_l\right)^\dagger \left(ig\tau_a W^{a\mu}\Phi_m\right) \delta^l_m \\ = \; & g^4 \eta_p \left[\Phi^\dagger_j \left(W^i_\mu\right)^\dagger \left(\tau^\dagger_i \tau_i\right) \left(W^{i\mu}\right) \Phi_k\right] \delta^j_k \left[\Phi^\dagger_l \left(W^a_\mu\right)^\dagger \tau^\dagger_a \tau_a \left(W^{a\mu}\right) \Phi_m\right] \delta^l_m \\ = \; & \frac{3\eta_p g^4}{16} \left[\Phi^\dagger_j \left(W^i_\mu\right)^\dagger \left(W^{i\mu}\right) \Phi_k\right] \delta^j_k \left[\Phi^\dagger_l \left(W^i_\mu\right)^\dagger \left(W^{i\mu}\right) \Phi_m\right] \delta^l_m \end{aligned}$$

η_p are the polarization degrees of freedom for gauge bosons. Moreover, from renormalization procedure, we find an additional factor of two. For the second rule $\left(W_\mu W^\mu \Phi^\dagger_j \Phi_k\right)$

$$\begin{aligned}\text{s-channel:} \quad & \frac{1}{2}\eta_p \left(ig\tau_i W^i_\mu \Phi_j\right)^\dagger \left(ig' Y B^\mu \Phi_k\right) \frac{1}{2}\left(ig\tau_i W^i_\mu \Phi_l\right)^\dagger \left(ig' Y B^\mu \Phi_m\right) \\ \text{t-channel:} \quad & \frac{1}{2}\eta_p \left(ig' Y B_\mu \Phi_j\right)^\dagger \left(ig\tau_i W^{i\mu}\Phi_k\right) \left(ig\tau_i W^i_\mu \Phi_l\right)^\dagger \left(ig' Y B^\mu \Phi_m\right) \\ \text{s}+\text{t channels} \; = \; & \frac{1}{16}\eta_p g^2 g'^2 \left[\Phi^\dagger_j \left(W^i_\mu\right)^\dagger B^\mu \Phi_k \Phi^\dagger_l B^\dagger_\mu W^{i\mu}\Phi_m\right] \delta^j_k \delta^l_m \\ + \; & \frac{1}{16}\eta_p g^2 g'^2 \left[\Phi^\dagger_j B^\dagger_\mu W^{i\mu}\Phi_k \Phi^\dagger_l \left(W^i_\mu\right)^\dagger B^\mu \Phi_m\right] \delta^l_k \delta^j_m \end{aligned}$$

Hence the contribution due to one W and one B fields inside the loop is finally

$$\text{s}+\text{t-channel: } 3g^2 g'^2 \delta^l_k \delta^j_m - \frac{3}{2} g^2 g'^2 \delta^j_k \delta^l_m \tag{3.2.11}$$

For the third rule $\left(B_\mu B^\mu \Phi^\dagger_j \Phi_k\right)$, it is possible to get

$$\text{s-channel: } \frac{\eta_p g'^4 Y^4}{16} \left(B_\mu \Phi_j\right)^\dagger \left(B^\mu \Phi_k\right) \left(B_\mu \Phi_l\right)^\dagger \left(B^\mu \Phi_m\right) \tag{3.2.12}$$

Therefore, the coefficients associated are a consequence of the gauge structure of the standard model and the multiplicity inside of the loop due to the gauge bosons.

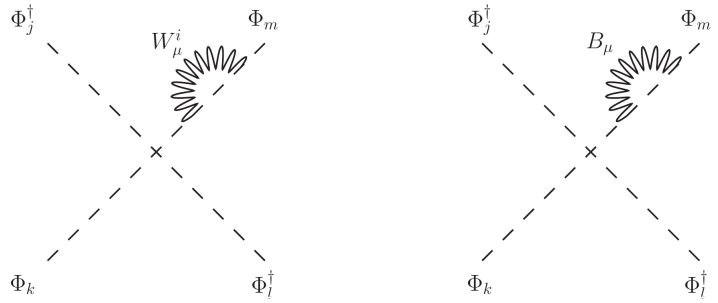

Figure 3.3.: *External corrections at one loop level to the scalar legs from gauge bosons (gauge eigenstates). Couplings among physical scalars of the doublets and gauge bosons are settled respecting charge conservation in each vertex.*

On the other side I_{EG} are the external corrections to the legs due to gauge bosons (Fig. 3.3):

$$I_{EG} = -\left(3\eta_p g^2 + \eta_p g'^2\right)\Lambda^{jl}_{km} \tag{3.2.13}$$

The first factor of three appears by the number of gauge of bosons, i.e. the number of group $SU(2)$ generators. These terms come from the Lagrangian (which describes the interactions among two scalar doubles and one gauge bosons)

$$\mathcal{L} = -\left(\partial_\mu \Phi_k\right)^\dagger \left(ig\tau_i W^{i\mu}\Phi_k\right) - \left(ig\tau_i W^i_\mu \Phi_k\right)^\dagger \left(\partial^\mu \Phi_k\right) - \frac{1}{2}\left(\partial_\mu \Phi_k\right)^\dagger \left(ig' Y B^\mu \Phi_k\right) - \frac{1}{2}\left(ig' Y B_\mu \Phi_k\right)^\dagger \left(\partial^\mu \Phi_k\right) \tag{3.2.14}$$

For fermions we get the box contributions (N_c is the number of colors)

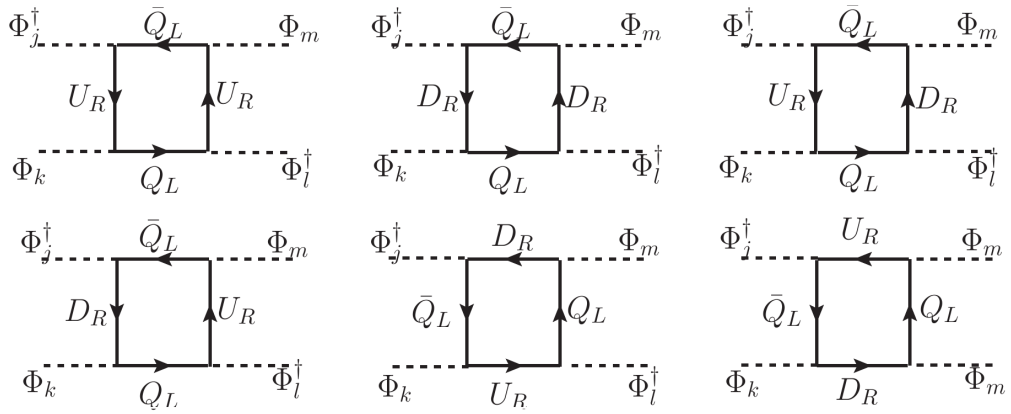

Figure 3.4.: *Fermion box corrections to quartic couplings. The contributions come from the general Yukawa couplings written regarding gauge eigenstates. Couplings between fermions and scalars presented by the specific components are respecting charge conservation in each vertex.*

$$\begin{aligned} I_{F_Q} \;=\; & -4N_c \mathrm{Tr}\left[Y_j^{d\dagger} Y_k^d Y_l^{d\dagger} Y_m^d + Y_k^{u\dagger} Y_j^u Y_m^{u\dagger} Y_l^u + Y_j^{d\dagger} Y_l^u Y_m^{u\dagger} Y_k^d \right. \\ & \left. + Y_k^{u\dagger} Y_m^d Y_l^{d\dagger} Y_j^u - Y_m^{u\dagger} Y_k^d Y_l^{d\dagger} Y_j^u - Y_j^{d\dagger} Y_l^u Y_k^{u\dagger} Y_m^d\right]. \end{aligned}$$

Likewise for leptons, we can obtain in a similar way

$$I_{F_l} = -4\mathrm{Tr}\left[Y_j^{e\dagger} Y_k^e Y_l^{e\dagger} Y_m^e\right]. \tag{3.2.15}$$

For fermion external legs corrections

$$I_{EF} = \sum_{p=1}^{2}\left(T_{mp}\Lambda^{jl}_{kp} + T_{kp}\Lambda^{jl}_{pm} + T^*_{jp}\Lambda^{pl}_{km} + T^*_{lp}\Lambda^{jp}_{km}\right). \tag{3.2.16}$$

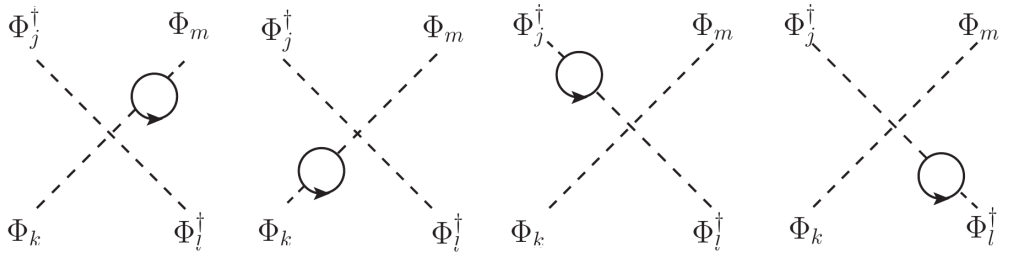

Figure 3.5.: *External corrections to scalar doublets from fermion loops. These contributions have been written regarding the gauge eigenstates of the Yukawa sector. Couplings among components of Higgs doublets with fermion doublets and fermion singlets respect charge conservation.*

with T_{ij} terms for traces with Yukawa couplings for quarks and leptons

$$T_{ij} = N_c \mathrm{Tr}\left[Y_i^{u\dagger} Y_j^u + Y_i^{d\dagger} Y_j^{d\dagger}\right] + \mathrm{Tr}\left[Y_i^{e\dagger} Y_j^e\right] \tag{3.2.17}$$

3.3. RGEs for Yukawa couplings

To find the RGEs for Yukawa coupling at one loop, we need to compute the three point Green function $G^{(3)}$. Taking propagator corrections into account, the full connected Green's function, at one loop level, has the overall form

$$G^{(3)} = \begin{pmatrix} \text{tree level} \\ \text{diagram} \end{pmatrix} + \begin{pmatrix} \text{external leg} \\ \text{corrections} \end{pmatrix} + \begin{pmatrix} \text{1PI loop} \\ \text{diagrams} \end{pmatrix} + \begin{pmatrix} \text{vertex} \\ \text{counterterm} \end{pmatrix}. \tag{3.3.1}$$

We often use the modified minimal subtraction; wherein one absorbs the divergent part plus a universal constant (which always arises along with the divergence in Feynman diagram calculations) into the counterterms. The contribution of three points structure is based on C-functions (3.1.1c) reduction.

In analogy with scalar couplings, the RGEs associated to the different Yukawa couplings can be written by

$$16\pi^2 \frac{dY}{dt} \equiv \mathcal{D}Y = \mathcal{Y}_{EL} + \mathcal{Y}_{EF} + \mathcal{Y}_V + \mathcal{Y}_G. \tag{3.3.2}$$

Here $\mathcal{Y}_{\mathcal{EL}}$ are the external corrections for scalars with fermionic loops. $\mathcal{Y}_{\mathcal{EF}}$ are the external corrections from fermionic legs with a scalar field. $\mathcal{Y}_{\mathcal{V}}$ are the vertex corrections to the respective Yukawa couplings. $\mathcal{Y}_{\mathcal{G}}$ are the contribution due to gauge bosons, whose contribution is the same of SM. The external corrections for scalars from fermionic loops $\mathcal{Y}_{\mathcal{EL}}$ in the scalar part are depicted in Fig. 3.6.

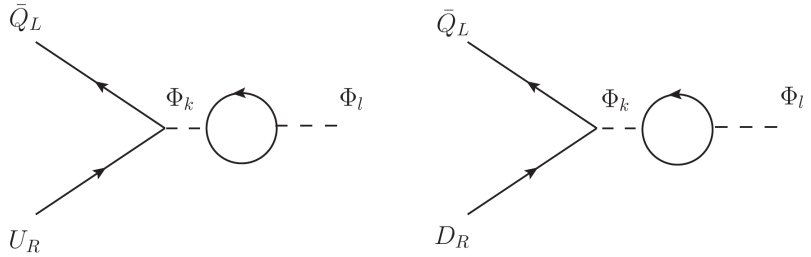

Figure 3.6.: *Diagrams contributing to the external corrections to the quarks Yukawa couplings from fermionic loops. Inside the fermionic loops exist contributions from quarks up and down, as well as charged leptons. Couplings among components of Higgs doublets with fermion doublets and fermion singlets respect charge conservation in each vertex.*

This part has been extrapolated from the analogous part in the correction of the quartic part of the Higgs potential presented in Eq. (3.2.16). In the fermionic loops exist contributions for quarks type up, down and leptonic sectors:

$$\mathcal{Y}_{EL} = \sum_{i=1}^{2} T_{ik} Y_k. \tag{3.3.3}$$

with

$$T_{ik} = N_c \mathrm{Tr}\left[Y_i^{u\dagger} Y_j^u + Y_i^{d\dagger} Y_j^{d\dagger}\right] + \mathrm{Tr}\left[Y_i^{e\dagger} Y_j^e\right]. \tag{3.3.4}$$

The external corrections for scalar doublets in the doublet and singlet parts are displayed in Fig. 3.7; which are part of the contribution $\mathcal{Y}_{EF}$ in the general RGE (3.3.2).

For Yukawa couplings renormalization, the external legs corrections have the contributions of the fermion field renormalization with diagrams (for instance D_R and U_R evolution) shown in the Figure 3.8. Moreover, we have the right part for both contributions (up and down singlets). The respective β function for these diagrams is

$$\beta_1 = 2 Y_k Y_k^\dagger \frac{1}{(4\pi)^2}. \tag{3.3.5}$$

Hence the respective contributions are namely

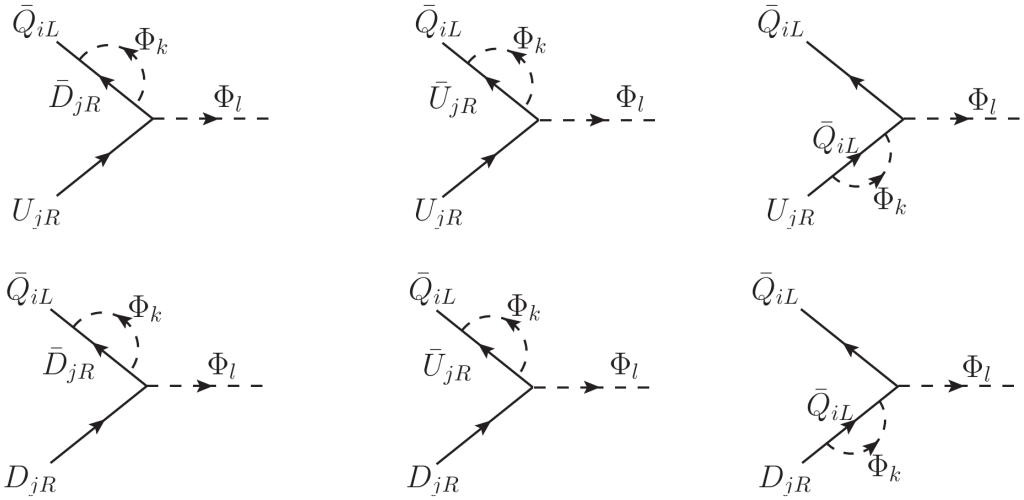

Figure 3.7.: *External corrections to the fermionic legs for up and down sectors from scalar doublets contributions. Couplings among components of Higgs doublets with fermion doublets and fermion singlets respect charge conservation in each vertex.*

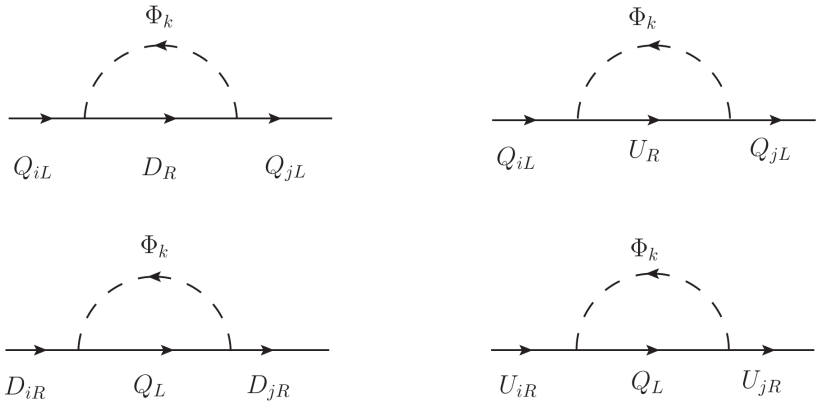

Figure 3.8.: *Analysis for external corrections (Fig. 3.7) to the fermionic (doublets and singlets respectively) part of the Yukawa couplings. Couplings among components of Higgs doublets with fermion doublets and fermion singlets respect charge conservation in each vertex.*

$$\mathcal{Y}_{EF} = \frac{1}{2} Y_j^d \sum_{k=1}^{2} \left(Y_k^u Y_k^{u\dagger} + Y_k^d Y_k^{d\dagger} \right) + \sum_{k=1}^{2} Y_k^d Y_k^{d\dagger} Y_j^d . \tag{3.3.6}$$

The 1PI diagrams for Y_l^d and Y_l^u vertices come from Figure 3.9. When the evolution in the RGE is for the Yukawa coupling Y_l^u (Y_l^d), the diagrams for up (down) type singlet inside the loop vanish by symmetry in the Yukawa couplings and their Hermitian conjugate. In other words, this contribution is antisymmetric to the exchange of two Yukawa couplings.

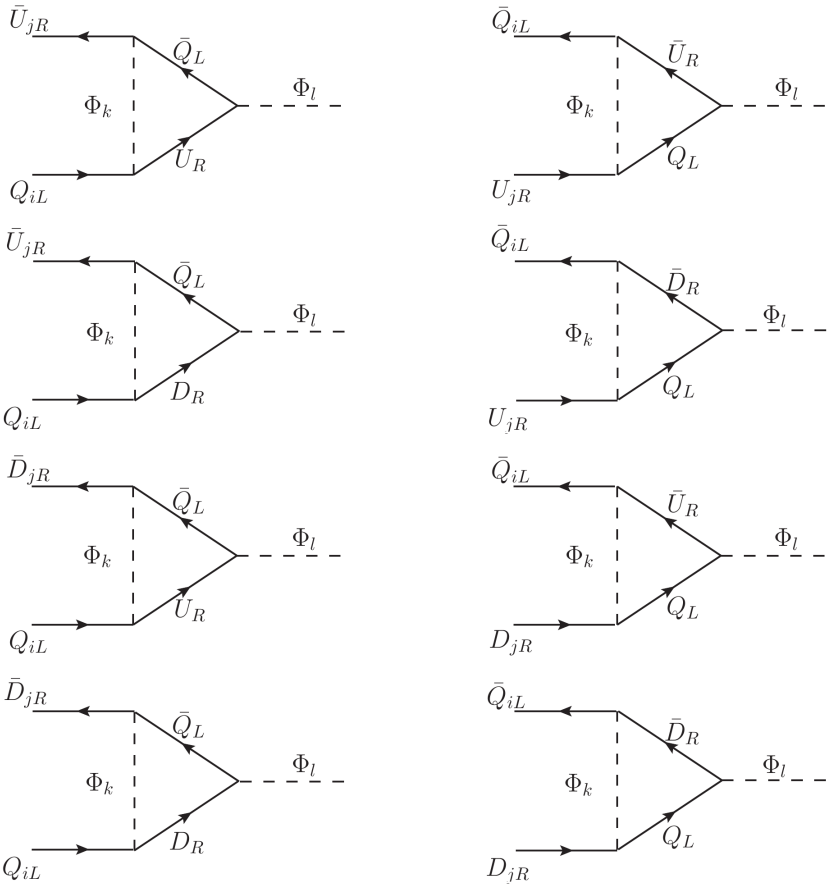

Figure 3.9.: *1PI vertex correction to Yukawa couplings for up and down quarks respectively. Topologies can also be extrapolated to the lepton sector in the massless neutrino regime. Couplings among components of Higgs doublets with fermion doublets and fermion singlets are in consistency with charge conservation in each vertex.*

In the same way, for $Y_l^{u(d)}$ vertex the contributions of up (down) type singlet have to vanish. This sector is represented by Y_V in the RGE (3.3.2). For leptons, due to there are no right-handed neutrinos in the EW scale at least, these kind of diagrams are not present in the 2HDM. The β_Y function associated to those diagrams is

$$\beta_Y = \frac{\partial}{\partial \ln M} \delta_Y = -2 Y_k Y_l^\dagger Y_k \frac{1}{(4\pi)^2} . \tag{3.3.7}$$

The contribution only from quarks up as external legs (first four diagrams left to right and up to down in Fig. 3.9)

$$\mathcal{Y}_V^u = -2 \sum_{k=1}^{2} \left(Y_k^u Y_j^{u\dagger} Y_k^u + Y_k^d Y_k^{u\dagger} Y_j^d \right) . \tag{3.3.8}$$

For down quarks in the external legs (later four diagrams left to right and up to down in Fig. 3.9), it is only necessary to change $u \leftrightarrow d$ in the product of Yukawa couplings [132]. Finally, we discuss how to get contributions to the β function

from couplings with the electroweak gauge bosons and gluons. Extrapolating the analog SM sector, we can write gauge interactions with fermions through

$$\begin{aligned}\mathcal{L} &= i\bar{Q}_{Li}\gamma^{\mu}\left(\partial_{\mu} - ig\tau_i W^i_{\mu} - \frac{ig'}{2}YB_{\mu}\right)Q_{L_i} + i\bar{L}_{Li}\gamma^{\mu}\left(\partial_{\mu} - ig\tau_i W^i_{\mu} - \frac{ig'}{2}YB_{\mu}\right)L_i \\ &+ i\bar{E}_{Ri}\gamma^{\mu}\left(\partial_{\mu} - \frac{1}{2}ig'B_{\mu}Y_L\right)E_{Ri} + i\bar{D}_{Ri}\gamma^{\mu}\left(\partial_{\mu} - \frac{1}{2}ig'B_{\mu}Y_D\right)D_{Ri} + i\bar{U}_{Ri}\gamma^{\mu}\left(\partial_{\mu} - \frac{1}{2}ig'B_{\mu}Y_U\right)U_{Ri}. \quad (3.3.9)\end{aligned}$$

Plus the QCD-SU(3) sector. The possible EW-NLO contributions are shown in Figs. 3.10-3.12. Similar topologies in Figs. 3.11-3.12 are presented by gluon-fermion-antifermion couplings. Again, we have chosen massless neutrinos. Thus the corresponding right-handed chiral component is absent in this minimal structure. With the last fact in mind, only is necessary change $D_R \leftrightarrow E_R$ and $Q_L \leftrightarrow L_L$

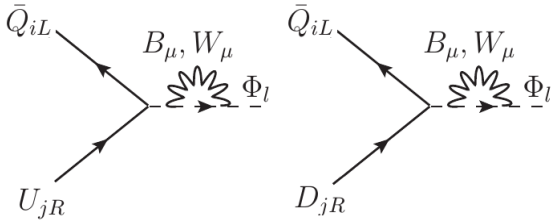

Figure 3.10.: *External corrections for Yukawa coupling from quark-gauge sector correction to the scalar propagator. Topologies can also be extrapolated to the lepton sector in the massless neutrino regime. Couplings among components of Higgs doublets with fermion doublets and fermion singlets are in consistency with charge conservation in each vertex.*

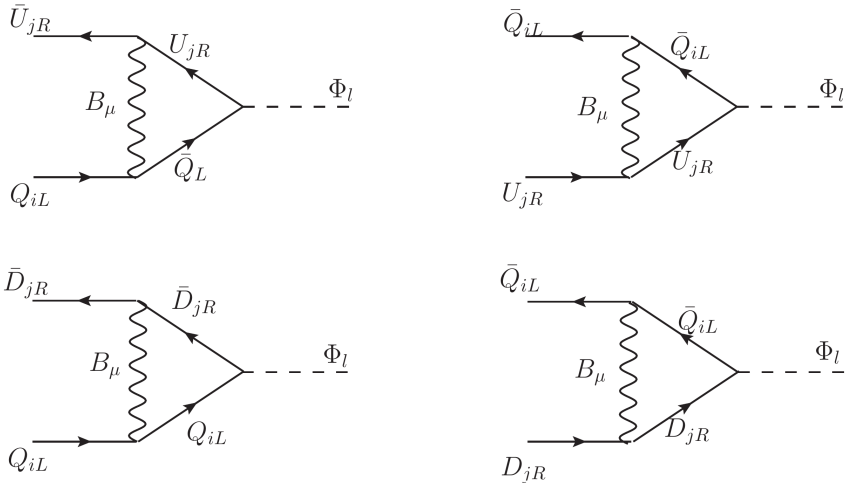

Figure 3.11.: *1PI vertex corrections for Yukawa coupling from quark-gauge sector interactions. Topologies can also be extrapolated to the lepton sector in the massless neutrino regime. Couplings among components of Higgs doublets with fermion doublets and fermion singlets are in consistency with charge conservation in each vertex.*

Taking into account these couplings, the contributions from the gauge part Y_G are given by

$$\mathcal{Y}_G = -A_{Q,l}Y_{Q,l} \quad (3.3.10)$$

where

$$A_Q = \begin{cases} 3\frac{N_C^2-1}{N_C}g_s^2 + \frac{9}{4}g^2 + \frac{17}{12}g'^2 & \text{for } Q = U \\ 3\frac{N_C^2-1}{N_C}g_s^2 + \frac{9}{4}g^2 + \frac{5}{12}g'^2 & \text{for } Q = D \end{cases} \quad (3.3.11)$$

$$A_l = \frac{9}{4}g^2 + \frac{15}{4}g'^2 \quad (3.3.12)$$

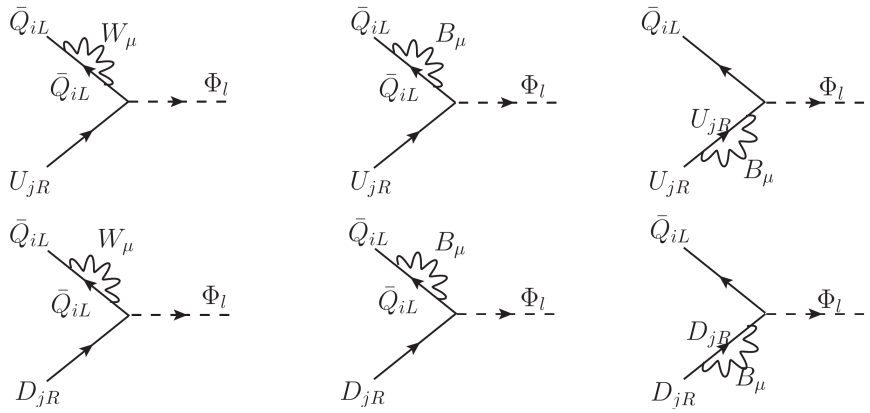

Figure 3.12.: *External corrections for Yukawa coupling from gauge sector interactions. Topologies can also be extrapolated to the lepton sector in the massless neutrino regime. Couplings among components of gauge bosons with fermion doublets and fermion singlets are in consistency with charge conservation in each vertex.*

3.3.1. RGE for bilinear couplings

From the Higgs potential given in notation (3.2.1), the couplings for the bilinear terms (m^2_{ij} and μ^j_k respectively) have the following RGE equation

$$16\pi^2 \frac{d\mu^j_k}{dt} \equiv \mathcal{D}\mu^j_k = 2 \sum_{p,q=1}^{2} \mu^q_p \left(2\Lambda^{jq}_{kp} + \Lambda^{jq}_{pk}\right). \tag{3.3.13}$$

This structure comes from the contributions from the diagram shown in Figure (3.13)

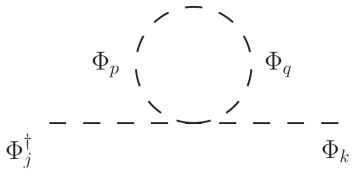

Figure 3.13.: *One loop correction to bilinear terms in the Higgs potential. Couplings among physical scalars of the doublets are done in consistency with charge conservation in each vertex.*

The RGE for μ^j_k comes from the correction to the momentum independent mass term of the Higgs potential and it is based on contributions regarding A_0-tadpole functions of standard integral (3.1.1a). This evolution will be substantial for the metastability analysis of the Higgs potential.

3.4. Explicit couplings evolution: Pure gauge sector in 2HDM

One-loop corrections are relatively easy to evaluate and visualize. In this section, we shall present an evaluation of RGEs in each sector, starting with whose independent of the evolution of remaining ones. Hence, for the gauge boson part, we have for 2HDMs

$$\frac{dg}{dt} = \frac{1}{16\pi^2}\left(\frac{4}{3}n_f + \frac{1}{6}n_H - \frac{22}{3}\right) g^3 = -3g^3, \tag{3.4.1}$$

$$\frac{dg'}{dt} = \frac{1}{16\pi^2}\left(\frac{20}{9}n_F + \frac{1}{6}n_H\right) g'^3 = 7g'^3, \tag{3.4.2}$$

$$\frac{dg_s}{dt} = \frac{1}{16\pi^2}\left(\frac{4}{3}n_f - 11\right) g_s^3 = -7g_s^3. \tag{3.4.3}$$

In the SM there are three families $N_{fam} = 3$ and one Higgs doublet $N_{Higgs} = 1$. From these formulae we see that the QCD coupling g_s is asymptotically free and is therefore weak in the UV. Besides, it runs to a strong coupling in the

IR. The $SU(2)$ coupling running, emulating a roughly asymptotic free behavior, is also affected by the Higgs mechanism which leads to SSB. The net effect on the RG evolution is to give a mass to the gauge bosons $W^{\pm}$ and Z^0. Denoting this as a collective mass scale called M, we analyze the following statements for gauge couplings runnings. For RG scales $\mu > M$, the $W^{\pm}$ and Z gauge bosons participate in the running of the gauge couplings as in the mathematical structures shown above. Nevertheless, for $\mu << M$, the $W^{\pm}$ and Z^0 gauge bosons decouple and can be integrated out. The appropiate gauge coupling controlating weak interaction at those scales no lunger runs and it frozen. This is the reason of why, unlike QCD coupling evolution, the weak relevant coupling does not become large in the IR. Besides, at charactering regimes, when weak gauge bosons are decoupled they leave relics in the low energy effective theory in the form of the weak four fermion interactions [133].

Since for 2HDM, $n_H = 2$ and $n_f = 3$ (the same fermionic content of SM). In all equations $t = \log \mu$. Figure 3.14 shows gauge couplings energy evolution: wherein exist a important set of attributes. One of them is that the GU triangle is located between $10^{17} \leq \mu\,(\text{GeV}) \leq 10^{22}$. The lower point correspond to the unification between $SU\,(3)$ and $SU\,(2)$, followed of the unification between $SU\,(3)$ and $U\,(1)$ and finally the unification between $SU\,(2)$ and $U\,(1)$ interactions. The last two points of unification are beyond of Planck scales; being an important problem for compatibility with physics from Cosmology. Indeed, in early Universe, we can interpret these evolution from possible phase transitions occurring at those energy scales. For instance, predictions from these running must be according to other effects that have been discarded in the foundations for those energy values, as mechanisms associated to Quantum Gravity. All these arguments are motivations to introduce NNLO corrections, which give information about UV completions for 2HDMs and their compatibility with cosmology.

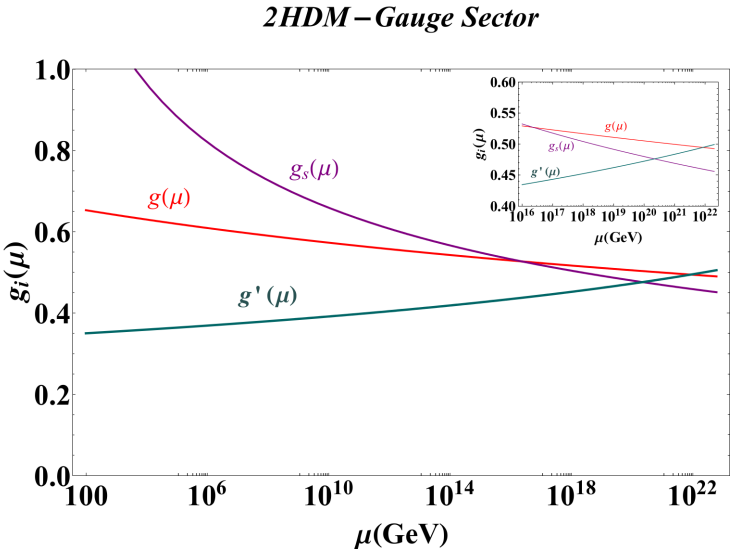

Figure 3.14.: *Evolution for gauge couplings in the 2HDM. Initial conditions for gauge couplings have been established in Tab. 3.1.*

As in the SM behavior, the NNLO corrections could set the GU triangle in lower energy scales, as can be seen in [6].

3.5. Explicit couplings evolution: Yukawa sector

The following sector to analyze is the Yukawa part. RGEs are dependent on symmetries implemented and gauge couplings evolution. However, RGE's structure at one loop level is independent of quartic couplings of the Higgs potential. Thus, we can extract some relevant information without involving many assumptions over another point in the parameter space. Indeed, RG evolution is a useful tool to analyze different 2HDMs on a reliability of underlying assumptions. A quick appearance of Landau poles or large deviations of diagonal Yukawa coupling under RG evolution may indicate the model is either fine tuned or incomplete, e.g., needing new particles appearing at high energy scales.

From our description and developments to suppress FCNC processes, we begin describing the type I and type II -2HDMs. Thus for Yukawa couplings of the type I-2HDM and from Eq. (3.3.2) and its explicit parts, the leptonic sector reads

$$\mathcal{D}\xi^L = A_l \xi^L + T_{11}\xi^L + \frac{3}{2}\xi^L \eta^{L\dagger}\eta^L. \tag{3.5.1}$$

Coupling (m_z)	Standard Expression	Numerical value	Updated Parameters (GeV)
$g_s\,(m_z)$	$4\pi\alpha_s\,(m_z)$	1.2367	
$g\,(m_z)$	$\left(\frac{4m_w^2}{v^2}\right)^{1/2}$	0.6504	$m_w = 80.385 \pm 0.015$
$g'\,(m_z)$	$\left(\frac{4m_z^2}{v^2} - \frac{4m_w^2}{v^2}\right)^{1/2}$	0.3560	$m_z = 91.1876 \pm 0.0021$
$\lambda\,(m_z)$	$\frac{m_h^2}{2v^2}$	$(0.1290 - 0.1312)$	$m_{h^o} = 125 - 126\,(125.7 \pm 0.4)$
$y_t\,(m_z)$	$\frac{\sqrt{2}m_t}{v}$	$(0.9922 - 0.9997)$	$m_t = 173.21 \pm 0.51 \pm 0.71$
$y_b\,(m_z)$	$\frac{\sqrt{2}m_b}{v}$	0.0240	$m_b = 4.18 \pm 0.03$
$y_\tau\,(m_z)$	$\frac{\sqrt{2}m_\tau}{v}$	0.0067	$m_\tau = 1.776 \pm 0.001$

Table 3.1.: *Initial conditions for running of RGE in the SM and 2HDMs. Only gauge part constraints are extrapolated to running couplings of 2HDMs. The parameters values are taken from [4].*

In the same way, for the down sector

$$\mathcal{D}\xi^D = A_D\xi^D + T_{11}\xi^D + \frac{3}{2}\xi^D\xi^{D\dagger}\xi^D - \frac{3}{2}\xi^U\xi^{U\dagger}\xi^D. \tag{3.5.2}$$

and for the up sector

$$\mathcal{D}\xi^U = A_u\xi^U + T_{11}\xi^U + \frac{3}{2}\xi^U\xi^{U\dagger}\xi^U - \frac{3}{2}\xi^D\xi^{D\dagger}\xi^U. \tag{3.5.3}$$

Here we have eliminated one coupling matrix. Since large part of the literature choose Φ_2, the doublet to be coupled fermions, in a general way, we shall take this prescription in non-inert models. Nevertheless, in the inert models, we adopt whose wherein only Φ_1 couples to fermions. This fact is due to vacuum structure where $\langle\Phi_1\rangle_0 = v/\sqrt{2}$ and $\langle\Phi_2\rangle_0 = 0$. This choice lead to establish the compatibility with symmetries to build up a Yukawa Lagrangian free of FCNCs. Therefore, for non-inert models, the Type I-RGEs are given by

$$\begin{aligned}
\mathcal{D}\xi_\tau &= A_\tau\xi_\tau + T_{11}\xi_\tau + \frac{3}{2}\xi_\tau^3 \\
\mathcal{D}\xi_b &= A_b\xi_b + T_{11}\xi_b + \frac{3}{2}\xi_b^3 - \frac{3}{2}\xi_t^2\xi_b \\
\mathcal{D}\xi_t &= A_t\xi_t + T_{11}\xi_t + \frac{3}{2}\xi_t^3 - \frac{3}{2}\xi_b^2\xi_t
\end{aligned}$$

Initial conditions for type I Yukawa couplings can be chosen in the following way (without QCD threshold corrections)

$$\eta_\tau(m_Z) = \frac{1}{\sin\beta}\frac{\sqrt{2}m_\tau}{v} \tag{3.5.4a}$$

$$\eta_b(m_Z) = \frac{1}{\sin\beta}\frac{\sqrt{2}m_b}{v} \tag{3.5.4b}$$

$$\eta_t(m_Z) = \frac{1}{\sin\beta}\frac{\sqrt{2}m_t}{v} \tag{3.5.4c}$$

Evolutions for relevant Yukawa couplings are depicted in Fig. 3.15.
In the same way for type II 2HDM, we finally get

$$\begin{aligned}
\mathcal{D}\eta_\tau &= a_e\eta_\tau + T_{22}\eta_\tau + \frac{3}{2}\eta_\tau^3 \\
\mathcal{D}\eta_b &= a_b\eta_b + T_{22}\eta_b + \frac{3}{2}\eta_b^3 + \frac{1}{2}\xi_t^2\eta_b \\
\mathcal{D}\xi_t &= a_t\xi_t + T_{11}\xi_t + \frac{3}{2}\xi_t^3 + \frac{1}{2}\eta_b^2\xi_t
\end{aligned}$$

With the initial conditions

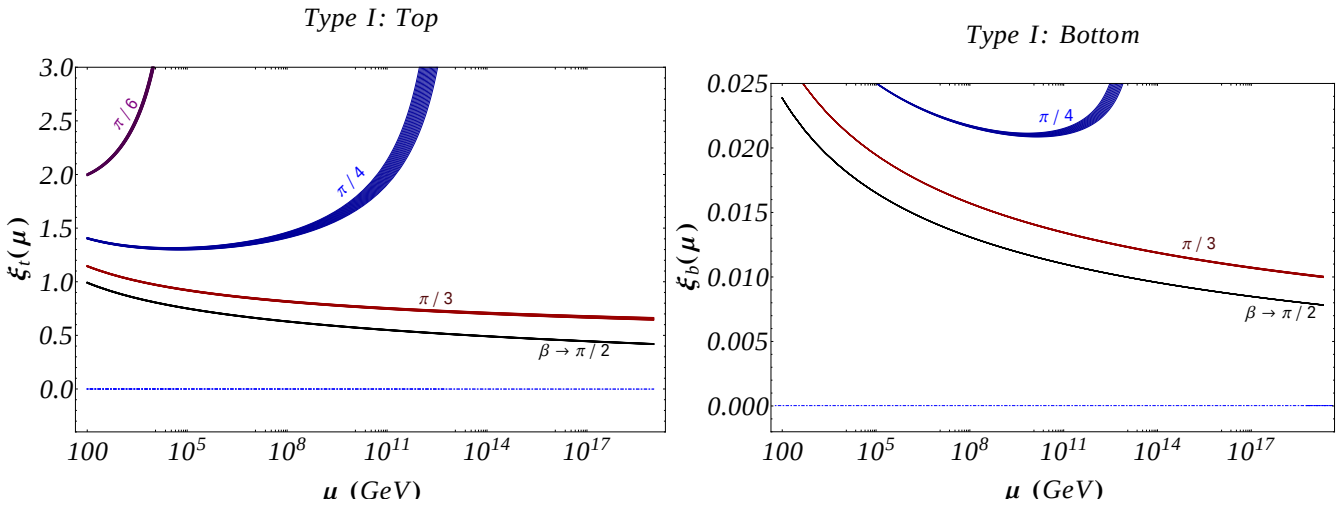

Figure 3.15.: *Yukawa couplings evolution for top (**Left**) and bottom (**Right**) quarks in the type I-2HDM. We have taken the initial conditions without threshold corrections given by QCD. Width in each curve is due to top quark uncertainty. In addition, we have varied β mixing angle in the following values $\pi/6, \pi/4, \pi/3, \to \pi/2$.*

$$\eta_\tau(m_Z) = \frac{1}{\cos\beta}\frac{\sqrt{2}m_\tau}{v} \tag{3.5.5a}$$

$$\eta_b(m_Z) = \frac{1}{\cos\beta}\frac{\sqrt{2}m_b}{v} \tag{3.5.5b}$$

$$\xi_t(m_Z) = \frac{1}{\sin\beta}\frac{\sqrt{2}m_t}{v} \tag{3.5.5c}$$

Figure 3.16 shows energy evolution of Yukawa couplings in the type II 2HDM. Because of initial conditions, there exist remarkable differences with the type I in the case of bottom quark evolution. In angles less to $\beta < \pi/4$ (at least) appear divergences, in particular values of μ_I, likewise in type I 2HDM. These possible Landau poles are essentially due to t-quark Yukawa evolution. Besides, at high energy values and for angles $\beta \geq \pi/3$, b-Yukawa couplings present asymptotic freedom. Differences regarding the type I arises, and just before of the non-analytic behavior, the relevant evolution is given for larger β mixing angles, as we expect by the initial conditions structure.

For the top quark evolution, significant differences arise for $\beta \geq \pi/3$, e.g. it is possible to see the distance between both curves ($\beta = \pi/3$ and $\beta \to \pi/2$) is highly reduced in comparison with the evolution of the type I scenario. This fact is an effect of $b-$ quark Yukawa evolution.

3.5.1. Yukawa evolution for the type III-2HDM

Employing Eq. (1.3.1) and taking the Higgs basis where Φ_1 generates mass terms and Φ_2 produces FCNC couplings (in the fundamental parameterization)[3], it is possible to get the general Yukawa couplings RGEs: In the case of the leptonic sector

$$\mathcal{D}\eta^L = a_e\eta^L + T_{11}\eta^L + T_{12}\xi^L + \frac{3}{2}\eta^L\eta^{L\dagger}\eta^L + \eta^L\xi^{L\dagger}\xi^L + \frac{1}{2}\xi^L\xi^{L\dagger}\eta^L \tag{3.5.6}$$

$$\mathcal{D}\xi^L = a_e\xi^L + T_{21}\eta^L + T_{22}\xi^L + \frac{3}{2}\xi^L\xi^{L\dagger}\xi^L + \xi^L\eta^{L\dagger}\eta^L + \frac{1}{2}\eta^L\eta^{L\dagger}\xi^L \tag{3.5.7}$$

for down-quarks sector

$$\begin{aligned}\mathcal{D}\eta^D = a_d\eta^D + T_{11}\eta^D + T_{12}\xi^D + \frac{3}{2}\eta^D\eta^{D\dagger}\eta^D - \frac{3}{2}\eta^U\eta^{U\dagger}\eta^D \\ - 2\xi^U\eta^{U\dagger}\xi^D + \frac{1}{2}\xi^U\xi^{U\dagger}\eta^D + \eta^D\xi^{D\dagger}\xi^D + \frac{1}{2}\xi^D\xi^{D\dagger}\eta^D\end{aligned} \tag{3.5.8}$$

[3]A detailed discussion of Type III and FCNC's origin is presented at Appendix C

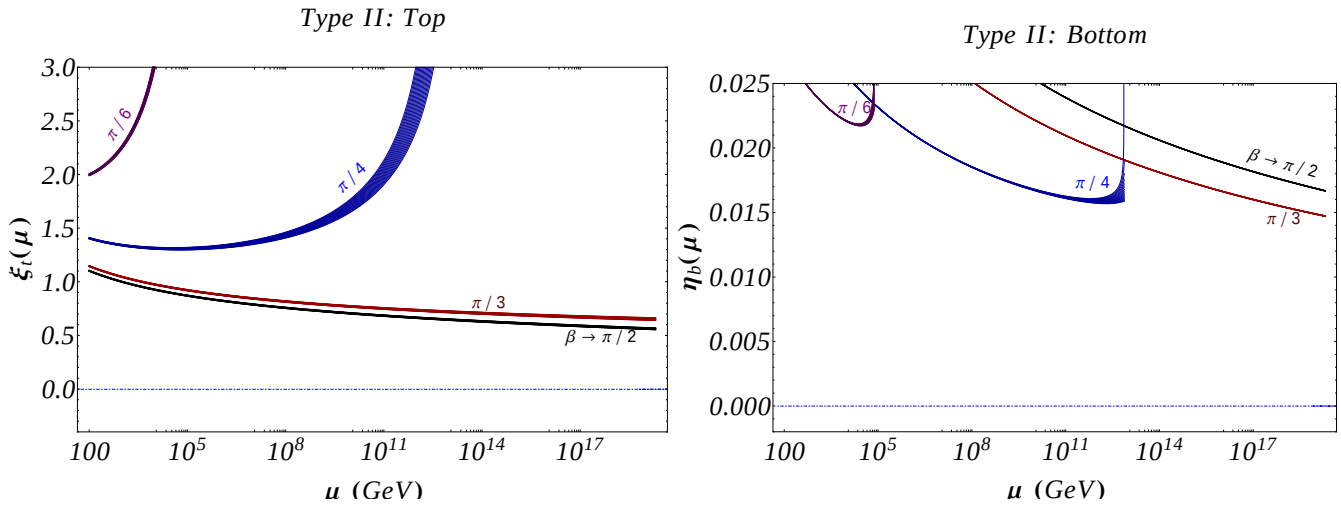

Figure 3.16.: *Yukawa couplings evolution for top (**Left**) and bottom (**Right**) quarks in the type II-2HDM. We have taken the initial conditions without threshold corrections given by QCD in the EW scale. The width in each curve is due to the minimum and maximum values taken for top masses* $(172.5 - 174.1\ GeV)$*. In addition, we have varied* β *mixing angle in the following values* $\pi/6, \pi/4, \pi/3, \to \pi/2$.

$$\begin{aligned}\mathcal{D}\xi^D &= a_d\xi^D + T_{21}\eta^D + T_{22}\xi^D + \frac{3}{2}\xi^D\xi^{D\dagger}\xi^D - \frac{3}{2}\xi^U\xi^{U\dagger}\xi^D \\ &- 2\eta^U\xi^{U\dagger}\eta^D + \frac{1}{2}\eta^U\eta^{U\dagger}\xi^D + \xi_2^D\eta^{D\dagger}\eta^D + \frac{1}{2}\eta^D\eta^{D\dagger}\xi^D \end{aligned} \tag{3.5.9}$$

and for up-quarks sector

$$\begin{aligned}\mathcal{D}\eta^U &= a_u\eta^U + T_{11}\eta^U + T_{12}\xi^U + \frac{3}{2}\eta^U\eta^{U\dagger}\eta^U - \frac{3}{2}\eta^D\eta^{D\dagger}\eta^U \\ &- 2\xi^D\eta^{D\dagger}\xi^U + \frac{1}{2}\xi^D\xi^{D\dagger}\eta^U + \eta^U\xi^{U\dagger}\xi^U + \frac{1}{2}\xi^U\xi^{U\dagger}\eta^U \end{aligned} \tag{3.5.10}$$

$$\begin{aligned}\mathcal{D}\xi^U &= a_u\xi^U + T_{21}\eta^U + T_{22}\xi^U + \frac{3}{2}\xi^U\xi^{U\dagger}\xi^U - \frac{3}{2}\xi^D\xi^{D\dagger}\xi^U \\ &- 2\eta^D\xi^{D\dagger}\eta^U + \frac{1}{2}\eta^D\eta^{D\dagger}\xi^U + \xi_2^U\eta^{U\dagger}\eta^U + \frac{1}{2}\eta^U\eta^{U\dagger}\xi^U \end{aligned} \tag{3.5.11}$$

For now and since Yukawa couplings, we consider the following textures for FCNC matrices (four zero textures)

$$\begin{aligned}\xi^U &= \begin{pmatrix} 0 & \times & 0 \\ \times & 0 & \times \\ 0 & \times & \times \end{pmatrix}. \\ \xi^D &= \begin{pmatrix} 0 & \times & 0 \\ \times & 0 & \times \\ 0 & \times & \times \end{pmatrix}. \\ \xi^L &= \begin{pmatrix} 0 & \times & 0 \\ \times & 0 & \times \\ 0 & \times & \times \end{pmatrix}. \end{aligned}$$

These FCNC matrices satisfy the typical form of Fritzsch structure [134, 135]. The Sher and Cheng anzats presents the assumption that the FCNC couplings are proportional to $\lambda_{ij}\sqrt{m_i m_j}$ with λ_{ij} couplings being the $O(1)$. That fact preserves the hierarchical structure of the Yukawa couplings in the mass couplings. Hence the simplest way to implement

the anzats in the case of the real Yukawa couplings is through the matrices

$$\begin{aligned}
\xi^U &= \frac{\sqrt{2}}{v}\begin{pmatrix} 0 & \lambda_{uc}\sqrt{m_u m_c} & 0 \\ \lambda_{uc}\sqrt{m_u m_c} & 0 & \lambda_{ct}\sqrt{m_c m_t} \\ 0 & \lambda_{ct}\sqrt{m_c m_t} & \lambda_{tt} m_t \end{pmatrix}. \\
\xi^D &= \frac{\sqrt{2}}{v}\begin{pmatrix} 0 & \lambda_{ds}\sqrt{m_d m_s} & 0 \\ \lambda_{ds}\sqrt{m_d m_s} & 0 & \lambda_{bs}\sqrt{m_b m_s} \\ 0 & \lambda_{bs}\sqrt{m_b m_s} & \lambda_{bb} m_b \end{pmatrix}. \\
\xi^L &= \frac{\sqrt{2}}{v}\begin{pmatrix} 0 & \lambda_{e\mu}\sqrt{m_e m_\mu} & 0 \\ \lambda_{e\mu}\sqrt{m_e m_\mu} & 0 & \lambda_{\mu\tau}\sqrt{m_\mu m_\tau} \\ 0 & \lambda_{\mu\tau}\sqrt{m_\mu m_\tau} & \lambda_{\tau\tau} m_\tau \end{pmatrix}.
\end{aligned}$$

The coefficients λ_{ij} are of order unity. Taking into account only the diagonal terms in the third family, we can summarize all RGEs for Yukawa couplings through

$$\begin{aligned}
\mathcal{D}\eta_\tau &= a_\tau\eta_\tau + \left(3\left(\eta_t^2+\eta_b^2\right)+\eta_\tau^2\right)\eta_\tau + \left(3\left(\eta_t\xi_{tt}+\eta_b\xi_{bb}\right)+\eta_\tau\xi_{\tau\tau}\right)\xi_{\tau\tau} \\
&\quad +\frac{3}{2}\eta_\tau^3 + \frac{3}{2}\xi_{\tau\tau}^2\eta_\tau \\
\mathcal{D}\xi_{\tau\tau} &= a_\tau\xi_{\tau\tau} + \left(3\left(\eta_t\xi_{tt}+\eta_b\xi_{bb}\right)+\eta_\tau\xi_{\tau\tau}\right)\eta_\tau + \left(3\left(\xi_{tt}^2+\xi_{bb}^2\right)+\xi_{\tau\tau}^2\right)\xi_{\tau\tau} \\
&\quad +\frac{3}{2}\xi_{\tau\tau}^3 + \frac{3}{2}\xi_{\tau\tau}\eta_\tau^2 \\
\mathcal{D}\eta_b &= a_b\eta_b + \left(3\left(\eta_t^2+\eta_b^2\right)+\eta_\tau^2\right)\eta_b + \left(3\left(\eta_t\xi_{tt}+\eta_b\xi_{bb}\right)+\eta_\tau\xi_{\tau\tau}\right)\xi_{bb} \\
&\quad +\frac{3}{2}\eta_b^3 - \frac{3}{2}\eta_t^2\eta_b - 2\xi_{bb}\eta_t\xi_{tt} + \frac{1}{2}\xi_{tt}^2\eta_b + \frac{3}{2}\xi_{bb}^2\eta_b \\
\mathcal{D}\xi_{bb} &= a_d\xi_{bb} + \left(3\left(\eta_t\xi_{tt}+\eta_b\xi_{bb}\right)+\eta_\tau\xi_{\tau\tau}\right)\eta_b + \left(3\left(\xi_{tt}^2+\xi_{bb}^2\right)+\xi_{\tau\tau}^2\right)\xi_{bb} \\
&\quad +\frac{3}{2}\xi_{bb}^3 - \frac{3}{2}\xi_{tt}^2\xi_{bb} - 2\eta_t\eta_b\xi_{tt} + \frac{1}{2}\eta_t^2\xi_{bb} + \frac{3}{2}\xi_{bb}\eta_b^2 \\
\mathcal{D}\eta_t &= a_t\eta_t + \left(3\left(\eta_t^2+\eta_b^2\right)+\eta_\tau^2\right)\eta_t + \left(3\left(\eta_t\xi_{tt}+\eta_b\xi_{bb}\right)+\eta_\tau\xi_{\tau\tau}\right)\xi_{tt} \\
&\quad +\frac{3}{2}\eta_t^3 - \frac{3}{2}\eta_b^2\eta_t - 2\xi_{bb}\eta_b\xi_{tt} + \frac{1}{2}\xi_{bb}^2\eta_t + \frac{3}{2}\xi_{tt}^2\eta_t \\
\mathcal{D}\xi_{tt} &= a_u\xi_{tt} + \left(3\left(\eta_t\xi_{tt}+\eta_b\xi_{bb}\right)+\eta_\tau\xi_{\tau\tau}\right)\eta_t + \left(3\left(\xi_{tt}^2+\xi_{bb}^2\right)+\xi_{\tau\tau}^2\right)\xi_{tt} \\
&\quad +\frac{3}{2}\xi_{tt}^3 - \frac{3}{2}\xi_{bb}^2\xi_{tt} - 2\eta_b\xi_{bb}\eta_t + \frac{1}{2}\eta_b^2\xi_{tt} + \xi_{tt}\eta_t^2 + \frac{1}{2}\eta_t^2\xi_{tt}
\end{aligned}$$

The solutions from these RGEs for top and bottom quarks are shown in Figs. 3.17-3.18. Here, we have used the following initial conditions for mass couplings

$$\xi_\tau(m_Z) = \frac{\sqrt{2}m_\tau}{v} \tag{3.5.12a}$$

$$\xi_b(m_Z) = \frac{\sqrt{2}m_b}{v} \tag{3.5.12b}$$

$$\xi_t(m_Z) = \frac{\sqrt{2}m_t}{v} \tag{3.5.12c}$$

In this step, we have not taken into account QCD corrections yet. Figures 3.17-3.18 show Yukawa couplings RG evolution for different choices of initial conditions of FCNC couplings. For the top quark scenario, we can see the influence of FCNC couplings in the mass term evolution in regimes where $\xi_{tt} > 0.6$ and $\mu > 10^{10}$ GeV. This effect can be extrapolated to the FCNC sector, where for high energy scales exist relevant discrepancies for couplings in $\xi_{tt}(m_z) > 0.5$. For lower values ξ_{tt}-evolution is approximately constant for fixed values of $\xi_{ii}(m_z)$.

The corresponding RG evolutions for bottom quark couplings are settled in Fig. 3.18. In this case discrepancies in the FCNC sector appears in low energy scales (as is shown in the right part). The evolution-ξ_{bb} become constant in high energy scales. Here, η couplings RG evolution are located in values of one order of magnitude below with respect the same mass coupling for the top quark. Meanwhile, FCNC couplings belong in the same scale. It is worthwhile to point

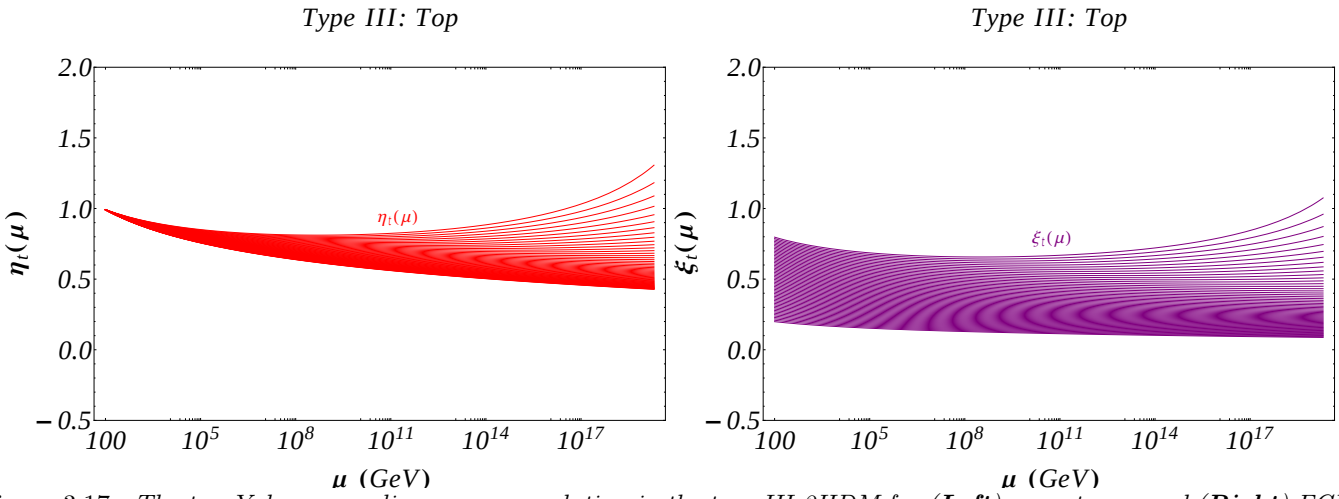

Figure 3.17.: *The top-Yukawa couplings energy evolution in the type III-2HDM for (**Left**) mass terms and (**Right**) FCNC couplings. The width in the family of curves is due to initial conditions in FCNC couplings* $0.2 \leq \xi_{tt}(m_z) \leq 0.8$. *In addition, we have taken* $\xi_{bb} = \xi_{\tau\tau} = 0.2$.

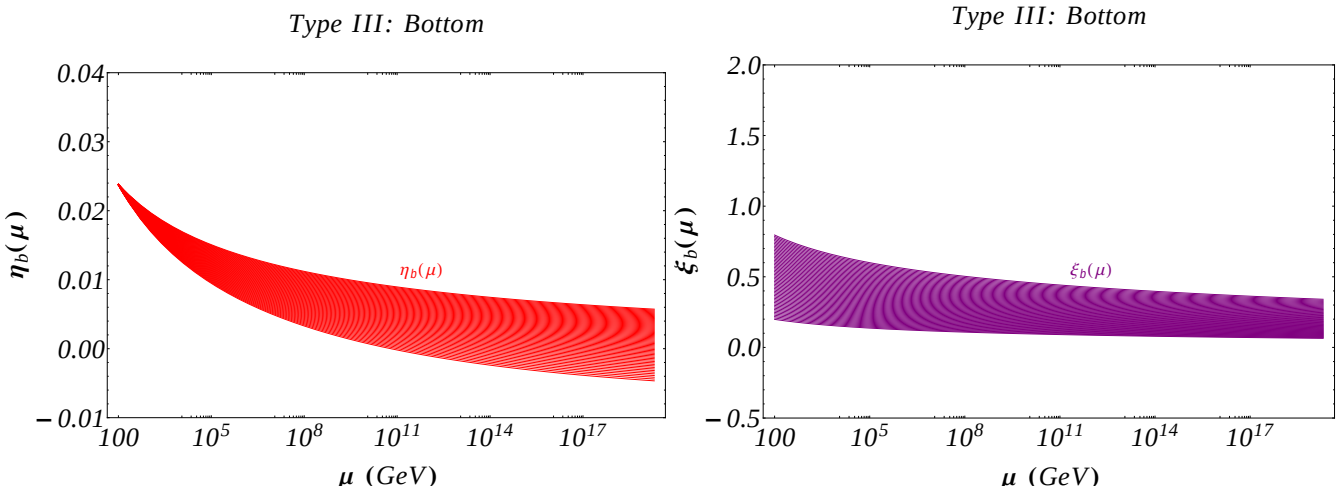

Figure 3.18.: *The bottom-Yukawa couplings energy evolution in the type III-2HDM for (**Left**) mass terms and (**Right**) FCNC couplings. The width in the family of curves is due to initial conditions in FCNC couplings* $0.2 \leq \xi_b(m_z) \leq 0.8$. *In addition, we have taken* $\xi_t(m_z) = \xi_{\tau\tau}(m_z) = 0.2$

out that any evolution in the type III scenario shows Landau poles up to Grand Unification or Planck scales; perhaps by taking FCNC coupling in m_z with higher values we might begin to see these divergences appearance. This fact gives us limiting values over those unknown structures, which must also be consistent with other theoretical analyses, like those coming from perturbative unitarity.

3.6. Inclusion of QCD improvements for Yukawa couplings

In this section, we make similar analysis to those presented in later sections, but introducing threshold corrections in the EW scale for Yukawa-quarks couplings given by QCD improvement. Our primary goal is to compute the influence of these corrections in perturbative analyses made above; to address the origin of these improvements in the Yukawa coupling definition for initial conditions.

The quark masses, in particular, the top and bottom quark masses are input parameters in SM and 2HDMs. Our prior discussions have been based on the fact these masses coming from Higgs mechanism in those models. Nevertheless, the value cannot be computed from SM or 2HDM foundations. Instead, quark masses have to be determined from the comparison between theoretical predictions and experimental behavior of several processes involving these particles.

It is relevant to stress that there is no a unique definition of quark masses. Because of quarks cannot be observed as

free particles like charged leptons, the quark mass is a theoretical concept and depends on the concept adopted for its right definition. The best-known definitions are the derived in the pole mass and the $\bar{M}S$ mass. The pole mass should not be used because it has the renormalon ambiguity and cannot be determined more accurately than $0.3-0.4$ GeV [4]. Actually and to establish the origin of renormalon ambiguity, we may relate the pole with some short distance mass scale like the $\bar{M}S$ mass scale μ_0 which for "large β_0" approximation by

$$m_{\text{pole}} = \mu_0 \left\{ 1 + \sum m_n \left(\frac{\beta_0 \alpha_s}{4\pi} \right)^n \right\} \tag{3.6.1}$$

We can see the meaning of this relation with the following statements [137]: Although the top quark lifetime is much less than the strong interaction time scale, Λ_{QCD}, there are non-perturbative contributions to the top-quark pole mass, just as in the case of a stable heavy quark. These non-perturbative contributions are signaled by the divergent behavior at large orders of an expansion in $a = \beta_0 \alpha_s(m_R)/4\pi$. This fact leads to an unavoidable ambiguity of $O(\Lambda_{QCD})$ in the pole mass of the top quark. The short-distance mass, such as the $\bar{M}S$ mass, can in principle be measured with arbitrary accuracy. This concept may require non-perturbative information, depending on the measurement. It is feasible to adopt the $\bar{M}S$ mass as the standard definition of the top-quark mass. The relation between the top-quark pole mass and the $\bar{M}S$ mass evaluated at the pole mass $\bar{m} = \bar{m}\left(m_{pole}\right)$ is known up to two loops

$$m_{\text{pole}} = \bar{m}\left(m_{pole}\right) \left[1 + \frac{4}{3} \frac{\bar{\alpha}_s(m_{pole})}{\pi} + 10.95 \left(\frac{\bar{\alpha}_s(m_{pole})}{\pi} \right)^2 + ... \right] + O(\Lambda_{QCD}) \tag{3.6.2}$$

where the last term reminds us that the pole mass has an unavoidable ambiguity of $O(\Lambda_{QCD})$. Given that the pole mass is ambiguous itself, we suggest as the standard $\bar{M}S$ mass evaluated at the $\bar{M}S$ mass, which is related to the pole mass by

$$m_{\text{pole}} = \bar{m}\left(\bar{m}\right) \left[1 + \frac{4}{3} \frac{\bar{\alpha}_s(\bar{m})}{\pi} + 8.28 \left(\frac{\bar{\alpha}_s(\bar{m})}{\pi} \right)^2 + ... \right] + O(\Lambda_{QCD}) \tag{3.6.3}$$

The difference in the coefficients of the two α_s^2 terms above is exactly $8/3$. Same appears to happen for all quark mass dependent observables. It is thus clear that pole mass is an irrelevant concept and leads to artificially significant corrections in higher orders. In areas of high energy physics, where heavy quark masses need to be known with uncertainties below GeV, short-distance frameworks for masses must be used. The short distance mass schemes have the following generic form

$$m^{sd}\left(\mu\right) = m^{\text{pole}} - R\left(\mu\right) \left[a_1 \frac{\alpha_s(\mu)}{4\pi} + a_2 \left(\frac{\alpha_s(\mu)}{4\pi} \right)^2 + ... \right] \tag{3.6.4}$$

In the $\bar{M}S$ scheme [5], $R = \bar{m}(\mu)$ and $a_1 = 16/3 + 4\ln\mu^2/m^2$. All a_i are chosen in such a way that renormalon ambiguity is removed of the respective quark mass definition.

3.6.1. RGEs evolution within $\bar{M}S$ scheme for quark masses definition

Taking as the basis our above discussion, and by means up to NLO terms in Eq. (3.6.4) in the $\bar{M}S$ scheme, the evaluation for RGEs of last sections is based on the new initial conditions:

[4] The top quark mass enters the relation between the electroweak precision observables indirectly through loop effects. The global electroweak fit of the SM requires having very accurate input data to make a constraint for the masses of undiscovered particles, such as Higgs bosons within 2HDM scalar spectrum. The increase in the accuracy of the top quark mass will improve the precision tests on the Higgs masses. This fact is important in the correct description of the phase diagram of stability in SM (presented in our Introduction) and 2HDM (following chapters). Besides, we can study possible deviations from the SM with the aid of anomalous couplings, CP violation or extra dimensions [136]

[5] This scheme is useful when involved processes have heavy quarks off-shell and with higher momentum (UV Regime). In a regime near to a single resonance, heavy quarks are very close to their mass shell and in this case $R = \Gamma_Q$ (i.e. the resonance width).

$$\xi_\tau(m_Z) = \frac{\sqrt{2}m_\tau}{v\sin\beta} \tag{3.6.5a}$$

$$\xi_b(m_Z) = \frac{\sqrt{2}m_b}{v\sin\beta}\left[1-\delta_{QCD}(m_z)\right] \tag{3.6.5b}$$

$$\xi_t(m_Z) = \frac{\sqrt{2}m_t}{v\sin\beta}\left[1-\delta_{QCD}(m_z)\right], \tag{3.6.5c}$$

in the type I scenario. Results are depicted in Fig. 3.19. Comparing with type I running evolution of Yukawa couplings without QCD corrections (Fig. 3.15), we see as the convergence of numerical evaluation increases in the energy scale for some values of β. For $\beta = \pi/4$, the energy value where possible Landau poles appear in η_b and ξ_t is now located in $\mu \sim 10^{16}$ GeV, which is four magnitude order above of the energy scale of divergences for the RG evolution without QCD threshold corrections. A less dramatic case occurs in $\pi/3$, where the increases of energy scale for perturbativity is only around of one magnitude order. For these β values, QCD correction additionally yields a broader dependence of top mass uncertainty for Yukawa couplings evolution. For $\beta \to \pi/2$, the effect of QCD improvement is negligible.

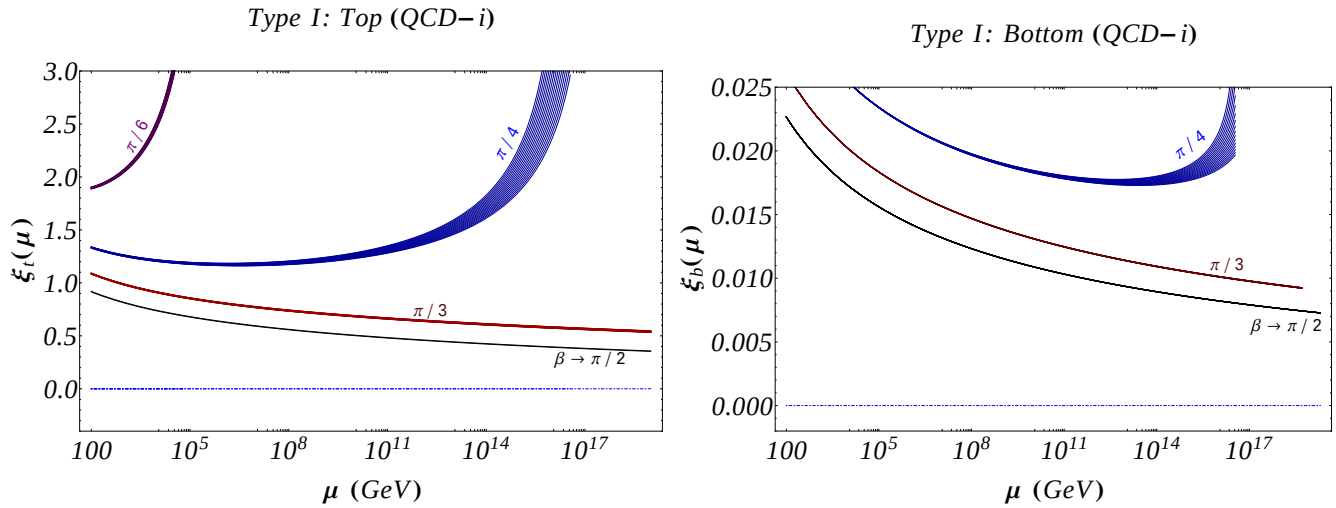

Figure 3.19.: *Yukawa couplings evolution for top (**Left**) and bottom (**Right**) quarks in the type I-2HDM. We have taken initial conditions with threshold corrections given by QCD in the EW scale. The width in each curve is due to the top mass uncertainty (*173.2 ± 0.9 *GeV-Tevatron) . In addition, we have varied β mixing angle in the following values $\pi/6, \pi/4, \pi/3, \to \pi/2$.*

For the type II case, the QCD corrections to initial conditions are

$$\eta_\tau(m_Z) = \frac{\sqrt{2}m_\tau}{v\cos\beta} \tag{3.6.6a}$$

$$\eta_b(m_Z) = \frac{\sqrt{2}m_b}{v\cos\beta}\left[1-\delta_{QCD}(m_z)\right] \tag{3.6.6b}$$

$$\xi_t(m_Z) = \frac{\sqrt{2}m_t}{v\sin\beta}\left[1-\delta_{QCD}(m_z)\right] \tag{3.6.6c}$$

Figure 3.20 shows the evolution of Yukawa couplings for top and bottom quarks. For $\beta = \pi/4$ in both evolutions, the scale of perturbativity changes in four order of magnitude, which is now $\mu_{pert} \leq 10^{16}$ GeV. For values $\beta \to \pi/2$, QCD corrections does not have a different effect on RGE evolution for top and bottom quarks.

In the type III scenario, QCD corrections on initial conditions in $\mu_0 = m_Z$ are given by

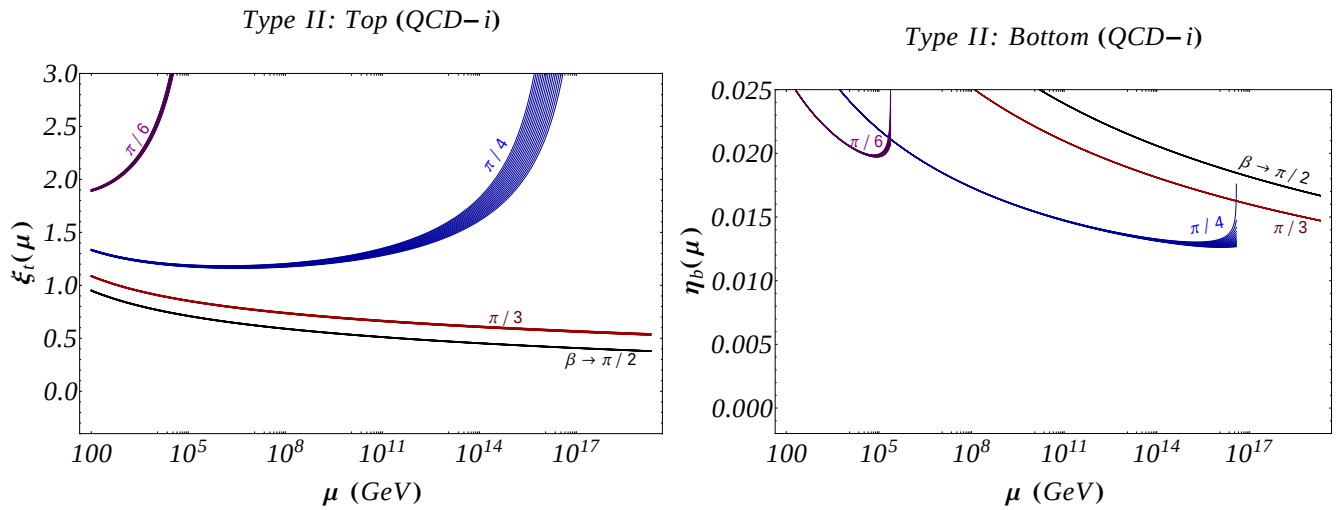

Figure 3.20.: *Yukawa couplings evolution for top (**Left**) and bottom (**Right**) quarks in the type II-2HDM. We have taken the initial conditions with threshold corrections given by QCD. The width in each curve is due to the top mass uncertainty (*173.3 ± 0.8 *GeV). In addition, we have varied* β *mixing angle in the following values* $\pi/6, \pi/4, \pi/3, \to \pi/2$.

$$\eta_\tau(m_Z) = \frac{\sqrt{2}m_\tau}{v} \tag{3.6.7a}$$

$$\eta_b(m_Z) = \frac{\sqrt{2}m_b}{v}\left[1 - \delta_{QCD}(m_Z)\right] \tag{3.6.7b}$$

$$\eta_t(m_Z) = \frac{\sqrt{2}m_t}{v}\left[1 - \delta_{QCD}(m_Z)\right] \tag{3.6.7c}$$

The influence of QCD corrections in type III scenario are shown in Figs. 3.21-3.22

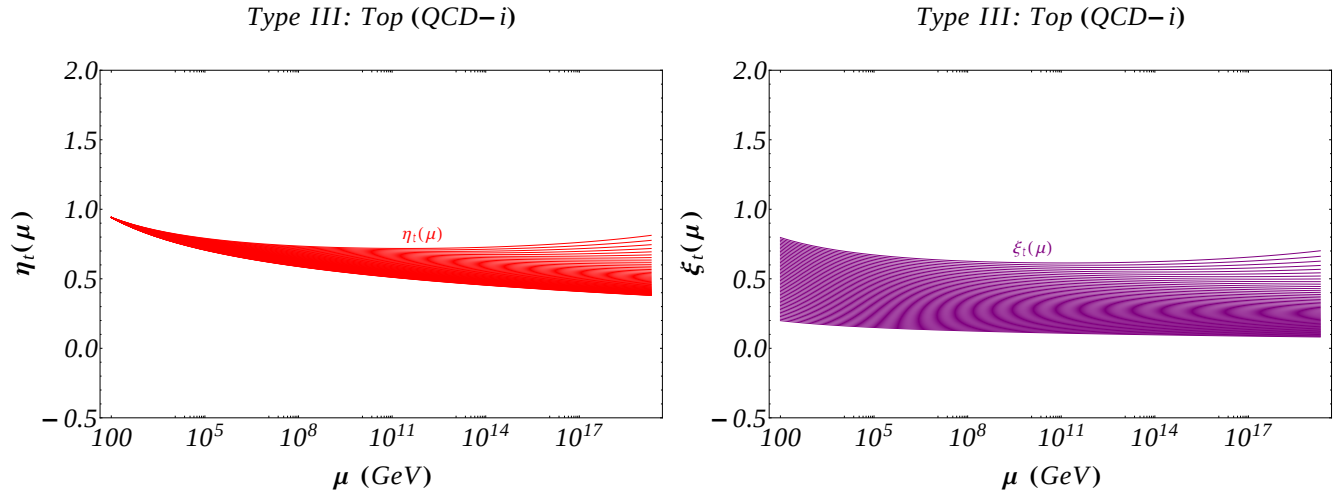

Figure 3.21.: *Yukawa evolution for top mass (**Left**) and top-FCNC (**Right**) couplings in the type III-2HDM. We have taken the initial conditions with threshold corrections given by QCD. The width in the family of curves is due to initial conditions in FCNC couplings* $0.2 \leq \xi_t(m_z) \leq 0.8$. *In addition, we have taken* $\xi_{bb} = \xi_{\tau\tau} = 0.2$.

We see as quark mass definition affects slightly RG evolution at high energy scales for top and bottom mass and FCNCs like couplings. In these behaviors for higher values of ξ_{tt}, new small discrepancies among different curves approaching the maximum value avoid non-perturbative behavior at larger scales. It is worthwhile to point out that FCNC evolution

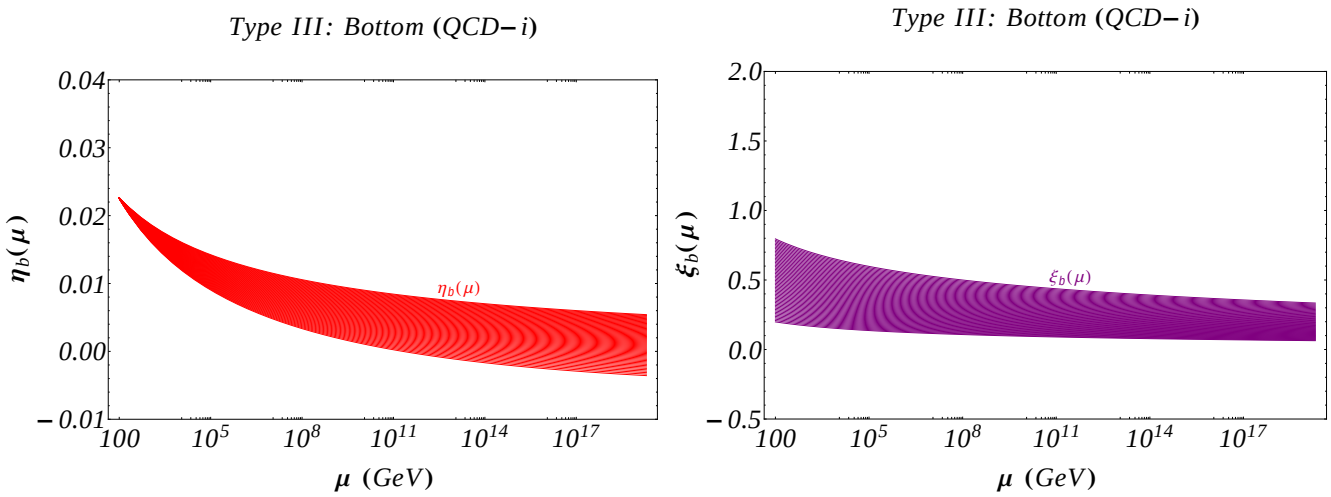

Figure 3.22.: *Yukawa evolution for bottom mass (**Left**) and bottom-FCNC (**Right**) couplings in the type III-2HDM. We have taken the initial conditions with threshold corrections given by QCD. The width in the family of curves is due to initial conditions in FCNC couplings* $0.2 \leq \xi_b(m_z) \leq 0.8$. *In addition, we have taken* $\xi_t(m_z) = \xi_{\tau\tau}(m_z) = 0.2$

depends on other Yukawa couplings evolution, and that initial conditions in EW scale give us relevant information for the study of these processes in cosmological scenarios (which can be belong at those energy values).

3.7. Structure of radiative corrections: A general overview

We have studied all relevant β functions and those independent of Higgs potential couplings have been evolving with energy scale. With the aim of establishing the influence of this evolution in particular models, from the fundamentals we study which is the structure of the effective Higgs potential [6]. Let us first review the form of the radiative corrections in the context of a theory with a single scalar field, the real scalar ϕ^4-model, with

$$V_{cl} = \frac{m^2}{2}\phi^2 + \frac{\lambda}{4!}\phi^4 \tag{3.7.1}$$

The effective Higgs potential up to one loop level is

$$V_{eff} = V_{cl} + \frac{V_{cl}^{''}(\phi)^2}{64\pi^2}\ln\left(\frac{V_{cl}^{''}(\phi)}{\mu^2}\right) + ... \tag{3.7.2}$$

If $m^2 > 0$, we should explore in what values of ϕ it is possible to compute V_{eff}. Suppose we have chosen a RG-scale $\mu \sim m$ and that λ is small on that scale so that perturbation theory in λ is valid. Then evidently we can calculate V as $\phi \to 0$ by just retaining $\mu \sim m$ since the one loop correction is obviously small. Thus the origin remains a minimum, as was the case for the tree potential.

Now, if $\phi >> m$,the one-loop correction now becomes large, because of the logarithm, so that one must improve on this perturbation expansion. RG improvement amounts, in fact, to exploiting the freedom to choose the renormalization scale to take $\mu^2 \sim V_{cl}^{''}(\phi)$, or $\phi \sim \mu$ for large ϕ. Then to a good approximation at large ϕ we will have

$$V = \frac{\lambda(\phi)}{4!}\phi^4 \tag{3.7.3}$$

and this will be perturbatively believable as long as $\lambda(\phi)$ is small. Now in this simple model λ becomes large at large scales, approaching to a Landau pole, and so perturbation breaks down eventually in spite of our RG improvement. Thus we cannot say what form the potential takes at sufficiently large ϕ.

In a more complicated theory, there are two main issues to take into consideration. Firstly, if the potential depends on more than one scalar field, it is not immediately apparent in which directions in field space we will be able to describe

[6] This discussion follows the formalism presented in [114]

the large-field potential since we have only one scale at our disposal. Secondly, the behavior of the $\lambda_i(\phi)$ for large ϕ may be quite different from that in the simple ϕ^4-model. In the SM, for instance, an appropriate direction is oriented with the one where the SSB occurs. Besides, fermions and vector gauge boson contribute to the second derivative of classical potential in the logarithmic part. Despite these issues, one loop RG improvement for Higgs potential can be computed directly knowing β_λ function, the anomalous dimension, and the function γ_m to one loop level

$$\begin{aligned} V_{RGI} &\simeq \frac{1}{2}m^2\left[1+\frac{12\lambda}{32\pi^2}\ln\left(\frac{\Lambda^2}{\mu^2}\right)\right]\phi_c^2(\mu) \\ &+\frac{1}{4}\left[\lambda+\frac{1}{16\pi^2}\left(12\lambda^2+\frac{3}{8}g^4+\frac{3}{16}\left(g^2+g'^2\right)-3j\eta_t^4\right)\ln\left(\frac{\Lambda^2}{\mu^2}\right)\right]\phi_c^4(\mu) \end{aligned}$$

where Λ is some energy scale much larger than μ (the scale that fixed the initial conditions of the ODEs).

In particular, in the 2HDM the large size of the top quark Yukawa coupling, and the sign of its contribution to the β-function of λ_1 drives down the value of that parameter as one goes up in renormalization scale μ. If the starting point of λ_1 is sufficiently small, λ_1 may become negative at a given high value of μ, which mean that any minimum present for lower renormalization scales would in fact be unstable. This fact drives out that the potential would either be unbounded from below or develop a much deeper minimum at large ϕ_1. In fact, for the kinds of theories we consider here, the latter is generally the scenario because the positive contribution of the gauge coupling contributions to their β-functions causes λ_i to recover to positive values at yet higher scales.

A traditional approach to correct the tree-level potential at one-loop is by adding to the tree level 2HDM Higgs potential the Coleman-Weinberg potential

$$V_{\text{1-loop}}(\phi)=\sum_i\frac{\pm n_i}{64\pi^2}m_i(\phi)^2\left(\frac{m_i(\phi)^2}{\mu^2}-\frac{1}{2}\right) \tag{3.7.4}$$

The overhead sign refers to bosons and the lower sign to fermions; we sum over all particles of the theory, n_i is the degree of freedom for particle i and $m_i(\phi)$ is its field dependent mass; μ is the renormalization scale. It is necessary adding counterterms to the potential,

$$V(\Phi)=\sum_{i,j=1}^{n_H=2}\delta\mu_{ij}\Phi_i^\dagger\Phi_j+\frac{1}{2}\sum_{m,j,k,l=1}^{n_H=2}\delta\Lambda_{km}^{jl}(\Phi_j^\dagger\Phi_k)(\Phi_l^\dagger\Phi_m), \tag{3.7.5}$$

to ensure that the minimum of the tree-level potential together with the scalar masses are not changed by the 1-loop correction. We have used the compact form of Eq. (1.2.2). This approach has two unappealing features. First of all, the choice of renormalization scale μ is rather arbitrary. The assumption behind this is that μ is a residual scale dependence which shows up because we are not performing a complete renormalization, in fact, we are only renormalizing at 1 loop. The choice of this scale should not affect the physics at one-loop, only at two loops levels and hence it should not matter at our order of accuracy. Nonetheless, we are focused on the location of the minimum of this potential and since the potential clearly depends on this scale. This arbitrary selection might affect final conclusions and results [138][7]. A second issue is that the conditions which fix the parameters introduced in equation (3.7.5) leads to several nonlinear equations (RGEs described above) which must be solved numerically. These forms strongly depend on treated model. A third caveat is that divergences show up when one is fixing the parameters. This fact is because we need to calculate derivatives of the potential in the Coleman-Weinberg form (3.7.4).

$$\left[\left(m_i(\phi)^2\right)^2\ln\left(\frac{m_i(\phi)^2}{\mu^2}\right)\right]''=2\left(m_i(\phi)^{2'}\right)^2\ln\left(\frac{m_i(\phi)^2}{\mu^2}\right)+... \tag{3.7.6}$$

where $m_i(\phi)^2$ can be zero values at the same time as derivative $m_i(\phi)'^2$ is different to zero. Taking a simple scalar-field theory [139], it is possible consider quantum corrections and conterterms by means of

$$V_{\text{1-loop}}(\phi)+V_{CT}(\phi)=\sum_i\frac{\pm n_i}{64\pi^2}m_i(\phi)^2\left[\left(\frac{m_i(\phi)^2}{m_i(v)^2}-\frac{3}{2}\right)+2m_i(\phi)^2m_i(v)\right]. \tag{3.7.7}$$

[7] In fact, as we will see in chapter 5, this occurs in the Inert-2HDM [34] where even nature of minima might change at one loop level.

We should to choose the counterterms such that the location of the minimum is the same as for the tree-level potential (as above), and that the tree level masses are preserved. Here v is the place of the minimum, which means that $m_i(v)$ is the physical mass of the particle. Note that all residual scale dependence vanishes from the potential, due to being absorbed in the added counterterms.

We shall assume that the stability conditions shown in Tab. 2.1 must hold at all renormalization scales μ up to the gauge unification or Planck scales. This fact will be sufficient to yield a Higgs potential bounded from below. Demanding the stability of the scalar potential at all energy scales will thus, typically, impose lower limits on the values of its quartic couplings.

Another way of defining the values of the λ_i is by requiring that they remain small enough for perturbative reliability at higher energy scales. Hence, if the initial values of λ_i are too large, their β-functions will be positive and their renormalization scale evolution will drive them to ever higher values. Requiring that the λ_i remain small at all energy scales will thus impose upper bounds on their values. How small should "small" be? Here we enter a somewhat arbitrary region, but requiring initially that all λ_i remain less than 4π at all renormalization scales seems a reasonable requirement. Nevertheless, our analyses are driven in such a way that numerical convergence could give values even smaller for couplings, and thus more constrained zones in different realizations of parameter space.

We will impose both stability and perturbativity bounds on the quartic parameters of the 2HDM at all scales between the weak-scale m_Z and m_U . Such analyses have been made before in the following works: these ideas were applied to the SM [11, 49, 140–143], SUSY models [5, 144, 145] and also to a simple 2HDM [20, 21, 33, 146, 147]. In this work we are interested in studying the differences that the application of these bounds will have on the several possible two-Higgs doublet models, and on the possible vacua therein.

3.8. Comments about NLO analyses

The presence of an additional doublet yields new zones in the parameter space to be analyzed by the behavior of extended quartic couplings. β functions at one loop level lead to study evolution of extended parameters concerning a UV energy scale μ. Vacuum analyses at this level are based on the fulfillment of constraints, gotten at tree level for a bounded from below extended Higgs potential, over quartic couplings now depending on μ. Moreover, possible divergences in the evolution of scalar couplings give us information of perturbation theory develops in the new Higgs sectors. Obtaining these evolutions require the simultaneous solution of all RGEs, i.e., scalar, gauge, and Yukawa sector. Since at one loop level gauge and extended Yukawa sectors are independent of scalar couplings, we obtained relevant information independent of symmetries in the Higgs potential over energy-evolution for these couplings. Due to its relevance in the vacuum and perturbativity analyses, we focused on the fermion-scalar sector wherein we analyzed couplings structures behavior for models with (type I-II) and without natural flavor conservation (type III). Furthermore, we study ambiguities-free definition of quark masses, which is crucial in the interpretation of RGEs results for vacuum stability. The strong dependence of these corrections is relevant in type I and II 2HDMs when $\tan\beta < 1$ due to for these values divergences appearance scale is shifted to values one to four magnitude orders upper. Therefore, we can see it as an improvement of energy scales for perturbation theory validity. Nevertheless, for models with alternative mechanism to suppress FCNCs, this QCD improvement for heavier quark masses is only relevant in the highest scales analyzed. However, these improvements in the evolution for FCNC couplings can be appropriate to study them in cosmological scenarios, where perhaps precision shall become relevant.

Finally with these developments in mind and from diagrammatic systematics here performed and from an algebraic approach to RGEs treated in Appendix J, symmetries, and vacuum choices leading construct well-motivated scalar models which will be studied regarding stability, metastability and perturbativity concepts in the next chapters. Before that, we will introduce perturbative unitarity from the S matrix, which are complementary studies to constrain and to interpret these models correctly.

4. $S-$matrix unitarity and constraints to 2HDM

Relativistic quantum field theories arise from different mathematical principles and systematics. These foundations allow analyzing several phenomenologies of elementary particles at a wide range of energy scales. One of them is the Poincaré's covariant construction of the space-time scenario where interactions take place. This relativistic invariance includes all translations, rotations and boosts in four dimensions operations leaving unaffected intervals between events. Besides, interactions what are described by quantum mechanics foundations must satisfy the probability conservation principle. Both statements, Poincaré's invariance and probability conservation, lead to define the scattering matrix or $S-matrix$ for interactions between elemental fields; which are intimately related each to other by the $S-$matrix unitarity properties itself. This picture for interactions is the traditional one based on the structure of the correlation functions of the bosons or fermion fields in the theory. Scattering matrix unitarity is a necessary and sufficient condition to ensure probability conservation in the Hilbert space and also allows to define to the S matrix as a space-temporal invariant. In this chapter, we discuss the fundamentals behind $S-matrix$ definition and the behavior of specific processes where unitarity has been implemented. To that end, we take into account some discussions of the perturbative character of the unitarity for realistic models in high energy physics, as well as the influence in the searching of possible strongly interacting sectors or dynamical resonances. Furthermore with these foundations, we incorporate the perturbative unitarity in scattering processes in a general and particular cases of 2HDMs. By using perturbative unitarity in models with SSB, we study potential mechanisms and models describing possible fermion mass scales using these analyses into the annihilation of two fermions in polarized gauge bosons. Having in mind the above discussions, we introduce the study of the behavior of general Yukawa couplings for 2HDMs in fermion-antifermion scattering.

4.1. $S-$matrix: The framework for the interactions in High Energy Physics

Our initial objective is to determine how asymptotic initial (e.g. two particles $k-momenta$) and final (multi-particle state with $p_i-momenta$) states develop in a scattering process. To compute the change, we initially take both states relating to a temporal translation:

$$\begin{aligned} {}_{out}\left\langle p_1 p_2 ... \right| \left. k_A k_B \right\rangle_{in} &= \lim_{T\to\infty} \underbrace{\left\langle p_1 p_2 ... \right.}_{T} \overbrace{\left| k_A k_B \right\rangle}^{-T} \\ &= \lim_{T\to\infty} \left\langle p_1 p_2 ... \right| e^{-iH(2T)} \left| k_A k_B \right\rangle . \end{aligned} \tag{4.1.1}$$

In the last line, both asymptotic states are referred to the same temporal system. Therefore, the *in* and *out* states are connected by a sequence of unitary operators. This set is called the S matrix:

$${}_{out}\left\langle p_1 p_2 ... \right| \left. k_A k_B \right\rangle_{in} \equiv \left\langle p_1 p_2 ... \right| S \left| k_A k_B \right\rangle . \tag{4.1.2}$$

In other words, the S-matrix transforms initial arbitrary free particle states

$$(in-states)|\alpha; ini\rangle = |k_1, ...k_n; ini\rangle. \tag{4.1.3}$$

into final particle states

$$(out-states)|\beta; out\rangle = |p_1, ...p_m; out\rangle. \tag{4.1.4}$$

Hence, it is possible to make

$$S_{\beta\alpha} \equiv \langle\beta; out|\alpha; in\rangle \Leftrightarrow \langle\beta; in|S = \langle\beta; out| \text{ and } |\alpha; in\rangle = S|\alpha; out\rangle, \tag{4.1.5}$$

The S-matrix has the following formal features: i) The vacuum is trivially invariant, i.e., $|S_{00}| = 1$. ii) The one particle state is also invariant. By definition, these invariances are a consequence of energy-momentum conservation and four-dimensional translation invariance of Poincaré group. iii) S is unitary, i.e., it conserves the scalar product from initial

to a final state; it is equivalent to say that in and out Hilbert spaces are isomorphic[1]. And finally, iv) The $S-$matrix is also Poincaré's invariant, i.e.

$$U(\omega,a)\,SU^{-1}(\omega,a)=S. \tag{4.1.6}$$

with $U(\omega,a)$ the unitary representation of the Poincaré's group, obtained exponentiating the algebra [148]:

$$U(\omega,a)=\exp\left(\frac{i}{2}\omega_{\mu\nu}M^{\mu\nu}+ia_{\mu}P^{\mu}\right). \tag{4.1.7}$$

The operators $M_{\mu\nu}$ generate the algebra $SO(d,1)$ of Lorentz (orthogonal) transformations in $d+1$ spacetime dimensions. The spatial components M_{jk} generate the algebra $SO(d)$ of rotations in d spatial dimensions. The overall representation includes $\mathrm{Spin}^{+}(d,1)$, the double cover of the proper orthochronous Lorentz group, along with translations.

4.2. S matrix unitarity

The S matrix unitarity reflects the fundamental principle of probability conservation in quantum mechanics. All relevant physical quantities are equivalent to positive-norm states preserved through their time evolution in, for instance, a scattering, annihilation or decay process. This fact has significant consequences in the computations of physical observables, like the optical theorem and dispersion relations. To see those relationships in detail, first we establish the restrictions imposed by $S-matrix$ unitarity:

$$SS^{\dagger}=S^{\dagger}S=I. \tag{4.2.1}$$

The S matrix is the identity when there are no interactions. Even under existence of interactions, the particles has a some probability to become lost one another, for instance through some mechanism breaking the initial correlations. It also yields a S matrix approximately equal to the identity. These facts lead to us to isolate the non trivial part, defined by the T-matrix

$$S=I+iT,\;\; S^{\dagger}=I-iT^{\dagger}. \tag{4.2.2}$$

Using those forms in unitarity relation for scattering matrix (4.2.1)

$$SS^{\dagger}=(I+iT)\left(I-iT^{\dagger}\right)=I-iT^{*}+iT+TT^{\dagger}=I, \tag{4.2.3}$$

hence

$$TT^{\dagger}=iT^{\dagger}-iT. \tag{4.2.4}$$

In a similar way and taking the second part in (4.2.1), another relation for T matrix becomes

$$T^{\dagger}T=iT^{\dagger}-iT. \tag{4.2.5}$$

Introducing four-momentum conservation between in i and out f multi-particle states,

$$\langle f|\,T\,|i\rangle=(2\pi)^{4}\delta^{4}(P_f-P_i)\mathcal{T}_{fi}. \tag{4.2.6}$$

Here $\mathcal{T}_{fi}$ is the matrix element. The $S-$matrix elements must be consistent with four-momentum conservation, whose dependence is in the $T-$matrix. From equation (4.2.4)

$$\langle f|\,T^{\dagger}\,T\,|i\rangle=i\,\langle f|\,T^{\dagger}\,|i\rangle-i\,\langle f|\,T\,|i\rangle=\sum_{n}\langle f|\,T^{\dagger}\,|n\rangle\,\langle n|\,T\,|i\rangle\,, \tag{4.2.7}$$

where we have used a completeness relation for intermediate states labeled by n. Employing four-momentum conservation, Eq. (4.2.7) acquires the following form

$$\langle f|\,T\,|i\rangle-\langle f|\,T^{\dagger}\,|i\rangle=(2\pi)^{4}\delta^{4}(P_f-P_i)(\mathcal{T}_{fi}-\mathcal{T}^{*}_{fi})=i\sum_{n}(2\pi)^{4}\delta^{4}(P_f-P_n)(2\pi)^{4}\delta^{4}(Pn-P_i)\mathcal{T}^{*}_{fn}\mathcal{T}_{ni}. \tag{4.2.8}$$

Since all intermediate states must also be compatible with the four-momentum conservation. Therefore both restrictions are equivalent to having a global four-momentum conservation

[1] It is natural to assume that outgoing particles of some scattering process can be used as incoming particles of another scattering process. Therefore the *in* and *out* spaces must be isomorphic.

$$\mathcal{T}_{fi} - \mathcal{T}^*_{fi} = i\sum_n (2\pi)^4 \delta^4(Pn - P_i)\mathcal{T}^*_{nf}\mathcal{T}_{ni}. \tag{4.2.9}$$

Involving all intermediate states $|n\rangle$ coupled to $|i\rangle$ and $\langle f|$. In practical cases, we seldom have two particle scatterings (or several cases can be reduced to two-particle scattering). As a first glance, identical particles are ignored. Besides, we take in (4.2.9) the elastic channel, i.e., $|i\rangle = |f\rangle$ states; corresponding to a forward scattering with the same spin and internal variables in the initial and final configurations. Assuming only short range interactions [149], it is possible to get

$$\mathcal{T}_{ii} - \mathcal{T}^*_{ii} = i\sum_n (2\pi)^4 \delta^4(Pn - P_i)\mathcal{T}^*_{ni}\mathcal{T}_{ni} \tag{4.2.10}$$

The left side in (4.2.9) is translated into

$$\mathcal{T}_{ii} - \mathcal{T}^*_{ii} = 2i\mathrm{Im}\mathcal{T}_{ii}. \tag{4.2.11}$$

From Fermi's golden rule, the right side of (4.2.11) is connected with the total cross section, additionally to a flux factor coming from the initial state. To see this fact, terms $(m_a, \mathtt{s}_a)$ and $(m_b, \mathtt{s}_b)$ denotes mass and spin of the particles in the initial state. Taking n intermediate states and from integral equation for two particles differential cross section[2]

$$d\sigma_{2\to n} = \frac{1}{4\left[(p_1\cdot p_2)^2 - m_1^2 m_2^2\right]^{1/2}} \int_\Delta d\tilde{p}_3 ... d\tilde{p}_{n+2} \left|\langle p_3 .. p_{n+2}|\ \mathcal{T}\ |p_1, p_2\rangle\right|^2 (2\pi)^4 \delta^4(p_1 + p_2 - p_3 - ... - p_{n+2}), \tag{4.2.13}$$

it is possible to find the structure for the total cross section

$$\sigma_{tot}(i) = \frac{1}{2\lambda^{1/2}(s, m_a^2, m_b^2)} \sum_n (2\pi)^4 \delta^4(Pn - P_i)\mathcal{T}^*_{ni}\mathcal{T}_{ni}, \tag{4.2.14}$$

where

$$\lambda(s, m_a^2, m_b^2) = \left(s^2 + m_a^4 + m_b^4\right) - 2sm_a^2 - 2m_a^2 m_b^2 - 2sm_b^2, \tag{4.2.15}$$

with a appropriate normalization in (4.2.14) has been used for an invariant phase space $d^3p/(2\pi)^3 2E$. The common 3-momentum in the center of mass frame $|\mathbf{p}|$ of the particles A and B is related to Mandelstam variable s by $4s\mathbf{p}^2 = \lambda(s, m_a^2, m_b^2)$. By meaning of (4.2.11) and (4.2.14), it is possible to find out the traditional form of the *optical theorem* in scattering theory [149]

$$\mathrm{Im}\mathcal{T}_{ii} = \lambda^{1/2}(s, m_a^2, m_b^2)\sigma_{tot}(i). \tag{4.2.16}$$

It is worth to see how $\mathcal{T}_{ii}$ amplitude enter in the elastic cross section. Assuming polarizations to be in such a way that initial state is invariant under rotations around incoming momentum, the elastic cross section can be integrated over azimuthal angle and expressed in terms of transfered momentum t, instead of scattering angle θ in the CM reference system. Hence, in the process $A + B \to A + B$ we call (p_a, p_b) and $\left(p_a^{'}, p_b^{'}\right)$ the initial and final momentum respectively and satisfying four momentum conservation, i.e., $p_a + p_b = p_a^{'} + p_b^{'}$.. The elastic cross section can thus be written by

$$\frac{d\sigma_{ela}(s,t)}{dt} = \frac{|\mathcal{T}(s,t)|^2}{16\pi\lambda(s, m_a^2, m_b^2)}. \tag{4.2.17}$$

The forward scattering is characterized by $t = 0$ and $\mathcal{T}(s, 0)$(denoted above as $\mathcal{T}_{ii}$). Consequently

[2]In this derivation, we will use the explicit forms of the Mandelstam variables

$$\begin{aligned} s &= (p_a + p_b)^2 = \left(p_a^{'} + p_b^{'}\right)^2. \\ t &= \left(p_a - p_a^{'}\right)^2 = \left(p_b - p_b^{'}\right)^2, \quad s + t + u = 2\left(m_a^2 + m_b^2\right). \\ u &= \left(p_a - p_b^{'}\right)^2 = \left(p_b - p_a^{'}\right)^2. \end{aligned} \tag{4.2.12}$$

$$\frac{d\sigma_{ela}(s,0)}{dt} = \frac{\left(\mathrm{Re}\mathcal{T}_{ii}\right)^2 + \left(\mathrm{Im}\mathcal{T}_{ii}\right)^2}{16\pi\lambda(s,m_a^2,m_b^2)}. \tag{4.2.18}$$

Utilizing optical theorem (4.2.16)

$$\begin{aligned}\frac{d\sigma_{ela}(s,0)}{dt} &= \frac{\left(\mathrm{Re}\mathcal{T}_{ii}\right)^2 + \left(\lambda^{1/2}(s,m_a^2,m_b^2)\sigma_{tot}(i)\right)^2}{16\pi\lambda(s,m_a^2,m_b^2)}, \\ &= \frac{\left(\mathrm{Re}\mathcal{T}_{ii}\right)^2}{16\pi\lambda(s,m_a^2,m_b^2)} + \frac{\sigma_{tot}^2(i)}{16\pi} > \frac{\sigma_{tot}^2(i)}{16\pi}.\end{aligned} \tag{4.2.19}$$

In high-energy collisions could happen in such a way that the imaginary parts of the forward scattering dominate to the real part ones. In that case, Eq. (4.2.19) might useful to normalize the differential cross section by assuming the total cross section to be known.

4.2.1. Generalized partial waves

It is possible to extract more observable consequences from unitarity condition when the operator T becomes diagonalized, at least partially. In the two particles scattering, this is achieved in angular momentum basis; being the Jacob-Wick formalism the most accurate method to do the corresponding projection between plane waves state and momentum angular ones (see discussion presented in Appendix K). Calling (λ_a,λ_b) and $(\lambda_a^{'},\lambda_b^{'})$ the helicities for particles in the initial and the final states respectively, referred to the center of mass frame (CM) where $\mathbf{p}_a+\mathbf{p}_b = \mathbf{p}_a^{'}+\mathbf{p}_b^{'}$[3]. For a two particles state in the CM system, let be θ and φ the polar and the azimuthal angles of the 3-momentum on a fixed z-axis. Considering $R_{\theta\varphi}$, the product of two transformations: a rotation in θ around y axis followed by a rotation in φ around z axis. This rotation transforms the unitary vector $\widehat{z}$ into the vector $\mathbf{p}/|\mathbf{p}|$. A state with angular momentum J and projection M along z axis is obtained as

$$|J,M;\lambda_a,\lambda_b\rangle = \left(\frac{2J+1}{4\pi}\right)^{1/2}\int d\varphi\sin\theta d\theta\mathcal{D}^J_{\lambda_a-\lambda_b}\left(R^{-1}_{\theta\varphi}\right)|p_a,\lambda_a;p_b,\lambda_b\rangle\,. \tag{4.2.23}$$

Phase conventions are selected in such a way that η_a and η_b are intrinsic parities of particles A and B; being the transformation of states under parity P and temporal inversion T, the following

$$P\,|J,M;\lambda_a,\lambda_b\rangle = \eta_a\eta_b\,(-1)^{J-S_a-S_b}\,|J,M;-\lambda_a,-\lambda_b\rangle\,. \tag{4.2.24}$$

$$T\,|J,M;\lambda_a,\lambda_b\rangle = (-1)^{J-M}\,|J,-M;-\lambda_a,-\lambda_b\rangle\,. \tag{4.2.25}$$

These relations reflect the fact helicity is odd under parity but even under temporal inversion. By using Wigner-Eckart theorem [4], the matrix element $\mathcal{T}_{fi}$ satisfy the following expansion

[3] We do it for two-particle states with definite momentum. For one-particle states, we use the normalization

$$\langle p'\lambda'|p\lambda\rangle = (2\pi)^3\,2E\delta_{\lambda\lambda'}\delta^3\left(\mathbf{p}-\mathbf{p}'\right) \tag{4.2.20}$$

so that the two-particle states are normalized as follows

$$\langle p_a'\lambda_a' p_b'\lambda_b'|p_a\lambda_a p_b\lambda_b\rangle = (2\pi)^6\,(2E_a)\,(2E_b)\,\delta_{\lambda\lambda'}\delta^3\left(\mathbf{p}_a-\mathbf{p}_a'\right)\delta^3\left(\mathbf{p}_b-\mathbf{p}_b\right) \tag{4.2.21}$$

The product of δ-function in the last equation can be redefined as

$$\delta^3\left(\mathbf{p}_a-\mathbf{p}_a'\right)\delta^3\left(\mathbf{p}_b-\mathbf{p}_b\right) = \Lambda\delta^4\left(p_a'+p_b'-p_a-p_b\right)\delta^2\left(\mathbf{n}-\mathbf{n}'\right) \tag{4.2.22}$$

where $\mathbf{n},\mathbf{n}$ are unit vectors in directions $\mathbf{p}_a$ and $\mathbf{p}_a'$ ($\delta^2(n-n)$ can be written in terms of angles (θ,φ) as $\delta\left(\cos\theta-\cos\theta'\right)\delta\left(\varphi-\varphi'\right)$). The Λ is a normalization factor given as $\Lambda = |\det(J)|$, where J is the Jacobian of the considered transformation.

[4] The Wigner-Eckart theorem comes from representation theory in group theory. For our particular case, it states that matrix elements of spherical tensor operators on the basis of angular momentum eigenstates can be expressed as the product of two factors, one of which is independent of angular momentum orientation, and the other a Clebsch-Gordan coefficient; i.e.

$$\langle jm|T^k_q|j^{'},m^{'}\rangle \tag{4.2.26}$$

where T^k_q is the qth component of a rank k spherical tensor, $|jm\rangle$ and $|j^{'}m^{'}\rangle$ are eigenstates of total angular momentum J^2 and its

$$\mathcal{T}_{fi} = \langle p_a^{'}, \lambda_a^{'}; p_b^{'}, \lambda_b^{'} | \mathcal{T} | p_a, \lambda_a; p_b, \lambda_b \rangle = 16\pi \sum_J (2j+1)\, \mathcal{T}^J_{\lambda_a' \lambda_b'; \lambda_a \lambda_b}(s) \mathcal{D}^{J*}_{\lambda_a - \lambda_b, \lambda_a' - \lambda_{b,}'}(\varphi, \theta, 0)\,. \tag{4.2.28}$$

In the last relation, rotational invariance has been taking into account. In Eq. (4.2.28) the z axis is chosen along the incident momentum p_a and θ,φ are the polar angles of $p_a^{'}$. Finally, the sum over J runs over integer or half-integer values according to whether an even or odd number of half spin is present in the incoming and outcoming states. Besides, Jacob-Wick expansion in (4.2.28) is generalized to an arbitrary two by two scattering process. In the helicity formalism, the spin degrees of freedom of the particle involved do not introduce any significant complication that brings a more intricate systematics with respect to spinless particles. By contrast, in the conventional approach with static spin labels for the particles, the relationship between " plane wave"and "angular momentum" states lead to multiple Clebsh-Gordan couplings coefficients for both the initial and the final states, and consequently the partial wave is much more complicated than that of spinless particles [111].

If invariance under parity applies, the reduced matrix element behaves as

$$\mathcal{T}^J_{\lambda_a', \lambda_b'; \lambda_a, \lambda_b}(s) = \mathcal{T}^J_{-\lambda_a'. -\lambda_b'; -\lambda_a, -\lambda_b}(s). \tag{4.2.29}$$

In the same way, if invariance under temporal inversion applies, we get

$$\mathcal{T}^J_{\lambda_a', \lambda_b'; \lambda_a, \lambda_b}(s) = \mathcal{T}^J_{\lambda_a, \lambda_b; \lambda_a', \lambda_b'}(s). \tag{4.2.30}$$

These relations are expressing the symmetry of the scattering matrix. When the total energy $s^{1/2}$ is below to the inelastic threshold only the initial two body channel contributes to the sum over intermediate states in (4.2.9). Projecting on angular momentum J results in the relation [5]

$$\mathcal{T}^J(s) - \mathcal{T}^{J\dagger}(s) = 2i\lambda^{1/2}(s, m_a^2, m_b^2) s^{-1} \mathcal{T}^J(s) \mathcal{T}^{J\dagger}(s), \tag{4.2.32}$$

where $\mathcal{T}^J(s)$ is considered as a matrix $(2S_a+1)(2S_b+1) \times (2S_a+1)(2S_b+1)$ in the helicity space. Invariance under time reversal can be applied to reexpress (4.2.32)

$$2i \mathrm{Im} \mathcal{T}^J(s) = 2i\lambda^{1/2}(s, m_a^2, m_b^2) s^{-1} \mathcal{T}^J(s) \mathcal{T}^{J\dagger}(s). \tag{4.2.33}$$

For spinless particles the develops are simplified considerably. In particular $\mathcal{D}^{J*}_{0,0}(\varphi, \theta, 0)$ is the Legendre polynomial $P_J(\cos\theta)$, while Eq. (4.2.32) is solved by introducing a phase shift $\delta_J(s)$ through

$$\frac{2\lambda^{1/2}}{s} \mathcal{T}^J(s) = -i\left(e^{2i\delta_J(s)} - 1\right) = 2e^{i\delta_J(s)} \sin\delta_J(s). \tag{4.2.34}$$

If the matrix $\mathcal{T}^J(s)$ is diagonal in some appropriate basis, the same expression is true for each diagonal element. Establishing the scopes and limitations of the overall approach is worthwhile. It is well known as the strong interactions as well as many scalar couplings coming from a Higgs mechanism satisfy all considerations established. By contrast, weak interactions violate parity conservation. Hence inversion temporal requirement is not exactly achieved in many processes. On the other hand, as electromagnetic interactions are of long range, generating possible correlation mechanism of in and out states and as first glance avoiding an analog treatment in, at least, an exact way. Having these facts in mind, we will consider unitarity constraints for particular gauge theories with extended Higgs sectors as 2HDM.

---

z-component J_z, $\langle j || T^k || j^{'} \rangle$ has a value which is independent of m and q, and

$$C^{jm}_{kqj'm'} = \langle j^{'} m^{'}; kq | jm \rangle \tag{4.2.27}$$

is the Clebsch-Gordan coefficient for adding $j^{'}$ and k to get j.

[5] Here the kinematical factor comes from

$$\int \frac{d^3p_a d^3p_b}{(2\pi)^3 (2E_a) (2\pi)^3 (2E_b)} (2\pi)^4 \delta^4(p_a + p_b - P) = \frac{\lambda^{1/2}(s, m_a^2, m_b^2)}{8s(2\pi)^2} d\Omega_p. \tag{4.2.31}$$

4.2.2. Unitarity Constraints

Our goal is to introduce the standard systematics to evaluate S matrix unitarity in an extensive set of high energy scatterings. In the last section, we see as the non-trivial part of the S-matrix can be projected into an appropriate momentum angular basis; where is possible to establish a meaningful set of symmetry and dynamical properties.

First of all, it starts defining the matrix element normalized with kinematical factors

$$\mathcal{M}^J(s) \equiv \mathcal{M}^J_{\lambda'_a\lambda'_b;\lambda_a\lambda_b}(s) = \frac{s^{1/2}}{\lambda^{1/4}(s,m_a^2,m_b^2)}\mathcal{T}^J_{\lambda'_a\lambda'_b;\lambda_a\lambda_b}(s). \tag{4.2.35}$$

with kinematical factor $\lambda(s,m_a^2,m_b^2) = \left(s^2+m_a^4+m_b^4\right) - 2sm_a^2 - 2m_a^2m_b^2 - 2sm_b^2$. If the initial and the final helicity states are zero (i.e. $\lambda_a = \lambda_b$ and $\lambda_c = \lambda_d$), the $\mathcal{D}$ functions in Eq. (4.2.28) are reduced to Legendre polynomials, being possible to compute coefficients associated to partial wave expansion using

$$\mathcal{M}^J(s) = \frac{1}{32\pi}\int_{-1}^{1}\mathcal{M}(s,\theta)P^J(\cos\theta)d(\cos\theta). \tag{4.2.36}$$

The unitarity limit over matrix elements $\mathcal{M}^J_{\lambda'_a\lambda'_b;\lambda_a\lambda_b}(s)$ in (4.2.35) could be get in a general way (for any helicity combination) by means of $S-$matrix unitarity related to the conditions (4.2.9). Taking the matrix element for two particles states in an elastic scattering,

$$\langle J,M,\lambda_a,\lambda_b|\,\mathcal{T}^{J\dagger}-\mathcal{T}^J\,|J,M,\lambda_a,\lambda_b\rangle = i\,\langle J,M,\lambda_a,\lambda_b|\,\mathcal{T}^{J\dagger}\mathcal{T}^J\,|J,M,\lambda_a,\lambda_b\rangle\,. \tag{4.2.37}$$

We note that the decomposition of the unitary operator contains not only the two-particle states (which are in the form $|J,M,\lambda_a,\lambda_b\rangle$), but it must involve a complete basis for Fock-space. By introducing a completeness relation of intermediate states, we find

$$\begin{aligned}
\langle J,M,\lambda_a,\lambda_b|\,\mathcal{T}^{J\dagger}-\mathcal{T}^J\,|J,M,\lambda_a,\lambda_b\rangle &= i\sum_\alpha \langle J,M,\lambda_a,\lambda_b|\,\mathcal{T}^{J\dagger}\,|J,M,\alpha\rangle\,\langle J,M,\alpha|\,\mathcal{T}^J\,|J,M,\lambda_a,\lambda_b\rangle\,,\\
&= i\sum_\alpha \langle J,M,\alpha|\,\mathcal{T}^J\,|J,M,\lambda_a,\lambda_b\rangle^\dagger\,\langle J,M,\alpha|\,\mathcal{T}^J\,|J,M,\lambda_a,\lambda_b\rangle\,,\\
&= i\sum_\alpha \left|\langle J,M,\alpha|\,\mathcal{T}^J\,|J,M,\lambda_a,\lambda_b\rangle\right|^2,
\end{aligned} \tag{4.2.38}$$

α refers to other important quantum numbers. Taking into account intermediate states with the same helicity, we arrive at the following inequality

$$\left|\langle J,M,\lambda_a,\lambda_b|\,\mathcal{T}^{J\dagger}-\mathcal{T}^J\,|J,M,\lambda_a,\lambda_b\rangle\right| \geq \left|\langle J,M,\lambda_a,\lambda_b|\,\mathcal{T}^J\,|J,M,\lambda_a,\lambda_b\rangle\right|^2. \tag{4.2.39}$$

Thus intermediate inelastic channels have not been considered yet. From relation (4.2.35), the last relation in $\mathcal{T}$ is converted into one to $\mathcal{M}$ through by

$$\left|\mathcal{M}^{J*}_{\lambda_a,\lambda_b,\lambda_a,\lambda_b} - \mathcal{M}^J_{\lambda_a,\lambda_b,\lambda_a,\lambda_b}\right| \geq \frac{\lambda^{1/4}(s,m_a^2,m_b^2)}{s^{1/2}}\left|\mathcal{M}^J_{\lambda_a,\lambda_b,\lambda_a,\lambda_b}\right|^2 \tag{4.2.40}$$

In the high energy limit the kinematical factor becomes $\lambda^{1/4}(s,m_a^2,m_b^2)\to s^{1/2}$. This fact leads to last relation to be translated into

$$\left|\mathcal{M}^{J*}_{\lambda_a,\lambda_b,\lambda_a,\lambda_b} - \mathcal{M}^J_{\lambda_a,\lambda_b,\lambda_a,\lambda_b}\right| \geq \left|\mathcal{M}^J_{\lambda_a,\lambda_b,\lambda_a,\lambda_b}\right|^2, \tag{4.2.41}$$

which is equivalent to $\left|\mathrm{Im}(\mathcal{M}^J)\right| \geq \left|\mathcal{M}^J\right|^2$. Moreover, Schwartz inequality reads $\left|\mathrm{Im}(\mathcal{M}^J)\right| \geq \left|\mathcal{M}^J\right|$; indicating finally the following relation for

$$\left|\mathcal{M}^J\right| \leq 1. \tag{4.2.42}$$

4.3. Interpretation of unitarity relations

Focusing our discussion in bounds and limits obtained from optical theorem with Jacob-Wick formalism for helicity waves, we consider the interpretations of these constraints in the case of a theory under a perturbative expansion for scattering processes. Expanding unitarity relations (4.2.42), it is possible to get

$$\left|\mathcal{M}^J\right|^2 = \left(\mathrm{Re}\mathcal{M}^J\right)^2 + \left(\mathrm{Im}\mathcal{M}^J\right)^2 \leq \left|\mathrm{Im}(\mathcal{M}^J)\right|, \tag{4.3.1}$$

$$\left(\mathrm{Re}\mathcal{M}^J\right)^2 \leq \left|\mathrm{Im}(\mathcal{M}^J)\right|\left(1-\left|\mathrm{Im}(\mathcal{M}^J)\right|\right) \leq \frac{1}{4}. \tag{4.3.2}$$

This relation can be drawn in an Argand's diagram, as the shown in Figure 4.1; where is possible to see as $\left(\mathrm{Re}\mathcal{M}^J\right)^2 \leq 1/2$. Geometrically (4.3.2) means that the eigenvalues of $\mathcal{M}^J$ lie on a circle of center $(0, 1/2)$ and radius $R = 1/2$ in the complex plane. It is important to note that (4.3.2) applies to the exact scattering matrix elements. However, in perturbation theory, the $\mathcal{M}^J$ matrices can be computed only up to a finite loop order. These approximated $\mathcal{M}^J$ do not lie on the Argand circle [150].

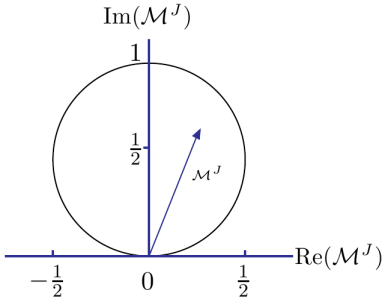

Figure 4.1.: *Argand diagram for the unitarity analysis of scattering amplitudes.*

In a unitary theory, the eigenvalues of all scattering matrices must lie on the Argand's circle. Since this requirement applies to the fully resumed scattering amplitudes, it is in general impossible to apply it directly. However in [151] a useful prescription to the unitarity requirement has been assumed to treat tree level scattering amplitudes with the further assumption that the theory is pertubative (there is not a strong regime for interactions or possible dynamical resonances in high energy scales).

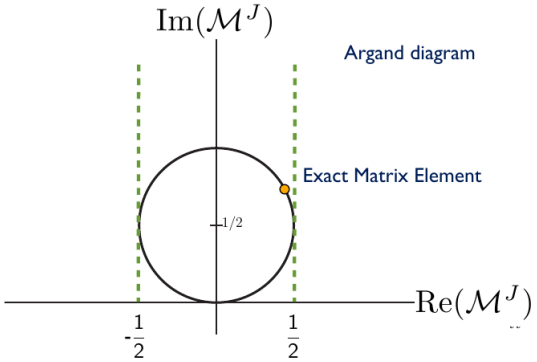

Figure 4.2.: *Tree-level value of the eigenvalues of M^J..*

In a unitary theory, the eigenvalues of all scattering matrices must lie on the Argand's circle. Since this requirement applies to the fully resumed scattering amplitudes, it is in general impossible to apply it directly. However in [151] a useful prescription to the unitarity condition has been assumed to treat tree-level scattering amplitudes with the further assumption that the theory is perturbative (there is not a strong regime for interactions or possible dynamical resonances in high energy scales).

$$\mathcal{M}(s,t) = \frac{g}{4m_w^2}(s+t). \tag{4.3.3}$$

Representation	Expression	Energy-Dependence
Dirac Spinors	$u(p), v(p)$	$\sqrt{E}$
Transverse Polarizations	$\varepsilon_T(p), \varepsilon_T^*(p)$	1
Longitudinal Polarizations	$\varepsilon_T(p), \varepsilon_L^*(p)$	E
Fermion Propagators	$(/q - m_f)^{-1}$	E^{-1}
Photon Propagator	$g^{\mu\nu} q^{-2}$	E^{-2}
Higgs Propagator	$\left(q^2 - m_H^2\right)^{-1}$	E^{-2}
3-Boson vertex function	$V_{\mu\nu\rho}$	E
Vector Boson Propagators	$\frac{-g_{\mu\nu}+q^\mu q^\nu/m_V^2}{q^2-m_V^2}$	1

Table 4.1.: *Energy dependence of gauge and scalar bosons and fermions representations inside scattering amplitudes. Gauge boson propagators are written in the unitary gauge, which is not manifestly renormalizable [44].*

By using restriction over Argand's diagram, energy behaves as

$$s \leq \frac{128 m_w^2}{g} \tag{4.3.4}$$

Thus we can conclude that outside this energy region, the use of perturbation theory is doubtful (the interaction of longitudinal W bosons is not "weak"at high energies). Within full SM, the problem of rapid growth of considered scattering amplitude is solved by including the Higgs boson exchange. In SM there are many individual diagrams whose contributions exhibit a polynomial growth in high-energy limit. All these "divergences" are caused by longitudinally polarized vector bosons or longitudinal parts of the corresponding massive propagators (see Table 4.1). However, in the sum of the diagrams contributing to a given process, such a power like growth is always compensated, and the result behaves as $O\left(E^0\right)$. It is notable that the same Higgs boson, which is related to the mass generation, is also essential in canceling the divergences due to vector boson scattering.

Moreover, there is another important aspect of perturbation expansion that should be mentioned separately. In higher orders of perturbation expansion, there appear closed-loop diagrams that lead to divergent integrals (ultraviolet divergences). Within some quantum field theory models, these can be tackled successfully with the aid of the renormalization procedure. It turns out that for a general model the non-renormalizability of ultraviolet divergences in higher orders of perturbation expansion are closely connected with the character of the high-energy behavior of scattering amplitudes at tree level: in particular, the power-like growth of a tree-level scattering amplitude implies non-renormalizability in higher orders [44].

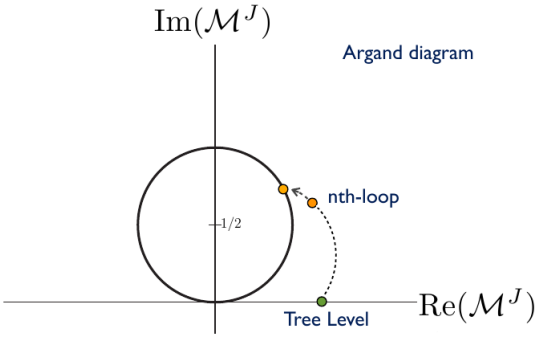

Figure 4.3.: *Tree-level value of the eigenvalues of M^J. The arrows show and paths how the loop corrections end up inside Argand's circle.*

Another way to see unitarity relations comes from the comprehensive study of the Argand circle; which is based on the fact the unitarity is only reliable for the full amplitude. However, it is possible to apply another prescription to interpret the unitarity requirement at tree level for models flat asymptotically [150,151] (amplitudes do not increase with energy indefinitely). The systematics belongs on the fact tree-level scattering are not subject to the unitarity requirement of optical theorem since they are real. Hence they belong on the real axis in the complex plane and might not reach the Argand circle. The loop corrections then play a crucial role in unitary theories. When perturbation assumption is implemented, loop corrections bring out the scattering amplitudes get closer to the Argand's circle, often following a

circuitous route, i.e., in which the loop corrections take the shortest possible path to the circle and are therefore minimal (see Fig. 4.3) [6].

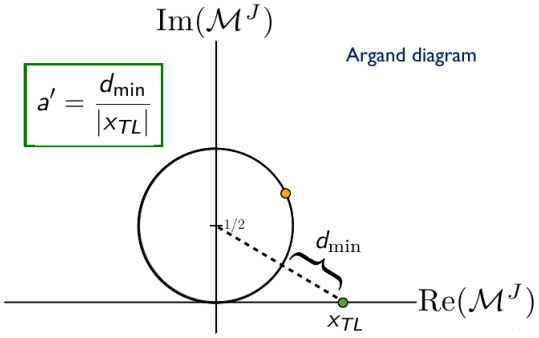

Figure 4.4.: *Optimistic case where the loop corrections take the shortest route to the Argand's circle. The orange point is the tree-level value of the T^J eigenvalue.*

In the optimistic case shown in Fig. 4.4, the size of the loop corrections can be computed using simple geometric arguments. The relative amount of loop corrections with respect to the tree-level value is given by

$$\mathsf{a} = \left| \frac{\mathcal{M}_{ii}^{J,exact} - \mathcal{M}_{ii}^{J,tree}}{\mathcal{M}_{ii}^{J,tree}} \right| = \frac{1}{|\mathcal{M}_{ii}^{J,tree}|} \left(\sqrt{(\mathcal{M}_{ii}^{tree})^2 + \frac{1}{4}} - \frac{1}{2} \right). \tag{4.3.5}$$

The ratio a represents the minimal relative amount of loop corrections needed to unitarize a given theory. Since it assumes that the loop corrections take the most direct route to the circle, this estimate is conservative. If a is close to one and the theory begins to be considered non-perturbative. Computing scattering amplitudes at tree-level allows determining when perturbativity is broken in a unitary theory.

Setting the maximal value for a which perturbativity is broken introduces some amount of arbitrariness in this approach. Nonetheless, this arbitrariness is widely limited [150, 151]. The following two requirements: $\mathsf{a} \leq 41\%$ and $\mathsf{a} \leq 20\%$, correspond respectively to demanding

$$\left| \mathcal{M}_{ii}^{J,tree}(s) \right| \leq \frac{1}{2} \text{ and } \left| \mathcal{M}_{ii}^{J,tree}(s) \right| \leq \frac{1}{4}. \tag{4.3.6}$$

These requirements hold for all center of mass energies $\sqrt{s}$. We show unitarity analyses for these additional two cases in the following sections. Although our study focuses on the 2HDM (as a simple extension of a minimal Higgs sector), the approach outlined here is universal and only assumes that the theory considered is unitary and perturbative (avoiding the presence of strong regime for interactions or possible dynamical resonances). Once a maximal ratio $\mathsf{a}_{\max}$ is selected, upper limits on the tree-level scattering amplitudes can be derived from (4.3.5) for any type of model respecting the former relevant assumptions.

4.4. Unitarity behavior for 2HDMs

To define an accurate model what describe realistic scattering processes, we demand that unitarity constraints be satisfied in all perturbative order of the theory. Unitarity is an essential framework which can be studied even at tree level with the fundamental assumption: Interactions are not strong enough in such a way the perturbativity is satisfied at this level. The possible fail or the accomplishment of this condition have been studied by the LHC employing effective couplings as presented in Fig. 1.1[7]. The systematic is based on the extrapolation of LQT method of the SM. The maximal mass for Higgs boson is achieved finding a saturation of the unitarity at tree level for partial waves coefficients $|\mathrm{Re}\mathcal{M}_0| \leq 1/2$. In this procedure, we use the regime for $\sqrt{s} >> m_w, m_z$, converting thus the vectorial scattering processes in the associated

[6] In effective theories, this procedure needs an additional step give by some unitarization method UM. Indeed, there are several UMs, which depending of interactions introduces one plausible characterization of effects like dynamical resonances or strongly interacting sectors for gauge bosons [152–154]. Perhaps ambiguities to define the minimal path can be present by non-renormalizability in such theories. See, for instance, discussion given in section 4.5

[7] Large deviation of SM prediction would indicate the presence of strong interacting gauge sectors. These effects have been described comprehensively in [152]

processes for Goldstone bosons using the equivalence theorem. Dominant couplings in this scattering processes are typically proportional to the scalar masses. Therefore, under the use of partial wave expansion, it is possible to constrain their values. This method based on unitarity has been applied in a generic structure to the 2HDM parameter space in [26,43]. We review this procedure formally, starting with the unitarity condition in the most conservative performance

$$|\mathcal{M}| \leq 1. \tag{4.4.1}$$

To take into account all possible processes in 2HDM, we should consider following matrix elements:

$$M_{ij} = \mathcal{M}_{i\to j}. \tag{4.4.2}$$

i, j labeling all possible two particle states. We consider only those processes involving the Higgs bosons masses directly. From equivalence theorem, we study processes with both physical and non-physical scalar states $w^{\pm}$, z, $H^{\pm}, A^0, H^0, h^0$. The eigenvalues of the matrices involving these relevant scattering processes will be bounded by the unitarity behavior of the higher one. The eigenvalues can be obtained on a particular basis and might be connected with the physical basis by a unitary transformation [19, 26, 37], as was discussed in section 2.3. To simplify the computations, we do it in a non-physical basis with gauge eigenstates $\phi_i^{\pm}, \eta_i, \xi_i$, To take into account all possible processes in 2HDM, we should consider following matrix elements:

$$\Phi_1 = \begin{pmatrix} \phi_1^+ \\ \eta_1 + i\xi_1 \end{pmatrix} \text{ and } \Phi_2 = \begin{pmatrix} \phi_2^+ \\ \eta_2 + i\xi_2 \end{pmatrix}. \tag{4.4.3}$$

by [23, 43], by means of the following procedure [26]:

- At high energy in scalar scattering processes, total weak isospin σ and the total hypercharge Y are conserved quantities, with values $\sigma = 0, 1$ and $Y = 0, 2, -2$:
- By considering states with $Y = 0$, and isospinors Φ_a ($a = 1, 2$ indicating doublet) they could be represented as columns, and $\Phi_a^\dagger$ can be represented as rows. Therefore the direct product $\Phi_{b\beta}\Phi^\dagger_{a\alpha}$ is translated into a 2×2 matrix for each pair a and b. Following an analog discussion presented in section 2.3 and since Pauli matrices plus identity build up a basis in the space of 2×2 hermitian matrices, it is possible to write

$$\Phi_{b\beta}\Phi^\dagger_{a\alpha} = A_0\delta_{\beta\alpha} + \overrightarrow{A}\cdot\overrightarrow{\tau}_{\beta\alpha}, \tag{4.4.4}$$

with $A_0 = (\Phi_a^\dagger\Phi_b)/2$ representing a *isoscalar* and $A_i = (\Phi_a^\dagger\tau^i\Phi_b)/2$ representing *isovector*. This lead to construct quartic dimension terms through

$$(\Phi^*_{a\alpha}\Phi_{b\alpha})(\Phi^*_{c\beta}\Phi_{d\beta}) = \frac{1}{2}\left[(\Phi^*_{a\alpha}\Phi_{d\alpha})(\Phi^*_{c\beta}\Phi_{b\beta}) + \sum_r \left(\Phi^*_{a\alpha}\tau^r_{\alpha\beta}\Phi_{d\beta}\right)\left(\Phi^*_{c\gamma}\tau^r_{\gamma\delta}\Phi_{bd}\right)\right]. \tag{4.4.5}$$

The complete set of all possible initial states with hypercharge $Y = 0$, which in our case these can be written as scalar products, transforming according to Z_2 symmetry as:

$$Y=0,\ \ \sigma=0: \quad \overbrace{\frac{1}{\sqrt{2}}\left(\Phi_1^\dagger\Phi_1\right)}^{Z_2\text{ even}},\ \overbrace{\frac{1}{\sqrt{2}}\left(\Phi_2^\dagger\Phi_2\right)}^{Z_2\text{ even}},\ \overbrace{\frac{1}{\sqrt{2}}\left(\Phi_1^\dagger\Phi_2\right)}^{Z_2\text{ odd}},\ \overbrace{\frac{1}{\sqrt{2}}\left(\Phi_2^\dagger\Phi_1\right)}^{Z_2\text{ odd}}, \tag{4.4.6a}$$

$$Y=0,\ \ \sigma=1: \quad \underbrace{\frac{1}{\sqrt{2}}\left(\Phi_1^\dagger\tau^i\Phi_1\right)}_{Z_2\text{ even}},\ \underbrace{\frac{1}{\sqrt{2}}\left(\Phi_2^\dagger\tau^i\Phi_2\right)}_{Z_2\text{ even}},\ \underbrace{\frac{1}{\sqrt{2}}\left(\Phi_1^\dagger\tau^i\Phi_2\right)}_{Z_2\text{ odd}},\ \underbrace{\frac{1}{\sqrt{2}}\left(\Phi_2^\dagger\tau^i\Phi_1\right)}_{Z_2\text{ odd}}, \tag{4.4.6b}$$

with $i = +, z, -$ labeling Pauli matrices representation. Now we consider states with $Y = 2$, where the following notation for the rows $\tilde{\Phi}_a = (i\tau_2\Phi_a)^T = (n_a, -\phi_a^+)$ and the columns $\tilde{\Phi}_a^\dagger = (i\tau_2\Phi_a)^*$ are introduced. The isoscalar $\tilde{\Phi}_{a\alpha}\Phi_{b\alpha}$ is antisymmetric under permutations $a \to b$, $\tilde{\Phi}_{a\alpha}\Phi_{b\alpha} = -\tilde{\Phi}_{b\alpha}\Phi_{a\alpha}$, while isovector is symmetric under by.

The entire set of initial states with hypercharge $Y = 2$, in analogy with (4.4.6a) can be written by

$$Y=2,\ \ \sigma=0: \qquad \overbrace{\text{absent}}^{Z_2\text{ even}}, \qquad \overbrace{\frac{1}{\sqrt{2}}\left(\tilde{\Phi}_1\Phi_2\right)}^{Z_2\text{ odd}} = -\overbrace{\frac{1}{\sqrt{2}}\left(\tilde{\Phi}_2\Phi_1\right)}^{Z_2\text{ odd}} \tag{4.4.7a}$$

$$Y=2,\ \ \sigma=1: \quad \underbrace{\frac{1}{2}\left(\tilde{\Phi}_1\tau^i\Phi_1\right)}_{Z_2\text{ even}}, \underbrace{\frac{1}{2}\left(\tilde{\Phi}_2\tau^i\Phi_2\right)}_{Z_2\text{ even}}, \qquad \underbrace{\frac{1}{\sqrt{2}}\left(\tilde{\Phi}_1\tau^i\Phi_2\right)}_{Z_2\text{ odd}} = \underbrace{\frac{1}{\sqrt{2}}\left(\tilde{\Phi}_2\tau^i\Phi_1\right)}_{Z_2\text{ odd}}. \tag{4.4.7b}$$

Factor 1/2 for the case Z_2 is due to the presence of two identical particles to the initial state. Z_2 even states with $Y=2$ and $\sigma=0$ are absent by virtue to the Bose-Einstein symmetry for identical scalars. States $Y=-2$ and $\sigma=1$ could be obtained from states with $Y=2$ by implementing a charge conjugation operator. Similarly, it is possible to write

$$\left(\Phi^*_{a\alpha}\Phi_{b\alpha}\right)\left(\Phi^*_{c\beta}\Phi_{d\beta}\right) = \frac{1}{2}\left[\left(\Phi^*_{a\alpha}\tilde{\Phi}^*_{c\alpha}\right)\left(\tilde{\Phi}_{d\beta}\tilde{\Phi}_{b\beta}\right) + \sum_r \left(\Phi^*_{a\alpha}\tau^r_{\alpha\beta}\tilde{\Phi}^*_{c\beta}\right)\left(\tilde{\Phi}_{d\gamma}\tau^r_{\gamma\delta}\Phi_{b\delta}\right)\right]. \tag{4.4.8}$$

Scattering matrices for each set of states with given quantum numbers Y and σ represented by (4.4.6a) and (4.4.7a)-(4.4.7b) at tree level are computed from potential (1.2.1) by means of the relations (4.4.5) and (4.4.8). Results can be represented by [26, 37]:

$$8\pi S_{Y=2,\sigma=1} = \begin{pmatrix} \lambda_1 & \lambda_5 & \sqrt{2}\lambda_6 \\ \lambda_5^* & \lambda_2 & \sqrt{2}\lambda_7^* \\ \sqrt{2}\lambda_6^* & \sqrt{2}\lambda_7 & \lambda_3+\lambda_4 \end{pmatrix}, \tag{4.4.9a}$$

$$8\pi S_{Y=2,\sigma=0} = \lambda_3 - \lambda_4, \tag{4.4.9b}$$

$$8\pi S_{Y=0,\sigma=1} = \begin{pmatrix} \lambda_1 & \lambda_4 & \lambda_6 & \lambda_6^* \\ \lambda_4 & \lambda_2 & \lambda_7 & \lambda_7^* \\ \lambda_6^* & \lambda_7^* & \lambda_3 & \lambda_5^* \\ \lambda_6 & \lambda_7 & \lambda_5 & \lambda_3 \end{pmatrix}, \tag{4.4.9c}$$

$$8\pi S_{Y=0,\sigma=0} = \begin{pmatrix} 3\lambda_1 & 2\lambda_3+\lambda_4 & 3\lambda_6 & 3\lambda_6^* \\ 2\lambda_3+\lambda_4 & 3\lambda_2 & 3\lambda_7 & 3\lambda_7^* \\ 3\lambda_6 & 3\lambda_7^* & \lambda_3+2\lambda_4 & 3\lambda_5^* \\ 3\lambda_6 & 3\lambda_7 & 3\lambda_5 & \lambda_3+2\lambda_4 \end{pmatrix}. \tag{4.4.9d}$$

In each matrix left sides to contain matrix elements for Z_2-even states, meanwhile in the lower right part belong Z_2-odd states; they are described employing λ_6 and λ_7 couplings. Unitarity bounds $|\mathcal{M}|<1$ are translated into eigenvalues for Λ matrices, in the most conservative case, the new condition is

$$|\Lambda| < \frac{1}{8\pi}. \tag{4.4.10}$$

By using perturbative prescription given in (4.3.6), where is possible set up loop corrections in a 41% and 21% to resumed amplitude with respect the tree level one, bound (4.4.10) is respectively translated into

$$|\Lambda| < \frac{1}{16\pi} \text{ and } |\Lambda| < \frac{1}{32\pi} \tag{4.4.11}$$

With an additional factor of two for indistinguishable final states in each case. For the general Higgs potential of (1.2.1), the eigenvalues equations for scattering matrices might become of third and fourth order, which is an intricate problem. By limiting the parameter space of the Higgs potential with reliable models, this issue can be avoided. For example, the models here considered are whose with a softly broken Z_2 symmetry (with a possible violation of the CP symmetry), within $\lambda_6=\lambda_7=0$. For this particular case, the matrices are diagonal by blocks leading to computing eigenvalues $\lambda^{Z_2}_{Y,\sigma\pm}$:

$$\Lambda^{even}_{21\pm} = \frac{1}{2}\left(\lambda_1+\lambda_2 \pm \sqrt{(\lambda_1-\lambda_2)^2+4\lambda_5^2}\right), \quad \Lambda^{odd}_{21} = \lambda_3+\lambda_4. \tag{4.4.12a}$$

$$\Lambda^{odd}_{20\pm} = \lambda_3-\lambda_4. \tag{4.4.12b}$$

$$\Lambda^{even}_{01\pm} = \frac{1}{2}\left(\lambda_1+\lambda_2 \pm \sqrt{(\lambda_1-\lambda_2)^2+4\lambda_4^2}\right), \quad \Lambda^{odd}_{01\pm} = \lambda_3 \pm \lambda_5. \tag{4.4.12c}$$

$$\Lambda^{even}_{00\pm} = \frac{1}{2}\left[3(\lambda_1+\lambda_2) \pm \sqrt{9(\lambda_1-\lambda_2)^2+4\left(2\lambda_3+\lambda_4\right)^2}\right], \quad \Lambda^{odd}_{00\pm} = \lambda_3+2\lambda_4 \pm 3\lambda_5. \tag{4.4.12d}$$

We shall use these eigenvalues in the following chapters to evaluate the perturbative unitarity behavior in λ couplings, which can be translated into bounds over scalar mass splittings in particular 2HDMs, in a joint study with vacuum stability analysis. For a Higgs potential with a complex value for λ_5 coupling, it is necessary replace $\lambda_5 \to |\lambda_5|$. For the general model with couplings of fourth dimension, where exist a hard violation of the Z_2 symmetry, extrapolation of the diagonalization lead to the following properties:

For a Hermitian matrix $\mathcal{M} = ||M_{ij}||$ with maximal and minimal eigenvalues Λ_+ and Λ_- respectively, all diagonal elements M_{ii} must belong between these eigenvalues[8]

$$\Lambda_- \leq M_{ii} \leq \Lambda_+. \tag{4.4.13}$$

By applying two steps is possible to achieve matrices diagonalization:

1. Corners for scattering matrices correspondent to terms are no violating the Z_2 symmetry. In this step, we get eigenvalues of the similar form (4.4.12a)-(4.4.12d).

2. By virtue of (4.4.13), the constraints (4.4.10) and (4.4.12) are necessary conditions for S-matrix unitarity. These increase due to the presence of λ_6 and λ_7 terms, which are related to the explicit break of the Z_2 symmetry and they accomplish with the assumption $|\lambda_{6,7}| \ll \Lambda^{Z_2}_{Y,\sigma}$.

Perhaps another effective manner to tackle the diagonalization problem is by using the re-parametrization invariants: As was discussed 2HDM have two doublets with the same quantum numbers (Φ_1, Φ_2). Therefore, their more general form must lead to global transformations mixing these fields and changing their phase relative. Each set of transformations yields a new Lagrangian with parameters coming from a first Lagrangian and whose generated by the first transformation. Details for this symmetry due to non-distinguishably for fields can be found widely in [58].

Eigenvalues of scattering matrices (4.4.12a)-(4.4.12d) are re-parametrization invariants by construction. The standard equations for eigenvalues of these matrices are also invariants under re-parametrization invariants by virtue construction from eigenvalues. Each matrix $n \times n$ $S_{Y,\sigma}$yields n invariant polynomials of λ_i. An appropriate choice is given by

$$\mathrm{Tr}\{S^k_{Y,\sigma}\} \;\; con \;\; k = 1, ..., n. \tag{4.4.14}$$

$\mathrm{Det}\,(S_{Y,\sigma})$ can also be used as invariant functions. Traces generate around of 12 non-independent invariants. Examples of four invariants, which are linear in λ_i and denoted as $I_{Y\sigma} \equiv 8\pi \mathrm{Tr}\{S_{Y\sigma}\}$ according their quantum numbers of hypercharge$Y$ and isospin σ

$$I_{21} = \lambda_1+\lambda_2+\lambda_3+\lambda_4, \tag{4.4.15a}$$

$$I_{20} = \lambda_3-\lambda_4, \tag{4.4.15b}$$

$$I_{01} = \lambda_1+\lambda_2+2\lambda_3, \tag{4.4.15c}$$

$$I_{00} = 3(\lambda_1+\lambda_2)+2\lambda_3+4\lambda_4, \tag{4.4.15d}$$

Only two are linearly independent combinations. This fact is due to two combinations linearly independent of λ_i parameters in the general Higgs potential for 2HDMs, corresponding to two scalars for the $SU(2) \times U(1)$ group which describes a re-parametrization transformation.

[8]This fact is obtained from extremal properties of the $n-$dimensional ellipsoid, described by $\Lambda_- \sum x_i^2 \leq \sum M_{ij}x_i x_j \leq \Lambda_+ \sum x_i^2$.

- Explicit relations in bounds for masses and mixing angles. Through searching explicit quantities, we would see as they are relations among masses and Higgs potential parameters in such a way that perturbative unitarity is preserved. To do it, in [23] considered a case with a Higgs potential with Z_2-symmetry and accomplishing with a CP symmetry. This fact was generalized in [43, 44], through

$$L_1 = \frac{1}{2v^2}\left[m_{H^0}^2\cos^2\alpha + m_{h^0}^2\sin^2\alpha + \frac{\sin 2\alpha}{2\tan\beta}\left(m_{h^0}^2 - m_{H^0}^2\right)\right] + \frac{m_{12}^2}{v^2\sin 2\beta}\left(1-\tan^2\beta\right), \tag{4.4.16a}$$

$$L_2 = \frac{1}{2v^2}\left[m_{H^0}^2\cos^2\alpha + m_{h^0}^2\sin^2\alpha + \frac{\sin 2\alpha\tan\beta}{2}\left(m_{h^0}^2 - m_{H^0}^2\right)\right] + \frac{m_{12}^2}{v^2\sin 2\beta}\left(1-\cot^2\beta\right), \tag{4.4.16b}$$

$$L_3 = \frac{1}{v^2\sin 2\beta}\left[\frac{\sin\alpha}{2}\left(m_{H^0}^2 - m_{h^0}^2\right) - m_{12}^2\right], \tag{4.4.16c}$$

$$L_4 = \frac{2m_{H^+}^2}{v^2}, \tag{4.4.16d}$$

$$L_5 = \frac{m_{12}^2}{v^2\sin 2\beta}, \tag{4.4.16e}$$

$$L_6 = \frac{2m_{A^0}}{v^2}. \tag{4.4.16f}$$

The L_i are functions of masses, α and β, and the softly broken parameter m_{12}^2. The unitarity limits are expressed regarding these quantities. From L_i expressions, quartic couplings inside Higgs potential can be written by

$$\lambda_1 = 2\left(L_1 + L_3\right), \tag{4.4.17a}$$

$$\lambda_2 = 2\left(L_2 + L_3\right), \tag{4.4.17b}$$

$$\lambda_3 = 2\left(L_3 + L_4\right), \tag{4.4.17c}$$

$$\lambda_4 = \frac{1}{2}\left(L_5 + L_6 - 2L_4\right), \tag{4.4.17d}$$

$$\lambda_5 = \frac{1}{2}\left(L_5 - L_6\right). \tag{4.4.17e}$$

- Mass limitations. By using L_i expressions (4.4.16a) between L_is with masses for the remain parameters of 2HDM, eigenvalues with unitarity restriction (4.4.10) and under the assumption of the Z_2-symmetry and for lower values of $\tan\beta$, following bounds can be gotten

$$m_{H^\pm} < 691 \text{ GeV}, \;\; m_{A^0} < 695 \text{ GeV}, \;\; m_h < 435 \text{ GeV}, \text{ and } m_{H^0} < 638 \text{ GeV}. \tag{4.4.18}$$

To higher values of $\tan\beta$ the upper limit becomes to be strong, going down to 100 GeV for $\tan\beta \simeq 6$, which is in conflict with exclusions regions from LEP, TEVATRON, and LHC for new Higgs bosons. Fixing, the lightest Higgs can change bounds over heaviest neutral Higgs dramatically. This effect can be seen from sum-rules for tree level unitarity [9]. On the other hand, presence of m_{12}^2 can relax the upper bounds for values big enough; for instance leading over m_{h^0} becomes independent of $\tan\beta$ and approximate equal to 670 GeV. This bound is compatible with the identification of this state with the scalar resonance found by CMS and Atlas collaborations [1, 2]. Unitarity

[9] Couplings from the kinetic sector of 2HDM satisfy some tree level unitarity bounds automatically. Since partial amplitudes cannot grow with energy, cancellations to avoid violation of perturbative unitarity are necessary. For instance, in the case of $V_LV_L \to V_LV_L$ scattering, the cancellation is possible in SM because the vertex is of the form $g_{\phi^0WW} = gm_w$. When a second or more doublets are added, saturation can be done by the sum of Higgs consistent with couplings nature and symmetries similar to SM ones:

$$\sum_i g_{h_i^0VV}^2 = g_{\phi^0VV}^2 \tag{4.4.19}$$

where i labels all neutral Higgs bosons of the extended Higgs sector, and ϕ^0 denotes the SM Higgs. On the other hand, ensuring $f\bar{f} \to V_LV_L$ unitarity demand for fermion and boson couplings

$$\sum_i g_{h_i^0VV}\, g_{h_i^0f\bar{f}} = g_{\phi^0VV}\, g_{\phi^0ff}. \tag{4.4.20}$$

Sum-rules have been discussed comprehensively in [61, 74, 155]

limits for 2HDMs require dependence on some additional parameters, but at the same time, they can be some restrictive, even after to run in all parameter space. This fact is due to the conflicts presented with exclusions regions for phenomenological searches. However, provided limits by perturbative unitarity are the most restrictive bounds at tree level for gauge models with extended Higgs sectors; by virtue to the closer relation with the internal consistency of the quantum field theory, which is indeed the fundamental background of a gauge field theory.

- Unitarity restrictions and strong interactions in the Higgs sector: For minimal-SM, the Higgs mass for the Higgs boson $m_h^2 = 2\lambda v^2$ meanwhile the decay rate Γ_H (mainly by associated channels to the longitudinal parts of the gauge bosons $W^\pm$ and Z^0) grows like $\Gamma_h \approx m_h^3$. Unitarity restrictions for this case are used in the limit when $\Gamma_H \approx m_h$, hence the Higgs boson disappears of the scalar spectrum. This fact leads to consider strong interactions in the Higgs sector realized as non-perturbative relations among W_L and Z_L at the regime $\sqrt{s} > v\sqrt{\lambda} \gtrsim v\sqrt{8\pi} \approx 1.2$ TeV. Therefore, if λ exceeds for unitarity at tree level, the discussion regarding observables could fail, and even it is necessary to construct a new framework to analyze scattering processes and the physics behind. The conventional methods of unitarization arise to explain all possible effects inside, as possible dynamical resonances. However, exploratory behavior and identification of scalar particle found in LHC with SM Higgs evade a strong interacting gauge sector [156].

  Correspondence among theoretical limits, dynamical resonances in the Higgs scattering and strong interactions for processes involving and W_LW_L and Z_LZ_L, can generally to be violated in the 2HDM if the values of different of λ_i at tree level differ considerably to the perturbative unitarity limits. The number of degrees of freedom for 2HDM yields situations wherein some Higgs bosons interacts perturbatively, meanwhile other scalars and W_L and Z_L components interact strongly at energies large enough (see table 4.1). Hence, in this procedure could happen that only longitudinal parts of gauge bosons hold for scattering processes, in a different way to SM Higgs-like, which can be decoupled of the spectrum. In such cases, unitarity limits work in a variety of ways for different physical channels. If 2HDM Higgs spectrum saturates unitarity sum rules (4.4.19) and (4.4.20), this situation can be avoided indeed. These non-perturbative values also drive out RGEs to possible Landau poles, which are related to dynamical divergences or strong interacting Higgs sectors. To evade this issue, one can argue that exist a non interacting Higgs sector, converting 2HDM in a trivial theory [157].

- This procedure introduced to other gauge models and multi-doublets extensions: The scheme here proposed can be extrapolated in the unitarity limits for scalar and gauge extensions for SM. To illustrate this, in the former case, a theory with a Higgs sector 2HDM-like plus a singlet ($\sigma = 0$) with $Y = 0$ can be described for the Higgs potential (1.2.1) plus additional terms[10]. In the case for scattering matrices $S_{Y=2,0}, S_{Y=0,\sigma=1}$ have the structure of (4.4.12a)-(4.4.12c), while the associated to $S_{Y=0,\sigma=0}$ can be obtained from the (4.4.12d) plus the addition of one column and one row. A new scattering matrix for $S_{Y=1,\sigma=1/2}$ appears in this case.

4.5. Fermion mass generation

As we have discussed in section 4.3, the upper limit on the scale of EW symmetry breaking could be achieved by describing the elastic scattering of longitudinal weak vector bosons. In the absence of an explicit scenario of electroweak symmetry breaking, this contribution increases quadratically with energy and violates unitarity at an energy $\Lambda_{EWSB} = \sqrt{8\pi v} \approx 1$ TeV, where $v = \left(\sqrt{2}G_F\right)^{-1/2} \approx 246$ GeV [4]. Interpretation of this fact comes from the scale of which the effective field theory of massive weak vector bosons is embedded by a deeper theory having a mechanism for EW-symmetry breaking and new physics effects, thereby generating the masses of the weak bosons.

These formulations can be extrapolated to understand the fermion mass generation, as was pointed out in [161, 162]. The amplitude for the scattering of a fermion-anti-fermion pair of the same helicity into a pair of longitudinal weak vector bosons, in the absence of an explicit model of fermion mass generation, is proportional to $m_f\sqrt{s}/v^2$

(where m_f is the fermion mass and $\sqrt{s}$ is the center-of-mass energy). This amplitude violates unitarity at the scale $\Lambda_f \approx v^2/m_f$, which varies with each fermion depending on its mass and is greater than EWSB for all known fermions. This energy range was interpreted as an upper bound on the scale of fermion mass generation.

It is known from [162] that there is no a model fermion mass generation that saturates the upper bound set by Λ_f. Hence this issue must be considered widely to search a valid explanation for fermion mass scale. Besides, Λ_f role in SM and 2HDMs should be tackled with the aid of proper foundations and with the help of effective theories interpretation.

[10] Singlet terms could be associated to SSB of another abelian gauge extended $U(1)_X$, being X a possible conserved quantum number. For instance, singlet scalar is needed to broke spontaneously the gauge group where $X = B - L$ where B is the baryonic number and L is the leptonic one. This gauge theory has dark matter candidates and, under an accurate See-Saw mechanism; it could be translated into a useful scenario to explain smallness of neutrino masses [158–160]

From discussion presented in section 4.2.2, we review the well established upper bound on the scale of electroweak symmetry breaking. Consider a $SU(2)_L \times U(1)_Y$ Yang-Mills gauge theory. Without an SSB, the boson vectors are massless to respect the gauge symmetry. Now add a bare mass for W and Z bosons,

$$\mathcal{L}_{mass}=m_w^2 W^{+\mu} W_\mu^- + \frac{1}{2}\frac{m_w^2}{\cos^2\theta} Z^\mu Z_\mu \tag{4.5.1}$$

where the relation $m_w^2 = m_z^2 \cos^2\theta$ is made explicit: since this relation arise to demand custodial symmetry. These terms violate the gauge symmetry, so one should question why it is legitimate to add them. The answer is that these terms correspond to the unitary gauge expression of an effective Lagrangian in which the gauge symmetry is non-linearly realized,

$$\mathcal{L} = \frac{v^2}{4}\mathrm{Tr}\left(D^\mu\Sigma\right)^\dagger \left(D_\mu\Sigma\right) \tag{4.5.2}$$

where

$$D^\mu\Sigma = \partial^\mu\Sigma + i\frac{g}{2}\sigma\cdot W^\mu\Sigma - i\frac{g^{'}}{2}\Sigma\sigma^3 B^\mu \tag{4.5.3}$$

and

$$\Sigma = \exp\left(\frac{i\sigma\cdot\pi}{v}\right) \tag{4.5.4}$$

contains the Goldstone bosons π^i of the spontaneously broken gauge symmetry [152]. This effective field theory is valid below of EW-symmetry breaking scale, but no above of it. One may the calculate the energy scale at which this effective field theory breaks down, Λ_{EWSB} [11]. The scenario containing this effective field theory and so on the physics of electroweak symmetry breaking must occur at or below of this scale. Thus Λ_{EWSB} represents an upper limit on the scale of electroweak symmetry breaking.

The scale which the effective field theory breaks down may be calculated using perturbative unitarity. The zeroth-partial-wave ($J=0$) elastic scattering amplitude for longitudinal weak vector bosons in proportional to s/v^2, where s is the square of the center of mass energy and $v=\left(\sqrt{2}G_F\right)^{-1/2}$ is the weak scale. Applying the elastic unitarity condition $\left|\mathrm{Re}\left(a_0^0\right)\right| \leq 1/2$ to the $J=0$ and $I=0$ partial waves amplitude yields the energy at which the effective field theory breaks down

$$\Lambda_{EWSB} \equiv \sqrt{8\pi v} \approx 1 \text{ TeV}. \tag{4.5.5}$$

This relation is the upper bound on the of electroweak symmetry breaking. In the SM at energies above the Higgs-boson mass, the elastic scattering amplitude for longitudinal weak vector bosons receives an additional contribution from the exchange of the Higgs boson. This contribution cancels the term proportional to s/v^2, leading behind factors that approach a constant at high energy values. Thus the effective field theory of massive weak vector bosons is contained by a more fundamental theory containing a Higgs boson in the scalar spectrum.

At energies operating above the Higgs mass scale, the Lagrangian for the essential theory has a linearly realized $SU(2)_L \times U(1)_Y$ gauge invariance, unlike the effective field theory of massive weak vector bosons working below the Higgs mass. The Lagrangian (4.5.2) is replaced by

$$\mathcal{L} = \left(D^\mu\Phi\right) D_\mu\Phi - \lambda\left(\Phi^\dagger\Phi - \frac{v^2}{2}\right)^2. \tag{4.5.6}$$

where Φ is the Higgs doublet field. One may recover the effective field theory of massive weak vector bosons at energies less than the Higgs mass, Eq. (4.5.5) , by integrating out the Higgs boson field h, contained in the Higgs doublet field

$$\Phi = \Sigma\begin{pmatrix} 0 \\ \frac{h+v}{\sqrt{2}} \end{pmatrix}. \tag{4.5.7}$$

The above considerations lead to the following definition: The scale of electroweak symmetry breaking is the minimum energy at which the Lagrangian has a linearly realized $SU(2)_L \times U(1)_Y$ gauge invariance. Instead in the SM, the Higgs boson is associated with the scale of electroweak symmetry breaking.

The Higgs boson mass is proportional to $\sqrt{\lambda v}$, where λ is the self-coupling in (4.5.6). Because the coupling is bounded to be at most of order 4π, the upper limit on the Higgs mass is close to $\sqrt{4\pi v}$ [10]. This number derives by requiring that

[11] In the context of an effective theory, the breaks down scale means that new degrees of freedom are relevant to take into account in the physical processes description.

the Higgs mass should be less than the ultraviolet cutoff of the theory, avoiding possible Landau poles. The upper bound on the m_{h^0} is parametrically equal to the higher bound on the scale of electroweak symmetry breaking, $\Lambda_{EWSB} = 8\pi v$, so the Higgs mass saturates this bound within a factor of order unity. A detailed study shows that the upper limit on the Higgs mass is close to 600 GeV.

As was pointed out in former sections, if there is no Higgs boson, then the effective field theory of massive weak vector bosons directly stops to give a valid description of nature above Λ_{EWSB} will not contain longitudinal weak vector bosons as weakly-coupled degrees of freedom. The SM (and extensions as 2HDM wherein that decouple [163] when the mass of the new physical scalars is taken to infinity) is the unique theory that contains longitudinal weak vector bosons as weakly-coupled degrees of freedom above Λ_{EWSB} [164]. Since a theory of Goldstone bosons, but no Higgs boson does not possess linearly-realized gauge symmetry, the scale of electroweak symmetry breaking typically saturates Λ_{EWSB} in such models. This an excellent motivation to introduce strongly coupled patterns in an effective way.

4.5.1. Scale of fermion mass generation

The limit on the scale of fermion mass generation, derived originally in [162], is generated on a calculation of $f_{\pm}\bar{f}_{\pm} \to V_L V_L$ (where V_L is a longitudinal weak vector boson and the subscripts on the fermion and anti-fermion indicate their helicities). The fermion mass is introduced via a bare mass term in the Lagrangian,

$$\mathcal{L} = -m_f \bar{f}_L f_R + h.c. \tag{4.5.8}$$

where the subscripts indicate chirality. This term violates the gauge symmetry since, in the standard model, f_L and f_R transform differently under $SU(2)_L \times U(1)_Y$ gauge transformations. Eq. (4.5.8) is the unitary gauge expression of a Lagrangian in which the gauge symmetry is nonlinearly realized,

$$\mathcal{L} = -m_f \bar{F}_L \Sigma \begin{pmatrix} 0 \\ 1 \end{pmatrix} f_R + h.c. \tag{4.5.9}$$

where F_L is a $SU(2)_L$-doublet fermion field whose lower component is f_L. Since the fermion mass employs a Yukawa coupling to the Higgs field, there is no diagram corresponding to the exchange of a Higgs boson in the s-channel, as there would be in the standard model. The resulting amplitude is proportional to the fermion mass and grows linearly with energy. Applying the inelastic unitarity condition $|a_{00}| \leq 1/2$ to the $J = 0, I = 0$, spin-zero, color-singlet amplitude for $f_{\pm}\bar{f}_{\pm} \to V_L V_L$ leads to an upper bound on the scale of fermion mass generation

$$\Lambda_f = \frac{8\pi v^2}{\sqrt{3N_c} m_f}. \tag{4.5.10}$$

where $N_C = 3$ for quarks and unity for leptons. However, Eq. (7) is not the strongest upper bound that one can derive, given the above framework. By considering $f_{\pm}\bar{f}_{\pm} \to V_{L1}V_{L2}....V_{Ln}$, with n particles in the final state one obtains an upper bound on the scale of fermion mass generation proportional to $(v^n/m_f)^{1/(n-1)}$. For arbitrarily large n, one obtains an upper bound close to the weak scale v for any value of m_f. We first derive this result and then discuss its implications by proposing some mechanism to describe these effects.

The easiest way to reproduce this effect is to consider the theory in the limit that the weak gauge coupling goes to zero, with v fixed. In this limit the weak vector bosons become massless, and the longitudinal weak vector bosons are represented by the Goldstone bosons $s^{\pm}, \chi$ contained in the field

$$\Sigma = \exp\left(\frac{i\sigma \cdot \pi}{v}\right). \tag{4.5.11}$$

where

$$s^{\pm} = -\frac{\left(\pi^1 \mp \pi^2\right)}{\sqrt{2}} \text{ and } \chi = -\pi^3. \tag{4.5.12}$$

The terms that grow with energy in the amplitudes are independent of the weak gauge coupling, so they survive in this limit. Thus the high-energy behavior of amplitudes with longitudinal weak vector bosons in the final state may be obtained from the amplitudes with the vector bosons replaced with the corresponding Goldstone bosons (times a factor of i $(-i)$ for each outgoing (incoming) longitudinal weak vector boson). This fact is the Goldstone-boson Equivalence Theorem.

The fermion interacts with the Goldstone bosons via the interaction of Eq. (4.5.9). Expanding the field in powers of the Goldstone-boson fields, we obtain an interaction such as that shown in Fig. 4.6, with n external Goldstone bosons.

The Feynman rule for this interaction is proportional to m_f/v^n. The amplitude for $f_\pm \bar{f}_\pm \to \pi\pi$ is therefore proportional to $m_f\sqrt{s}/v^n$. The relevant unitarity condition on this inelastic amplitude is

$$\sigma_{inel}\,(2 \to n) \leq \frac{4\pi}{s}, \tag{4.5.13}$$

where $\sigma_{inel}\,(2 \to n)$ is the total cross section for $f_\pm \bar{f}_\pm \to \pi\pi...\pi$. Since the phase space for a n particle final state is proportional to at high energies, one finds that the unitarity condition, Eq. (4.5.13), is violated at an energy proportional to $(v^n/m_f)^{1/(n-1)}$, as stated above.

We see that $f_\pm \bar{f}_\pm \to V_L V_L ... V_L$, with $n > 2$ particles in the final state, leads to a stronger upper bound than Eq. (4.5.10), which is based on the case $n = 2$. Thus, the Appelquist-Chanowitz bound is subsumed by this stronger bound, which is of order the weak scale, v, for n large, independently of m_f. Since we already know that there must be new physics at the weak scale, namely the physics of electroweak symmetry breaking, the consideration of fermion-anti-fermion scattering into longitudinal weak vector bosons does not reveal a new energy scale for interactions. This claiming is supported by the fact the upper bound is independent of the fermion mass. Thus, there is no maximum limit on the range of fermion mass generation. therefore proportional to $m_f\sqrt{s}/v^n$. The relevant unitarity condition on this inelastic amplitude is

4.5.2. Standard Model and Scale of Fermion Mass Generation

The derivation in the previous section of $f_\pm \bar{f}_\pm \to V_L V_L ... V_L$, with n particles in the final state, tacitly assumes that the longitudinal weak vector bosons are weakly-coupled degrees of freedom. As discussed before, this is not reliable in general above $\Lambda_{EWSB} \approx \sqrt{8\pi}v$. In order to justify the calculation of $f_\pm \bar{f}_\pm \to V_L V_L ... V_L$ above Λ_{EWSB} [12], one must specify the mechanism of electroweak symmetry breaking such that the longitudinal weak vector bosons remain weakly-coupled degrees of freedom above Λ_{EWSB}. The only theory that contains longitudinal weak vector bosons as a weakly-coupled scenario to arbitrarily high energies is the standard model with a Higgs boson (or with scalar extensions). Having these foundations in mind, in this section, we consider the scale of fermion mass generation in SM.

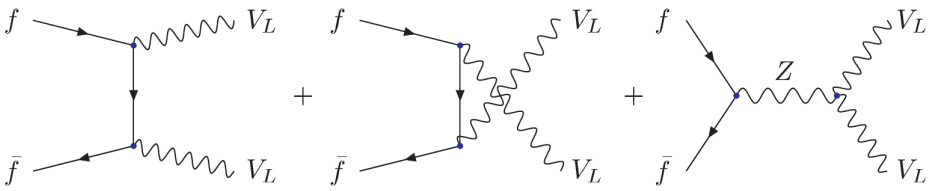

Figure 4.5.: *Feynman diagrams contributing to the inelastic amplitude for $f\bar{f} \to V_L V_L$ in unitary gauge, where off-shell Goldstone bosons are vanished.*

In a first glance, we consider the model treated in Ref. [162], in which the weak-vector-boson masses are generated through an explicit model of SSB, but fermions described with concerning their bare masses. As an example of this, one could imagine the standard Higgs model, but with the fermion Yukawa interactions replaced by bare fermion masses, Eq. (4.5.8). However, even in this scenario, the considerations of the previous section continue to apply. The calculation of $f_\pm \bar{f}_\pm \to V_L ... V_L$, with n particles in the final state, continues to violate unitarity at the scale of electroweak symmetry breaking for large n. Thus unitarity of this process does not reveal a new energy scale beyond that of EW-symmetry breaking.

The theory that is valid above the scale of electroweak symmetry breaking has a linearly-realized gauge invariance. Thus the fermion mass, Eq. (4.5.9), must be described by a Yukawa interaction written in the form

$$\mathcal{L} = -y_f \bar{F}_L \phi f_R + h.c. \tag{4.5.14}$$

This Lagrangian contains a Yukawa interaction of the fermion with the Higgs boson and yields the diagram in Fig. 4.7. This diagram, when added to the diagrams in Fig. 4.5, cancels the term that grows linearly with energy, leaving behind terms that fall like an inverse power of energy at high energy. A similar cancellation occurs for all processes of the type $f_\pm \bar{f}_\pm \to V_L V_L ... V_L$.

[12] In [165], we have presented the first nontrivial calculation at one loop level of the inverse process, i.e., a realistic computation of $t\bar{t}$ production amplitudes from longitudinal WW, ZZ within the HEFT framework. Besides we have extended it to the resonance region by using new unitarization methods.

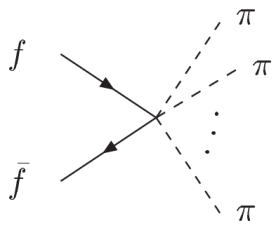

Figure 4.6.: *Feynman diagram for the interaction of a fermion with n Goldstone bosons.*

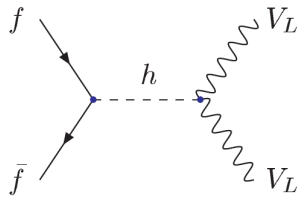

Figure 4.7.: *New diagram involving the exchange of a Higgs boson that contributes to the amplitude for $f\bar{f} \to V_L V_L$. This contribution cancels the terms that grow with an energy resulting from the diagrams in Fig. 4.6.*

It is tempting to quantify the scale of fermion mass generation with the energy at which the amplitude for $f_\pm \bar{f}_\pm \to V_L V_L$ ceases to increase with energy, specifically the Higgs mass. However, the Higgs mass corresponds to the scale of EW-symmetry breaking, it is not the value of fermion mass generation. The reason for the amplitude for $f_\pm \bar{f}_\pm \to V_L V_L$ increases with energy below the Higgs mass is because the fermion mass is described in one theory with a non-linearly realized gauge invariance, Eq. (4.5.9). Above the Higgs mass, the amplitude for $f_\pm \bar{f}_\pm \to V_L V_L$ falls off with energy and unitarity rules at all energies. Thus, in the SM there is no scale treating with fermion mass generation. We will support this claiming by considering extensions of the SM in which there is a well-defined energy scale of fermion mass generation.

A possible way to circumvent the above arguments is to introduce a new Higgs doublet field of some scenario for 2HDM, such that longitudinal weak vector bosons are weakly coupled above the EW-scale, but to forbid the Higgs field from coupling to fermions. This fact can be tackled, for instance, by imposing the discrete symmetry Z_2 $\Phi_i \to -\Phi_i$. However, this also has the consequence of forbidding a gauge-invariant mass for the fermion, so the scale of fermion mass generation is questionable. One might also take into account a model with two Higgs doublets where only one doublet couples to fermions, as we will see it in the next section.

In this part of the dissertation, we have argued that there is no scale of fermion mass generation in the standard model. However, Yukawa couplings are not asymptotically free in general, so the energy at which a Yukawa coupling becomes strong also indicates an upper bound on the scale of fermion mass generation. In SM and 2HDM (using the minimality principle), only the top quark Yukawa coupling is not asymptotically free. All other Yukawa couplings are asymptotically free under the fermion's gauge interactions. The top quark's Yukawa coupling is sufficiently large that it eventually overwhelms the gauge interactions, causing it to become strong at high energies. However, for $m_t = 173.2$ GeV, the energy at which the top quark's Yukawa coupling becomes strong is many orders of magnitude above the Planck scale and is, therefore, irrelevant to a real discussion. If a quark of mass over 225 GeV existed, its Yukawa coupling would become strong below the grand unification scale [161, 162].

The upper limit describing the scale of fermion mass generation derives from the dimensionality of the interaction yielding the fermion mass. The upper bound is correspondingly proportional to

$$\Lambda_f \propto \left(\frac{v^3}{m_f}\right)^{\frac{1}{d-4}} \tag{4.5.15}$$

4.5.3. 2HDM and Fermion Mass Scale Generation

To study more fact about a fermion scale mass generation, we consider a particular case of 2HDM in a decoupling regime. We impose a Z_2-like symmetry, where for instance $\Phi_1 \to -\Phi_1$, such that only Φ_2 couples to a given fermion (2HDM

Type I). The Higgs potential invariant under this symmetry plus a violation soft term

$$\begin{aligned} V\left(\Phi_1,\Phi_2\right) &= m_{11}^2\Phi_1^\dagger\Phi_1 + m_{22}^2\Phi_2^\dagger\Phi_2 - m_{12}^2\left(\Phi_1^\dagger\Phi_2 + \Phi_2^\dagger\Phi_1\right) + \frac{1}{2}\lambda_1\left(\Phi_1^\dagger\Phi_1\right)^2 + \frac{1}{2}\lambda_2\left(\Phi_2^\dagger\Phi_2\right)^2 \\ &\quad +\lambda_3\left(\Phi_1^\dagger\Phi_1\right)\left(\Phi_2^\dagger\Phi_2\right) + \lambda_4\left(\Phi_1^\dagger\Phi_2\right)\left(\Phi_2^\dagger\Phi_1\right) + \frac{1}{2}\lambda_5\left[\left(\Phi_1^\dagger\Phi_2\right)^2 + \left(\Phi_2^\dagger\Phi_1\right)^2\right]. \end{aligned} \tag{4.5.16}$$

Where the λ_i are real, and where the discrete symmetry is softly broken by the term proportional to m_{12}^2. The coupling of a fermion f to the Higgs field Φ_2 is given by a dimension four Yukawa interaction

$$\mathcal{L} = -y_f\bar{F}_L\Phi_2 f_R + h.c., \tag{4.5.17}$$

where F_L is a $SU\left(2\right)_L -$ doublet fermion field whose lower component is f_L. We study the decoupling limit in a simple way, by integrating out one of the Higgs-doublet fields. A convenient way to accomplish this is to make a rotation in Higgs-doublet-field space such that the mass matrix is diagonal. Thus we define fields, Ψ, Ξ given by

$$\begin{pmatrix} \Psi \\ \Xi \end{pmatrix} = \begin{pmatrix} \cos\alpha & \sin\alpha \\ -\sin\alpha & \cos\alpha \end{pmatrix}\begin{pmatrix} \Phi_1 \\ \Phi_2 \end{pmatrix}. \tag{4.5.18}$$

which is a basis transformation as presented in Eq. (1.2.7). The angle α, defined in the rotations of scalar neutral eigenstates, is chosen to eliminate the off-diagonal term in the mass matrix (which are proportional to m_{12}^2). The resulting scalar potential has the following structure

$$V\left(\Psi,\Xi\right) = -\mu^2\Psi^\dagger\Psi + M^2\Xi^\dagger\Xi + ... + \tilde{\lambda}_6\left[\left(\Psi^\dagger\Psi\right)\left(\Psi^\dagger\Xi\right) + h.c.\right] \tag{4.5.19}$$

with

$$\tilde{\lambda}_6 = \frac{1}{2}\sin 2\alpha\left[\lambda_3 + \lambda_4 + \lambda_5 + \cos^2\alpha\left(\lambda_2 - 2\left(\lambda_3 + \lambda_4 + \lambda_5\right)\right) - \lambda_1\sin^2\alpha\right]. \tag{4.5.20}$$

We have suppressed all quartic interactions except a term linear in Ψ, which is induced by the rotation in Higgs-field space. This is the unique term linear in Ψ; its coefficient $\tilde{\lambda}_6$ is a linear combination of the $\lambda_i^{'}$ see Eq. (4.5.20).

Considering the decoupling limit in $\mu^2 << M^2$, and integrating out Ξ field, the Lagrangian (4.5.17) becomes:

$$\begin{aligned} \mathcal{L} &= -y_f\cos\alpha\bar{F}_L\Psi f_R - y_f\sin\alpha\bar{F}_L\Xi f_R + h.c. \\ &= -y_f^{'}\bar{F}_L\Psi f_R - \frac{c}{M^2}\bar{F}_L\Psi f_R\Psi^\dagger\Psi + h.c. \end{aligned} \tag{4.5.21}$$

where $y_f^{'} = y_f\sin\alpha\cos\alpha$ and $c = -y_f\tilde{\lambda}_6\sin\alpha$. This interaction is exactly of the form of the standard model plus the dimension-six term[13], where M is identified with the mass of the heavy Higgs field.

The decoupling limit of a two-Higgs-doublet model was studied in an attempt to find a model in which the scale of fermion mass generation saturates the Appelquist-Chanowitz bound, $\Lambda_f \simeq v^2/m_f$. The mass value of the heavy neutral Higgs scalar could be identified as the energy scale of fermion mass generation. Nevertheless, it must be considered the scale of new physics; and hence there is no scale of fermion mass generation since the fermion mass arises in part from a renormalizable interaction [161, 167]. This dimension six operator affects the fermion mass definition when the second double decouples of field spectrum.

These statements lead to define the fermion mass scale as: *The energy value of fermion mass generation is the minimum energy at which the fermion mass arises from a renormalizable interaction.* In SM and 2HDMs, the fermion mass is caused by a renormalizable interaction at all energies (above the Higgs mass), so there is no scale of fermion mass generation. Based on this definition, one could argue that the Higgs mass is the energy magnitude of fermion mass generation in the SM or 2HDMs. However, as was pointed out above, the Higgs mass must be regarded as the scale of EW-symmetry breaking, but not the energy magnitude of fermion mass generation.

[13]There are a large number of interactions of dimension six available with the field content of the standard model, nonetheless there is only one that contributes to fermion masses, given by [166]

$$\mathcal{L}_6 = -\frac{c}{M^2}\bar{F}_L\Psi f_R\Psi^\dagger\Psi + h.c. \tag{4.5.22}$$

4.6. Fermion-anti-fermion scattering

One important benchmark what we have learned is that in perturbative unitarity analysis, the optical theorem discriminates as boson scattering or annihilation at one specific order in perturbation theory is connected with the processes at a lower level; such that allowed channels are those where cuadri-momentum conservation is always ensured. Having analyzed unitarity constraints interpretation for tree level matrix elements and clarified facts over fermion mass generation in SM and 2HDMs, we proceed to study other processes that can be treated from S-matrix unitarity formalism. It is clear that in 2HDMs do not exist a scale of fermion mass generation since that mass terms come from renormalizable interactions. Nevertheless, 2HDM scenarios give us more information about non-mass-like couplings which are associated with phenomena involving FCNCs. To describe unitarity behavior over these particular Yukawa couplings, we compute fermion-antifermion scattering processes at tree level, taking into account models without natural flavor conservation, in such a way that FCNC couplings are present in the matrix elements (in a controlled way using Sher and Cheng anzats). Finally, we put those matrix elements in the unitarity constraints from Argand diagram; also interpreting them as perturbative limits over respective Yukawa couplings.

4.6.1. Neutral channels

In the following, we consider the tree level matrix elements for the process $f\bar{f} \to f\bar{f}$ at the high energy limit under the helicity spinors formalism. The neutral Higgs (η^0) contributions are shown in Fig. 4.8.

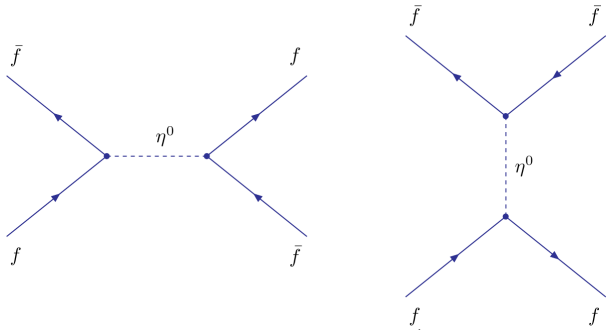

Figure 4.8.: *Diagrams at the tree-level with scalar contribution (neutral Higgs bosons) for $f\bar{f} \to f\bar{f}$ processes.*

First, we write the invariant amplitude in the CP-conserving frame:

$$\begin{aligned}\mathcal{M}(f\bar{f} \to f\bar{f}) = &\sum_{\eta^0_{CP-even}} \left(\bar{v}_2 i\chi^{\eta^0}_{ff} u_1 \frac{1}{s - m^2_{\eta^0}} \bar{u}_3 i\chi^{\eta^0}_{ff} v_4 + \bar{v}_2 i\chi^{\eta^0}_{ff} v_4 \frac{1}{t - m^2_{\eta^0}} \bar{u}_3 i\chi^{\eta^0}_{ff} u_1 \right) \\ &+ \sum_{\phi^0_{CP-odd}} \left(\bar{v}_2 i\chi^{\phi^0}_{ff} \gamma_5 u_1 \frac{1}{s - m^2_{\phi^0}} \bar{u}_3 i\chi^{\phi^0}_{ff} \gamma_5 v_4 + \bar{v}_2 i\chi^{\phi^0}_{ff} \gamma_5 v_4 \frac{1}{t - m^2_{\phi^0}} \bar{u}_3 i\chi^{\phi^0}_{ff} \gamma_5 u_1 \right),\end{aligned} \tag{4.6.1}$$

here $\chi^{\eta^0}_{ff}(\chi^{\phi^0}_{ff})$ are the couplings between fermions and CP-even (CP-odd) neutral Higgs bosons. For different helicity combinations that satisfy the relations $\lambda_a = \lambda_b$ and $\lambda_c = \lambda_d$, we get the following non-zero coupled channels (see appendix in [168])

$$\mathcal{M}(f_\uparrow \bar{f}_\uparrow \to f_\uparrow \bar{f}_\uparrow) = -\sqrt{2} G_f m_f^2 \sum_{\eta^0_{all}} \left(\Xi^{\eta^0}_{ff} \right)^2 \left(\frac{s}{s - m^2_{\eta^0}} \right) \tag{4.6.2}$$

$$\mathcal{M}(f_\downarrow \bar{f}_\downarrow \to f_\uparrow \bar{f}_\uparrow) = -\sqrt{2} G_f m_f^2 \sum_{\eta^0_{all}} \left(\Xi^{\eta^0}_{ff} \right)^2 \left(\frac{s}{s - m^2_{\eta^0}} - \frac{t}{t - m^2_{\eta^0}} \right), \tag{4.6.3}$$

where s and t are Mandelstam variables and Ξ_s are relative Yukawa couplings of neutral Higgs bosons concerning SM. The input associated with the pseudoscalar sector is the same as to the scalar sector, because in the high energy limit the eigenspinors are also chiral eigenstates (see appendix in [168]).

There are other channels, e.g. $\mathcal{M}(f_\downarrow \bar{f}_\downarrow \to f_\downarrow \bar{f}_\downarrow)$ and $\mathcal{M}(f_\uparrow \bar{f}_\uparrow \to f_\downarrow \bar{f}_\downarrow)$, which just differ by a minus sign from amplitudes (4.6.2) and (4.6.3) respectively. Therefore, they would not provide new information about unitarity bounds.

The $J = 0$ partial wave coefficient is given by (4.2.36). From the definition of the Mandelstam variables, we have in the high energy limit

$$a^0 \equiv \mathcal{M}^{J=0}(s) = \frac{1}{16\pi s}\int_{-s}^{0} \mathcal{M}(s,t)dt. \tag{4.6.4}$$

Therefore, in the regime of $s >> m_{\eta^0}^2$ and for elastic scattering channels (e.g. $f_i \bar{f}_i \to f_i \bar{f}_i$), the non-zero matrix elements lead us to the following coefficients

$$a^0(f_\uparrow \bar{f}_\uparrow \to f_\uparrow \bar{f}_\uparrow) = -\frac{\sqrt{2}G_f m_f^2}{16\pi}\sum_{\eta^0_{all}} \left(\Xi^{\eta^0}_{ff}\right)^2 \tag{4.6.5}$$

$$a^0(f_\downarrow \bar{f}_\downarrow \to f_\uparrow \bar{f}_\uparrow) = 0. \tag{4.6.6}$$

For the 2HDM type III (in the fundamental parametrization i.e. $\tan\beta = 0$) the Yukawa couplings for neutral interactions are displayed in table 4.2.

Coupling/Model	2HDM III (up-sector)	2HDM III (down-sector)
$\Xi^{H^0}_{q_i\bar{q}_j}$	$\left(\delta_{ij}\cos\alpha + \frac{\xi^U_{ij}\sin\alpha}{\sqrt{2m_{u_i}m_{u_j}}}v\right)$	$\left(\delta_{ij}\cos\alpha + \frac{\xi^D_{ij}\sin\alpha}{\sqrt{2m_{d_i}m_{d_j}}}v\right)$
$\Xi^{h^0}_{q_i\bar{q}_j}$	$\left(-\delta_{ij}\sin\alpha + \frac{\xi^U_{ij}\cos\alpha}{\sqrt{2m_{u_i}m_{u_j}}}v\right)$	$\left(-\delta_{ij}\sin\alpha + \frac{\xi^D_{ij}\cos\alpha}{\sqrt{2m_{d_i}m_{d_j}}}v\right)$
$\Xi^{A^0}_{q_i\bar{q}_j}$	$-i\frac{\xi^U_{ij}}{\sqrt{2m_{u_i}m_{u_j}}}v\gamma_5$	$i\frac{\xi^D_{ij}}{\sqrt{2m_{d_i}m_{d_j}}}v\gamma_5$

Table 4.2.: *Yukawa couplings structure for 2HDM III (neutral Higgs with quarks and charged leptons) in the fundamental parametrization. α is the mixing angle between neutral gauge eigenstates and mass eigenstates (CP-even) [61].*

By using the Cheng-Sher parametrization Eq. (1.5.4) for diagonal couplings, we obtain the unitarity constraints by combining Eqs. (4.2.1), (4.6.4) and (4.6.5). They are given by

$$|\lambda^{U,D}_{ii}| \leq \left(\frac{2\sqrt{2}\pi}{G_f m_f^2} - \frac{1}{2}\right)^{1/2}. \tag{4.6.7}$$

These relations lead to upper bounds for the fermion generations. We obtain them by taking the input parameters in [4], and they are specified in the caption of Table 4.3.

$\lambda^{U,D}_{ii}$	$\lvert\lambda_{ii}\rvert_{unit}$	$\lvert\lambda_{ii}\rvert_{unit}$ ($\mathsf{a} \leq 41\%$)	$\lvert\lambda_{ii}\rvert_{unit}$ ($\mathsf{a} \leq 20\%$)	$\sim \mathcal{O}$
λ_{tt}	5	3.5	2.4	$\mathcal{O}(1)$
λ_{bb}	208	147	104	$\mathcal{O}(10^2)$
λ_{cc}	687	486	343	$\mathcal{O}(10^2)$
λ_{ss}	8.6×10^3	6.1×10^3	4.3×10^3	$\mathcal{O}(10^3)$
λ_{uu}	$(2.6\text{-}5.1)\times10^5$	$(1.87-3.6)\times10^5$	$(1.3-2.5)\times10^5$	$\mathcal{O}(10^5)$
λ_{dd}	$(1.5\text{-}2.1)\times10^5$	$(1.0\text{-}1.5)\times10^5$	$(0.75-1.0)\times10^5$	$\mathcal{O}(10^5)$
$\lambda_{\tau\tau}$	491	347	245	$\mathcal{O}(10^2)$
$\lambda_{\mu\mu}$	8.3×10^3	5.8×10^3	4.1×10^3	$\mathcal{O}(10^3)$
λ_{ee}	1.7×10^6	1.2×10^6	0.8×10^6	$\mathcal{O}(10^6)$

Table 4.3.: *Bounds on Yukawa couplings from relation (4.6.7) for elastic processes $f_i\bar{f}_i \to f_i\bar{f}_i$ in the 2HDM type III. Here, perturbativity parameter a is considered in the way to obtain unitarity bounds. The parameters were taken from [4] (central values): $m_t = 172\ GeV$, $m_b = 4.19\ GeV$, $m_c = 1.27\ GeV$, $m_s = 0.101\ GeV$, $m_d = (0.0041-0.0058)\ GeV$, $m_u = (0.0017-0.0033)\ GeV$, $m_\tau = 1.776\ GeV$, $m_\mu = 0.106\ GeV$ and $m_e = 0.00051\ GeV$.*

In the same way, for non-diagonal couplings, the upper bounds become

$$|\lambda_{ij}^{U,D}| \leq \left(\frac{2\sqrt{2}\pi}{G_f m_i m_j}\right)^{1/2}, \tag{4.6.8}$$

and they are evaluated numerically in table 4.4.

$\lambda_{ij}^{U,D}$	$\lvert\lambda_{ij}\rvert_{unit}$	$\sim \mathcal{O}$
λ_{tc}	59	$\mathcal{O}(10)$
λ_{tu}	$1.2 - 1.6 \times 10^3$	$\mathcal{O}(10^3)$
λ_{bs}	1.3×10^3	$\mathcal{O}(10^3)$
λ_{bd}	$5.6 - 6.6 \times 10^3$	$\mathcal{O}(10^3)$
$\lambda_{\tau\mu}$	2.0×10^3	$\mathcal{O}(10^3)$
$\lambda_{\tau e}$	2.9×10^4	$\mathcal{O}(10^4)$
$\lambda_{\mu e}$	1.2×10^5	$\mathcal{O}(10^5)$

Table 4.4.: *Bounds on Yukawa couplings from (4.6.8) for mixed channels $f_i\bar{f}_j \to f_i\bar{f}_j$ in the 2HDM type III. The parameters were taken from [4], and they are specified in the caption of table 4.3.*

All unitarity constraints compete with those coming from perturbativity, in which we require that the running coupling constants of the Higgs self-couplings and the Yukawa couplings do not blow up below a certain energy scale $\Lambda : \lambda_i(\mu) < 8\pi$ and $(g_f^{\eta}(\mu))^2 < 4\pi$, for a renormalization scale μ less than Λ [169][14]. If these couplings were higher of this value, the respective β-functions would be positive, and their renormalization scale evolution will drive them to even higher values [20, 114] .

With mixed channels (e.g. $f_i\bar{f}_i \to f_j\bar{f}_j$), the partial wave coefficients (4.6.4) are transformed into

$$a^0(f_\uparrow\bar{f}_\uparrow \to f_\uparrow\bar{f}_\uparrow) = -\frac{\sqrt{2}G_f m_i m_j}{16\pi}\sum_{\eta^0_{all}}\left(\Xi^{\eta^0}_{f_if_i}\Xi^{\eta^0}_{f_jf_j}\right), \tag{4.6.9}$$

$$a^0(f_\downarrow\bar{f}_\downarrow \to f_\uparrow\bar{f}_\uparrow) = -\frac{\sqrt{2}G_f m_i m_j}{16\pi}\sum_{\eta^0_{all}}\left[\Xi^{\eta^0}_{f_if_i}\Xi^{\eta^0}_{f_jf_j} - \left(\Xi^{\eta^0}_{f_if_j}\right)^2\right]. \tag{4.6.10}$$

From which the unitarity limits become

$$\sum_{\eta^0}\Xi^{\eta^0}_{f_if_i}\Xi^{\eta^0}_{f_jf_j} \leq \frac{8\sqrt{2}\pi}{G_f m_i m_j}, \tag{4.6.11}$$

$$\sum_{\eta^0}\left[\Xi^{\eta^0}_{f_if_i}\Xi^{\eta^0}_{f_jf_j} - \left(\Xi^{\eta^0}_{f_if_j}\right)^2\right] \leq \frac{8\sqrt{2}\pi}{G_f m_i m_j}. \tag{4.6.12}$$

The sum runs over all neutral Higgs states (CP-even and CP-odd). In the particular case of the 2HDM type III (from couplings in table 4.2), these relations regarding Sher-Cheng couplings satisfy

$$\lambda_{ii}^{U,D}\lambda_{jj}^{U,D} \leq \frac{4\sqrt{2}\pi}{G_f m_i m_j} - \frac{1}{2}, \tag{4.6.13}$$

$$\lambda_{ii}^{U,D}\lambda_{jj}^{U,D} - \left(\lambda_{ij}^{U,D}\right)^2 \leq \frac{4\sqrt{2}\pi}{G_f m_i m_j} - \frac{1}{2}. \tag{4.6.14}$$

Where the products are only by pairs either $\lambda_{ii}^{U}\lambda_{jj}^{U}$ or $\lambda_{ii}^{D}\lambda_{jj}^{D}$. The numerical evaluations of these crossed products for FCNC couplings are displayed in Table 4.2. It worths saying that if some of these couplings were determined, these limits could help in restricting the remaining ones.

[14] In particular, from pseudoscalar-fermion couplings perturbativity requires that: $\xi_{ij}^2 < 4\pi$. It is is translated into $\lambda_{ij} < \left(\frac{\sqrt{2}\pi}{G_f m_i m_j}\right)^{1/2}$. Since the scalar couplings depend on the mixing angle α as well as on the elements λ_{ij}, the perturbative constraints depend on more degrees of freedom.

$\lambda_{ii}^{U,D}\lambda_{jj}^{U,D}$	$\lambda_{ii}^{U,D}\lambda_{jj}^{U,D}-\left(\lambda_{ij}^{U,D}\right)^2$	Bound	$\sim\mathcal{O}$
$\lambda_{tt}\lambda_{cc}$	$\lambda_{tt}\lambda_{cc}-\lambda_{tc}^2$	7.0×10^3	$\mathcal{O}(10^3)$
$\lambda_{tt}\lambda_{uu}$	$\lambda_{tt}\lambda_{uu}-\lambda_{tu}^2$	$(2.7\text{-}5.2)\times10^6$	$\mathcal{O}(10^6)$
$\lambda_{bb}\lambda_{ss}$	$\lambda_{bb}\lambda_{ss}-\lambda_{bs}^2$	3.6×10^6	$\mathcal{O}(10^6)$
$\lambda_{bb}\lambda_{dd}$	$\lambda_{bb}\lambda_{dd}-\lambda_{bd}^2$	$(6.3\text{-}8.8)\times10^7$	$\mathcal{O}(10^7)$
$\lambda_{\tau\tau}\lambda_{\mu\mu}$	$\lambda_{\tau\tau}\lambda_{\mu\mu}-\lambda_{\tau\mu}^2$	8.2×10^6	$\mathcal{O}(10^6)$
$\lambda_{\tau\tau}\lambda_{ee}$	$\lambda_{\tau\tau}\lambda_{ee}-\lambda_{\tau e}^2$	1.7×10^9	$\mathcal{O}(10^9)$
$\lambda_{\tau\tau}\lambda_{ee}$	$\lambda_{\tau\tau}\lambda_{ee}-\lambda_{\tau e}^2$	2.8×10^{10}	$\mathcal{O}(10^{10})$

Table 4.5.: *Bounds on Yukawa couplings from (4.6.13) and (4.6.14) for mixed channels $f_i\bar{f}_i\to f_j\bar{f}_j$ in the 2HDM type III. The parameters was taken from [4], and they are specified in table 4.3.*

In the same way, in which the unitarity constraints are interpreted for self-couplings of the Higgs potential, these Yukawa couplings constraints can be treated (without the inclusion of new physics) as the upper values for which the perturbation theory will become reliable at all energy scales.

4.6.2. Charged channels

It is also possible to evaluate the contribution from charged channels (final and initial charged states) to the unitary amplitude. It is worthwhile to observe that the matrix elements ξ_{ij} modify the charged Higgs couplings:

$$\chi_{f_if_j}^{H^\pm}=(K_{ik}\xi_{kj}^{D}P_R-\xi_{ik}^{U}K_{kj}P_L),$$

for the fundamental parametrization [19,61], where K is the Kobayashi Maskawa matrix and $P_{L(R)}$ are the Left (Right) projection operators. Hence, there are two facts to point out i) the flavor changing charged currents (FCCC) in the quark sector are modified by the same matrix that produces FCNC, ii) in the lepton sector FCCC are generated by the matrix that makes FCNCs multiplied by Pontecorvo-Maki-Nakawaga-Sakata matrix. A typical charged scattering process at the tree level for the scalar sector has two contributions: the first one associated with $H^\pm$ states in the propagator for the s-channel and the second one with neutral scalar states in the propagator for the t-channel:

$$\mathcal{M}(f_i\bar{f}_j\to f_i\bar{f}_j)=\sum_{\eta_{H^\pm}}\left(\bar{v}_2\chi_{f_if_j}^{H^\pm}u_1\frac{1}{s-m_{\eta_{H^\pm}}^2}\bar{u}_3\chi_{f_if_j}^{H^\pm}v_4\right)+\sum_{\eta^0}\left(\bar{v}_2 i\chi_{f_jf_j}^{\eta^0}v_4\frac{1}{t-m_{\eta^0}^2}\bar{u}_3 i\chi_{f_if_i}^{\eta^0}u_1\right).$$

Assuming diagonal textures for both flavor matrices in 2HDM type III (quark sector) and using the systematic got in the last section, the amplitudes for the polarized process $f_{i\uparrow}\bar{f}_{j\uparrow}\to f_{i\uparrow}\bar{f}_{j\uparrow}$ becomes

$$\mathcal{M}(f_{i\uparrow}\bar{f}_{j\uparrow}\to f_{i\uparrow}\bar{f}_{j\uparrow})=\bar{v}_{2_\uparrow}\chi_{f_if_j}^{H^\pm}u_{1_\uparrow}\frac{1}{s-m_{H^\pm}^2}\bar{u}_{3_\uparrow}\chi_{f_if_j}^{H^\pm}v_{4_\uparrow}=\xi_{ii}^{U}\xi_{jj}^{D}K_{ij}^2\frac{s}{s-m_{H^\pm}^2}. \tag{4.6.15}$$

where $i=u,c,t$ and $j=d,s,b$. We have used the CKM hierarchy and the assumption of universality deviation in the same generation. Here $u_{1\uparrow},\bar{v}_{2\uparrow},\bar{u}_{3\uparrow}$ and $v_{4\uparrow}$ are the eigenspinors as (right-handed) helicity states. Since $\bar{u}_{3_\uparrow}u_{1_\uparrow}=0$ at the high energy limit (appendices in [168]), the neutral channel does not have a contribution for this helicity choice. From Cheng-Sher anzats for diagonal couplings, the partial wave coefficient has the unitarity bound

$$\lambda_{ii}^{U}\lambda_{jj}^{D}\leq\frac{2\sqrt{2}\pi}{G_f m_i m_j K_{ij}^2}. \tag{4.6.16}$$

We have summarized these bounds in the table 4.6. If some of these couplings were determined (say couplings from the up sector), these limits could help in restricting the remaining ones (say couplings from the down sector)[15].

[15]For instance, the process $b\to s\gamma$ could determine the value of λ_{tt}, from which our present bounds would help in obtaining the associated λ_{bb}.

$\lambda^U_{ij}\lambda^D_{jj}$	Bound	$\sim \mathcal{O}$
$\lambda_{tt}\lambda_{bb}$	1055	$\mathcal{O}(10^3)$
$\lambda_{cc}\lambda_{ss}$	5.9×10^6	$\mathcal{O}(10^6)$
$\lambda_{uu}\lambda_{dd}$	(0.4-1.1) $\times 10^{11}$	$\mathcal{O}(10^3)$

Table 4.6.: *Bounds on Yukawa couplings from (4.6.16) for mixed channels $f_i\bar{f}_j \to f_i\bar{f}_j$ in the 2HDM type III. The parameters was taken from [4].*

4.7. Remarks on S-matrix and perturbative unitarity

S-matrix connects asymptotic multiparticle states incoming and emerging of a scattering process through a transformation presented by a sequence of unitary operators. Unitarity and Poincaré's invariance are two relevant properties accomplished by the S matrix. The first feature ensures the fundamental principle of probability conservation and reflects significant consequences for dispersion theory. One of them is the saturating behavior for the cross section in the two particles states scattering. Another feature is associated with the optical theorem, which relates processes occurring in a given perturbative order with the scattering annihilation o decays in a lower level.

Unitarity constraints at tree level arise using the optical theorem in the S-matrix description using partial waves. The traditional way to implement it in gauge theories is demanding that the model has only weakly interacting degrees of freedom at high energy limit. In these weakly coupled theories, higher order contributions to S-matrix become smaller compared to the leading order. It is then possible to require for S-matrix to be unitary from the tree level of the theory. To circumvent strong assumption to apply optical theorem at tree level, we also considered a complementary prescription where is defined a parameter measuring the ratio between the partial wave of full amplitude and the partial wave of the tree-level element. This setting ends up to measure the inherent difference that drives out the latter (i.e., tree-level contribution) to enter in the Argand's diagram, satisfying the optical theorem. This convert to unitarity constraint to be stronger than the traditional conservative systematics.

Constraints based on unitarity to 2HDM are obtained using the Ivanov's formalism, within scattering amplitudes, and partial waves are computed on a non-physical basis. There, interactions are simplest than a physical basis. This procedure leads to imposing different bounds for quartic couplings in various channels of scattering processes for $Z_2 - symmetry$ behavior, based on high energy quantum conserved numbers of hypercharge and isospin.

Perturbative unitarity allows study the fermion mass scale generation defined as The minimum energy at which a renormalizable interaction generates the fermion mass. Under this definition, in SM and 2HDMs there is no such scale since fermion masses are caused by a renormalizable interaction at all energies above the Higgs mass (considered as the scale of EW-SSB).

Under the use of a general expansion of partial waves, we obtain unitarity constraints over fermionic scattering processes in 2HDM type III. The method relies on a diagonalization (at least partial) in the angular momentum basis of the $\widehat{S}$ matrix for the scattering of two particles in the center of mass frame and the appropriate choice of helicity states. In the helicity formalism, the spin degrees of freedom of the particle involved do not introduce any significant complication concerning spinless particles, at least when $\lambda_a = \lambda_b$ (initial helicities) and $\lambda_c = \lambda_d$ (final helicities). In fact, this particular case recovers the traditional partial wave expansion as well as its unitary conditions over the coefficients expansion. This scenario leads to build up a well-grounded formalism to impose the unitary constraints over spin $1/2$ states or in general states of any spin. The primary assumption for unitarity bound is that the 2HDM is a valid description of physics up to very high energy scales where new or non-perturbative physics of some kind must be taken into account.

Due to the universality deviation by the presence of FCNC vertices for fermionic interactions with scalars in the type III 2HDM, this formalism is applied in all its generality to get unitary constraints over Yukawa couplings values under Cheng and Sher parametrization. The constraints obtained are indeed independent of other parameters of the Higgs sector, i.e. the scalar masses and mixing angles.

In the case of elastic scattering processes, diagonal Yukawa couplings constraints (coming from $f_i\bar{f}_i \to f_i\bar{f}_i$) are more stringent that non-diagonal couplings (coming from $f_i\bar{f}_k \to f_i\bar{f}_k$). Besides, these unitarity limits compete with those imposed from perturbative interactions, which could introduce more parameters. Moreover, our limitations compete with current phenomenological constraints ($\bar{B}^0 - B^0$ mixing, $(g-2)_\mu$ factor) for heavy fermionic masses, e.g. the top mass. It is worthwhile emphasizing that the phenomenological constraints demand the use of several parameters like scalar masses or mixing angles. Further, those computations lie on two-loop radiative corrections to the physical processes unlike the unitary constraints, which unfold naturally at the tree level. Finally, this systematic might be extrapolated to other fermionic sectors such as the minimal supersymmetric standard model, minimal $B - L$ extension of the SM, the SM with fourth generations, etc.

5. The prototypical model: The Inert-2HDM

From all fundamentals and developments previously introduced, we study the vacuum behavior at one loop level in extended Higgs sectors with two doublets (2HDM), where $U(1)$ and Z_2 symmetries are considered to protect the CP symmetry in the Higgs potential and to avoid Flavor Changing Neutral Currents at tree level in the Yukawa sector. In the Inert Higgs Model case, a detailed comparison is made between both models by using the energy evolution of couplings, which should satisfy energy scale dependent relations deduced for minima and stationary points of the Higgs potential at tree level. Besides, perturbative unitarity constraints at tree level are considered to generate the allowed parameter space compatible with perturbativity (absence of Landau poles). Our studies illustrate exclusion regions for Higgs masses and other combinations of couplings in the scalar sector, in particular for splittings of mass square for neutral scalars A^0 and H^0, as well as the difference between the sum of these and the charged Higgs mass square. From the vacuum stability for inert-2HDM at the tree and one loop levels, analyses lead us to find out new hierarchical structures for scalar masses. To complete vacuum studies on the Inert model, and based on reparameterization invariance of the Higgs potential, we compute original discriminants that allow ensuring the presence of a global electroweak minimum at tree level. Moreover, the behavior in high energy scales drives out analyzing criticality phenomena for the additional parameters of extended Higgs sectors. Finally, and using the consistency with the electroweak precision analyses of oblique parameters, we describe several implications from different regimes of the inert model on charged and pseudoscalar Higgs searches[1].

To incorporate all these concepts, we organize this chapter as follows: In section 5.1, we discuss particular cases of Z_2 and $U(1)$ global symmetries of the Inert Two Higgs Doublet Model. Additionally, we after discussing positivity constraints as well as conditions for the presence of a global minimum in the Higgs potential at tree level. Mass eigenstates and splittings among scalars in the inert 2HDM will be given in the same section. In section 5.2, we describe perturbative unitarity constraints to the scalar sector for both models. In section 5.3, contours and the corresponding analyses of couplings are considered in several energy-scales from Electroweak up to GUT and Planck scales- for type I Yukawa Lagrangian. At the same time in those studies, we find compatibility with perturbative unitarity behavior for scalar couplings. Tree level regions compatible to get one global electroweak minimum are described in section 5.4. According to the restrictions obtained, in section 5.5, EW-oblique parameters are computed regarding $S-T$ values to establish the compatibility between vacuum behavior predictions and phenomenological observables.

5.1. Inert Two Higgs Doublet Model (IHDM)

Preserving the SM content of fermionic and bosons fields, the Inert Two Higgs Doublet Model contains additionally a doublet Φ_2 with a VEV equal to zero. The model has a general Z_2-invariance, under which Φ_2 transforms odd, and the remaining fields change even. At tree level, Φ_2 is not coupled with fermions. The physical parametrization of the Higgs doublets is

$$\Phi_1 = \begin{pmatrix} G^+ \\ \frac{1}{\sqrt{2}}\left(v + h^0 + iG^0\right) \end{pmatrix} \text{ and } \Phi_2 = \begin{pmatrix} H^+ \\ \frac{1}{\sqrt{2}}\left(H^0 + iA^0\right), \end{pmatrix} \tag{5.1.1}$$

featuring five Higgs bosons $(h^0, H^0, A^0, H^\pm)$ and three Goldstone bosons $(G^0, G^\pm)$. The vacuum expectation value for the first doublet is located in $\langle\Phi_1\rangle_0 = v = 246$ GeV. Fields h^0 and H^0 are defined as scalars transforming to CP symmetry in a even way, meanwhile A^0 is a pseudoscalar field changing odd under CP symmetry. Finally, fields $H^\pm$ are the charged Higgs bosons.

The scalar field h^0 emulates SM Higgs boson in mass and couplings with fermionic and gauge bosonic fields, trivially satisfying an *alignment regime* in the scalar sector[2]. The Higgs potential in this context takes the following form:

[1] This chapter is mainly based on developments presented systematically in [170]

[2] In the general alignment regimen, the remaining scalars can be located in any energy scale fulfilling the electroweak oblique parameters [171]

$$V_H = m_{11}^2\Phi_1^\dagger\Phi_1 + m_{22}^2\Phi_2^\dagger\Phi_2 + \frac{1}{2}\lambda_1\left(\Phi_1^\dagger\Phi_1\right)^2 + \frac{1}{2}\lambda_2\left(\Phi_2^\dagger\Phi_2\right)^2 + \lambda_3\left(\Phi_1^\dagger\Phi_1\right)\left(\Phi_2^\dagger\Phi_2\right) + \lambda_4\left(\Phi_1^\dagger\Phi_2\right)\left(\Phi_2^\dagger\Phi_1\right) + \frac{1}{2}\lambda_5\left[\left(\Phi_1^\dagger\Phi_2\right)^2 + \left(\Phi_2^\dagger\Phi_1\right)^2\right]. \tag{5.1.2}$$

We have considered a CP conserving Higgs potential by taking all couplings in (2.3.1) as real quantities. Under an Abelian theory, a global $U(1)$-symmetry excludes λ_5 coupling in V_H. If we choose an inert second doublet, i.e. $\langle\Phi_2\rangle_0 = 0$, Higgs masses acquire the following structure:

$$m_{h^0}^2 = \lambda_1 v^2, \tag{5.1.3}$$

$$m_{H^0}^2 = m_{22}^2 + \frac{1}{2}\lambda_3 v^2 + \frac{1}{2}\left(\lambda_4 - \lambda_5\right)v^2 + \lambda_5 v^2 = m_{A^0}^2 + \lambda_5 v^2, \tag{5.1.4}$$

$$m_{A^0}^2 = m_{22}^2 + \frac{1}{2}\lambda_3 v^2 + \frac{1}{2}\left(\lambda_4 - \lambda_5\right)v^2 = m_{H^\pm}^2 + \frac{1}{2}\left(\lambda_4 - \lambda_5\right)v^2, \tag{5.1.5}$$

$$m_{H^\pm}^2 = m_{22}^2 + \frac{1}{2}\lambda_3 v^2. \tag{5.1.6}$$

From this settlement of equations, we realize that the mass eigenstates are independent of λ_2. This fact prevents to constraint λ_2 with phenomenology for scalar boson h^0 directly because production or decay rates with λ_2 depend on new physics Higgs bosons H^0, A^0 and $H^\pm$. This fact motivates to vacuum stability and perturbativity analyses since these approaches are meaningful ways to give feasible values for this particular coupling. Besides, λ_5 coupling prevents mass degeneracy between H^0 and A^0 scalars. This regime of degeneracy will be present in a Higgs potential with $U(1)$ symmetry [3]. In the last scenario, a remarkable fact observed is the non-appearance of an axion with $m_{A^0} = 0$ (emerging when a continuous global symmetry becomes spontaneously broken), which is due to the choice of an inert doublet makes that the $U(1)$-global symmetry remains unbroken. Because of the relation of λ_5 with the scalar masses, it is possible to define the splitting among masses of pseudoscalar and the heaviest neutral Higgs by:

$$\lambda_5 = \frac{m_{H^0}^2 - m_{A^0}^2}{v^2} \equiv \Delta S_0^2. \tag{5.1.7}$$

For λ_4, relation with the scalar masses induces a splitting between neutral and charged scalars:

$$\lambda_4 = \frac{m_{H^0}^2 + m_{A^0}^2 - 2m_{H^\pm}^2}{v^2} \equiv \Delta S_1^2. \tag{5.1.8}$$

It is also convenient to define the difference between charged Higgs mass and m_{22}^2 parameter

$$\lambda_3 = \frac{2\left(m_{H^\pm}^2 - m_{22}^2\right)}{v^2} \equiv \Delta S_2^2. \tag{5.1.9}$$

5.1.1. Vacuum Stability Behavior

To ensure a bounded from below Higgs potential, it is necessary the exigence that V_H in Eq. (2.3.1) must always be positive for large field values along all possible directions of the (Φ_1, Φ_2) space. At tree level and from studies presented in section 2.3.2, this is translated into the following inequalities

$$\lambda_1 + \lambda_2 > |\lambda_1 - \lambda_2|, \tag{5.1.10}$$

which is equivalent to $\lambda_1 > 0$ and $\lambda_2 > 0$ in the individual directions of Φ_1 and Φ_2 directions. In the plane $\Phi_1 - \Phi_2$, the positivity conditions are

[3] Moreover, extending the Higgs potential to be invariant under a global $SU(2)$ acting on Φ_2 makes both $\lambda_4 = \lambda_5 = 0$ and forces all three inert scalars degenerate. This fact motivates a *compressed*-IHDM where all inert scalars have almost degenerated masses and where $SU(2)$ global symmetry is an approximated symmetry of the Higgs potential [172].

$$\lambda_3 > -\sqrt{\lambda_1\lambda_2}, \tag{5.1.11}$$
$$\lambda_4 + \lambda_3 + \lambda_5 > -\sqrt{\lambda_1\lambda_2}, \tag{5.1.12}$$
$$\lambda_4 + \lambda_3 - \lambda_5 > -\sqrt{\lambda_1\lambda_2}. \tag{5.1.13}$$

These inequalities (5.1.10)-(5.1.13) ensure absolute stability for the electroweak vacuum by defining a bounded from below Higgs potential. However, possible metastable scenarios arise when a second inert-like extremum is specified by a VEV v_2 non-zero and $v_1 = 0$. In this stationary point, the Z_2 symmetry of the Higgs potential is conserved by this state; however, the Z_2 symmetry of the Lagrangian become spontaneously violated. In this framework, fermions are massless since they uniquely couple to Φ_1. Therefore, this non-physical behavior must be excluded from a plausible parameter space when this extremum point become one global minimum of the theory. Two necessary conditions for the simultaneous existence of both minima is that i) $m_{11}^2 < 0$ and $m_{22}^2 < 0$ or ii) $\lambda_3 + \lambda_4 + \lambda_5 > 0$ [34].

One condition to ensure that the inert vacuum would be the global minimum of the Higgs potential is [26, 118]

$$\frac{m_{11}^2}{\sqrt{\lambda_1}} < \frac{m_{22}^2}{\sqrt{\lambda_2}}. \tag{5.1.14}$$

To determine if the EW-minimum (inert) is a global one, we calculate a new set of inequalities relating to quartic and bilinear couplings with critical points in the Higgs potential. The new discriminants, encouraging a global minimum in the Higgs potential, are computed for IHDM from the respective Hessian in the gauge orbit field using the general reparameterization group $SO(1,3)^+$ evaluated in the inert-stationary point[4]:

$$-\sqrt{\lambda_1\lambda_2} < \frac{2m_{22}^2}{v^2} < \sqrt{\lambda_1\lambda_2}, \tag{5.1.15}$$
$$-(\lambda_3 + \lambda_4 + \lambda_5) < \frac{2m_{22}^2}{v^2} < \sqrt{\lambda_1\lambda_2}, \tag{5.1.16}$$
$$-(\lambda_3 + \lambda_4 - \lambda_5) < \frac{2m_{22}^2}{v^2} < \sqrt{\lambda_1\lambda_2}. \tag{5.1.17}$$

Computation has been described in appendix L. We focus only on the implications that new discriminants have over parameters at tree level. Possible studies might be done in the future by exploring the consequences at one loop level since many phenomena over nature of minima seem to show intriguing effects of the effective Higgs potential at NLO [34].

Despite in 2HDMs at tree level two minima that break different symmetries cannot coexist, a global minimum with charge violation can appear if quartic couplings satisfy [118]- [173]

$$\lambda_4 - \lambda_5 > 0 \text{ and } \lambda_5 + \lambda_4 > 0 \text{ and } \lambda_3 - \sqrt{\lambda_1\lambda_2} > 0. \tag{5.1.18}$$

Mass eigenstates and conditions to avoid charge violation vacua lead to study possible sequences for scalar masses. For instance, from $\lambda_4 + \lambda_5 < 0$, we can infer the hierarchy $m_{H^\pm} > m_{H^0}$ for scalar masses, which is also inherited by a $U(1)$ Higgs potential with the additional consequence of degeneracy between H^0 and A^0. By contrast, $\lambda_4 - \lambda_5 > 0$ implies $m_{A^0} > m_{H^\pm}$ for the Z_2 invariant model. With these constraints in mind, we shall study their compatibility level with stability and unitarity bounds.

5.2. Unitarity constraints

Unitarity constraints at tree level arise using the optical theorem in the S-matrix description with generalized partial waves for scalar scattering processes. The traditional way to implement it in gauge theories is demanding that the model has only weakly interacting degrees of freedom at high energy limit. In these weakly coupled theories, higher order contributions to S-matrix become smaller compared to the leading order. It is then possible to require for S-matrix to be unitary from the tree level of the theory.

[4] Our computations are based on new methods for searching stationary points in 2HDMs, which are defined systematically in [29]

We concentrate on scalar processes coming from Higgs potentials with $U(1)$ and Z_2 symmetries. In a generic basis of the Higgs potential Eq. (2.3.1), processes labeling total isospin σ and hypercharge Y lead to construct the following transition matrices for the particular case of a Z_2 invariant Higgs potential (see section 4.4):

$$8\pi\tilde{S}_{Y=2,\sigma=1} = \begin{pmatrix} \lambda_1 & \lambda_5 & 0 \\ \lambda_5 & \lambda_2 & 0 \\ 0 & 0 & \lambda_3+\lambda_4 \end{pmatrix}, \tag{5.2.1a}$$

$$8\pi\tilde{S}_{Y=2,\sigma=0} = \lambda_3 - \lambda_4, \tag{5.2.1b}$$

$$8\pi\tilde{S}_{Y=0,\sigma=1} = \begin{pmatrix} \lambda_1 & \lambda_4 & 0 & 0 \\ \lambda_4 & \lambda_2 & 0 & 0 \\ 0 & 0 & \lambda_3 & 0 \\ 0 & 0 & 0 & \lambda_3 \end{pmatrix}, \tag{5.2.1c}$$

$$8\pi\tilde{S}_{Y=0,\sigma=0} = \begin{pmatrix} 3\lambda_1 & 2\lambda_3+\lambda_4 & 0 & 0 \\ 2\lambda_3+\lambda_4 & 3\lambda_2 & 0 & 0 \\ 0 & 0 & \lambda_3+2\lambda_4 & 3\lambda_5 \\ 0 & 0 & 3\lambda_5 & \lambda_3+2\lambda_4 \end{pmatrix}. \tag{5.2.1d}$$

In each matrix, left sides contain matrix elements for $Z_2 - even$ states, meanwhile in the lower right part they belong to $Z_2 - odd$ states. Unitarity bounds over partial waves $|\mathcal{M}| < 1$ are translated into eigenvalues $\mathbf{\Lambda}$ for $\tilde{S}$ matrices, hence the new condition is

$$|\mathbf{\Lambda}| < \frac{1}{8\pi\xi}, \tag{5.2.2}$$

with ξ an indistinguishability factor. As was discussed above, this upper bound corresponds to equal the $\mathcal{M}$-matrix with the tree-level elements by disregarding higher order corrections. For the Higgs potential (2.3.1), the matrices in (5.2.1) are block-diagonal facilitating the computation of the eigenvalues $\mathbf{\Lambda}^{Z_2}_{Y,\sigma\pm}$:

$$\mathbf{\Lambda}^{even}_{2,1\pm} = \frac{1}{2}\left(\lambda_1+\lambda_2 \pm \sqrt{(\lambda_1-\lambda_2)^2+4\lambda_5^2}\right), \quad \mathbf{\Lambda}^{odd}_{21} = \lambda_3+\lambda_4. \tag{5.2.3a}$$

$$\mathbf{\Lambda}^{even}_{2,0\pm} = \lambda_3 - \lambda_4. \tag{5.2.3b}$$

$$\mathbf{\Lambda}^{even}_{0,1\pm} = \frac{1}{2}\left(\lambda_1+\lambda_2 \pm \sqrt{(\lambda_1-\lambda_2)^2+4\lambda_4^2}\right), \quad \mathbf{\Lambda}^{odd}_{01\pm} = \lambda_3 \pm \lambda_5. \tag{5.2.3c}$$

$$\mathbf{\Lambda}^{even}_{0,0\pm} = \frac{1}{2}\left[3(\lambda_1+\lambda_2) \pm \sqrt{9(\lambda_1-\lambda_2)^2+4\left(2\lambda_3+\lambda_4\right)^2}\right], \quad \mathbf{\Lambda}^{odd}_{00\pm} = \lambda_3+2\lambda_4 \pm 3\lambda_5. \tag{5.2.3d}$$

These constraints will be used to see the compatibility between vacuum predictions and perturbative unitarity, as well as relationships with the possible presence of Landau poles in the parameter space.

5.3. One loop level analysis

As a first proof of the influence of the scalar extended Higgs sector in the vacuum stability scenario, we consider the running coupling for λ_1 which could be compared with $\lambda_{SM}(\mu)$ through the appropriate limits of the theory. Indeed the numerical evaluation of Renormalization Group Equations (RGEs) for the 2HDM type I (they are depicted in J) allows computing the vacuum behavior and perturbative realization in field and parameter space for an $U(1)$-invariant model. This evolution can also be seen in a Z_2 invariant model with $\lambda_5(m_Z) = 0$. Figure 5.1- shows energy scale evolution for $\lambda_1(\mu)$ with different values of the remaining scalar couplings. $\lambda_2(\mu_0)$ coupling is settled in such a way that its vacuum constraint satisfies, i.e. $\lambda_2(\mu_0) > 0$ (with $\mu_0 = m_Z$ the initial scale). For the initial conditions taken there over other couplings, the vacuum instabilities are suppressed in the Φ_1 direction between $10^3 - 10^{19}$ GeV. Then, criticality presented in the SM at energies close to GUT and Planck scales for values of $\lambda_1(m_Z)$ could be avoided in an extensive regime of the parameter space for an inert 2HDM type I.

With the general condition $\lambda_3(\mu) + \lambda_4(\mu) - |\lambda_5(\mu)| > -\sqrt{\lambda_1(\mu)\lambda_2(\mu)}$ at specific energies, we get the contours for $\lambda_4(m_Z) = \left(m^2_{A^0} + m^2_{H^0} - 2m^2_{H^\pm}\right)/v^2$ vs $\lambda_1(m_Z) = m^2_{h^0}/v^2$ and $\lambda_4(m_Z) = \left(m^2_{A^0} + m^2_{H^0} - 2m^2_{H^\pm}\right)/v^2$ vs $\lambda_5(m_Z) =$

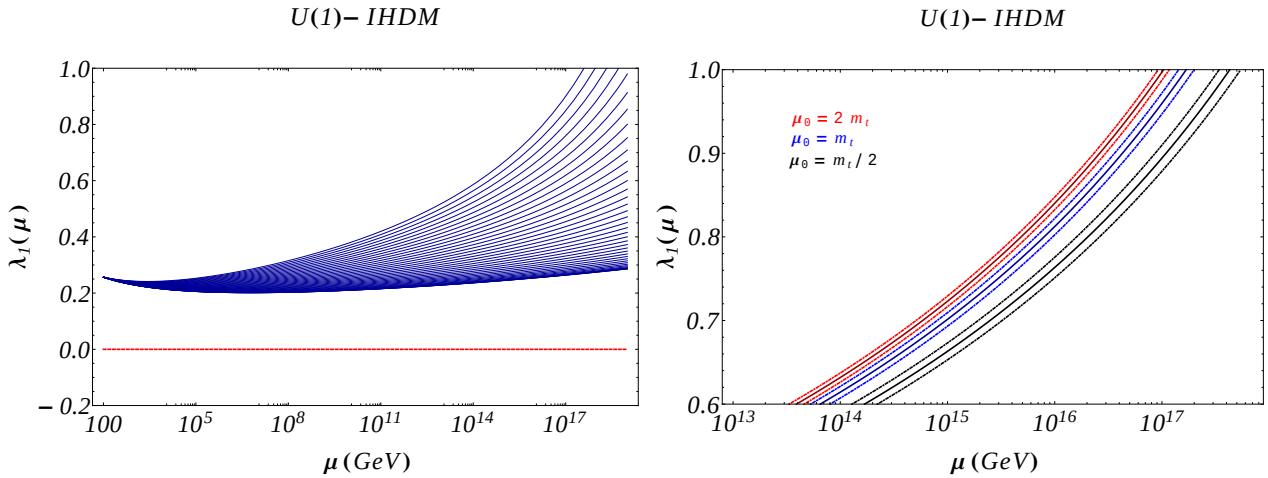

Figure 5.1.: (**Left**) Energy scale evolution for λ_1 coupling with $m_{h^0} = 125.04$ GeV and $m_t = 173.34$ GeV. Evolution of $\lambda_1(\mu)$ is made fixing the remaining initial conditions $\lambda_i(\mu_0 = m_z)$'s. Initial gauge couplings have been taken at m_Z-scale. Here $-0.4 \leq \lambda_4(m_Z) \leq 0.0$, $-0.2 \leq \lambda_3(m_Z) \leq 0$ and $0.0 \leq \lambda_2(m_Z) \leq 0.2$, and the assumption of $\lambda_2(m_z) = |\lambda_4(m_z)|/2$ and $\lambda_3(m_z) = \lambda_4(m_z)/2$. Each curve is varying in 0.02 units in those intervals. (**Right**) Maximum curve lying in such ranges that specifies the top quark mass uncertainty [174] ($m_t = 173.34 \pm 0.76$ GeV) leading to corrections for $\lambda_1(\mu)$ ($\mu = 10^{17}$ GeV) around 4%. Henceforth, numerical analysis are based on these central values of Higgs boson and top quark masses, likewise for gauge couplings in m_Z scale [50] and we have varied the matching condition $\mu_0 = \{\frac{m_t}{2}, m_t, 2m_t\}$. To assess the uncertainty on the coupling, we have followed the prescription presented in [10]

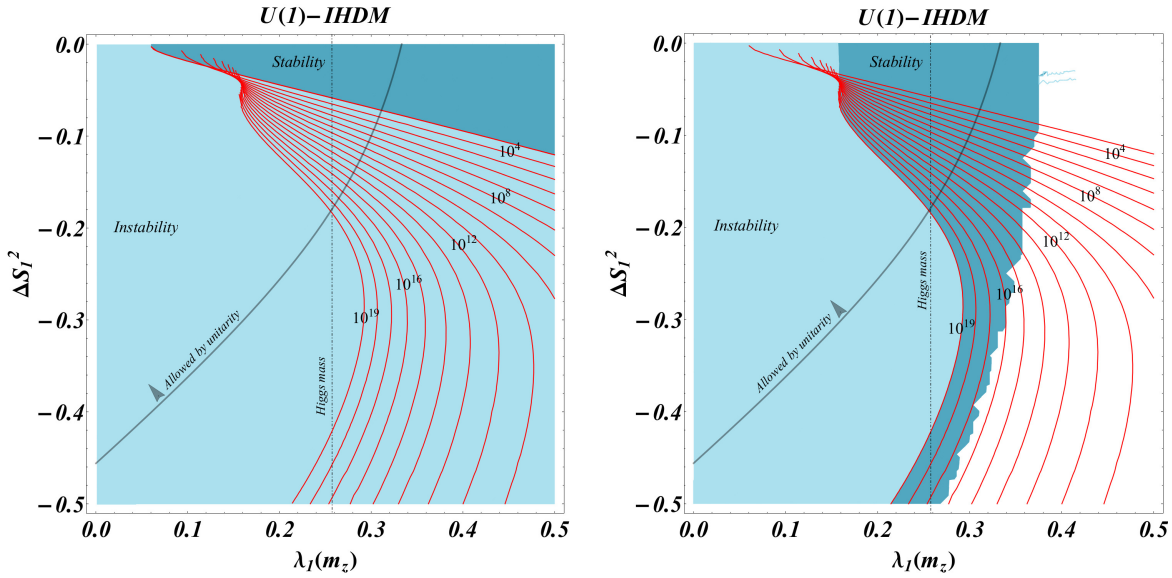

Figure 5.2.: *Phase diagrams with the evolution of contours from $\mu = 10^3$ GeV (**Background-Left**) up to $\mu = 10^{19}$ GeV (**Background-Right**) in the ΔS_1^2 versus $\lambda_1(m_Z)$ plane. Here $0 \leq \lambda_2(m_Z) \leq 0.25$ and $0 \leq \lambda_3(m_Z) \leq 0.25$, starting with $|\lambda_3(m_Z)| = \lambda_2(m_Z)$ and $\lambda_3(m_Z) = \lambda_4(m_Z)/2$. Red lines are the remaining contours between $\mu = 10^3$ and 10^{19} GeV. Dashed line indicates the experimental value for the ratio in $\lambda_1(m_Z)$ for a Higgs with a mass near to 125 GeV [3]. For red contours initial points mark the final zone of instability scenario. Gray curve encloses the region compatible with the strongest unitarity bound given by the eigenvalue $\mathbf{\Lambda}_{00}^{even+}$ in Eq. (5.2.3d) .*

$\left(m^2_{H^0} - m^2_{A^0}\right)/v^2$. For all phase diagrams for stability-instability (blue and light-blue areas respectively), we have also taken two particular backgrounds at $\mu = 10^3$ GeV (Left-panels) and $\mu = 10^{19}$ GeV (Right panels), and analyzing as critical zones (or criticality in our context) evolves with energy scales between these backgrounds.

For instance in the $U(1)$ case, contours in the $\lambda_1(m_Z) - \lambda_4(m_Z)$ plane are depicted in Fig. 5.2. Here evolution of contours of stability and instability are considered in the scales between 10^3 GeV and 10^{19} GeV for sundry values of $\lambda_3(m_Z)$ and $\lambda_2(m_Z)$. Similarly, for the $U(1)$-case, we consider in (Fig. 5.3) the $\lambda_3(m_Z) - \lambda_4(m_Z)$ plane, which yields vacuum analysis for splittings $m^2_{H^\pm} - m^2_{22}$ and $m^2_{A^0,H^0} - m^2_{H^\pm}$ for different energy regimes. Contours have taken values around of the central ones for fermion and boson particles in the current phenomenological analyses considered in [50, 174]. We take as our input parameters $m_t = 173.34$ GeV, $m_b = 4.2$ GeV, $m_{h^0} = 125.04$ GeV, $m_W = 80.36$ GeV, $m_Z = 91.18$ GeV [50].

There are regions phenomenologically relevant since they could be easily recognizable by exclusion zones for observed or new resonances. For instance, in the $U(1)-$model, relevant regimes are: (a) the scenario with A^0-axion appearance ($m^2_{H^\pm} = -\lambda_4 v_1^2/2$) or (b) the limit for the *compressed* regime with triply degenerate scalars (i.e $m_{H^0} = m_{A^0} = m_{H^\pm}$). The latter occurs when $\lambda_4(m_Z) = 0$. The first regime would also have as a consequence $m_{H^0} = 0$, which is phenomenologically unwanted and from theoretical point of view this limit is forbidden by the model foundations. Another important region corresponds to identify m_{h^0} with the experimental resonance in the mass range of 125.04 ± 0.64 GeV. The theoretical framework for this assumption is the alignment regime [88, 171], which is satisfied trivially in the inert 2HDM. The zone consistent with vacuum stability and the value $\lambda_1(m_Z) \simeq 0.258$ (for central value of Higgs mass) in Fig. 5.2 and 5.4 will be given as a dashed line crossing the respective parameter space.

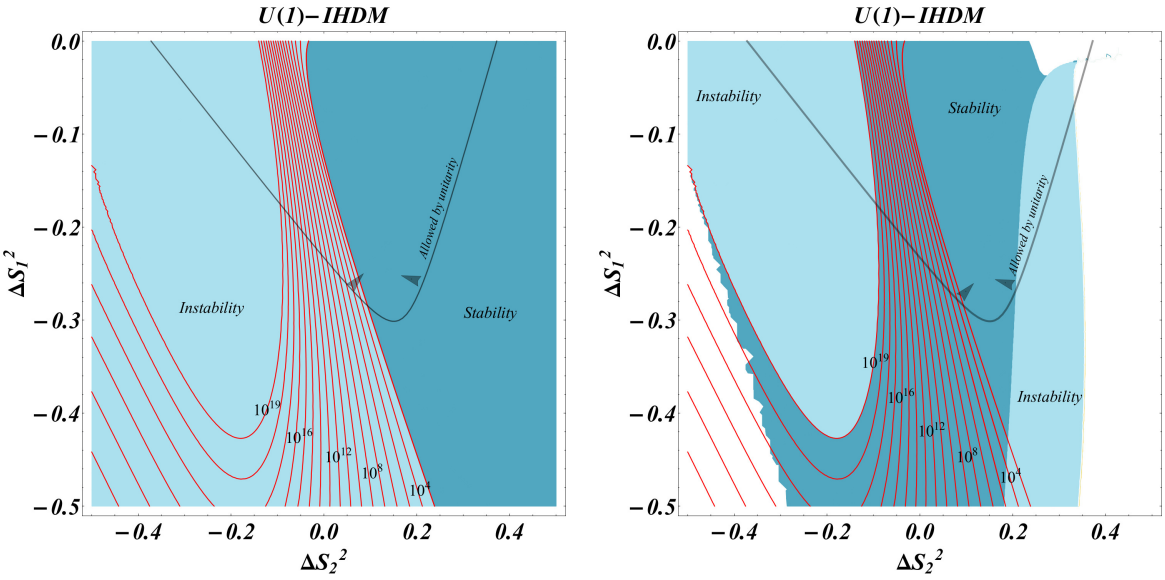

Figure 5.3.: *Phase diagram with evolution of stability and instability contours from* $\mu = 10^3$ *GeV (**Background-Left**) up to* $\mu = 10^{19}$ *GeV (**Background-Right**) in the* ΔS_1^2 *versus* ΔS_2^2 *plane. Red lines show the evolution of the remaining contours between* $\mu = 10^3$ *and* 10^{19} *GeV. Here* $0 \leq \lambda_2(m_Z) \leq 0.25$*, starting with* $\lambda_2(m_Z) = |\lambda_4(m_Z)|/2$*. Gray curve encloses region compatible with the strongest unitarity bound given by eigenvalue* $\mathbf{\Lambda}_{00}^{even+}$.

Constraint $\lambda_3(\mu) + \lambda_4(\mu) - |\lambda_5(\mu)| > -\sqrt{\lambda_1(\mu)\lambda_2(\mu)}$ contains the positivity conditions $\lambda_1(\mu) > 0$ and $\lambda_2(\mu) > 0$ in an independent form, because of the well defined behavior of the root square. The RGE of $\lambda_2(\mu)$ is not widely relevant, because the Yukawa structure leads to an evolution which does not involve strong sources of instabilities. Hence positivity of this product correspond to ensure positivity of λ_1. This correspondence between conditions can be seen in the contours through regions for small values of $\lambda_1(m_Z)$, which will not be relevant since these regimes are located apart from phenomenological identification of m_{h^0}.

Correspondingly, contours in the Z_2-model are shown in Figs. 5.4-5.6, from which we can study stability behavior in $\lambda_1(m_Z) - \lambda_4(m_Z)$ and $\lambda_1(m_Z) - \lambda_4(m_Z)$ planes. As in the $U(1)$ case, dashed line indicates m_{h^0} identification with Higgs-like scalar observed in LHC. In Fig. 5.6 we show the variation of vacuum stability and instability zones for $\lambda_3(\mu) + \lambda_4(\mu) - |\lambda_5(\mu)| > -\sqrt{\lambda_1(\mu)\lambda_2(\mu)}$ contour with respect to the energy scale in $\lambda_5(m_Z) - \lambda_4(m_Z)$ plane, which leads to determine the mass splittings influence in vacuum stability for the Z_2 case.

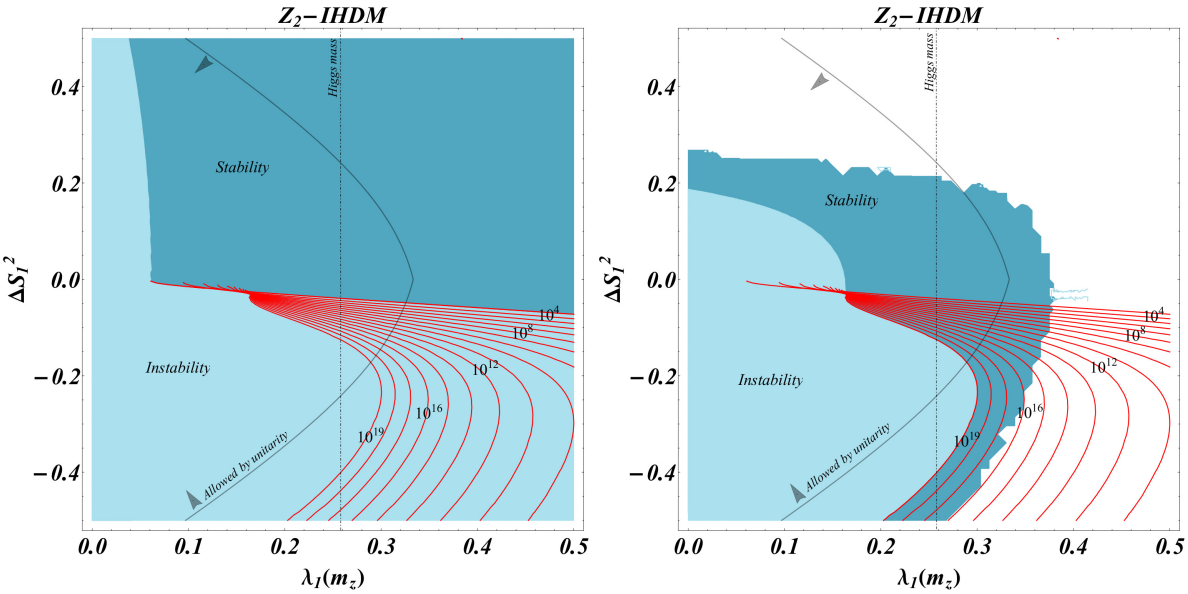

Figure 5.4.: *Phase diagrams with the evolution of contours from* $\mu = 10^3$ *GeV* (***Background-Left***) *up to* $\mu = 10^{19}$ *GeV* (***Background-Right***) *in the* ΔS_1^2 *versus* $\lambda_1\,(m_Z)$ *plane. Here* $0 \leq \lambda_2(m_Z) \leq 0.25$ *and* $-0.25 \leq \lambda_{3,4}(m_Z) \leq 0.25$, *starting with* $\lambda_{3,4}(m_Z) = \lambda_5(m_Z)/2$ *and* $\lambda_{34}(m_Z) = |\lambda_2(m_Z)|$. *Red lines are the remaining contours between* $\mu = 10^3$ *and* 10^{19} *GeV. Dashed line indicates the experimental value for the ratio in* $\lambda_1(m_Z)$ *for a Higgs with a mass near to* 125 *GeV [3]. Gray curve encloses region compatible with the strongest unitarity bound given by the eigenvalue* $\mathbf{\Lambda}_{00}^{even+}$.

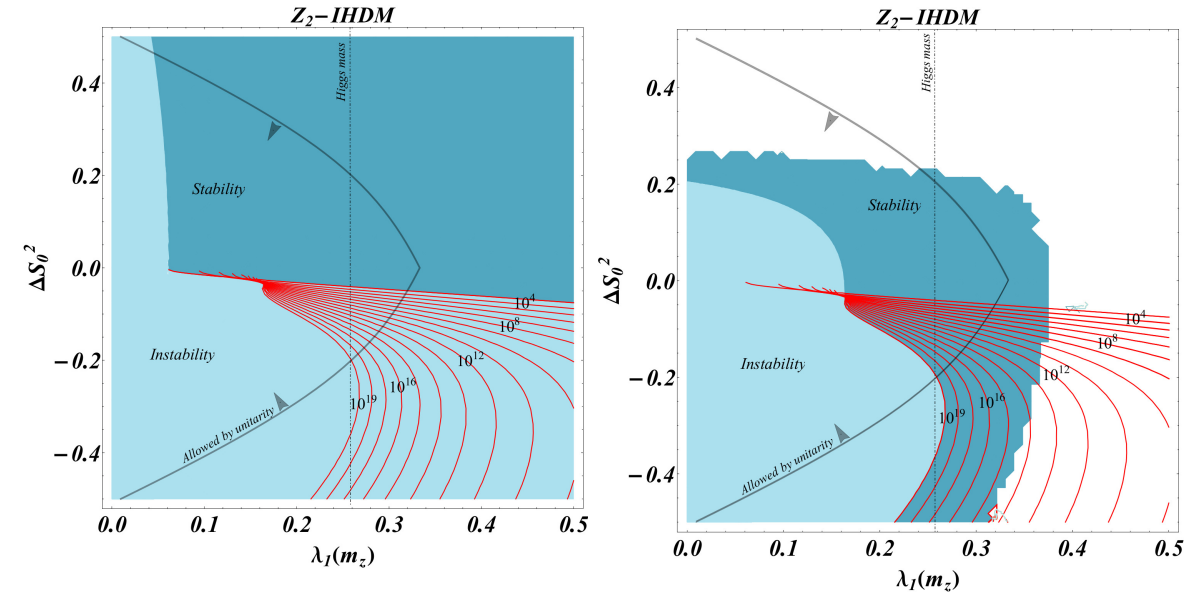

Figure 5.5.: *Phase diagrams with the evolution of contours from* $\mu = 10^3$ *GeV* (***Background-Left***) *up to* $\mu = 10^{19}$ *GeV* (***Background-Right***) *in the* ΔS_0^2 *versus* $\lambda_1\,(m_Z)$ *plane. Here* $0 \leq \lambda_2(m_Z) \leq 0.25$ *and* $-0.25 \leq \lambda_{3,4}(m_Z) \leq 0.25$, *starting with* $\lambda_{3,4}(m_Z) = \lambda_5(m_Z)/2$ *and* $\lambda_{34}(m_Z) = |\lambda_2(m_Z)|$. *Red lines are the remaining contours between* $\mu = 10^3$ *and* 10^{19} *GeV. Dashed line indicates the experimental value for the ratio in* $\lambda_1(m_Z)$ *for a Higgs with a mass near to* 125 *GeV [3]. Gray curve encloses the region compatible with the strongest unitarity bound given by the eigenvalue* $\mathbf{\Lambda}_{00}^{even+}$.

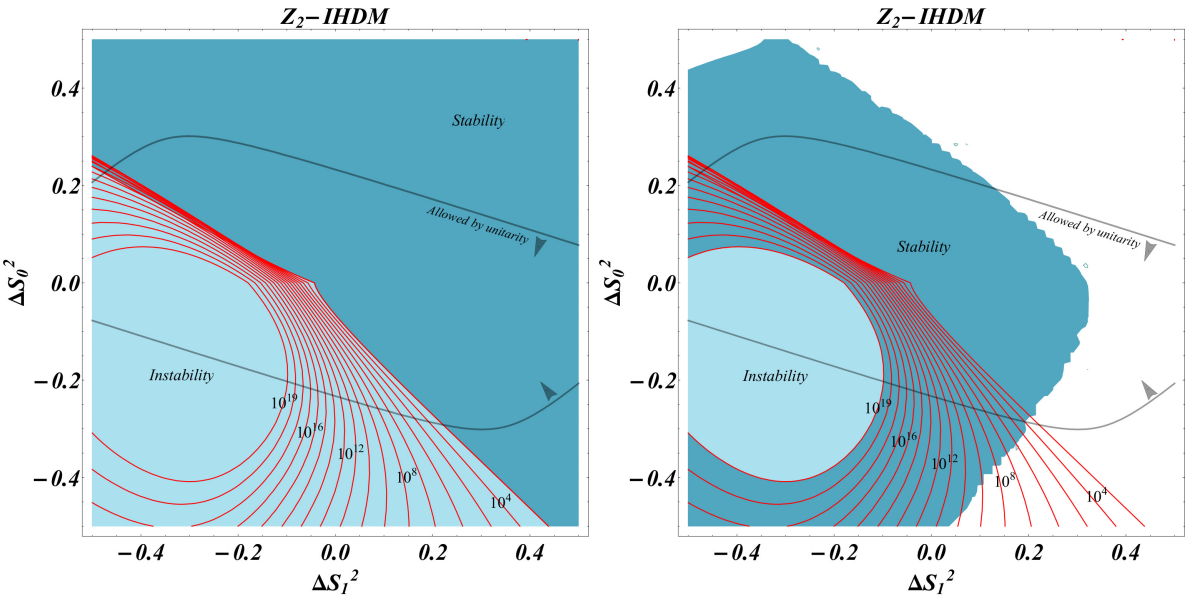

Figure 5.6.: *Phase diagram with evolution of stability and instability contours from* $\mu = 10^3$ *GeV* (***Background-Left***) *up to* $\mu = 10^{19}$ *GeV* (***Background-Right***) *in the* ΔS_0^2 *versus* ΔS_1^2 *plane. Here* $0 \leq \lambda_2(m_Z) \leq 0.25$ *and* $-0.25 \leq \lambda_3(m_Z) \leq 0.25$*, starting with* $\lambda_3(m_Z) = \lambda_5(m_Z)/2$ *and* $\lambda_2(m_Z) = |\lambda_3(m_Z)|$*. Red lines show the evolution of the remaining contours between* $\mu = 10^3$ *and* 10^{19} *GeV. Gray curves enclose the region compatible with the strongest unitarity bound of the eigenvalue* $\mathbf{\Lambda}_{00}^{even}$*.*

Our phase diagrams lead us to verify some limits for the perturbative validity of the both models (Z_2 -$U(1)$) in the field space. It can be seen due to solutions for RGEs present possible Landau poles. These non-perturbative zones are identified with white areas, as it is shown on the right side of Figs. 5.2-5.6 for the background of $\mu = 10^{19}$ GeV.

5.3.1. Implications of vacuum behavior in Z_2-2HDM and $U\,(1)\,-$2HDM

In the SM, the positivity of the scalar boson mass-squared and bounded from below potential implies that $\lambda > 0$. To ensure vacuum stability for all scales up to μ_I, one must have $\lambda\,(\mu) > 0$ for all μ between m_Z and μ_I. Similarly, to ensure vacuum stability in the 2HDM up to μ_I, effective Higgs potential must require that all of the five constraints be valid up to μ_I. At one loop level, this can be rendered as a threshold effect for SM vacuum. If the condition $\lambda_1\,(\mu) > 0$ or $\lambda_2\,(\mu) > 0$ is violated, the potential will be unstable in the Φ_1 or Φ_2 direction respectively. These threshold corrections at one loop increase the Higgs potential stability by the introduction of new fields and couplings among them, which in the SM is lost even from scales around $\mu = 10^{11}$ GeV [6]. Although in this case, new physics improves vacuum stability in Φ_1 in particular limits compatible with the SM behavior, other directions can be affected by the fields and couplings added to the spectrum.

In other directions of the extended field space, the statement of instability works as follows: if the conditions $\lambda_4\,(\mu) + \lambda_5\,(\mu) < 0$, $\lambda_3\,(\mu) + \lambda_4\,(\mu) - |\lambda_5\,(\mu)| + \sqrt{\lambda_1\,(\mu)\,\lambda_2\,(\mu)} > 0$ or $\lambda_3\,(\mu) + \sqrt{\lambda_1\,(\mu)\,\lambda_2\,(\mu)} > 0$ are not accomplished one by one or simultaneously, the potential will be unstable in the Φ_1-Φ_2 plane. At the same time, it is viable to require that all λ's be finite (or perturbative) up to Λ in order to avoid possible Landau poles.

Numerical analyses start with quartic couplings defined at the electroweak scale $\mu_{ew} = m_Z$. With these initial conditions, the RGEs are integrated out to search whether one of the bounds for positivity is violated or whether any of the couplings become non-perturbative before reaching a $\mu_{\rm crit} \equiv \Lambda$ (procedure established in [20]). By sweeping different zones in the parameter space, it is possible to describe contours as a function of scalar mass splittings. The contours built up, interpreted as phase diagrams, yield information about how instabilities arise in the Higgs potential at an energy scale and a field-space direction given.

Minimality principle and vacuum relations could be studied by some limits between the SM and the inert-2HDM. For instance, the parameter space compatible with h^0 emulating to SM-Higgs boson is non-suppressed even at Planck scales for positive values of $\lambda_5, \lambda_4, \lambda_3$ as it is shown in vacuum stability analyses. This regime implies that, for $\lambda_1\,(m_Z)$ identified with the Higgs mass and with initial conditions, $\lambda_5\,(m_Z)$ must be positive and whose inferior limit close to 0.0.. The limit superior belongs in $\lambda_5(m_Z) \simeq 0.2$, which is also compatible with unitarity perturbative bounds. In the

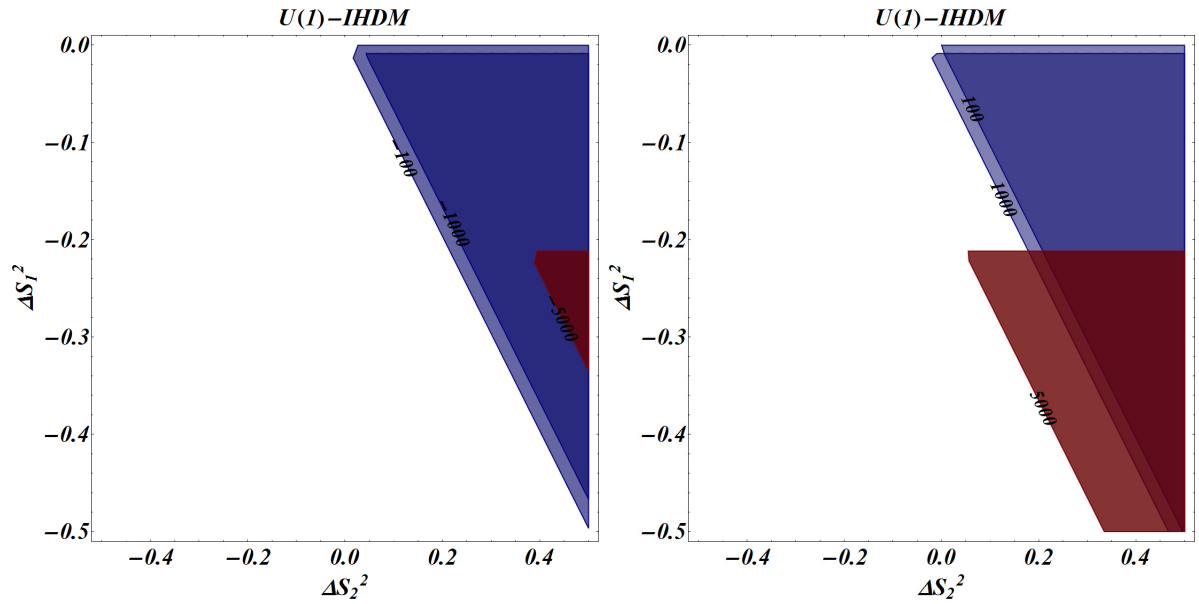

Figure 5.7.: *Global minimum for* $\Delta S_1^2 - \Delta S_0^2$ *zones in different values of* ***(Left)*** $m_{22}^2\left(GeV^2\right) = -100, -1000, -5000$ *and* ***(Right)*** $m_{22}^2\left(GeV^2\right) = 100, 1000, 5000$. *Here* $0 \leq \lambda_2 \leq 0.25$, *starting with* $\lambda_2 = |\lambda_4|/2$.

Z_2 case, this stable zone is consistent with a spectrum where $m_{H^0} > m_{A^0}$ for all energy scales. Nonetheless, this region will be suppressed by condition $\lambda_4 > \lambda_5$.

Vacuum stability and perturbative unitarity bounds are compatible with $\Delta S_0^2 > 0$ (in a wide zone), while there also exist a reduced zone where $\Delta S_0^2 < 0$ is allowed by both analyses. The last result is compatible with the tree level analysis where $\lambda_4 > \lambda_5$. From plane $\lambda_4\left(m_Z\right) - \lambda_1\left(m_Z\right)$, a similar restriction over ΔS_1^2 implies $2m_{H^\pm}^2 < m_{H^0}^2 + m_{A^0}^2$. Compatibility among $\lambda_4 + \lambda_5 < 0$ $\lambda_4 - \lambda_5 > 0$ and vacuum stability scenario gives an advantage for regions where $\lambda_4 > 0$ and $\lambda_5 < 0$, with small splittings. The last fact is a radical difference between both models, because in the $U(1)$-2HDM and to avoid vacuum configurations with charge violation, the model demands $\lambda_4 < 0$.

Non-perturbative values are driven out for $\lambda_{1,2}\left(m_Z\right) \sim 0.25$ (even incompatible with perturbative unitarity) and $\lambda_3\left(m_Z\right) \sim -0.35$ and $\lambda_{3,4,5}\left(m_Z\right) \sim 0.25$, being determined by regions where numerical solutions of RGEs were finite. As it was pointed out, these non-perturbative zones are also strongly disfavored by unitarity constraints of scalar scattering processes.

5.4. Tree level contours for metastability analyses

To search the compatibility between splittings allowed by vacuum analyses and the presence of a global minimum in these scenarios, we take into account the restrictions obtained in Eqs (5.1.15)-(5.1.17). For instance, in the $U(1)$-model, we evaluate the metastability constraints over $\Delta S_1^2 - \Delta S_2^2$ plane in Fig. 5.7. We see as negative and positive values of m_{22}^2 favor positive zones for ΔS_2^2, relating to $m_{H^\pm}^2 > m_{22}^2$ hierarchy. These compatible zones are larger for $|m_{22}^2| < 5000$ GeV^2. Particularly values $|m_{22}^2| > 7500$ GeV^2 will enter in higher values of ΔS_2^2, which are related to non-perturbative or unstable zones in the Higgs potential. Compressed models with an approximate degeneracy between $m_{H^\pm} = m_{A^0, H^0}$ become incompatible with a global minimum in $|m_{22}^2| > 1000$ GeV^2.

In the Z_2 case, in Fig. 5.8 global minima zones are drawn over $\Delta S_1^2 - \Delta S_0^2$ plane for different values of m_{22}^2, which generate a global minimum in positive values of ΔS_1^2. Those regimens are compatible with assumptions from conditions to avoid a charge violation minimum (before introducing vacuum and mass eigenstates structures for scalar sector). Another important point is that compressed models become incompatible with a EW-global minimum for $|m_{22}^2| > 2500$ GeV^2. Explicitly, in $m_{22}^2 = 5000$ GeV^2 just values of $|\Delta S_0^2| > 0.2$ are compatible with a global minimum structure, but incompatible with a mass degeneracy between A^0 and H^0.

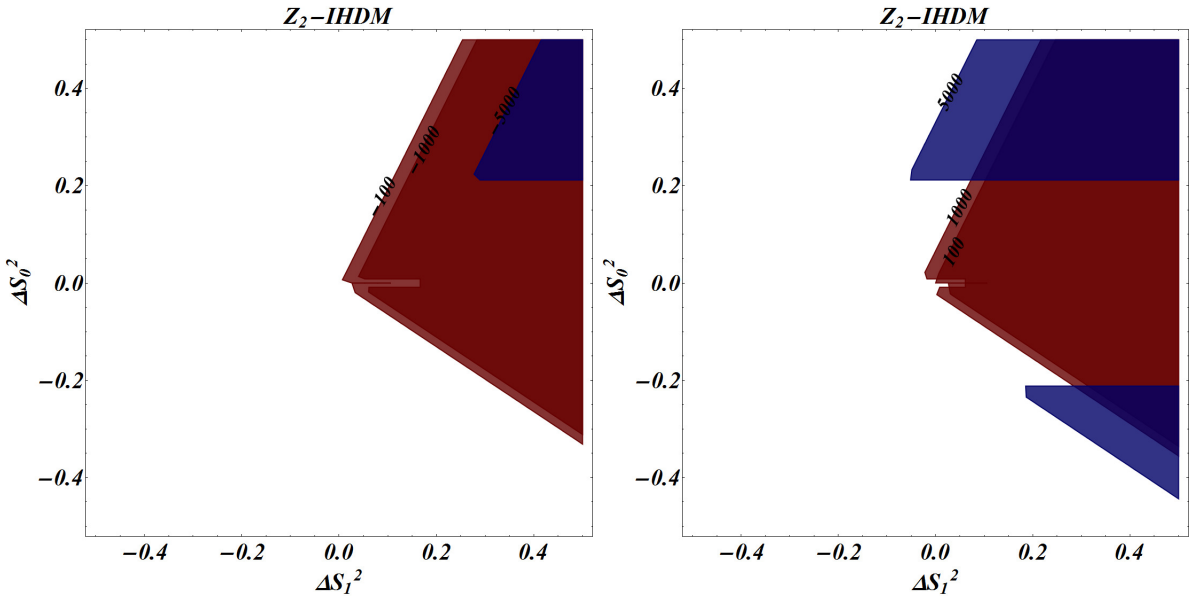

Figure 5.8.: *Global minimum for* $\Delta S_0^2 - \Delta S_1^2$ *zones in different values of* (***Left***) $m_{22}^2\left(GeV^2\right) = -100, -1000, -5000$ *and* (***Right***) $m_{22}^2\left(GeV^2\right) = 100, 1000, 5000$. *Here* $0 \leq \lambda_2 \leq 0.25$ *and* $-0.25 \leq \lambda_3 \leq 0.25$, *starting with* $\lambda_3 = \lambda_5/2$ *and* $\lambda_2 = |\lambda_3|$.

5.5. Oblique parameters and observables influence

From vacuum and metastability analyses, it is possible to make a major comparison with electroweak precision parameters since they are highly sensitive to mass splittings [117]. It is well known that oblique parameters are designed to constrain models of new physics from the electroweak precision observables. It is assumed that the effects of new physics only appear through vacuum polarization and therefore enables us to modify oblique parameters. Most of the effects on electroweak precision observables can be parameterized by three gauge self-energy parameters (S, T, U) introduced by Peskin and Takeuchi [175–178] (see discussion presented in the final part of chapter 1). Hence, the correlation among the parameters above could be given regarding electroweak observables and leads to analyses some precision physics, useful to constraint phenomenology from new physics mechanisms. For instance, S or $S+U$ describe new physics contributions to neutral or charged current processes at several energy scales; while T measures the difference between the new physics contributions of neutral and charged current processes at low energies (i.e., sensitive to isospin violation) close to EW cut [179]. Indeed, this parameter is related to the commonly used parameter $\rho_0 = \rho/\rho_{SM}$ through $\rho_0 = 1/\left(1 - \alpha T\right)$; encoding the departure from the SM value of $\rho_0 = 1$. By contrast, U is only constrained by the W boson mass and its total width. Likewise, U is seldom small in new physics models, and therefore, the STU parameter space can often be projected down to a two-dimensional parameter space in which the experimental constraints are easy to visualize [179] [5].

Constraints on the STU parameters are derived from a fit to the precision electroweak data (more details can be found in the most current articles [81–85]). Besides, in the STU parameters the floating fit values are $m_Z = 91.1873 \pm 0.0021$ GeV, $\Delta\alpha_{had}(m_Z^2) = 0.02757 \pm 0.00010$, and $\alpha_s(m_Z^2) = 0.1192 \pm 0.0033$. The following fit results are determined from a fit for a reference Standard Model with $m_{t,ref} = 173$ GeV and $m_{H,ref} = 125$ GeV and fixing $U = 0$: giving $S_{U=0} = 0.06 \pm 0.09$ and $T_{U=0} = 0.10 \pm 0.07$, with a correlation coefficient of $+0.91$. The general procedure to measure oblique parameters relies on a global fit to the high-precision electroweak observables coming from particle collider experiments (mostly the Z pole data from the CERN-LEP collider) and atomic parity violation [81, 175]. Every step presented here would be a valuable tool to measure the compatibility level of the vacuum behavior predictions with the EW observables and precision tests.

Despite at this level, these computations do not distinguish among fermionic couplings, the plane of correlations gives information about scalar states splitting and how it could be restricted from EW measurements. Definitions of S and T parameters for 2HDM-Inert case read [22, 24]:

[5] In fact, U quantity is related to a dimension-eight operator, while S and T can be given concerning six dimension operators.

$$S_{In} = \frac{1}{2\pi}\left[\frac{1}{6}\ln\left(\frac{m_{H^0}^2}{m_{H^\pm}^2}\right) + \frac{1}{3}\frac{m_{H^0}^2 m_{A^0}^2}{\left(m_{A^0}^2 - m_{H^0}^2\right)^2} + \frac{1}{6}\frac{m_{A^0}^4\left(m_{A^0}^2 - 3m_{H^0}^2\right)}{\left(m_{A^0}^2 - m_{H^0}^2\right)^3}\ln\left(\frac{m_{A^0}^2}{m_{H^0}^2}\right) - \frac{5}{36}\right], \tag{5.5.1}$$

$$T_{In} = \frac{1}{32\pi\alpha^2 v^2}\left[F\left(m_{H^\pm}, m_{H^0}\right) + F\left(m_{H^\pm}, m_{H^0}\right) - F\left(m_{A^0}, m_{H^0}\right)\right], \tag{5.5.2}$$

with F a masses symmetric function defined by

$$F(m_1, m_2) \equiv \frac{m_1^2 + m_2^2}{2} - \frac{m_1^2 m_2^2}{m_1^2 - m_2^2}\ln\left(\frac{m_1^2}{m_2^2}\right). \tag{5.5.3}$$

From the equations for S and T written through $m_{H^\pm}$ and ΔS_1^2 variables, we can verify the compatibility level under electroweak observables of regions once studied from vacuum behavior. Figure 5.9 shows the oblique parameter constraints from the electroweak precision and how it translates data into constraints on the masses or their splittings for the extended sector for $U(1)$ and Z_2 models. In these two cases, there are regimes compatible between the experimental fits and the inert-2HDM predictions over S, T parameters, so that a variety of model configurations exhibits an intimate relation with the electroweak precision observables [24].

Splittings between m_{A^0} and m_{H^0}, characterized by their respective ratio $k_S \equiv m_{A^0}/m_{H^0}$, have a high level of compatibility when $\Delta S_1^2 \to 0$ when k_S is close to degeneracy. For $k_s > 1$, compatible zones are reduced when k_S increases, being large splittings in ΔS_0^2 compensated with large splittings in ΔS_1^2, which are suppressed by perturbativity analyses. The quasi-degeneracy between neutral states is excluded for large splittings among them and charged Higgs mass. In the $U(1)$ case, 99% fit contours are approximately symmetric in ΔS_1^2 splittings, implying that ST parameters do not distinguish relative sign between sum of neutral states masses and charged Higgs mass. For ΔS_2^2 close to zero only splittings with $\Delta S_1^2 \approx 0^-$ are allowed. Hence, in the particular limit of $m_{22}^2 \simeq m_{H^\pm}^2$, a *compressed* scenario for IHDM (quasi-degeneracy in masses of the inert scalar states) is favored by systematics of ST oblique parameters.

In terms of direct masses of scalar spectrum, oblique parameters fits at 99% yield constrained regions showed in Fig. 5.10. With the global $U(1)$-symmetry, both possible hypothesis for scalar hierarchies, $m_{H^\pm} > m_{A^0,H^0}$ or $m_{H^\pm} < m_{A^0,H^0}$ are consistent with fits for ST oblique parameters[6]. Here scalars states are organized near to the maximal compressed scenario with $m_{H^\pm} \simeq m_{A^0,H^0}$. Heavier neutral states in a quasi degeneracy are also allowed, if charged Higgs is also heavy with a mass near to those neutral states. Meanwhile, in the Z_2-scenario, we can see as for $k_s < 1$ (i.e $m_{A^0} < m_{H^0}$), compatible regions prefer $m_{H^\pm} > m_{A^0}$ hierarchy. Most constrained region in this set is present for $k_s = 0.2$, where only zones with $m_{H^\pm} < 250$ GeV and $m_{A^0} < 250$ GeV are consistent with the fits for ST parameters. For $k_s > 1$, the most favored hierarchy is $m_{A^0} > m_{H^\pm}$. Heavier states are thus inconsistent only by unitarity and perturbative analyses. It is also explicit how compressed scenario is consistent with ST plane for $k_s > 0.4$.

Above all, it seems pertinent to point out that vacuum analysis as well as oblique parameters allow to determine space parameters compatible with phenomenology coming from colliders searches and dark matter studies. In the first case, in the quasi-degeneracy case of neutral states, LEP II analysis excludes the region of masses where simultaneously: $m_{H^0} < 80$ GeV, $m_{A^0} < 100$ GeV and $m_A - m_H > 8$ GeV ($m_{H^0}(\text{ GeV}) > 8/(k_s - 1)$, with $k_s = m_{A^0}/m_{H^0}$) [181]. For $m_{H^0}(\text{ GeV}) < 8/(k_s - 1)$, the LEP I limit $m_{H^0} + m_{A^0} > m_{Z^0}$ applies, preventing invisible $Z^0 \to A^0 H^0$ channel [182,183]. In terms of h^0 mass and for $m_{A^0,H^0} < m_{h^0}$, precision tests predict that $h^0 \to A^0 A^0$ and $h^0 \to H^0 H^0$ decays shall be dominant channels. In particular, for the $U(1)$ case both decays are invisible, meanwhile in the Z_2 case the $h^0 \to H^0 H^0$ decay will be the invisible one. These effects can be ruled out by the Run 2 in the LHC, if the properties of the scalar Higgs boson with $m_h = 125$ GeV are still compatible with the ones predicted by SM.

For the charged Higgs boson and owing to the kinetic-gauge interactions, the dominant decays are $H^\pm \to W^\pm H^0$ and $H^\pm \to W^\pm A^0$. In degeneracy limit, both channels can be distinguished by precision tests over parity and spin of possible subsequent final decays [1–3]. In the Z_2 case, $m_{A^0} > m_{H^\pm}$ hierarchy forbids the last decay channel at least as an on shell one. Nevertheless, there are also trilinear gauge couplings among charged Higgs boson and neutral gauge bosons leading to new decays channels which can compete with decays involving Z_2 odd scalar states.

Finally, we discuss some consequence of our results in front of dark matter phenomenology for the IHDM. Measured relic abundance density for dark matter is $\Omega_{cdm}h^2 = 0.1199 \pm 0.0022$ [184]. This selects distinct zones in the parameter space for new physics [126][7]: i) *Low mass regime*: $m_{H^0} < m_{h^0}/2$. The Dark matter pair-annihilation predominantly

[6] The former has been used in the vacuum analysis as a input assumption. This can be seen as a limit case avoiding the presence of a vacuum with charge violation

[7] In [126] is discussed the possible origin of a strong phase transition in the inert-2HDM required in baryogenesis processes; being it possible when the resonant scenario is considered.

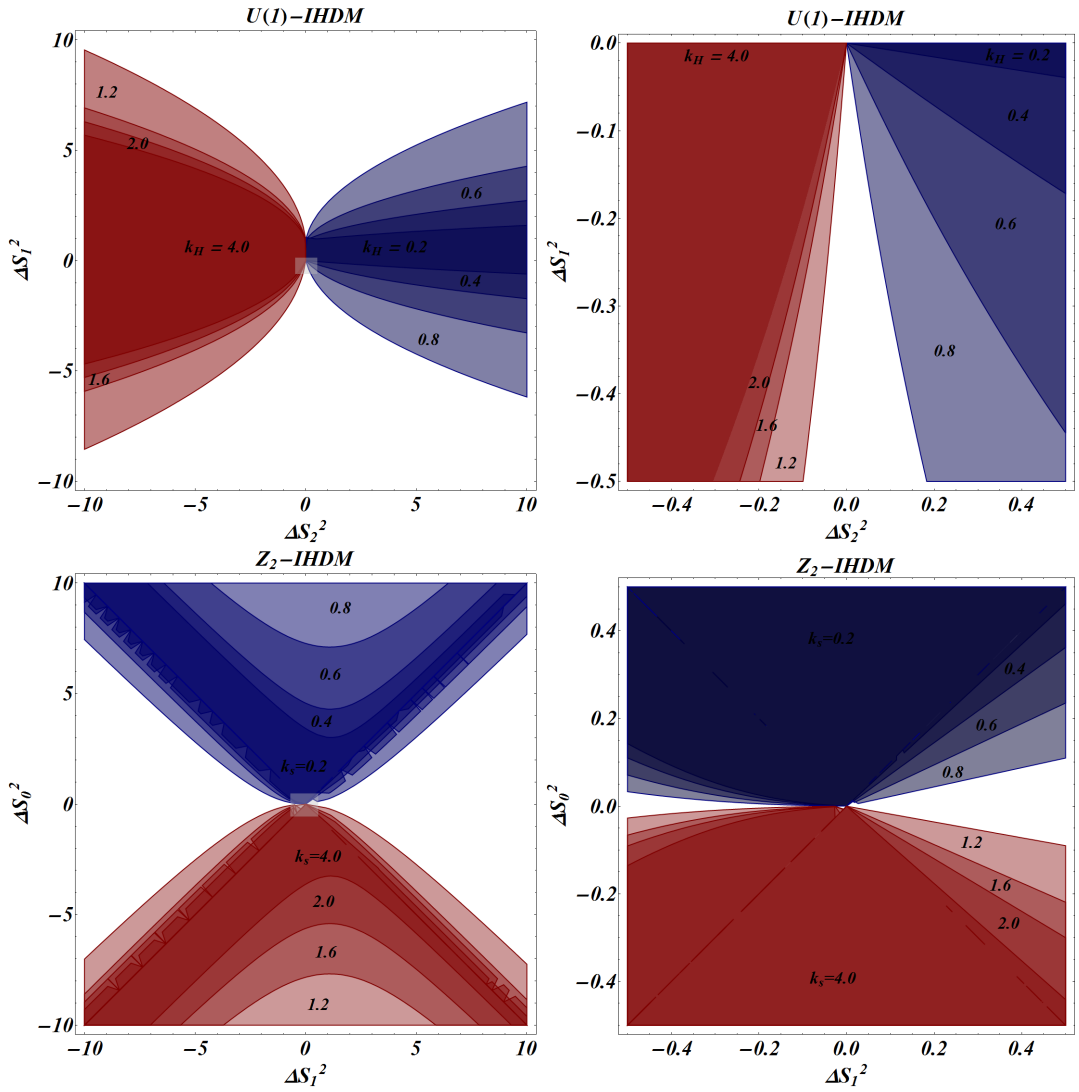

Figure 5.9.: Oblique parameters in the inert-Higgs doublet model with the S, T fit results (with $U = 0$) at 99 % CL for $U(1)$ (**Up**) and Z_2 (**Down**) symmetries. The model area is obtained with the use of the mass parameter splittings and defining $k_H^2 \equiv m_{22}^2/m_{H^\pm}^2$ ($U(1)$ case) and $k_s \equiv m_{A^0}/m_{H^0}$ (Z_2 case) ratios. Plots in right side are zoomed regions compatible with vacuum stability analyses. Computations over ST plane have used Mathematica module described in [180].

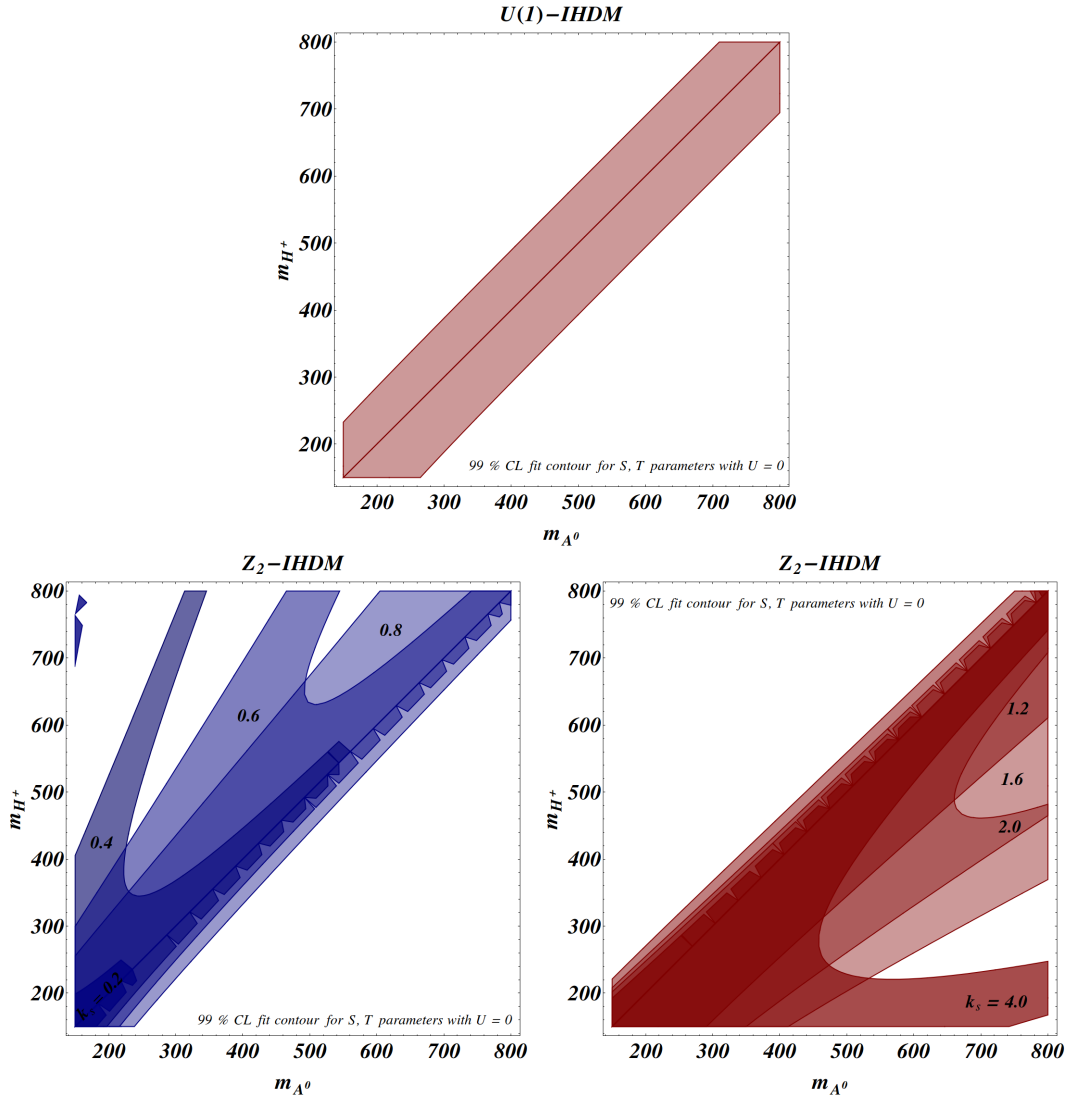

Figure 5.10.: *Oblique parameters in the inert-Higgs doublet model with the* S, T *fit results (with* U = 0*) at 99 % CL for* $U(1)$ *(**Up**) and* Z_2 *(**Down**) symmetries. The model area constraining direct masses is obtained by defining* $k_s \equiv m_{A^0}/m_{H^0}$ *(Z_2 case) ratios. Computations over ST plane have used Mathematica module described in [180].*

proceeds via the pair production of the b quarks and τ leptons; being SM-like Higgs boson the dark matter portal. ii) *Resonant regime*: $m_{H^0} \sim m_{h^0}/2$. This scenario produces a viable mass around a pole leaving even an unconstrained window close to 10-15 GeV around of $m_{h^0}/2$ [185]. iii) *Intermediate mass regime*: $m_{h^0}/2 << m_{H^0}(\text{GeV}) < 500$. Here H^0 pair annihilation to gauge bosons becomes significant, such that the thermal relic density is systematically below the universal dark matter density for any combination of model parameters, excluding the presence of dark matter constituents [51,54]. Moreover, as the charged Higgs holds $m_{H^\pm} > m_{H^0}$ in both models (with Z_2 and $U(1)$ symmetries), zone approaching to the upper bound is also incompatible with EW-ST parameters. iv) *Heavy mass regime*: $m_{H^0} \gtrsim 500$ GeV. This scenario, in the lower bound, can be rendered as a decoupling among Z_2 odd scalars and h^0 wherein there is no relic density enough. If couplings with h^0 are driven out away from zero cancellations, it is possible leads to achieve the correct relic density for mass values from the lower bound slightly different up to heavy scalar settled in TeV scale. Again incompatibility of this scenario comes from oblique quantities and unitarity constraints, which can be evaded if this inert model is considered as an effective theory of a strong interacting sector with new physics set up in the TeV energy [186]. Taking into account the $U(1)$ case, all these constraints in the different scenarios must also be satisfied by pseudoscalar Higgs boson. This fact can yields discrepancies in the matching of the relic density value since direct dark matter with spin-independent searches put limits over the degeneracy between H^0 and A^0 [187,188]. Nevertheless, from quantum gravity analyses, a recent approach [189] has discarded likely dark matter candidates for a 2HDM with a global $U(1)$-symmetry.

5.6. Addendum: Two photon decay in the IHDM

In this section, we describe how precision tests over Higgs decays leading to constrain the extended space of parameters of IHDM. In the two photon decay, new physics implemented by charged Higgs couplings gives us information on phenomenological reliability of the model in front of data for run I of LHC. Likelihood proof for this decay channel has been treated in Appendix M.

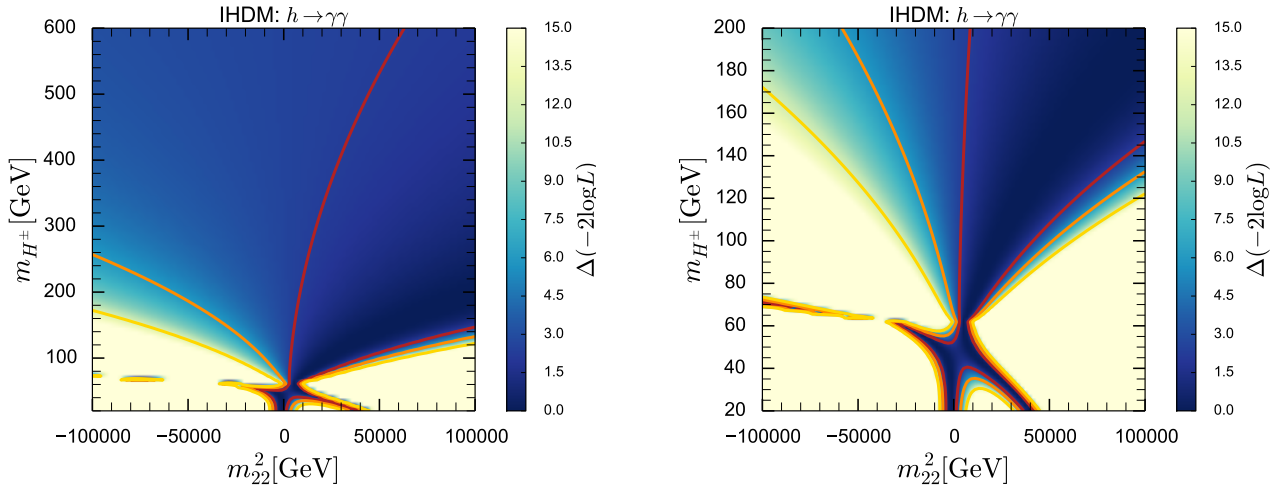

Figure 5.11.: *Likelihood analysis in the IHDM for the $m_{H^\pm} - m^2_{22}$ plane in the diphotonic channel. Here h^0 SM-like Higgs has a mass of 125 GeV. The red, orange and yellow lines correspond to the allowed boundaries of 68%, 95% and 99.7% CL regions, respectively. The right figure is the zoomed area for the most constrained scenario in the same plane (lower masses for charged Higgs boson).*

Contours and analyses made with `Lilith` in Fig. 5.11-5.12 work in the following way [35]: From definitions of effective coupling among two photons and one Higgs h^0 at LO of (M.1.4), likewise $-2\log(C_\gamma)$ correspondingly defined in Appendix M, we scan the 2-dimensional parameter space in $m_{H^\pm} - m^2_{22}$ plane. This 2-dimensional grid scan is performed over the parameters defining $\lambda_3(m^2_{22},\ m_{H^\pm})$ coupling between charged Higgs and h^0. For each couple $(m^2_{22},\ m_{H^\pm})$, the corresponding $\Delta(-2\log L(C_\gamma))$ is obtained according to C_γ in Eq. (M.1.4). In this scanning out, charged Higgs masses below 100 GeV are highly suppressed beyond contours at 99% C.L.. Zones between $-10000 < m^2_{22}(\text{GeV}) < 10000$ have zones compatible with experimental data in $m_{H^\pm} > 20$ GeV. A region at $\Delta(-2\log L) < 2.3$ is given in $m^2_{22} > 0$ in $m_{H^\pm} > 150$ GeV. This plot gives us additional information to control quadratic parameter, which from theoretical point of view is important to feature metastability scenario between inert and inert like vacuum structures.

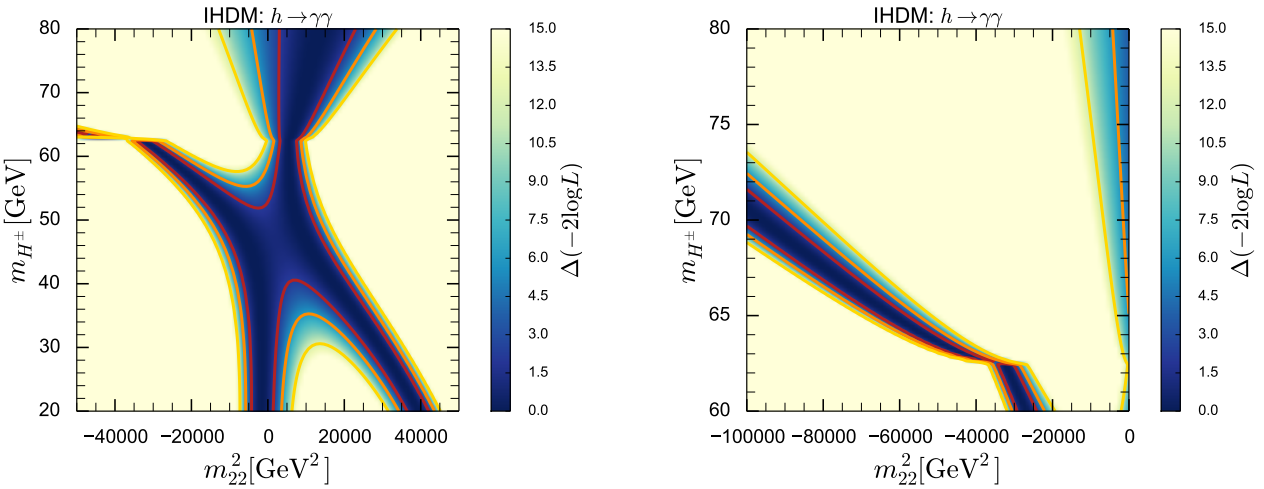

Figure 5.12.: *Likelihood analysis in the IHDM for the $m_{H^\pm} - m^2_{22}$ plane in the diphotonic channel. Here h^0 SM-like Higgs has a mass of 125 GeV, presenting specific and zoomed zones of Fig. 5.11. Once again, the red, orange and yellow lines correspond to the allowed boundaries of 68%, 95% and 99.7% CL regions, respectively. The right figure is the zoomed region for the most constrained scenario in the same plane (even lower masses for charged Higgs boson and negative values of m^2_{22}).*

Two caveats can complement these analyses. In the diphotonic channel, and despite the charged scalar loop can interfere either constructively or destructively with the SM contribution, it is possible to see how decoupling of charged Higgs is consistent with precision measurements (beyond of $m_{H^\pm} > 300$ GeV). This behavior occurs even at 99.7% CL and independently of values taken for m^2_{22}. Secondly, the total decay width $\Gamma^{IHDM}(h)$ can be increased concerning the SM scenario due to the existence of the invisible decays: $h^0 \to H^0 H^0$ and $h^0 \to A^0 A^0$. Nevertheless, they have not been considered in those analyses. Therefore our scanning can be modified by introducing possible invisible decays. However, observing Fig. 5.13, contributions from invisible decays are expected to no exceed $\mathcal{B}(h^0 \to \text{Invisible}) < 0.28$ at 99.7% C.L. of total branching ratio for decays of scalar boson founded in LHC.

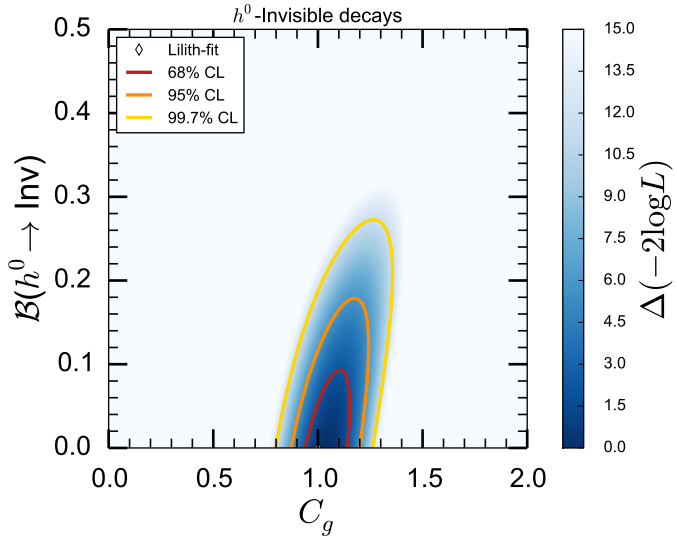

Figure 5.13.: *Likelihood analysis for invisible decays from $\mathcal{B}\left(h^0 \to Invisible\right)$ vs effective coupling to C_g. The red, orange and yellow regions are 68%, 95% and 99.7% CL regions, respectively. Here we have used monojets constraints ($gg \to h^0 + 1 - 2j, VBF$ where $R_{invisible} \equiv \left(\frac{2}{3}C^2_{ggh} + \frac{1}{3}C^2_{VBF}\right)\mathcal{B}_{inv} < 1.1$ at 95%) [190, 191].*

6. Models with soft breaking of a $U(1)$ global symmetry

We now continue to study the vacuum behavior of an extended Higgs sector with two doublets in a scenario with a softly broken $U(1)$ global symmetry. The soft-term is introduced to avoid massless-axion particles arising when the global symmetry becomes spontaneously broken. This model has metastable states through the possible presence of multiple non-degenerate minima, which is unwanted from the phenomenological point of view if the metastable state is not long-lived enough. The analysis of this fact leads to find possible exclusion limits over parameter space of quartic couplings. It can be translated into improving the individual behavior of initial conditions for renormalization group equations; also determining unstable zones for the Higgs potential at one loop level. Besides vacuum stability analyses, the influence of absence of charge violation minima is considered in all studies. Extremal cases for the model as well as criticality phenomena are comprehensively discussed using relations among Higgs masses or splittings among them. From vacuum behavior and LHC results, phenomenological aspects in the searching of charged and heavier Higgs bosons are considered to evaluate the scalar alignment regimen of the two Higgs doublet model[1].

To describe all these concepts systematically, we organize this chapter as follows. In section 6.1 and under symmetries and basis invariant transformations in 2HDMs, we use formalism presented in [36] to find out positivity constraints in this simple $U(1)$ scalar sector with a soft-violation term. The systematic begins with a general way to write a more compact form for the Higgs potential which is invariant under a unique parameterization of type Lorentz group. Under impositions over doublets and its extrapolation into Minkowskian space is possible to find out vacuum stability constraints associated with the requirement at tree level for a bounded from below Higgs potential in regimes of the field space associated with points or orbits here defined. Moreover, that covariant structure of the Higgs potential returns an appropriate frame to analyze the possibility to reach metastable states in vacua with two normal minima (where VEVs are real). On the other hand, bilinears form of the Higgs potential carries out information about structures of critical conditions compatible with a complete SSB and one neutral vacuum. These conditions can be considered from a precise point of view; studying when possible critical points are minima indeed. For these purposes, we first find eigenstates masses for scalars in 6.2. The phenomenological starting point to interpret a model realization, the alignment regimen is studied in 6.3. Then, in section 6.4, we review the problem for critical conditions of a Higgs potential with a softly broken $U(1)$-symmetry. Some general phenomenological aspects of these models are reviewed in section 6.5. In 6.7, we compute the vacuum behavior at tree level and for different combinations of the parameter space. Meanwhile, NLO calculations have been studied in section 6.8. Likelihood proofs for two photons decay, and oblique parameters analyses are established in 6.9 with the aim to see the compatibility of vacuum studies with models in the alignment scenario for 2HDMs. Finally, in conclusions and remarks, we describe the relevance of our treatment in the interpretation of vacuum and metastability analyses and the compatibility with Electroweak precision tests and likelihood proofs in the two photons decay channel.

6.1. Vacuum behavior and positivity constraints in a 2HDM with a softly violation for $U(1)$ symmetry

This section is devoted to introducing generalities of the Real $U(1)$-2HDM, as well as its theoretical constraints. The 2HDM potential concerning doublets with a soft breaking of a $U(1)$ global symmetry is

$$\begin{aligned} V_H = {} & m_{11}^2 \Phi_1^\dagger \Phi_1 + m_{22}^2 \Phi_2^\dagger \Phi_2 - m_{12}^2 \left(\Phi_1^\dagger \Phi_2 + \Phi_2^\dagger \Phi_1 \right) \\ & + \frac{1}{2}\lambda_1 \left(\Phi_1^\dagger \Phi_1 \right)^2 + \frac{1}{2}\lambda_2 \left(\Phi_2^\dagger \Phi_2 \right)^2 + \lambda_3 \left(\Phi_1^\dagger \Phi_1 \right) \left(\Phi_2^\dagger \Phi_2 \right) + \lambda_4 \left(\Phi_1^\dagger \Phi_2 \right) \left(\Phi_2^\dagger \Phi_1 \right). \end{aligned} \tag{6.1.1}$$

[1] This chapter is mainly based on the results presented in [192]

By using reparametrization invariance [36] given by $SO(1,3)$ group transformations, Higgs potential can be written in terms of gauge orbit vectors r^μ, i.e.

$$V_H = -M_\mu r^\mu + \frac{1}{2}\Lambda_{\mu\nu} r^\mu r^\nu, \tag{6.1.2}$$

with $r^\mu = (r^0, r^i) = (\mathbf{\Phi}^\dagger \mathbf{\Phi}, \mathbf{\Phi}\sigma_i \mathbf{\Phi})$ and where

$$\mathbf{\Phi} = \begin{pmatrix} \Phi_1 \\ \Phi_2 \end{pmatrix}. \tag{6.1.3}$$

Here $\mathbf{\Phi}$ is a 2-dimensional vector and σ_i are the Pauli matrices. In this particular case, cuadrivector of bilinears couplings is

$$M_\mu = \left(\frac{m_{11}^2 + m_{22}^2}{2}, \mathrm{Re}\left(m_{12}^2\right), 0, \frac{m_{11}^2 - m_{22}^2}{2} \right). \tag{6.1.4}$$

In the scenario of a $U(1)-$ Higgs potential, diagonal $\Lambda_{\mu\nu}$ tensor of quartic couplings has the following form

$$\Lambda = \frac{1}{2} \begin{pmatrix} \lambda_3 + \sqrt{\lambda_1 \lambda_2} & 0 & 0 & 0 \\ 0 & -\lambda_4 & 0 & 0 \\ 0 & 0 & -\lambda_4 & 0 \\ 0 & 0 & 0 & \lambda_3 - \sqrt{\lambda_1 \lambda_2} \end{pmatrix}. \tag{6.1.5}$$

A bounded from below Higgs potential demands $\Lambda_{\mu\nu}$ must be positive definite in the future light cone LC^+, i.e., $r_\mu r^\mu \geq 0$. Employing this formalism for reparametrization of the Higgs potential, it is possible to find out the Higgs potential positivity constraints in the fourth dimension terms:

$$\lambda_1 + \lambda_2 > |\lambda_1 - \lambda_2|. \tag{6.1.6}$$

which is equivalent to $\lambda_1 > 0$ and $\lambda_2 > 0$. And

$$\lambda_3 > -\sqrt{\lambda_1 \lambda_2}. \tag{6.1.7a}$$

$$\lambda_4 + \lambda_3 > -\sqrt{\lambda_1 \lambda_2}. \tag{6.1.7b}$$

In addition to the traditional relations for vacuum stability at tree-level, the absence of charge violation vacua yields to one possible condition $\lambda_4 < 0$. Despite in 2HDMs at tree level two minima that break different symmetries cannot coexist, this situation can be rendered as a limiting hypothesis for our assumption of neutral vacua. This fact has significant phenomenological consequences and which will be treated exhaustively in the following sections, as in to describe possible hierarchical structures in the masses for scalar states.

On the other hand, unitarity constraints can be obtained from the following eigenvalues $\mathbf{\Lambda}^{Z_2}_{Y,\sigma\pm}$[2] of scattering matrices:

$$\mathbf{\Lambda}^{even}_{2,1\pm} = \frac{1}{2}\left(\lambda_1 + \lambda_2 \pm \sqrt{(\lambda_1 - \lambda_2)^2}\right), \tag{6.1.8a}$$

$$\mathbf{\Lambda}^{even}_{2,0\pm} = \lambda_3 - \lambda_4. \tag{6.1.8b}$$

$$\mathbf{\Lambda}^{even}_{0,1\pm} = \frac{1}{2}\left(\lambda_1 + \lambda_2 \pm \sqrt{(\lambda_1 - \lambda_2)^2 + 4\lambda_4^2}\right), \tag{6.1.8c}$$

$$\mathbf{\Lambda}^{even}_{0,0\pm} = \frac{1}{2}\left[3(\lambda_1 + \lambda_2) \pm \sqrt{9(\lambda_1 - \lambda_2)^2 + 4\left(2\lambda_3 + \lambda_4\right)^2}\right]. \tag{6.1.8d}$$

which have already been treated in chapter 4. The perturbative unitarity bound can be written by

$$|\mathbf{\Lambda}| < \frac{1}{8\xi\pi} \tag{6.1.9}$$

$\xi = 2$ is a factor for indistinguishable particles present in the initial or final states.

[2]Matrices are constructed from Isospin σ and Hypercharge Y, which are conserved quantities of scalar scattering at high energies.

6.2. Softly broken $U(1)-$Higgs Potential: Mass Eigenstates

In the following, mass eigenstates and respective relations among Higgs potential couplings are considered. To that end, we describe the standard parametrization of Higgs doublets regarding physical mass eigenstates introduced in chapter 1

$$\Phi_1 = \frac{1}{\sqrt{2}} \begin{pmatrix} \sqrt{2}\left(G^{\pm}\cos\beta - H^{+}\sin\beta\right) \\ v\cos\beta - h^0\sin\alpha + H^0\cos\alpha + i\left(G^0\cos\beta - A^0\sin\beta\right) \end{pmatrix}. \tag{6.2.1}$$

$$\Phi_2 = \frac{1}{\sqrt{2}} \begin{pmatrix} \sqrt{2}\left(G^{\pm}\sin\beta + H^{+}\cos\beta\right) \\ v\sin\beta + h^0\cos\alpha + H^0\sin\alpha + i\left(G^0\sin\beta + A^0\cos\beta\right) \end{pmatrix}. \tag{6.2.2}$$

Where $-\pi/2 \leq \alpha \leq \pi/2$ and $0 < \beta < \pi/2$. The Higgs masses and Higgs eigenstates are defined concerning parameters m_{ij}^2 and λ_i from the potential (6.1.1), and consequently, depend on the symmetries to write the Higgs potential indeed. Moreover, the mass matrix depends on the normal vacuum structure selected in the above parameterization,

$$\langle\Phi_1\rangle_0 = \frac{1}{\sqrt{2}}\begin{pmatrix}0\\ v_1\end{pmatrix} \text{ and } \langle\Phi_2\rangle_0 = \frac{1}{\sqrt{2}}\begin{pmatrix}0\\ v_2\end{pmatrix} \tag{6.2.3}$$

where $v_1 = v\cos\beta$ and $v_2 = v\sin\beta$. In the case of a Higgs potential with soft breaking of a $U(1)-$*symmetry*, relations among quartic couplings and masses are given by

$$\lambda_1 = \frac{1}{v^2\cos^2\beta}\left(\cos^2\alpha m_{H^0}^2 + \sin^2\alpha m_{h^0}^2 - m_{12}^2\tan\beta\right) \equiv \Delta S_1^2, \tag{6.2.4a}$$

$$\lambda_2 = \frac{1}{v^2\sin^2\beta}\left(\sin^2\alpha m_{H^0}^2 + \cos^2\alpha m_{h^0}^2 - m_{12}^2\cot\beta\right) \equiv \Delta S_2^2, \tag{6.2.4b}$$

$$\lambda_3 = \frac{2m_{H^{\pm}}^2 - m_{A^0}^2}{v^2} + \frac{\sin 2\alpha\left(m_{H^0}^2 - m_{h^0}^2\right)}{v^2} \equiv \Delta S_3^2, \tag{6.2.4c}$$

$$\lambda_4 = \frac{2m_{A^0}^2 - 2m_{H^{\pm}}^2}{v^2} \equiv \Delta S_4^2. \tag{6.2.4d}$$

and

$$m_{A^0}^2 = \frac{m_{12}^2}{\sin\beta\cos\beta} = \frac{2m_{12}^2}{\sin(2\beta)}. \tag{6.2.4e}$$

These arrays of equations are valid for $0 < \beta < \pi/2$, excluding inert models for 2HDM since impossibility of diagonalizing mass eigenstates at the same time that stationary conditions be preserved.

6.3. Alignment regime and relations for global minimum discriminant

The scalar *alignment regime*, where the lighter Higgs CP-even behaves as SM Higgs, independently of masses for remaining scalars is aimed to establish compatibility between theoretical analysis and precision searches for beyond SM physics. Despite phenomenologically it seems likely that alignment will only be realized approximately, rather than exactly, it can be translated in ground studies to interpret scalar signal at 125 GeV results from extended models like 2HDMs. The decoupling limit, where the low-energy spectrum contains only the SM Higgs and no new light scalars, is only a subset of one more general alignment limit [171]. As a first view, we present a study where the exact alignment is achieved for our model.

First, for that the alignment emulates couplings of SM Higgs boson with fermions and gauge bosons is required $\cos(\beta-\alpha) \approx 0$. For the Higgs potential described in (6.1.1), we extrapolate the alignment scenario using the conditions over lighter Higgs boson h^0:

$$m_h^2 = v^2\left(\lambda_1\cos^2\beta + (\lambda_3+\lambda_4)\sin^2\beta\right), \tag{6.3.1a}$$

$$m_h^2 = v^2\left(\lambda_2\sin^2\beta + (\lambda_3+\lambda_4)\cos^2\beta\right). \tag{6.3.1b}$$

If there is a $\tan\beta$ satisfying the above equations, then the alignment limit would occur for arbitrary values of m_{A^0} and does not require non-SM-like scalars to be heavy. In our analyses, we scan out the parameter space in such way that both conditions are satisfied simultaneously:

$$\tan^2\beta = \frac{\lambda_1 - \lambda_3 - \lambda_4}{\lambda_2 - \lambda_3 - \lambda_4}. \tag{6.3.2}$$

In the limit of $\beta \to 0$, both conditions have a natural solution only if $\lambda_1 = \lambda_3 + \lambda_4$. On the other hand, $\tan\beta \to 1$, implies $\lambda_1 = \lambda_2$. With the stationary conditions of Eq.(H.1.14)-(H.1.15) and relations for couplings in terms of Higgs masses (6.2.4), we evaluate the behavior of these alignment cases for $\tan\beta$ in the global minimum discriminant (6.4.6):

- $\tan\beta \to 0$ ($v_2 << v_1$) gives

$$\mathcal{D} \simeq -\left(m_{11}^2 - \kappa^2 m_{22}^2\right)\kappa \tag{6.3.3}$$

  Here, alignment takes place when $\alpha \to \pi/2$ (i.e. $\cos(\beta-\alpha) \simeq 0$). In this regimen and with $\tan^2\beta \to 0$, $\kappa \simeq 0$ and thus $\mathcal{D} \simeq 0$. Higgs potentital couplings perturbativity in this case demands also that $m_{12}^2 << v_1$.

- $\tan\beta = 1$ and $\lambda_1 = \lambda_2$ (alignment) implies

$$\mathcal{D} = 0 \tag{6.3.4}$$

  In particular, the complete alignment arises when $\alpha = -\pi/4$. Independently of $\cos(\beta-\alpha) \simeq 0$ condition for alignment in fermionic and gauge couplings, Eq. (6.3.2) belongs in the boundary separating global minimum regimen of multiple minima presence.

- $\tan\beta >> 1$ ($v_2 >> v_1$)

$$\mathcal{D} \simeq (m_{11}^2 - m_{22}^2)\tan\beta \tag{6.3.5}$$

  Perturbativity of λ_1, λ_2 couplings demands $\kappa \sim O(1)$[3] and $m_{12}^2 << v_2^2$. Complete alignment arises when $\alpha \to 0$ and from equation (6.3.2), alignment also needs to satisfy $\lambda_2 = \lambda_3 + \lambda_4$. With all conditions, discriminant gives $\mathcal{D} \simeq 0$

For these regimes in $\tan\beta$, we show as alignment and perturbativity are suffiency conditions to explain $\mathcal{D} \simeq 0$ scenario.

6.4. Metastability theorems: Particular cases

We briefly discuss the origin of multiple stationary points in the 2HDM by considering tadpoles at tree level equations for the Higgs potential and through of a revision of systematics developed comprehensively in last chapters. We additionally have reviewed this systematic in Appendix H. Firstly, we consider the critical points equations (i.e. non-trivial tadpoles at tree level) for Higgs potential (6.1.1) that give rise to the different stationary points (based on a normal vacuum):

$$T_1 \equiv 2m_{11}^2 v_1 - 2m_{12}^2 v_2 + \lambda_1 v_1^3 + \lambda_4 v_1 v_2^2 + \lambda_3 v_1 v_2^2 = 0. \tag{6.4.1a}$$
$$T_2 \equiv 2m_{22}^2 v_2 - 2m_{12}^2 v_1 + \lambda_2 v_2^3 + \lambda_4 v_1^2 v_2 + \lambda_3 v_1^2 v_2 = 0. \tag{6.4.1b}$$

Notice that one cannot have solutions of the form $\{v_1 = 0, v_2 \neq 0\}$ or $\{v_1 \neq 0, v_2 = 0\}$, unless that $m_{12}^2 = 0$. Those are the natural inert models discussed broadly in the last chapter. A trivial solution of these equations is clearly $v = 0$, equivalent to one theory without EW symmetry breaking. Excluding that case, the stationarity conditions (6.4.1a) and (6.4.1b) become

$$v^2 + \frac{2m_{11}^2 - 2m_{12}^2\tan\beta}{\lambda_1\cos^2\beta + \lambda_4\sin^2\beta + \lambda_3\sin^2\beta} = 0. \tag{6.4.2a}$$
$$\left(2m_{11}^2 - 2m_{12}^2\tan\beta\right)\left(\lambda_2\tan^2\beta + \lambda_4 + \lambda_3\right) - \left(2m_{11}^2 - 2m_{12}^2\cot\beta\right)\left(\lambda_1\cot^2\beta + \lambda_4 + \lambda_3\right)\tan\beta = 0 \tag{6.4.2b}$$

We have also been following discussion and formalism presented in [30]. Equation. (6.4.2a) tells us that, other than its sign, the value of VEV v is given unequivocally by $\tan\beta$ function. Eq. (6.4.2b) is an equation of fifth order on $\tan\beta$,

[3] Indeed, perturbative limits are established to avoid divergences in the renormalization group equations. The reason is that the value of quartic coupling cannot exceed the bound of 4π since beyond this limit the possibility to find out some Landau pole in energy couplings evolution is significantly greater [169].

having at most five possible real solutions. These two equations describe therefore ten possible solutions $\{v_1, v_2\}$, due to the ambiguity on the sign of v; since 2HDM potential in Eq. (6.1.1) is also invariant under the transformation $\Phi_1 \to -\Phi_1$ and $\Phi_2 \to -\Phi_2$. These ten solutions correspond to only four different physical scenarios. Adding the trivial solution $v_1 = v_2 = 0$ (no EW symmetry), we have a total of eleven solutions.

There are at most two different values of $\tan\beta$ which satisfy both equations. This fact means that exist a maximum of six stationary points. Indeed, it could lead more than one normal minimum, with different depths. To establish it formally is necessary to make use of Morse's systematics [30, 193]: For a given real function of two variables, let η_0, η_1 and η_2 be the number of its minima, saddle points, and maximums inside in the Higgs potential, respectively. For a polynomial function in v_1 and v_2, bounded from below, such as the one we are dealing with, Morse's inequalities state that:

- $\eta_0 \geq 1$.
- $\eta_1 \geq \eta_0 - 1$.
- $\eta_0 - \eta_1 + \eta_2 = 1$.

The foundations of Morse's inequalities give bounds over critical points, in particular over minima behavior in the Higgs potential and its influence in stationary conditions and mass matrices. The 2HDM potential in Eq (6.1.1) has $\eta_0 + \eta_1 + \eta_2 = 2n + 1$ stationary solutions, $n = 0, ..., 5$: at most $2n$ real roots of eqs. (H.1.18), (H.1.19) plus the trivial solution $v_1 = v_2 = 0$ (No EW symmetry breaking). We can use Morse's inequalities to get $\eta_0 + \eta_2 = n + 1$. We analyze several possibilities for the number of minima η_0, depending on the number of real solutions n. By counting extremal cases, all the different combinations of stationary points leads to find the following general aspects: There are critical points without symmetry breaking associated to every case of maximums, minima or saddle points combinations. Thus, typical situations of SSB with a global minimum are given for $1 \leq n \leq 2$. Meanwhile, for $n = 3$ and using Morse's inequalities: $\eta_0 + \eta_2 = 4$ yields a SSB scenario plus a trivial minimum located at the origin. The $n = 4$ case translates in two pairs of degenerate minima away from the origin. It is not mandatory that these two pairs of minima to have the same depth. Therefore as first glance, we might have one normal minimum deeper than another. Finally, the higher order in n solutions yields trivial plus global and non-global minima.

Hence if there are more than two solutions for v_2/v_1 ratio, which said the 2HDM might have more than one normal minimum away from the origin with different depths. However, no more than two of such minima can exist by physical grounds (for a non-long-lived enough minimum state). The analysis of non-global minimum structures must be seen as potential exclusion regions in the parameter spaces for these particular cases of 2HDM.

From the form of critical points and Morse's inequalities, we can see as multiple non-degenerate minima can be present in the Higgs potential. It is worthwhile now to analyze where can be ensured the existence of one and only one global minimum. For this purpose, we restrict the following phenomenological study to avoid two minima with different depths. Taking the case of four real solutions, in [25, 27] have shown that the difference in the values of the potential in those two normal vacuum structures N_1 and N_2 is given by

$$V_{N_2} - V_{N_1} = \frac{1}{4}\left[\left(\frac{m_{H^\pm}^2}{v^2}\right)_{N_1} - \left(\frac{m_{H^\pm}^2}{w^2}\right)_{N_2}\right](v_1 w_2 - v_2 w_1)^2 . \tag{6.4.3}$$

with $v^2 = v_1^2 + v_2^2$ in N_1 and $w^2 = w_1^2 + w_2^2$ in N_2. N_2 structure can be seen interchanging $v_i \to w_i$ in the VEVs for respective doublets of (6.2.3). Nothing establishes how to carry out the computations to determine which is the overall sign in the difference. Another aspect of this result is that starting with the same Higgs potential, the demonstration depends on only of vacuum structure in both minima. The following discriminant, written regarding tensor matrix of the Higgs potential (6.1.2), ensures the existence of one and only one global minimum in the theory [29][4]

$$\mathcal{D} \equiv -\det(\Lambda_E - \zeta I). \tag{6.4.4}$$

ζ is an auxiliary function introduced in the Higgs potential to determine stationary conditions. This Lagrange multipliers is related with $\sum_{i=1}^{2} \Phi_i^\dagger \Phi_i \geq 0$ constraint. Λ_E is $\Lambda_{\mu\nu}$ of Higgs potential (6.1.2) expressed by an Euclidean-metric and I is the four dimensional identity matrix. In the diagonal basis ($\Lambda_E \to \text{diag}(\Lambda_0, \Lambda_1, \Lambda_2, \Lambda_3)$), the global minimum discriminant reads

[4] $\mathcal{D}$-discriminant, encouraging a global minimum in the Higgs potential, has been computed for 2HDMs from Hessian of the Higgs potential in the gauge orbit field using the reparameterization group $SO(1,3)$, as is shown in Appendix I.

$$\mathcal{D} \equiv (\Lambda_0 - \zeta)(\zeta - \Lambda_1)(\zeta - \Lambda_2)(\zeta - \Lambda_3). \tag{6.4.5}$$

Concerning the parameters inside of the Higgs potential with a softly breaking of $U(1)$-symmetry (6.1.1).

$$\mathcal{D} = \left(m_{11}^2 - \kappa^2 m_{22}^2\right)(\tan\beta - \kappa) > 0. \tag{6.4.6}$$

with $\kappa = (\lambda_1/\lambda_2)^{1/4}$. By the implications of stationary conditions (H.1.14) and (H.1.15), we exclude $\beta = 0$ and $\beta = \pi/2$ values in the parameter space. Only we approach to them by means of their limit values, which bring out to some couplings in non-perturbative regions. In terms of scalar masses this discriminant takes the form is

$$\mathcal{D} = \left[1 - \frac{m_{A^0}^2}{m_{h^0}^2 m_{H^0}^2}\left(m_{H^0}^2\cos^2(\alpha+\beta) + m_h^2\sin^2(\alpha+\beta)\right)\right]\frac{m_{A^0}^2 m_{h^0}^2 m_{H^0}^2}{4v^8\cos^2\beta\sin^2\beta}.. \tag{6.4.7}$$

Regarding splitting parameter k_S, this condition can be translated into

$$k_S < \frac{1}{\left(\frac{m_{H^0}^2}{m_{h^0}^2}\left(1 - \sin^2(\beta+\alpha)\right) + \sin^2(\beta+\alpha)\right)}. \tag{6.4.8}$$

This bound has been evaluated in the plane $m_{H^0} - \sin(\beta+\alpha)$ as is depicted in Fig. (6.1). For our purposes, both structures for metastability discriminant are useful in determining regions of parameter space compatible with vacuum stability. The second one give us direct information about scalar mass, while the former give us information about Higgs mass splittings. $\mathcal{D} > 0$ ensure a global minimum in the theory. If $\mathcal{D} < 0$, additional computations are necessary to discriminate between both vacuum structures.

6.5. Phenomenological aspects of theories with softly breaking of $U(1)$

The 2HDM model with Abelian global symmetries has been used as a ground basis to explain CP violation phases in strong interactions employing Peccei Quinn mechanism [194, 195]. When the global symmetry is spontaneously broken, the new scalar spectrum should contain an axion with zero mass, which is not wanted by theoretical facts [64, 66]. If a massless (o with a mass of small size) scalar particle exist its detection and precision measurements are a real challenge; the phenomenological compatibility to explain strong CP phases is not accurate yet so far [65]. Furthermore, topological defects as vortices are generated in this regime when the global symmetry has been broken. To avoid those issues and to improve experimental level of accuracy of the Peccei-Quinn models, a dimension two term of $U(1)$ symmetry violation, is introduced in the Higgs potential. This term has a small impact on the evolution of Renormalization Group Equations[5] computations about stability and metastability: It also yields a non-zero mass term for pseudoscalar particle A^0 (see Eq. 6.2.4e).

It is worth to say that the presence of dimension two-term as well as the stationary conditions exclude the possibility of an inert vacuum in some doublet. Hence inert cases are just accomplished in an approximate way for fractions of $v_2/v_1 \to 0$ (quasi-inert regimen); having many phenomenological consequences in dark matter searches [118, 173] and for the description of viable mass terms for neutrinos [68, 130].

As was pointed out above, an outstanding aspect of general 2HDM is the presence of metastable states with two normal vacuum structures; what is a consequence of the solutions of stationary conditions combinations of Eqs. (H.1.18)-(H.1.19). The simplest case is such where a soft term appears in the Higgs potential invariant under a continuous global symmetry. Nevertheless, 2HDM nature restricts facts as the coexistence of minima of different depths and different origins (CP breaking and charge breaking -CB- vacuum structures) [25]. Besides, whenever a normal minimum exists in the 2HDM, the global minimum of the potential is a normal one, and no tunneling to a deeper CB or CP minimum is allowed [67]. On the other hand, if a CP (CB) violating minimum exist in the 2HDM, it is the global minimum of the theory, and so stable, and no tunneling to a deeper normal or CB (CP) minimum can occur [19]. Hereafter, we are only focused on normal behavior of EW vacuum and its phenomenological consequences.

[5] In the softly broken $U(1)$-model, $\bar{m}_{12}^2$ has the following RGE

$$16\pi^2\frac{d}{d\log\mu^2}\bar{m}_{12}^2 = (2\lambda_3 + \lambda_4)\,\bar{m}_{12}^2.$$

It is possible to see as radiative corrections to m_{12}^2 are proportional to m_{12}^2 itself and are only logarithmically sensitive to the cutoff μ.

With this phenomenological approach, our primary goal is to compute the regions where the metastability due to two normal vacua in EW scale arise; determining allowed scenarios in experimental data (e.g. diphotonic decays for SM like-Higgs) and thus improving vacuum analysis carried out at NLO level.

6.6. Global minimum behavior in $m_{H^0} - \sin(\alpha+\beta)$ plane

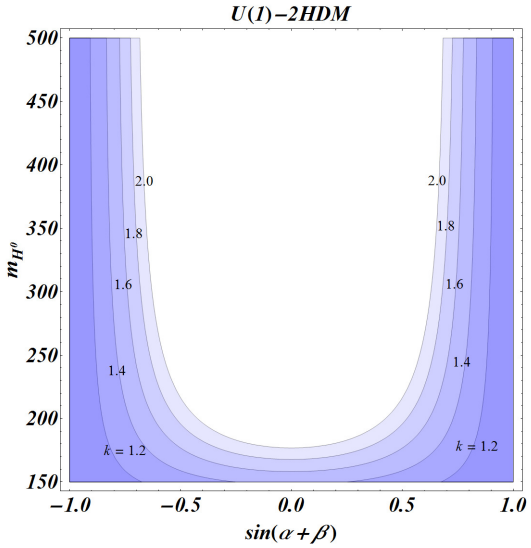

Figure 6.1.: *Metastability behavior for $m_{H^0} - \sin(\alpha+\beta)$ plane represented by shadowed zones. Each scenario is characterized by ratio $k_S = m^2_{A^0}/m^2_{H^0}$.*

Considering Eq. (6.4.7) is possible to establish the zones where absolute stability could be in conflict with the presence of a second minimum. Ratio between Higgs eigenstates $k = m^2_{A^0}/m^2_{H^0}$ has been used to compare different regions in the plane $m_{H^0} - \sin(\alpha+\beta)$, as is despited in Fig. (6.1)

More generally and to avoid multiple minima at tree level, the lower limit on m_{H^0} becomes weaker as $\sin(\alpha+\beta) \to 0$. Moreover, metastable states appear in a wide zone of $m_{H^0} - \sin(\beta+\alpha)$ when $k_s > 1$ increases. In addition when $k_s < 1$, the parameter space does not show exclusion zones. Finally, metastable states dominate all values of m_{H^0} when $|\sin(\beta+\alpha)| = 1$.

6.7. Exclusion regions by stability and metastability analyses: $0 \leq \alpha \leq \pi/2$

Discrimination of exclusion zones from metastability in particular regions of parameter space is relevant to estimate vacuum behavior for the theory at NLO. Typical constraints found out involve many parameters of the Higgs potential. Thus, to extract phenomenological information, we analyze particular models. To that end, we have listed in Tab. 6.1 some limiting models for specific values of α and β angles by using expressions of Higgs eigenstates given in section (6.2).

Particularly, alignment regime for couplings ($\cos(\beta-\alpha) \to 0$) is present in A_{III} and C_I models. For model A_{III}, condition (6.3.2) implies besides $\lambda_1 = \lambda_3 + \lambda_4$. Finally, fulfillment of alignment regime in model C_I is achieved when $\lambda_2 = \lambda_3 + \lambda_4$. Other models taking into account h^0 with the mass of 125 GeV, but they do not emulate the same Higgs couplings as in the SM case.

Figure 6.2 shows a set of contours to see metastability states in the parameter space and for particular cases depicted in Tab. 6.1. With this in mind, the plane $\Delta S_1^2 - \Delta S_2^2$ is the first candidate to observe exclusion zones using discriminant 6.4.6. By a counting of parameters, metastability zones end up into depending on mixing angles α, β, quartic couplings λ_1 and λ_2, and from m_{h^0} values. Given this context, we fixed the mass value for a lighter Higgs in 125 GeV, appealing to a searching of a complete alignment scenario for 2HDM. Here the lighter Higgs is identified with the SM Higgs boson and the remaining scalars could be set at any energy scale, even in the EW regime. Having this exclusion analysis, we proceed to evaluate the RGE's evolution to describe initial conditions influence in the global solution in the face of vacuum behavior. Here the contours are interpreted from the minimum values obtained from the discriminant in such a way that the presence of another minimum has been identified as a possible appearance of metastable states.

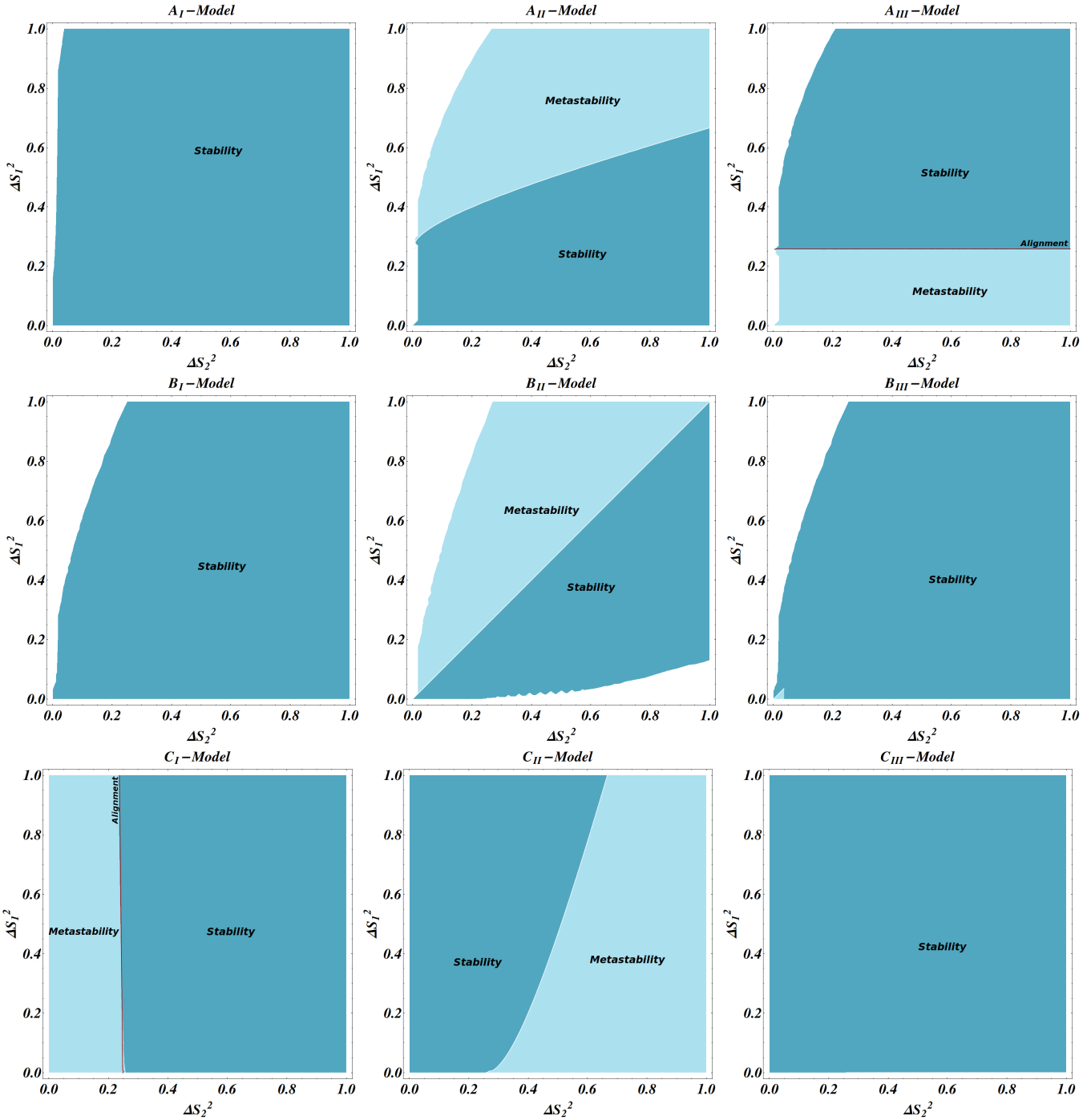

Figure 6.2.: *Metastability and absolute stability region in $\Delta S_1^2 - \Delta S_2^2$ plane for A_i, B_i and C_i models with $i = I, II, III$ described in Table 6.1. Red lines in A_{III} and C_I models give information about as alignment regime behaves in those parameter spaces where $\cos(\beta - \alpha) \approx 0$. Zones with $\mathcal{D} < 0$ (Light-Blue) where the chance of finding two non-degenerate minima pairs is greater, will be labeled as "metastable" ones.*

Model	$\tan\beta$	α	$\Delta S_1^2 v^2$	$\Delta S_2^2 v^2$	$\Delta S_3^2 v^2$
A_I	10^{-3}	0	$m^2_{H^0}$	$\xi_0\left(m^2_{h^0} - m^2_{A^0}\right)$	$2m^2_{H^\pm} - m^2_{A^0}$
A_{II}	10^{-3}	$\to \pi/4$	$\frac{1}{2}\left(m^2_{H^0} + m^2_{h^0}\right)$	$\frac{\xi_0}{2}\left(m^2_{H^0} + m^2_{h^0} - 2m^2_{A^0}\right)$	$2m^2_{H^\pm} + m^2_{H^0} - m^2_{A^0} - m^2_{h^0}$
A_{III}	10^{-3}	$\pi/2$	$m^2_{h^0}$	$\xi_0\left(m^2_{H^0} - m^2_{A^0}\right)$	$2m^2_{H^\pm} - m^2_{A^0}$
B_I	1	0	$\left(2m^2_{H^0} - m^2_{A^0}\right)$	$\left(2m^2_{h^0} - m^2_{A^0}\right)$	$2m^2_{H^\pm} - m^2_{A^0}$
B_{II}	1	$\to \pi/4$	$\left(m^2_{H^0} + m^2_{h^0} - m^2_{A^0}\right)$	$\frac{1}{2}\left(m^2_{H^0} + m^2_{h^0} - m^2_{A^0}\right)$	$2m^2_{H^\pm} + m^2_{H^0} - m^2_{A^0} - m^2_{h^0}$
B_{III}	1	$\pi/2$	$\left(2m^2_{h^0} - m^2_{A^0}\right)$	$\left(2m^2_{H^0} - m^2_{A^0}\right)$	$2m^2_{H^\pm} - m^2_{A^0}$
C_I	10^2	0	$\simeq \xi_1(m^2_{H^0} - m^2_{A^0})$	$\simeq m^2_{h^0}$	$2m^2_{H^\pm} - m^2_{A^0}$
C_{II}	10^2	$\to \pi/4$	$\simeq \frac{\xi_1}{2}\left(m^2_{H^0} + m^2_{h^0} - 2m^2_{A^0}\right)$	$\simeq \frac{1}{2}\left(m^2_{H^0} + m^2_{h^0}\right)$	$2m^2_{H^\pm} + m^2_{H^0} - m^2_{A^0} - m^2_{h^0}$
C_{III}	10^2	$\pi/2$	$\simeq \xi_1\left(m^2_{h^0} - m^2_{A^0}\right)$	$\simeq m^2_{H^0}$	$2m^2_{H^\pm} - m^2_{A^0}$

Table 6.1.: *Splittings among Higgs mass eigenstates for different models, which are varying mixing angles α and β ($\tan\beta$); being $\lambda_4 = 2\left(m^2_{A^0} - m^2_{H^\pm}\right)/v^2 \equiv \Delta S_4^2$ independent of those parameters. ξ_0 and ξ_1 are related to values of $\cot\beta$ and $\tan\beta$ respectively. Moreover, they are introduced to conserve perturbative behavior of λ's couplings, i.e., $\lambda_i \sim O(1)$. From stability conditions of $\lambda_1 > 0$ and $\lambda_2 > 0$, it is also possible to infer a set of features of each model.*

Metastability and absolute stability region in $\Delta S_1^2 - \Delta S_2^2$ plane for A_i, B_i and C_i models with $i = I, II, III$ described in Table 6.1. Red lines in A_{III} and C_I models give information about as alignment regime behaves in those parameter spaces where $\cos(\beta - \alpha) \approx 0$.

- A_I model. Metastable states are suppressed in the plane $\Delta S_1^2 - \Delta S_2^2$. Model has only instabilities for the effective Higgs potential. To maintain perturbativity in the scenario with $m_{A^0} \sim m_{h^0}$ (Φ_2-direction) and to avoid minima with charge violation, scalar spectrum behaves as $m_{h^0,A^0} < m_{H^0}$ and $m_{A^0} < m_{H^\pm}$. This scenario embodies a non-alignment case, where H^0 saturates couplings with SM bosons and fermions.

- A_{II} model (limit case). Stable zones dominate over broad regions in the respective plane. Metastable zones start to appear in values of $\Delta S_1^2 > 0.258$ and ΔS_2^2 approaching to zero. Non-perturbative zones are excluded when $2m_{A^2} \sim m^2_{H^0} + m^2_{h^0}$, which is not compatible with stable zones at tree level (presence of one global minimum in the EW theory).

- A_{III} model. Metastable zones dominate both directions $\Phi_1 - \Phi_2$. In the limit, a small stable zone is located $\Delta S_1^2 > 0.258$. The lower bound corresponds to the observed Higgs mass of $m_{h^0} \approx 125$ GeV and that has been identified with parameters associated with h^0. This choice is the alignment regimen defining a boundary between stable and metastable scenarios. Non-perturbativity zones are present unless $m_{H^0} \sim m_{A^0}$. This limit model emulates important features of a $U(1)$-Inert 2HDM, like the hierarchy in the scalar spectrum: $m_{H^\pm} > m_{A^0,H^0}$. As well as in the inert model and since fulfillment of an alignment regime, H_0 and A_0 would behave as likely dark matter candidates. It is worthwhile to describe that all these Abelian models with softly breaking terms can not be reduced down at all to an inert 2HDMs since stationary-conditions (H.1.14) do not satisfy the choice of $v_2 = 0$ simultaneously.

- B_I model. Metastability is absent in the plane $\Delta S_1^2 - \Delta S_2^2$ for zones compatible with SSB. In addition, and in the same space parameter, vacuum stability at tree level imposes $2m^2_{H^0} > m^2_{A^0}$ and $2m^2_{h^0} > m^2_{A^0}$. Thus $A^0 \to h^0 h^0$ and $A^0 \to H^0 H^0$ decays are suppressed.

- B_{II} model. Metastability appears in this parameter space significantly, with a scenario where $\Delta S_1^2 > \Delta S_2^2$. From vacuum stability conditions, it is inferred that $m^2_{H^0} + m^2_{h^0} > m^2_{A^0}$. Non alignment scenario is present since $\cos(\beta - \alpha) \simeq 1$, thus H^0 impersonates to couplings SM Higgs with fermions and gauge bosons.

- B_{III} model. Stability through just one global minimum is ensured in almost all parameter space. Tiny zones of non-stability are encoded for values of $\lambda_1 \to 0$. Here the scalar spectrum inherits an analog behavior for that obtained in the B_I model, i.e., $2m^2_{H^0} > m^2_{A^0}$ and $2m^2_{h^0} > m^2_{A^0}$. The hierarchy structure for scalars spectrum saves a similar pattern that in the B_I model.

- Model C_I: One stable global minimum broadly dominates parameter space. Presence of one and only global minimum is ensured for $\Delta S_1^2 \geq 0.258$. By providing perturbativity in the scalar sector, spectrum should satisfy

Model	$\tan\beta$	α	$\Delta S_1^2 v^2$	$\Delta S_2^2 v^2$	$\Delta S_3^2 v^2$
D_I	10^{-3}	$\to -\pi/4$	$\frac{1}{2}\left(m_{H^0}^2 + m_{h^0}^2\right)$	$\frac{\xi_1}{2}\left(m_{H^0}^2 + m_{h^0}^2 - 2m_{A^0}^2\right)$	$2m_{H^\pm}^2 + m_{h^0}^2 - m_{A^0}^2 - m_{H^0}^2$
D_{II}	10^{-3}	$\to -\pi/2$	$m_{h^0}^2$	$\xi_1\left(m_{H^0}^2 - m_{A^0}^2\right)$	$2m_{H^\pm}^2 - m_{A^0}^2$
E_I	1	$\to -\pi/4$	$\frac{1}{2}\left(m_{H^0}^2 + m_{h^0}^2 - m_{A^0}^2\right)$	$\frac{1}{2}\left(m_{H^0}^2 + m_{h^0}^2 - m_{A^0}^2\right)$	$2m_{H^\pm}^2 + m_{h^0}^2 - m_{A^0}^2 - m_{H^0}^2$
E_{II}	1	$\to -\pi/2$	$\left(2m_{h^0}^2 - m_{A^0}^2\right)$	$\left(2m_{H^0}^2 - m_{A^0}^2\right)$	$2m_{H^\pm}^2 - m_{A^0}^2$
F_I	10^2	$\to -\pi/4$	$\simeq \frac{\xi_0}{2}\left(m_{H^0}^2 + m_{h^0}^2 - 2m_{A^0}^2\right)$	$\simeq \frac{1}{2v^2}\left(m_{H^0}^2 + m_{h^0}^2\right)$	$2m_{H^\pm}^2 + m_{h^0}^2 - m_{A^0}^2 - m_{H^0}^2$
F_{II}	10^2	$\to -\pi/2$	$\simeq \xi_0\left(m_{h^0}^2 - m_{A^0}^2\right)$	$\simeq m_{H^0}^2$	$2m_{H^\pm}^2 - m_{A^0}^2$

Table 6.2.: *Splittings among Higgs mass eigenstates for different models, which are varying mixing angles α and β ($\tan\beta$); being $\lambda_4 = 2\left(m_{A^0}^2 - m_{H^\pm}^2\right)/v^2 \equiv \Delta S_4^2$ independent of those parameters. ξ_0 and ξ_1 are related to values of $\cot\beta$ and $\tan\beta$ respectively. Moreover, they are introduced to conserve perturbative behavior of λ's couplings, i.e., $\lambda_i \sim O(1)$. From stability conditions of $\lambda_1 > 0$ and $\lambda_2 > 0$, it is possible to infer a set of features of each model.*

$m_{H^0} \sim m_{A^0}$; being both scalars plausible dark matter candidates. Once again, this model can emulate a pseudo-inert scenario with $v_1 = 0$. It also contains an alignment scenario delimiting the boundary between stable and possible metastable states.

- Model C_{II}: Metastable zones are present in values starting in $\Delta S_2^2 \approx 0.258$ for small values of ΔS_1^2, but other metastable zones are also present in lower values of ΔS_1^2. Together with avoiding non perturbative scenarios, structure of mass eigenstates implies $m_{h^0}^2 + m_{H^0}^2 \sim 2m_{A^0}^2$.

- Model C_{III}: Large areas of stability are present in this particular parameter space. Non-perturbative scenarios appear unless that $m_{h^0} \sim m_{A^0}$, with a small splitting preferring $m_{A^0}^2 - m_{h^0}^2 < 0$. Here H^0 can be identified with possible values taken by λ_2. In comparison to cases A_{III}, B_{II} and C_I, C_{III} model ensures a non-alignment regime where couplings to SM bosons and fermions are dominated by H^0, meanwhile h^0 is approximately decoupled of them. Perhaps, this model has many strong constraints from the phenomenological point of view [171].

And from construction of mass eigenstates, there is another relevant phenomenological zone where $-\pi/2 < \alpha < 0$, with limit values of $\alpha \to -\pi/2$ and $\alpha \to -\pi/4$.

There are two alignment regimes given by the D_{II} and E_I models. From Fig. 6.3 and mass eigenstates behavior described in Table 6.2, we can extract the following features:

- D_I-model: Despite this choice contains a metastable zone for lower values of $\Delta S_1^2 < 0.258$, global-minimum presence dominates this parameter space. The most stringent bound from metastable behavior is also in lower values of ΔS_2^2. Moreover by perturbativity $m_{h^0}^2 + m_{H^0}^2 \sim 2m_{A^0}^2$; being slightly greater the sum of CP even states.

- D_{II}-model: A metastable zone is set in $\Delta S_1^2 \geq 0.258$. By virtue of identification of h^0 with SM Higgs, alignment regime is developed over this value separating global minima and metastability behavior. In addition $m_{H^0} \sim m_{A^0}$ condition coming from perturbativity request. In this model $A^0 \to H^0 H^0$ decays are forbidden.

- E_I model: A broad zone of metastability is present for $\Delta S_2^2 \geq \Delta S_1^2$, developing an alignment regime in the limit where both parameters are equal. Hence alignment scenario defines a boundary between a theory with a global minimum and one model with more of two minima. By the form of the couplings, alignment seems to be the best limit in the parameter space. Stability in the Φ_1 and Φ_2 directions leads to $m_H^0 + m_{h^0} > m_{A^0}$.

- E_{II}-model: Parameter space compatible with SSB does not contain metastable states for any combination of couplings. In this scenario $2m_{h^0}^2 > m_{A^0}^2$ and $2m_{H^0}^2 > m_{A^0}^2$; avoiding $A^0 \to h^0 h^0$ and $A^0 \to H^0 H^0$ decays. Thus $m_{A^0} < 176$ GeV. This model shares some features of metastability and phenomenology with the B_I and B_{III}-models.

- F_I-model: Metastability zones are developed in lower values of $\Delta S_2^2 < 0.258$ extending roughly in all values of ΔS_1^2. In this parameter space, perturbativity demands $m_{H^0}^2 + m_{h^0}^2 \sim 2m_{A^0}^2$.

- F_{II}-model: Stable zones are in almost all parameter space. This a scenario of non-alignment since H^0 emulates the couplings among SM-Higgs with fermions and bosons. To avoid non-perturbative scenarios for quartic couplings, h^0 and A^0 should be almost degenerate in mass.

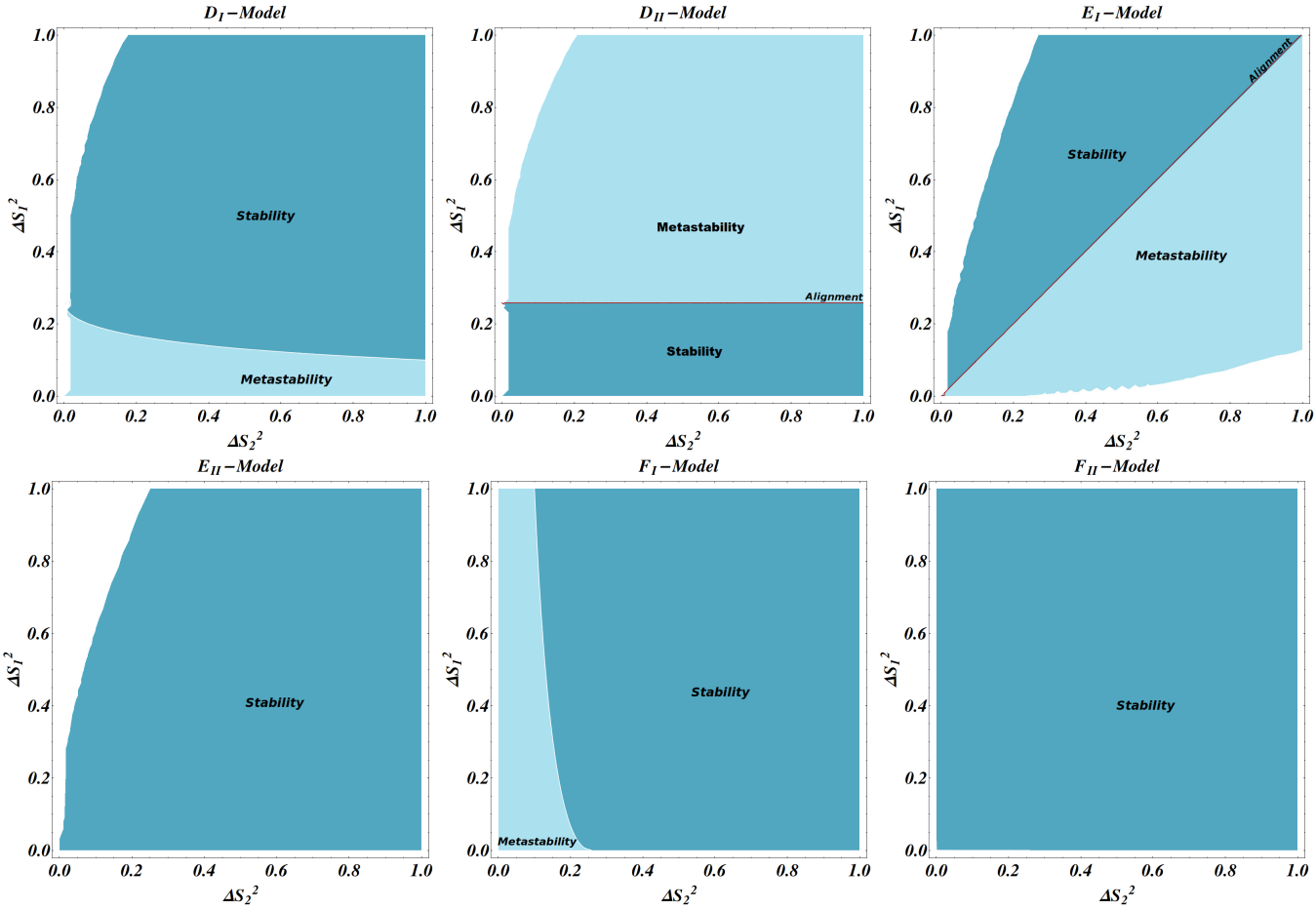

Figure 6.3.: *Metastability and absolute stability region in* $\Delta S_1^2 - \Delta S_2^2$ *plane for* D_i, E_i *and* F_i *models with* $i = I, II$ *described in Table 6.2. Red lines in* D_{II} *and* E_I *models give information about as alignment regime behaves in those parameter spaces where* $\cos(\beta - \alpha) \approx 0$.

Finally, we note the strong dependence and sensitivity of a unique global solution with the $\tan\beta$ when $\beta \to 0$ and $\pi/2$. Therefore, in these zones and models, a more carefully analysis must be done to describe the real behavior of metastable states and global minimum.

6.8. One loop analysis for quartic couplings for $B-E$ and $C-F$ like models

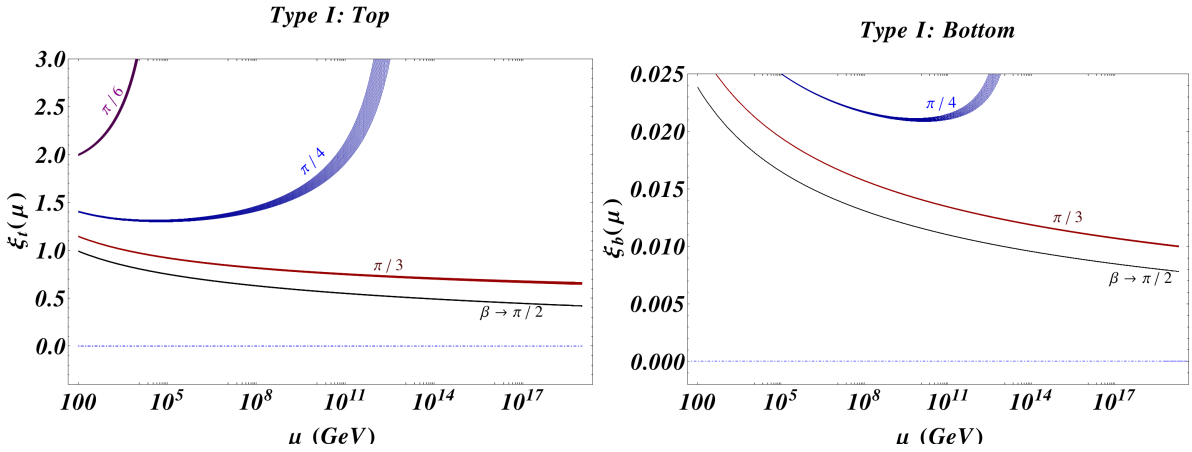

Figure 6.4.: *Top and bottom Yukawa couplings evolution are varying mixing angle β in the initial condition 3.5.4a. Width in each evolution is due to top mass (pole) uncertainty $m_t = (173.34 \pm 0.76)$ GeV [174]. As was explained in Chapter 3, at one loop level RGEs for Yukawa couplings, are independent of scalar couplings. These plots are extrapolations of the already obtained ones in section 3.5.*

From the possible presence of two non-degenerate minima in the Higgs potential at tree level, it is feasible to extract the following consequences. Firstly, metastable states are strongly dependent on α and β angles, and secondly, the alignment regime, where it is reliable, is the boundary between absolute-stable zones and metastable zones. By the form of Yukawa couplings evolution *A-D* models could be ruled highly constrained from vacuum stability analyses. Non-perturbative zones exclude models with $\tan\beta < 1$ since compatible areas with stability are highly reduced[6]. This argument comes from top-Yukawa couplings given in Fig. 6.4 evolution and structure of stability contours in *B-E* models shown in Fig. 6.5, which are inconsistent with perturbative unitarity in the $\lambda_1 - \lambda_2$ plane.

One relevant scenario is presented when $\tan\beta \to 1$ and $\alpha \to \pi/4, -\pi/4$, where the improvement under metastability forbids every zone allowed by stability at one loop level; being restricted by perturbativity and unitarity analyses as well. In addition, when $\alpha = \pi/4$ (non-alignment) this zone is also forbidden by divergent solutions for metastability discriminant (6.4.6). Alignment scenario is present when $\alpha \to \pi/4$, where metastability does not allow zones where $\Delta S_1^2 < \Delta S_2^2$. Despite perturbative unitarity is consistent with stable zones at 10^{11} GeV in $\Delta S_4^2 - \Delta S_3^2$, at 10^3 GeV unitarity exclude all possible stable zones in the $\Phi_1 - \Phi_2$ plane.

At one loop level, instabilities in the 2HDM type I in *C-E* models are present among in intermediate energies and GUT and Planck scales. Hence we focused on $10^3 \leq \mu(\text{ GeV }) \leq 10^{19}$ scenario. By crossing stability and metastability analyses, it is possible to find out stronger exclusion regions. This procedure can be seen as an improvement of stability analysis to eliminate the possibility of having two minima in the EW scale.

On the other hand, *C-F* models are broadly compatible with perturbative unitarity and vacuum stability analysis. For instance in the plane $\Delta S_1^2 - \Delta S_2^2$, stable zones shown in Fig. 6.6 are also consistent with unitarity analysis for lower values of ΔS_1^2. In the Φ_1 direction, values beyond 0.4 are non-perturbative. This zone is compatible with alignment regime given by the C_I model. In the $\Delta S_4^2 - \Delta S_3^2$ exist zones compatible with stability and perturbative unitarity for considered energy scales. However they are broadly suppressed and have set in $\Delta S_3^2 > 0$ and $-0.35 < \Delta S_4^2 < -0.1$; which can enter in conflict with *ST* oblique parameters [170]. By ΔS_3^2 results, a new hierarchical structure appears in mass eigenstates for F_I and C_{II} models: $2m_{H^\pm}^2 > m_{A^0}^2 + m_{H^0}^2 - m_{h^0}^2$. Stability analyses in the λ_3 coupling for F_{II} and C_{II} models are also consistent with hypothesis avoiding charge breaking minima i.e. $m_{A^0} < m_{H^\pm}$.

One reference point to study is the limit of a quasi-inert case, where one vacuum expectation value emulates the unique VEV of SM vacuum, and the remaining one is equal to zero. This case is recovered when $\tan\beta >> 1$ and

[6]Explicit RGEs can be obtained from those presented in Appendix J by taking the limit of $\lambda_5 \to 0$

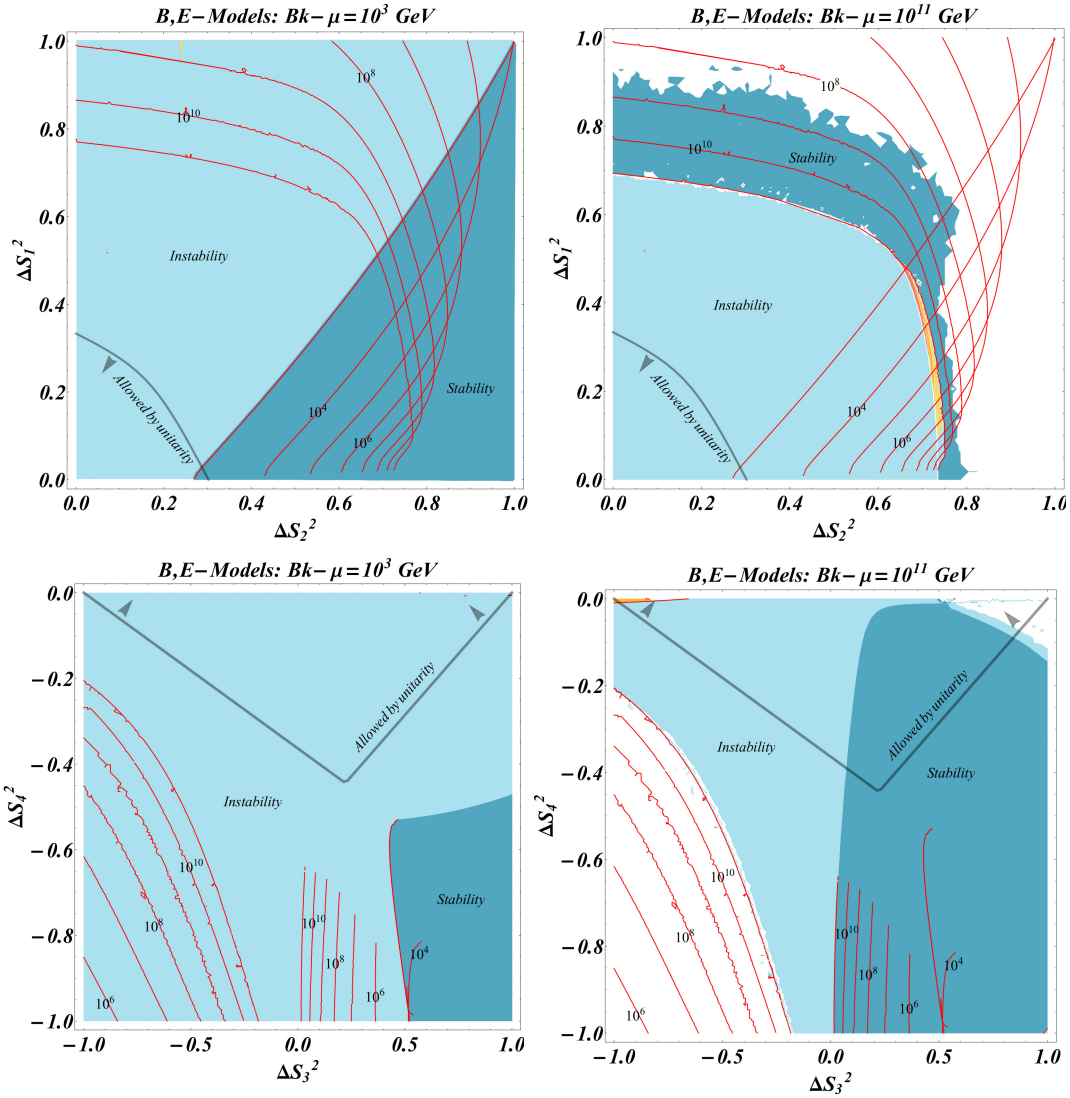

Figure 6.5.: *(**Up**) Phase diagrams with the evolution of contours from $\mu = 10^3$ GeV (**Background-Left**) up to $\mu = 10^{11}$ GeV (**Background-Right**) in the ΔS_1^2-ΔS_2^2 plane for B-models. Here $-0.25 \leq \lambda_{3,4}(m_Z) \leq 0$ and starting with $\lambda_{3,4}(m_Z) = -\lambda_2(m_Z)/2$. Red lines are the remaining contours between $\mu = 10^3$ and 10^{11} GeV. (**Down**) Phase diagrams with the evolution of contours from $\mu = 10^3$ GeV (**Background-Left**) up to $\mu = 10^{11}$ GeV (**Background-Right**) in the ΔS_4^2-ΔS_3^2 plane for B-models. Here $0 \leq \lambda_{1,2}(m_Z) \leq 0.25$ and starting with $\lambda_{1,2}(m_Z) = \lambda_3(m_Z)$. Red lines are the remaining contours between $\mu = 10^3$ and 10^{11} GeV. Higher values of μ are incompatible with perturbativity and RGEs convergence. We have taking into account quark top mass in the pole for Yukawa evolution.*

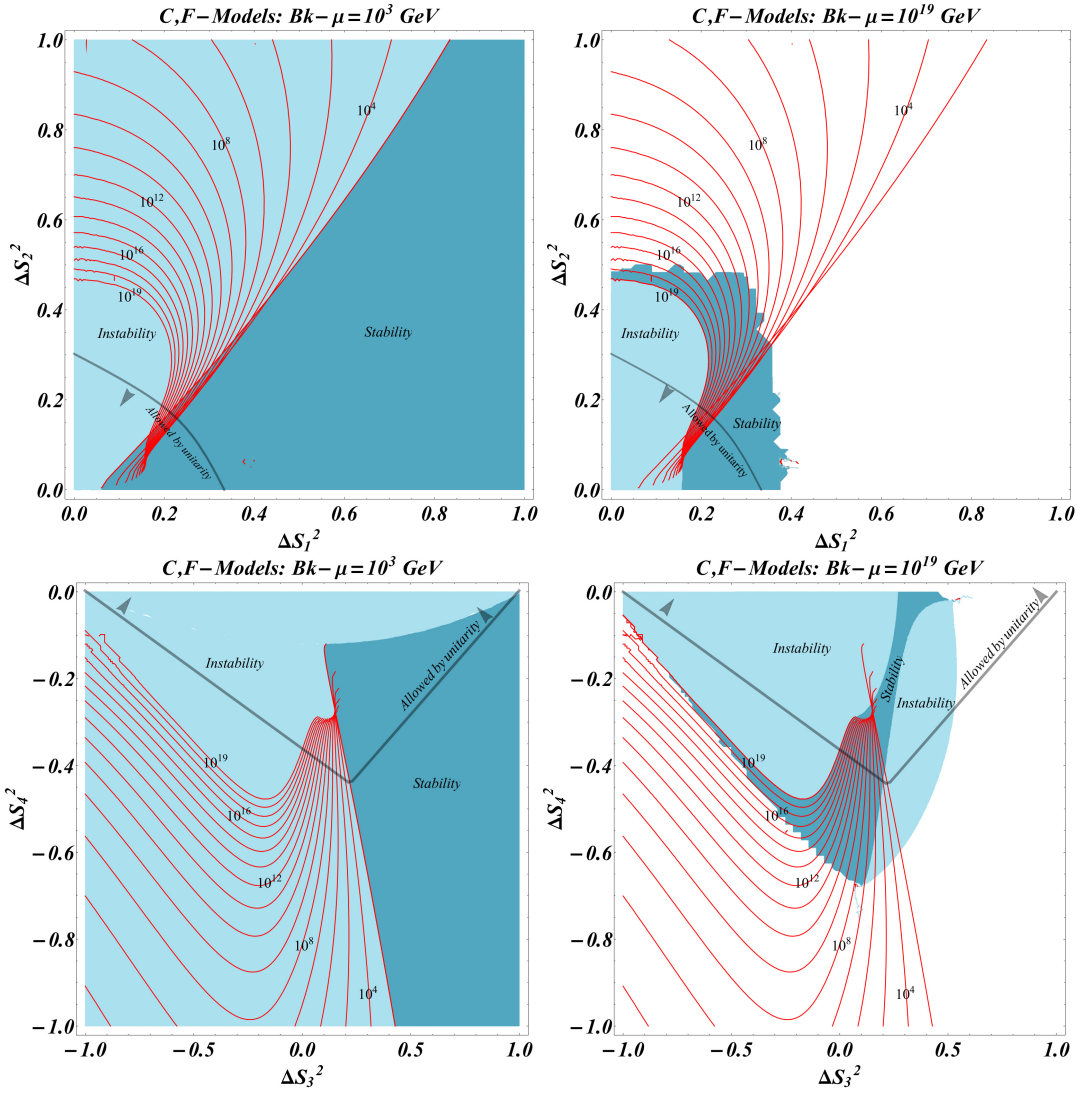

Figure 6.6.: *(**Up**) Phase diagrams with the evolution of contours from $\mu = 10^3$ GeV (**Background-Left**) up to $\mu = 10^{19}$ GeV (**Background-Right**) in the ΔS_1^2-ΔS_2^2 plane for C-models. Here $-0.25 \leq \lambda_{3,4}(m_Z) \leq 0$ and starting with $\lambda_{3,4}(m_Z) = -\lambda_2(m_Z)/2$. Red lines are the remaining contours between $\mu = 10^3$ and 10^{19} GeV. (**Down**) Phase diagrams with the evolution of contours from $\mu = 10^3$ GeV (**Background-Left**) up to $\mu = 10^{19}$ GeV (**Background-Right**) in the ΔS_4^2-ΔS_3^2 plane for C-models. Here $0 \leq \lambda_{1,2}(m_Z) \leq 0.25$ and starting with $\lambda_{1,2}(m_Z) = \lambda_3(m_Z)$. Red lines are the remaining contours between $\mu = 10^3$ and 10^{19} GeV.*

$\alpha \to 0$; identifying highly compatibility from metastability at tree level. It is worthwhile to say that this scenario is perturbatively reliable, and RGEs can be solved if and only if there is a degeneracy between H^0 and A^0. This quasi-inert limit can easily be identified with the scalar sector for neutrino-specific 2HDMs considered broadly in [68,130]; which are motivated to introduce naturally neutrino masses if one VEV acquires a small enough value in the scale of eV compatible with cosmological and experimental constraints.

6.9. Phenomenological aspects in the alignment regime

We analyze phenomenological compatibility in the alignment regimen with the likelihood proof for two photons decay and the oblique parameters realization in the ST plane. In the former case, contours built from `Lilith` in Fig. 6.7 operates with the method: From definitions of effective coupling C_γ among two photons and one Higgs h^0 at LO given in appendix M, likewise of $-2\log(C_\gamma)$ relation, we scan the 2-dimensional parameter space in the $m_{H^\pm} - m_{A^0}$ plane fixing $\beta \to 0, \pi/4, \pi/2$ in contours. We study particularly an alignment scenario where $\cos(\beta-\alpha) \approx 0$ (A_{III}, C_I, D_{II} and E_I models). In addition for E_I model, in each contour of Fig. 6.9 we are varying $k_S = m^2_{A^0}/m^2_{H^0}$ ratio. The 2-dimensional $68\%, 95\%, 99.7\%$ CL regions in the plane $(m_{H^\pm} - m_{A^0})$ are obtained with $\Delta(-2logL) < 2.3, 5.99, 11.83$, respectively.

On the other hand, the systematic with oblique parameters in the S, T plane works in the following way: Taking the experimental constraints $S = (0.05 \pm 0.11)$ and $T = (0.09 \pm 0.13)$, we examine 99% CL contours for model predictions in splittings and direct masses. The ST formulas for 2HDMs have been extracted from Appendix B.

In the alignment regime for ACD models, perturbativity analysis presented in the section 6.7, demands that A^0 and H^0 to have small splittings ($k_S \approx 1$). Likelihood proof (figure 6.7) shows as states where $m_{H^\pm} > m_{H^0}$ are compatible with a Gaussian distribution of the measurements in the diphotonic channel. At this level, hypothesis to avoid charge vacua where $m_{H^\pm} > m_{A^0}$ becomes consistent with phenomenological approach of this two photon decay for a SM like Higgs (in the range of $\Delta(-2logL) < 2.3$). However, regions with $m_{H^\pm} < m_{A^0}$ splittings are still compatible with measurements for $h \to \gamma\gamma$ decay. Finally, zones with $m_{A^0,H^0} > 500$ GeV and $m_{H^\pm} < 150$ GeV are excluded at 99.7 % of C.L.

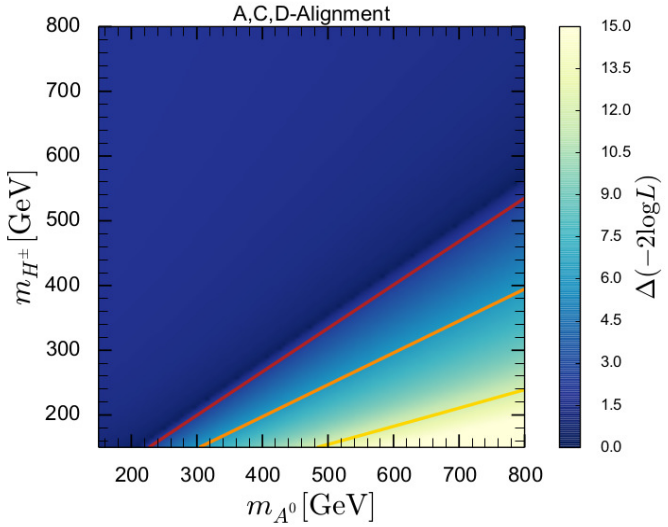

Figure 6.7.: *Likelihood analysis in the alignment regime described by the A_{III}, C_I and D_{II} models in the $m_{H^\pm} - m_{A^0}$ plane in the diphotonic channel. Here h^0-SM-like Higgs has a mass of 125 GeV. The red, orange and yellow lines correspond to the allowed boundaries of 68%, 95% and 99.7% CL regions, respectively. Only $k_S = 1$ is taken by the perturbativity argument given in Tab. 6.1.*

The oblique parameters in the C_I-model are depicted in Fig 6.8 in terms of compatible contours at 99% for splittings and masses (taking $m_{H^\pm} > m_{A^0,H^0}$). These analyses shows how masses for charged Higgs are highly constrained for $m_{H^\pm} > 700$ GeV. In the same way, at this level, pseudoscalar masses are excluded for $m_{A^0} > 400$ GeV.

From vacuum stability and perturbativity analyses, one of the most stable models is the C_I scenario, requiring additionally a degeneracy between m_{A^0} and m_{H^0} yielding $k_S \approx 1$; thus alignment regime requires more information to probe $\lambda_4 < 0$ constraint. On the other hand, ST-oblique parameters plane at 99% CL and shown in Fig. 6.8 yields two zones of compatibility for the C_I model. Here we have taken the hypothesis $m_{H^\pm} > m_{A^0}$. These zones are consistent with the

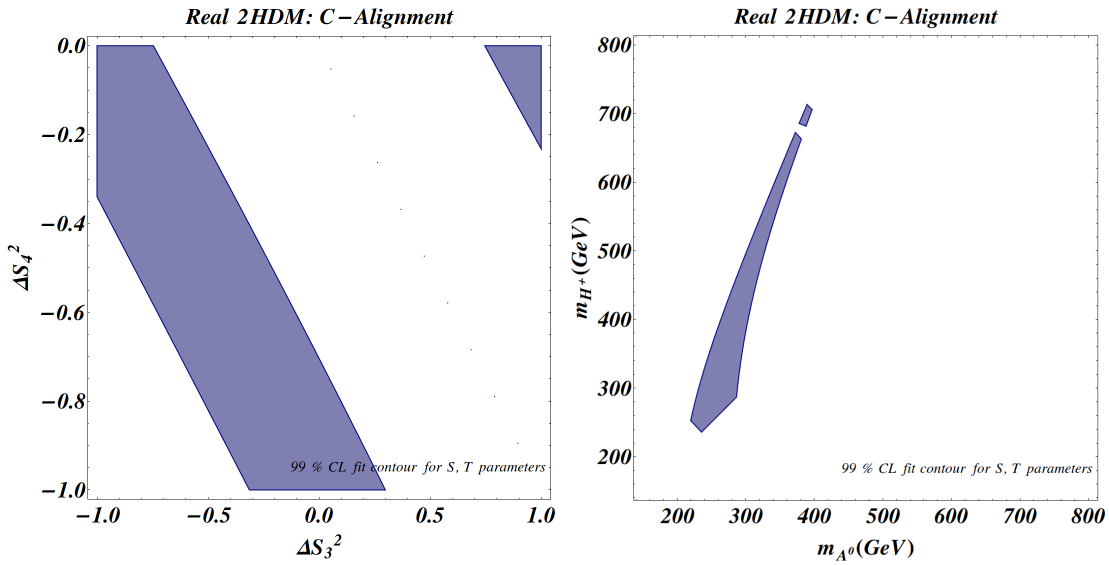

Figure 6.8.: *Oblique parameters in the 2HDM-U*(1) *with the* S, T *fit results for softly breaking of* $U(1)$ *symmetry in the alignment regime given by the* C_I *model; in terms of splittings (**Left**) and in terms of masses for scalar states (**Right**). Computations over ST plane have used* `Mathematica` *module described in [180].*

stable regions in the plane $\Delta S_4^2 - \Delta S_3^2$ from scales of $\mu = 10^5$ up to scales 10^{19} GeV in values of $\Delta S_4^2 < -0.4$ (Fig 6.6). However, these zones are outside of unitarity behavior and perturbativity regime for λ_4 and λ_3 couplings at high energy scales. Oblique parameters ST at 99% CL, locate pseudoscalar and H^0 Higgs with masses in $200 < m_{A^0,H^0}(\text{GeV}) < 400$, meanwhile the charged Higgs mass satisfies $200 < m_{H^\pm}(\text{GeV}) < 700$.

On the other hand, a most constrained parameter space comes from likelihood analysis for the alignment regime given in the E_I model as is shown in Fig. 6.9. For $k_S > 1$ choice and at least at 68% C.L. hypothesis where $m_{H^\pm} < m_{H^0}$ is excluded from the compatibility of the diphotonic decay for a SM-like Higgs boson. Nevertheless, this model has a stringent zone for stability and no-metastability at tree level. Therefore, even though the model is highly compatible with measurements and likelihood hypothesis, stability can be ruled out broadly zones of the respective parameter space.

In the aligned A_{III}, D_{II} and E_I models, oblique parameters at 99% C.L. exclude masses for pseudoscalar Higgs of $m_{A^0} > 400$ GeV when $k_s = 0.4, 0.6$ (Fig. 6.10). In that regimen, charged Higgs mass could get up values up to of 800 GeV. When $k_s = 1.2, 2.0$, pseudoscalar Higgs boson has a maximum mass close to 480 GeV, with a mass for charged Higgs close to 800 GeV.

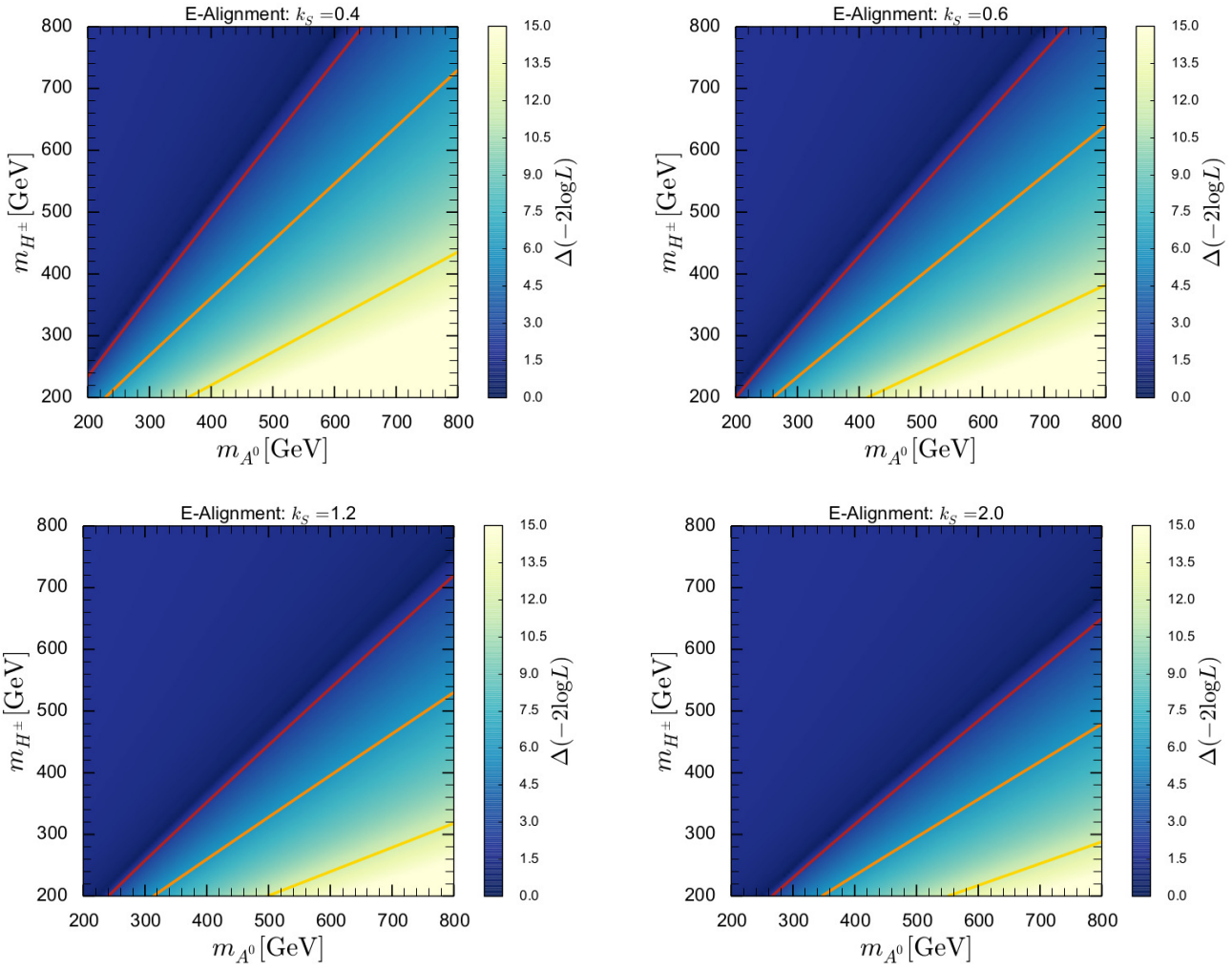

Figure 6.9.: *Likelihood analysis in the alignment scenario described by E_I model in the $m_{H^\pm} - m_{A^0}$ plane in the diphotonic channel and varying $k_S = m^2_{A^0}/m^2_{H^0}$ ratio. Here h^0-SM-like Higgs has a mass of 125 GeV. The red, orange and yellow lines correspond to the allowed boundaries of 68%, 95% and 99.7% CL regions, respectively.*

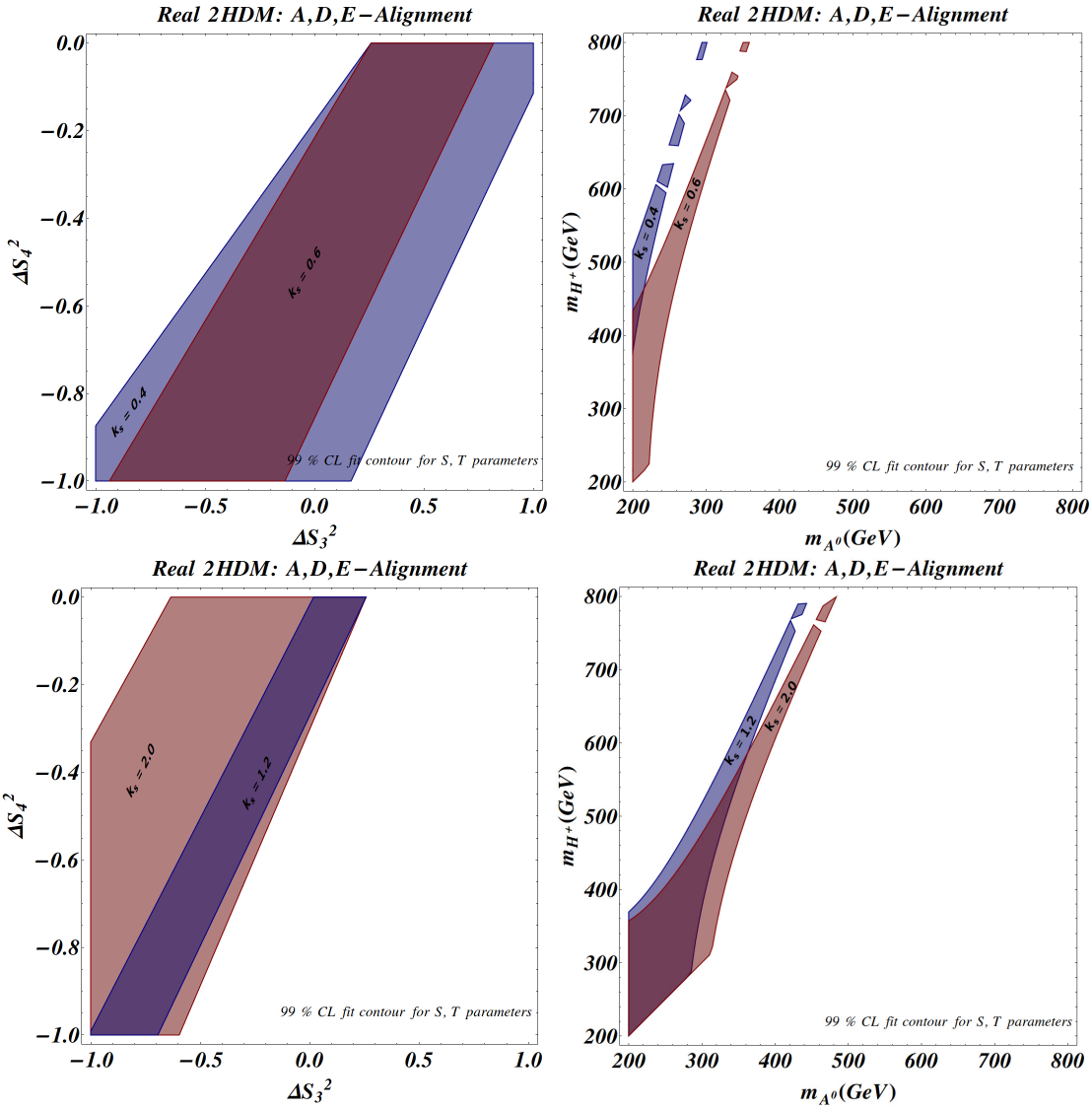

Figure 6.10.: *Oblique parameters in the 2HDM-U(1) with the* S, T *fit results for softly breaking of* $U(1)$ *symmetry in the alignment regime given by the* A_{III}, D_{II} *and* E_I *models (varying* k_s*); in terms of splittings (**Left**) and in terms of masses for scalar states (**Right**). Computations over ST plane have used* `Mathematica` *module described in [180].*

Concluding Remarks

We have presented a unified study of theoretical constraints for non-minimal Higgs sector formed by two scalar doublets. Several motivations to introduce this non-trivial extension for Higgs sector in SM electroweak gauge group arise from the following facts: Firstly, observations in cosmology and astrophysics deduce a necessary amount of non-baryonic dark matter abundance, which has not any candidate from SM spectrum. Also, matter-antimatter asymmetry can not be compatible with current experimental limits for precision tests in SM. Perhaps, the most outstanding discrepancy from SM grounds is the neutrino oscillations, yielded by their small masses. Neutrino masses and their smallness is a problem did not consider by old SM formalisms. Besides, not only the unnatural hierarchy in masses is present in neutrino sector, for instance, but also the third family also depicts a big difference between top quark and bottom quark masses; being this an evidence strong enough of isospin violation phenomenon. This effect can not be explained by only an EW- Higgs doublet generating a SSB simultaneously in all sector for fermions. Secondly, new kind of phenomenology is drawn by 2HDM fundamentals, as the generation of either CP spontaneous or/and explicit violation in all sectors of Lagrangian. These effects can be relevant mechanisms to interpret baryogenesis or leptogenesis scenarios explaining matter-antimatter surplus. Moreover, 2HDMs predict possible Flavor Changing Neutral Currents, which are actively suppressed in a sort of experiments (e.g. in $K^0 - \bar{K}^0$ mixing), but there are not successful reasons to avoid them from a fundamental point of view. Finally, 2HDMs can be compatible effective theories in the scalar sector for a low energy limit of models with extended gauge implementations (e.g. GUT or Left-Right Models) or extended symmetries of space-time (e.g. Super Symmetry).

Benchmarks scenarios for physics beyond the SM have changed from the Higgs boson discovery by CMS and ATLAS collaborations in LHC. The region mass compatible with the scalar signal measured is around 125 GeV. This scale shows outstanding features related to vacuum behavior according to the model background. In minimal SM, computations at NNLO exclude absolute stability at 95% C.L. for the current mass region in $m_t - m_h$; plane; showing a preference for a metastable Higgs potential for high energy scales. Hence the Higgs self-coupling approaches to zero in Planck energies, involving a critical phase that could be explained by either dynamical or symmetry reasons. The above argument is related to new fields interaction at vanishing scale even as threshold corrections, meanwhile the last fact arises from radiative corrections for classical Lagrangian parameters.

In our studies, these possibilities are encoded in extended Higgs sectors, where threshold vacuum behavior comes from corrections at one loop level for 2HDM type I with one inert doublet (i.e. $\langle \Phi_2 \rangle_0 = 0$). We are additionally taking into account $U(1)$ and Z_2 global symmetries for the Higgs potential, since these preclude the occurrence of FCNC processes at tree level (highly constrained by experiments). The global $U(1)$ symmetry yields a degeneracy between A^0 and H^0. Even though, degeneracy among neutral eigenstates is also avoided by the presence of λ_5 coupling, which comes from considering a general Z_2 symmetric Higgs potential.

The constraints at tree level for a bounded from below potential are computed with the formalism of Ivanov [26], where the $SL(2, C)$ reparametrization symmetry of 2HDM is considered in all its extension. In addition to the standard constraints over quartic couplings of the Higgs potential, the formalism, as a limiting case, for Z_2-symmetry avoiding charge breaking minima provides $\lambda_4 + \lambda_5 < 0$ and $\lambda_4 - \lambda_5 > 0$ bounds. These conditions are translated into mass eigenstates through $m_{A^0} > m_{H^\pm} > m_{H^0}$ restriction. On the other hand, for the Higgs potential with a $U(1)$ symmetry, this condition for scalar spectrum implies $\lambda_4 < 0$, leading to charged Higgs to be the heaviest scalar state in the spectrum of the inert-2HDM since $m_{H^0} = m_{A^0}$.

Since EHS as 2HDMs contains a bigger parameter space, a strong first order phase transition could take place, which is relevant to achieve a successful BAU via baryogenesis. Thus, they are basic models to address the matter-antimatter asymmetry of the universe. This fact is an additional motivation to study vacuum structures of 2HDMs at tree level and with radiative corrections since our analyses are inspired in quantifying the threshold effects for stability and exploring their impact on the Higgs sector for these two limiting models.

For the $U(1)$ and Z_2 cases for IHDM, contours in the planes $\lambda_1(m_Z) - \lambda_{3,4,5}(m_Z)$ were considered when the vacuum positivity relations are elevated to be accomplished with the effective quartic couplings in the Higgs potential at one loop level. Those structures allow studying the new sources of instabilities in the Φ_1, Φ_2 directions or in the $\Phi_1 - \Phi_2$ plane of the 2HDM-field space. And they are translated into constraints over scalar masses or more particular in splitting

between them; where the discovered scalar state in LHC has been identified with the lightest scalar CP even of 2HDM. The last regime is interpreted as the alignment limit, where the mass scale of the remaining scalars could even be at EW scale. Fixing the minimality principle and vacuum behavior of the model, we look for the scalar mass values compatible with perturbative unitarity constraints and EW precision tests by oblique parameters realization.

The 2HDM-type I threshold corrections at one loop increase energy scale for Higgs potential stability by the introduction of new fields and couplings among them, all compared with the vacuum behavior in the SM minimal (with Higgs masses of order of the central value of the current experimental signal $m_h = 125.04$ GeV). However new sources of instabilities in those scales appear in the $\Phi_1 - \Phi_2$ plane by the evolution of the remaining quartic couplings, which has many implications for the behavior of mass eigenstates. For instance, in the splitting between states $m^2_{H^\pm}$ and $\bar{m}^2_{22}$ evolution (encoded in λ_3), is shown as positive zones are favored for the reference value in EW scale (m_Z). Moreover, this zone is also compatible with perturbative unitarity behavior of scalar scattering. All results favor the scenario in which the charged Higgs is the heaviest mass state present in the $U(1)$ invariant Higgs potential for an inert vacuum. Meanwhile, A^0 is the heaviest one in Z_2 theory, with $m_{A^0} > m_{H^\pm} > m_{H^0}$. Both statements come mainly from also avoiding a charge violation minimum.

Behavior of SM parameters could be extrapolated to the inert 2HDM. Particularly, in the 2HDM type I, strong instability sources come from $\lambda_1(\mu)$ evolution. These instability zones could be present even in $\mu = 10^3$ GeV for some zones of the parameter space. For instance, in ΔS_1^2 (when $\lambda_1(m_Z) = m^2_{h^0}/v^2 \simeq 0.258$), stability zone is located at $-0.06 \lesssim \lambda_4(m_Z) \lesssim 0$. However, these zones near to $\Delta S_1^2 = 0$ could be evaluated with custodial symmetry behavior at one loop level; being this fact determined from ST-electroweak parameters (for $U = 0$). Meanwhile, non-critical values for $\lambda_1(\mu)$ at Planck scales are compatible with $S-T$ fit contours at 99% C.L. in values $m^2_{H^\pm} > m^2_{22}$. In the Z_2 scenario, analyses favored small splittings between the mass of A^0 and H^0, making more compatible the $m^2_{A^0}/m^2_{H^0} > 1$ condition. The compressed scenario, with an approximated degeneracy between m_{A^0} and m_{H^0} is not ruled out in the $S-T$ plane at 99% C.L. for $\Delta S_1^2 < 0.5$ and $\Delta S_0^2 < 0.25$. Nonetheless, presence of a global minimum analyses exclude this compressed regime for $|m^2_{22}| > 2500$ GeV^2. Finally, global minimum belongs in $m^2_{H^\pm} > m^2_{22}$, which is in consistency with vacuum analyses.

Vacuum stability systematics discriminate between the most general form for Higgs potentials in both cases, with Z_2 and $U(1)$ symmetries because of hierarchy for mass eigenstates obtained is distinct from those models. From a recent discussion, in the first case the pseudoscalar A^0 arises as the heaviest scalar particle, meanwhile in the $U(1)$-model, charged Higgs boson plays this role. Hence in the Z_2 case, the most natural dark matter candidate is H^0 and, by contrast, in the $U(1)$ case both A^0 and H^0 might be good prospects. However, models with a $U(1)$-symmetry have been ruled out from quantum gravity analyses [189]; excluding the presence of plausible dark matter candidates for these models with abelian global symmetries.

In the inert-2HDM happens that the parameter space compatible with the simultaneous existence of both vacua is larger than the predicted by tree-level analyses. In this direction, new featured constraints to describe one global minimum has been computed using re-parametrization group theorems. It can be a useful aid to investigate the metastable behavior at NLO, due to the effective potential predictions the nature of vacuum can change at one loop level concerning established at the tree level. The last can be interpreted as quantum corrections trigger phase transitions between Inert and Inert-like vacuum structures. Hence possible zones investigated by vacuum stability and precision observables can be excluded by the presence of an inert-like vacuum at one loop level. This effect is an important issue that should be addressed using properties here computed about features of a global minimum at tree level.

We know well that the Standard Model with a light Higgs boson in a mass around of 125 GeV provides an accurate description of a significant quantity of experimental data associated with the Spontaneous Symmetry Breaking mechanism. The consistency of the precision EW observables with predictions of SM suggest that, if new physics is present at the EW scale, it is most probably weakly interacting and consistent with the presence of a light Higgs boson in the spectrum. Extensions with these features are the Two Higgs Doublet Models with a softly broken global symmetry implementing an additional hypothesis of alignment for scalar states.

Based on the vacuum behavior of SM, we comprehensively study metastable and stable states in the model with softly breaking of a $U(1)$ global symmetry in the 2HDM. Initially, softly terms are implemented to forbid massless axion-like particles. Besides, these components are related to metastable states at tree level in the field space. If these minima are not long-lived enough, dramatical consequences forbid a well-grounded theory. Thus, we consider this fact as possible exclusions for different configurations of parameter space. Metastability behavior searches are based on Minkowskian formalism of reparameterization group of the Higgs potential to search one global minimum in the theory, which are strongly dependent on $\tan\beta$ and α mixing. There is a high sensitivity of discriminant in zones approaching to $\beta \to 0$ and $\pi/2$, and when $\beta \to \pi/4$ and $\alpha \to \pi/4$. The alignment scenarios present in the parameters sweeping define the boundary between stable and metastable zones, being important to characterize possible phase transitions due to formation the

multiple local minima in the Higgs potential.

Once studied possible exclusion regions for metastability behavior, we describe vacuum analyses at one loop level for the models with $\tan\beta = 1$ and $\tan\beta >> 1$, for different crucial values of mixing angle α. Regimes for $\tan\beta < 1$ are highly non-perturbative and drive out rapidly to instabilities in the Higgs potential. This effect is a consequence of initial conditions for Yukawa dynamics for type I 2HDM. Besides of this model with $v_1 = v_2$ present most stringent regions for parameter space. On the other hand, analyses for $\tan\beta >> 1$ leads to study, in a perturbative reliable theory, regions where instabilities in the Higgs potential appears in different directions of the field space.

Likewise, the hypothesis to avoid electromagnetically charged vacua are proved in a phenomenological point of view, employing the likelihood proof of charged Higgs boson influence in the triangle loop corrections of the diphotonic decay of SM Higgs. In this direction, run 1 data of LHC strongly favored scenarios where $m_{H^\pm} > m_{A^0}$, which is also a necessary exigency from couplings in the Higgs potential to get one neutral minimum consistent with the EW symmetry breaking. The chance of finding a stationary point with charge breaking, before constructing mass eigenstates, is greater when all space like couplings in the Λ diagonalized tensor are negative. Studying Λ positivity from Silvester criterion drive out to the same conditions to avoid charge stationary oints, however the full demostration is on road. Notwithstanding stringent behavior from vacuum analyses, the alignment scenario with $v_2 = v_1$ is phenomenological compatible by likelihood proofs with the normal vacuum hypothesis for charged Higgs boson with the highest mass value in the scalar spectrum.

Within all frameworks here presented, these limits provide a test into the scale characterizing possible sources of instabilities or new physics energies in several zones of the parameter space in both cases. Although the additional heavy scalars may improve the behaviour of running Higgs self-coupling at large field values, we prove that they can destabilise the vacuum in other field directions even in scales related to EW-scenario. Our systematic also lead to determine the evolution of unstable levels for different regions of field space, complementing previous studies in vacuum behavior in IHDM. However, these analyses deal open questions about the possible additional threshold contributions from the 2HDM to explain the criticality in SM from the input of more general Higgs potentials. Nevertheless, when more precision tests are performed at LHC, and with most accurate values of parameters, the extension to analyses must be introduced to explain issues related to a stable, effective Higgs potential, baryonic asymmetry of the universe, and the dark matter origin. Perhaps in those scenarios, higher radiative corrections beyond NLO for 2HDM couplings should be considered and hence studies about vacuum nature and its behavior might be completed.

All these studies leave open some issues about new physics effects to vacuum stability and the relation with metastable states. For instance, implications over explanation of baryonic asymmetry of the universe. The influence of this analysis tackling baryogenesis processes must be addressed soon since accurate descriptions of these effects require of a correct definition of vacuum states in the Higgs potential. On the other hand, leptogenesis in 2HDMs needs additional fermionic fields considered as TeV completions via RH-neutrinos for the effective Higgs sector. Notwithstanding, in leptogenesis mechanism we are focused in massive neutrino decays, these processes depend on a workable definition of a Higgs potential to describe the phase space allowed for new leptons, and especially, thermal effects are incorporated to provide enough out of equilibrium processes.

Other aspects are related with how strong gravity sources (e.g. black holes) could change time rates between EW minimum (as a local stationary point) and one deepest minimum. In this direction and using a thin-wall bubble approximation for the nucleation process (which is possible when generic quantum gravity corrections are added to the Higgs potential), in [196–198] has been demonstrated that primordial black holes can stimulate vacuum decay. The lifetime predicted is in millions of Planck times rather than billions of years. One future research might be associated with the effects over 2HDMs effective Higgs potentials in the presence of a black hole. These results can be seen as the solution not only aspect related to particle physics, but as a way to analyze tunneling rates near to event horizon of one black hole. These studies allow describing not only a possible cosmological scenario for 2HDMs but also to determine possible restrictions in the parameter spaces in extended Higgs sectors from black holes searches in the LHC.

A. Alignment Regimen

A.1. Scalar Alignment in 2HDMs

In the light of results of LHC, it is convenient to translate general analysis into a particular scenario strongly compatible with experimental observables. One possible hypothesis is the impersonating the scalar signal found by CMS and ATLAS collaborations at LHC with the lightest Higgs boson of 2HDM. Meanwhile, the remain scalar spectrum might be coupled with the same scale energy. Therefore oblique corrections could come in the threshold achieved by precision observables and thus the couplings among fermions and boson with h^0 do not have significant deviations from whose arising in the SM.

In this section we discussed systematically as *Alignment Regime* can be achieved from stationary and mass matrices; from the general Higgs potential presented in (1.2.1), and by imposing a CP-conserving scenario we consider that vacuum has the following structure

$$\Phi_1 = \frac{1}{\sqrt{2}}\begin{pmatrix} 0 \\ v_1 \end{pmatrix} \text{ and } \Phi_2 = \frac{1}{\sqrt{2}}\begin{pmatrix} 0 \\ v_2 \end{pmatrix}$$

being v_i are real. The non trivial tadpoles at tree level are

$$m_{11}^2 v_1 - m_{12}^2 v_2 + \frac{1}{2}\left(\lambda_1 v_1^3 + 3\lambda_6 v_1^2 v_2 + \lambda_{345} v_1 v_2^2 + \lambda_7 v_2^3\right) = 0 \tag{A.1.1}$$

$$m_{22}^2 v_2 - m_{12}^2 v_1 + \frac{1}{2}\left(\lambda_2 v_2^3 + 3\lambda_7 v_2 v_1^2 + \lambda_{345} v_1^2 v_2 + \lambda_6 v_1^3\right) = 0 \tag{A.1.2}$$

If some of the VEVs is zero (say $v_i = 0$), associated stationary equation in m_{ii}^2 becomes trivial. This scenario is the case of Inert models, whose construction regarding an additional trivial tadpole at tree-level. It is convenient to introduce the $\tan\beta$ parameter, using VEVs ratio

$$\tan\beta = \frac{v_2}{v_1} \text{ and } v^2 = v_1^2 + v_2^2 \simeq (246)^2 \text{ GeV}^2$$

In terms of $\tan\beta$, stationary conditions (A.1.1) and (A.1.2) behave as

$$\begin{aligned} m_{11}^2 - m_{12}^2 \tan\beta + \frac{1}{2}v^2 \cos^2\beta \left(\lambda_1 + 3\lambda_6 \tan\beta + \lambda_{345}\tan^2\beta + \lambda_7 \tan^3\beta\right) &= 0 \\ m_{22}^2 - m_{12}^2 \tan^{-1}\beta + \frac{1}{2}v^2 \sin^2\beta \left(\lambda_2 + 3\lambda_7 \tan^{-1}\beta + \lambda_{345}\tan^{-2}\beta + \lambda_6 \tan^{-3}\beta\right) &= 0 \end{aligned}$$

In both equation we have assumed that $v_i \neq 0$ in the respective relation for m_{ii}^2. The matrix mass in the CP even sector is

$$M^2 = \begin{pmatrix} M_{11}^2 & M_{12}^2 \\ M_{21}^2 & M_{22}^2 \end{pmatrix} = m_A^2 \begin{pmatrix} \sin^2\beta & -\sin\beta\cos\beta \\ -\sin\beta\cos\beta & \cos^2\beta \end{pmatrix} + v^2 \begin{pmatrix} L_{11} & L_{12} \\ L_{21} & L_{22} \end{pmatrix}.$$

with the mass of the pseudoscalar [132]

$$m_A^2 = \frac{2m_{12}^2}{\sin 2\beta} - \frac{1}{2}v^2\left(2\lambda_5 + \lambda_6 \tan^{-1}\beta + \lambda_7 \tan\beta\right) \tag{A.1.3}$$

where

$$L_{11} = \lambda_1 \cos^2\beta + 2\lambda_6 \sin\beta\cos\beta + \lambda_5 \sin^2\beta \tag{A.1.4}$$
$$L_{22} = (\lambda_3 + \lambda_4)\sin\beta\cos\beta + \lambda_6 \cos^2\beta + \lambda_7 \sin^2\beta \tag{A.1.5}$$
$$L_{12} = \lambda_2 \sin^2\beta + 2\lambda_7 \sin\beta\cos\beta + \lambda_5 \cos^2\beta \tag{A.1.6}$$

The mixing angle for the CP-even sector is defined as

$$\begin{pmatrix} H \\ h \end{pmatrix} = \begin{pmatrix} \cos\alpha & \sin\alpha \\ -\sin\alpha & \cos\alpha \end{pmatrix} \begin{pmatrix} \phi_1^0 \\ \phi_2^0 \end{pmatrix} \equiv \mathrm{R}(\alpha) \begin{pmatrix} \phi_1^0 \\ \phi_2^0 \end{pmatrix}$$

This leads to

$$R^T(\alpha) \begin{pmatrix} m_H^2 & 0 \\ 0 & m_h^2 \end{pmatrix} R(\alpha) = \begin{pmatrix} \mathcal{M}_{11}^2 & \mathcal{M}_{12}^2 \\ \mathcal{M}_{12}^2 & \mathcal{M}_{22}^2 \end{pmatrix} \tag{A.1.7}$$

From the component $(1,2)$ in the above equation, mass states are related by

$$(m_{H^0}^2 - m_{h^0}^2)\sin\alpha\cos\alpha = \mathcal{M}_{12}^2 \tag{A.1.8}$$

By virtue of $m_{H^0} > m_{h^0}$, implying $\sin\alpha\cos\alpha$ has the same sign as $\mathcal{M}_{12}^2$.
There are two possible sign choices:

- $-\frac{\pi}{2} \leq \alpha \leq \frac{\pi}{2}$: $\cos\alpha \geq 0$ and $\mathrm{Sign}(\sin\alpha) = \mathrm{Sign}\left(\mathcal{M}_{12}^2\right)$
- $0 \leq \alpha \leq \pi$: $\sin\alpha \geq 0$ and $\mathrm{Sign}(\cos\alpha) = \mathrm{Sign}\left(\mathcal{M}_{12}^2\right)$

We will work with these choices for mixing angle α in our phenomenological and theoretical analyses.
The eigenvector corresponding to eigenvalue m_h^2 is associated to the second row in $R(\alpha)$ from Eq. (A.1.7), satisfies indeed

$$\begin{pmatrix} \mathcal{M}_{11}^2 & \mathcal{M}_{12}^2 \\ \mathcal{M}_{12}^2 & \mathcal{M}_{22}^2 \end{pmatrix} \begin{pmatrix} -\sin\alpha \\ \cos\alpha \end{pmatrix} = m_{h^0}^2 \begin{pmatrix} -\sin\alpha \\ \cos\alpha \end{pmatrix} \tag{A.1.9}$$

A.2. Generalities and Definitions for Alignment Regimen

Our aim is to find the general conditions obtaining alignment without a decoupling of the scalar spectrum. We are interested in the alignment limit, where the lightest CP-even Higgs mimics the SM one and remain scalars might be set even in the same EW scale. We will begin by solving for the conditions for which the Higgs couplings to fermions have the same magnitude as in the SM: $|g_{huu}/g_f| = |g_{hdd}/g_f| = 1$. The decoupling limit, where the low-energy spectrum contains only the SM and no new light scalars, is only a subset of the more general alignment limit for fermions couplings [171]:

- i) $g_{hdd} = g_{huu} = \pm g_f$
- ii)$g_{hdd} = -g_{huu} = \pm g_f$

  Demanding case i) leads to

$$\sin\alpha = \mp\cos\beta \text{ and } \cos\alpha = \pm\sin\beta \tag{A.2.1}$$

  which then implies

$$\cos(\beta - \alpha) = 0 \text{ and } \sin(\beta - \alpha) = \pm 1 \tag{A.2.2}$$

  Couplings of the CP-even Higgs bosons now become

$$g_{hVV} \to \pm g_V,\ g_{hff} \to \pm g_f,\ g_{HVV} \to 0,\ g_{Hdd} \to \pm\tan\beta g_f,\ g_{Huu} \to \mp\tan^{-1}\beta\ g_f \tag{A.2.3}$$

where the upper and lower signs correspond to $\sin(\beta-\alpha)=1$ and -1, respectively. This choice is the alignment limit. The heavy CP-even Higgs couplings to SM gauge bosons vanish in this limit since it does not acquire a VEV. In other words, the alignment limit is the regimen where the mass eigenbasis in the CP-even sector coincides with the basis which the gauge bosons receive all of their masses from one of the doublets. As such, the non-SM-like CP-even Higgs does not couple to the gauge bosons at the tree-level. However, on this basis H still has non-vanishing couplings to SM fermions

On the other hand, fulfillment of case ii) requires

$$\sin\alpha = \mp\cos\beta \text{ and } \cos\alpha = \mp\sin\beta \tag{A.2.4}$$

which gives

$$\cos(\beta-\alpha) = \mp\sin 2\beta \text{ and } \sin(\beta-\alpha) = \pm\cos 2\beta$$

We see that the hVV coupling does not tend to the SM value in this case and alignment is not reached.

The decoupling limit, where the low-energy spectrum contains only the SM and no new light scalars, is only a subset of the more general alignment limit in Eq. (A.2.2). In particular, quite generically, there exist regions of parameter space where one attains the alignment limit with new light scalars not far above $m_{h^0}=125$ GeV.

It is illustrative to derive the alignment limit in the usual decoupling regime but in a slightly different reasoning. Consider the eigenvalue equation of the CP-even Higgs mass matrix, rewriting Eq. (A.1),

$$\begin{pmatrix} \mathcal{M}_{11}^2 & \mathcal{M}_{12}^2 \\ \mathcal{M}_{12}^2 & \mathcal{M}_{22}^2 \end{pmatrix} \equiv m_{A^0}^2 \begin{pmatrix} \sin^2\beta & -\sin\beta\cos\beta \\ -\sin\beta\cos\beta & \cos^2\beta \end{pmatrix} + v^2 \begin{pmatrix} L_{11} & L_{12} \\ L_{12} & L_{22} \end{pmatrix} \tag{A.2.5}$$

which using Eq. (A.1.9), above relation becomes

$$\begin{aligned} \begin{pmatrix} \sin^2\beta & -\sin\beta\cos\beta \\ -\sin\beta\cos\beta & \cos^2\beta \end{pmatrix} \begin{pmatrix} -\sin\alpha \\ \cos\alpha \end{pmatrix} &= \frac{1}{m_{A^0}^2} \begin{pmatrix} \mathcal{M}_{11}^2 & \mathcal{M}_{12}^2 \\ \mathcal{M}_{12}^2 & \mathcal{M}_{22}^2 \end{pmatrix} \begin{pmatrix} -\sin\alpha \\ \cos\alpha \end{pmatrix} \\ &- \frac{v^2}{m_{A^0}^2} \begin{pmatrix} L_{11} & L_{12} \\ L_{12} & L_{22} \end{pmatrix} \begin{pmatrix} -\sin\alpha \\ \cos\alpha \end{pmatrix} \end{aligned}$$

$$\begin{pmatrix} \sin^2\beta & -\sin\beta\cos\beta \\ -\sin\beta\cos\beta & \cos^2\beta \end{pmatrix} \begin{pmatrix} -\sin\alpha \\ \cos\alpha \end{pmatrix} = \frac{m_h^2}{m_{A^0}^2} \begin{pmatrix} -\sin\alpha \\ \cos\alpha \end{pmatrix} - \frac{v^2}{m_{A^0}^2} \begin{pmatrix} L_{11} & L_{12} \\ L_{12} & L_{22} \end{pmatrix} \begin{pmatrix} -\sin\alpha \\ \cos\alpha \end{pmatrix} \tag{A.2.6}$$

Decoupling is defined by taking all non-SM-like scalar masses to be much heavier than the SM-like Higgs mass, $m_{A^0}^2 >> v^2, m_h^2$. Then we see that at leading order in $v^2/m_{A^0}^2$ and $m_h^2/m_{A^0}^2$ the right side of Eq. (A.2.6) can be ignored, and the eigenvalue equation becomes

$$\begin{pmatrix} -\sin\alpha\sin^2\beta - \sin\beta\cos\beta\cos\alpha \\ \sin\beta\cos\beta\sin\alpha + \cos^2\beta\cos\alpha \end{pmatrix} \approx 0 \tag{A.2.7}$$

thus

$$\cos(\beta-\alpha) \approx 0. \tag{A.2.8}$$

Here we make the critical observation that while decoupling achieves alignment by neglecting the right-hand side of Eq (A.2.6), alignment can also be obtained if the right-hand side of Eq. (A.2.6) vanishes identically, independent of m_A scale:

$$\begin{aligned} m_h^2 \begin{pmatrix} -\sin\alpha \\ \cos\alpha \end{pmatrix} &= v^2 \begin{pmatrix} L_{11} & L_{12} \\ L_{12} & L_{22} \end{pmatrix} \begin{pmatrix} -\sin\alpha \\ \cos\alpha \end{pmatrix} \\ &= v^2 \begin{pmatrix} \cos\alpha L_{12} - \sin\alpha L_{11} \\ \cos\alpha L_{22} - \sin\alpha L_{12} \end{pmatrix}. \end{aligned} \tag{A.2.9}$$

More explicitly, since $\sin\alpha = -\cos\beta$ in the alignment limit, we can re-write the above matrix equation as two algebraic equations

$$m_h^2 = v^2 L_{11} + \tan\beta v^2 L_{12} = v^2\left(\lambda_1\cos^2\beta + 3\lambda_6\sin\beta\cos\beta + \lambda_{345}\sin^2\beta + \lambda_7\tan\beta\sin^2\beta\right), \tag{A.2.10}$$

$$m_h^2 = v^2 L_{22} + \tan^{-1}\beta v^2 L_{12} = v^2\left(\lambda^2\sin^2\beta + 3\lambda_7\sin\beta\cos\beta + \lambda_{345}\cos^2\beta + \lambda_6\tan^{-1}\beta\cos^2\beta\right). \tag{A.2.11}$$

Above equations have been broadly used in vacuum analysis to establish the compatibility level between a parameter space allowed by positivity constraints and an alignment scenario. All statements done in this appendix have been settled in Fig. A.1, wherein Higgs states are located with respect to different planes in the spectrum of several effective theories of scalar sector for 2HDM. In addition, we put the decoupling limit as the final plane of the "cascade" of effective theories that can be considered in the 2HDM.

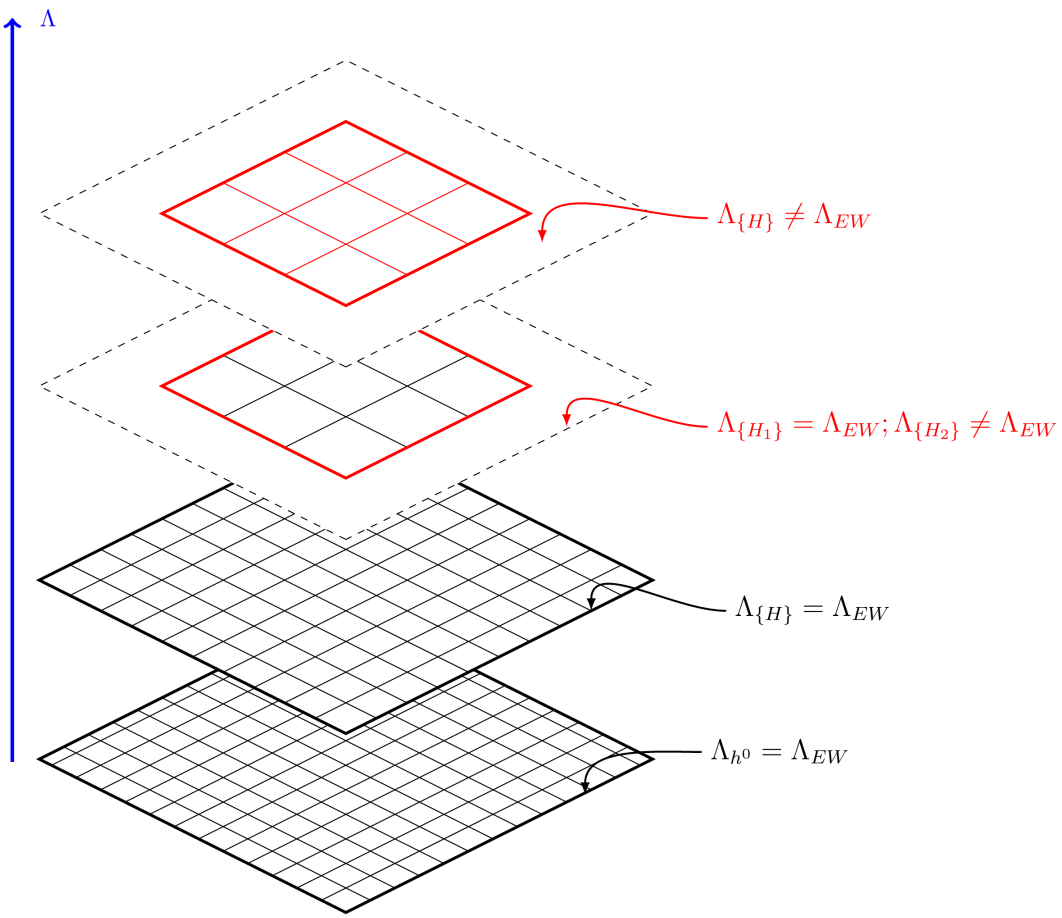

Figure A.1.: *Alignment cascade of scalar states with respect of energy regimen* Λ. $\{H\} = A^0, H^0, H^\pm$ *are the remaining Higgses of 2HDM* (H_1, H_2 *are subsets of them). The higher plane (red) refers to the* decoupling limit *where all remaining scalars belong in* $\Lambda > \Lambda_{EW}$.

B. Oblique parameters definitions

B.1. Oblique parameters fundamentals and definitions

Oblique parameters are designed to constrain models of new physics from the electroweak precision observables. It is assumed that the effects of new physics only appear through vacuum polarization and therefore lead to modifying oblique parameters. Most of the effects on electroweak precision observables can be parameterized by three gauge self-energy parameters *(S, T, U)* introduced by Peskin and Takeuchi [175]. Hence, the correlation among these parameters could be given regarding electroweak observables and leads to analyze precision physics, useful to constraint new phenomena. STU parameters are mainly focused on different contributions for observables of physics beyond, as follows

- $S(S+U)$ value describes new physics contributions to neutral (charged) current processes at different energy scales.
- T parameter measures the difference between the new physics contributions of neutral and charged current processes at low energies. This effect is related to isospin violation at the EW scale. The T parameter is also linked to the commonly used custodial-parameter $\rho \equiv m_W^2/m_Z^2 \cos^2\theta_w$ (which is close to 1)

$$\rho_0 = \frac{\rho}{\rho_{SM}}. \tag{B.1.1}$$

  Using,

$$\rho_0 = \frac{1}{1-\alpha T}, \tag{B.1.2}$$

  we can evaluate deviations from the SM value of $\rho_0 = 1$.

- U is only constrained by the W boson mass and its total width. Besides, the U parameter is often a small quantity in new physics models because of it is associated with an eight-dimension effective operator. Therefore, the STU parameter space can seldom be projected into a two-dimensional parameter space, in which the experimental constraints are easy to describe in the $S-T$ plane. T parameter measures the difference between the new physics contributions of neutral and charged current processes at low energies. This effect is related to isospin violation at the EW scale. The T parameter is also linked to the commonly used custodial-parameter $\rho \equiv m_W^2/m_Z^2 \cos^2\theta_w$ (which is close to 1)

The 2HDM contributions are defined from relations [199]

$$S = \frac{16\pi \cos\theta_w^2}{g^2}\left\{\frac{\bar{A}_{Z^0Z^0}(m_Z^2) - \bar{A}_{Z^0Z^0}(0)}{m_Z^2} - \left.\frac{\partial \bar{A}_{\gamma\gamma}(q^2)}{\partial q^2}\right|_{q^2=0} + \frac{\cos^2\theta_w - \sin^2\theta}{\sin\theta_w\cos\theta_w}\left.\frac{\partial \bar{A}_{\gamma Z^0}(q^2)}{\partial q^2}\right|_{q^2=0}\right\} \tag{B.1.3}$$

$$T = \frac{4\pi}{g^2 \sin^2\theta_w}\left[\frac{\bar{A}_{W^+W^-}(0)}{m_W^2} - \frac{\bar{A}_{Z^0Z^0}}{m_Z^2}\right] \tag{B.1.4}$$

$$U = \frac{16\pi}{g^2}\left\{\frac{\bar{A}_{W^+W^-}(m_W^2) - \bar{A}_{W^+W^-}(0)}{m_W^2} - \cos\theta_w^2\frac{\bar{A}_{Z^0Z^0}(m_Z^2) - \bar{A}_{Z^0Z^0}}{m_Z^2} - \sin^2\theta_w\left.\frac{\partial \bar{A}_{\gamma\gamma}(q^2)}{\partial q^2}\right|_{q^2=0}\right.$$
$$\left. + 2\cos\theta_w\sin\theta_w\left.\frac{\partial \bar{A}_{\gamma Z^0}(q^2)}{\partial q^2}\right|_{q^2=0}\right\}. \tag{B.1.5}$$

Here the $A_{VV'}$ are the coefficients for $g^{\mu\nu}$ in the vacuum polarization tensors

$$\Pi^{\mu\nu}_{VV'}(q) = g^{\mu\nu}A_{VV'}(q^2) + q^\mu q^\nu B_{VV'}(q^2). \tag{B.1.6}$$

With the subtraction from the SM contribution, we have

$$\bar{A}_{VV''}(q^2) = A_{VV'}(q^2)|_{2HDM} - A_{VV'}(q^2)|_{SM}. \tag{B.1.7}$$

For the T parameter, we have the formula [199]:

$$\begin{aligned} T = \frac{g^2}{64\pi^2 m_W^2}\Bigg\{ &\sum_{k=1}^{3}|C_k|^2 F(m_{H^+}^2, m_{H^k}^2) - \sum_{k=1}^{2}|C_k|^2 F(m_{H^k}^2, m_{A^0}^2) \\ &+ 3\sum_{k=1}^{2}|C_{3-k}|^2\left[F(m_Z^2, m_{H_k}^2) - F(m_W^2, m_{H_k}^2)\right] - 3\left[F(m_Z^2, m_{h_{ref}}^2) - F(m_W^2, m_{h_{ref}}^2)\right]\Bigg\}, \end{aligned} \tag{B.1.8}$$

where m_{H_k} $(k = 1, 2, 3)$ denotes scalar masses, and $m_{H_{ref}}$ is the SM Higgs. The latter terms isolate the new physics effect through the subtraction of the SM equivalent. The F function is given by

$$F(x,y) = \begin{cases} \frac{x+y}{2} - \frac{xy}{x-y}\ln\frac{x}{y}; & \text{for } x \neq y \\ 0; & \text{for } x = y \end{cases}, \tag{B.1.9}$$

Couplings between EW bosons to a pair of scalars are summarized by the following arrangement:

$$C_k = \{\cos(\beta-\alpha),\ \sin(\beta-\alpha),\ 1\}. \tag{B.1.10}$$

Here α is the diagonalization angle in the real part of the neutral components in the doublets, while β is the diagonalization angle for "charged" fields in the doublets. β is also related to vacuum structure since $\tan\beta = v_2/v_1$. For the inert model, $\alpha = \pi/2$ and β is equal to zero due to its vacuum realization; being this choice compatible with an alignment regime (for fermionic and bosonic couplings) since $\cos(\beta-\alpha) \approx 0$ [171]. To find other two parameters, S and U, we define G and $\widehat{G}$ structures. The former functions are [37]

$$G(x,y,Q) = -\frac{16}{3} + \frac{5(x+y)}{Q} - \frac{2(x+y)^2}{Q^2} + \frac{3}{Q}\left[\frac{x^2+y^2}{x-y} - \frac{x^2-y^2}{Q} + \frac{(x-y)^3}{3Q^2}\right]\ln\frac{x}{y} + \frac{r}{Q^3}f(t,r), \tag{B.1.11}$$

with $t \equiv x+y-Q$, $r \equiv Q^2 - 2Q(x+y) + (x-y)^2$, and

$$f(t,r) = \begin{cases} \sqrt{r}\ln\left|\frac{t-\sqrt{r}}{t+\sqrt{r}}\right| & r > 0 \\ 0 & r = 0 \\ 2\sqrt{-r}\arctan\frac{\sqrt{-r}}{t} & r < 0. \end{cases} . \tag{B.1.12}$$

The latter $\widehat{G}$ function is given by

$$\widehat{G}(x,Q) = G(x,Q,Q) + \tilde{G}(x,Q,Q), \tag{B.1.13}$$

and

$$\tilde{G}(x,y,Q) = 12\left[\frac{x-y}{Q} - \frac{x+y}{x-y}\right]\ln\frac{x}{y} + \frac{12}{Q}f(t,r) - 24. \tag{B.1.14}$$

Hence the $S-$parameter can be described from

$$S = \frac{g^2}{384\pi^2 \cos\theta_w^2}\left\{ \left(\sin^2\theta_w - \cos^2\theta_w\right)^2 G(m^2_{H^\pm}, m^2_{H^\pm}, m^2_Z) + \sum_{k=1}^{2} |C_k|^2 G(m^2_{H_k}, m^2_A, m^2_Z) \right.$$
$$- 2\ln m^2_{H^+} + \sum_{k=1}^{3} \ln m^2_{H_k} - \ln m^2_{H_{ref}}$$
$$\left. + \sum_{k=1}^{2} |C_{3-k}|^2 \widehat{G}(m^2_{H_k}, m^2_Z) - \widehat{G}\left(m^2_{H_{ref}}, m^2_Z\right) \right\}. \tag{B.1.15}$$

And the $U-$parameter is

$$U = \frac{g^2}{384\pi^2}\left\{ \sum_{k=1}^{3} |C_k|^2 G(m^2_{H^+}, m^2_{H_k}, m^2_W) - \left(\sin^2\theta_w - \cos^2\theta_w\right)^2 G(m^2_{H^\pm}, m^2_{H^\pm}, m^2_Z) \right.$$
$$- \sum_{k=1}^{2} |C_k|^2 G(m^2_{H_k}, m^2_{A^0}, m^2_W)$$
$$\left. + \sum_{k=1}^{2} |C_{3-k}|^2 \left[\widehat{G}(m^2_{H_k}, m^2_W) - \widehat{G}(m^2_{H_k}, m^2_Z)\right] - \widehat{G}(m^2_{H_{ref}}, m^2_W) + \widehat{G}(m^2_{H_{ref}}, m^2_Z) \right\}. \tag{B.1.16}$$

Constraints on the STU oblique observables are derived from a fit to the electroweak precision data, more details can be found in the most current articles [81–83]. Besides, in the STU parameters the floating fit values are $m_Z = 91.1873 \pm 0.0021$ GeV, $\Delta\alpha_{had}(m^2_Z) = 0.02757 \pm 0.00010$, and $\alpha_s(m^2_Z) = 0.1192 \pm 0.0033$. The following fit results are determined from a fit for a reference Standard Model with $m_{t,ref} = 173$ GeV and $m_{H,ref} = 125$ GeV:

$$\begin{aligned} S &= 0.05 \pm 0.11 \\ T &= 0.09 \pm 0.13 \\ U &= 0.01 \pm 0.11 \end{aligned} \tag{B.1.17}$$

with correlation coefficients of $+0.90$ between S and T, $-0.59(-0.83)$ between S and U (T and U). Fixing $U{=}0$ one obtains $S_{U=0} = 0.06 \pm 0.09$ and $T_{U=0} = 0.10 \pm 0.07$, with a correlation coefficient of $+0.91$. The general procedure to measure oblique parameters is extracted from a global fit to the high-precision electroweak data from particle collider experiments (mostly the Z pole data from the CERN-LEP collider) and atomic parity violation [200]. Every step presented here would be an important tool to measure the compatibility level of the vacuum behavior predictions with the EW observables and precision tests.

C. Type III Lagrangian for 2HDMs: FCNCs

C.1. Type III-2HDMs: Mass Eigenstates and FCNC couplings

In this appendix, we explore realizations for the type III-2HDM. This model has general couplings between fermions and both doublets. We start with the Higgs doublets and their VEVs, which can be defined by

$$\Phi_i' = \begin{pmatrix} \phi_i^+ \\ \phi_i^0 \end{pmatrix} = \frac{1}{\sqrt{2}} \begin{pmatrix} \phi_1^i + i\phi_2^i \\ \phi_3^i + i\phi_4^i \end{pmatrix}, \quad \langle \Phi_i' \rangle = \frac{1}{\sqrt{2}} \begin{pmatrix} 0 \\ v_i e^{i\varphi_i} \end{pmatrix} \tag{C.1.1}$$

The phases φ_i are sources of spontaneous CP violation from the purely scalar sector [1]. This fact is a radical difference between 2HDM and the minimal SM. The Yukawa Lagrangian has the general form:

$$-\mathcal{L}_Y = \tilde{\eta}^{U,0}_{i,j} \bar{Q}^0_{iL} \tilde{\Phi}_1' U^0_{jR} + \tilde{\eta}^{D,0}_{i,j} \bar{Q}^0_{iL} \Phi_1' D^0_{jR} + \tilde{\xi}^{U,0}_{i,j} \bar{Q}^0_{iL} \tilde{\Phi}_2' U^0_{jR} + \tilde{\xi}^{D,0}_{i,j} \bar{Q}^0_{iL} \Phi_2' D^0_{jR} + \tilde{\eta}^{E,0}_{i,j} \bar{L}^0_{iL} \Phi_1' E^0_{jR} + \tilde{\xi}^{E,0}_{i,j} \bar{L}^0_{iL} \Phi_2' E^0_{jR} + h.c. \tag{C.1.2}$$

In the leptonic sector, we have taken what there are no right handed singlets neutrinos at electroweak scale. Hence they remain massless. We can redefine the scalar doublets by the following way:

$$\begin{aligned} \begin{pmatrix} H_1 \\ H_2 \end{pmatrix} &= \begin{pmatrix} \cos\theta & e^{-i\varphi}\sin\theta \\ -\sin\theta & e^{-i\varphi}\cos\theta \end{pmatrix} \begin{pmatrix} \Phi_1' \\ \Phi_2' \end{pmatrix} \\ \varphi &= \varphi_2 - \varphi_1 \end{aligned}$$

This rotation (or combinations) do not have physical consequences since it is basically a change of basis. Therefore, it is possible to choice the reasoning in which Φ_1' to be responsible for the fermion masses, and Φ_2' with its couplings to the fermions yields FCNC terms. The original Yukawa Lagrangian density can be defined regarding these primed scalar fields as

$$-\mathcal{L}_Y = \eta^U_{i,j} \bar{Q}_{iL} \tilde{H}_1 U_{jR} + \eta^D_{i,j} \bar{Q}_{iL} H_1 D^0_{jR} + \xi^U_{i,j} \bar{Q}_{iL} \tilde{H}_2 U_{jR} + \xi^D_{i,j} \bar{Q}_{iL} H_2 D_{jR} + \eta^E_{i,j} \bar{L}_{iL} H_1 E_{jR} + \xi^E_{i,j} \bar{L}_{iL} H_2 E_{jR} + h.c. \tag{C.1.3}$$

In this basis, only the Yukawa couplings of the doublet H_1, *viz* the η, generate fermion masses; those may be bi-diagonalized, and they do not lead to tree-level FCNC. Therefore

$$\begin{aligned} \eta^U &= \frac{\sqrt{2}}{v} M^U = \tilde{\eta}^U \cos\beta + \tilde{\xi}^U e^{-i\varphi} \sin\beta \\ \eta^D &= \frac{\sqrt{2}}{v} M^D = \tilde{\eta}^D \cos\beta + \tilde{\xi}^D e^{i\varphi} \sin\beta \end{aligned}$$

and

$$\begin{aligned} \xi^U &= -\tilde{\eta}^U \sin\beta + \tilde{\xi}^U e^{-i\varphi} \cos\beta \\ \xi^D &= -\tilde{\eta}^D \sin\beta + \tilde{\xi}^D e^{i\varphi} \cos\beta \end{aligned}$$

By a bi-unitary transformation involving the matrices

$$V_L^U, V_R^U, V_L^D \text{ and } V_R^D,$$

[1] This discussion can find out in a complete form in [61]. Here is considered again under multiple analyses carried out where FCNC's processes were involved.

the Yukawa parameters can be expressed in the mass basis of the fermions, where the (rescaled) mass matrices $\bar{\eta}^U$ and $\bar{\eta}^D$ are diagonal and real:

$$\begin{aligned}\bar{\eta}^U &= \frac{\sqrt{2}}{v}M^U = V_L^U \eta^U V_R^{U\dagger}, \quad M_{ij}^U = \delta_{ij} m_i^u \\ \bar{\eta}^D &= \frac{\sqrt{2}}{v}M^D = V_L^D \eta^D V_R^{D\dagger}, \quad M_{ij}^D = \delta_{ij} m_i^d\end{aligned}$$

and

$$\begin{aligned}\bar{\xi}^U &= V_L^U \xi^U V_R^{U\dagger} \\ \bar{\xi}^U &= V_L^D \xi^D V_R^{D\dagger}\end{aligned}$$

Finally, to convert the Lagrangian (C.1.2) into mass eigenstates we make the unitary transformations over singlets

$$\begin{aligned}D_{L,R} &= V_{L,R}^D D_{L,R}^0 \\ U_{L,R} &= V_{L,R}^U U_{L,R}^0\end{aligned}$$

When that bi-diagonalization is performed, the neutral flavor changing neutral couplings become

$$\mathcal{L}_{FCNC} = \bar{\xi}_{i,j}^U \bar{Q}_{iL} \tilde{H}_2 U_{jR} + \bar{\xi}_{i,j}^D \bar{Q}_{iL} H_2 D_{jR} + \bar{\xi}_{i,j}^E \bar{L}_{iL} H_2 E_{jR} + h.c$$

Since V_R is completely unknown and the $\widehat{\xi}$ are arbitrary, these $\xi^{U;D,L}$ coefficients are arbitrary. To look at specific processes, we make some assumptions about their magnitudes. The most outstanding feature of the fermion mass form is its hierarchical structure indeed. Hence the argument to impose a texture for FCNC scalar-mediated couplings is the following [91]: The flavor changing couplings should be of the order of the geometric mean of the Yukawa couplings of the two fermions. This fact is equivalent to

$$\xi_{ij} = \lambda_{ij} \frac{\sqrt{2 m_i m_j}}{v}$$

where $\lambda_{ij} \sim O(1)$. That fact is called the Sher-Cheng anzats. Since the most strict bounds on FCNC arise from the first two generations and this anzats especially suppresses the Yukawa couplings of those generations. Therefore, it is possible to write the Lagrangian (C.1.3) concerning its neutral current part in the fermion mass basis

$$-\mathcal{L}_{Y(\text{neutral})} = \frac{1}{\sqrt{2}}\sum_{i=1}^{3}\left[\eta_{ii}^D \bar{D}_{iL} D_{iR}\left(\phi_1^0\right) + \eta_{ii}^U \bar{U}_{iL} U_{iR}\left(\phi_1^0\right)^* + h.c.\right] + \frac{1}{\sqrt{2}}\sum_{i.j=1}^{3}\left[\xi_{ij}^D \bar{D}_{iL} D_{jR}\left(\phi_2^0\right) + \xi_{ij}^U \bar{U}_{iL} U_{jR}\left(\phi_2^0\right)^* + h.c.\right]$$

We have used the parametrization (C.1.1). On the other hand, the charged current part of the Lagrangian density in the fermion mass basis is

$$\begin{aligned}-\mathcal{L}_{Y(\text{charged})} = &\frac{1}{\sqrt{2}}\sum_{i=1}^{3}\left[\left(K\eta_{ij}^D\right)\bar{U}_{iL} D_{jR}\left(\phi_1^+\right) + \left(K\eta_{ij}^U\right)\bar{D}_{iL} U_{jR}\left(\phi_1^+\right)^* + h.c.\right] \\ &+ \frac{1}{\sqrt{2}}\sum_{i.j=1}^{3}\left[\left(K\xi_{ij}^D\right)\bar{U}_{iL} D_{jR}\left(\phi_2^+\right) + \left(K\xi_{ij}^U\right)\bar{D}_{iL} U_{jR}\left(\phi_2^+\right)^* + h.c.\right]\end{aligned}$$

V is the CKM matrix. These terms arise from

$$V_L^{D\dagger} V_L^D \tilde{\eta}_{i,j}^{D,0} V_R^{+D} V_R^D V_L^{U\dagger} V_L^U \bar{Q}_{iL}^0 \Phi_1' V_R^{D\dagger} V_R^D D_{jR}^0 = V_L^{D\dagger} \eta_{i,j}^D V_R^D V_L^{U\dagger} \bar{Q}_{iL} \Phi_1' V_R^{D\dagger} D_{jR}$$

After expanding the Lagrangian in the fundamental parametrization (CP-conserving frame) we get

$$\begin{aligned}-\mathcal{L}_Y = &\frac{g}{2M_w}\bar{D}M_D D\left(H^0\cos\alpha - h^0\sin\alpha\right) + \frac{1}{\sqrt{2}}\bar{D}\xi^D D\left(H^0\sin\alpha + h^0\cos\alpha\right) \\ &+\frac{g}{2M_w}\bar{U}M_U U\left(H^0\cos\alpha - h^0\sin\alpha\right) + \frac{1}{\sqrt{2}}\bar{U}\xi^U U\left(H^0\sin\alpha + h^0\cos\alpha\right) \\ &+\frac{i}{\sqrt{2}}\bar{D}\xi^D\gamma^5 D - \frac{i}{\sqrt{2}}\bar{U}\xi^U\gamma^5 U + \frac{ig}{2M_w}\bar{D}M_D\gamma^5 D G_z^0 - \frac{ig}{2M_w}\bar{U}M_D\gamma^5 U G_z^0 \\ &+\bar{U}\left(K\xi^D P_R - \xi^U K P_L\right) D H^+ + \bar{U}\left(K M_D P_R - M_U K P_L\right) D G_w^+ \\ &+\text{Leptonic sector} + h.c.\end{aligned}$$

D. Normal minimum and bilinears notation

D.1. Bilinears notation: Normal minimum

This appendix is devoted to defining the bilinear notation for Higgs potential and their important features as well as its importance finding vacuum structures. We now consider the case wherein $\lambda_6 \neq 0$, $\lambda_7 \neq 0$ and $\lambda_5 \neq 0$ with $\lambda_6, \lambda_{7,}\lambda_5 \in \mathbb{R}$. We describe the bilinear

$$x_1 = \left(\Phi_1^\dagger \Phi_1\right),\ x_2 = \left(\Phi_2^\dagger \Phi_2\right),\ x_3 = \frac{1}{2}\left(\Phi_1^\dagger \Phi_2 + \Phi_2^\dagger \Phi_1\right) \text{ and } x_4 = \frac{1}{2i}\left(\Phi_1^\dagger \Phi_2 - \Phi_2^\dagger \Phi_1\right). \tag{D.1.1}$$

Therefore, the most general Higgs potential renormalizable and gauge invariant is the following

$$\begin{aligned} V &= a_1 x_1 + a_2 x_2 + a_3 x_3 + a_4 x_4 + b_{11} x_1^2 + b_{22} x_2^2 + b_{33} x_3^2 + b_{44} x_4^2 \\ &\quad + b_{12} x_1 x_2 + b_{13} x_1 x_3 + b_{23} x_2 x_3 + b_{14} x_1 x_4 + b_{24} x_2 x_4 + b_{34} x_3 x_4. \end{aligned} \tag{D.1.2}$$

This potential has ten independent parameters. By renormalizability, the parameters a_i have mass dimension and the b_i ones are dimensionless. Moreover, the terms linear in x_4 are those that break CP explicitly. In a general way, we can parametrize the doublets present in the bilinear by

$$\Phi_1 = \begin{pmatrix} \phi_1 + i\phi_2 \\ \phi_3 + i\phi_4 \end{pmatrix} \text{ and } \Phi_2 = \begin{pmatrix} \phi_5 + i\phi_6 \\ \phi_7 + i\phi_8 \end{pmatrix}. \tag{D.1.3}$$

The fields ϕ_i inside doublets are real functions. From ϕ_i fields, bilinear can be decomposed as

$$x_1 = \left(\Phi_1^\dagger \Phi_1\right) = \phi_1^2 + \phi_2^2 + \phi_3^2 + \phi_4^2, \tag{D.1.4}$$

$$x_2 = \left(\Phi_2^\dagger \Phi_2\right) = \phi_5^2 + \phi_6^2 + \phi_7^2 + \phi_8^2, \tag{D.1.5}$$

$$x_3 = \mathrm{Re}\left(\Phi_1^\dagger \Phi_2\right) = \phi_1\phi_5 + \phi_2\phi_6 + \phi_3\phi_7 + \phi_4\phi_8, \tag{D.1.6}$$

$$x_4 = \mathrm{Im}\left(\Phi_1^\dagger \Phi_2\right) = \phi_1\phi_6 - \phi_2\phi_5 + \phi_3\phi_8 - \phi_4\phi_7. \tag{D.1.7}$$

Expanding the Higgs potential in terms of fields ϕ_i , we find out

$$\begin{aligned} V(\phi_i) &= a_1\left(\phi_1^2 + \phi_2^2 + \phi_3^2 + \phi_4^2\right) + a_2\left(\phi_5^2 + \phi_6^2 + \phi_7^2 + \phi_8^2\right) \\ &\quad + a_3\left(\phi_1\phi_5 + \phi_2\phi_6 + \phi_3\phi_7 + \phi_4\phi_8\right) + a_4\left(\phi_1\phi_6 - \phi_2\phi_5 + \phi_3\phi_8 - \phi_4\phi_7\right) \\ &\quad + b_{11}\left(\phi_1^2 + \phi_2^2 + \phi_3^2 + \phi_4^2\right)^2 + b_{22}\left(\phi_5^2 + \phi_6^2 + \phi_7^2 + \phi_8^2\right)^2 \\ &\quad + b_{33}\left(\phi_1\phi_5 + \phi_2\phi_6 + \phi_3\phi_7 + \phi_4\phi_8\right)^2 + b_{44}\left(\phi_1\phi_6 - \phi_2\phi_5 + \phi_3\phi_8 - \phi_4\phi_7\right)^2 \\ &\quad + b_{12}\left(\phi_1^2 + \phi_2^2 + \phi_3^2 + \phi_4^2\right)\left(\phi_5^2 + \phi_6^2 + \phi_7^2 + \phi_8^2\right) \\ &\quad + b_{13}\left(\phi_1^2 + \phi_2^2 + \phi_3^2 + \phi_4^2\right)\left(\phi_1\phi_5 + \phi_2\phi_6 + \phi_3\phi_7 + \phi_4\phi_8\right) \\ &\quad + b_{23}\left(\phi_5^2 + \phi_6^2 + \phi_7^2 + \phi_8^2\right)\left(\phi_1\phi_5 + \phi_2\phi_6 + \phi_3\phi_7 + \phi_4\phi_8\right) \\ &\quad + b_{14}\left(\phi_1^2 + \phi_2^2 + \phi_3^2 + \phi_4^2\right)\left(\phi_1\phi_6 - \phi_2\phi_5 + \phi_3\phi_8 - \phi_4\phi_7\right) \\ &\quad + b_{24}\left(\phi_5^2 + \phi_6^2 + \phi_7^2 + \phi_8^2\right)\left(\phi_1\phi_6 - \phi_2\phi_5 + \phi_3\phi_8 - \phi_4\phi_7\right) \\ &\quad + b_{34}\left(\phi_1\phi_5 + \phi_2\phi_6 + \phi_3\phi_7 + \phi_4\phi_8\right)\left(\phi_1\phi_6 - \phi_2\phi_5 + \phi_3\phi_8 - \phi_4\phi_7\right). \end{aligned} \tag{D.1.8}$$

We consider an notation that will be extremely useful. By defining a vector A and a square symmetric matrix B as

$$\mathcal{A} = \begin{pmatrix} a_1 \\ a_2 \\ a_3 \\ a_4 \end{pmatrix}, \quad \mathcal{B} = \begin{pmatrix} 2b_{11} & b_{12} & b_{13} & b_{14} \\ b_{12} & 2b_{22} & b_{23} & b_{24} \\ b_{13} & b_{23} & 2b_{33} & b_{34} \\ b_{14} & b_{24} & b_{34} & 2b_{44} \end{pmatrix}. \tag{D.1.9}$$

Defining a new four-vector

$$\mathcal{X} = \begin{pmatrix} x_1 \\ x_2 \\ x_3 \\ x_4 \end{pmatrix}. \tag{D.1.10}$$

We can write the Higgs potential (D.1.2) in a more compact form given by

$$\begin{aligned} V &= \mathcal{A}^T\mathcal{X} + \frac{1}{2}\mathcal{X}^T\mathcal{B}\mathcal{X}. \\ &= \begin{pmatrix} a_1 & a_2 & a_3 & a_4 \end{pmatrix} \begin{pmatrix} x_1 \\ x_2 \\ x_3 \\ x_4 \end{pmatrix}. \\ &\quad + \frac{1}{2} \begin{pmatrix} x_1 & x_2 & x_3 & x_4 \end{pmatrix} \begin{pmatrix} 2b_{11} & b_{12} & b_{13} & b_{14} \\ b_{12} & 2b_{22} & b_{23} & b_{24} \\ b_{13} & b_{23} & 2b_{33} & b_{34} \\ b_{14} & b_{24} & b_{34} & 2b_{44} \end{pmatrix} \begin{pmatrix} x_1 \\ x_2 \\ x_3 \\ x_4 \end{pmatrix}. \end{aligned} \tag{D.1.11}$$

E. Mass matrices

E.1. Generalities for Mass Matrices in 2HDM

The normal vacuum will be treated from the minimization conditions for the general Higgs potential, through

$$\begin{aligned} V = {} & a_1 x_1 + a_2 x_2 + a_3 x_3 + a_4 x_4 + b_{11} x_1^2 + b_{22} x_2^2 + b_{33} x_3^2 + b_{44} x_4^2 \\ & + b_{12} x_1 x_2 + b_{13} x_1 x_3 + b_{23} x_2 x_3 + b_{14} x_1 x_4 + b_{24} x_2 x_4 + b_{34} x_3 x_4, \end{aligned} \tag{E.1.1}$$

which in the minimum is

$$V|_{\text{min}} = a_1 v_1^2 + a_2 v_2^2 + a_3 v_1 v_2 + b_{11} v_1^4 + b_{22} v_2^4 + b_{33} v_1^2 v_2^2 + b_{12} v_1^2 v_2^2 + b_{13} v_1^3 v_2 + b_{23} v_2^3 v_1 \tag{E.1.2}$$

Hence

$$\frac{\partial V}{\partial v_1} = 2a_1 v_1 + a_3 v_2 + 4b_{11} v_1^3 + 2b_{33} v_1 v_2^2 + 2b_{12} v_1 v_2^2 + 3b_{13} v_1^2 v_2 + b_{23} v_2^3 = 0 \tag{E.1.3}$$

$$\frac{\partial V}{\partial v_2} = 2a_2 v_2 + a_3 v_1 + 4b_{22} v_2^3 + 2b_{33} v_1^2 v_2 + 2b_{12} v_1^2 v_2 + b_{13} v_1^3 + 3b_{23} v_2^2 v_1 = 0 \tag{E.1.4}$$

The normal vacua, with VEVs which do not have any complex relative phase and can thus be trivially rendered real:

$$\langle \Phi_1 \rangle = \frac{1}{\sqrt{2}} \begin{pmatrix} 0 \\ v_1 \end{pmatrix} \text{ and } \langle \Phi_2 \rangle = \frac{1}{\sqrt{2}} \begin{pmatrix} 0 \\ v_2 \end{pmatrix} \tag{E.1.5}$$

with $v = \sqrt{v_1^2 + v_2^2} = 246$ GeV. This solution is the 2HDM equivalent to SM vacuum indeed. We can distinguish a special case here, in which the minimization conditions allow for one of the VEVs to be zero. These are called inert models, which has been studied broadly in 5. Unlike the passage to the Higgs basis, where in one doublet acquire VEV zero, the inert vacua are found on the basis where a Z_2 (or perhaps a most restrictive $U(1)$-invariance) symmetry is manifest.

To determine the nature of the stationary points one must analyze the second derivatives of the potential, which is to say, the scalar squared mass matrices. They are given by

$$\left[M_{ij}^2\right] = \frac{\partial^2 V}{\partial \phi_i \partial \phi_j}$$

As is traditional, the Higgs potential is expanded in terms of fields ϕ_i

$$\begin{aligned} V = {} & a_1 \left(\phi_1^2 + \phi_2^2 + \phi_3^2 + \phi_4^2\right) + a_2 \left(\phi_5^2 + \phi_6^2 + \phi_7^2 + \phi_8^2\right) \\ + {} & a_3 \left(\phi_1\phi_5 + \phi_2\phi_6 + \phi_3\phi_7 + \phi_4\phi_8\right) + a_4 \left(\phi_1\phi_6 - \phi_2\phi_5 + \phi_3\phi_8 - \phi_4\phi_7\right) \\ & + b_{11} \left(\phi_1^2 + \phi_2^2 + \phi_3^2 + \phi_4^2\right)^2 + b_{22} \left(\phi_5^2 + \phi_6^2 + \phi_7^2 + \phi_8^2\right)^2 + b_{33} \left(\phi_1\phi_5 + \phi_2\phi_6 + \phi_3\phi_7 + \phi_4\phi_8\right)^2 \\ & + b_{44} \left(\phi_1\phi_6 - \phi_2\phi_5 + \phi_3\phi_8 - \phi_4\phi_7\right)^2 + b_{12} \left(\phi_1^2 + \phi_2^2 + \phi_3^2 + \phi_4^2\right) \left(\phi_5^2 + \phi_6^2 + \phi_7^2 + \phi_8^2\right) \\ & + b_{13} \left(\phi_1^2 + \phi_2^2 + \phi_3^2 + \phi_4^2\right) \left(\phi_1\phi_5 + \phi_2\phi_6 + \phi_3\phi_7 + \phi_4\phi_8\right) \\ & + b_{23} \left(\phi_5^2 + \phi_6^2 + \phi_7^2 + \phi_8^2\right) \left(\phi_1\phi_5 + \phi_2\phi_6 + \phi_3\phi_7 + \phi_4\phi_8\right) \\ & + b_{14} \left(\phi_1^2 + \phi_2^2 + \phi_3^2 + \phi_4^2\right) \left(\phi_1\phi_6 - \phi_2\phi_5 + \phi_3\phi_8 - \phi_4\phi_7\right) \\ & + b_{24} \left(\phi_5^2 + \phi_6^2 + \phi_7^2 + \phi_8^2\right) \left(\phi_1\phi_6 - \phi_2\phi_5 + \phi_3\phi_8 - \phi_4\phi_7\right) \\ & + b_{34} \left(\phi_1\phi_5 + \phi_2\phi_6 + \phi_3\phi_7 + \phi_4\phi_8\right) \left(\phi_1\phi_4 - \phi_2\phi_5 + \phi_3\phi_8 - \phi_4\phi_7\right) \end{aligned} \tag{E.1.6}$$

Therefore the mass matrix can be shown in the following way,

$$M^2 = \begin{pmatrix} M_{11}^2 & 0 & 0 & 0 & M_{15}^2 & M_{16}^2 & 0 & 0 \\ 0 & M_{22}^2 & 0 & 0 & M_{25}^2 & M_{26}^2 & 0 & 0 \\ 0 & 0 & M_{33}^2 & M_{34}^2 & 0 & 0 & M_{37}^2 & M_{38}^2 \\ 0 & 0 & M_{34}^2 & M_{44}^2 & 0 & 0 & M_{47}^2 & M_{48}^2 \\ M_{15}^2 & M_{25}^2 & 0 & 0 & M_{55}^2 & 0 & 0 & 0 \\ M_{16}^2 & M_{26}^2 & 0 & 0 & 0 & M_{66}^2 & 0 & 0 \\ 0 & 0 & M_{37}^2 & M_{47}^2 & 0 & 0 & M_{77}^2 & M_{78}^2 \\ 0 & 0 & M_{38}^2 & M_{48}^2 & 0 & 0 & M_{78}^2 & M_{88}^2 \end{pmatrix}$$

where all entries are given by

$$\begin{aligned} M_{78}^2 &= b_{24}v_1v_2 + 2b_{34}v_1^2 \\ M_{88}^2 &= a_2 + 2b_{22}v_2^2 + b_{44}v_1^2 + b_{12}v_1^2 + b_{23}v_1v_2 \\ M_{77}^2 &= a_2 + 2b_{22}v_2^2 + b_{33}v_1^2 + b_{12}v_1^2 + b_{23}v_1v_2 \\ M_{66}^2 &= a_2 + 2b_{22}v_2^2 + b_{12}v_1^2 + b_{23}v_1v_2 \\ M_{55}^2 &= a_2 + 2b_{22}v_2^2 + b_{12}v_1^2 + b_{23}v_1v_2 \\ M_{48}^2 &= a_3 + 2b_{33}v_1v_2 + b_{13}v_1^2 + b_{23}v_2^2 - 2b_{44}v_1v_2 \\ M_{47}^2 &= -a_4 - b_{14}v_1^2 - b_{24}v_2^2 - b_{34}v_1v_2 \\ M_{45}^2 &= 0 \\ M_{46}^2 &= 0 \end{aligned}$$

and

$$\begin{aligned} M_{54}^2 &= 0 \\ M_{11}^2 &= a_1 + 2b_{11}v_1^2 + b_{12}v_2^2 + b_{13}v_1v_2,\ M_{12}^2 = 0,\ M_{13}^2 = 0,\ M_{14}^2 = 0 \\ M_{15}^2 &= a_3 + b_{13}v_1^2 + b_{23}v_2^2 + 2b_{33}v_1v_2,\ M_{16}^2 = a_4 + b_{14}v_1^2 + b_{24}v_2^2,\ M_{17}^2 = 0,\ M_{18}^2 = 0 \\ M_{21}^2 &= 0,\ M_{22}^2 = a_1 + 2b_{11}v_1^2 + b_{12}v_2^2 + b_{13}v_1v_2,\ M_{23}^2 = 0,\ M_{24}^2 = 0 \\ M_{25}^2 &= -a_4 - b_{14}v_1^2 - b_{24}v_2^2 - b_{34}v_1v_2,\ M_{26}^2 = a_3 + 2b_{33}v_1v_2 + b_{13}v_1^2 + b_{23}v_2^2,\ M_{27}^2 = 0,\ M_{28}^2 = 0 \\ M_{31}^2 &= 0,\ M_{32}^2 = 0,\ M_{33}^2 = a_1 + 2b_{11}v_1^2 + b_{12}v_2^2 + b_{13}v_1v_2,\ M_{34}^2 = -b_{14}v_1v_2 - b_{34}v_2^2 \\ M_{35}^2 &= 0,\ M_{36}^2 = 0,\ M_{37}^2 = a_3 + 2b_{33}v_1v_2 + 2b_{12}v_1v_2 + b_{13}v_1^2 + b_{23}v_2^2,\ M_{38}^2 = b_{14}v_1^2 + b_{24}v_2^2 + b_{34}v_1v_2 \\ M_{41}^2 &= 0,\ M_{42}^2 = 0,\ M_{43}^2 = M_{34}^2 = -b_{14}v_1v_2 - b_{34}v_2^2,\ M_{44}^2 = a_1 + 2b_{11}v_1^2 + b_{12}v_2^2 + b_{13}v_1v_2 \end{aligned} \tag{E.1.7}$$

E.1.1. Extension a VEV in Complex Components: Spontaneous CP Violation

We use another method to obtain the mass matrix. The second derivatives of the potential can be written by using Fa di Bruno's formula [201]

$$\frac{\partial^2 V}{\partial\phi_i\partial\phi_j} = \sum_k \frac{\partial V}{\partial x_k}\frac{\partial^2 x_k}{\partial\phi_i\partial\phi_j} + \sum_{k,l}\frac{\partial^2 V}{\partial x_k\partial x_l}\frac{\partial x_k}{\partial\phi_i}\frac{\partial x_l}{\partial\phi_j} \tag{E.1.8}$$

We again define

$$V_i' = \frac{\partial V}{\partial x_i} \tag{E.1.9}$$

The first term in (E.1.8) is written as an 8×8 matrix of the form

$$M^2 = \begin{pmatrix} M_{11}^2 & 0 \\ 0 & M_{12}^2 \end{pmatrix} \tag{E.1.10}$$

With M_{11}^2 a 4×4 matrix, which comes from

$$\sum_k \frac{\partial V}{\partial x_k}\frac{\partial^2 x_k}{\partial\phi_i\partial\phi_j} = V_1'\frac{\partial^2 x_1}{\partial\phi_i\partial\phi_j} + V_2'\frac{\partial^2 x_2}{\partial\phi_i\partial\phi_j} + V_3'\frac{\partial^2 x_3}{\partial\phi_i\partial\phi_j} + V_4'\frac{\partial^2 x_4}{\partial\phi_i\partial\phi_j} \tag{E.1.11}$$

Remembering bilinear form in terms of ϕ_i-fields

$$\begin{aligned} x_1 &= \left(\Phi_1^\dagger \Phi_1\right) = \phi_1^2 + \phi_2^2 + \phi_3^2 + \phi_4^2 \\ x_2 &= \left(\Phi_2^\dagger \Phi_2\right) = \phi_5^2 + \phi_6^2 + \phi_7^2 + \phi_8^2 \\ x_3 &= \mathrm{Re}\left(\Phi_1^\dagger \Phi_2\right) = \phi_1\phi_5 + \phi_2\phi_6 + \phi_3\phi_7 + \phi_4\phi_8 \\ x_4 &= \mathrm{Im}\left(\Phi_1^\dagger \Phi_2\right) = \phi_1\phi_6 - \phi_2\phi_5 + \phi_3\phi_8 - \phi_4\phi_7 \end{aligned} \tag{E.1.12}$$

From these relations, it is possible to get

$$\begin{aligned} M_{11}^2 &= V_1' \frac{\partial^2 x_1}{\partial\phi_1\partial\phi_1} = 2V_1' \\ M_{12}^2 &= V_1' \frac{\partial^2 x_1}{\partial\phi_1\partial\phi_2} = 0 \\ M_{15}^2 &= V_3' \frac{\partial^2 x_3}{\partial\phi_1\partial\phi_5} = V_3' \\ M_{15}^2 &= V_4' \frac{\partial^2 x_4}{\partial\phi_1\partial\phi_6} = V_4' \\ M_{22}^2 &= V_1' \frac{\partial^2 x_1}{\partial\phi_2\partial\phi_2} = 2V_1' \\ M_{25}^2 &= V_4' \frac{\partial^2 x_4}{\partial\phi_2\partial\phi_5} = -V_4' \\ M_{26}^2 &= V_3' \frac{\partial^2 x_3}{\partial\phi_2\partial\phi_6} = V_3' \\ M_{55}^2 &= V_2' \frac{\partial^2 x_2}{\partial\phi_5\partial\phi_5} = 2V_2' \\ M_{66}^2 &= V_2' \frac{\partial^2 x_2}{\partial\phi_6\partial\phi_6} = 2V_2' \end{aligned} \tag{E.1.13}$$

These elements are the associated to the charged part of the doublets. We can arrange these components in the next submatrix

$$M_{H^\pm}^2 = \frac{1}{2}\begin{pmatrix} 2V_1' & 0 & V_3' & V_4' \\ 0 & 2V_1' & -V_4' & V_3' \\ V_3' & -V_4' & 2V_2' & 0 \\ V_4' & V_3' & 0 & 2V_2' \end{pmatrix} \tag{E.1.14}$$

The eigenvalues are:

$${}^0\lambda_1 = \frac{1}{2}\left(V_1' + V_2'\right) + \frac{1}{2}\sqrt{(V_1')^2 - 2V_1'V_2' + (V_2')^2 + (V_3')^2 + (V_4')^2}, \tag{E.1.15}$$

$${}^0\lambda_2 = \frac{1}{2}\left(V_1' + V_2'\right) - \frac{1}{2}\sqrt{(V_1')^2 - 2V_1'V_2' + (V_2')^2 + (V_3')^2 + (V_4')^2} \tag{E.1.16}$$

From (F.1.11) for a normal minimum, $V_4' = 0$, and from

$$4V_2'V_1' = 4V_3'\frac{v_2}{2v_1}V_3'\frac{v_1}{2v_2} = \left(V_3'\right)^2$$

The eigenvalues acquire the form

$$\lambda' = \left(V_1' + V_2'\right),\ \lambda'' = 0$$

The second degenerate eigenvalue corresponds to the Goldstone Bosons $G^\pm$. We can see that the non-zero eigenvalue of this matrix is $M_{H^\pm}^2$

$$M_{H^\pm}^2 = V_1' + V_2' = V_3'\frac{v_2}{2v_1} + V_3'\frac{v_1}{2v_2} = \frac{1}{2}\frac{V_3'}{v_1v_2}\left(v_1^2 + v_2^2\right) = \frac{1}{2}\frac{V_3'}{v_1v_2}v^2$$

If N_1 is a minimum, then all of the squared scalar masses are positive, and so this quantity is also positive.

We know to focus on the minima N_2. A priori there is no reason why the 2HDM potential cannot have, simultaneously, both "normal"minima, so the question arises, can the potential be in an N_2 minimum that is not deeper than a CB stationary point? The answer is no, and the demonstration follows very closely the one we just concluded. Returning to (E.1.14), and by using (F.1.11)

$$V' = -\frac{V_3'}{2v_1'v_2'}\begin{pmatrix} v_2^{'2} \\ v_1^{'2}+\delta^2 \\ -2v_1'v_2' \\ 2\delta v_2' \end{pmatrix} \tag{E.1.17}$$

$$M^2_{H^\pm} = \frac{1}{2}\begin{pmatrix} 2V_1' & 0 & V_3' & V_4' \\ 0 & 2V_1' & -V_4' & V_3' \\ V_3' & -V_4' & 2V_2' & 0 \\ V_4' & V_3' & 0 & 2V_2' \end{pmatrix} \tag{E.1.18}$$

The first eigenvalue (the non trivial one) in Eq. (E.1.15) is given by

$$\begin{aligned}
&\frac{1}{2}V_1' + \frac{1}{2}V_2' + \frac{1}{2}\sqrt{(V_1')^2 - 2V_1'V_2' + (V_2')^2 + (V_3')^2 + (V_4')^2} = \\
&= -\frac{V_3'}{4v_1'v_2'}\left(v_2^{'2} + v_1^{'2} + \delta^2 + \sqrt{(v_2^{'2})^2 - 2v_2^{'2}\left(v_1^{'2}+\delta^2\right) + (v_1^{'2}+\delta^2)^2 + (2v_1'v_2')^2 + (2\delta v_2')^2}\right) \\
&= -\frac{V_3'}{4v_1'v_2'}\left(v_2^{'2} + v_1^{'2} + \delta^2 + \sqrt{(v_2^{'2})^2 + 2v_2^{'2}\left(v_1^{'2}+\delta^2\right) + (v_1^{'2}+\delta^2)^2}\right) \\
&= -\frac{V_3'}{4v_1'v_2'}\left(v_2^{'2} + v_1^{'2} + \delta^2 + (v_1^{'2} + v_2^{'2} + \delta^2)\right) \\
&= -\frac{V_3'}{2v_1'v_2'}v^{'2}
\end{aligned}$$

with $v'^2 = v_2^{'2} + v_1^{'2} + \delta^2$. Hence

$$M^2_{H^\pm} = -\frac{V_3'}{2v_1'v_2'}v^{'2} \tag{E.1.19}$$

$$\left(\frac{M^2_{H^\pm}}{v^{'2}}\right)_{N_1} = -\frac{V_3'}{2v_1'v_2'} \tag{E.1.20}$$

F. Metastability Theorems

F.1. Metastability theorems and vacuum structures

From bilinear notation presented in Appendix D is straightforward to show as metastable states arise in the minima of the Higgs potential. This appendix is dedicated to studying the parameter space related with this behavior in the Higgs potential employing different theorems related to the possible existence of several minima from stationary conditions. Indeed, we based this appendix in an extension of the article [202].

Theorem 1 *If one of the normal minima exists, it is certainly deeper than the charge or CP breaking ones.*

Proof: Let be V' a vector defined by its components

$$V'_i = \left.\frac{\partial V}{\partial x_i}\right|_{N_1} . \tag{F.1.1}$$

evaluated in the N_1 minimum. At N_1 the non-zero vevs are

$$\phi_3 = v_1,\ \phi_7 = v_2 \tag{F.1.2}$$

Equivalently, the normal minimum is located inside doublets in

$$\langle 0\,|\phi_3|\,0\rangle = v_1,\ \ \langle 0\,|\phi_7|\,0\rangle = v_2,\ \text{and}\ \ \langle 0\,|\phi_i|\,0\rangle = 0 \text{ for } i \neq 3,7 \tag{F.1.3}$$

From above definitions of bilinear x_i in Eq. (D.1.1)

$$x_1|_{\min} = v_1^2\ ,\ \ x_2|_{\min} = v_2^2,\ \ x_3|_{\min} = v_1 v_2 \text{ and } \ x_4|_{\min} = 0. \tag{F.1.4}$$

From VEVs, we can write the relevant minimization conditions as

$$\frac{\partial V}{\partial v_1} = \frac{\partial V}{\partial x_1}\frac{\partial x_1}{\partial v_1} + \frac{\partial V}{\partial x_3}\frac{\partial x_3}{\partial v_1} = 0 \tag{F.1.5}$$

$$\frac{\partial V}{\partial v_2} = \frac{\partial V}{\partial x_2}\frac{\partial x_2}{\partial v_2} + \frac{\partial V}{\partial x_3}\frac{\partial x_3}{\partial v_2} = 0 \tag{F.1.6}$$

Explicitly the vector V' of Eq. (F.1.1), with tadpoles at tree level as components, is given by,

$$V' = \begin{pmatrix} V'_1 \\ V'_2 \\ V'_3 \\ V'_4 \end{pmatrix} = \left.\begin{pmatrix} \frac{\partial V}{\partial x_1} \\ \frac{\partial V}{\partial x_2} \\ \frac{\partial V}{\partial x_3} \\ \frac{\partial V}{\partial x_4} \end{pmatrix}\right._{\langle 0\,|\phi_3|\,0\rangle = v_1,\ \langle 0\,|\phi_7|\,0\rangle = v_2} \tag{F.1.7}$$

Hence, from (F.1.5)-(F.1.6) we have in the respective tadpoles

$$V'_1 = -V'_3\frac{v_2}{2v_1} \tag{F.1.8}$$

$$V'_2 = -V'_3\frac{v_1}{2v_2} \tag{F.1.9}$$

$$V'_4 = 0 \tag{F.1.10}$$

In fact we can arrange the vector V' of Eq. (F.1.7)

$$V' = -\frac{V_3'}{2v_1v_2}\begin{pmatrix} v_2^2 \\ v_1^2 \\ -2v_1v_2 \\ 0 \end{pmatrix} \tag{F.1.11}$$

Therefore V_1' and V_2' have the same sign. Hereafter we will use $\mathcal{X}_{N_1}$ to designate the vector $\mathcal{X}$ evaluated at the minimum N_1, that is,

$$\mathcal{X}_{N_1} = \begin{pmatrix} v_1^2 \\ v_2^2 \\ v_1v_2 \\ 0 \end{pmatrix}. \tag{F.1.12}$$

We can verify easily the relation

$$\mathcal{X}_{N_1}^T V' = -\frac{V_3'}{2v_1v_2}\begin{pmatrix} v_1^2 & v_2^2 & v_1v_2 & 0 \end{pmatrix}\begin{pmatrix} v_2^2 \\ v_1^2 \\ -2v_1v_2 \\ 0 \end{pmatrix} = 0. \tag{F.1.13}$$

Direct analysis of the potential (D.1.2) also shows that we can write V' in matrix form as

$$V' = \mathcal{A} + \mathcal{B}\mathcal{X}_{N_1}, \tag{F.1.14}$$

$$= \begin{pmatrix} a_1 & a_2 & a_3 & 0 \end{pmatrix} + \begin{pmatrix} 2b_{11} & b_{12} & b_{13} & 0 \\ b_{12} & 2b_{22} & b_{23} & 0 \\ b_{13} & b_{23} & 2b_{33} & 0 \\ 0 & 0 & 0 & 2b_{44} \end{pmatrix}\begin{pmatrix} v_1^2 \\ v_2^2 \\ v_1v_2 \\ 0 \end{pmatrix}. \tag{F.1.15}$$

The potential (D.1.2) is a sum of quadratic and quartic polynomials,

$$V = V_2 + V_4 \tag{F.1.16}$$

By performing the sum with the minimization conditions

$$V|_{\min} = a_1v_1^2 + a_2v_2^2 + a_3v_1v_2 + b_{11}v_1^4 + b_{22}v_2^4 + b_{33}v_1^2v_2^2 + b_{12}v_1^2v_2^2 + b_{13}v_1^3v_2 + b_{23}v_2^3v_1 \tag{F.1.17}$$

Driven out to stationary conditions behave as

$$v_1\frac{\partial V}{\partial v_1} = 2a_1v_1^2 + a_3v_2v_1 + 4b_{11}v_1^4 + 2b_{33}v_1^2v_2^2 + 2b_{12}v_1^2v_2^2 + 3b_{13}v_1^3v_2 + b_{23}v_2^3v_1, \tag{F.1.18}$$

$$v_2\frac{\partial V}{\partial v_2} = 2a_2v_2^2 + a_3v_1v_2 + 4b_{22}v_2^4 + 2b_{33}v_1^2v_2^2 + 2b_{12}v_1^2v_2^2 + b_{13}v_1^3v_2 + 3b_{23}v_2^3v_1,$$

$$v_1\frac{\partial V}{\partial v_1} + v_2\frac{\partial V}{\partial v_2} = 2\left(a_1v_1^2 + a_2v_2^2 + a_3v_1v_2\right) \tag{F.1.19}$$

$$+4\left(b_{11}v_1^4 + b_{22}v_2^4 + b_{33}v_1^2v_2^2 + b_{12}v_1^2v_2^2 + b_{13}v_1^3v_2 + b_{23}v_2^3v_1\right) = 0. \tag{F.1.20}$$

From the last relation, minimum condition implies that

$$2\,V_2|_{\min} + 4V_4|_{\min} = 0. \tag{F.1.21}$$

The Higgs potential is

$$V_{N_1} \equiv V|_{\min} = A^T\mathcal{X}_{N_1} + \frac{1}{2}\mathcal{X}_{N_1}^T B\mathcal{X}_{N_1} = A^T\mathcal{X}_{N_1} - \frac{1}{2}A^T\mathcal{X}_{N_1} = \frac{1}{2}A^T\mathcal{X}_{N_1} \tag{F.1.22}$$

$$V_{N_1} \equiv V|_{\min} = -\mathcal{X}_{N_1}^T B\mathcal{X}_{N_1} + \frac{1}{2}\mathcal{X}_{N_1}^T B\mathcal{X}_{N_1} = -\frac{1}{2}\mathcal{X}_{N_1}^T B\mathcal{X}_{N_1}. \tag{F.1.23}$$

It is primary to point out that although we have been considering the normal minimum, it is clear that the conditions (F.1.5) and (F.1.6) only assure that the potential has a stationary point. To encourage a minimum in the theory, we must analyze the second derivatives of V, i.e., the matrix of the squared scalar masses. After, we reject all combinations of parameters with structure $\{a_i, b_{jk}\}$ for which any of the non-zero eigenvalues are negative (this matrix has three zero eigenvalues corresponding to the Goldstone bosons, see Appendix E). Mainly, the charged Higgs mass obtained in Eq. (E.1.20), satisfy

$$m^2_{H^\pm} = V_1' + V_2' > 0 \tag{F.1.24}$$

Being the last condition a necessary one for the existence of a normal minimum. Additionally, we have shown that V_1' and V_2' have the same sign. Thus both are positive in fact. Therefore for tadpole at tree level labeled by 1

$$V_1' = \left(-\frac{V_3'}{2v_1v_2}\right) v_2^2 > 0 \tag{F.1.25}$$

Being the quantity in parenthesis a positive quantity. This procedure will be substantial in our demonstrations.

F.2. Charge breaking minima

For a charge breaking minimum, the fields with non-zero VEVs are given by

$$\phi_3 = w_1, \quad \phi_7 = w_2 \text{ and } \phi_5 = \alpha \tag{F.2.1}$$

Defining the $\mathcal{Y}$ to be equal to the vector $\mathcal{X}$ evaluated in this configuration for minimum

$$\mathcal{Y} = \begin{pmatrix} w_1^2 \\ w_2^2 + \alpha^2 \\ w_1 w_2 \\ 0 \end{pmatrix} \tag{F.2.2}$$

Stationary conditions are now translated into the following tadpoles at tree level

$$\frac{\partial V}{\partial w_1} = 0 \leftrightarrow \frac{\partial V}{\partial x_1}\frac{\partial x_1}{\partial w_1} + \frac{\partial V}{\partial x_3}\frac{\partial x_3}{\partial w_1} \leftrightarrow V_1' = -V_3' \frac{\frac{\partial x_3}{\partial w_1}}{\frac{\partial x_1}{\partial w_1}} = -V_3' \frac{w_2}{2w_1} \tag{F.2.3}$$

$$\frac{\partial V}{\partial w_2} = 0 \leftrightarrow \frac{\partial V}{\partial x_2}\frac{\partial x_2}{\partial w_2} + \frac{\partial V}{\partial x_3}\frac{\partial x_3}{\partial w_2} \leftrightarrow V_2' = -V_3' \frac{\frac{\partial x_3}{\partial w_2}}{\frac{\partial x_2}{\partial w_2}} = -V_3' \frac{w_1}{2w_2} \tag{F.2.4}$$

For charge and CP breaking VEVs

$$\frac{\partial V}{\partial \alpha} = 0 \leftrightarrow V_2' \frac{\partial x_2}{\partial \alpha} = 0 \leftrightarrow V_2' = 0 \tag{F.2.5}$$

$$\frac{\partial V}{\partial \phi_4} = 0 \leftrightarrow \frac{\partial V}{\partial x_4}\frac{\partial x_4}{\partial \phi_4} = 0 \leftrightarrow V_4' = 0 \tag{F.2.6}$$

Thus, in CB stationary point $V_i' = 0$. The equation determining Y is simply

$$\mathcal{A} + \mathcal{B}\mathcal{Y} = 0. \tag{F.2.7}$$

This linear relation implies that if CB stationary point exists, this is unique. This behavior for a CB stationary point is a clear difference with the normal vacuum, because, from the second case the extremal conditions (F.1.18)-(F.1.19)

yield two cubic equations, which in principle lead multiple solutions. Returning to CB case and using the fact $\mathcal{B}$ is invertible, linear relation (F.2.7) implies

$$\mathcal{Y} = -\mathcal{B}^{-1}\mathcal{A}. \tag{F.2.8}$$

Also, to CB stationary exist two first component in $\mathcal{Y}$ must be positive. Nevertheless, not all choices of A and B will yield a result as given in (F.2.8). The last fact can be demonstrated from Minkowskian treatment of the Higgs potential considered extensively in section 2.4.

As was shown in the previous part, in the minimum Higgs potential in its respective quadratic and quartic parts satisfies

$$2\ V_2|_{min} + 4\ V_4|_{min} = 0. \tag{F.2.9}$$

Designating V_{CB} as the Higgs potential evaluated in the CB minimum

$$V_{CB} = V|_{min} = \mathcal{A}^T\mathcal{Y}_{CB} + \frac{1}{2}\mathcal{Y}_{CB}^T B\mathcal{Y}_{CB} = A^T\mathcal{Y}_{CB} - \frac{1}{2}\mathcal{A}^T\mathcal{Y}_{CB} = \frac{1}{2}\mathcal{A}^T\mathcal{Y}_{CB} \tag{F.2.10}$$

We have used Eq. (F.2.9). Equivalently in terms of the quartic part

$$V_{CB} = V|_{min} = \mathcal{A}^T\mathcal{Y}_{CB} + \frac{1}{2}\mathcal{Y}_{CB}^T B\mathcal{Y}_{CB} = -\mathcal{Y}_{CB}^T B\mathcal{Y}_{CB} + \frac{1}{2}\mathcal{Y}_{CB}^T B\mathcal{Y}_{CB} = -\frac{1}{2}\mathcal{Y}_{CB}^T B\mathcal{Y}_{CB} \tag{F.2.11}$$

Tadpoles matrix behaves according to neutral vacuum considered in Eq. (F.1.12)

$$V' = \mathcal{A} + \mathcal{B}\mathcal{X}_N = -\mathcal{B}\mathcal{Y} + B\mathcal{X}_N \tag{F.2.12}$$

Orthogonality properties over neutral minima, quoted in Eq. (F.1.13), given by $\mathcal{X}_N^T V' = 0$, apply in (F.2.12) as

$$\mathcal{X}_N^T V' = -\mathcal{X}_N^T\mathcal{B}\mathcal{Y} + \mathcal{X}_N^T B\mathcal{X}_N = 0 \tag{F.2.13}$$

Which is equivalent to

$$\mathcal{X}_N^T\mathcal{B}\mathcal{Y} = \mathcal{X}_N^T B\mathcal{X}_N = -2V_N. \tag{F.2.14}$$

In the last step, we have used (F.1.23). In the same way, we can compute from (F.2.12)

$$\mathcal{Y}^T V' = -\mathcal{Y}^T\mathcal{B}\mathcal{Y} + \mathcal{Y}^T\mathcal{B}\mathcal{X}_N \tag{F.2.15}$$

With this, it is possible to build up

$$\mathcal{Y}^T\mathcal{B}\mathcal{Y} = -2V_{CB}. \tag{F.2.16}$$

In the same way for the neutral case, we have used (F.2.11). Computing the difference between both potentials given by (F.2.14) and (F.2.16) in the minima, we find out

$$\mathcal{Y}^T V' = -\mathcal{Y}^T\mathcal{B}\mathcal{Y} + \mathcal{Y}^T\mathcal{B}\mathcal{X}_N = 2V_{CB} - 2V_N \tag{F.2.17}$$

In the last relation, $\mathcal{B}$ matrix-invertibility property has been applied. Finally, all is translated into

$$V_{CB} - V_N = \frac{1}{2}\mathcal{Y}^T V' = \frac{1}{2}\begin{pmatrix} w_1^2 & w_2^2+\alpha^2 & w_1 w_2 & 0 \end{pmatrix}\begin{pmatrix} V_1' \\ V_2' \\ V_3' \\ V_4 \end{pmatrix} \tag{F.2.18}$$

V_i' components behave as

$$V' = -\frac{V_3'}{2\omega_1\omega_2}\begin{pmatrix} v_2^2 \\ v_1^2 \\ v_1 v_2 \\ 0 \end{pmatrix} \tag{F.2.19}$$

The product is thus

$$-\frac{1}{2}\frac{V_3'}{2v_1v_2}\begin{pmatrix} w_1^2 & w_2^2+\alpha^2 & w_1 w_2 & 0 \end{pmatrix}\begin{pmatrix} v_2^2 \\ v_1^2 \\ -2v_1v_2 \\ 0 \end{pmatrix} = -\frac{1}{2}\frac{V_3'}{2v_1v_2}\left[w_1^2v_2^2 + w_2^2v_1^2 + v_1^2\alpha^2 - 2v_1v_2w_2w_1\right] \tag{F.2.20}$$

Charged Higgs mass is defined in the normal vacua, quoting (E.1.20),

$$V_{CB} - V_N = \frac{1}{2}\left(\frac{m_{H^\pm}^2}{v^2}\right)\left[(w_1v_2 - w_2v_1)^2 + v_1^2\alpha^2\right] \tag{F.2.21}$$

This relation has worth consequences:

- If N_1 is a minimum of the theory, CB stationary points are located above of N_1. N_1 is thus the global minimum of the theory.
- Potential positivity ensures to CB stationary point to be a saddle point.

F.3. CP breaking minimum

By following a similar procedure, we can consider stationary points associated to one CP breaking minimum. In this case, let $\mathcal{Z}_{CP}$ be the $\mathcal{X}$ vector defined in the vacua

$$\phi_3 = z_1, \quad \phi_4 = \delta, \quad \phi_7 = z_2. \tag{F.3.1}$$

using

$$\mathcal{Z}_{CP} = \begin{pmatrix} z_1^2 + \delta^2 \\ z_2^2 \\ z_1 z_2 \\ 0 \end{pmatrix}. \tag{F.3.2}$$

Thus, calculating the Higgs potential in the stationary point and using uniqueness solution for this configuration, is possible arrives to

$$V_{CP} - V_N = \frac{1}{2}Z_{CP}^T V' = -\left(\frac{V_3'}{2v_1v_2}\right)\left[(z_1v_2 - z_2'v_1)^2 + \delta^2 v_2^2\right]. \tag{F.3.3}$$

Since Eq. (F.1.25) is possible to conclude

$$V_{CP} - V_N > 0 \tag{F.3.4}$$

In other words, the normal vacuum is always deeper that the CP- breaking stationary point is. The matrix of quartic couplings $\mathcal{B}_{CP}$ is not positive definite, implying that CP extremal point is necessarily a saddle point [67, 202].

F.4. Two normal vacua

Perhaps ambiguity to define the global minimum in the theory is the most interesting feature present in the vacuum of the general extended Higgs sectors models. This fact describes the possibility of having two possible vacua N_1-N_2 states compatible with gauge foundations of the theory. Unfortunately, we cannot apply the procedure gotten so far to realize whether one of the both minima is deeper than the other. Nevertheless, it is possible to point out structure of the difference of Higgs potential in both minima [202]

$$V_{N_2} - V_{N_1} = \frac{1}{2}\left[\left(\frac{m^2_{H^\pm}}{v^2}\right)^2_{N_1} - \left(\frac{m^2_{H^\pm}}{v^2}\right)^2_{N_2}\right]\left[\left(v_1' v_2 - v_2' v_1\right)^2\right]. \tag{F.4.1}$$

where v_1' and v_2' are VEVs in the second minima N_2, meanwhile v_1, v_2 are VEVs defined in the first minimum N_1. We can extract the following features from (F.4.1)

- Nothing define the overall sign in the difference, $V_{N_2} - V_{N_1}$. Thus, it is impossible to say, in this stage, which is the deeper minimum.
- We have excluded the possibility of one vacuum has spontaneous CP violation. However, this relation can describe for this additional structure of the vacuum. In this case, it is also impossible to determine whether one minimum is the truth vacuum state of the theory.

G. Minkowskian properties of the Higgs Potential: Diagonalization of $\Lambda^{\mu\nu}$

G.1. Generalities

Reparameterization invariance of the Higgs potential drive out to new interesting features for field and parameter spaces for Higgs potential in 2HDMs. In this appendix, we treat with the properties and definitions of four-dimensional formalism focusing in positivity conditions over the $SO(1,3)$ invariant Higgs potential

$$V = -M_\mu r^\mu + \frac{1}{2}\Lambda_{\mu\nu} r^\mu r^\nu,$$

where gauge orbit space is defined by the cuadrivector

$$r_\mu = (r_0, r_1, r_2, r_3) = \left(\Phi_1^\dagger\Phi_1 + \Phi_2^\dagger\Phi_2, 2\mathrm{Re}\left(\Phi_1^\dagger\Phi_2\right), 2\mathrm{Im}\left(\Phi_1^\dagger\Phi_2\right), \Phi_1^\dagger\Phi_1 - \Phi_2^\dagger\Phi_2\right). \tag{G.1.1}$$

From the general Higgs potential 2.3.1, rank one and two components are defined by

$$M_\mu = \left(-\frac{m_{11}^2 + m_{22}^2}{2}, \mathrm{Re}\left(m_{12}^2\right), -\mathrm{Im}\left(m_{12}^2\right), -\frac{m_{11}^2 - m_{22}^2}{2}\right), \tag{G.1.2}$$

$$\Lambda^{\mu\nu} = \frac{1}{2}\begin{pmatrix} \frac{\lambda_1+\lambda_2}{2} + \lambda_3 & -\mathrm{Re}\left(\lambda_6+\lambda_7\right) & \mathrm{Im}\left(\lambda_6+\lambda_7\right) & -\frac{\lambda_1+\lambda_2}{2} \\ -\mathrm{Re}\left(\lambda_6+\lambda_7\right) & \lambda_4 + \mathrm{Re}\lambda_5 & -\mathrm{Im}\lambda_5 & \mathrm{Re}\left(\lambda_6-\lambda_7\right) \\ \mathrm{Im}\left(\lambda_6+\lambda_7\right) & -\mathrm{Im}\lambda_5 & \lambda_4 - \mathrm{Re}\lambda_5 & -\mathrm{Im}\left(\lambda_6-\lambda_7\right) \\ -\frac{\lambda_1+\lambda_2}{2} & -\mathrm{Re}\left(\lambda_6-\lambda_7\right) & -\mathrm{Im}\left(\lambda_6-\lambda_7\right) & \frac{\lambda_1+\lambda_2}{2} - \lambda_3 \end{pmatrix} \tag{G.1.3}$$

The mixed tensor, which is important in our discussion, is given by

$$\Lambda_E = \Lambda^\mu{}_\nu = \frac{1}{2}\begin{pmatrix} \frac{1}{2}\left(\lambda_1+\lambda_2\right) + \lambda_3 & \mathrm{Re}\left(\lambda_6+\lambda_7\right) & -\mathrm{Im}\left(\lambda_6+\lambda_7\right) & \frac{1}{2}\left(\lambda_1-\lambda_2\right) \\ -\mathrm{Re}\left(\lambda_6+\lambda_7\right) & -\lambda_4 - \mathrm{Re}\left(\lambda_5\right) & \mathrm{Im}\left(\lambda_5\right) & -\mathrm{Re}\left(\lambda_6-\lambda_7\right) \\ \mathrm{Im}\left(\lambda_6+\lambda_7\right) & \mathrm{Im}\left(\lambda_5\right) & -\lambda_4 + \mathrm{Re}\left(\lambda_5\right) & \mathrm{Im}\left(\lambda_6-\lambda_7\right) \\ -\frac{1}{2}\left(\lambda_1-\lambda_2\right) & -\mathrm{Re}\left(\lambda_6-\lambda_7\right) & \mathrm{Im}\left(\lambda_6-\lambda_7\right) & -\frac{1}{2}\left(\lambda_1+\lambda_2\right) + \lambda_3 \end{pmatrix} \tag{G.1.4}$$

From these definitions, this appendix is devoted to showing the properties to get a bounded from below Higgs potential. Moreover, the same formalism leads us to demonstrate properties of charge breaking minima in 2HDMs. Finally, these developments will be used to study the metastability in the Higgs potential in Appendix F.

G.2. Higgs potential behavior

We first show some basic facts on diagonalization of the real symmetric tensor $\Lambda^{\mu\nu}$ in the Minkowski space following [36]. $\Lambda^{\mu\nu}$ can be viewed as an operator acting on vectors in the Minkowski space. The (right) eigenvector p^μ with eigenvalue Λ satisfy

$$\begin{aligned} \Lambda^{\mu\rho} g_{\rho\nu} v^\nu &= \Lambda p^\mu, \\ \Lambda^\mu{}_\nu v^\nu &= \Lambda p^\mu. \end{aligned} \tag{G.2.1}$$

Thus the characteristic equation for the eigenvalues is

$$\begin{aligned} \det(\Lambda^{\mu\rho} g_{\rho\nu} - \Lambda g^{\mu\rho} g_{\rho\nu}) &= 0, \\ \det(\Lambda^{\mu}{}_{\nu} - \Lambda \delta^{\mu}_{\nu}) &= 0. \end{aligned} \tag{G.2.2}$$

Tensor $\Lambda^{\mu}{}_{\nu}$ that enters into the characteristic equation is still real, but not symmetric anymore. Therefore from a general point of view, its eigenvalues are, in general, complex. If this is the case, the transformation that diagonalizes $\Lambda^{\mu\nu}$ would involve a complex transformation matrix (every real symmetric matrix is Hermitian, and therefore all its eigenvalues are real.), which does not belong to the $SO(1,3)$ group. This fact means that exploiting only the proper Lorentz group of transformations, one might not be able to diagonalize to $\Lambda^{\nu\mu}$[1].

The demonstration can be easily shown due to the requirement that $\Lambda^{\mu\nu}$ is positive definite on the future light cone (gauge orbit field space).

Proposition 1: Tensor $\Lambda^{\mu\nu}$ is positive definite[2] on the future light cone LC^{+} if and only if the following three conditions hold:

1. $\Lambda^{\mu\nu}$ is diagonalizable by a $SO(1,3)$ transformation,
2. The timelike eigenvalue Λ_0 is positive,
3. All spacelike eigenvalues Λ_i are smaller than Λ_0.

Proof: If $\Lambda^{\mu\nu}$ satisfies conditions $(1)-(3)$, then the positive definiteness follows immediately:

- After $\Lambda_{\mu\nu}$ diagonalization by a transformation T of $SO\,(1,3)$, $\bar{V} \equiv \Lambda_{\mu\nu} r^{\mu} r^{\nu}$ can be expressed by

  $$\bar{V} = \Lambda_0 r_0^2 - \sum_i \Lambda_i r_i^2.$$

  Thus, $\Lambda_{\mu\nu}$ can be seen as a new metric in the space of vector r^{μ}.

- In the frame where $r_i = (0,0,0)$ and from the fact $r_0^2 > 0$, it is necessary that the temporal like component behaves as

  $$\Lambda_0 > 0.$$

- Meanwhile, employing relation in the gauge orbit field space

  $$r_0^2 - r_i^2 \geq 0$$

  and from a corresponding normalization, we arrive at

  $$\frac{\bar{V}}{\Lambda_0} = r_0^2 - \sum_i \left(\frac{\Lambda_i}{\Lambda_0}\right) r_i^2$$

  If $\Lambda_i < \Lambda_0$, the relation for $\bar{V}$ can be easily identified with the properties

  $$\bar{V} > 0$$

  where, we have used the condition over temporal part of the diagonalized couplings tensor i.e. $\Lambda_0 > 0$.

[1] The finite-dimensional spectral theorem states that any symmetric matrix with real entries can be diagonalized by an orthogonal matrix. In other words, for every symmetric real matrix A there exists a real orthogonal matrix Q such that $D = Q^T A Q$ is a diagonal matrix. Every symmetric matrix is thus, up to the choice of an orthonormal basis, a diagonal matrix. Also, every real symmetric matrix is Hermitian, and therefore all its eigenvalues are real. (In fact, the eigenvalues are the entries in the diagonal matrix D (above), and therefore D is uniquely determined by A up to the order of its entries.) Essentially, the feature of being symmetric for real matrices it is equivalent to the property of being Hermitian for complex matrices [203].

[2] In linear algebra, one symmetric $n \times n$ real matrix M is positive definite if $z^T M z$ is positive for every non-zero column vector z of n real numbers. More generally, a $n \times n$ Hermitian matrix M is said to be positive definite if $z^* M z$ is real and positive for all non-zero complex vectors z. Here z^* denotes the conjugate transpose of z.

Now, it is necessary to prove that conditions $(1)-(3)$ are a consequence from the positive definiteness of $\Lambda_{\mu\nu}$. Despite *tensor* $\Lambda^{\mu\nu}$ being real and symmetric, its eigenvalues can be complex because of the non-Euclidean metric; hence it is convenient to clarify the mean of this metric. Indeed, the Minkowski metric is a *pseudo-Riemannian* metric, more precisely, a more specifically a*Lorentzian metric*, or more deep the *Lorentz metric*, reserved for 4-dimensional flat space-time with the remaining ambiguity only being the signature convention ($+2$ or -2). A *pseudo-Riemannian* manifold (M, g) is a differentiable manifold M implemented with a non-degenerate, smooth, and symmetric metric tensor g. Such a metric is denominated a pseudo-Riemannian metric, and its entries could be positive, negative or zero. The signature of a *pseudo-Riemannian* metric is (p, q), where both p and q are non-negative. A Lorentzian manifold is an particular case of a pseudo-Riemannian manifold in which the signature of the metric is $(1, n-1)$ (or sometimes $(n-1, 1)$) [204].

Having clarified the realization of a Lorentzian metric, now the first step is now to prove that the positive definiteness in the future lightcone LC^+ implies that all the eigenvalues of $\Lambda^{\mu\nu}$ are real. For this purpose, we suppose that there is a pair of complex eigenvalues, λ and λ^*, with respective complex eigenvectors p_μ and q_μ:

$$\Lambda^\mu{}_\nu p^\nu = \lambda p^\mu \text{ and } \Lambda^\mu{}_\nu q^\nu = \lambda^* q^\mu. \tag{G.2.3}$$

It is possible show that there can be only one pair of complex eigenvalues, thus, λ is non-degenerate. Since $\Lambda^\mu{}_\nu$ is real, $q^\mu \propto p^{\mu *}$ (and can be taken equal to $p^{\mu *}$). These eigenvectors are orthogonal,

$$p^\mu q_\mu = 0, \tag{G.2.4}$$

(it follows from the standard argument due to $\lambda \neq \lambda^*$) and can be normalized so

$$p^\mu p_\mu = q^\mu q_\mu = 1. \tag{G.2.5}$$

Consider now a real vector r^μ, which can be written by

$$r^\mu = cp^\mu + c^* p^{\mu *}. \tag{G.2.6}$$

Supposing that

$$r^\mu r_\mu = \left(cp^\mu + c^* p^{\mu *}\right)\left(cp_\mu + c^* p^*_\mu\right) = c^2 + c^{*2} = 2\left|c\right|^2 \cos\left(2\phi_c\right) > 0, \tag{G.2.7}$$

The coefficients behave as

$$\begin{aligned} c &= |c|\, e^{i\phi_c} \rightarrow c^2 = |c|^2 e^{2i\phi_c}, \\ c^* &= |c|\, e^{-i\phi_c} \rightarrow c^{*2} = |c|^2 e^{-2i\phi_c}. \end{aligned}$$

so that either r_μ or $-r_\mu$ lie inside the forward lightcone LC^+. Then, the corresponding quadratic form is now

$$\Lambda_{\mu\nu} r^\mu r^\nu = \lambda c^2 + \lambda^* c^{*2} = 2\left|\lambda\right|\left|c\right|^2 \cos\left(2\phi_c + \phi_\lambda\right). \tag{G.2.8}$$

We have used the parameterization $\lambda = |\lambda| e^{i\phi_\lambda}$ and $\lambda^* = |\lambda| e^{-i\phi_\lambda}$. Due to the phase shift $\phi_\lambda \neq 0$ one can always find ϕ_c such that

$$\cos\left(2\phi_c\right) > 0. \tag{G.2.9}$$

but

$$\cos(2\phi_c + \phi_\lambda) < 0. \tag{G.2.10}$$

i.e. one can always find a $r_\mu \in LC^+$ such that $\Lambda_{\mu\nu} r^\mu r^\nu < 0$, which contradicts the primary first assumption. Since all the eigenvalues of $\Lambda_{\mu\nu}$ are real; the eigenvectors also can be chosen all real and orthogonal. One can show that they can be normalized so that one of the eigenvectors, for the temporal part, has a positive norm, $p_0 p^0 = 1$, while the spatial components have negative norm, i.e., $p_i p^i = -1$ for each $i = 1, 2, 3$. Thus the transformation matrix T that diagonalizes $\Lambda_{\mu\nu}$ is real, and after diagonalization $\Lambda_{\mu\nu}$ takes the following form

$$\text{diag}(\Lambda_0, -\Lambda_1, -\Lambda_2, -\Lambda_3). \tag{G.2.11}$$

Note that transformation T also conserves norm, $r^\mu r_\mu = $cte. It means that T can be realized as a transformation from the proper Lorentz group $SO\left(1,3\right)$.

Now, the requirement that $\Lambda_{\mu\nu}$ is positive definite in LC^+ means

$$\Lambda_0 - \rho\left(\Lambda_1 \sin\theta\cos\phi + \Lambda_2 \sin\theta\sin\phi + \Lambda_3 \cos\theta\right) > 0. \tag{G.2.12}$$

for $0 < \rho < 1$, $0 < \theta < \pi$ and $0 < \phi < 2\pi$. This holds when Λ_0 is positive and is larger than all Λ_i. Note that since $\Lambda_{\mu\nu}$ is a linear operator, it maps points inside some surface S into points that also lie inside the image of this surface S'.

G.2.1. Positivity of $\Lambda_{\mu\nu}$ and Formalism Applications

The positivity conditions in the form of inequalities among λs can be readily obtained from the last statements. Here we reproduce the standard set of positivity conditions for a model with explicit Z_2-symmetry, i.e. when $\lambda_6 = \lambda_7 = 0$. The $\Lambda^{\mu\nu}$ of this particular model has the following form

$$\Lambda^{\mu\nu} = \frac{1}{2}\begin{pmatrix} \frac{\lambda_1+\lambda_2}{2}+\lambda_3 & 0 & 0 & -\frac{\lambda_1-\lambda_2}{2} \\ 0 & \lambda_4+\mathrm{Re}\,(\lambda_5) & -\mathrm{Im}\,(\lambda_5) & 0 \\ 0 & -\mathrm{Im}\,(\lambda_5) & \lambda_4-\mathrm{Re}\,(\lambda_5) & 0 \\ -\frac{\lambda_1-\lambda_2}{2} & 0 & 0 & \frac{\lambda_1+\lambda_2}{2}-\lambda_3 \end{pmatrix}. \tag{G.2.13}$$

By taking $\lambda_5 = \lambda_5^*$,

$$\Lambda^{\mu\nu} = \frac{1}{2}\begin{pmatrix} \frac{\lambda_1+\lambda_2}{2}+\lambda_3 & 0 & 0 & -\frac{\lambda_1-\lambda_2}{2} \\ 0 & \lambda_4+\lambda_5 & 0 & 0 \\ 0 & 0 & \lambda_4-\lambda_5 & 0 \\ -\frac{\lambda_1-\lambda_2}{2} & 0 & 0 & \frac{\lambda_1+\lambda_2}{2}-\lambda_3 \end{pmatrix}. \tag{G.2.14}$$

The covariant-contravariant form of this tensor is given by

$$\begin{aligned} \Lambda^{\nu}{}_{\mu} &= g^{\nu}{}_{\sigma}\Lambda^{\mu\sigma} \\ &= \frac{1}{2}\begin{pmatrix} \frac{\lambda_1+\lambda_2}{2}+\lambda_3 & 0 & 0 & \frac{\lambda_1-\lambda_2}{2} \\ 0 & -(\lambda_4+\lambda_5) & 0 & 0 \\ 0 & 0 & -(\lambda_4-\lambda_5) & 0 \\ -\frac{\lambda_1-\lambda_2}{2} & 0 & 0 & -\left(\frac{\lambda_1+\lambda_2}{2}-\lambda_3\right) \end{pmatrix}. \end{aligned} \tag{G.2.15}$$

Diagonalizing this matrix we find

$$\Lambda = \frac{1}{2}\begin{pmatrix} \lambda_3+\sqrt{\lambda_1\lambda_2} & 0 & 0 & 0 \\ 0 & \lambda_3-\sqrt{\lambda_1\lambda_2} & 0 & 0 \\ 0 & 0 & \lambda_5-\lambda_4 & 0 \\ 0 & 0 & 0 & -\lambda_4-\lambda_5 \end{pmatrix}. \tag{G.2.16}$$

Also from positive definite of Λ, its leading principal minors are all positive. The k^{th} leading principal minor of a matrix Λ is the determinant of its upper-left k by k sub-matrix. It turns out that a matrix is positive definite if and only if all these determinants are positive (well known as Silvester's criterion)[3]. From this property

$$\det K_1 > 0 : \lambda_3+\sqrt{\lambda_1\lambda_2} > 0, \tag{G.2.17}$$

$$\det K_2 > 0 : \lambda_3^2-\lambda_1\lambda_2 > 0, \tag{G.2.18}$$

$$\det K_3 > 0 : \left(\lambda_3^2-\lambda_1\lambda_2\right)(\lambda_5-\lambda_4) > 0 \to (\lambda_5-\lambda_4) > 0, \tag{G.2.19}$$

$$\det K_4 > 0 : \left(\lambda_3^2-\lambda_1\lambda_2\right)(\lambda_4+\lambda_5)(\lambda_4-\lambda_5) > 0 \to -(\lambda_4+\lambda_5) > 0. \tag{G.2.20}$$

And we know particular features of Λ

1. $\Lambda^{\mu\nu}$ is diagonalizable by a $SO(1,3)$ transformation,
2. The timelike eigenvalue Λ_0 is positive,
3. All spacelike eigenvalues Λ_i are smaller than Λ_0. From this property, we find out

$$\lambda_5-\lambda_4-\lambda_3 < \sqrt{\lambda_1\lambda_2} \to \lambda_4+\lambda_3-\lambda_5 > -\sqrt{\lambda_1\lambda_2}. \tag{G.2.21}$$

$$-\lambda_4-\lambda_5-\lambda_3 < \sqrt{\lambda_1\lambda_2} \to \lambda_4+\lambda_3+\lambda_5 > -\sqrt{\lambda_1\lambda_2}. \tag{G.2.22}$$

Which are associated with the traditional conditions for a potential bounded from below shown in Table 2.1.

[3] Exist some caveats in the preceding discussion. The Sylvester's criterion is applicable only to Hermitian matrices in the R^N or C^N with a usual metric. Moreover, this condition checks the positive definiteness of a matrix in the entire space. In our case, we have a symmetric matrix with non-euclidean space, or, a non-symmetric matrix in a euclidean space, so that the criterion cannot be applied directly. We need to check for positive definiteness, not in the entire r^μ space, but only within the lightcone. But Sylvester's criterion, or its possible generalization, does not encode information about the region of the space over which we check the matrix. When these issues become circumvent, It would especially be useful for NHDM (N-Higgs Doublet Model) beyond two doublets, where no necessary and sufficient criterion is known at all. Although it looks like a purely mathematical exercise, the answer would be useful for model builders, especially because community slowly starts to study phenomenology of 3HDM (Three Higgs Doublet Model)

G.3. Charge Breaking Minima

Having proved stability conditions as a result of $\Lambda_{\mu\nu}$ properties in the future cone light, this formalism also allows demonstrating what scenario for parameter space is consistent with a charge breaking minima. In this direction, we need to prove the following statements [36]:

1. *Any $SL(2,C)$ transformation of the Higgs field preserves the positive (semi)-definiteness of the second derivative matrix*
$$M_{ab} = \frac{1}{2}\frac{\partial^2 V}{\partial\phi_a \partial\phi_b},\ a = 1, ..., 8. \tag{G.3.1}$$
where ϕ_a are the neutral scalar fields parameterizing in a general way the doublets in the Higgs potential V.

2. *Charge breaking stationary points exist if and only if M^μ lies inside the image lightcone LC', which is defined by*
$$LC' = \left\{ r^{\mu'} | r^{\mu'} = \Lambda^{\mu\nu} r_\nu \text{ for all } r^\mu \in LC^+ \right\}.$$

3. *The charge-breaking stationary point is a minimum if and only if $\Lambda^{\mu\nu}$ is positive definite in the entire Minkowski space.*

To show the first proposition is necessary to introduce the form in which mass matrix and kinetic term of the model transform under $SL(2,C)$. For the kinetic sector, a cuadrivector ρ^μ is introduced in the form

$$\rho^\mu = (\partial_\alpha \Phi)^\dagger \sigma^\mu (\partial^\alpha \Phi), \text{ with } \Phi = \begin{pmatrix} \Phi_1 \\ \Phi_2 \end{pmatrix}$$

where α gives the space-time coordinates. It is possible rewrite the kinetic term as

$$K = K_\mu \rho^\mu.$$

$K_\mu = (1,0,0,0)$ sets a preferred reference frame in the space of ρ^μ and therefore in the gauge orbit space. In general, a transformation of $SL(2,C)$ for the Higgs fields could convert spatial components of K_μ in non-zero values. Thus, the canonical form of K could be broken. The structure of kinetic sector has the following properties

- The number of stationary points is not affected by the structure of K since this uniquely depend on Higgs potential form.
- Nonetheless, it can affect the localization of these stationary points and the matrix of second derivatives of Eq. (G.3.1) computed from these values.

The important point is that (G.3.1) represents the truth mass matrix of the Higgs bosons only when is computed in the above-preferred reference frame of K_μ. Despite this break of Lorentz invariance, the true mass matrix and the Hessian of the Higgs potential (Second derivative matrix) in any Lorentz frame are characterized by a significant property: both are always positive definite matrices independent of the reference frame. This fact is the spirit of the statement number one.

Demonstration 1) With these definitions in mind, the proof of proposition 1 is in order. In advance, we consider each of the complex Higgs fields as a pair of real ones ϕ_a. In this scenario, $SL(2,C)$ transformations are equivalent to rotations with a $SL(4,R)$ structure over ϕ_a,

$$\phi_a \to \phi'_a = R_{aa'}\phi_{a'}$$

The mass matrix of Eq. (G.3.1) is then transformed as

$$M_{ab} \to M'_{ab} = R^{-1}_{a'a} M_{ab} R_{bb'}$$

If M'_{ab} is positive (semi)definite ,

$$q_a M'_{ab} q_b > 0,\ (\text{or } \geq 0) \text{ for any vector } q_a$$

By defining the rotation of $q-$vectors as

$$Q_a = q_{a'} R^{-1}_{a'a}$$

Since map $R_{a'a}$ is surjective[4], then

$$Q_a M_{ab} Q_b > 0, (\text{or } \geq 0) \text{ for any vector } Q_a.$$

Therefore, M_{ab} is also positive (semi) definite. Hence, the physical interpretation of the proposition number one is the fact that a local minimum remains local under any rotation and stretching of the coordinates in the space of Higgs fields.

Demonstration 2) For the demonstration of the second proposition, we express the charge breaking stationary point by means of

$$\Lambda_{\mu\nu} r^\nu = M_\mu, \tag{G.3.2}$$

which defines an inhomogeneous system of linear equations. A point lies inside of a closed Minkowski structure I if and only if the image of this point lies inside of the image of this closed Minkowski structure I'. Since r^μ lies inside LC^+, $\Lambda_{\mu\nu} r^\nu$ lies inside LC'. Therefore, existence of physical solutions of (G.3.2) bring out that M^μ lies inside of LC'.

Demonstration 3) By using proposition 1 and a convenient $SO(1,3)$ transformation of a charge breaking minima, it is possible to get a demonstration of the third statement. Since charged vacuum, defined in r^μ_{ch}, lies inside of the LC^+, it is always possible to perform a $SO(1,3)$ rotation defining the stationary point as

$$r^\mu_{ch} = \left(u^2, 0, 0, 0\right).$$

where $u \in$R. The proposition 1 ensures the freedom to choose a particular representing point over the r^μ space by performing a convenient EW rotation. For instance,

$$\Phi_1 = \frac{1}{\sqrt{2}} \begin{pmatrix} 0 \\ u \end{pmatrix}, \text{ and } \Phi_2 = \frac{1}{\sqrt{2}} \begin{pmatrix} u \\ 0 \end{pmatrix}.$$

The Higgs modes in this charge vacuum have the next Hessian matrix

$$\left(M^2_{ij}\right)_{ch} \equiv \left(\frac{1}{2}\frac{\partial^2 V}{\partial\phi_i \partial\phi_j}\right)_{ch} = 2u^2 \begin{pmatrix} \langle e_0|e_0\rangle & \langle e_0|e_1\rangle & \langle e_0|e_2\rangle & \langle e_0|e_3\rangle \\ \langle e_1|e_0\rangle & \langle e_1|e_1\rangle & \langle e_1|e_2\rangle & \langle e_1|e_3\rangle \\ \langle e_2|e_0\rangle & \langle e_2|e_1\rangle & \langle e_2|e_2\rangle & \langle e_2|e_3\rangle \\ \langle e_3|e_0\rangle & \langle e_3|e_1\rangle & \langle e_3|e_2\rangle & \langle e_3|e_3\rangle \end{pmatrix}, \tag{G.3.3}$$

where the unit vectors are defined by

$$\begin{aligned} e_0^\mu &= (1,0,0,0), \\ e_1^\mu &= (0,1,0,0), \\ e_2^\mu &= (0,0,1,0), \\ e_3^\mu &= (0,0,0,1). \end{aligned}$$

with the notation

$$\langle e|e\rangle \equiv e_\mu e_\nu \Lambda^{\mu\nu}.$$

$\rightarrow$Supposing that $p_i = (p_0, p_1, p_2, p_3)$ is a normalized eigenvector of (G.3.3), with eigenvalue $\left(M^2\right)_{ch}$. Then

$$\left(M^2\right)_{ch} = \left(M^2_{ij}\right)_{ch} p_i p_j = u^2 \Lambda^{\mu\nu} P_\mu P_\nu$$

where

$$P^\mu \equiv p_0 e_0^\mu + p_1 e_1^\mu + p_2 e_2^\mu + p_3 e_3^\mu$$

Hence, if $\Lambda_{\mu\nu}$ is positive definite in the entire Minkowski space,

$$\Lambda^{\mu\nu} P_\mu P_\nu > 0$$

and all eigenvalues of the Hessian matrix are positive. The stationary point is, therefore, a minimum, and according to the statement 1, it remains a minimum when is transformed to the preferred frame, with the canonical kinetic term.

$\leftarrow$In the other direction, if $\Lambda^{\mu\nu}$ is not defined positive, then exist a Q_μ such that

$$\Lambda^{\mu\nu} Q_\mu Q_\nu < 0$$

[4]If $f: X \to Y$, then f is said to be surjective if $\forall\, y \in Y$, $\exists\, x \in X$, such that $f(x) = y$

The vector Q^μ can be represented as

$$Q^\mu = q_0 e_0^\mu + q_1 e_1^\mu + q_2 e_2^\mu + q_3 e_3^\mu.$$

since $\{e_0^\mu, e_1^\mu, e_2^\mu, e_3^\mu\}$ form a basis in the Minkowski space. Therefore the property for the Hessian implies

$$u^2 \Lambda^{\mu\nu} Q_\mu Q_\nu = \left(M_{ij}^2\right)_{ch} q_i q_j$$

q_i can be represented in the basis of eigenvectors $\left\{p_i^{(a)}\right\}$ of the mass matrix

$$q_i = \sum_a c_a p_i^a$$

it is possible to simplify

$$u^2 \Lambda^{\mu\nu} Q_\mu Q_\nu = \left(M_{ij}^2\right)_{ch} q_i q_j = \sum_a \left(M_a^2\right)_{ch} c_a^2 < 0$$

which implies that at least one of mass matrix eigenvalues is negative. Contradicting the fact the stationary point associated with a charge breaking one is a minimum.

Corollary 1) In order to get a charge breaking stationary point as a minimum of the theory, all spatial like components Λ_i must be non-positive.

H. Morse's Inequalities

Employing bilinears form of the Higgs potential, we shall study the realization of different normal minima by counting the number of solutions of respective stationary conditions. Applying the so-called Morse's inequalities, we can say the structure of minima and their degeneracy inside Higgs potential.

H.1. Morse's Inequalities in the stationary conditions

Let us now consider the stationarity equations that give rise to the different critical points that we have been discussing. We have mentioned that the CB and CP stationary points are unique since they are obtained from linear equations on the vevs. However, this is not true for the normal stationary point. Let us begin with the most general 2HDM potential

$$\begin{aligned} V_H &= a_1 x_1 + a_2 x_2 + a_3 x_3 + a_4 x_4 + b_{11} x_1^2 + b_{22} x_2^2 + b_{33} x_3^2 + b_{44} x_4^2 \\ &\quad + b_{12} x_1 x_2 + b_{13} x_1 x_3 + b_{23} x_2 x_3 + b_{14} x_1 x_4 + b_{24} x_2 x_4 + b_{34} x_3 x_4, \end{aligned} \tag{H.1.1}$$

which written in a basis where $a_3 = a_4 = 0$, it is simply translated to

$$\begin{aligned} V_H &= a_1 x_1 + a_2 x_2 + b_{11} x_1^2 + b_{22} x_2^2 + b_{33} x_3^2 + b_{44} x_4^2 \\ &\quad + b_{12} x_1 x_2 + b_{13} x_1 x_3 + b_{23} x_2 x_3 + b_{14} x_1 x_4 + b_{24} x_2 x_4 + b_{34} x_3 x_4, \end{aligned} \tag{H.1.2}$$

We can parametrize the doublets by

$$\Phi_1 = \begin{pmatrix} \phi_1 + i\phi_2 \\ \phi_3 + i\phi_4 \end{pmatrix} \text{ and } \Phi_2 = \begin{pmatrix} \phi_5 + i\phi_6 \\ \phi_7 + i\phi_8 \end{pmatrix} \tag{H.1.3}$$

The fields ϕ_i are real functions. The bilinears are

$$x_1 = \left(\Phi_1^\dagger \Phi_1\right) = \phi_1^2 + \phi_2^2 + \phi_3^2 + \phi_4^2 \tag{H.1.4}$$

$$x_2 = \left(\Phi_2^\dagger \Phi_2\right) = \phi_5^2 + \phi_6^2 + \phi_7^2 + \phi_8^2 \tag{H.1.5}$$

$$x_3 = \mathrm{Re}\left(\Phi_1^\dagger \Phi_2\right) = \phi_1\phi_5 + \phi_2\phi_6 + \phi_3\phi_7 + \phi_4\phi_8 \tag{H.1.6}$$

$$x_4 = \mathrm{Im}\left(\Phi_1^\dagger \Phi_2\right) = \phi_1\phi_6 - \phi_2\phi_5 + \phi_3\phi_8 - \phi_4\phi_7 \tag{H.1.7}$$

In the stationary point

$$x_1|_0 = v_1^2 \tag{H.1.8}$$

$$x_2|_0 = v_2^2 \tag{H.1.9}$$

$$x_3|_0 = v_1 v_2 \tag{H.1.10}$$

$$x_4|_0 = 0 \tag{H.1.11}$$

The Higgs potential in terms of $v's$ is

$$\begin{aligned}
V &= a_1\left(\phi_1^2+\phi_2^2+\phi_3^2+\phi_4^2\right)+a_2\left(\phi_5^2+\phi_6^2+\phi_7^2+\phi_8^2\right)\\
&+a_3\left(\phi_1\phi_5+\phi_2\phi_6+\phi_3\phi_7+\phi_4\phi_8\right)+a_4\left(\phi_1\phi_6-\phi_2\phi_5+\phi_3\phi_8-\phi_4\phi_7\right)\\
&+b_{11}\left(\phi_1^2+\phi_2^2+\phi_3^2+\phi_4^2\right)^2+b_{22}\left(\phi_5^2+\phi_6^2+\phi_7^2+\phi_8^2\right)^2\\
&+b_{33}\left(\phi_1\phi_5+\phi_2\phi_6+\phi_3\phi_7+\phi_4\phi_8\right)^2+b_{44}\left(\phi_1\phi_6-\phi_2\phi_5+\phi_3\phi_8-\phi_4\phi_7\right)^2\\
&+b_{12}\left(\phi_1^2+\phi_2^2+\phi_3^2+\phi_4^2\right)\left(\phi_5^2+\phi_6^2+\phi_7^2+\phi_8^2\right)\\
&+b_{13}\left(\phi_1^2+\phi_2^2+\phi_3^2+\phi_4^2\right)\left(\phi_1\phi_5+\phi_2\phi_6+\phi_3\phi_7+\phi_4\phi_8\right)\\
&+b_{23}\left(\phi_5^2+\phi_6^2+\phi_7^2+\phi_8^2\right)\left(\phi_1\phi_5+\phi_2\phi_6+\phi_3\phi_7+\phi_4\phi_8\right)\\
&+b_{14}\left(\phi_1^2+\phi_2^2+\phi_3^2+\phi_4^2\right)\left(\phi_1\phi_6-\phi_2\phi_5+\phi_3\phi_8-\phi_4\phi_7\right)\\
&+b_{24}\left(\phi_5^2+\phi_6^2+\phi_7^2+\phi_8^2\right)\left(\phi_1\phi_6-\phi_2\phi_5+\phi_3\phi_8-\phi_4\phi_7\right)\\
&+b_{34}\left(\phi_1\phi_5+\phi_2\phi_6+\phi_3\phi_7+\phi_4\phi_8\right)\left(\phi_1\phi_4-\phi_2\phi_5+\phi_3\phi_8-\phi_4\phi_7\right) \qquad \text{(H.1.12)}
\end{aligned}$$

The no- trivial tadpoles at tree level are

$$\begin{aligned}
\frac{\partial V}{\partial\phi_3} &= 2a_1\phi_3+a_3\phi_7+a_4\phi_8\\
&+4b_{11}\left(\phi_1^2+\phi_2^2+\phi_3^2+\phi_4^2\right)\phi_3+2b_{33}\left(\phi_1\phi_5+\phi_2\phi_6+\phi_3\phi_7+\phi_4\phi_8\right)\phi_7\\
&+2b_{44}\left(\phi_1\phi_6-\phi_2\phi_5+\phi_3\phi_8-\phi_4\phi_7\right)\phi_8+2b_{12}\phi_3\left(\phi_5^2+\phi_6^2+\phi_7^2+\phi_8^2\right)\\
&+2b_{13}\phi_3\left(\phi_1\phi_5+\phi_2\phi_6+\phi_3\phi_7+\phi_4\phi_8\right)+b_{13}\left(\phi_1^2+\phi_2^2+\phi_3^2+\phi_4^2\right)\phi_7\\
&+b_{23}\left(\phi_5^2+\phi_6^2+\phi_7^2+\phi_8^2\right)\phi_7+2b_{14}\phi_3\left(\phi_1\phi_6-\phi_2\phi_5+\phi_3\phi_8-\phi_4\phi_7\right)\\
&+b_{14}\left(\phi_1^2+\phi_2^2+\phi_3^2+\phi_4^2\right)\phi_8+b_{24}\left(\phi_5^2+\phi_6^2+\phi_7^2+\phi_8^2\right)\phi_8\\
&+b_{34}\phi_7\left(\phi_1\phi_4-\phi_2\phi_5+\phi_3\phi_8-\phi_4\phi_7\right)+b_{34}\left(\phi_1\phi_5+\phi_2\phi_6+\phi_3\phi_7+\phi_4\phi_8\right)\phi_8 \qquad \text{(H.1.13)}
\end{aligned}$$

We make $\phi_3=v_1$ and $\phi_7=v_2$, therefore

$$\frac{\partial V}{\partial\phi_3} = 2a_1v_1+a_3v_2+2b_{11}v_1^3+b_{33}v_1v_2^2+b_{12}v_1v_2^2+\frac{3}{2}b_{13}v_1^2v_2+\frac{1}{2}b_{23}v_2^3=0 \qquad \text{(H.1.14)}$$

$$\frac{\partial V}{\partial\phi_7} = 2a_2v_2+a_3v_1+2b_{22}v_2^3+b_{33}v_1^2v_2+b_{12}v_1^2v_2+\frac{1}{2}b_{13}v_1^3+\frac{3}{2}b_{23}v_1v_2^2=0 \qquad \text{(H.1.15)}$$

and

$$\frac{\partial V}{\partial\phi_4} = v_1\left(b_{14}v_1^2+b_{24}v_2^2+b_{34}v_1v_2\right)=0 \qquad \text{(H.1.16)}$$

$$\frac{\partial V}{\partial\phi_4} = -v_2\left(b_{14}v_1^2+b_{24}v_2^2+b_{34}v_1v_2\right)=0 \qquad \text{(H.1.17)}$$

Notice that one cannot have solutions of the form $\{v_1=0,v_2\neq0\}$ or $\{v_1\neq0,v_2=0\}$, unless some parameters of the potential are set to zero (a_3,b_{23}, b_{24} and b_{13}, b_{14} respectively). Since there is no symmetry forcing those parameters to be zero, they have to be present in the potential. We now define the usual polar coordinates $v_1=v\cos\beta$ and $v_2=v\sin\beta$. A trivial solution of these equations is clearly $v=0$. Excluding that case, the stationarity conditions (H.1.14) and (H.1.15) become

$$v^2=-\frac{1}{\cos^2\beta}\frac{2a_1}{\left(4b_{11}+b_{23}\tan^3\beta+3b_{13}\tan\beta+2b_{12}\tan^2\beta+2b_{33}\tan^2\beta\right)} \qquad \text{(H.1.18)}$$

$$\begin{aligned}
&2a_1\left(b_{13}\cot\beta+4b_{22}\tan^2\beta+2b_{12}+3b_{23}\tan\beta+2b_{33}\right)\\
&-2a_2\left(4b_{11}+b_{23}\tan^3\beta+3b_{13}\tan\beta+2b_{12}\tan^2\beta+2b_{33}\tan^2\beta\right)=0
\end{aligned} \qquad \text{(H.1.19)}$$

And both equations (H.1.16) and (H.1.17) reduce to

$$\left(b_{14}v_1^2+b_{24}v_2^2+b_{34}v_1v_2\right)=0$$

since v_1, v_2 can not be equal to zero simultaneously.

$$\left(b_{14} + b_{24}\tan^2\beta + b_{34}\tan\beta\right) = 0 \tag{H.1.20}$$

Eq. (H.1.18) tells us that, other than its sign, the value of v is determined unequivocally by $\tan\beta$. Eq. (H.1.19) is a quartic equation on $\tan\beta$, having at most four possible real solutions. These two equations describe therefore eight possible solutions $\{v_1, v_2\}$, due to the ambiguity on the sign of v. The 2HDM potential

$$\begin{aligned} V &= a_1x_1 + a_2x_2 + a_3x_3 + a_4x_4 + b_{11}x_1^2 + b_{22}x_2^2 + b_{33}x_3^2 + b_{44}x_4^2 \\ &\quad + b_{12}x_1x_2 + b_{13}x_1x_3 + b_{23}x_2x_3 + b_{14}x_1x_4 + b_{24}x_2x_4 + b_{34}x_3x_4, \end{aligned}$$

is however invariant under the transformation $\Phi_1 \to -\Phi_1$ and $\Phi_2 \to -\Phi_2$, so that these eight solutions correspond to only four different physical scenarios. Adding the trivial solution $v_1 = v_2 = 0$, we have a total of nine solutions. However, we must contend with eq. (H.1.20) as well, which is a quadratic equation on $\tan\beta$.

Then, there are at most two different values of $\tan\beta$ which satisfy all equations. This fact means that we have a maximum of five stationary points. For potentials with explicit CP conservation, equations (H.1.16) and (H.1.17) are trivially satisfied, since $b_{14} = b_{24} = b_{34} = 0$. Therefore, equation (H.1.20) does not exist and the potential could have a total of nine stationary points.

At this stage, it is possible to see Higgs potential have more than one normal minimum, with different depths?. To establish this formally, we can use of Morse's inequalities [205, 206]: for a given real function of two variables, let η_0, η_1 and η_2 be the number of its minima, saddle points, and maximums, respectively [1]. For a polynomial function in v_1 and v_2, bounded from below, such as the one we are dealing with, Morse's inequalities state that:

- $\eta_0 \geq 1$
- $\eta_1 \geq \eta_0 - 1$
- $\eta_0 - \eta_1 + \eta_2 = 1$.

  We know that the 2HDM potential has $\eta_0 + \eta_1 + \eta_2 = 2n + 1$ stationary solutions, $n = 0, ..., 4$: at most $2n$ real roots of eqs. (H.1.18), (H.1.19) and (H.1.20) plus the trivial solution $v_1 = v_2 = 0$. Hence we find that $\eta_0 + \eta_2 = n + 1$. $(\eta_0 + \eta_0 + \eta_2 - 1 + \eta_2 = 2n + 1, 2\eta_0 + 2\eta_2 = 2n + 2)$ .Let us analyze the several possibilities for the number of minima η_0, depending on the number of solutions n. Simply counting all the different combinations of extrema leads us to:

- $n = 0$,

  $$\eta_0 + \eta_2 = 1 \text{ and } \eta_0 \geq 1 \to \eta_0 = 1$$

  The minimum is unique but has its localization at the origin, $v_1 = v_2 = 0$, which means that there is no $SU(2)_L \times U(1)_Y$ symmetry breaking. This case is excluded or not considered on physical grounds (i.e. it is not relevant for our treatment).

[1] For a differentiable continuous function, at least of C_2-type, of a set of real variables, a point P is critical or an extremum if all of the partial derivatives of the function are zero at P, in other words, if its gradient is zero. The critical values are evaluated at the extremal points, i.e., vacuum definition in our treatment.

If the function is smooth, or, at least twice continuously differentiable C_2-type, a critical point may be either a local maximum, a local minimum or a saddle point. The several cases may be discriminated by considering the eigenvalues of the Hessian matrix of second derivatives of the Higgs potential, in our case.

A critical point at which the Hessian matrix is nonsingular is said to be non-degenerate, and the signs of the eigenvalues of the Hessian determine the local behavior of the function. In the case of a function of a single variable, the Hessian is simply the second derivative, viewed as a 1×1-matrix, which is nonsingular if and only if it does not vanish. In this particular case, a non-degenerate extremum point is a local maximum or a local minimum, depending on the sign of the second derivative. The sign is positive for a local minimum and negative for a local maximum. If the second derivative is null, the critical point is an inflection point, but may also be an undulation point, which may be a local minimum or a local maximum depending on the direction in the n-dimensional space.

On the other hand, for a function of n variables, the number of negative eigenvalues of the Hessian matrix at a critical point is called the index of the extremum point. A non-degenerate critical point is a local maximum if and only the index is n, or, i.e., if the Hessian matrix is negative definite; it is a local minimum if the index n is equal zero, or, equivalently, if the Hessian matrix is positive definite. For the other n-index values, a non-degenerate critical point is a saddle point; that is a point which is a maximum in some directions and a minimum in others [207].

- $n = 1$

  $$\eta_0 + \eta_2 = 2 \text{ and } \eta_0 \geq 1$$

  we have two possibilities

  $$\eta_0 = 1 \text{ and } \eta_0 = 2$$

  The first one is the previous case. And the second one which means two degenerate minima away from the origin, related to one another by a change of sign of the vevs. This situation corresponds to an acceptable symmetry breaking, and it means that there are no normal minima with different depths. This would be the "standard" situation.

  - $n = 2$

    $$\eta_0 + \eta_2 = 3 \text{ and } \eta_0 \geq 1$$

    there are three possibilities:

    $-\eta_0 = 1$ or 2 are like the previous cases.

    $-\eta_0 = 3$ One uninteresting minimum at the origin and two degenerate ones away from it. This situation would also be the "standard" one, as there would be no normal minima with different depths.

  - $n = 3$

    $$\eta_0 + \eta_2 = 4 \text{ and } \eta_0 \geq 1$$

    $-\eta_0 = 1, 2$, or 3 are like the previous cases.

    $-\eta_0 = 4$ This case corresponds to two pairs of degenerate minima away from the origin. Nothing forces these two pairs of minima to have the same depth. We might, therefore, have one normal minimum deeper than another.

  - $n = 4$

    $$\eta_0 + \eta_2 = 5 \text{ and } \eta_0 \geq 1$$

    $-\eta_0 = 1, 2, 3$, or 4 like above

    $-\eta_0 = 5$ This case is similar to the $\eta_0 = 4$ case examined above, with an extra minimum present at the origin.

    This little analysis shows us that, if there are more than two solutions for $\tan\beta$, then the 2HDM may have more than one normal minimum away from the origin at different depths. However, no more than two such minima can exist.

I. Discriminant for global minimum

In this appendix, we show how is possible constructing a formalism and one discriminant ensuring that a particular stationary point is a global minimum in the Higgs potential. For this purpose, Hessian formalism and convex forms for C_2 functions will be used [1].

I.1. Global minimum criteria

We start with the $SO(1,3)$ Higgs potential defined in a normal minimum

$$\bar{V} = -M_\mu r^\mu + \frac{1}{2}\Lambda_{\mu\nu} r^\mu r^\nu - \frac{1}{2}\zeta g_{\mu\nu} r^\mu r^\nu \tag{I.1.1}$$

ζ is a Lagrange multiplier enforcing to $\langle \widehat{r}^\mu \rangle$ to reside in the surface of the LC^+. This point will be shown below The contravariant vector r^μ is

$$r^\mu = (r_0, r_1, , r_2, r_3) = \left(\Phi_1^\dagger\Phi_1 + \Phi_2^\dagger\Phi_2, 2\mathrm{Re}\left(\Phi_1^\dagger\Phi_2\right), 2\mathrm{Im}\left(\Phi_1^\dagger\Phi_2\right), \Phi_1^\dagger\Phi_1 - \Phi_2^\dagger\Phi_2\right).$$

and

$$M_\mu = \left(-\frac{m_{11}^2 + m_{22}^2}{2}, \mathrm{Re}\left(m_{12}^2\right), -\mathrm{Im}\left(m_{12}^2\right), -\frac{m_{11}^2 - m_{22}^2}{2}\right).$$

$\Lambda_{\mu\nu}$ is a symmetric matrix. The mixed tensor $\Lambda^\mu{}_\nu = g^{\mu\alpha}\Lambda_{\alpha\nu}$ can be treated as a matrix in Euclidean space:

$$\Lambda_E = \Lambda^\mu{}_\nu = \frac{1}{2}\begin{pmatrix} \frac{1}{2}(\lambda_1+\lambda_2)+\lambda_3 & \mathrm{Re}(\lambda_6+\lambda_7) & -\mathrm{Im}(\lambda_6+\lambda_7) & \frac{1}{2}(\lambda_1-\lambda_2) \\ -\mathrm{Re}(\lambda_6+\lambda_7) & -\lambda_4-\mathrm{Re}(\lambda_5) & \mathrm{Im}(\lambda_5) & -\mathrm{Re}(\lambda_6-\lambda_7) \\ \mathrm{Im}(\lambda_6+\lambda_7) & \mathrm{Im}(\lambda_5) & -\lambda_4+\mathrm{Re}(\lambda_5) & \mathrm{Im}(\lambda_6-\lambda_7) \\ -\frac{1}{2}(\lambda_1-\lambda_2) & -\mathrm{Re}(\lambda_6-\lambda_7) & \mathrm{Im}(\lambda_6-\lambda_7) & -\frac{1}{2}(\lambda_1+\lambda_2)+\lambda_3 \end{pmatrix}.$$

As this matrix in its generic version is not symmetric, its eigenvalues can be complex leading to unbounded from below potentials (see appendix G). A change of basis yields

$$\Phi_i' = U_{ij}\Phi_j.$$

Choosing the matrix U in $U(2)$ guarantees that the kinetic terms retain their canonical form. However as was pointed in later sections, these transformations are only a subset of more general changes given by $SO(1,3)$ rotations; indeed this is a symmetry of re-parameterizing of the Higgs potential in the 2HDM. An important feature on these transformations is that Λ_E can be diagonalized into

$$\Lambda_E \to \mathrm{diag}\left(\Lambda_0, \Lambda_1, \Lambda_2, \Lambda_3\right).$$

Hence, stability conditions require

$$\Lambda_0 > 0, \text{ and } \Lambda_0 > \Lambda_k;\ k = 1, 2, 3.$$

After SSB, the fields acquire vacuum expectation values

$$\langle\Phi_1\rangle = \frac{1}{\sqrt{2}}\begin{pmatrix} 0 \\ v_1 \end{pmatrix} \text{ and } \langle\Phi_2\rangle = \frac{1}{\sqrt{2}}\begin{pmatrix} 0 \\ v_2 e^{i\delta} \end{pmatrix}.$$

[1] We follow the systematic presented by Ivanov et al in [29, 31]

r^μ in the vacuum is thus

$$\begin{aligned}\mathfrak{r}^\mu &\equiv \langle r^\mu\rangle = \frac{1}{2}\left(v_1^2+v_2^2, 2v_1v_2\cos\delta, 2v_1v_2\sin\delta, v_1^2-v_2^2\right).\\ \mathfrak{r}^\mu\mathfrak{r}_\mu &= \frac{1}{4}\left[\left(v_1^2+v_2^2\right)^2 - 4v_1^2v_2^2 - \left(v_1^2-v_2^2\right)^2\right] = 0.\end{aligned}$$

Besides in a general way

$$r_0 \geq 0 \text{ and } r_\mu r^\mu \geq 0.$$

Corresponding to the forward light cone LC^+. The $SU(2)\times U(1)$ symmetric vacuum lies at the apex, the surface corresponds to neutral vacua, while any point in the interior of LC^+ represents a charge breaking vacua. Henceforth, with this formalism will describe the way to determine if a stationary point is a global minimum or a saddle point.

Discriminating a minimum from a saddle point requires of the Hessian definition

$$H_{ab} \equiv \frac{1}{2}\frac{\partial^2 V}{\partial\varphi_a\partial\varphi_b}$$

where φ_i, $i = 1,...,8$ are the real fields parameterizing the doublets. Due to Goldstone bosons, the Hessian is a positive semi-definite matrix. Apart from this sector, the Hessian is positive definite in the Higgs field space. For a neutral stationary point, the charged and neutral fields decouple, and one is regarding on H_{ab} in the four-dimensional subspace of neutral Higgs modes. $(a,b=1,2,3,4)$.

The $SO(1,3)$ formalism gives us information how ζ, with respect to Λ_k and Λ_0, is related with minimum versus saddle point assignments. Therefore we use instead the basis invariant approach to Higgs masses, which allow us to switch to the $\Lambda_{\mu\nu}-$diagonal basis. In this particular basis, the Hessian in the 4D space of neutral modes takes the following form

$$H_{ab} = \left(R^T\right)_{a\alpha} S_{\alpha\beta} R_{\beta b}$$

with

$$R_{a\alpha} = \frac{1}{2}\langle\frac{\partial r_\alpha}{\partial\varphi_a}\rangle$$

There are two different spaces to taking into account in the formalism. One of them, labeled with Greek letters α,β, is related to the space of bilinears from we erased the Minkowski space metric. The second of them refers to the space of neutral modes at the extremum (labeled by a,b). Both subspaces and the connection through R are shown in the Fig. I.1

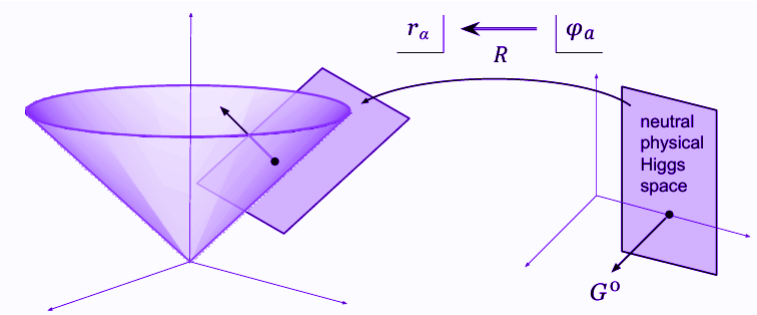

Figure I.1.: *R transformation acting over neutral Higgs modes maps the complement of physical space onto a 3D plane tangent to the forward lightcone in the r_α space at the extremum point. Figure taken from [29]*

To compute the Hessian in a Minkowskian subspace, we use

$$S_{\mu\nu} \equiv \frac{\partial V}{\partial r^\mu \partial r^\nu} = \Lambda_{\mu\nu} - \zeta g_{\mu\nu}$$

From this matrix structure, we obtain in a diagonal basis

$$\begin{aligned}S &= \Lambda^\mu{}_\nu - \zeta g^\mu{}_\nu = \Lambda_E - \zeta 1\\ &= \begin{pmatrix}\Lambda_0-\zeta & 0 & 0 & 0\\ 0 & \zeta-\Lambda_1 & 0 & 0\\ 0 & 0 & \zeta-\Lambda_2 & 0\\ 0 & 0 & 0 & \zeta-\Lambda_3\end{pmatrix}.\end{aligned}$$

The matrix S signature Sig$S$ and the matrix $S_E = \Lambda_E - \zeta 1$ is originating from the same $\Lambda_{\mu\nu} - \zeta g_{\mu\nu}$: Sig$S$ is obtained by erasing the Minkowski metric and S_E matrix is achieved by lowering one index. This fact leads to defining

$$D \equiv \det S$$

It is worthwhile to make some annotations over physical significance of the *Hessian* over gauge orbit space. Indeed, the extended reparameterization group $SL\,(2, C)$ modifies the Higgs kinetic term since space-like components become altered under proper operations. Despite the structure of the kinetic term does not affect the number of stationary points in the Higgs potential, but it does change the position of these extremal points, and then the form of the Hessian elements are calculated around them. Nonetheless, any $SL(2, C)$ transformation of the Higgs fields preserves the positive (semi) of the Hessian (see Proposition 1 in appendix G). Then any rotation or stretching operation over Higgs space leaves invariant the signature of the Hessian,i.e., the signs of its eigenvalues. Therefore, Sig$S$ represents of the masses squared of the four neutral scalar degrees of freedom.

We must also search for the link between the sign of eigenvalues in H_{ab} and S. The transformation matrix associated to R is singular ($\det R = 0$). This scenario is an indication that one of the four directions in the scalar field space in φ_a is a would be Goldstone boson G^0. The orthogonal plane to it represents the $3D$ physical neutral Higgs space. This physical Higgs space is mapped by R onto the $3D$ subspace in the r_α space tangent to LC^+ at the extremum point. If this mapping is not realized, the presence of a Goldstone boson does not lead to analyze the Hessian criteria, since the presence of an eigenvalue equals to zero. Therefore to discriminate between a saddle point or a minimum, in addition to the full signature of S, we need to know the signature of this restriction onto this $3D$ subspace.

The relation between signatures of H_{ab} and S describes the cases

- If S has the signature $(+, +, +, +)$ then H_{ab} is positive definite in the physical Higgs space; settled at a minimum. In this case also $D > 0$.
- If S has the signature $(-, +, +, +)$ up to permutations, then H_{ab} is not positive definite in the r_α space. But it might still be positive definite when to become restricted to the physical Higgs space. In this case $D < 0$, but deciding whether we are at a minimum or a saddle point requires further analysis.
- If S has the signature $(-, -, +, +)$ up to permutations. Then H_{ab} cannot be positive definite even when projected onto the physical Higgs space. Using dimension counting, in the r_α space, there exists a 2D subspace of negative,

  $$S_{\alpha\beta} r_\alpha r_\beta,$$

  intersecting a 3D subspace tangent to the light cone. So even with a $D > 0$, but this stationary point cannot be a minimum. The same conclusion holds for the signature $(-, -, -, -)$.

Therefore, a minimum with positive $D > 0$ can take place if and only if S has signature $(+, +, +, +)$. This occurs when

$$\Lambda_0 > \zeta > \Lambda_1, \Lambda_2, \Lambda_3$$

This fact also satisfies the typical conditions for bounded from below Higgs potential. We proceed to show as in this region exist only one stationary point and that this point is a global minimum.

I.1.1. General treatment for stationary points nature

Criteria for extremal points, in perhaps a stronger formulation, are established in the following statements: Let $A \subseteq R^n$ be an open convex set and let $f : A \to R$ be twice differentiable [207, 208]. Write $H(x)$ for the Hessian matrix of A at $x \in A$.

- If the Hessian is positive definite (equivalently, all $H-$eigenvalues are positive) at x, then f attains a local minimum at x.
- If the Hessian is negative definite (equivalently, all $H-$eigenvalues are negative) at x, then f attains a local maximum at x.
- If the Hessian has both positive and negative eigenvalues then x is a saddle point for f (this is true even if x is degenerate).

- If $H(x)$ is positive semidefinite for all $x \in A$, then f is convex and has a strict global extremal-minimum at any x for which $f'(x) = 0$ and $H(x)$ is positive definite.
- If $H(x)$ is negative semidefinite for all $x \in A$, then f is concave and has a strict global maximum at any x for which $f'(x) = 0$ and $H(x)$ is negative definite.

  Naively in our case

  $$\Lambda_0 > \zeta,\ \zeta > \Lambda_1,\ \zeta > \Lambda_2 \text{ and } \zeta > \Lambda_3.$$

  There is a milder condition related to being H a positive definite quantity if the subspace tangent to the stationary point, i.e., in the space of r^μ. Therefore, H to carry out minima, it must be positive definite in LC^+,

  $$\begin{aligned} i)\Lambda_0 - \zeta &> 0 \\ ii)\Lambda_0 - \zeta &> \zeta - \Lambda_i \end{aligned}$$

- On the other hand, to avoid a saddle point, the determinant of the Hessian matrix must satisfy

  $$D = (\Lambda_0 - \zeta)(\zeta - \Lambda_1)(\zeta - \Lambda_2)(\zeta - \Lambda_3) > 0$$

- By using the bounded from below constraints, $D > 0$ condition ensures that we are in a global minimum of the theory.

J. $\beta-$Functions structure in the 2HDM

J.1. The one loop $\beta-$functions in 2HDM

The energy behavior of the parameters in all interaction sectors and relations among them are computed through the Renormalization Group Equations (RGEs). At higher levels in perturbation theory, quartic coupling depends on the energy scale μ employing procedure renormalization, which is introduced in the regularization of ultraviolet divergences in loop integrals. With aim to evaluate the presence of instabilities in all field space, those energy-scale dependent couplings must satisfy the same constraints obtained at tree level in section 2.3.2, ensuring a bounded effective Higgs potential from below and preventing a possible decay of EW minima.

Besides the importance of the vacuum behavior, the RGE are worth tools to determine by the triviality principle energy bounds of the parameters and perturbative validity of the model. In a practical sense, to numerically evaluate the energy dependence of the quartic couplings one loop level, it is necessary to consider RGEs of all remain couplings, i.e., the gauge group couplings g', g, g_s of the symmetry groups $U(1)$, $SU(2)$, $SU(3)$, the vacuum expectation values v_1, v_2, and the Yukawa couplings of the top and the down quark sectors η_{tt}, η_{bb} and $\eta_{\tau\tau}$ (couplings to Φ_1 doublet) and ξ_{tt}, ξ_{bb} and $\xi_{\tau\tau}$ (couplings to Φ_2 doublet) respectively are computed in Refs [120,121]. The one loop RGEs for a general gauge theory are presented in [113, 122, 123] and for NHDM theory with gauge group $SU(2)_L \times U(1)_Y$ were computed in [124, 125]. For the particular inert-2HDM, RGEs can be found in [126]. They have also been proved with `SARAH`-package [127].

In this section, we describe an algebraic form to get β structures with the aid of scale invariant effective Higgs potential formalism. This systematic is an additional method to obtain RGEs besides to the diagrammatic form presented in chapter 3. This part is based mainly on the structure followed by [209].

At one loop, the effective potential $V_{eff}(\Phi)$ for a scalar theory

$$V_{eff}(\Phi) = V_0(\Phi) + V_1(\Phi) + ...$$

$V_0(\Phi)$ is the tree level Higgs potential given in Eq. (1.2.1). The Higgs potential up to one loop ($M\bar{S}$ scheme) defined by

$$V_1(\Phi) = \frac{1}{4}\frac{1}{16\pi^2}\mathrm{STr}\left(M^4\right)\ln\left(\frac{M^2(\Phi)}{\mu^2} - C\right)$$

M includes all possible contributions to the scalar, fermion and vector masses, being Str the spin-weighted trace (with arbitrary background values of scalar fields). The supertrace operator counts positively (negatively) the number of degrees of freedom for the different bosonic and fermionic fields. C is a (constant) diagonal matrix which depends on the renormalization scheme, and finally μ is the mass scale. In the Landau gauge, V_{eff} obeys the following RGE

$$\left[\mu\frac{\partial}{\partial\mu} + \sum_i \beta_i\frac{\partial}{\partial\lambda_i} - \left(\Phi\gamma\frac{\partial}{\partial\Phi} + \text{c.c.}\right)\right]V_{eff} = 0$$

where the $\lambda_i$include all mass parameters and coupling constants, and γ is the matrix of anomalous dimensions of the scalar fields. Defining $n-$derivative operator $\mathcal{D}$ as

$$\mathcal{D}^{(n)} = \sum_i \beta_i^{(n)}\frac{\partial}{\partial\lambda_i} - \left(\Phi\gamma^{(n)}\frac{\partial}{\partial\Phi} + \text{c.c.}\right)$$

For $n = 1$, we have

$$\mathcal{D}^{(1)}V_1 = -\mu\frac{\partial}{\partial\mu}V_1 = \frac{1}{2}\frac{1}{16\pi^2}\mathrm{Str}\left(M^4\right) \tag{J.1.1}$$

By comparing coefficients of the various Φ terms on the two sides of Eq. (J.1.1) and knowing γ, it is possible to determine all the one-loop β functions.

Setting Yukawa and gauge couplings equal to zero

$$M^2 = \begin{pmatrix} A & B \\ C & D \end{pmatrix}$$

where

$$\begin{aligned} A &= \begin{pmatrix} \frac{\partial^2 V}{\partial\phi_i\partial\phi^{\dagger j}} & \frac{\partial^2 V}{\partial\phi_i\partial\xi^{\dagger j}} \\ \frac{\partial^2 V}{\partial\xi_i\partial\phi^{\dagger j}} & \frac{\partial^2 V}{\partial\xi_i\partial\xi^{\dagger j}} \end{pmatrix} \\ B &= \begin{pmatrix} \frac{\partial^2 V}{\partial\phi_i\partial\phi_j} & \frac{\partial^2 V}{\partial\phi_i\partial\xi_j} \\ \frac{\partial^2 V}{\partial\xi_i\partial\phi_j} & \frac{\partial^2 V}{\partial\xi_i\partial\xi_j} \end{pmatrix} \\ C &= \begin{pmatrix} \frac{\partial^2 V}{\partial\phi^{\dagger i}\partial\phi^{\dagger j}} & \frac{\partial^2 V}{\partial\phi^{\dagger i}\partial\xi^{\dagger j}} \\ \frac{\partial^2 V}{\partial\xi^{\dagger i}\partial\phi^{\dagger j}} & \frac{\partial^2 V}{\partial\xi^{\dagger i}\partial\xi^{\dagger j}} \end{pmatrix} \\ D &= \begin{pmatrix} \frac{\partial^2 V}{\partial\phi^{\dagger i}\partial\phi_j} & \frac{\partial^2 V}{\partial\phi^{\dagger i}\partial\xi_j} \\ \frac{\partial^2 V}{\partial\xi^{\dagger i}\partial\phi_j} & \frac{\partial^2 V}{\partial\xi^{\dagger i}\partial\xi_j} \end{pmatrix}. \end{aligned}$$

Here $i,j=1,2$ are $SU(2)$ indices and we have defined $\phi\equiv\Phi_1$ and $\xi\equiv\Phi_2$. For instance the $1,1$ matrix element of A

$$\frac{\partial^2 V}{\partial\phi_i\partial\phi^{\dagger j}} = \delta^i{}_j\left(\lambda_1\phi^\dagger\phi+\lambda_3\xi^\dagger\xi+\lambda_6\left(\phi^\dagger\xi+\xi^\dagger\phi\right)\right)+\lambda_1\phi^{\dagger i}\phi_j+\lambda_4\xi^{\dagger i}\xi_j+\lambda_6\left(\phi^{\dagger i}\xi_j+\xi^{\dagger i}\phi_j\right)$$

Since we are neglecting gauge and Yukawa terms, there are no contributions to γ. Hence, from Eq. (J.1.1), we have that

$$\begin{aligned} \frac{1}{2}\mathrm{STr}\left(M^4\right) &= \frac{1}{2}\left[\mathrm{Tr}\left(A^2\right)+2\mathrm{Tr}\left(BC\right)+\mathrm{Tr}\left(D^2\right)\right] \\ &= \frac{\beta_{\lambda_1}}{2}\left(\phi^\dagger\phi\right)^2+\frac{\beta_{\lambda_2}}{2}\left(\xi^\dagger\xi\right)^2+\beta_{\lambda_3}\left(\phi^\dagger\phi\right)\left(\xi^\dagger\xi\right)+\beta_{\lambda_4}\left(\phi^\dagger\xi\right)\left(\xi^\dagger\phi\right) \\ &\quad+\left\{\frac{\beta_{\lambda_5}}{2}\left(\phi^\dagger\xi\right)^2+\left[\beta_{\lambda_6}\left(\phi^\dagger\phi\right)+\beta_{\lambda_7}\left(\xi^\dagger\xi\right)\right]\left(\phi^\dagger\xi+\xi^\dagger\phi\right)\right\} \end{aligned}$$

We have assumed that all λ_i and $m_{ij}\in$R. By direct straightforward calculations, we can get the following β functions

$$\begin{aligned} \beta_{\lambda_1} &= 12\lambda_1^2+4\lambda_3^2+4\lambda_3\lambda_4+2\lambda_4^2+2\lambda_5^2+24\lambda_6^2 \\ \beta_{\lambda_2} &= 12\lambda_2^2+4\lambda_3^2+4\lambda_3\lambda_4+2\lambda_4^2+2\lambda_5^2+24\lambda_6^2 \\ \beta_{\lambda_3} &= \left(\lambda_1+\lambda_2\right)\left(6\lambda_3+2\lambda_4\right)+4\lambda_3^2+2\lambda_4^2+2\lambda_5^2+4\lambda_6^2+16\lambda_6\lambda_7+4\lambda_7^2 \\ \beta_{\lambda_4} &= 2\left(\lambda_1+\lambda_2\right)\lambda_4+8\lambda_3\lambda_4+4\lambda_4^2+8\lambda_5^2+10\lambda_6^2+4\lambda_6\lambda_7+10\lambda_7^2 \\ \beta_{\lambda_5} &= 2\left(\lambda_1+\lambda_2\right)\lambda_5+8\lambda_3\lambda_5+12\lambda_4\lambda_5+10\lambda_6^2+4\lambda_6\lambda_7+10\lambda_7^2 \\ \beta_{\lambda_6} &= 12\lambda_1\lambda_6+6\lambda_3\left(\lambda_6+\lambda_7\right)+8\lambda_4\lambda_6+4\lambda_4\lambda_7+10\lambda_5\lambda_6+2\lambda_5\lambda_7 \\ \beta_{\lambda_7} &= 12\lambda_2\lambda_7+6\lambda_3\left(\lambda_6+\lambda_7\right)+4\lambda_4\lambda_6+8\lambda_4\lambda_7+2\lambda_5\lambda_6+10\lambda_5\lambda_7 \end{aligned}$$

Including gauge contributions at order $O\left(g^4,g^2g^{'2},g^{'4}\right)$ are described by the following matrix

$$M_V^2 = \begin{pmatrix} \frac{1}{2}g^2\phi^\dagger\left\{\tau^a,\tau^b\right\}\phi+\frac{1}{2}g^2\xi^\dagger\left\{\tau^a,\tau^b\right\}\xi & \frac{1}{2}gg^{'}\phi^\dagger\tau^a\phi+\frac{1}{2}gg^{'}\xi^\dagger\tau^a\xi \\ \frac{1}{2}gg^{'}\phi^\dagger\tau^a\phi+\frac{1}{2}gg^{'}\xi^\dagger\tau^a\xi & \frac{1}{2}g^{'2}\phi^\dagger\phi+\frac{1}{2}g^{'2}\xi^\dagger\xi \end{pmatrix}$$

Using the following features

$$\begin{aligned} \left\{\tau^a,\tau^b\right\} &= 2\delta^{ab} \\ \left(\tau^a\right)^i_j\left(\tau^b\right)^k_l &= 2\delta^i_l\delta^j_k-\delta^i_j\delta^k_l \end{aligned}$$

The spin-weighted super trace is given by

$$\begin{aligned}\mathrm{STr}\left(M_V^4\right) &= 3\left(\frac{3}{4}g^4+\frac{1}{4}g^{'4}\right)\left[\left(\phi^\dagger\phi\right)^2+\left(\xi^\dagger\xi\right)^2+2\phi^\dagger\phi\xi^\dagger\xi\right]\\ &+\frac{3}{2}g^2g^{'2}\left[\left(\phi^\dagger\phi\right)^2+\left(\xi^\dagger\xi\right)^2+4\phi^\dagger\xi\xi^\dagger\phi-2\phi^\dagger\phi\xi^\dagger\xi\right]\end{aligned}$$

The factor 3 coming from polarization degrees of freedom of the gauge vector bosons. The $O\left(\eta_t^4\right)$ contributions from the top mass

$$M_t^2=\eta_t^2\phi^\dagger\phi$$

In this particular case, the top quark has just been coupled to the first doublet ϕ. So that

$$\mathrm{STr}\left(M^4\right)=-12j\eta_t^4\left(\phi^\dagger\phi\right)^2$$

The minus sign comes from Fermi-Dirac statistic. A factor of 3 is by the color degeneracy of top quark and 4 is the spin counting factor. The remaining mixed contributions of $O\left(\lambda_i\eta_t^2,\lambda_ig^2,\lambda_ig^{'2}\right)$ come from the anomalous dimension terms in Eq. (J.1.1), which in the Landau gauge are

$$\begin{aligned}\gamma_\phi &= 3\eta_t^2-\frac{9}{4}g^2-\frac{3}{4}g^{'2}\\ \gamma_\xi &= -\frac{9}{4}g^2-\frac{3}{4}g^{'2}\end{aligned}$$

With all contributions, $\beta-functions$ changing into

$$\begin{aligned}\beta_{\lambda_1} &\to \beta_{\lambda_1}+\frac{3}{4}\left(3g^4+g^{'4}+2g^2g^{'2}\right)-3\lambda_1\left(3g^2+g^{'2}-4\eta_t^2\right)-12j\eta_t^4\\ \beta_{\lambda_2} &\to \beta_{\lambda_2}+\frac{3}{4}\left(3g^4+g^{'4}+2g^2g^{'2}\right)-3\lambda_2\left(3g^2+g^{'2}\right)\\ \beta_{\lambda_3} &\to \beta_{\lambda_3}+\frac{3}{4}\left(3g^4+g^{'4}-2g^2g^{'2}\right)-3\lambda_3\left(3g^2+g^{'2}-2\eta_t^2\right)\\ \beta_{\lambda_4} &\to \beta_{\lambda_4}+3g^2g^{'2}-3\lambda_4\left(3g^2+g^{'2}-2\eta_t^2\right)\\ \beta_{\lambda_5} &\to \beta_{\lambda_5}-3\lambda_5\left(3g^2+g^{'2}-2\eta_t^2\right)\\ \beta_{\lambda_6} &\to \beta_{\lambda_6}-3\lambda_6\left(3g^2+g^{'2}-3\eta_t^2\right)\\ \beta_{\lambda_7} &\to \beta_{\lambda_7}-3\lambda_7\left(3g^2+g^{'2}-\eta_t^2\right)\end{aligned}$$

The Renormalization Group Equations for gauge sector at one loop level are given by

$$\frac{dg}{dt} = \frac{1}{16\pi^2}\left(\frac{4}{3}n_f+\frac{1}{6}n_H-\frac{22}{3}\right)g^3=-3g^3, \tag{J.1.2}$$

$$\frac{dg'}{dt} = \frac{1}{16\pi^2}\left(\frac{20}{9}n_F+\frac{1}{6}n_H\right)g^{'3}=7g^{'3}, \tag{J.1.3}$$

$$\frac{dg_s}{dt} = \frac{1}{16\pi^2}\left(\frac{4}{3}n_f-11\right)g_s^3=-7g_s^3. \tag{J.1.4}$$

Since for 2HDM, $n_H=2$ and $n_f=3$ (the same fermionic content of SM). In all equations $t=\log\mu$.

K. Scattering states for massive fermions and bosons

K.1. Fundamentals of two particle scattering

We consider the scattering of two particles in the center of mass reference. This general treatment has been used in the description of unitarity behavior of different scatterin processes (See Chapter 4). To create states of definite total angular momentum (which is conserved in all physical processes) one must combine the"orbital" and the "static spin" degrees of freedom by the traditional rules of the addition of angular momentum. One starts with a standard physical state in the center-of-mass frame of the two particles involving particle 1 moving (in the z-direction) with momentum $p\widehat{z}$, helicity λ_a, and particle 2 moving in the opposite direction with momentum $-p\widehat{z}$ and helicity λ_b,

$$|p\widehat{z},\lambda_a\lambda_b\rangle = |p\widehat{z},\lambda_a\rangle \times U(=,\pi,0)|p\widehat{z},\lambda_b\rangle, \tag{K.1.1}$$

where $U(0,\pi,0)$ is a matrix rotation. Total helicity of the two-particles system is defined as

$$\Lambda = \Lambda_1 + \Lambda_2 = \mathbf{J}_1\cdot\widehat{p}_1 + \mathbf{J}_2\cdot\widehat{p}_2 = (\mathbf{J}_1 - \mathbf{J}_2)\cdot\widehat{p}. \tag{K.1.2}$$

It is also useful to define the relative helicity of the two-particles system as

$$\mathbf{J}\cdot\widehat{p} = (\mathbf{J}_1 + \mathbf{J}_2)\cdot\widehat{p} = \Lambda_1 - \Lambda_2 \tag{K.1.3}$$

Now, we can construct two-particle helicity states [111] in the same way we obtained the one-particle helicity states above. First, we define two-particle plane wave states in the CM-frame. However, there is a subtle question of phases that must first be addressed. As in the derivation of the one-particle helicity states, one begins from the state moving along the z-direction and rotates to the desired orientation. But, in the two-particle state in the CM-frame, if $\mathbf{p}_1 = p\widehat{z}$ then $\mathbf{p_2} = -p\widehat{z}$. Thus we must define the state $|-p\widehat{z},\lambda\rangle$. This fact can be done in two different ways. (i) Start in the rest frame with a state of helicity, boosted along the positive z-direction and then rotate to the negative z-axis, or (ii) start in the rest frame with a state of helicity and boost along the negative z-axis. These two results yield states that differ by a phase, so a convention is required. We shall choose the Jacob-Wick second particle protocol which defines a helicity state of a particle of spin s moving in the negative z-direction to be

$$|-p\widehat{z},\lambda\rangle = (-1)^{s-\lambda}e^{i\pi J_y}|p\widehat{z},\lambda\rangle \tag{K.1.4}$$

J_y is the rotation generator in the y-axis (Euler's angle θ). This definition implies

$$\lim_{p\to 0}\langle p\widehat{z},-\lambda|-p\widehat{z},\lambda\rangle \tag{K.1.5}$$

The phase factor in Eq. (K.1.4) comes from

$$e^{-i\pi J_y}|J,M\rangle = (-1)^{J-M}|J,-M\rangle. \tag{K.1.6}$$

The two-particle plane-wave state is then defined by

$$|\mathbf{p};\lambda_a\lambda_b\rangle \equiv U\left[R(\phi,\theta\phi)\right]|p\widehat{z},\lambda_a\rangle \times |-p\widehat{z},\lambda_2\rangle. \tag{K.1.7}$$

It follows from Eq. (K.1.3) that

$$\mathbf{J}\cdot\widehat{p}|\mathbf{p},\lambda_a,\lambda_b\rangle = \lambda|\mathbf{p},\lambda_a\lambda_b\rangle, \lambda = \lambda_a - \lambda_b, \tag{K.1.8}$$

Likewise for one particle state, we can obtain the angular momentum projection

$$|p, J, M, \lambda_a\lambda_b\rangle = \sqrt{\frac{2J+1}{4\pi}} \int d\Omega D^{(J)}_{M\lambda}(R)^* |\mathbf{p}, \lambda_a\lambda_b\rangle. \tag{K.1.9}$$

The angular momentum states $\{|p, J, M, \lambda\rangle\}$ also form a basis in the space of single particle states. Hence we can invert (K.1.9) to obtain

$$|p, \theta, \phi, \lambda\rangle = \sum_{J,M} |p, J, M, \lambda\rangle D^{(J)}(\theta, \phi, 0)^M_\lambda . \tag{K.1.10}$$

In particular, the "standard state" is given by

$$|p\widehat{z}, \lambda\rangle = \sum_J |p, J, \lambda, \lambda\rangle. \tag{K.1.11}$$

From the expression for the two-particle helicity state given in Eqs. (K.1.10)-(K.1.11), it is straightforward to derive formula for scattering amplitudes in terms of helicity amplitudes [111, 149].

K.2. Jacob-Wick Formalism

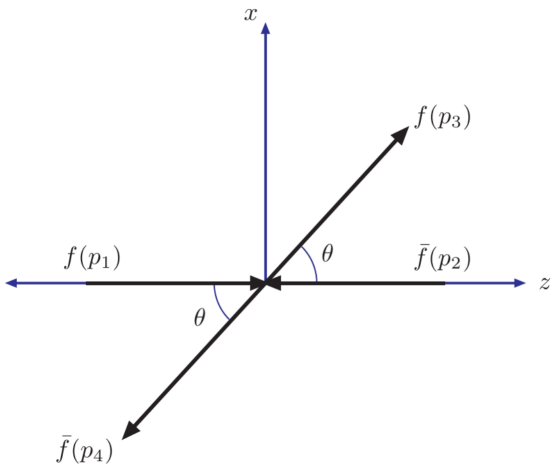

Figure K.1.: *Two particle scattering in the center of mass reference.*

In the follows, we reconstruct Jacob Wick formalism, which is based on diagonalization of S- matrix in the angular momentum basis. Starting with the invariant matrix element defined as

$$\langle f|\widehat{T}|i\rangle = (2\pi)^2\delta^4(P_f - P_i)\mathcal{M}_{fi}. \tag{K.2.1}$$

being $\widehat{T} = i(\widehat{S} - 1)$, and $|i\rangle$, $|f\rangle$ represent initial and final states respectively. For instance

$$|i\rangle = |p_a, \lambda_a; p_b, \lambda_b\rangle, \tag{K.2.2}$$
$$|f\rangle = |p_c, \lambda_c; p_d, \lambda_d\rangle. \tag{K.2.3}$$

In the definition of the matrix element appears the δ-functions corresponding to the energy-momentum conservation. To get the desired constraints, we reduce our Hilbert space to a subspace H_s with given total energy and momentum. By reducing $|i\rangle$ and $|f\rangle$ into H_s the δ function is automatically taken into account. We do it from two-particle states with definite momentum. For one-particle states, we use the normalization

$$\langle p', \lambda'|p, \lambda\rangle = 2E\delta_{\lambda\lambda'}\delta^3(p - p). \tag{K.2.4}$$

so that the two-particle states are normalized as follows

$$\langle p_c\lambda_c; p_d\lambda_d|p_a\lambda_a; p_b\lambda_b\rangle = (2E_a)(2E_b)(2\pi)^6\delta^3(\mathbf{p}_c - \mathbf{p}_a)\,\delta^3(\mathbf{p}_d - \mathbf{p}_b). \tag{K.2.5}$$

The product of δ function can be recast as

$$\delta^3\left(\mathbf{p}_c-\mathbf{p}_a\right)\delta^3\left(\mathbf{p}_d-\mathbf{p}_b\right)=\Lambda\delta^4\left(p_c+p_d-p_a-p_d\right)\delta^2\left(\mathbf{n}'-\mathbf{n}\right). \tag{K.2.6}$$

where $\mathbf{n},\mathbf{n}'$ are unit vectors in directions p_a and p_c ($\delta^2(n-n')$ can be written in terms of angles (θ,φ) as $\delta(\cos\theta'-\cos\theta)\delta\left(\varphi'-\varphi\right)$. The Λ is a normalization factor given as $\Lambda\equiv|\det(J)|$, where J is Jacobian of the considered transformation. In our case we have (denoting $\mathbf{p}_a=(p_{a1},p_{a2},p_{a3})$ and $\mathbf{p}_b=(p_{b1},p_{b2},p_{b3})$) [44]

$$\begin{array}{llll} p_{a1} & & & p_{a1}+p_{b1} \\ p_{a2} & \boldsymbol{p}_a+\boldsymbol{p}_b= & & p_{a2}+p_{b2} \\ p_{a3} & & & p_{c3}+p_{c3} \\ p_{b1} & E_a+E_b= & & \sqrt{p_{a1}^2+p_{a2}^2+p_{a3}^2+m_a^2}+\sqrt{p_{b1}^2+p_{b2}^2+p_{b3}^2+m_b^2} \\ p_{b2} & \cos\theta= & & \frac{p_{a3}}{\sqrt{p_{a1}^2+p_{a2}^2+p_{a3}^2}} \\ p_{b3} & \mathrm{Tan}\phi= & & \frac{p_{a1}}{p_{a2}} \end{array} \tag{K.2.7}$$

The Jacobian has the form

$$J_{ij}=\frac{\partial p'_{ij}}{\partial p_{ij}}. \tag{K.2.8}$$

The determinant J_{ij} become

$$|\det J|=\left(\frac{p_{a1}^2+p_{a2}^2+p_{a3}^2}{\sqrt{p_{a1}^2+p_{a2}^2+p_{a3}^2+m_a^2}}-\frac{p_{a1}p_{b1}+p_{a2}p_{b2}+p_{a3}p_{b3}}{\sqrt{p_{b1}^2+p_{b2}^2+p_{b3}^2+m_b^2}}\right)\left(p_{a1}^2+p_{a2}^2+p_{a3}^2\right)^{3/2}. \tag{K.2.9}$$

and this can be expressed in the c. m. system (where $\boldsymbol{p}_a=-\boldsymbol{p}_b$ and $s=\left(E_a+E_b\right)^2$)

$$|\det J|=\frac{1}{|\boldsymbol{p}|^3}\left(\frac{|\boldsymbol{p}|^2}{E_a}+\frac{|\boldsymbol{p}|^2}{E_b}\right)=\frac{\sqrt{s}}{E_aE_b|\boldsymbol{p}|}. \tag{K.2.10}$$

Using this relation, we can transform the normalization (K.2.5) as

$$\begin{aligned} \langle p_c\lambda_c;p_d\lambda_d|p_a\lambda_a;p_b\lambda_b\rangle &= (2E_a)(2E_b)(2\pi)^6\delta^3\left(\mathbf{p}_c-\mathbf{p}_a\right)\delta^3\left(\mathbf{p}_d-\mathbf{p}_b\right)\delta_{\lambda_c,\lambda_a}\delta_{\lambda_d,\lambda_b} \\ &= \frac{4\left(2\pi\right)^2\sqrt{s}}{|\boldsymbol{p}|}\left(2\pi\right)^4\delta^4\left(p_c+p_d-p_a-p_b\right)\delta\left(\mathbf{n}'-\mathbf{n}\right). \end{aligned} \tag{K.2.11}$$

In our treatment

$$\int\delta^2\left(\mathbf{n}-\mathbf{n}'\right)f\left(\mathbf{n}\right)d\Omega=f\left(\boldsymbol{n}'\right). \tag{K.2.12}$$

We see that in (K.2.11) the total four-momentum conservation is factored out. Thus we can reduce the state vectors to the H_s (our kets and bras contain a subindex s indicating operations in the respective Hilbert subspace). With aim to fix the normalization, the scalar product is defined as

$${}_s\langle p_c\lambda_c;p_d\lambda_d|p_a\lambda_a;p_b\lambda_b\rangle_s=\delta\left(\boldsymbol{n}-\boldsymbol{n}'\right). \tag{K.2.13}$$

However, in doing this, one must be careful when reducing operators, since there can appear some extra factor. Restricting the unit operator to our subspace with (K.2.11) and dropping $\left(2\pi\right)^4\delta^4\left(P_f-P_i\right)$, one is left with the factor

$$\frac{4\left(2\pi\right)^2\sqrt{s}}{|\mathbf{p}|}. \tag{K.2.14}$$

and a delta function, which represents $\widehat{I}$ in our new basis. Such a factor appears in the expression for invariant amplitude on H_s.

$$\mathcal{M}_{fi}\left(s,\Omega\right)=4\left(2\pi\right)^2\frac{\sqrt{s}}{|\mathbf{p}|}\,{}_s\langle p_c,\lambda_c;p_d,\lambda_d|\mathcal{T}|p_a,\lambda_a;p_b,\lambda_b\rangle_s \tag{K.2.15}$$

where $\mathcal{T}$ is the reduction of the original transition operator T. In a similar way, it is possible to reduce the angular momentum and for the states characterized by the angular momentum J and its projection M along the axis z, as Eq (K.1.9):

$$|p,J,M,\lambda_a,\lambda_b\rangle = \sqrt{\frac{2J+1}{4\pi}}\int d\Omega \mathcal{D}^{(J)}_{M\lambda}(R)^*|\mathbf{p},\lambda_a,\lambda_b\rangle \tag{K.2.16}$$

which has been written in the CM of reference. Let us now transform the matrix element to the eigenstates (K.2.16), by using orthogonality relations fro $D-$Wigner representations

$$\delta_{\lambda_a,\lambda_b}\sum_{J,M}\left(\frac{2J+1}{4\pi}\right)^{1/2}\mathcal{D}^{J}_{\lambda_a-\lambda_b,M}\left(R^{-1}_{\theta,\varphi}\right)D^{J}_{\lambda_a-\lambda_b,M}\left(R^{-1}_{\theta,\varphi}\right)=\delta\left(\mathbf{n}-\mathbf{n}'\right) \tag{K.2.17}$$

Therefore, the momentum eigenstates can be expressed as

$$|\mathbf{p},\lambda_a,\lambda_b\rangle = \sum_{J,M}\left(\frac{2J+1}{4\pi}\right)^{1/2}\mathcal{D}^{J*}_{\lambda_a-\lambda_b,M}|p,J,M,\lambda_a,\lambda_b\rangle \tag{K.2.18}$$

Thus the elements of $\widehat{T}$ become

$$\langle \mathbf{p}_i,\lambda_a,\lambda_b|\mathcal{T}|\mathbf{p}_f,\lambda_c,\lambda_d\rangle = \sum_{J,M}\left(\frac{2J+1}{4\pi}\right)\mathcal{D}^{J}_{\lambda_a-\lambda_b,M}\left(R^{-1}_{\theta',\varphi'}\right)\mathcal{D}^{J}_{\lambda_c-\lambda_d,M}\left(R^{-1}_{\theta,\varphi}\right)\ {}_s\langle \mathbf{p}_i,J,M,\lambda_c,\lambda_d|\mathcal{T}|\mathbf{p}_f,J,M,\lambda_c,\lambda_d\rangle_s \tag{K.2.19}$$

The commutation relation $[S_i,J_i]=0$ (which is satisfied also in the subspace H_s), implies that the $\mathcal{T}$ is a scalar under rotations. Then, using Wigner theorem, one has

$${}_s\langle J_f,M_f,\lambda_c,\lambda_d|\mathcal{T}|J_i,M_i,\lambda_a,\lambda_b\rangle_s = \langle\lambda_c\lambda_d||\mathcal{T}_{IJ}(s)||\lambda_a\lambda_b\rangle\delta^{J_F}_{J}\delta^{M_f}_{M_i}\delta^{J}_{J_i} = \delta^{J_f}_{J_I}\delta^{M'}_{M}\mathcal{T}^{J}_{\lambda_c\lambda_d,\lambda_a\lambda_b}. \tag{K.2.20}$$

There is another very useful identity for $D-$functions, namely

$$\sum_{M=-J}^{J}\mathcal{D}^{J}_{m',M}(R')\,\mathcal{D}^{J}_{M,m}(R)=\mathcal{D}^{J}_{m',m}(R'R) \tag{K.2.21}$$

$$\langle \mathbf{p}_i,\lambda_a,\lambda_b|T|\mathbf{p}_f,\lambda_c,\lambda_d\rangle = \sum_{J,M}\frac{2J+1}{4\pi}D^{J*}_{\lambda_c-\lambda_d,\lambda_a-\lambda_b}(\varphi,\theta,0)\,T^{J}_{\lambda_c\lambda_d,\lambda_a\lambda_b}(s) \tag{K.2.22}$$

where φ,θ now denote the transformation angles between $\mathbf{n}$ and $\mathbf{n}$. In terms of invariant amplitude

$$\mathcal{M}(s,\theta)=32\pi\sum_{J,M}(2J+1)\,\mathcal{D}^{J*}_{\lambda_c-\lambda_d,\lambda_a-\lambda_b}(\varphi,\theta,0)\,\mathcal{M}^{J}_{\lambda_c\lambda_d,\lambda_a\lambda_b}(s) \tag{K.2.23}$$

K.2.1. Helicity states

One processes in which we are focused is the annihilation of a pair fermion-anti fermion into two spinless particles. In addition to the isospin quantum numbers and momentum, initial states are labeled with the letters (a,b) for helicities. In the center-of-mass frame, the initial and final momenta in the scattering plane are depicted in Fig. K.1. The initial two-particle system can be characterized as

$$|\mathbf{p}_i,I,\lambda_a,\lambda_b\rangle = \sum_{J}|p_i,I,J,M=\lambda_a-\lambda_b,\lambda_a,\lambda_b\rangle D^{(J)}(\phi,\Theta,0)^{\lambda_a-\lambda_b}_{\lambda_a-\lambda_b}. \tag{K.2.24}$$

For $\Theta=0$ under alignment of the initial process with z axis, D-Wigner representation at equal M is unity ($D^{(J)}(\phi,\Theta,0)^{\lambda_a-\lambda_b}_{\lambda_a-\lambda_b}=\widehat{I}$). The final two particles[1]

$$|\mathbf{p}_f,I,\lambda_c,\lambda_d\rangle = \sum_{J,M}|p_f,I,J,M,\lambda_c,\lambda_d\rangle D^{J}(\phi,\theta,0)^{M}_{\lambda_c-\lambda_d}. \tag{K.2.26}$$

[1]These $D-$functions satisfy the following orthogonality relation

$$\int D^{*(j_1)}_{m_1m_1'}D^{*(j_2)}_{m_2m_2'}\frac{d\Omega}{4\pi}=\frac{1}{2j_1+1}\delta_{m_1m_2}\delta_{m_1'm_2'}\delta_{j_1j_2} \tag{K.2.25}$$

where we have assumed that the initial states have been "prepared" with well-defined values of helicity (hence there is no sum over M) while the final states do not have a clearly defined helicity. Since all known interactions are invariant under spatial rotations, the scattering matrix conserves total angular momentum. According to the Wigner-Eckart theorem (for the scalar particular case),

$$\langle \mathbf{p}_f, I_f, J_f, M_f, \lambda_c, \lambda_d | T | \mathbf{p}_i, I_i, J_i, M_i, \lambda_a, \lambda_b \rangle = \langle \lambda_c \lambda_d || T_{IJ}(s) || \lambda_a \lambda_b \rangle \delta_J^{J_F} \delta_{M_i}^{M_f} \delta_{J_i}^J. \tag{K.2.27}$$

where s is the root square of the total energy of the system and the first factor on the right-hand side is the "reduced matrix element" depending only on the variables explicitly displayed. Combining Eqs (K.2.24)-(K.2.27) in terms of the invariant amplitude, we find

$$\mathcal{M}(s,\Omega) = \sum_J \langle \lambda_c \lambda_d || M_{IJ}(s) || \lambda_a \lambda_b \rangle d^J(\theta)^{\lambda_a - \lambda_b}_{\lambda_c - \lambda_d} e^{i(\lambda_a - \lambda_b)\phi}, \tag{K.2.28a}$$

$$\mathcal{M}(s,\theta,\phi) = 32\pi \sum_J (2J+1)\, \mathcal{M}^{IJ}_{\lambda_a,\lambda_b,\lambda_c,\lambda_d}(s)\, d^J(\theta)^{\lambda_a - \lambda_b}_{\lambda_c - \lambda_d} e^{i(\lambda_a - \lambda_b)\phi}. \tag{K.2.28b}$$

where we have used

$$\mathcal{M}^{IJ}_{\lambda_a,\lambda_b,\lambda_c,\lambda_d}(s) = \frac{\sqrt{s}}{4|\mathbf{p}|} \mathcal{T}^{IJ}_{\lambda_a,\lambda_b,\lambda_c,\lambda_d}(s) \tag{K.2.29}$$

where s is the root square of the total energy of the system and the first factor on the right-hand side is the "reduced matrix element" depending only on the variables explicitly displayed. Combining Eqs (K.2.24)-(K.2.27) regarding the invariant amplitude, we find

$$d^J(\theta)^M_0 = \left[\frac{(J-M)!}{(J+M)!}\right]^{1/2} (-1)^M P_{JM}(\theta). \tag{K.2.30}$$

With P_{JM} is the associated Legendre function. By defining

$$\mathcal{M}^{I,J}_{\lambda_a,\lambda_b}(s,\phi) = e^{i(\lambda_a - \lambda_b)\phi} \mathcal{M}^{I,J}_{\lambda_a,\lambda_b,0,0}(s), \tag{K.2.31}$$

it is possible to find an explicit form for the coefficients of partial waves

$$\begin{aligned} \mathcal{M}^{I,J}_{\lambda_a\lambda_b}(s) &= \frac{1}{32\pi} \int \mathcal{M}(s,\theta)\, d^J(\theta)^{\lambda_a - \lambda_b}_0\, d(\cos\theta) \\ &= \frac{1}{32\pi} \int \mathcal{M}(s,\theta) \left[\frac{(J+\lambda_b-\lambda_a)!}{(J+\lambda_a-\lambda_b)!}\right]^{1/2} (-1)^{\lambda_a - \lambda_b} P_{J,\lambda_a-\lambda_b}(\cos\theta)\, d(\cos\theta) \end{aligned} \tag{K.2.32}$$

L. Inert Higgs Doublet Model: Eigenstates and Metastability relations

L.1. Mass eigenstates in the IHDM

In this appendix, we discuss the origin of the critical conditions and so on the mass of physical states in the Inert Higgs Doublet Model (IHDM). For this purpose, we start our development by building a Z_2-invariant Higgs potential:

$$\begin{aligned} V_H &= m_{11}^2\Phi_1^\dagger\Phi_1 + m_{22}^2\Phi_2^\dagger\Phi_2 + \frac{1}{2}\lambda_1\left(\Phi_1^\dagger\Phi_1\right)^2 + \frac{1}{2}\lambda_2\left(\Phi_2^\dagger\Phi_2\right)^2 \\ &\quad +\lambda_3\left(\Phi_1^\dagger\Phi_1\right)\left(\Phi_2^\dagger\Phi_2\right) + \lambda_4\left(\Phi_1^\dagger\Phi_2\right)\left(\Phi_2^\dagger\Phi_1\right) + \frac{1}{2}\lambda_5\left[\left(\Phi_1^\dagger\Phi_2\right)^2 + h.c.\right]. \end{aligned} \tag{L.1.1}$$

where $\lambda_5 \in$Re. From a general point of view, the doublets can be parameterized by

$$\Phi_1 = \begin{pmatrix} \phi_1 + i\phi_2 \\ \phi_3 + i\phi_4 \end{pmatrix} \text{ and } \Phi_2 = \begin{pmatrix} \phi_5 + i\phi_6 \\ \phi_7 + i\phi_8 \end{pmatrix},$$

where ϕ_i's are real fields. Concerning ϕ_i fields, the Higgs potential in (L.1.1) can be translated into

$$\begin{aligned} V_H &= m_{11}^2\left(\phi_1^2+\phi_2^2+\phi_3^2+\phi_4^2\right) + m_{22}^2\left(\phi_5^2+\phi_6^2+\phi_7^2+\phi_8^2\right) \\ &\quad +\frac{1}{2}\lambda_1\left(\phi_1^2+\phi_2^2+\phi_3^2+\phi_4^2\right)^2 + \frac{1}{2}\lambda_2\left(\phi_5^2+\phi_6^2+\phi_7^2+\phi_8^2\right)^2 \\ &\quad +\lambda_3\left(\phi_1^2+\phi_2^2+\phi_3^2+\phi_4^2\right)\left(\phi_5^2+\phi_6^2+\phi_7^2+\phi_8^2\right) \\ &\quad +\left(\lambda_4+\lambda_5\right)\left(\phi_1\phi_5+\phi_2\phi_6+\phi_3\phi_7+\phi_4\phi_8\right)^2. \end{aligned}$$

The inert vacuum structure is chosen using

$$\langle\Phi_1\rangle_0 = \frac{v}{\sqrt{2}} \rightarrow \phi_3 = \frac{v}{\sqrt{2}}, \{\phi_1,\phi_2,\phi_4\} = 0 \text{ and } \langle\Phi_2\rangle_0 = 0 \rightarrow \{\phi_5,\phi_6,\phi_7,\phi_8\} = 0.$$

Under this selection, the single non-trivial tadpole (stationary conditions) at tree-level is given by

$$\left.\frac{\partial V_H}{\partial\phi_3}\right|_{\phi_3=\frac{v}{\sqrt{2}}} = 2m_{11}^2\frac{v}{\sqrt{2}} + \lambda_1\frac{v^3}{\sqrt{2}} = 0.$$

Therefore our stationary condition is indeed

$$m_{11}^2 = -\frac{1}{2}\lambda_1 v^2 < 0. \tag{L.1.2}$$

L.1.1. Mass matrices

To compute scalar masses, we make the following physical parameterization for doublets

$$\Phi_1 = \begin{pmatrix} G^+ \\ \frac{h+v+iG^0}{\sqrt{2}} \end{pmatrix} \text{ and } \Phi_2 = \begin{pmatrix} H^+ \\ \frac{H^0+iA^0}{\sqrt{2}} \end{pmatrix}. \tag{L.1.3}$$

The Higgs potential in Eq. (L.1.1) is now expanded regarding physical eigenstates

$$\begin{aligned}
V_H &= m_{11}^2\left(G^+G^- + \frac{h^2+v^2}{2} + hv + \frac{G^0G^0}{2}\right) + m_{22}^2\left(H^+H^- + \frac{H^0H^0}{2} + \frac{A^0A^0}{2}\right) \\
&+\frac{1}{2}\lambda_1\left(G^+G^- + \frac{h^2+v^2}{2} + hv + \frac{G^0G^0}{2}\right)^2 + \frac{1}{2}\lambda_2\left(H^+H^- + \frac{H^0H^0}{2} + \frac{A^0A^0}{2}\right)^2 \\
&+\lambda_3\left(G^+G^- + \frac{h^2+v^2}{2} + hv + \frac{G^0G^0}{2}\right)\left(H^+H^- + \frac{H^0H^0}{2} + \frac{A^0A^0}{2}\right) \\
&+\lambda_4\left(G^-H^+ + \frac{(h+v)\,H^0}{2} + \frac{G^0A^0}{2} + i\frac{(h+v)\,A^0}{2} - i\frac{G^0H^0}{2}\right) \\
&\times\left(G^+H^- + \frac{(h+v)\,H^0}{2} + \frac{G^0A^0}{2} - i\frac{(h+v)\,A^0}{2} + i\frac{G^0H^0}{2}\right) \\
&+\frac{1}{2}\lambda_5\left(G^-H^+ + \frac{(h+v)\,H^0}{2} + \frac{G^0A^0}{2} + i\frac{(h+v)\,A^0}{2} - i\frac{G^0H^0}{2}\right)^2 \\
&+\frac{1}{2}\lambda_5\left(G^-H^+ + \frac{(h+v)\,H^0}{2} + \frac{G^0A^0}{2} - i\frac{(h+v)\,A^0}{2} + i\frac{G^0H^0}{2}\right)^2 . \qquad \text{(L.1.4)}
\end{aligned}$$

Physical mass terms are easily obtained by making the following partial derivatives

$$m_{h^0}^2 = \frac{\partial V_H}{\partial h^2} = m_{11}^2 + \frac{3}{2}\lambda_1 v^2 = \lambda_1 v^2 \qquad \text{(L.1.5)}$$

$$m_{H^0}^2 = \frac{\partial V_H}{\partial H^2} = m_{22}^2 + \frac{1}{2}\left(\lambda_3+\lambda_4+\lambda_5\right)v^2 \qquad \text{(L.1.6)}$$

$$m_{A^0}^2 = \frac{\partial V_H}{\partial A^2} = m_{22}^2 + \frac{1}{2}\left(\lambda_3+\lambda_4-\lambda_5\right)v^2 \qquad \text{(L.1.7)}$$

$$m_{H^\pm}^2 = \frac{\partial V_H}{\partial H^+\partial H^-} = m_{22}^2 + \frac{1}{2}\lambda_3 v^2. \qquad \text{(L.1.8)}$$

In the term associated with $m_{h^0}^2$, we have used the stationary condition in Eq. (L.1.2).

L.2. Metastability in the Inert 2HDM

The vacuum structure in the IHDM is concentrated in the first doublet, i.e., $\langle\Phi_1\rangle_0 = v/\sqrt{2}$, yielding the stationary condition (L.1.2) and masses given by Eqs. (L.1.5)-(L.1.8). Under this choice, Z_2 symmetry is preserved in the Higgs potential and Yukawa sector after SSB, providing a conserved quantum number as we will just point out: real part neutral field inside the first doublet is identified with h^0, right part of (L.1.3). The remaining components are the Goldstone boson G^0 in this case, and the $G^\pm$ for the charged part of Φ_1. On the other hand Φ_2 yields the remaining physical degrees, $H^\pm, H^0$ and A^0. None of these extra fields is coupled to fermions, which is originated by the effect of an *intact* Z_2-symmetry and so on exists a conserved quantum number in scattering processes. The consequence of this intact symmetry is that extra scalars within Φ_2 are always produced by pairs. Hence, the lightest scalar in Φ_2 is a feasible dark matter candidate.

All these described features define an Inert vacuum. This state is however only a possible case for most general stationary conditions with general VEVs in both doublets. By assuming a normal vacuum, doublets in general stationary points behave as

$$\langle\Phi_1\rangle = \frac{1}{\sqrt{2}}\begin{pmatrix}0\\ v\end{pmatrix},\ \langle\Phi_2\rangle = \frac{1}{\sqrt{2}}\begin{pmatrix}0\\ v_I\end{pmatrix}.$$

The stationary conditions are given by two cubic coupled equations

$$\begin{aligned}
2m_{11}^2 v^2 + \lambda_1 v^3 + \left(\lambda_3+\lambda_4+\lambda_5\right)v_I^2 &= 0 \\
2m_{22}^2 v_I^2 + \lambda_2 v_I^3 + \left(\lambda_3+\lambda_4+\lambda_5\right)v^2 &= 0.
\end{aligned}$$

where the first vacuum structure is whose obtained by the formulation of an inert-global model in the last section. Nevertheless, a new scenario can be achieved by considering $v = 0$ and $v_I \neq 0$; an inert like structure for stationary

points. The stationary relation between mass and quartic couplings satisfies

$$m_{22}^2 = -\frac{1}{2}\lambda_2 v_I^2.$$

In this case, since only doublet Φ_1 is coupled of matter spectrum, all fermions are massless, obtaining thus an unphysical scenario for nature. Our choice of parameter is such that this regime must be avoided. Because of Inert and Inert like scenarios preserve Z_2 symmetry in the Higgs potential, both structures could exist simultaneously as vacua in the model[1]. Two just necessary conditions, ensuring the existence of simultaneous inert vacua, are given by the following statements [34]:

- *Inert and Inert like minima can coexist in the Higgs potential if* $m_{11}^2 < 0$ *and* $m_{22}^2 < 0$
- *Inert and Inert like minima can coexist in the Higgs potential* $\lambda_3 + \lambda_4 + \lambda_5 > 0$

The relation between depths can be obtained from the discussion presented in Appendix F. There, we give a link between two normal vacua eq (F.4.1),

$$V_N - V_{N_2} = \frac{1}{2}\left[\left(\frac{m_{H^\pm}}{v}\right)_{N_2}^2 - \left(\frac{m_{H^\pm}}{v}\right)_{N_1}^2\right]\left[v_1' v_2 - v_2' v_1\right]^2,$$

which in terms of charged Higgs masses at each minimum inert and inert like,

$$\begin{aligned}
V_I - V_{IL} &= \frac{1}{4}\left[\left(\frac{m_{H^\pm}^2}{v_I^2}\right)_{IL} - \left(\frac{m_{H^\pm}^2}{v^2}\right)_{I}\right] v_I^2 v^2 \\
|V_I - V_{IL}| &= \frac{1}{4}\left|\left(\frac{m_{11}^2 + \frac{1}{2}\lambda_3 v_I^2}{v_I^2}\right) - \left(\frac{m_{22}^2 + \frac{1}{2}\lambda_3 v^2}{v^2}\right)\right| v_I^2 v^2. \\
&= \frac{1}{4}\left|\left(\frac{m_{11}^2}{v_I^2}\right) v_I^2 v^2 - \left(\frac{m_{22}^2}{v^2}\right) v_I^2 v^2\right|. \\
&= \frac{1}{4}\left|m_{11}^2 v^2 - m_{22}^2 v_I^2\right|.
\end{aligned}$$

Replacing VEVs relation with couplings through stationary conditions for both vacua

$$\begin{aligned}
|V_I - V_{IL}| &= \frac{1}{4}\left|-2\left(\frac{m_{11}^4}{\lambda_1}\right) + 2\left(\frac{m_{22}^4}{\lambda_2}\right)\right| \\
&= \frac{1}{2}\left|\left(\frac{m_{22}^4}{\lambda_2}\right) - \left(\frac{m_{11}^4}{\lambda_1}\right)\right|.
\end{aligned}$$

In the particular case for inert and inert like vacua

$$|V_I - V_{IL}| = \frac{1}{2}\left|\frac{m_{22}^4}{\lambda_2} - \frac{m_{11}^4}{\lambda_1}\right|.$$

Therefore, the inert vacuum is the global minimum if

$$V_I - V_{IL} = -\left(\frac{m_{22}^4}{\lambda_2} - \frac{m_{11}^4}{\lambda_1}\right) < 0,$$

which is equivalent to

$$\frac{m_{11}^2}{\sqrt{\lambda_1}} < \frac{m_{22}^2}{\sqrt{\lambda_2}}.$$

In a first view, there is no a way to determine which is the deepest minimum. Parameters set up will determine the minimum in the theory. On the other hand, it is useful to describe the possibility of having one inert vacuum enough lived, in such a way perhaps the inert like minima will be the deepest structure, but it will be suppressed by quantum tunneling effects. This is the aim of the following sections.

[1] In 2HDM at tree level, the minima that break different symmetries of the Higgs potential cannot coexist. If a minimum exists with an exclusive breaking pattern, other stationary points are at most saddle points.

L.2.1. Computing ζ in the Inert 2HDM

From the reparameterization group formalism and systematics presented in appendixes G-I, we proceed to compute ζ in the IHDM. The stationary conditions, from constrained Higgs potential in Eq. (I.1.1), are given by

$$\Lambda^{\mu}{}_{\nu} r^{\nu} - M^{\mu} = \zeta r^{\mu}$$

In the diagonal basis

$$\begin{aligned} \Lambda_0 r^0 - M^0 &= \zeta r^0 \\ \Lambda_k r^k - M^k &= \zeta r^k \end{aligned}$$

with $k = 1, 2, 3$. In the inert Higgs model, r^{μ} and M^{μ} acquire the form

$$\begin{aligned} r^{\mu} &= (r_0, r_1, , r_2, r_3) = \left(\Phi_1^{\dagger}\Phi_1 + \Phi_2^{\dagger}\Phi_2, 2\mathrm{Re}\left(\Phi_1^{\dagger}\Phi_2\right), 2\mathrm{Im}\left(\Phi_1^{\dagger}\Phi_2\right), \Phi_1^{\dagger}\Phi_1 - \Phi_2^{\dagger}\Phi_2\right) \\ M^{\mu} &= (M_0, M_1, M_2, M_3) = \left(-\frac{m_{11}^2 + m_{22}^2}{2}, 0, 0, -\frac{m_{11}^2 - m_{22}^2}{2}\right) \end{aligned}$$

The stationary condition are translated into

$$\begin{aligned} \Lambda_0\left(\Phi_1^{\dagger}\Phi_1 + \Phi_2^{\dagger}\Phi_2\right) - \frac{m_{11}^2 + m_{22}^2}{2} &= \zeta\left(\Phi_1^{\dagger}\Phi_1 + \Phi_2^{\dagger}\Phi_2\right) \\ 2\Lambda_1\mathrm{Re}\left(\Phi_1^{\dagger}\Phi_2\right) &= 2\zeta\mathrm{Re}\left(\Phi_1^{\dagger}\Phi_2\right) \\ 2\Lambda_2\mathrm{Im}\left(\Phi_1^{\dagger}\Phi_2\right) &= 2\zeta\mathrm{Im}\left(\Phi_1^{\dagger}\Phi_2\right) \\ \Lambda_3\left(\Phi_1^{\dagger}\Phi_1 - \Phi_2^{\dagger}\Phi_2\right) - \frac{m_{11}^2 - m_{22}^2}{2} &= \zeta\left(\Phi_1^{\dagger}\Phi_1 - \Phi_2^{\dagger}\Phi_2\right) \end{aligned}$$

Summing 0 and 3

$$\begin{aligned} (\Lambda_0 + \Lambda_3)\left(\Phi_1^{\dagger}\Phi_1\right) + (\Lambda_0 - \Lambda_3)\left(\Phi_2^{\dagger}\Phi_2\right) + m_{22}^2 &= 2\zeta\left(\Phi_1^{\dagger}\Phi_1\right) \\ (\Lambda_0 + \Lambda_3)\left(\Phi_2^{\dagger}\Phi_2\right) + (\Lambda_0 - \Lambda_3)\left(\Phi_1^{\dagger}\Phi_1\right) + m_{11}^2 &= 2\zeta\left(\Phi_2^{\dagger}\Phi_2\right) \end{aligned}$$

In the inert vacuum, the first condition is propitious to determine ζ

$$(\Lambda_0 + \Lambda_3)\frac{v^2}{2} + m_{22}^2 = 2\zeta\frac{v^2}{2},$$

knowing $2\Lambda_0 = \lambda_3 + \sqrt{\lambda_1\lambda_2}$ and $2\Lambda_3 = \lambda_3 - \sqrt{\lambda_1\lambda_2}$, this equation can be translated into

$$m_{H^{\pm}}^2 = \zeta v^2 = \frac{1}{2}\lambda_3 v^2 + m_{22}^2.$$

We have used eigenstates equations for masses. Hence, our minimum is global if

$$\begin{aligned} \frac{1}{2}\left(\lambda_3 + \sqrt{\lambda_1\lambda_2}\right) &> \frac{1}{2}\lambda_3 + \frac{m_{22}^2}{v^2} \\ \frac{1}{2}\sqrt{\lambda_1\lambda_2} &> \frac{m_{22}^2}{v^2} \end{aligned} \tag{L.2.1}$$

and

$$\begin{aligned} \frac{1}{2}\lambda_3 + \frac{m_{22}^2}{v^2} &> -\frac{1}{2}(\lambda_4 + \lambda_5) \\ \frac{1}{2}\lambda_3 + \frac{m_{22}^2}{v^2} &> -\frac{1}{2}(\lambda_4 - \lambda_5) \\ \frac{1}{2}\lambda_3 + \frac{m_{22}^2}{v^2} &> \frac{1}{2}\left(\lambda_3 - \sqrt{\lambda_1\lambda_2}\right) \end{aligned} \tag{L.2.2}$$

From (L.2.1) and (L.2.2), we found finally

$$-\sqrt{\lambda_1\lambda_2} < \frac{2m_{22}^2}{v^2} < \sqrt{\lambda_1\lambda_2}$$

M. Higgs decay in two photons and likelihood proof

M.1. Two photon decay in 2HDMs

It is known from 2HDM fundamentals that charged Higgs might have substantial contribution to the $h \to \gamma\gamma$ decay rate. Since this channel has been an important scenario for Higgs like scalar detection in LHC-experiments, constraints on the parameters controlling this new contribution can therefore be obtained from the Higgs precision measurements. We consider an IHDM and one 2HDM with a softly broken $U(1)$ symmetry in the Higgs potential and Yukawa Lagrangian and assume that the only deviation from a SM-like Higgs behavior comes from the contribution of charged Higgs to the loop-induced process $h \to \gamma\gamma$. More precisely, in these particular models other scalar states are decoupled and only the charged scalar contribution is present[1]. In this case, the contribution from status to the $h \to \gamma\gamma$ decay width is parameterized by charged Higgs mass. The corresponding amplitude at LO reads

$$\mathcal{M}_{h\gamma\gamma}^{H^\pm} = \frac{v^2 g\left(m_{H^\pm}\right)}{2m_{H^\pm}^2} A_0^h\left(\tau_{H^\pm}\right),\ \tau_{H^\pm} = \frac{m_h^2}{4m_{H^\pm}^2}. \tag{M.1.1}$$

where $g\left(m_{H^\pm}\right)$ is the h, H^+H^- coupling and $A_0^h\left(m_h^2/4m_{H^\pm}^2\right)$ form factor. In the Inert 2HDM, $g_I\left(m_{H^\pm}\right) \equiv g\left(m_{H^\pm}\right)$

$$g_I\left(m_{H^\pm}\right) = \lambda_3 \tag{M.1.2}$$

See appendix L at Eq. (L.1.4). For lower values in $\cos\left(\beta-\alpha\right) \approx 0$ (alignment scenario), $g_R\left(H^\pm\right) = g\left(H^\pm\right)$ coupling [88]

$$g_R\left(H^\pm\right) = -\frac{1}{4}\sin^2 2\beta\left(\lambda_1+\lambda_2-2\lambda_{34}\right)-\lambda_3 \tag{M.1.3}$$

The effective Higgs-$\gamma\gamma$ coupling can therefore be expressed by

$$C_\gamma = \frac{|\mathcal{M}_{h\gamma\gamma}^{SM} + \mathcal{M}_{h\gamma\gamma}^{H^\pm}|}{|\mathcal{M}_{h\gamma\gamma}^{SM}|}. \tag{M.1.4}$$

Note that the SM amplitude $h^0\gamma\gamma$ appears both in the numerator and denominator of Eq. (M.1.4) since SM tree-level couplings are assumed. This part for SM contribution has the following terms

$$\mathcal{M}_{h\gamma\gamma}^{SM} = \sum_f N_c Q_f^2 g_{hff} A_{1/2}^h\left(\tau_f\right) + g_{hVV} A_1^h\left(\tau_w\right). \tag{M.1.5}$$

g_{hff} and g_{hVV} are the reduced couplings couplings among Higgs and fermion or vector boson respectively. The form factors in Eq. (M.1.1) are described by

$$A_0^h\left(\tau_{H^\pm}\right) = -\left[\tau_{H^\pm} - f\left(\tau_{H^\pm}\right)\right]\tau_{H^\pm}^{-1}. \tag{M.1.6}$$

$$A_{1/2}^h\left(\tau_f\right) = 2\left[\tau_f + \left(\tau_f-1\right) f\left(\tau_f\right)\right]\tau_f^{-2}. \tag{M.1.7}$$

$$A_1^h\left(\tau_w\right) = -\left[2\tau_w^2 + 3\tau_w + 3\left(2\tau_w-1\right) f\left(\tau_w\right)\right]\tau_w^{-2}. \tag{M.1.8}$$

where equivalently to charged Higgs

$$\tau_f = \frac{m_h^2}{4m_f^2} \text{ and } \tau_w = \frac{m_{h^0}^2}{4m_W^2} \tag{M.1.9}$$

[1] For both models, this assumptions is accomplished by virtue of alignment regimen. In the Inert case, the alignment is achieved trivially, meanwhile in the real 2HDM, we analyze scenarios where this regimen is satisfied at all

Finally the complex functions $f(\tau)$ is itself given by the integral

$$f(\tau) = -\frac{1}{2}\int_0^1 \frac{dy}{y}\ln\left[1-4\tau y(1-y)\right] = \begin{cases} \arcsin^2\left(\sqrt{\tau}\right); & \tau \leq 1 \\ -\frac{1}{4}\left[\ln\left(\frac{\sqrt{\tau}+\sqrt{\tau-1}}{\sqrt{\tau}-\sqrt{\tau-1}}\right) - i\pi\right]^2 & \tau > 1 \end{cases} \tag{M.1.10}$$

M.2. Likelihood proof

We study the likelihood proof used by the code `Lilith` to search a compatibility level between new physics effects with the current data in LHC [35]. Indeed, the searches for the Higgs boson performed by the Run I[2] for ATLAS and CMS collaborations are divided into individual analysis, usually focusing on a single decay mode. For example golden channels in Higgs detection: $i)h \to \gamma\gamma$ (Diphotonic) and $ii)h \to ZZ^* \to 4l$ (Four lepton channels). Within each analysis several event categories are then computed and stored. Among other reasons, these are designed to optimize the sensitivity to the different production mechanisms of the SM Higgs boson (hence, they have different reduced efficiencies eff_{XY}). In order to put constraints on new physics couplings from the results in a given event category, it is necessary to extract the measurement of the signal strength and the relevant eff_{XY} information from the experimental results. For example, measurements of the CMS $h \to \gamma\gamma$ analyses, in terms of signal strengths for all categories With the addition of the reduced efficiencies $\text{eff}_{X,\gamma\gamma}$, also given in Ref. [210], combinations of $\sigma(X)\,B(h \to \gamma\gamma)$ can be constrained.

However, several problems arise when constructing a likelihood measurement. First of all, only two pieces of information are given: the best fit to the data, that will be denoted as $\widehat{\mu}$ in the following, and the 68% confidence level (CL) interval or 1σ interval. Since the full likelihood function category per category is never given, it is necessary to assume that the measurements are approximately Gaussian, it is however possible to reconstruct a simple likelihood, $L(\mu)$, from this information. In that case, $-2\log L(\mu)$ follows a χ^2 law. From the boundaries of the 68% CL interval, left and right uncertainties at 68% CL, $\Delta\mu^-$ and $\Delta\mu^+$, with respect to the best fit point can be derived. The likelihood can then be defined as [35]

$$-2\log L(\mu) = \begin{cases} \left(\frac{\mu-\widehat{\mu}}{\Delta\mu^-}\right)^2 & \text{if } \mu < \widehat{\mu} \\ \left(\frac{\mu-\widehat{\mu}}{\Delta\mu^+}\right)^2 & \text{if } \mu > \widehat{\mu} \end{cases} \tag{M.2.1}$$

with $\Delta\mu^- = \Delta\mu^+$ in the Gaussian regime. While this is often a valid approximation to the likelihood, it should be pointed out that signal strength measurements are not necessarily Gaussian, depending in particular on the size of the event sample. Constraining new physics from a single LHC Higgs category can already be a non-trivial task and come with some uncertainty because the full information is not provided category per category. However, more severe complications typically arise when using several categories/searches at the same time, as is needed for a global fit to the Higgs data. The simplest solution is to define the full likelihood as the product of individual likelihoods

[2]The likelihood obtained from the LHC Run I measurements has been well validated against ATLAS and CMS results, however this could change with LHC Run II results where systematic uncertainties are expected to dominate over the statistical ones, i.e., with more data to be collected during LHC Run II, the construction of a combined likelihood would require more detailed experimental inputs.

Bibliography

[1] S. Chatrchyan and et al. *Observation of a new boson at a mass of 125 GeV with the CMS experiment at the LHC. Phys. Lett. B*, 716(1):30–61, 2012.

[2] G. Aad and et al. *Observation of a new particle in the search for the Standard Model Higgs boson with the ATLAS detector at the LHC. Phys. Lett. B*, 716(1):1–29, 2012.

[3] et al Aad G. Combined measurement of the higgs boson mass in pp collisions at $\sqrt{s} = 7$ and 8 tev with the ATLAS and CMS experiments. *Phys. Rev. Lett.*, 114:191803, May 2015.

[4] et al Beringer J. *Review of Particle Physics. PRD*, 86(1), 2012.

[5] Quiros M. Casas J., Espinosa J. *Improved Higgs mass stability bound in the standard model and implications for supersymmetry . PLB*, 342:171–179, 1995.

[6] J. Elias-Miro J., Espinosa, G. Giudice, F. Isidori, A. Riotto, and A. Strumia. *Higgs mass and vacuum stability in the Standard Model at NNLO. JHEP* **1208**, *098*, 2012. CERN-PH-TH/2012-134, RM3-TH/12-9. arxiv:1205497 [hep-ph].

[7] G. Ridolfi G. Isidori and A. Strumia. *On the metastability of the Standard Model vacuum. Nuc. Phys. B.*, 609:387–409, 2001.

[8] Espinosa J. Burgess C., Di Clemente V. *Effective operators and vacuum instability as heralds of new physics. Journal of High Energy Physics*, 0201:041, 2002.

[9] Joan Elias-Miro, Jose R. Espinosa, Gian F. Giudice, Gino Isidori, Antonio Riotto, and Alessandro Strumia. *Higgs mass implications on the stability of the electroweak vacuum. Phys. Lett.*, B709:222–228, 2012. arXiv:hep-ph/1112.3022.

[10] Joan Elias-Miro, Jose R. Espinosa, Gian F. Giudice, Gino Isidori, Antonio Riotto, and Alessandro Strumia. *Higgs mass implications on the stability of the electroweak vacuum. Phys. Lett.*, B709:222–228, 2012.

[11] F. Bezrukov and M. Shaposhnikov. *Standard Model Higgs boson mass from inflation: Two loop analysis. JHEP*, 07:089, 2009. arXiv:hep-ph/0904.1537.

[12] Vincenzo Branchina, Emanuele Messina, and Marc Sher. *Lifetime of the electroweak vacuum and sensitivity to Planck scale physics. Phys. Rev.*, D91:013003, 2015. arXiv:hep-ph/1408.5302.

[13] Dario Buttazzo, Giuseppe Degrassi, Pier Paolo Giardino, Gian F. Giudice, Filippo Sala, Alberto Salvio, and Alessandro Strumia. *Investigating the near-criticality of the Higgs boson. JHEP*, 12:089, 2013. arXiv:hep-ph/1307.3536.

[14] Vincenzo Branchina and Emanuele Messina. *Stability, Higgs Boson Mass and New Physics. Phys. Rev. Lett.*, 111:241801, 2013.

[15] M. Laine and K. Rummukainen. *Two Higgs doublet dynamics at the electroweak phase transition: A Nonperturbative study. Nucl.Phys.*, B597:23–69, 2001. arXiv:hep-lat/0009025.

[16] James M. Cline, Kimmo Kainulainen, and Axel P. Vischer. *Dynamics of two Higgs doublet CP violation and baryogenesis at the electroweak phase transition. Phys.Rev.*, D54:2451–2472, 1996. arXiv:hep-ph/9506284.

[17] Vasilios Zarikas. *The Phase transition of the two Higgs extension of the standard model. Phys.Lett.*, B384:180–184, 1996. arXiv:hep-ph/9509338.

[18] S. L. Glashow and S. Weinberg. *Natural conservation laws for neutral currents. PRD*, 15(7):1958–1965, 1977.

[19] G. C. Branco, P. M. Ferreira, L. Lavoura, M. N. Rebelo, M. Sher, and J. P. Silva. *Theory and phenomenology of two-Higgs-doublet models. Physics Reports*, 516(1-2):1–102, 2012.

[20] Shuquan Nie and Marc Sher. *Vacuum stability bounds in the two Higgs doublet model*. *Phys.Lett.*, B449:89–92, 1999. arXiv:hep-ph/9811234.

[21] Shinya Kanemura, Takashi Kasai, and Yasuhiro Okada. *Mass bounds of the lightest CP even Higgs boson in the two Higgs doublet model*. *Phys.Lett.*, B471:182–190, 1999. arXiv:hep-ph/9903289.

[22] Riccardo Barbieri, Lawrence J. Hall, and Vyacheslav S. Rychkov. *Improved naturalness with a heavy Higgs: An Alternative road to LHC physics*. *Phys. Rev.*, D74:015007, 2006. arXiv:hep-ph/0603188.

[23] S. Kanemura, T. Kubota, and E. Takasugi. *Lee-Quigg-Thacker bounds for Higgs boson masses in a two-doublet model. Phys. Lett. B*, 313(1-2):155–160, 1993. arXiv:hep-ph/9303263.

[24] M. Baak, M. Goebel, J. Haller, A. Hoecker, D. Ludwig, K. Moenig, M. Schott, and J. Stelzer. *Updated Status of the Global Electroweak Fit and Constraints on New Physics*. *Eur. Phys. J.*, C72:2003, 2012. arXiv:hep-ph/1107.0975.

[25] P. M. Ferreira, R. Santos, and A. Barroso. *Stability of the tree-level vacuum in two Higgs doublet models against charge or CP spontaneous violation. PLB*, 603(3-4):219–229, 2004. arXiv:hep-ph/0406231v2.

[26] I. F. Ginzburg and I. P. Ivanov. *Tree-level unitarity constraints in the most general two Higgs doublet model. PRD*, 72(11), 2005. arxiv:hep-ph/0508020v1.

[27] J. Velhinho, R. Santos, and A. Barroso. *Tree level vacuum stability in two Higgs doublet models*. *Phys.Lett.*, B322:213–218, 1994.

[28] A. Barroso, P. M. Ferreira, R. Santos, and Joao P. Silva. *Stability of the normal vacuum in multi-Higgs-doublet models*. *Phys. Rev.*, D74:085016, 2006.

[29] I. P. Ivanov and Joao P. Silva. *Tree-level metastability bounds for the most general two Higgs doublet model*. 2015. arXiv:hep-ph/1507.05100, CFTP-15-007.

[30] A. Barroso, P. M. Ferreira, and R. Santos. *Neutral minima in two-Higgs doublet models*. *Phys. Lett.*, B652:181–193, 2007. arXiv: hep-ph/0702098.

[31] A. Barroso, P.M. Ferreira, I. Ivanov, R. Santos, and João P. Silva. *Avoiding Death by Vacuum*. *J.Phys.Conf.Ser.*, 447:012051, 2013. arXiv:hep-ph/1305.1906.

[32] A. Barroso, P.M. Ferreira, I.P. Ivanov, and Rui Santos. *Metastability bounds on the two Higgs doublet model. JHEP*, 1306:045, 2013. arXiv:hep-ph/1303.5098.

[33] Dipankar Das and Ipsita Saha. Search for a stable alignment limit in two-Higgs-doublet models. *Phys. Rev.*, D91(9):095024, 2015.

[34] P. M. Ferreira and Bogumila Swiezewska. *One-loop contributions to neutral minima in the inert doublet model. JHEP*, 04:099, 2016. arXiv:hep-ph/1511.02879.

[35] Jeremy Bernon and Beranger Dumont. *Lilith: a tool for constraining new physics from Higgs measurements*. *Eur. Phys. J.*, C75(9):440, 2015. arXiv:hep-ph/1502.04138.

[36] I.P. Ivanov. *Minkowski space structure of the Higgs potential in 2HDM*. *Phys.Rev.*, D75:035001, 2007. arXiv:hep-ph/0609018.

[37] D. Eriksson, J. Rathsman, and O. Stal. *2HDMC - two-Higgs-doublet model calculator. Computer Physics Communications*, 181(1):189–205, 2010. arXiv:hep-ph/0902.0851.

[38] M. Peskin and D. Schroeder. *An introduction to Quantum field Theory.* Westview Press., Cambridge, 1995.

[39] L Ryder. *Quantum field theory.* Cambridge University Press, Cambridge, 1996.

[40] S. Weinberg. *The quantum theory of fields.* Cambridge University Press, Cambridge, 2005.

[41] D. A. Dicus and V. S. Mathur. *Upper bounds on the values of masses in unified gauge theories*. *Phys. Rev.*, D7:3111–3114, 1973.

[42] B. W. Lee, C. Quigg, and H. B. Thacker. *Strength of weak interactions at very high energies and the Higgs boson mass. Physical Review Letters*, 38(16):883–885, 1977.

[43] A. G Akeroyd, A. Arhrib, and E. Naimi. *Note on tree-level unitarity in the general two Higgs doublet model. PLB*, 490(1-2):119–124, 2000. arXiv:hep-ph/0006035.

[44] Horejsi,J. and Kladiva, M. *Tree-unitarity bounds for THDM Higgs masses revisited*. *European Physical Journal C*, 46(1):81–91, 2006.

[45] M. Jacob and G. Wick. *On the general theory of collisions for particles with spin*. *Annals of Physics*, 7:404, 1959.

[46] SNO collaboration. *Measurement of the Cosmic Ray and Neutrino-Induced Muon Flux at the Sudbury Neutrino Observatory.* July 2009. http://www.osti.gov/accomplishments/documents/fullText/ACC0524.pdf.

[47] et al T. Kajita. *Atmospheric $\nu_e\nu_\mu$ ratio in the multi-GeV energy range*. *Physics Letters B*, 335(2):237 – 245, 1994.

[48] et al T. Kajita. *Atmospheric neutrino results from Super-Kamiokande and Kamiokande - Evidence for ν_μ oscillations*. *Nuclear Physics B - Proceedings Supplements*, 77(1-3):123–132, 1999.

[49] M. Sher. *Electroweak Higgs potential and vacuum stability. PR*, 179:273–418, 1989.

[50] K. A. et al Olive. *Review of Particle Physics*. *Chin. Phys.*, C38:090001, 2014.

[51] A. Goudelis, B. Herrmann, and O. Stal. *Dark matter in the Inert Doublet Model after the discovery of a Higgs-like boson at the LHC*. *JHEP*, 09:106, 2013.

[52] P. Ko, Yuji Omura, and Chaehyun Yu. *Higgs and dark matter physics in the type-II two-Higgs-doublet model inspired by E_6 GUT*. *JHEP*, 06:034, 2015. arXiv:hep-ph/1502.00262.

[53] K. S. Babu, Shreyashi Chakdar, and Rabindra N. Mohapatra. *Warm Dark Matter in Two Higgs Doublet Models*. *Phys. Rev.*, D91(7):075020, 2015. arXiv:hep-ph/1412.7745.

[54] James M. Cline and Kimmo Kainulainen. *Improved Electroweak Phase Transition with Subdominant Inert Doublet Dark Matter*. *Phys. Rev.*, D87(7):071701, 2013. arXiv:hep-ph/1302.2614.

[55] Debasish Borah and James M. Cline. *Inert Doublet Dark Matter with Strong Electroweak Phase Transition*. *Phys.Rev.*, D86:055001, 2012. arXiv:hep-ph/1204.4722.

[56] Carlos G. Tarazona, Rodolfo A. Diaz, John Morales, and Andres Castillo. *Phenomenology of the new physics coming from 2HDMs to the neutrino magnetic dipole moment*. 2015. arXiv:hep-ph/1512.07722.

[57] Carlos G. Tarazona, Rodolfo A. Diaz, John Moralesa, and Andrés Castillo. *Contribution to the neutrino magnetic moment coming from 2HDM in presence of magnetic fields*. In *38th International Conference on High Energy Physics (ICHEP 2016) Chicago, IL, USA, August 03-10, 2016*, 2016. arXiv:hep-ph/1611.01135.

[58] I. F. Ginzburg and M. Krawczyk. *Symmetries of two Higgs doublet model and CP violation. PRD*, 72(11), 2005. arXiv:hep-ph/0408011.

[59] F. J. Botella and Joao P. Silva. *Jarlskog - like invariants for theories with scalars and fermions*. *Phys. Rev.*, D51:3870–3875, 1995.

[60] P. M. Ferreira, H. E. Haber, and J. P. Silva. *Generalized "CP" symmetries and special regions of parameter space in the two-Higgs-doublet model. PRD*, 79(11), 2009. arXiv:hep-ph/0902.1537 .

[61] R. A. Diaz. *Phenomenological Analysis of the Two-Higgs-Doublet Model.* PhD thesis, arxiv: hep-ph/0212237.

[62] T.D. Lee and G.C. Wick. *Negative metric and the unitarity of the S-matrix . Nuclear Physics B*, 9(2):209 – 243, 1969.

[63] T. D. Lee and G. C. Wick. *Finite Theory of Quantum Electrodynamics. PRD*, 2:1033–1048, Sep 1970.

[64] Jihn E. Kim. *A Review on axions and the strong CP problem*", booktitle = "Proceedings, 7th International Conference on Supersymmetry and the Unification of Fundamental Interactions (SUSY09). *AIP Conf. Proc.*, 1200:83–92, 2010. arxiv:hep-ph/0909.3908.

[65] Jihn E. Kim. *A Review on axions and the strong CP problem*. *AIP Conf. Proc.*, 1200:83–92, 2010. arXiv:hep-ph/0909.3908.

[66] RobertoD. Peccei. The strong cp problem and axions. In Markus Kuster, Georg Raffelt, and Berta Beltran, editors, *Axions*, volume 741 of *Lecture Notes in Physics*, pages 3–17. Springer Berlin Heidelberg, 2008. arXiv:hep-ph/0607268.

[67] P. M. Ferreira, R. Santos, and A. Barroso. *Erratum: Stability of the tree-level vacuum in two Higgs doublet models against charge or CP spontaneous violation (Physics Letters B (2004) 603 (219)*. 629(2-4):114, 2005. arxiv:hep-ph/0406231.

[68] Shainen M. Davidson and Heather E. Logan. *Dirac neutrinos from a second Higgs doublet*. *Phys. Rev.*, D80:095008, 2009. arxiv:hep-ph/0906.3335.

[69] Alejandro Ibarra and Cristoforo Simonetto. *Understanding neutrino properties from decoupling right-handed neutrinos and extra Higgs doublets*. *JHEP*, 11:022, 2011. arXiv:hep-ph/1107.2386.

[70] Susmita Bhowmik Duari and U. A. Yajnik. *Bubble wall dynamics, generalized Yukawa couplings and adequate electroweak baryogenesis in two Higgs doublet model*. *Mod. Phys. Lett.*, A11:2481–2488, 1996.

[71] E. Rodriguez-Jauregui. *Implications of maximal Jarlskog invariant and maximal CP violation*. 2001.

[72] Henning Flacher, Martin Goebel, Johannes Haller, Andreas Hocker, Klaus Monig, et al. *Revisiting the Global Electroweak Fit of the Standard Model and Beyond with Gfitter*. *Eur.Phys.J.*, C60:543–583, 2009. arxiv/hep-ph:0811.0009.

[73] M. Baak, M. Goebel, J. Haller, A. Hoecker, D. Ludwig, et al. *Updated Status of the Global Electroweak Fit and Constraints on New Physics*. *Eur.Phys.J.*, C72:2003, 2012. arxiv/hep-ph:1107.0975.

[74] J. F. Gunion, H. E. Haber, G. L. Kane, and S. Dawson. *The Higgs Hunter's Guide*, 1990.

[75] Alex Pomarol and Roberto Vega. *Constraints on CP violation in the Higgs sector from the rho parameter*. *Nucl. Phys.*, B413:3–15, 1994.

[76] J. M. Gerard and M. Herquet. *A Twisted custodial symmetry in the two-Higgs-doublet model*. *Phys. Rev. Lett.*, 98:251802, 2007.

[77] M.E. Peskin and T. Takeuchi. *Estimation of oblique electroweak corrections*. *Phys. Rev. D.*, 46:381–409, July 1992.

[78] J. L. Hewett. *The Standard model and why we believe it*. In *Supersymmetry, supergravity and supercolliders. Proceedings, Theoretical Advanced Study Institute in elementary particle physics, TASI'97, Boulder, USA, June 2-27, 1997*, pages 3–83, 1997.

[79] I. Maksymyk, C. P. Burgess, and D. London. *Beyond S, T, and U. Phys. Rev. D.*, 50(1):529–535, 1994. arXiv:hep-ph/9306267.

[80] M. Baak, J. Cúth, J. Haller, A. Hoecker, R. Kogler, K. Mönig, M. Schott, and J. Stelzer. *The global electroweak fit at NNLO and prospects for the LHC and ILC*. *Eur. Phys. J.*, C74:3046, 2014.

[81] M. Awramik, M. Czakon, A. Freitas, and G. Weiglein. *Precise prediction for the W boson mass in the standard model*. *Phys. Rev.*, D69:053006, 2004. arxiv:hep-ph/0311148.

[82] M. Awramik, M. Czakon, and A. Freitas. *Electroweak two-loop corrections to the effective weak mixing angle*. *JHEP*, 11:048, 2006. arXiv/hep-ph/0608099.

[83] M. Awramik, M. Czakon, A. Freitas, and B. A. Kniehl. *Two-loop electroweak fermionic corrections to* $\sin^2\theta b$ *anti-b(eff)*. *Nucl. Phys.*, B813:174–187, 2009. arXiv:hep-ph/0811.1364.

[84] Ayres Freitas. *Higher-order electroweak corrections to the partial widths and branching ratios of the Z boson*. *JHEP*, 04:070, 2014. arXiv:hep-ph/"1401.2447.

[85] P. A. Baikov, K. G. Chetyrkin, J. H. Kuhn, and J. Rittinger. *Complete $\mathcal{O}(\alpha_s^4)$ QCD Corrections to Hadronic Z-Decays*. *Phys. Rev. Lett.*, 108:222003, 2012. arXiv:hep-ph/1201.5804.

[86] Jeremy Bernon, Beranger Dumont, and Sabine Kraml. *Status of Higgs couplings after run 1 of the LHC*. *Phys. Rev.*, D90:071301, 2014.

[87] CMS collaboration. *Summary results of high mass BSM Higgs searches using CMS run-I data*.

[88] Jérémy Bernon, John F. Gunion, Howard E. Haber, Yun Jiang, and Sabine Kraml. *Scrutinizing the alignment limit in two-Higgs-doublet models: m_h=125 GeV*. *Phys. Rev.*, D92(7):075004, 2015. arXiv:hep-ph/1507.00933.

[89] S. L. Glashow, J. Iliopoulos, and L. Maiani. *Weak Interactions with Lepton-Hadron Symmetry*. *Phys. Rev.*, D2:1285–1292, 1970.

[90] Bruce McWilliams and Ling-Fong Li. *Virtual effects of Higgs particles*. *Nuclear Physics B*, 179(1):62 – 84, 1981.

[91] T. P. Cheng and Marc Sher. *Mass-matrix ansatz and flavor nonconservation in models with multiple Higgs doublets*. *PRD*, 35:3484–3491, Jun 1987.

[92] Farvah Mahmoudi and Oscar Stal. *Flavor constraints on the two-Higgs-doublet model with general Yukawa couplings*. *Phys.Rev.*, D81:035016, 2010.

[93] Enrico Lunghi and Amarjit Soni. *Footprints of the Beyond in flavor physics: Possible role of the Top Two Higgs Doublet Model*. *JHEP*, 09:053, 2007. arXiv:hep-ph/0707.0212.

[94] Rick S. Gupta and James D. Wells. *Next Generation Higgs Bosons: Theory, Constraints and Discovery Prospects at the Large Hadron Collider*. *Phys. Rev.*, D81:055012, 2010. arXiv:hep-ph/0912.0267.

[95] Bernard Aubert et al. *Search for the decay $B^+ \to K^+\tau^\mp\mu^\pm$*. *Phys. Rev. Lett.*, 99:201801, 2007.

[96] Eugene Golowich, JoAnne Hewett, Sandip Pakvasa, and Alexey A. Petrov. *Implications of D^0 - $\bar{D}^0$ Mixing for New Physics*. *Phys. Rev.*, D76:095009, 2007.

[97] Zhen-jun Xiao and Libo Guo. *B^0 -$\bar{B}^0$ mixing and $B \to X(s)$ gamma decay in the third type 2HDM: Effects of NLO QCD contributions*. *Phys. Rev.*, D69:014002, 2004. arXiv:hep-ph/0309103.

[98] Zhen-jun Xiao and Ci Zhuang. *Exclusive $B \to (K^*, \rho)\gamma$ decays in the general two Higgs doublet models*. *Eur. Phys. J.*, C33:349–368, 2004. arXiv:hep-ph/0310097.

[99] Rodolfo A. Diaz, R. Martinez, and Carlos E. Sandoval. *Flavor changing neutral currents from lepton and B decays in the two Higgs doublet model*. *Eur. Phys. J.*, C41:305–310, 2005. arXiv:hep-ph/0406265.

[100] Rodolfo A. Diaz, R. Martinez, and Jairo Alexis Rodriguez. *Phenomenology of lepton flavor violation in 2HDM type III from (g-2)μ and leptonic decays*. *Phys. Rev.*, D67:075011, 2003. arXiv:hep-ph/0208117.

[101] Andreas Crivellin, Christoph Greub, and Ahmet Kokulu. *Flavour-violation in two-Higgs-doublet models*. *PoS*, EPS-HEP2013:338, 2013.

[102] Malte Buschmann, Joachim Kopp, Jia Liu, and Xiao-Ping Wang. *New Signatures of Flavor Violating Higgs Couplings*. 2016.

[103] Dhiman Chakraborty. *Charged Higgs boson searches at the LHC*. *Nuclear and Particle Physics Proceedings*, 260:216 – 220, 2015. The 13th International Workshop on Tau Lepton PhysicsThe 13th International Workshop on Tau Lepton Physics (Tau2014).

[104] Georges Aad et al. *Search for charged Higgs bosons in the $H^\pm \to tb$ decay channel in pp collisions at $\sqrt{s} = 8$ TeV using the ATLAS detector*. 2015.

[105] *Search for charged Higgs bosons: Preliminary combined results using LEP data collected at energies up to 209-GeV*. In *Lepton and photon interactions at high energies. Proceedings, 20th International Symposium, LP 2001, Rome, Italy, July 23-28, 2001*, 2001.

[106] T. Aaltonen et al. *Search for charged Higgs bosons in decays of top quarks in p anti-p collisions at s**(1/2) = 1.96 TeV*. *Phys. Rev. Lett.*, 103:101803, 2009.

[107] V. M. Abazov et al. *Search for Charged Higgs Bosons in Top Quark Decays*. *Phys. Lett.*, B682:278–286, 2009.

[108] Georges Aad et al. *Search for charged Higgs bosons decaying via $H^{\pm} \to \tau^{\pm}\nu$ in fully hadronic final states using pp collision data at $\sqrt{s} = 8$ TeV with the ATLAS detector*. *JHEP*, 03:088, 2015.

[109] Georges Aad et al. *Search for a multi-Higgs-boson cascade in $W^+W^?b\bar{b}$ events with the ATLAS detector in pp collisions at $\sqrt{s} = 8\,TeV$*. *Phys. Rev.*, D89(3):032002, 2014.

[110] Vardan Khachatryan et al. *Search for a pseudoscalar boson decaying into a Z boson and the 125 GeV Higgs boson in $l^+l^-b\bar{b}$ final states*. *Phys. Lett.*, B748:221–243, 2015.

[111] Wu-Ki Tung. *Group Theory in Physics*. World Scientific Publishing, Cambridge, 2003.

[112] S.R. Juarez W., D. Morales C., and P. Kielanowski. *Outlook on the Higgs particles, masses and physical bounds in the Two Higgs-Doublet Model*. 2012. arxiv/hep-ph:1201.1876.

[113] S. R. Juarez W., D. Morales C., and P. Kielanowski. *Outlook on the Higgs particles, masses and physical bounds in the Two Higgs-Doublet Model*. 2012.

[114] P. M. Ferreira and D. R. T. Jones. *Bounds on scalar masses in two Higgs doublet models*. *JHEP*, 08:069, 2009. arxiv:hep-ph/0903.2856.

[115] Igor P. Ivanov. *Minkowski space structure of the Higgs potential in 2HDM. II. Minima, symmetries, and topology*. *Phys.Rev.*, D77:015017, 2008. arXiv:hep-ph/0710.3490.

[116] A. Barroso, P. M. Ferreira, I. P. Ivanov, and Rui Santos. *Metastability bounds on the two Higgs doublet model*. *JHEP*, 06:045, 2013. arXiv:hep-ph/1303.5098.

[117] M. Maniatis, A. von Manteuffel, O. Nachtmann, and F. Nagel. *Stability and symmetry breaking in the general two-Higgs-doublet model*. *Eur. Phys. J.*, C48:805–823, 2006. arXiv:hep-ph/0605184.

[118] I. F. Ginzburg, I. P. Ivanov, and K. A. Kanishev. *The Evolution of vacuum states and phase transitions in 2HDM during cooling of Universe*. *Phys. Rev.*, D81:085031, 2010.

[119] I. F. Ginzburg and I. P. Ivanov. *Tree-level unitarity constraints in the most general 2HDM*, year=2005, journal=Phys.Rev.D, volume=72, note=arXiv:hep-ph/0508020 and arXiv:hep-ph/0312374,.

[120] C. R. Das and M. K. Parida. *New formulas and predictions for running fermion masses at higher scales in SM, 2 HDM, and MSSM*. *Eur. Phys. J.*, C20:121–137, 2001.

[121] H. Arason, D. J. Castaño, B. Kesthelyi, S. Mikaelian, E. J. Piard, P. Ramond, and B. D. Wright. *Renormalization-group study of the standard model and its extensions: The standard model*. *PRD*, 46:3945–3965, Nov 1992.

[122] T. P. Cheng, E. Eichten, and Ling-Fong Li. *Higgs phenomena in asymptotically free gauge theories*. *PRD*, 9:2259–2273, Apr 1974.

[123] Marie E. Machacek and Michael T. Vaughn. *Two-loop renormalization group equations in a general quantum field theory (II). Yukawa couplings* . *Nuclear Physics B*, 236(1):221 – 232, 1984.

[124] Howard E. Haber and Ralf Hempfling. *The Renormalization group improved Higgs sector of the minimal supersymmetric model*. *Phys. Rev.*, D48:4280–4309, 1993.

[125] Walter Grimus and Luis Lavoura. *Renormalization of the neutrino mass operators in the multi-Higgs-doublet standard model*. *Eur. Phys. J.*, C39:219–227, 2005.

[126] Nikita Blinov, Stefano Profumo, and Tim Stefaniak. *The Electroweak Phase Transition in the Inert Doublet Model*. *JCAP*, 1507(07):028, 2015. arXiv:hep-ph/1504.05949.

[127] Florian Staub. *SARAH 4 : A tool for (not only SUSY) model builders*. *Comput. Phys. Commun.*, 185:1773–1790, 2014.

[128] R. Keith Ellis, Zoltan Kunszt, Kirill Melnikov, and Giulia Zanderighi. *One-loop calculations in quantum field theory: from Feynman diagrams to unitarity cuts*. *Phys. Rept.*, 518:141–250, 2012. arXiv:hep-ph/1105.4319.

[129] Jorge Romao. Modern Techniques for One-Loop Calculations. http://porthos.ist.utl.pt/OneLoop/one-loop.pdf.

[130] Shainen M. Davidson and Heather E. Logan. *LHC phenomenology of a two-Higgs-doublet neutrino mass model*. *Phys. Rev.*, D82:115031, 2010. arxiv:hep-ph/1009.4413.

[131] Walter Grimus and Luis Lavoura. *Renormalization of the neutrino mass operators in the multi-Higgs-doublet standard model*. *Eur.Phys.J.*, C39:219–227, 2005. arXiv:hep-ph/0409231.

[132] Howard E. Haber and Ralf Hempfling. *The Renormalization group improved Higgs sector of the minimal supersymmetric model*. *Phys.Rev.*, D48:4280–4309, 1993. arXiv:hep-ph/9307201.

[133] Timothy. Hollowod. *Renormalization Group and Fixed Points in Quantum Field Theory*. Springer Briefs in Physics, London, 2013.

[134] Zhi-zhong Xing and Zhen-hua Zhao. *On the four-zero texture of quark mass matrices and its stability*. *Nucl. Phys.*, B897:302–325, 2015. arXiv:hep-ph/1501.06346.

[135] Manmohan Gupta and Gulsheen Ahuja. *Flavor mixings and textures of the fermion mass matrices*. *Int. J. Mod. Phys.*, A27:1230033, 2012. arXiv:hep-ph/1302.4823.

[136] S. Groote O. Yakovlev. Top quark production near threshold at NLC. UM-TH-00-22, CLNS 00/1690.

[137] Martin C. Smith and Scott S. Willenbrock. Top quark pole mass. *Phys. Rev. Lett.*, 79:3825–3828, 1997. arXiv:hep-ph/9612329.

[138] Johan Löfgren. *Electroweak phase transitions in two Higgs doublet models*. Ph.D Thesis, https://www.diva-portal.org/smash/get/diva2:833479/FULLTEXT01.pdf.

[139] James M. Cline and Pierre-Anthony Lemieux. *Electroweak phase transition in two Higgs doublet models*. *Phys. Rev.*, D55:3873–3881, 1997.

[140] Zaglauer H. Lindner M., Sher M. *Probing vacuum stability bounds at the fermilab collider* . *PLB*, 228:139–143, 1989.

[141] Isidori G. Altarelli G. *Lower limit on the Higgs mass in the standard model: An update*. *PLB*, 337:141–144, 1994.

[142] N. Cabibbo, L. Maiani, G. Parisi, and R. Petronzio. *Bounds on the fermions and Higgs boson masses in grand unified theories*. *Nucl. Physics, Sect. B*, 158(2-3):295–305, 1979.

[143] Pham Quang Hung. *Vacuum instability and new constraints on fermion masses*. *Phys. Rev. Lett.*, 42(14):873–876, 1979.

[144] Jose Eliel Camargo-Molina, Ben O'Leary, Werner Porod, and Florian Staub. *On the vacuum stability of SUSY models*. *PoS*, EPS-HEP2013:265, 2013. arXiv:hep-ph/1310.1260.

[145] J. E. Camargo-Molina, B. O'Leary, W. Porod, and F. Staub. *Stability of the CMSSM against sfermion VEVs*. *JHEP*, 12:103, 2013. arXiv:hep-ph/1309.7212.

[146] Georg Kreyerhoff and R. Rodenberg. *Renormalization Group Analysis of Coleman-Weinberg Symmetry Breaking in Two Higgs Models*. *Phys.Lett.*, B226:323, 1989.

[147] Boris M. Kastening. Bounds from stability and symmetry breaking on parameters in the two Higgs doublet potential. 1992. arXiv:hep-ph/9307224.

[148] Matthew D. Schwartz. *Quantum Field Theory and the Standard Model*. Cambridge University Press., 2013.

[149] C. Itzykson and J.B. Zuber. *Quantum Field Theory*. Dover Books on Physics. Dover Publications, 2012.

[150] Kassahun Betre, Sonia El Hedri, and Devin G. E. Walker. *Perturbative Unitarity Constraints on the NMSSM Higgs Sector*. 2014. arXiv:hep-ph/1410.1534.

[151] Alexander Schuessler and Dieter Zeppenfeld. *Unitarity constraints on MSSM trilinear couplings*. In *SUSY 2007 proceedings, 15th International Conference on Supersymmetry and Unification of Fundamental Interactions, July 26 - August 1, 2007, Karlsruhe, Germany*, 2007. arXiv:hep-ph/0710.5175.

[152] Rafael L. Delgado, Antonio Dobado, and Felipe J. Llanes-Estrada. *Unitarity, analyticity, dispersion relations, and resonances in strongly interacting W_LW_L, Z_LZ_L, and hh scattering*. *Phys. Rev.*, D91(7):075017, 2015. arXiv:hep-ph/1502.04841.

[153] Rafael L. Delgado, Antonio Dobado, and Felipe J. Llanes-Estrada. *A Strongly Interacting Electroweak Symmetry Breaking Sector with a Higgs-like light scalar*. In *11th Conference on Quark Confinement and the Hadron Spectrum (Confinement XI) St. Petersburg, Russia, September 8-12, 2014*, 2014. arXiv:hep-ph/1412.3277.

[154] Antonio Dobado, Rafael L. Delgado, and Felipe J. Llanes-Estrada. *Strongly Interacting Electroweak Symmetry Breaking Sector with a Higgs-like light scalar*. *AIP Conf. Proc.*, 1606:151–158, 2014. arXiv:hep-ph/1402.0666.

[155] Tyler Corbett, O.J.P. Éboli, and M.C. Gonzalez-Garcia. *Unitarity Constraints on Dimension-Six Operators*. *Phys. Rev.*, D91(3):035014, 2015. arXiv:hep-ph/1411.5026.

[156] Gerhard Buchalla and Oscar Cata. *Effective Theory of a Dynamically Broken Electroweak Standard Model at NLO*. *JHEP*, 07:101, 2012. arXiv:hep-ph/1203.6510.

[157] J Maalampi, J Sirkka, and I Vilja. *Tree level unitarity and triviality bounds for two-Higgs models* . *PLB*, 265(34):371 – 376, 1991.

[158] Lorenzo Basso. *Phenomenology of the minimal B-L extension of the Standard Model at the LHC*. PhD thesis, Southampton University., 2011. arXiv:hep-ph:1106.4462.

[159] Lorenzo Basso, Stefano Moretti, and Giovanni Marco Pruna. *Theoretical constraints on the couplings of non-exotic minimal Z' bosons*. *JHEP*, 08:122, 2011. arXiv:hep-ph/1106.4762.

[160] Lorenzo Basso, Stefano Moretti, and Giovanni Marco Pruna. *The Pure $B-L$ Model and Future Linear Colliders: the Higgs Sector*. In *International Workshop on Future Linear Colliders (LCWS11) Granada, Spain, September 26-30, 2011*, 2012. arXiv:hep-ph/1201.5355.

[161] F. Maltoni, J. M. Niczyporuk, and S. Willenbrock. *The Scale of fermion mass generation*. *Phys. Rev.*, D65:033004, 2002. arXiv:hep-ph/0106281.

[162] T. Appelquist and M. S. Chanowitz. Unitarity bound on the scale of fermion mass generation. *Phys. Rev. Lett.*, 59:2405–2407, Nov 1987.

[163] Thomas Appelquist and J. Carazzone. *Infrared singularities and massive fields. PRD*, 11:2856–2861, May 1975.

[164] C.H. Llewellyn Smith. High energy behaviour and gauge symmetry. *Physics Letters B*, 46(2):233 – 236, 1973.

[165] Andrés Castillo, Rafael L. Delgado, Antonio Dobado, and Felipe J. Llanes-Estrada. *Top-antitop production from $W_L^+W_L^-$ and Z_LZ_L scattering under a strongly-interacting symmetry-breaking sector*. 2016. arXiv:hep-ph/1607.01158.

[166] Mitchell Golden. *Unitarity and fermion mass generation*. *Phys. Lett.*, B338:295–300, 1994. arXiv:hep-ph/9408272.

[167] Sally Dawson and Scott Willenbrock. *Radiative Corrections to Longitudinal Vector Boson Scattering*. *Phys.Rev.*, D40:2880, 1989.

[168] Andrés Castillo, Rodolfo A. Diaz, and Jhon Morales. *Unitarity constraints for Yukawa couplings in the two-Higgs-doublet model type III. International Journal of Modern Physics A*, 29(18):1450085, 2014. arxiv: hep-ph/1309.0831.

[169] Shinya Kanemura, Takashi Kasai, and Yasuhiro Okada. *Upper bounds and lower bounds of the lightest CP even Higgs boson in the two Higgs doublet model*. 1999. arXiv:hep-ph/9911312.

[170] Andrés Castillo, Rodolfo A. Diaz, John Morales, and Carlos G. Tarazona. *Study of vacuum behavior for inert models with discrete Z_2-like and abelian $U(1)$ symmetries*. 2015. arXiv:hep-ph/1510.00494.

[171] Marcela Carena, Ian Low, Nausheen R. Shah, and Carlos E. M. Wagner. *Impersonating the Standard Model Higgs Boson: Alignment without Decoupling*, 2013. arxiv/hep-ph:1310.2248.

[172] Nikita Blinov, Jonathan Kozaczuk, David E. Morrissey, and Alejandro de la Puente. Compressing the Inert Doublet Model. *Phys. Rev.*, D93(3):035020, 2016.

[173] I. F. Ginzburg, K. A. Kanishev, M. Krawczyk, and D. Sokolowska. *Evolution of Universe to the present inert phase*. *Phys. Rev.*, D82:123533, 2010.

[174] *First Combination of Tevatron and LHC Measurements of the Top-Quark Mass*. 2014. arxiv:hep-ph/1403.4427.

[175] Michael E. Peskin and Tatsu Takeuchi. *A New constraint on a strongly interacting Higgs sector*. *Phys.Rev.Lett.*, 65:964–967, 1990.

[176] W.J. Marciano and J.L. Rosner. *Atomic parity violation as a probe of new physics*. *Physical Review Letters*, 65:2963–2966, December 1990.

[177] W.J. Marciano and J.L. Rosner. *Erratum: " Parity violation as a probe of new physics*. *Physical Review Letters*, 68:898, February 1992.

[178] M. Baak, M. Goebel, J. Haller, A. Hoecker, D. Kennedy, K. Mönig, M. Schott, and J. Stelzer. *Updated status of the global electroweak fit and constraints on new physics. European Physical Journal C*, 72(5):1–35, 2012. arXiv:hep-ph/1107.0975.

[179] Martin Goebel. *Global Fits of the electroweak Standard Model and beyond with Gfitter*. In *Proceedings, 44th Rencontres de Moriond on Electroweak Interactions and Unified Theories*, pages 65–70, 2009. arXiv:hep-ph/0905.2488.

[180] Gerhardt Funk, Deva O'Neil, and R. Michael Winters. *What the Oblique Parameters S, T, and U and Their Extensions Reveal About the 2HDM: A Numerical Analysis*. *Int. J. Mod. Phys.*, A27:1250021, 2012.

[181] Erik Lundstrom, Michael Gustafsson, and Joakim Edsjo. *The Inert Doublet Model and LEP II Limits*. *Phys. Rev.*, D79:035013, 2009.

[182] Michael Gustafsson, Erik Lundstrom, Lars Bergstrom, and Joakim Edsjo. *Significant Gamma Lines from Inert Higgs Dark Matter*. *Phys. Rev. Lett.*, 99:041301, 2007.

[183] Qing-Hong Cao, Ernest Ma, and G. Rajasekaran. *Observing the Dark Scalar Doublet and its Impact on the Standard-Model Higgs Boson at Colliders*. *Phys. Rev.*, D76:095011, 2007.

[184] P. A. R. Ade et al. *Planck 2015 results. XIII. Cosmological parameters*. 2015.

[185] Abdesslam Arhrib, Yue-Lin Sming Tsai, Qiang Yuan, and Tzu-Chiang Yuan. *An Updated Analysis of Inert Higgs Doublet Model in light of the Recent Results from LUX, PLANCK, AMS-02 and LHC*. *JCAP*, 1406:030, 2014.

[186] Adrian Carmona and Mikael Chala. *Composite Dark Sectors*. *JHEP*, 06:105, 2015.

[187] Joachim Kopp, Thomas Schwetz, and Jure Zupan. *Global interpretation of direct Dark Matter searches after CDMS-II results*. *JCAP*, 1002:014, 2010. arXiv:hep-ph/0912.4264.

[188] D. S. Akerib et al. *Limits on Spin-Independent Wimp-Nucleon Interactions from the Two-Tower Run of the Cryogenic Dark Matter Search*. *Phys. Rev. Lett.*, 96:011302, 2006.

[189] Yann Mambrini, Stefano Profumo, and Farinaldo S. Queiroz. *Dark Matter and Global Symmetries*. 2015. arXiv:hep-ph/1508.06635.

[190] G. Belanger, B. Dumont, U. Ellwanger, J. F. Gunion, and S. Kraml. *Status of invisible Higgs decays*. *Phys. Lett.*, B723:340–347, 2013. arXiv:hep-ph/1302.5694.

[191] Abdelhak Djouadi, Adam Falkowski, Yann Mambrini, and Jeremie Quevillon. *Direct Detection of Higgs-Portal Dark Matter at the LHC*. *Eur. Phys. J.*, C73(6):2455, 2013. arXiv:hep-ph/1205.3169.

[192] Andrés Castillo, Rodolfo A. Diaz, John Morales, and Carlos G. Tarazona. *Phenomenological aspects from vacuum stability and metastability in models with soft breaking of a U* (1) *global symmetry*. 2016. arXiv:hep-ph/1607.07972.

[193] Pete. Gabor. Morse theory. In University Cambridge, editor, *Morse Theory*, Lecture Notes, pages 1–51. 2001.

[194] R. D. Peccei and H. R. Quinn. *Constraints imposed by "CP" conservation in the presence of pseudoparticles. Phys. Rev. D.*, 16(6):1791–1797, 1977.

[195] R. D. Peccei and H. R. Quinn. *"CP" conservation in the presence of pseudoparticles. PRL*, 38(25):1440–1443, 1977.

[196] Philipp Burda, Ruth Gregory, and Ian Moss. *Vacuum metastability with black holes. JHEP*, 08:114, 2015. arXiv:hep-th/1503.07331.

[197] Philipp Burda, Ruth Gregory, and Ian G. Moss. *Gravity and the Stability of the Higgs Vacuum. Phys. Rev. Lett.*, 115:071303, 2015. arXiv:hep-th/1501.04937.

[198] Philipp Burda, Ruth Gregory, and Ian Moss. *The fate of the Higgs vacuum. JHEP*, 06:025, 2016.

[199] W. Grimus, L. Lavoura, O. M. Ogreid, and P. Osland. *The oblique parameters in multi-Higgs-doublet models. NPB*, 801(1-2):81–96, 2008. arXiv:hep-ph/0802.4353v1-2.

[200] Johannes Haller. *Fits of the Electroweak Standard Model and Beyond using Gfitter*. 2008. arXiv:hep-ph/0810.3664.

[201] Alex D. D. Craik. *Prehistory of Faà di Bruno's Formula. The American Mathematical Monthly*, 112(2):119–130, 2005.

[202] A. Barroso, P.M. Ferreira, and R. Santos. *Some remarks on tree-level vacuum stability in two Higgs doublet models. Afr.J.Math.Phys.*, 3:103–109, 2006. arXiv:hep-ph/0507329.

[203] George Simons. *Introduction to Topology and Modern Analysis.* Robert E. Creiger Publishing Company, 1983.

[204] Barret O'Neill. *Semi-Riemannian Geometry.* Academic Press, 1983.

[205] Igor Prokhorenkov. *Witten's Proof of Morse Inequalities.* 2012. http://faculty.tcu.edu/richardson/Seminars.

[206] Gabor Pete. *Morse Theory.* Trinity College, University of Cambridge, UK, Bolyai Institute, University of Szeged, Hungary, 2001.

[207] James J. Callahan. *Advanced Calculus: A Geometric View.* Springer, 2010.

[208] *Hessian matrices*: https://wj32.org/wp/2013/02/26/convex-functions-second-derivatives-and-hessian-matrices. Accessed: 2016-06-30.

[209] P. M. Ferreira and D. R. T. Jones. *Bounds on scalar masses in two Higgs doublet models. JHEP*, 08:069, 2009.

[210] Vardan Khachatryan et al. *Observation of the diphoton decay of the Higgs boson and measurement of its properties. Eur. Phys. J.*, C74(10):3076, 2014. arXiv:hep-ph/1407.0558.

Index

UNIVERSIDAD
NACIONAL
DE COLOMBIA

Grupo de Campos y Partículas
Facultad de Ciencias